Université de Liège – University of Liège

Faculté des Sciences – Faculty of Sciences

PhD Thesis

Study of Marine Heatwaves in a semi-enclosed coastal area: detection, formation, drivers and impacts, using a combination of satellite and in situ data

Cécile Pujol

En vue de l'obtention du diplôme – Submitted in fulfilment of the requirements for

Doctorat en Océanographie – Doctor of Sciences in Oceanography

Années académiques – Academic years: 2021-2025

Promotrice – Supervisor: Aida Alvera-Azcárate *(GeoHydrodynamics and Environment Research, Liège, Belgium)*
Co-promoteur – Co-supervisor: Alexander Barth *(GeoHydrodynamics and Environment Research, Liège, Belgium)*

Cette thèse a débuté le 1er octobre 2021 et a été défendue le 23 octobre 2025.

This PhD Thesis started on October 1st, 2021, and finished on October 23th, 2025.

Membres du jury   –   Jury members

Sylvie Gobert (President) – *University of Liège, Belgium*

Aida Alvera-Azcárate – *University of Liège, Belgium*

Alexander Barth – *University of Liège, Belgium*

Iván Pérez Santos – *Universidad de Los Lagos, Chile*

Carole Rougeot – *University of Liège, Belgium*

Robert Schlegel – *Sorbonne University, France*

UNIVERSITY OF LIÈGE

Faculty of Sciences

Department of Astrophysics, Geography and Oceanography

Abstract

PhD Thesis in Oceanography

Study of Marine Heatwaves in a semi-enclosed coastal area: their detection, formation, drivers and impacts, using a combination of satellite and in situ data

by Cécile Pujol

Marine heatwaves (MHWs) and marine cold spells (MCSs) are discrete temperature anomalies events that can persist for weeks or months, often causing severe ecological and socio-economic impacts. This thesis investigates the development, drivers and consequences of MHWs and MCSs in Central and Southern Chile (29°S-55°S), with a particular focus on Northern Patagonia, a region of oceanographic interest and of an economic importance due to intensive aquaculture activity. The main objective is to characterise the surface and subsurface dynamics of MHWs and MCSs, assess their spatial variability among large basins and narrow fjords, identify their drivers, and evaluate their ecological implications.

A multi-scale approach was applied, moving from offshore to coastal environments and from surface to subsurface layers. At large scale, satellite reanalysis data at low resolution (0.25°) were used to identify patterns, long-term trends and main drivers of MHWs in Central and Southern Chile, regions previously unexplored in this context. At finer scale, a novel methodology was developed, merging over three decades of in situ observations with satellite products to generate high-resolution (900 m) temperature fields for Northern Patagonia. This allowed the detection of extreme events across fjords and basins and the assessment of their spatial and temporal variability. Subsurface dynamics where also explored with a hydrodynamic model to evaluate the vertical extent of MHWs and MCS and the relation between surface and subsurface events. Additionally, the potential role of MHWs in promoting harmful algal blooms (HABs) was investigated.

Results show that Central Chile and Northern and Southern Patagonia experienced more than 70 MHWs over the past four decades. Northern Patagonia displays the strongest warming trends and is the only subregion with a significant increase in MHW frequency, with more than 30 events in the past decade alone, while MCSs show an overall decline. In this region, the spatial heterogeneity is particularly pronounced, depending mostly on the topography and stratification: stratified fjords experienced stronger anomalies (up to 5°C), whereas more homogeneous basins exhibited weaker events (below 2°C). Major

MHWs occurred in 1997-98, 2008 and 2016-17, with contrasting subsurface penetration. The 1997-98 event shown rapid propagation to the bottom layers, while the 2016-17 event remained confined to the upper layers. Similarly, a prolonged series of MCSs affected intermediate layers from 2019 to 2024, while the main events were registered in 2007-08. For both MHWs and MCSs, subsurface anomalies were generally more intense below the low-salinity surface layer and considerably longer-lasting than those at the surface, with events extending over several months or years, with the extreme example of a MCS that lasted from 2022 to 2024 in the deep layers of Reloncaví Sound. Atmospheric forcings, particularly wind and solar radiation, were identified as key local drivers, while large-scale climate modes such as El Niño Southern Oscillation (ENSO) and Southern Annular Mode (SAM) amplified event intensity and duration. Finally, a link was established between MHWs and HAB development, with evidence that MHWs act as a catalyst for *A. catenella* blooms by creating favourable environmental conditions when sufficient nutrients are available.

This work provides the first integrated assessment of MHWs and MCSs in Central and Southern Chile, particularly in Northern Patagonia, demonstrating the importance of high-resolution approaches for capturing their complexity in coastal systems and highlighting implications for ecosystem functioning, fisheries and aquaculture management.

Key words: Marine heatwave, Marine cold spell, Sea temperature, Climate change, Patagonia, Chile, Aquaculture

Résumé

Doctorat en Océanographie

Study of Marine Heatwaves in a semi-enclosed coastal area: their detection, formation, drivers and impacts, using a combination of satellite and in situ data

Par Cécile Pujol

Les vagues de chaleur marines (MHWs) et les vagues de froid marines (MCSs) sont des évènements discrets d'anomalies de température qui peuvent persister plusieurs semaines, voire plusieurs mois, ayant de sévère répercussions environnementales et socio-économiques. Cette thèse analyse le développement, les causes et les conséquences des MHWs et MCSs dans le centre et le sud du Chili (29°S-55°S) avec une attention particulière sur le nord de la Patagonie, une région d'importance économique en raison de la présence de nombreux centres aquacoles. L'objectif principal de la thèse est de caractériser les dynamiques de surface et de subsurface de ces évènements extrêmes, de comprendre leur variabilité spatiale et temporelle entre les grands bassins et les fjords étroits, d'identifier leurs causes ainsi que leurs impacts.

Une approche multi-échelle a été adoptée, allant des zones océaniques offshores jusqu'aux écosystèmes côtiers, et de la surface vers les fonds marins. A grande échelle, un produit satellitaire de réanalyse à faible résolution (0,25°) a été utilisé pour identifier les patterns, les tendances à long terme et les facteurs des MHWs dans le centre et le sud du Chili, des régions qui n'avaient jamais été étudiées sous cet angle. A plus fine échelle, une nouvelle méthodologie a été développée, combinant plus de trois décennies de données in situ et des observations satellitaires pour générer des champs de température de l'eau à une résolution de 900 m pour la Patagonie du Nord. Cette approche a permis de détecter les évènements extrêmes dans les fjords et les bassins, ainsi que d'établir leur variabilité spatio-temporelle. La dynamique de subsurface a également été explorée à l'aide d'un modèle hydrodynamique afin d'évaluer la propagation verticale des MHWs et MCSs et leur relation avec les évènements de surface. Enfin, le rôle potentiel des MHWs dans le développement d'efflorescences d'algues toxiques (HABs) a été examiné.

Les résultats montrent que le centre du Chili et la Patagonie ont subi plus de 70 MHWs au cours des quatre dernières décennies. Le nord de la Patagonie se distingue par des

tendances de réchauffement particulièrement marquées et constitue la seule sous-région où la fréquence des MHWs augmente avec plus de 30 évènements sur la seule dernière décennie, tandis que les MCSs y présentent une tendance à la diminution. Dans cette même région, l'hétérogénéité spatiale est particulièrement importante, et résulte surtout de la topographie et de la stratification : les fjords, fortement stratifiés, sont touchés par des intensités beaucoup plus marquées (jusqu'à 5°C) que les bassins plus homogénéisés (moins de 2°C). Les MHWs les plus importantes se sont produites en 1997-98, 2008 et 2016-17, avec schémas de propagation verticale différents : celle de 1997-98 a très rapidement atteint les couches de subsurface, tandis que celle de 2016-17 est restée confinée à la superficie. De manière similaire, une série de MCSs s'est produite dans les couches intermédiaires entre 2019 et 2024, tandis que les évènements les plus importants ont été observées en 2007-08. Pour les MHWs comme pour les MCSs, les anomalies situées sous la couche de surface peu saline sont plus intenses. Les évènements de subsurface, sont également considérablement plus longs que ceux en surface, avec certains épisodes qui durent plusieurs mois voire plusieurs années. Cela a notamment été le cas lors d'une MCS présente pendant trois ans, de 2022 à 2024, dans le Golfe de Reloncaví. Les forçages atmosphériques, en particulier les vents et le rayonnement solaire, jouent un rôle déterminant, tandis que les modes climatiques à grande échelle, tels que El Niño Southern Oscillation (ENSO) and Southern Annular Mode (SAM), amplifient l'intensité et la durée des évènements. Enfin, un lien a été mis en évidence entre les MHWs et la prolifération de HABs d'*Alexandrium catenella,* qui trouvent dans ces conditions un environnement favorable à leur développement.

Ce travail propose la première évaluation des MHWs et MCSs dans le centre et le sud du Chili, en particulier dans le nord de la Patagonie, mettant en évidence l'importance d'utiliser des approches à haute résolution pour observer la complexité de ces évènements dans les environnements côtiers et souligne leurs conséquences potentielles sur le fonctionnement des écosystèmes ainsi que sur les secteurs de la pêche et de l'aquaculture.

Mots-clés : Vague de chaleur marine, Vague de froid marine, Changement climatique, Température des océans, Patagonie, Chili, Aquaculture

Resumen

Tesis de Doctorado en Oceanografía

Study of Marine Heatwaves in a semi-enclosed coastal area: their detection, formation, drivers and impacts, using a combination of satellite and in situ data

Por Cécile Pujol

Las Olas de Calor Marinas (MHWs) y Olas de Frio (MCSs) son diferentes eventos anómalos de temperatura que pueden persistir por semanas o meses, a menudo causando severos impactos ecológicos y socio-economicos. Esta tesis investiga el desarrollo, causas y consecuencias de MHWs y MCSs en el centro y sur de Chile (29°S-55°), enfocándose particularmente en la Patagonia Norte de Chile, una región de interés oceanográfico y de importancia económica debido a la acuicultura. El objetivo principal de este trabajo es caracterizar las dinámicas de las MHWs y MCSs en superficie y subsuperficie, evaluar su variabilidad espacial entre cuencas y fiordos, identificando sus causas y evaluando sus implicaciones ecológicas.

Una aproximación multiescalar fue aplicada, moviéndose desde mar abierto hacia ambientes costeros y desde la superficie hacia capaz subsuperficiales. A gran escala, reanálisis de datos satelitales en baja resolución (0.25°) fueron usados para identificar patrones, tendencias a largo plazo y principales causas de MHWs en el centro y sur de Chile, región no estudiada en esta materia. A fina escala, una novedosa metodología fue desarrollada, uniendo tres décadas de observaciones in situ con productos satelitales para generar una alta resolución (900 m) en campos de temperatura para la Patagonia Norte de Chile. Esto permitió la detección de eventos extremos a través de los fiordos y cuencas, y la evaluación de su variabilidad espacial y temporal. Las dinámicas subsuperficiales también fueron investigadas con un modelo hidrodinámico para evaluar la extensión vertical de MHWs y MCSs y la relación entre los eventos superficiales y subsuperficiales, además del rol potencial de MHWs en promover floraciones algales nocivas (HABs).

Los resultados muestran que la zona central, en conjunto con el norte y sur de la Patagonia de Chile experimentaron alrededor de 70 MHWs en las últimas cuatro décadas. La Patagonia Norte de Chile demuestra fuertes tendencias al calentamiento, siendo la única subregión con un incremento significativo en la frecuencia de MHWs, con más de 30 eventos solamente en la última década, mientras que MCSs muestran una

disminución en general. En esta región, la espacialidad heterogénea es particularmente pronunciada, despendiendo mayoritariamente de la topografía y estratificación: los fiordos estratificados experimentaron fuertes anomalías (sobre 5°C), mientras que cuencas más homogéneas presentaron eventos débiles (bajo los 2°C). Las MHWs más intensas ocurrieron en 1997-98, 2008 y 2016-17, con diferentes niveles de penetración subsuperficial. El evento de 1997-98 indico una rápida propagación hacia capas profundas, mientras que el evento de 2016-17 se mantuvo confinado en capas superiores. Similarmente, una serie prolongada de MCSs afectó las capas intermediarias desde 2019 a 2024, pero los principales eventos fueron registrados en 2007-08. Para ambos (MHWs y MCSs), las anomalías subsuperficiales fueron generalmente mas intensas debajo de la capa superficial de baja salinidad y considerablemente mas duraderas que las superficiales, con eventos extendidos por varios meses o años, con el ejemplo extremo de una MCSs desde 2022 a 2024 en capas profundad del Seno Reloncaví. Forzantes atmosféricos, particularmente vientos y radiación solar, fueron identificados como causas locales claves, mientras que eventos climáticos a gran escala como El Niño (ENSO) y el Modo Anular del Sur (SAM) amplifican la intensidad y duración de los eventos. Finalmente, se encontró una conexión entre MHWs y desarrollo de HABs, con evidencia que las MHWs actúan como precursor de la proliferación de *Alexamdrium catenella*, creando condiciones ambientales favorables cuando la suficiente cantidad de nutrientes son disponibles.

Este trabajo promueve la primera evaluación integrada de MHWs y MCSs en el centro y sur de Chile, particularmente en la Patagonia Norte, demostrando la importancia de la alta resolución aproximada para capturar la complejidad de su sistema de costas y resalta las implicaciones para los ecosistemas, pesquería y acuicultura.

Palabras claves: Ola de calor marina, Ola de frio marina, Cambio climático, Temperatura del mar, Patagonia, Chile, Acuicultura

Acknowledgments

I would like to particularly thank my thesis directors, Aida and Alex, for their constant help and support during these last four (and even more) years. I would like to particularly thank you Aida for trusting me and giving me the chance to do a PhD with you (and for your kindness ❤️).

Special thanks go to Iván who also supervised me and welcomed me two times into the i~mar research institute. I am especially grateful to him for bringing me on the amazing Patagonia cruise, and to all the very kind persons who shared this adventure with me: Sara, Patricio, Camila, Pili, Guido, Cesar, and obviously Iván.

I would also like to thank all my friends and colleagues, particularly Séverine (Merlin), Juan and Manal who helped me to achieve this thesis. Remerciements spéciaux à mon streamer préféré Basile, on a glandouillé bien assez dans la réalité pour qu'on puisse se permettre d'optimiser le fictionnel.

Je voudrais également remercier ma famille, mes parents et mon frère d'abord, mais aussi mes grands parents et ma tante qui m'ont toujours soutenue et encouragée, et enfin ma chienne Flipie qui m'a toujours accompagnée.

Je souhaiterais également remercier Jeanne qui m'a beaucoup encouragé dans les derniers moments de ma thèse. Malgré notre amitié à distance, parfois sans se parler pendant plusieurs mois ou années, je n'ai jamais douté de notre amitié et ait souvent pensé très fort à toi bien que je n'aie pas été capable de te le montrer ❤️

Guido, te agradezco muchísimo por todos los sacrificios que hiciste, por cocinarme todos los días, apoyarme tanto, y por darme tanto amor. Espero poder devolverte todo eso algún día ❤️.

CONTENTS

FIGURES

TABLE OF ABBREVIATIONS

EBUS	Eastern Boundary Upwelling System
ENSO	El Niño Southern Oscillation
ESSW	Equatorial Subsurface Water
EW	Estuarine Waters
GPD	Gross Domestic Product
HAB	Harmful Algal Bloom
IOD	Indian Ocean Dipole
ISA	Infectious Salmon Anaemia
MHW	Marine Heatwave
MJO	Madden-Jullian Oscillation
MCS	Marine Cold Spell
MSAAW	Modified SubAntacrtic Water
OAX	Ocean Acidity Extreme
OMZ	Oxygen Minimum Zone
PDO	Pacific Decadal Oscillation
SAAW	SubAntacrtic Water
SAM	Southern Annular Mode
SPSA	South Pacific Subtropical Anticyclone
SST	Sea Surface Temperature

CHAPTER 1.   INTRODUCTION

1.1. General context and state of the art

1.1.1. Marine Heatwaves and Marine Cold spells

1.1.1.1. Definitions

Marine heatwaves (MHWs) and marine cold spells (MCSs) are discrete oceanic events characterised by respectively anomalously warm or cold water, that can persist from days to months. MHWs were formally defined for the first time by Hobday et al. (2016) as prolonged, discrete periods of anomalously warm sea surface temperature (SST), basing this definition on the one long used to define atmospheric heatwaves (Perkins and Alexander, 2013). Although extreme ocean temperature anomalies have been observed for decades (e.g. Cerrano et al., 2000; McPhaden, 1999; Mills et al., 2013; Olita et al., 2007), the standardised definition of MHWs in 2016 by Hobday et al. greatly stimulated research on the topic: while less than 10 publication used the term "marine heatwave" or "marine heat wave" in their title prior to 2016, over 1400 papers have since been published, with more than 450 in 2024 alone. By analogy, MCSs are defined as "discrete, prolonged periods of anomalously cold ocean temperatures" (Schlegel et al., 2021). In contrast to MHWs, MCSs remain understudied, with only around 40 publications titled "marine cold spell" to date.

Both MHWs and MCSs are defined relative to local daily long-term climatology, typically calculated over a minimum 30-year baseline (Hobday et al., 2016; Schlegel et al., 2021). According to that same definition, a MHW occurs when daily SST exceeds the 90th percentile of the seasonally varying climatological distribution for at least five consecutive days, with no more than two consecutive days below the threshold (Hobday et al., 2016). This five-day minimum accounts for the ocean's slower thermal response compared to the atmosphere, where heatwaves are commonly defined over three days (Hobday et al., 2016; Perkins and Alexander, 2013). MCSs are similarly defined, but as periods where SST falls below the 10th percentile threshold, again lasting a minimum of five days with no more than two below threshold days (Schlegel et al., 2021). MHWs and MCSs are inherently discrete events, implying a return to normal conditions once the anomalies recede (Hobday et al., 2016). According to that definition (threshold calculated depending on a climatology), severity of the MHWs depends on both absolute SST and on local seasonal SST variability.

MHWs and MCSs are described, identified and characterised using standard metrics: the start and end dates, duration (days), mean and maximum intensity (°C above or below climatology, relying on the SST anomaly), cumulative intensity (°C.day), spatial extent (km^2), and rates of onset and decline (°C/day) (Hobday et al., 2016). Generally, the maximum spatial extent and highest
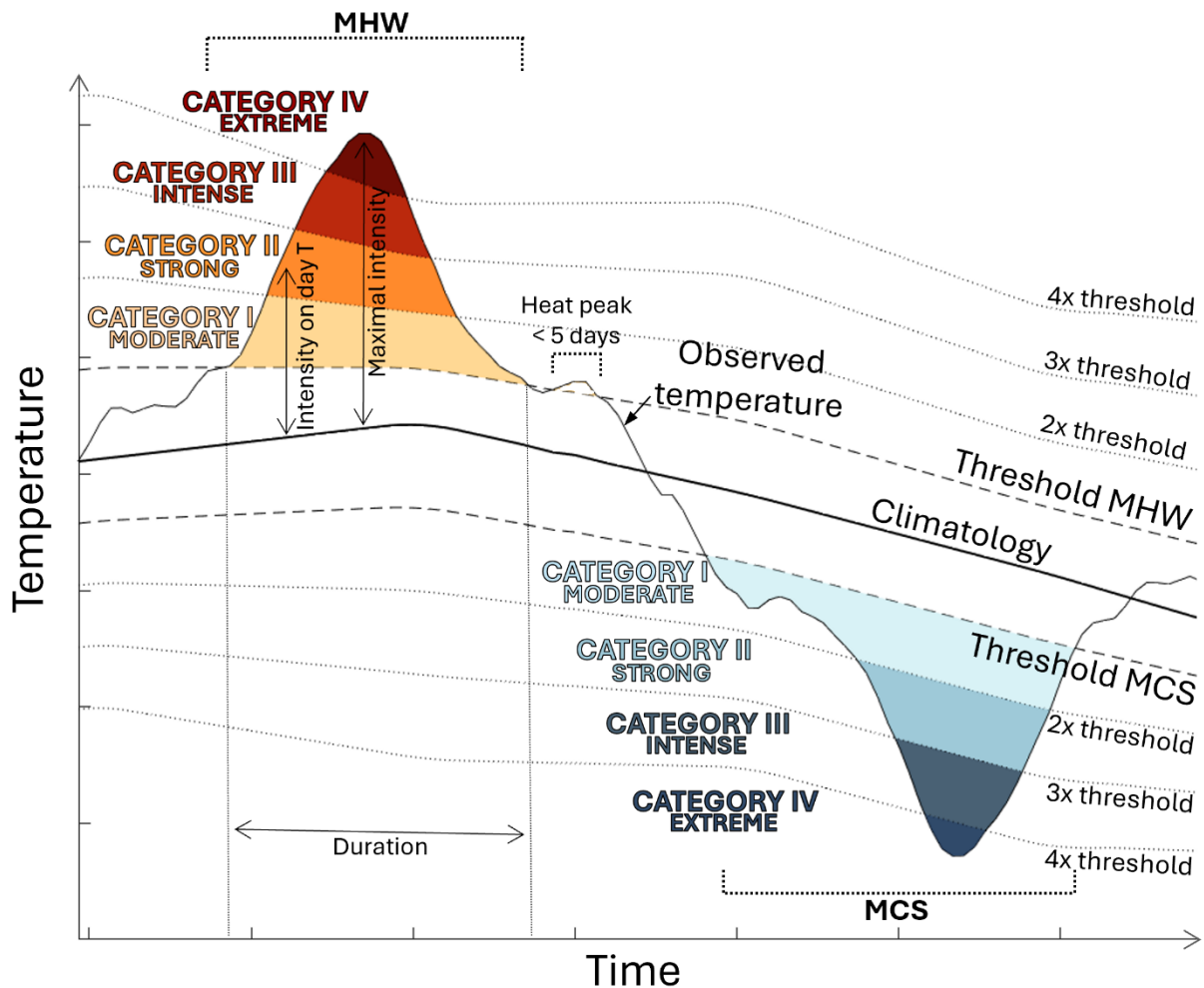
Figure 1: Suggestion of the temporal evolution of a marine heatwave (MHW) and of a marine cold spell (MCS). They are both determined according to the local climatology and thresholds. When the local temperature exceeds multiples of the threshold, it reaches the corresponding category, traditionally represented in shades of red for MHWs and in shades of blue for MCSs. If the local temperature exceeds the threshold during less than 5 days, it is considered as a heat or cold peak. Different metrics can be determined: the intensity on day T, the maximal intensity reached at the peak of the event, and the duration of the event (applicable to both MHW and MCS). This temporal representation can be from a unique location or a spatial average over a larger area.

intensities are reached around the centre of the event life cycle (Sun et al., 2023a). These different metrics allow comparison between events, across regions and time periods (Fig. 1). To facilitate communication, public understanding and to better understand harmfulness of such events on ecosystems, Hobday et al. (2018) proposed a classification scheme for MHWs with four categories based on maximal intensity reached by the event. Schlegel et al. (2021) extended this categorisation to MCSs, though their intensities are expressed as negative, since based on temperature anomalies. The categories are calculated as multiples of the difference between the climatology and the threshold (10th or 90th percentile). If the maximal intensity reached is between 1 and 2 time the difference, it is considered as a Category I (Moderate) event, if it is between 2 and 3 times the difference it is a Category II (Strong) event, if it is between 3 and 4 times the difference it is a Category III (Severe) event, and if it exceeds 4 times the difference it is a Category IV (Extreme) event (Table 1).

Table 1: Categorization of marine heatwaves and cold spells, according to Hobday et al., 2018

Multiple of the difference between climatology and threshold	Category	Intensity of the MHW/MCS
0 to <1	No MHW	No event
1 to <2	Category I	Moderate
2 to <3	Category II	Strong
3 to <4	Category III	Severe
> 4	Category IV	Extreme

The historical study of MHWs focused first on their surface signature (e.g. Di Lorenzo and Mantua, 2016; Frölicher et al., 2018; Hobday et al., 2016a; Holbrook et al., 2019; Oliver et al., 2018a; Smale et al., 2019). MHWs and MCSs tend to show similar spatial patterns, nonetheless showing differences in spatial variation and intensity (Yao et al., 2022). However, studies rapidly revealed that their subsurface counterparts can be longer and more intense than at the surface (Amaya et al., 2023b; Elzahaby and Schaeffer, 2019; Hu et al., 2021; Zhang et al., 2023), sometimes extending vertically over hundreds of meters (Chen et al., 2023; Fragkopoulou et al., 2023). Eventually, subsurface MHWs can be disconnected from surface, occurring at depth only, potentially due to the subduction of warmer sea surface waters and adiabatic processes (Amaya et al., 2023b; Guo et al., 2024). Approximately half of MHWs show continuous surface signals throughout their life cycles, while one third are confined to the subsurface only (Sun et al., 2023b). Due to the higher thermic capacities of deep waters, while MHWs are dissipating in surface, warm-water anomalies can persist over several years at depth (e.g. Jackson et al., 2018). Generally, the maximal intensity reached by a MHW is around 100m depth (peaking on average at 1.6°C), with an increasing intensity from surface to that depth, and then decreasing with depth (Guo et al., 2024). The frequency of the events is more linear, being higher in the surface layer (1.8 event per year on average globally), and slowly decreasing with depth (1.4 event per year at 1000m depth) (Guo et al., 2024).

1.1.1.2. MHWs and MCSs in a global warming context

The frequency, duration, intensity and spatial extent of MHWs have increased significantly over recent decades, primarily due to anthropic global warming (IPCC, 2021; Laufkötter et al., 2020; Oliver et al., 2018a; Peal et al., 2023). From 1925 to 2016, annual MHW days rose by approximately 50% (Oliver et al., 2018a), with the frequency doubling since the 1980s and projected to increase, particularly in coastal regions (Frölicher et al., 2018; IPCC, 2021). For example, during the years 2015-2016, at least one fourth of the oceans experienced a MHW (Oliver et al., 2017). Recent analyses indicate that 87% of present-day MHWs are attributable to human-induced warming, and projected to approach 100% under scenarios exceeding 2°C of global warming (Frölicher et al., 2018). By the end of the 21st century, many ocean regions could experience near-permanent MHWs conditions, especially under high-emission scenarios (Cheng et al., 2023; Oliver et al., 2019; Yao et al., 2022). Longer-lasting MHW events tend to be larger in spatial extent and vice versa, whereas intensity is nearly independent from the duration and spatial extent (Sun et al., 2023a). The increase in mean intensity and in annual MHW days should concern a big part of the water column, from surface to at least 1000m (Guo et al., 2024). Guo et al., (2024) project that globally, in the first 50m of the water column, MHWs annual days and mean intensity to increase by about 1.4 days and 0.13°C by the end of the century. For their part, Tanaka & Van Houtan (2022) estimate

that during the last 150 years, the Arctic Ocean has been the most impacted by increasing MHWs trends, whereas the Northern Atlantic has been the least affected. These increasing trends are mainly driven by increases in mean ocean temperature rather than changes in temperature variability, at both surface and depth (Oliver et al., 2019; Sun et al., 2023b). Other factors such as the shoaling of the mixed layer, changes in low-cloud cover and advection of warm air by anomalous winds are also likely to contribute to the MHWs amplification (Athanase et al., 2024). Model projections suggest that the annual occurrence of surface, mixed layer and subsurface MHWs will continue to increase globally, with stronger trends near the surface (Guo et al., 2024; Sun et al., 2023a). Deser et al., (2024) also suggest that MHWs and MCSs are more likely to intensify particularly in the northern extra-tropics and to weaken in the tropics, in relation to ENSO. Subsurface MHWs used to reach peak intensity at depths around 100m, but because of the intensification of the surface warming, an upward shift of the peak intensity is observed (Guo et al., 2024).

In contrast, the global frequency, duration and intensity of MCSs are declining everywhere, except in polar oceans, where unique oceanographic conditions can still promote their occurrence (Peal et al., 2023; Schlegel et al., 2021; Wang et al., 2022c). This reduction is primarily driven by the long-term warming of the oceans, which shifts the baseline upward, leaving fewer opportunities for anomalously cold events, and are expected to continue to decrease (Schlegel et al., 2021; Wang et al., 2022c). In the Northern Atlantic Ocean, MCSs will probably by enhanced by the weakening of the Atlantic Meridional Overturning in the subpolar Atlantic Ocean (Yao et al., 2022). While MHW and MCS spatial distributions overlap in certain ocean regions, such as the eastern tropical Pacific and mid-latitude Southern Hemisphere, their opposing trends underscore the asymmetric impact of global warming on extreme thermal events (Yao et al., 2022).

In summary, the intensification and near-permanence of MHWs alongside the decline of MCSs are clear indicators of an ocean increasingly influenced by anthropogenic climate change (Oliver et al., 2019; Venegas et al., 2023). The understanding of such events at both surface and subsurface is critical for predicting their ecological and climatic impacts under future warming scenarios, as large marine ecosystems regions are projected to face intensified threats from more extreme events (Guo et al., 2024), and probably pushing marine organisms and ecosystems to their resilience limits (Frölicher et al., 2018).

1.1.1.3. Focus on the importance of baselines in MHW and MCS detection

Accurate detection of MHWs and MCSs requires robust datasets. Satellite observations provide high spatial coverage and temporal resolution, but with moderate length records. Hobday et al. (2016) suggested the use of the NOAA SST reanalysis product (OISSTv2, Huang, Liu, et al., 2021) that has a resolution of 0.25°, becoming therefore one of the most used products for MHWs detection (e.g. Holbrook et al., 2019; Schlegel et al., 2021; Smale et al., 2019; Sun et al., 2023a). The historical study of MHWs have mostly relied on satellite derived SST products combined with near-surface in situ data, that provide daily measurements over several decades, as is the OISST product, but as well for instance the Operational SST and Ice Analysis product (OSTIA, European Union-Copernicus Marine Service, 2015; Capotondi et al., 2024). In situ measurements can offer longer time series and, when using autonomous sensors or mooring, they can achieve high temporal resolution, even though limited spatial coverage (Hobday et al., 2016). Few studies have used in situ data for MHWs detection, because of the limited spatial coverage. Some of them, however, used long-term mooring to calculate locally MHWs (Cook et al., 2022; Dabulevičienė and Servaitė, 2024). Global or regional models complement these sources, offering high-resolution products, especially

offshore. Models have been more and more used for MHWs detection, as they provide information on ocean temperature at both surface and depth, and are particularly useful for future MHWs projection and prediction (Oliver et al., 2018b; Pilo et al., 2019; Plecha and Soares, 2020; Vogt et al., 2022; Wang et al., 2023).

The choice of the baseline and threshold (thus the choice of the temperature dataset) should align with the different ecological problematics. Therefore, different adaptations have been proposed across the years to better understand MHWs and MCSs consequences on ecosystems and oceans properties. The most common approach for MHWs and MCSs detection involves identifying temperature anomalies that exceed a given statistical threshold, typically set at a high percentile, such as the 90th in the case of MHWs, or the 10th percentile in the case of MCSs (Hobday et al., 2016; Schlegel et al., 2021). For the detection of MHWs, some studies use higher percentiles in order to focus only on the strongest events and not on what could be considered as "normally warm", since 90th percentile might result in "too frequent" events that would not respect the rare nature of extreme events (Holbrook et al., 2019; Rosselló et al., 2023; Tanaka and Van Houtan, 2022). For instance, in the case of atmospheric cold and warm waves, the IPCC defines them with 10th and 90th percentile thresholds, but they are not necessarily considered as extreme events (Field et al., 2012). For MHWs, the 95th, 98th, 99th, and even 99.99th percentiles are sometimes used in order to focus only on the most extreme events (Darmaraki et al., 2019; Frölicher et al., 2018; Huang et al., 2021b). Others use an absolute temperature as threshold that can be ecologically meaningful for species with clear thermal tolerance limits. For instance, Marbà & Duarte (2010) used 28°C as threshold for MHWs impacts on the seagrass *Posidonia oceanica*, the temperature above which shoot mortality was observed. Similarly, some studies suggest that using a monthly baseline would be useful to detect only the most extreme events, in both intensity and duration, especially when studying MHWs and MCSs over historical periods (Jacox et al., 2020; Tanaka and Van Houtan, 2022). The definition of thresholds and baselines is therefore not trivial and should be context-dependent, reflecting the environmental adaptation capacities of the relevant ecosystems (Holbrook et al., 2020b).

One of the most central methodological challenges when defining MHWs and MCSs is the treatment of the baseline period used to calculate anomalies (Smith et al., 2025). Using a historical (fixed) baseline captures both long-term warming trends and short-term variability, thus providing insights into both the displacement of mean conditions and the occurrence of extreme events (Jacox et al., 2020). However, as ocean temperatures continue to rise due to anthropogenic climate change, relying on a fixed baseline risks saturating the definition of MHWs, eventually leading to a situation where nearly the entire year could be classified as a MHW (Jacox et al., 2020). This outcome would not fit to the notion of a "wave", which implies a deviation from a norm, rather than a new constant state (Jacox et al., 2020; Rosselló et al., 2023). To address this issue, some studies advocate for the use of a moving baseline that shifts with contemporary climatological conditions (Smith et al., 2025). This approach preserves a consistent frequency of extremes through time and prevents saturation in the count of MHW days (Rosselló et al., 2023). Nonetheless, a moving baseline may mask the absolute thermal stress experienced by marine ecosystems, which remains ecologically important for MHW mitigation (Scannell et al., 2016). Therefore, detrending SST data has been proposed to effectively isolate transient extremes from long-term warming signals (Amaya et al., 2023b; Holbrook et al., 2019; Smith et al., 2025). As Amaya et al. (2023b) underlined, the term "marine heatwave" should be deserved for temporary, extreme warm events relative to an evolving, recent climatological norm, whereas long-term trends describe the persistent background warming.

In practice, both fixed and moving baselines can be applied, depending on the research objective. Fixed baselines help illustrate the cumulative impacts of warming and are a tool for assessing changes over decades (Rosselló et al., 2023). In contrast, moving baselines highlight short-term extremes relative to relatively recent conditions, better reflecting the contemporary thermal stress face by organisms, and preventing saturation in MHW day-count per year in the context of warming seas (Holbrook et al., 2020b; Rosselló et al., 2023). The use of fixed threshold might lead to over or lower detection of MHWs and MCSs events, as a it assumes a stationary climate where the mean, scale and shape of temperature distributions remain constant, which is not consistent with increasing trends of ocean temperatures (Rosselló et al., 2023; Venegas et al., 2023). Consequently, the probability of exceeding a fixed threshold increases, not being coherent with the notion of rarity that defines the concept of extreme event (Rosselló et al., 2023). For example, (Rosselló et al., 2023) shown that in the Mediterranean Sea, the use of a moving baseline results in 12% of the year being classified as a MHW, whereas 24% of the year was under MHW conditions when using a fixed baseline. Recent work advocates the use of a moving baseline definition for identifying MHWs to better distinguish transitory extremes from long-term warming (Amaya et al., 2023b).

The length of the baseline period is also a crucial parameter in MHWs and MCSs detection. The World Meteorological Organisation recommends for both atmospheric and oceanic studies 30-years long period updated every decade to maintain relevance (WMO, 2023). Schlegel et al. (2019) warn on the use of time series shorter than 30 years that risk biased estimates of frequency, duration and intensity, and do not recommend to use time series as short as 10 years. Decreasing the length of the climatological baseline can lead to a decrease in the frequency, duration and intensity of both surface and subsurface MHWs (Lien et al., 2024; Schlegel et al., 2019). However, in the context of rapid ocean warming, shorter periods (such as 20-years period) might be more appropriate to avoid inflating the frequency of extremes due to outdated "cooler" reference years, and ensures to better reflects the characteristics of a specific period under recent climate conditions (Fernández-Álvarez et al., 2025; Rosselló et al., 2023).

Finally, the shifting baseline illustrates how each generation accepts the conditions of the environment they grew up with as "normal", raising the question of which state should be considered as "normal" for each ecosystems and individual species (Soga and Gaston, 2018), underlining the importance of clearly specifying the baseline when studying MHW and MCS impacts.

1.1.1.4. Drivers of MHWs and MCSs

MHWs and MCSs are driven by both atmospheric and oceanographic factors that have different spatial and temporal scales. In most of the cases, global, regional and local processes interplay together to trigger, exacerbate, maintain, and dissipate MHWs and MCSs events. However, although the different processes are well known, the way they interplay to interact with MHWs and MCSs remain uncertain.

At mid and high-latitudes, MHWs are often associated with large scale atmospheric pressure anomaly, typically high-pressure systems bringing warm air, weakening the winds and often reducing cloud cover and precipitations (Black et al., 2004; Holbrook et al., 2019; Sen Gupta et al., 2020). It often results in a reduction of the turbulent mixing and of the heat loss by the ocean towards the atmosphere, favouring the sea surface warming and/or the maintain or an already present heat (Black et al., 2004; Bond et al., 2015; Olita et al., 2007; Sen Gupta et al., 2020). The suppression of turbulent fluxes is probably on of the main driver for MHWs formation, whereas

the increase of turbulent fluxes is probably the main cause of their dissipation (Sen Gupta et al., 2020). Direct increase of solar radiation, local suppression of latent and/or sensible heat loss from the ocean, eddies, and water column stratification are other factors that can also contribute to the development and maintain of MHWs (Pujol et al., 2025; Rathore et al., 2022). Heat fluxes budget overall is one of the main driver of MHWs (Liu et al., 2024). The weakening of local or regional winds is also very important in the initiation and maintain of MHWs (Benthuysen et al., 2014). This combination of atmospheric factors is often observed in MHW formation (e.g. Xu et al., 2024) and resulted in some of the most emblematic MHWs ever studied as the very strong MHWs in the North-East Pacific Ocean in 2013-15 (Bond et al., 2015), and the 2003 MHW in the Western Mediterranean Sea that had enormous impacts on local ecosystems (Garrabou et al., 2009; Schär et al., 2004). MHWs are often associated to a shallower mixed layer depth and higher stratification, and the shallowing is more intense when the MHW's intensity is higher and if the MHW is associated to an anticyclonic eddy (Sun et al., 2024a). On the contrary, MCSs are generally associated with lower air temperature (e.g. Liu et al., 2024), stronger winds (e.g. Shen et al., 2020), increase of the cloud cover (Liu et al., 2024), depression systems (Liu et al., 2024), resulting in higher turbulent mixing and shallower mixed layer (Sun et al., 2024a), as well the heat fluxes play an important role (Liu et al., 2024).

Oceanic processes can also trigger MHWs and MCSs: the advection of warm or cold currents to respectively cooler and warmer regions (generally at higher latitudes in the case of a warming) lead to sea temperature anomalies and therefore to MHWs or MCSs conditions (e.g. Liu et al., 2024). On the other hand, the weakening or the suppression of ocean advection can also cause a MHW because of the more stagnant presence of water reducing the heat loss, as it has for instance been observed in the North Pacific Ocean in 2013-15 (Bond et al., 2015). Stronger cooler currents have been associated to the formation of MCSs (Lian et al., 2024). MHWs triggered by oceanic processes have already been observed for instance in Australia in 2011 (Benthuysen et al., 2014). When the region is favourable to the presence of eddied, MHWs and MCSs can be prolonged over time, deepen, or intensified by respectively anticyclonic and cyclonic eddies (Xu et al., 2024), as it has been for instance observed in Indonesia with 77% of MHWs associated to anticyclonic eddies and 75% of MCSs to cyclonic eddies (Napitupulu, 2025). Upwellings might be also a determinant factor, triggering a MHW when they are weaker than usual, or on the contrary promoting a MCS when they are stronger than usual (Reyes−Mendoza et al., 2022; Walter et al., 2024).

Retroactions between ocean and atmosphere can also contribute to the maintain of MHWs: positive sea temperatures might induce an increase of the air temperature, reducing the cloud coverage, weakening the wind speed, and initiating a positive thermodynamic feedback between the ocean and the atmosphere (Di Lorenzo and Mantua, 2016). This kind of interaction might be very important at low latitude regions where the heat budget can easily be modify by the solar radiation (Myers et al., 2018).

In addition to the different drivers cited above, remote sources such as ENSO (El Niño Southern Oscillation), PDO (Pacific Decadal Oscillation), SAM (Southern Annular Mode), IOD (Indian Ocean dipole), Rossby waves, MJO (Madde-Jullian Oscillation), have often played an important role in the development of MHWs and MCSs (Dalsin et al., 2023; Hamdeno et al., 2022; Piñones et al., 2024; Rodrigues et al., 2019; Schlegel et al., 2021). Propagation of planetary waves in the atmosphere or in the ocean can modify cloud cover, winds force and/or circulation, thermocline depth, or modify local circulation by an augmentation or reduction of the currents advection (Holbrook et al., 2019). ENSO phases have for instance often been associated to very large and long MHWs, such as in 2011 in Australia, for witch a La Niña event modified currents' circulation, and in 2013-15 in the

Pacific Ocean where a strong El Niño maintained and forced a MHW (Jacox et al., 2016). Monsoons have also been linked to the development of MCS in the West Pacific and MHWs in the Bay of Bengal (Lian et al., 2024; Zhou et al., 2025).

1.1.1.5. MHWs and MCSs consequences

MHWs have strong impacts on ocean's properties: by increasing temperature and consequently the stratification, MHWs can result in a diminution of the nutrients flux from deeper layers to the surface (Wyatt et al., 2022), or to diminish oxygen dissolution, possibly leading to hypoxic or anoxic conditions (e.g. Brauko et al., 2020; Fan et al., 2025; Shunk et al., 2024). In other cases, MHWs might modify carbon cycle by reducing carbon intake (Egea et al., 2023; Mignot et al., 2022; Yu et al., 2024) or by releasing stored carbon to the atmosphere when for instance seagrass meadows are killed (Arias-Ortiz et al., 2018; Serrano et al., 2021). The reduced carbon sequestration can also be due to the reduction of the species productivity, or to the increased remineralization of the carbon facilitated by the heat (Gao et al., 2021). Modification of the sea ice formation has also been observed in the Arctic and Antarctic Oceans after MHWs prevented water cooling (Carvalho et al., 2021; Meehl et al., 2019).

It has also been shown that MHWs and MCSs can interact with atmospheric phenomena. For instance, MHWs have been linked to terrestrial droughts, highlighting the interconnections between oceanic and terrestrial environments (Rodrigues et al., 2019; Shi et al., 2021; Yu et al., 2024). MHWs and MCSs have been associated with changes in regional precipitation regimes. For example, off the coast of tropical southwest Africa, MCSs are associated to reduced rainfalls over certain regions, whereas MHWs can be associated to increase in precipitations (Lutz et al., 2015). Along the Japanese Kuroshio Current, a MHW enhanced atmospheric instabilities, by modifying the near-surface atmosphere by increasing surface heat fluxes, resulting in that region in increased precipitations (Hirata et al., 2025). Moreover, MHWs play a critical role in the intensification of extreme weather events such as tropical cyclones, medicanes (Mediterranean hurricanes) and typhoons (Choi et al., 2024; Jangir et al., 2024; Pun et al., 2023). The increased latent heat flux associated with MHWs, primarily through enhanced evaporation, intensifies precipitation near tropical cyclones, which in turn amplifies the cyclone's strength and influence their trajectories (Androulidakis and Pytharoulis, 2025; Choi et al., 2024; Jangir et al., 2024). In this case, the relationship can be reciprocal: while MHWs supply heat and a steep temperature gradient that fosters cyclone formation and rapid intensification, the strong winds of the cyclone dissipated the MHW by increasing ocean mixing, deepening the mixing layer, and transferring the heat from the ocean to the atmosphere (Rathore et al., 2022). Androulidakis & Pytharoulis (2025) shown that the magnitude of the SST anomaly associated with the MHW is linked to the cyclone intensity. Anomalous heat loss from ocean to the atmosphere and elevated latent heat fluxes were also key factors in the formation of Medicane Scott in 2019 (Hamdeno and Alvera-Azcaráte, 2023). Similarly, the preconditioning effect of MHWs by elevating SST can significantly boost the total heat flux available for typhoons (Pun et al., 2023). Additionally, it has been observed that MHWs can influence urban areas by increasing air temperature and moisture (Hu, 2021).

The modifications of ocean's properties and atmospheric conditions (especially changes in heat fluxes) lead to consequences on ecosystems. Overall, the knowledge about MHWs consequences on ecosystems have been acquired through the study of major MHW events, and focusing on mainly emblematic species such as coral reefs, kelp forests or whales (Barlow et al., 2023; Benthuysen et al., 2021; Diehl et al., 2021; Leggat et al., 2019; McPherson et al., 2021; Santora et al., 2020; Spillman and Smith, 2021), or on valuable species such as salmons, mussels, lobsters or cod

(Barbeaux et al., 2020; Brooks et al., 2025; Greenhough et al., 2025; Traiger et al., 2022; Villaseñor-Derbez et al., 2024). However, MHWs do not affect all species the same way. On one hand, mobile species can migrate latitudinally (poleward) or vertically (deepward; Barange & Cochrane, 2018; Deutsch et al., 2015; Rutterford et al., 2015), and can be distinguished in two types of migrators: forced migration with species escaping the thermal stress (e.g. Mills et al., 2013), and opportunist migration of warm-water species taking advantage of the warmer temperatures to extend their geographical distribution (Jacox et al., 2020; Lonhart et al., 2019; Miyama et al., 2021; Wernberg et al., 2013). Sessile or sedentary organisms (corals, seagrass, bivalves, eels, etc) are much more vulnerable to increases of the temperature since they cannot migrate (e.g. A. Pearce et al., 2011). MHWs may lead to their habitat reduction over temporary or long-term periods (Smale and Wernberg, 2013), growth modification (Wade et al., 2019), failure in reproduction (Barlow et al., 2023; Wild et al., 2019), genetic loss or tropicalization (Coleman et al., 2020), or to mass mortality induced by either thermal stress (Couch et al., 2017; Oliver et al., 2017; Tietbohl et al., 2025) or modification of the food-chain assemblage (Cavole et al., 2016). Furthermore, it has been shown that in coastal environment, the heat generated by the MHW can even spread to the sediment, participating in the seagrass meadows dieback and other benthic organisms, modifying the composition of the sediment itself (Palmas et al., 2025; Tassone and Pace, 2024; Zhou et al., 2023).

Overall, 72% of MHWs events have been associated with low-chlorophyll-*a* concentrations (Sen Gupta et al., 2020). They can trigger extreme mortality of various species by limiting food availability for higher trophic levels, such as sea birds, crabs, shellfishes, sea lions and whales (Cavole et al., 2016; Gomes et al., 2024; Hart et al., 2020; Jones et al., 2018, 2019; Szuwalski et al., 2023), cause the migration of planktivorous fishes and of other species that try to escape heat and starvation, lead reproductive failure of sea birds (Jones et al., 2018; Piatt et al., 2020), and shifts in phytoplankton and zooplankton communities (Cavole et al., 2016; Yang et al., 2018). The mechanisms behind the co-occurrence of MHW and low-chlorophyll events are not fully studied, but it has often been associated to ENSO variations (Chen et al., 2023; Hamdeno et al., 2022; Le Grix et al., 2021). It has been observed that these events are more frequent at higher and equatorial latitudes, and less intense in tropical and mid-latitudes (Le Grix et al., 2021). Yet, not all MHWs lead to chlorophyll decline, and some are even associated with increase of chlorophyll concentration (Chen et al., 2024), and some species could beneficiate from MHWs increasing temperatures, by being more productive at the expanse of more thermal sensitive species (Egea et al., 2023; Piatt et al., 2020; Thompson et al., 2022).

All of those consequences might lead to shifts in ecosystems communities and assemblages due to the dieback of key species and to the arriving of new ones (Arafeh-Dalmau et al., 2019; Pellizzari et al., 2025). Overall, the consequences of MHWs on ecosystems also depend on their timing, as the season can affect their consequences, if occurring during a sensitive life stage or reproduction period of the different species (Bass and Falkenberg, 2024; Bruning et al., 2024; Tala et al., 2016).

The consequences of MCSs on ecosystems are however much less studied. Yet, similar consequences as for the MHWs can be observed: mass mortality of fishes, coral, sponges, molluscs, reptiles, mammals, etc (Avens et al., 2012; Laboy-Nieves et al., 2001; Mazzotti et al., 2016; Pirhalla et al., 2015; Shen et al., 2020), earlier spawning migrations having consequences for fisheries (Sims et al., 2004), reduction of spawning stocks (Millner and Whiting, 1996), coral bleaching (Rich et al., 2022), modification of species' growth rate and reproduction period (Bennett et al., 2019), increased primary production (Muller-Karger, 2000). The reduction of MCS events might also lead to poleward or deepward extension range of warmer water species (Cavanaugh et al., 2014; Sorte et al., 2010).

By affecting environmental conditions and ecosystems, MHWs and MCSs have strong repercussions on fisheries and aquaculture. Indeed, it has been shown that MHWs exacerbate the already existing stressing factors caused by global warming (Cheung and Frölicher, 2020). For instance, fish captures were seriously reduced by species migration, species community shifts and mass mortality during strong and/or long MHWs (Barbeaux et al., 2020; Caputi et al., 2016; Villaseñor-Derbez et al., 2024). Latitudinal migrations of some predator species have caused concurrence with fishermen (Santora et al., 2020; Tanaka et al., 2021); however, it has been observed higher catch rates during some MHWs because of the migration of commercial species closer to the coast (Cavole et al., 2016). Regarding aquaculture, MHWs can induced to heat vulnerable species a cessation of food intake, a reduced growth induced by thermal stress, and in several cases to mass mortality of the stocks associated to high economic losses (Oliver et al., 2017; Pearce and Feng, 2013; Wade et al., 2019). Recreational fishing has also been impacted by MHWs and MCSs with shifts in the species catches (Free et al., 2023; Santos et al., 2016). Reported economic loss involving MCSs are very rare, but it is however possible to cite a loss of 10 million US$ in fisheries in Taiwan and 1 million US$ in mariculture.

1.1.1.6. Compound events

Recent studies have increasingly focused on the occurrence of compound events, in this case MHW or MCS occurring with another extreme phenomenon. Evidences suggests that the global frequency of such compound events is rising worldwide (Gruber et al., 2021). Although compound events with MHWs are well studied, very little is known on compound events with MCS. While the effects of compound events on ecosystems and organisms remain poorly understood, short-term impacts may not exceed organisms' tolerance or capacity of acclimation, but long-term impacts can include misfunction of the organism's fitness, affecting processes such as reproduction and growth (Gruber et al., 2021). Due to the brief and intense nature of MHWs, there is often insufficient time for physiological adaptations (Gruber et al., 2021). However, facing two different stressors simultaneously may be even more harmful for the species (Kendrick et al., 2019; Rogers-Bennett and Catton, 2019). Among the different extreme events that occur with MHWs, it is possible to cite low-acidity, low oxygen, low chlorophyll concentration or atmospheric heatwaves. Some of them are detailed here and linked to their consequences.

MHWs frequently coincide with low-acidity extremes (commonly abbreviated AOX) at higher rates than it would be expected if the events were independent (Burger et al., 2022). Studies have shown that MHWs and OAX are prevalent at subtropical latitudes, and approximately one fourth of MHWs is a compound event MHW-AOX (Burger et al., 2022). They are often driven by wind-induced upwellings that bring deeper waters with lower pH (i.e. higher concentration in H+) to the surface (Gruber et al., 2021). Although the individual impact of MHWs and AOX on ecosystems have been studied, the consequences of compound event remain poorly understood. Nonetheless, observations indicate shifts in species composition towards organisms more tolerant of warmer and more acidic conditions (Gao et al., 2021). These kind of shifts have lead to a decrease in carbon sequestration, as it was for instance the case when a kelp forest-based ecosystem has been progressively replaced by seagrass turf (Gao et al., 2021). Additionally, certain microalgae may benefit from lower pH levels, outcompeting other species such as *Alexandrium catenella* (Seto et al., 2019).

Another frequently observed compound event is the simultaneous occurrence of MHW and low oxygen concentration, which are being reported with increasing frequency (Li et al., 2024). Ocean warming leads to a reduction of dissolved oxygen through the reduction of the solubility of

dissolved oxygen in warmer water and enhanced stratification limiting water column ventilation, phenomenon intensified by MHWs (Fan et al., 2025; Keeling et al., 2010). Oxygen depletion becomes particularly critical when organisms approach their upper thermal tolerance limit (Gruber et al., 2021). A notable triple compound event has even been observed during the famous Blob event (2013-2015) in the Northeast Pacific Ocean: MHW, low oxygen and AOX occurred at the same time, impacting the water column over 100m depth (Gruber et al., 2021).

MHWs increasing the water temperature and stratification is also particularly favourable to HAB development and/or proliferation (Smith et al., 2021). MHWs associated to HABs have caused among others mass mortality (e.g. Roberts et al., 2019) or changes in migration route (e.g. Santora et al., 2020). When occurring near to aquaculture farms, they can cause direct losses of fishes and molluscs by thermal stress, and contribute to the spread of pathogens (Green, 2014; Oliver et al., 2017; Sae-Lim et al., 2017). For human health and food security, some molluscs containing toxins emitted during HAB are withdraw from sales, causing for instance in the English Channel a loss of 1 millions £ (Ross Brown et al., 2022), or in Chile where a MHW coupled with HAB caused the death of 100 000 tonnes of salmon and trout, equivalent of 800 million USD$ (Clement et al., 2016; Trainer et al., 2020). The forced closure of recreational and commercial fisheries also induced million dollars economic losses (Cavole et al., 2016). It is also a problem for food safety since humans deaths have been reported after eating algae-contaminated molluscs (Trainer et al., 2020). However, it appeared that even if the prolonged-heat period caused by MHWs can trigger HABs, their triggering will also grandly depends on the availability in nutrient already present in the environment (Hayashida et al., 2020a).

The co-occurrence of atmospheric and marine heatwaves has caused mass mortality and shifts in species distribution in both terrestrial and marine environments, as for the famous 2003 event in the Mediterranean Sea where deaths were reported across thousands of kilometres (Garrabou et al., 2009; Ruthrof et al., 2018). These events pose higher risks of stress level, particularly in coastal environment, due to elevated heat and humidity, including implications for human health (Raymond et al., 2020). Such events are often associated with persisting high-pressure systems, reduced winds and increased solar radiation (Olita et al., 2007; Rodrigues et al., 2019). Moreover, terrestrial heatwaves are more likely to occur when there is a coastal MHW is present (Pathmeswaran et al., 2022). MHWs associated with droughts have also been observed (Rodrigues et al., 2019; Yu et al., 2024), which in turn can reduce CO_2 uptake by the ocean (Yu et al., 2024).

In contrast, compound events involving MCSs are almost unstudied. However, it has been shown that there is a prevalence between MCS and hypoxia in upwelling systems, as the upwelling brings cold and low-oxygenated waters closer to the surface (Walter et al., 2024). MHWs combined to hypoxia and lower salinity has also lead to the formation of phytoplanktonic blooms and mucilaginous aggregates that caused massive deaths in a coral reef (Laboy-Nieves et al., 2001).

1.1.2. Chile

Chile extends over more than 4300 km, from 17°S to 56°S, with an average width of approximately 180 km (Fig. 2). It shares borders with Argentina, Bolivia and Peru. It is divided into 16 administrative regions, among them, the regions of Los Lagos, Aysén and Magallanes, which together form the area known as Chilean Patagonia. Chile's narrow continental shelf places it in close proximity the Peru-Chile trench, a subduction zone, causing significant volcanic activity and frequent earthquakes all over the country, sometimes accompanied by tsunamis (Gironás et al., 2021).

Northern and Central Chile (18.4°S-41.5°S) are characterised by a relatively straight coastline featuring cliffs, dune fields, wetlands, peninsulas and bays (Pantoja et al., 2011). In contrast, Southern Chile, also known as Chilean Patagonia (41.5°S-56°S), presents a more complex geography, with a highly fragmented coastline forming one of the largest fjord and channel system in the world with more than 100 000km of coastline (Pantoja et al., 2011). Chile is bordered to the west by the Pacific Ocean and to the east by the Andean Cordillera. The Andes plays a crucial role in regulating the climate, creating altitudinal gradient and strongly interacting with atmospheric circulation, isolating Chile from the rest of the South American continent (Aceituno et al., 2021).

The Andes are the primary regulator of precipitation, generating a hyper-arid climate in the north, a mediterranean climate in central Chile, a hyper-humid climate in the south with precipitations between 3000 mm/year in Northern Patagonia and 7000 mm/year in central Patagonia, with a west-east gradient caused by orographic effect (Aceituno et al., 2021; Castro and Gironás, 2021; Fernández and Gironás, 2021; Pantoja et al., 2011; Viale and Garreaud, 2015), and temperate wet and glacial environments in Central and South Patagonia (McPhee et al., 2021). The Cordillera plays therefore a fundamental role in Chile's hydrology, as most rivers originate from glacial melting, with an increasing number of rivers further south (McPhee et al., 2021).

Chilean climate and oceanic circulation are primarily force by two large-scale atmospheric systems: the mid-latitude Westerly Winds belt and the basin-scale South Pacific Subtropical Anticyclone (SPSA), also known as South Pacific High. The Westerly Winds are characterised by strong eastward blowing jet streams at mid-latitudes across the South Pacific Ocean, driving the South Pacific Current from New-Zealand to Chile that forms the southern branch of the South Pacific Gyre (Stramma et al., 1995; Strub et al., 2019). Upon reaching the Chilean coast between 40°S and 50°S, the South Pacific Current splits into two branches going in opposite directions: the poleward-flowing Cap Horn Current, and the equatorward Humboldt Current System (Aguirre et al., 2012; Thiel et al., 2007). The Humboldt System Current is one of the four major eastern boundary current system, marked by cold, nutritious-rich and equatorward-flowing current, bounded to the north by the equatorial current (Thiel et al., 2007). It supports one of the most productive wind-driven upwelling systems in the world, mainly off the coasts of Peru and extreme northern Chile (Chavez et al., 2008). Conversely, the Cap Horn Current is a buoyancy-driven, downwelling favourable current, flowing poleward along Patagonian coast, and being more intense during winter due to increased river runoff (Thiel et al., 2007). The SPSA is a permanent anticyclone extending over the tropical and subtropical southeast Pacific Ocean, governing the temperature distribution over the Southeast Pacific Ocean and Chile, inducing relatively warm summers and cooler winters (Ancapichún and Garcés-Vargas, 2015). It is the main forcing of the subtropical oceanic gyre, bounded on its east by the Humboldt System Current (Ancapichún and Garcés-Vargas, 2015). Due to the constraint of the Andes on its eastern margin, strong equatorward jet-like winds are generated along the Chilean coasts (Montecinos and Gomez, 2010). In addition, the SPSA contributes to the marked seasonality of rainfall in Central Chile (30-40°S), more intense during the austral winter (Aceituno et al., 2021).

Both the Westerly Winds and the SPSA are subject to coordinated north-south seasonal variations forced by solar radiation. They migrate together southward during summer and northward during winter (Rahn and Garreaud, 2014; Thiel et al., 2007). They are also influenced by interannual and decadal variability forced by ENSO, SAM and PDO (Ancapichún and Garcés-Vargas, 2015; Thompson and Wallace, 2000). During the austral summer and spring, the SPSA reaches its southernmost point, centred around 100°W, 35°S, and at its northernmost point around 90°W, 27°S in winter (Rahn and Garreaud, 2014). The seasonal cycle of the Westerly Winds mirrors that of

the SPSA, shifting southward to around 45°S in summer and northward to 35-40°S in winter (Thiel et al., 2007). This latitudinal migration strongly influences ocean currents, shifting the trajectory of the South Pacific Current and altering the region it impacts the Chilean coast. Consequently, currents directions off Northern Patagonia change seasonally, flowing northward in summer and southward in winter (Strub et al., 2019; Thiel et al., 2007). To summarise, currents tend to flow equatorward north of 37°S, poleward south of 46°S and alternating between 37°S and 46°S (Pizarro A et al., 1994; Sobarzo et al., 2007; Strub et al., 2019; Thiel et al., 2007). This intermediate « transition zone » (Strub et al., 2019) is associated with cold SST and high chlorophyll-a concentration in summer, and downwelling-favourable conditions during winter with opposite features (Rahn and Garreaud, 2014; Strub et al., 2019). While seasonal currents variation in North-Central Chile exists south of 30°S, studies indicate that north of 37°S, winds and currents are consistently equatorward and upwelling-favourable (Sobarzo et al., 2007). Wind-driven upwellings in the northern part of Chile are also more intense during winter due to the convergence of the SPSA
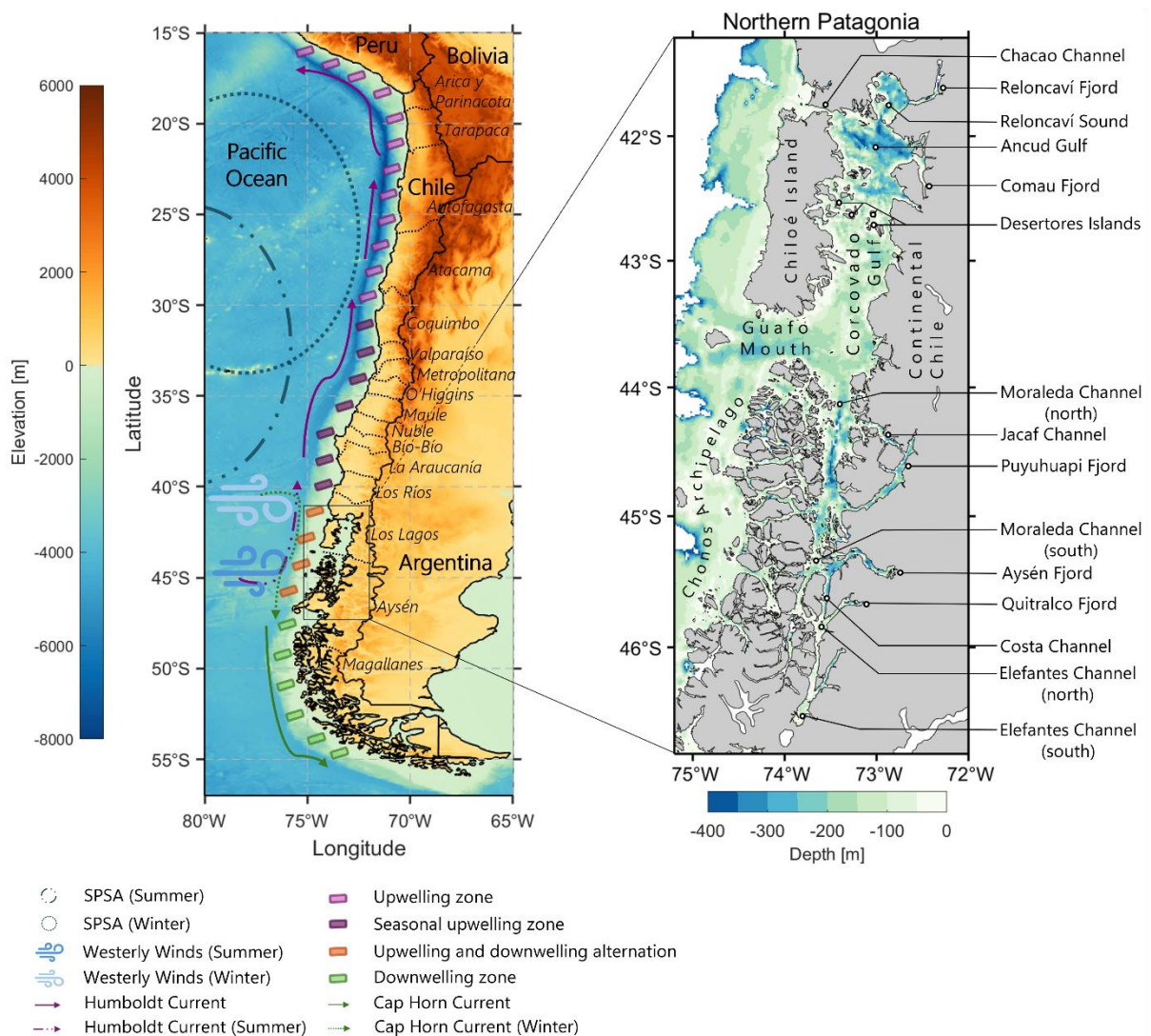
Figure 2: Left: Map of Chile showing topography and bathymetry. Chilean administrative regions are indicated in italic. Key atmospheric and oceanic features are indicated: Southeast Pacific Subtropical Anticyclone (SPSA) with its seasonal position shift, Westerly Winds with south/north migration in summer and winter, the Humboldt and Cap Horn currents, as well as major zones of upwelling and downwelling zones. Right: Zoom on Northern Patagonia, showing bathymetry and highlighting the major gulfs, channels and fjords.

closer to the coast (Fig. 2; Ancapichún and Garcés-Vargas, 2015).

In addition to these atmospheric factors, Chile is strongly shaped by large-scale remote drivers that interact over different timescales. Among these, the El Niño Southern Oscillation (ENSO) is perhaps the most important. It is an irregular cyclic phenomenon occurring every 2 to 7 years, primarily affecting the equatorial Pacific Ocean but with global repercussion (Chen et al., 2019). It is driven by the Walker Circulation, which results from a pressure gradient from the eastern and western Pacific, generating strong westward trade winds (Chen et al., 2019). This circulation maintains coastal upwelling and shallow thermocline along the coast of Central and South America, while warm water accumulates with deeper thermocline in the western Pacific (Chen et al., 2019). ENSO has two phases: the warm phase (El Niño), characterised by weaker trade winds, a reduced pressure gradient, a deeper thermocline and weakened upwelling, and a shallower thermocline and intensified upwelling (Santoso et al., 2017). In Chile, El Niño (La Niña) events weaken (enhance) the SPSA and deepen (shallow) the thermocline, reducing (strengthening) upwelling and bringing dryer (wetter) summer conditions due to weaker (enhanced) Westerly Winds (Ancapichún and Garcés-Vargas, 2015; Montecinos and Gomez, 2010; Rind et al., 2001)

The Pacific Decadal Oscillation (PDO) is an ENSO-like pattern operating over longer timescales, typically 20 to 30 years (Mantua et al., 1997; Mantua and Hare, 2002; Newman et al., 2016). The PDO can amplify or diminish ENSO's impacts depending on whether their phases align or oppose each other (Yáñez et al., 2017a). The cold (warm) phase of the PDO brings drought (wet) atmospheric conditions over Central Chile, a strengthening of the SPSA and causes its southward shift, intensifying equatorward winds and enhanced upwelling south of 33°S, which in turn lowers SSTs in north-central Chile (Ancapichún and Garcés-Vargas, 2015; Schneider et al., 2017).

Finally, the Southern Annular Mode (SAM), or Antarctic Oscillation, is the leading mode of atmospheric variability in the Southern Hemisphere's extratropic (Estay and Lima, 2010; Lee et al., 2019). It reflects the large-scale alternation of atmospheric masses between Antarctica and mid-latitudes (Gong and Wang, 1999; Reboita et al., 2009; Thompson and Wallace, 2000). SAM is defined by opposing geopotential height anomalies over Antarctica and mid-latitudes, causing the mid-latitude Westerly Winds to shift poleward or equatorward, having in return an impact in climate (Thompson and Wallace, 2000). When SAM is in its positive phase, lower pressure over Antarctica and higher pressure at mid-latitudes push the Westerly Winds poleward and weaken them near 40°S, leading to reduced precipitation and warmer conditions over western Patagonia. On the contrary, the negative phase shifts the Westerly Winds equatorward and strengthens them, bringing cooler, wetter conditions (Garreaud, 2018b; Gong et al., 2010; Lee et al., 2019). When ENSO and SAM coincide, their impacts can reinforce each other, leading to compounded effects on wind patterns, precipitations and SSTs, particularly over northern and central Patagonia (Garreaud, 2018b).

1.1.2.1. Chilean Patagonia

Chilean Patagonia spans over 240 000 km², stretching from the Reloncaví Fjord (41.4°S) to Cape Horn (55.9°S). It possesses a very complex coastline of 84 000 km, featuring a network of fjords and channels (Pantoja et al., 2011). The region is estuarine, fed by numerous rivers, high precipitation and glacial melt (Pantoja et al., 2011; Valle-Levinson et al., 2007). Characterised by a hyper-humid climate, Patagonia receives over 2 000 mm of precipitations annually, being locally superior to 7 000 mm, with a pronounced west-east gradient due to orographic effect (Garreaud et al., 2013a; Lenaerts et al., 2014; Valdés-Pineda et al., 2018; Varas and Varas, 2021). In some areas, especially around glaciers, precipitations exceed 10 metres in water equivalent (Lenaerts et al.,

2014). These conditions foster unique ecosystems adapted to extreme humidity, including peatlands and evergreen forests (Castilla et al., 2023), leading terrestrial Patagonia to stock very high quantities of carbon per hectare, that would be higher than the Amazon rainforest (Perez-Quezada et al., 2023).

1.1.2.2. Geography of Northern Patagonia

Northern Patagonia extends approximately from 41.4°S to 46.7°S and from 72°W to 74°W, covering the northern half of the Chilean Patagonia. Bordered by the Andean Cordillera to the east, Chiloé Island to the northwest, and the Chonos Archipelago to the southwest, the region features a highly fragmented coastline shaped by glacial erosion. This has produced a complex network of sounds, fjords, channels, islands and semi-enclosed basins (Fig. 2).

The northernmost section of Norther Patagonia, called the Inner Sea of Chiloé, extends from Reloncaví Sound to the southern end of Chiloé Island. It delimitates approximately the administrative region of Los Lagos, while the southern part of Northern Patagonia delimitates the administrative region of Aysén. While most Northern Patagonia has depths that do not exceed 300 m, some basins and channels are deeper, notably in Reloncaví Sound, Ancud Gulf, Comau Fjord, and channels south of Corcovado Gulf, including Moraleda Channel. The Corcovado Gulf is quite shallow, with a maximal depth of about 200 m (Rodrigo, 2008). To the west, the continental shelf drops sharply to 2 000 m due to the presence of the Peru-Chile Trench. This topography creates a complex coastline, sheltering some basins from the Pacific Ocean by different island chains.

The main geographical features of Northern Patagonia are described bellow:

- Reloncaví Sound (or Gulf) and Fjord: marks the northern boundary of Patagonia, with the fjord draining into it. This area is known for its strong estuarine circulation (Valle-Levinson et al., 2007), and significant tidal influence with amplitude reaching up to 6 metres (Fierro, 2008; Strub et al., 2019).
- Ancud Gulf: receives freshwater inputs from the Comau Fjord and connects to the Pacific Ocean via the Chacao Channel, which lies between Chiloé Island and the mainland.
- Corcovado Gulf: separated from the Ancud Gulf by the Desertores Islands, the Corcovado Gulf it is the primary gateway to the open ocean. The Guafo Mouth, its main passage, facilitates oceanic exchanges and is the key entry point for tidal currents (Fierro, 2008).
- Desertores Islands: they act as a barrier separating younger (Corcovado Gulf) and older (Ancud Gulf) waters. The waters passing by Desertores Islands renew the gulfs and fjords of the northern Sea of Chiloé (Pinilla et al., 2021).
- Chonos Archipelago: composed of a thousand of islands, it delimits the southeastern part of Northern Patagonia. It is greatly influenced by the fluctuations of the Humboldt Current and by the Westerly Winds that bring cold and wet conditions to the islands (Haberle, 2004).
- Moraleda Channel: this longitudinal corridor connects the Corcovado Gulf to several fjords and channels, including (from north to south) Jacaf Channel, Puyuhuapi Fjord, Aysén Fjord and Quitralco Fjord. It acts as a transition zone between high-salinity and elevated nutrient ocean waters and low-salinity continental waters. Its tidal amplitude can reach up to 3m (Fierro, 2008; Fuentes-Grünewald et al., 2008; Silva et al., 1998).
- Elefantes Channel: The southernmost channel in the region, it connects several fjords and channels and terminated at the San Rafael Lagune via a narrow passage.

Northern Patagonia is a particularly narrow region, being on average around 50 km wide, with the widest section slightly surpassing 70 km, and stretching 800 km in length, from Reloncaví Sound to Elefantes Channel. The particularly complex geography, with numerous fjords, channels, islands and gulfs, poses significant challenges for observation and analysis. Coarse resolution satellite products and global models often lack the spatial details needed to accurately capture the processes occurring in its narrowest and most intricate areas. Even higher resolution products may still struggle to resolve all the intricate coastal features of Northern Patagonia. For example, the widest fjord of the region is the Puyuhuapi Fjord, reaching a maximum width of only about 8 km, while its mouth narrows to just 3 km. Many other fjords and channels are even narrower, as for instance Reloncaví Fjord being maximum 3 km wide, or one of the major connection between Moraleda and Elefantes Channels is inferior to 2.5 km wide, making it challenging for remote sensing data and models to fully capture their dynamics and local processes. In addition to its fragmented and intricate coastal features, Northern Patagonia is a particularly cloudy and rainy region (Fernández and Gironás, 2021; Viale et al., 2019; Vimeux et al., 2011). Persistent cloud cover, frequent rainfall and fog make it particularly challenging to obtain clear satellite imagery, further limiting the availability of high-quality observations.

1.1.2.3. Oceanography and circulation

Offshore, Northern Patagonia acts as a transition zone between south-central Chile and Southern Patagonia, with north-south alternating currents (Strub et al., 2019). Inshore, hydrodynamics are highly influenced by interactions between oceanic and fresh waters, and waters are therefore governed by a stratified layer system (León-Muñoz et al., 2024). Closer to the continent and in continental channels regions, this layered structure is reinforced (Sievers, 2008).

The upper layer, generally described as 20 to 30 m thick (Pérez-Santos et al., 2014; Sievers, 2008; Sievers and Silva, 2008), sometimes 50 m (Pinilla et al., 2021), is strongly influenced by estuarine waters (Fig. 3). It is mainly governed by solar radiation, wind induced vertical mixing, colder freshwater inputs from precipitations, rivers and glaciers (Pérez-Santos et al., 2014; Sievers, 2008). This layer flows (10 to 20 cm/s) from Reloncaví Sound and the continent to Guafo Mouth following the continent, and a minor part exits passing by the channels of Chonos Archipelago (Pinilla et al., 2021; Sievers and Silva, 2008). A northward countercurrent flows along south of Chiloé Island (Pinilla et al., 2021). In Moraleda Channel, surface currents flows southward on the eastern side of the channel with a cyclonic eddy at its centre; on the contrary, in Elefantes Channel, currents are going northward (Pinilla et al., 2021).

The intermediate layer, named SubAntacrtic Water (SAAW), is present up to 150 m (Fig. 3). It is oxygen-rich and enters through Bocal del Guafo, although a small portion enters through the channels of Chonos Archipelago (Pérez-Santos et al., 2014; Sievers and Silva, 2008). It splits into two branches, one going northward up to Reloncaví Sound, and the other one southward up to Elefantes Channel, and fill the different basins of Northern Patagonia. During its trip, it eventually mixes with surface freshwater to become Modified SubAntarctic Water (MSAAW, Sievers & Silva, 2008). Desertores Islands act as a barrier separating younger (Corcovado Gulf) and older (Ancud Gulf) waters. The waters passing by Desertores Islands renew the gulfs and fjords of the northern Sea of Chiloé (Pinilla et al., 2021). Modified SubAntarctic Water are very important for deep ventilation processes, renewing fjords with deep oxygenated waters (Pérez-Santos, 2017).

The bottom layer, named Equatorial Subsurface Water (Fig. 3), originates in the Equatorial Pacific Oxygen Minimum Zone (OMZ), making it inherently low-oxygenated (Linford et al., 2023; Palma and Silva, 2004). It also enters through Boca del Guafo, but contrary to the intermediate waters that

flow everywhere, it is constrained by the topography and can flow only into the deepest basins (superior to 150 m) like the southern part of Corcovado Gulf, Moraleda and Jacaf Channels, and Puyuhuapi Fjord (Sievers and Silva, 2008). Because of its shallower topography, the Equatorial Subsurface Water cannot enter the Inner Sea of Chiloé (Sievers and Silva, 2008).

Northern Patagonia exhibits also significant spatial variability across its basins. The northern basins of Ancud and Reloncaví Gulfs, and Moraleda Channel display greater seasonal temperature variations, a pattern also observed offshore Chiloé Island, and high salinity
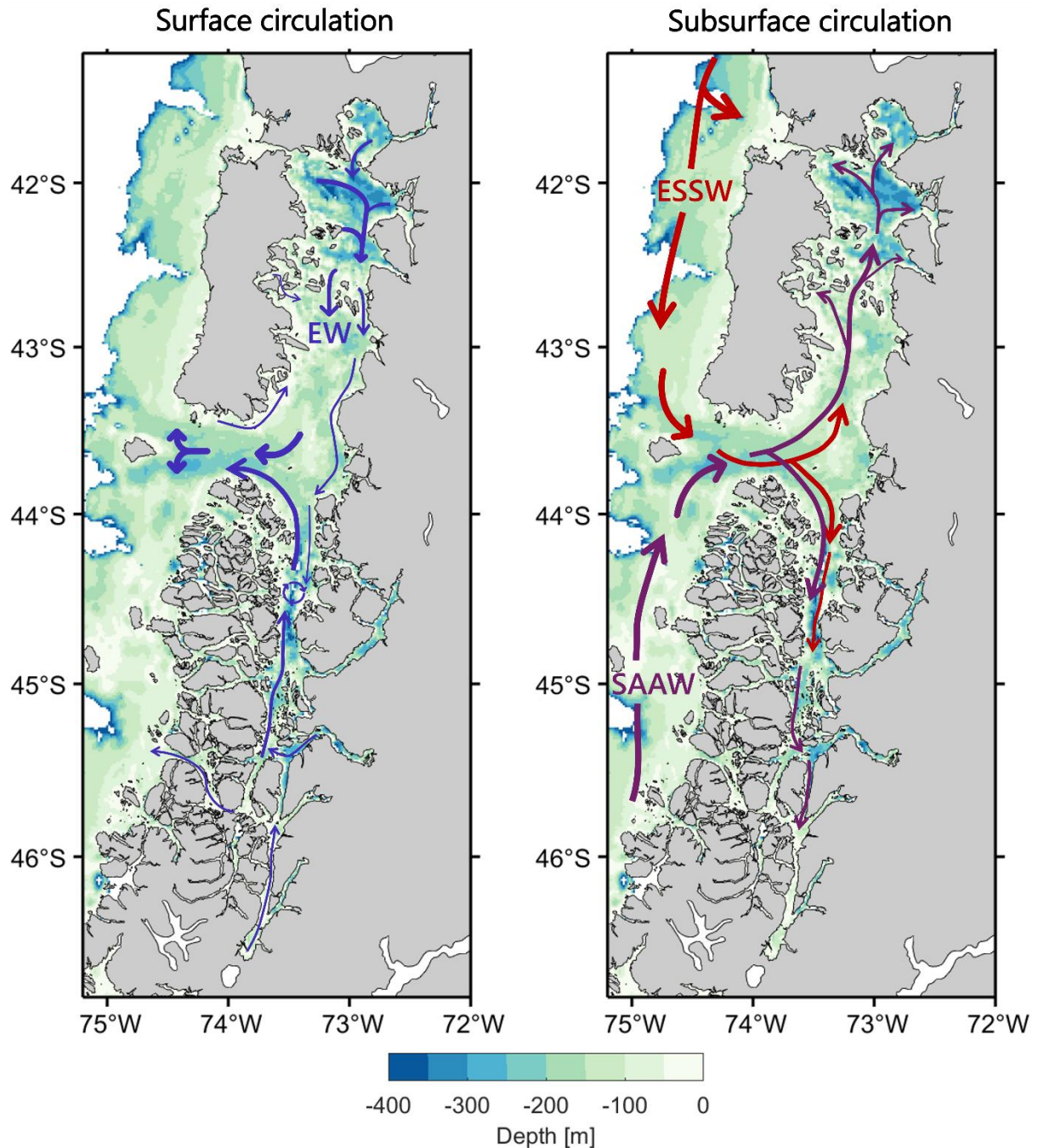
Figure 3:Water masses circulation in Northern Patagonia. Left: surface Estuarine Waters (EW, surface to ~30 m) flowing from the coast to the open ocean. Right: subsurface Subantarctic Waters (SSAW, ~30 m to ~150 m depth) renewing water in the different basins and the bottom layer Equatorial Subsurface Water (ESSW, ~150 m to the bottom) flowing only in the deepest basins.

variations du to higher freshwater inputs (Narváez et al., 2019; Strub et al., 2019; Vásquez et al., 2021). In contrast, Corcovado Gulf experiences lower variability (Narváez et al., 2019; Strub et al., 2019). However, in winter, the spatial distribution of the temperature become notably homogeneous across the region (Saldías et al., 2021; Strub et al., 2019). Likewise, chlorophyll concentration follow a similar pattern: higher levels in Ancud, Reloncaví and Moraleda, while lower values characterise the Corcovado Gulf and Desertores Islands (Lara et al., 2016; Strub et al., 2019; Vásquez et al., 2021). Nutrients concentration varies also spatially, being quite homogeneous through the water column in Corcovado Gulf, while showing greater surface variability in Ancud Gulf (Vásquez et al., 2021). This disparity originates from enhanced wind and tidal-induced mixing Corcovado Gulf and around Desertores Islands, which promotes a higher homogenisation of the water column (Strub et al., 2019). Notably, Corcovado Gulf has an homogenisation of its entire water column (100 to 150m), whereas Reloncaví and Ancud develop a pronounced thermocline, especially during summer (Sievers, 2008).

The vertical structure Northern Patagonia water column also shows great variability. The surface layer exhibits significantly greater variability compared to the deeper layer, which displays more homogeneous vertical distribution (Sievers and Silva, 2008). This stratified structure is marked by sharp gradients, including the presence of a pycnocline, a nutricline, a pHcline and an oxycline (Sievers, 2008). Dissolved oxygen distribution reinforces this layering, with a well-oxygenated and high pH surface layer (30 to 50 m thick) that overlies a deeper layer (75 m to bottom) where oxygen concentration decreases progressively (Sievers, 2008). However, it has been observed that in the deepest parts of some fjords and channels, particularly in Puyuhuapi, Aysén, Quitralco, Comau and Pupquelán Fjords, and in Jacaf and Moraleda Channels, oxygen levels become notably reduced, sometime reaching hypoxic conditions (Silva, 2008). Nonetheless, the past decade has seen a measurable decline in dissolved oxygen throughout Northern Patagonia, attributed to changing currents patterns that enhance the intrusion of low-oxygenated Equatorial Subsurface Water through Boca del Guafo (Linford et al., 2023; Palma and Silva, 2004).

1.1.3. Aquaculture in Chile

Chilean Patagonia, with stable cold temperate-oceanic climate and with a high proportion of estuarine systems, is particularly favourable to aquaculture. Chile has largely developed its production of aquaculture in sea, brackish and fresh water ecosystems, representing in 2024 0.9% of its GPD (Subsecretaría del Trabajo, Gobierno de Chile and Observatorio Laboral de la Región de Aysén, 2024). In 2024, Chile was the eighth largest global aquaculture producer, rising to the fifth position when considering marine production alone, with a total production of 1 509 000 tonnes in 2024. This production volume establishes Chile as the leading aquaculture producer in the Americas, having tripled its production over the past two decades (FAO, 2024). The country is also the second world largest producer of molluscs after China, with a production of 434 000 tonnes in 2024 (FAO, 2024).

Chile's aquaculture production is mainly based on fishes, representing 70.4% of the total production, followed by molluscs (28.9%) and algae (0.8%) (FAO, 2024; SUBPESCA, 2025). In 2022, Chile was the 5th biggest exporter of aquaculture products, representing around 8.5 billions USD$ (FAO, 2024). Tree species represent more than 94% of the total Chilean production: the Atlantic salmon (*Salmo salar*) accounting for 49.5% of the total production, the Chilean mussel (*Mytilus chilensis*) representing 28.4%, and the Coho salmon (*Oncorhynchus kisutch*) counting for 16.3% (SUBPESCA, 2025). Chile's salmon farming has grown almost uninterruptedly since 1978, positioning the country since 1991 as the world's second largest producer after Norway

(Buschmann et al., 2023). The Chilean mussel production is particularly noteworthy as it constitutes 98.5% of the total mollusc production, with all cultivation being realised in Los Lagos Region (SUBPESCA, 2025). Geographically, the industry shows remarkable concentration, the Los Lagos Region alone representing 65.5% of the total production, Northen Patagonia (Los Lagos and Aysén Regions) supports 91.9% of Chile's total aquaculture production in 2024, while the entire Patagonian region (Los Lagos, Aysén and Magallanes Regions) accounts for 99.4% (SUBPESCA, 2025). The aquaculture industry represents 17.6% of the regional GPD of the three administrative regions of Patagonia (Subsecretaría del Trabajo, Gobierno de Chile and Observatorio Laboral de la Región de Aysén, 2024).

The sector faces significant challenges from climate-change, including alteration in sea temperature, salinity, declines in oxygen concentrations, occurrences of HABs and spread of diseases (Díaz et al., 2019; Soto et al., 2019). Furthermore, the intensive nature of aquaculture has raised environmental concerns, with evidences suggesting these practices may contribute to ecosystem eutrophication, representing a potential threat to marine environmental quality (Quiñones et al., 2019)

1.1.4. Chile facing climate change

With large arid and semi-arid regions prone to extend under global warming, precipitations mostly dependent on westerly winds and glacier melting, Chile is particularly vulnerable to climate change (Yáñez et al., 2017a). In the future, floodings and droughts would be the largest risks for Chile (Cortina and Madeira, 2023). The global warming effects on Patagonia have not been fully studied, but the general results are that Patagonia would experience drier conditions and weak warming (Boisier et al., 2016; Garreaud et al., 2013b), as already observed since 2010 with more frequent long drought periods (Garreaud, 2018b; Winckler-Grez et al., 2020). Between 1950s and 2010s, Patagonia experienced a warming of +0.6°C, with the Aysén Region being the most impacted (+0.9°C) (Cortina and Madeira, 2023). Models show that Patagonia would experience a warming of between 0.9 and 1.4°C and reduced precipitations by 2070 (Marquet et al., 2023), and would even rise by more than 3°C by the end of the century according to the IPCC scenario (Marquet et al., 2023; WBG, 2021). Precipitations have already decrease by 14 mm on average in Patagonia between 1950s and 2010s, with Los Lagos Region being the most impacted with a diminution of 29 mm, and a projected decline by -10 to -30% by the end of the century (Salazar et al., 2024; WBG, 2021). The probability of atmospheric heatwave would also increase by 8% by 2040s (WBG, 2021).

Those climate changes are mainly due to the weakening of the Westerly Winds attributed to SAM positive trends and anthropogenic climate change (Garreaud et al., 2013b; Gillett and Thompson, 2003), and to the poleward migration and strengthening of the SPSA since the 1990s (Aguirre et al., 2018; Ancapichún and Garcés-Vargas, 2015; Winckler-Grez et al., 2020; Zou and Xi, 2021). Indeed, the Westerly Winds are the main precipitation driver (León-Muñoz et al., 2018), whereas the SPSA brings warm dry air (Ancapichún and Garcés-Vargas, 2015), intensifying the warm and drought episodes (Flores-Aqueveque et al., 2020). Decrease of precipitations reduces rivers discharge, strongly impacting human freshwater resources but also coastal ecosystems, especially fjords, by modifying salinity, turbidity and nutrient supply (Soto et al., 2019; Winckler-Grez et al., 2020). The glaciers melting can also contribute to the modification of the ecosystems, for the same reasons cited before (Rivera et al., 2023).

The warming of the Patagonia would lead different kind of consequences, as the decrease of the dissolve oxygen, in addition to the already hypoxic conditions that exist in some fjords (Schneider

et al., 2014; Silva and Vargas, 2014), a modification of the currents circulation associated to the modification of the winds, reduced freshwater inputs, increasing salinity, modification of nutrient supply, and more globally ocean chemistry (Yáñez et al., 2017a). HABs are also already often present in Patagonia, and warmer waters and stratification would be even more favourable to HAB formation (León-Muñoz et al., 2018). Different kind of HAB exists according to Lipiatou & Granéli (2002), based on the different kind of microalgae responsible of the bloom. It includes toxin-producing microalgae that accumulates through the food chain, high-biomass bloom-forming microalgae which, although non-toxic, might alter the environment's physicochemical conditions, and fish-killing microalgae. In Chile, mollusc aquaculture is facing threats from toxin-producing microalgae, accumulating the toxins in their organism and being a threat for human consumption (Schloss et al., 2023), whereas the salmon industry suffers mainly from fish-killing algae killing directly the organisms (Marquet et al., 2023). The main threats that is facing Chilean aquaculture is the decrease of oxygen concentration, HAB proliferation and the increasing incidence of pathogens (Soto et al., 2019), which all of them can be exacerbated by MHWs. In 2009, a bloom of *Alexandrium catenella* caused the loss of 10 million US$ (Mardones et al., 2010). Economic loss provoke by the compound event MHW, drought and HAB has been registered in summer 2015-16 causing an estimated loss of 200 million US$ for salmon industry only (León-Muñoz et al., 2018; Pujol et al., 2022; Yáñez et al., 2017a).

1.1.5. MHWs in Chile

The study of MHWs in Chile has historically been limited and mainly focuses on one of the world's most productive coastal upwelling system: the Peru-Chile Current, which forms part of the Humboldt Current System (Cooley et al., 2022; Marin et al., 2021; Pietri et al., 2021; Varela et al., 2021). Pietri et al. (2021) examined MHWs within this current system, and showed that the extreme northern Chile is exposed to increasing "short duration" MHWs (lasting 30 to 100 days), and to greater thermal impact. They also stated that these MHWs are linked to weaker upwelling-favourable winds. Cooley et al., (2022) studied anomalously warm SST events from 1980 to 2019 near the central Chile upwelling zone. They found that MHWs in this region typically peak during summer, and that SST anomalies can cover areas over thousands of kilometres. These events are linked to weakened surface wind stress, which reduces the entrainment of colder subsurface waters and diminishes the upwelling strength. In central-northern Chile, Carrasco et al. (2023) described MHWs with typical spatial extents of 100 km^2, mixing layer temperature anomalies between 1 and 1.3°C, and durations ranging from 10 to 40 days, although exceptional cases may persist for several months. MHWs in this region are strongly linked to ENSO cycles, with El Niño events increasing the likelihood of high-intensity and long-duration MHWs (Carrasco et al., 2023). They identified three dominant mechanisms driving MHWs in this region: diminished oceanic heat loss due to lower evaporation combined with increased insolation, which is the most common MHW driver, heat advection mainly caused by eastward surface currents anomalies, and events driven by a combination of positive air-sea heat fluxes anomalies and heat advection, which tend to exhibit the greatest spatial extent, intensity and duration (Carrasco et al., 2023).

Trends in MHWs frequency in central-northern Chile are predominantly negative in coastal regions, with coastal upwelling moderating SST trends and reducing the occurrence of MHWs compared to adjacent offshore waters that relatively neutral trends (Varela et al., 2021). For example, in the coastal area, MHW occurrence decreases by 7.43 MHW days per year per decade, whereas offshore a decrease of only -0.47 days per year per decade is observed (Varela et al., 2021).

Overall, MHWs have been little studied in Chile, and generally focused on the Humboldt Current System and its associated upwellings. To our knowledge, no studies have been conducted in Chilean Patagonia.

1.2. Research Problems and Objectives of the thesis

Marine heatwaves (MHWs) and marine cold spells (MCSs) have increasingly attracted scientific interest because MHWs are becoming more frequent, longer-lasting, and more intense, while MCSs are generally decreasing in frequency. These contrasting trends, combined with their severe impacts on marine ecosystems, biogeochemical cycles, fisheries and aquaculture, explain why researchers are increasingly focused on studying them. Yet, the southeast Pacific, and particularly the coastal regions of Central and Southern Chile, remain largely unstudied despite their high vulnerability to both phenomena. These regions support extensive aquaculture activities, reliant on cold-water species and are already experiencing the consequences of climate change through droughts, changes in large-scale ocean-atmosphere forcings, toxic algal blooms, reduced freshwater inputs and hypoxic events. Given these stressors, a deeper understanding of both MHWs and MCSs in this sensitive region is urgently needed.

The principal objectives of this thesis are described below (Fig. 4):

Objective 1: Assess large-scale patterns and drivers of surface MHWs by quantifying their occurrence, intensity and trends along Central and Southern Chilean coast over the past four decades, and identify the atmospheric and oceanic mechanisms behind their variability.

Objective 2: Develop and implement high-resolution approaches to detect and characterise both MHWs and MCSs in complex coastal fjord system by combining in situ and satellite observations to capture fine-scale spatial and temporal variability that cannot be resolved by global-scale models.

Objective 3: Characterise the spatial variability of surface MHWs and MCSs at high spatial resolution across regions, basins and fjords, highlighting differences in occurrence, intensity and duration, and identifying areas of relative stability or enhanced vulnerability.

Objective 4: Investigate subsurface dynamics of MHWs and MCSs, linking surface and subsurface development to local hydrography, salinity, stratification and topographic constraints, in order to better understand the vertical structure and persistence of thermal events.

Objective 5: Examine the ecological implications of thermal extremes with a particular focus on the relationship between MHWs and harmful algal blooms (HABs), and the potential consequences for ecosystems, aquaculture and fisheries in Northern Patagonia.
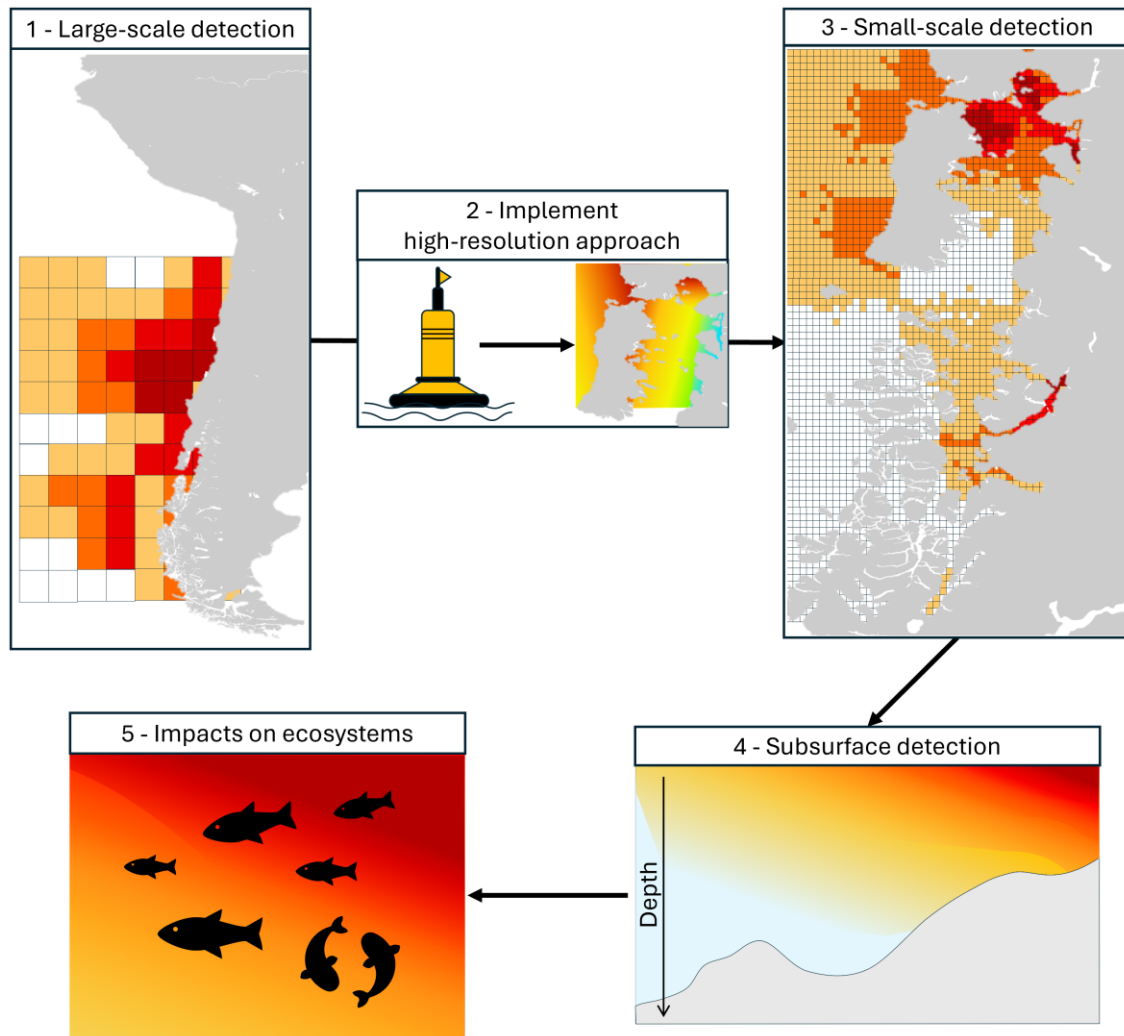
Figure 4: Schematic overview of the objectives of this thesis.

To address these objectives, the thesis is organised into seven main chapters:

Chapter 1 provides a general introduction to MHWs and MCSs, outlining their drivers and consequences, and gives a complete description of the study area.

Chapter 2 presents the first comprehensive large-scale assessment of MHWs along the coasts of central and southern Chile. It provides a global overview of MHWs and their characteristics in this unexplored region. The analysis covers the period from 1982 to 2020 and spans three subregions: Central Chile (29°S to 38°S), Northern Patagonia (38°S to 46°S) and Southern Patagonia (46°S to 55°S). To achieve this, daily reanalysis data at 0.25° spatial resolution are employed to ensure consistent coverage over the entire area.

Chapter 3 develops an innovative strategy to detect MHWs and MWSs at high spatial resolution in Northern Chilean Patagonia, a region characterised by narrow fjords, channels and limited water circulation, making it highly sensitive to thermal extremes. This chapter combines in situ observations with high-resolution satellite products to build a robust baseline with a spatial resolution of 900 m to characterise surface MHWs and MCSs from 2003 to 2023 and assess their trends, drivers and spatial variability across basins in this complex environment.

Chapter 4 explores the vertical dimension of MHWs and MCS using a hydrodynamic model with a horizontal resolution of about 8 km from 1993 to 2024. It characterises subsurface variability across basins and examines how local hydrography and topography shape their development. It establishes also the links between MHW and MCS development, with the salinity and water masses.

Chapter 5 explores the influence of MHWs on the occurrence and severity of HABs in Northern Patagonia, a global hotspot for HABs that poses significant risks to coastal ecosystems, aquaculture operations, and human health. Although the co-occurrence of MHWs and HABs is well documented elsewhere, this link remains unexplored for Northern Patagonia. This chapter focuses on the toxic dinoflagellate *Alexandrium catenella*, responsible for major economic losses and human health intoxications in Chile over recent decades.

Chapter 6 synthesises the results obtained, situating them together with the methodology within broader context of existing literature. It also provides insights into how both native and farmed species may respond to thermal extremes.

Chapter 7 presents the overall conclusions of the thesis and outlines perspectives for future research.

CHAPTER 2.   LARGE SCALE ASSESSMENT OF MHWS OFFSHORE CENTRAL AND SOUTH CHILE

Foreword

This chapter presents the first large-scale assessment of MHWs offshore Central and Southern Chile, a region where no previous studies have addressed this phenomenon. Establishing a broad overview is crucial, as the occurrences of MHWs in these waters remain largely unknown and form the basis for more detailed analyses.

The main objectives are to characterise the spatial and temporal variability of MHWs along the Chilean coast, to highlight regional differences in their frequency, intensity and duration, and to provide a baseline to understand how these extreme events interact with distinct oceanographic and atmospheric regimes that trigger and sustain their development. For this purpose, the area was divided into three large (eco)regions, each influenced by specific climatic and oceanographic conditions. The first one is Central Chile, defined by warm temperate to Mediterranean climate and dominated by persistent northward winds and currents, and characterised by upwellings, the second one Northern Patagonia that experiences a colder, humid temperate climate and where winds and currents alternate between northward and southward directions, and finally a third region, Southern Patagonia, which is shaped by cold tundra to polar conditions, with strong southward winds and currents, and mostly dominated by downwellings.

To achieve this, the NOAA OISSTv2 dataset, which provides daily SST data at spatial resolution of 0.25° was used. Although this dataset cannot resolve the intricate inner seas, fjords and channels of Patagonia, it offers a robust foundation for a first-order assessment at a large spatial scale.

By examining how MHWs manifest in each region and identifying their drivers, this chapter seeks to identify large-scale patterns and establish a reference point for finer-scale and subsurface analysis.

This paper was published in *Frontiers in Marine Science* in 2022.

Pujol, C., Pérez-Santos, I., Barth, A., & Alvera-Azcárate, A. (2022). Marine Heatwaves Offshore Central and South Chile : Understanding Forcing Mechanisms During the Years 2016-2017. Frontiers in Marine Science, 9, 800325. https://doi.org/10.3389/fmars.2022.800325

2.1. Introduction

Extreme warming events in the oceans have become more frequent over the years (Oliver et al., 2018a), partly due to human induced global warming (Laufkötter et al., 2020). Lima and Wethey (2012) estimated that between the 1980s and the 2010s, 38% of the world's coastal zones suffered from an increase of extremely warm SST events. More recently, the IPCC has estimated in 2021 that the frequency of marine heatwaves (MHWs) has doubled since the 1980s and is believed to continue to increase, particularly in the coastal zones (IPCC, 2021). Considered as anomalously warm events, MHWs are described by their duration, intensity, rate of evolution and spatial extent. Their severity depends on both absolute SST and on local seasonal SST variability, meaning that a high temperature above the threshold does not always imply a severe MHW. Diverse factors, both atmospheric (e.g. reduced winds, higher air temperatures) and oceanographic (e.g. advection of warm waters, weaker than usual upwellings) ones with different time and spatial scales can lead to ocean's mixed layer warming, inducing formation, maintenance and disappearance of MHWs (e.g. Holbrook et al., 2019). However, although the mechanisms that contribute to the formation of such events are becoming well known, the way they interplay to initiate and maintain MHWs remains uncertain.

The consequences of such extreme events, which can extend up to 100 m depth (e.g. Pearce and Feng, 2013; Jackson et al., 2018; Su et al., 2021a), are diverse, ranging from ecosystems damages such as mass mortality, species migrations, ecosystem's communities shifts (e.g. Smale et al., 2019), to reduced fisheries and aquaculture production (e.g. Oliver et al., 2017; Cheung and Frölicher, 2020), to modifications of the ocean's properties (e.g. altering carbon cycle and water column stratification, reducing dissolved oxygen concentration or preventing sea ice formation (Brauko et al., 2020; Carvalho et al., 2021; Mignot et al., 2022).

The Chilean Patagonia, extending from 41.5° S to 56° S and bordered by the Southeast Pacific Ocean, is characterised by a complex fragmented coast forming one of the largest fjord regions in the world (Pantoja et al., 2011). Freshwater inputs through the fjords and the relatively cold and stable coastal oceanic conditions confers to Patagonia an ideal environment for aquaculture farming (Iriarte, 2018; FAO, 2019), thus being a region with a major importance in the country's economy. Due to its sensitive environment and its economic importance, this region is particularly vulnerable to global warming (Castilla et al., 2021; Soto et al., 2021; Yáñez et al., 2017a). Patagonia has already experienced the global change consequences in the form of melting glaciers (e.g. Porter and Santana, 2014), reduced precipitations (Boisier et al., 2016; León-Muñoz et al., 2018; Aguayo et al., 2021) associated with more frequent droughts (Garreaud, 2018b; Winckler-Grez et al., 2020), reduced river discharge modifying nutrient supply, turbidity and salinity (e.g. Soto et al., 2019; Winckler-Grez et al., 2020) and harmful algal blooms (HABs; León-Muñoz et al., 2018). More precisely, during the first half of 2016, Patagonia experienced very uncommon conditions with warmer temperatures, a severe drought which had reduced the streamflow by -30% to -60%, and experienced a very strong HAB development (Garreaud, 2018b) in a global context of drought in subtropical Southeast Pacific Ocean since 2010 partly due to large-scale climate forcings (Garreaud et al., 2020). However, to the best of our knowledge, MHWs have not been studied yet in this region, despite the ecosystem's vulnerability. The first objective of this study is to realise a global assessment of the MHWs that have occurred off Central and South Chile over the last 4 decades (1982 to 2020). The second objective is to analyse the metrics of those MHWs (frequency of the events, duration and average and maximal intensity) in order to determine when the most important events occurred and if long-term trends can be observed. In addition, decadal trends of the MHWs' metrics and of the SST will also be assessed. The third objective of this study is to have a better understanding of the factors that contribute to the formation of exceptional MHW conditions that have occurred during the 2016-2017 period, as the MHWs observed at that time were particularly intense and long.

This paper is organised as follows: in section 2.2, we describe the data used for the MHWs detection and for the understanding of the atmospheric and oceanic context while the MHWs were occurring. An overview of the MHWs that have occurred between 1982 and 2020 is presented in section 2.3, as well as a focus on the MHW conditions and their forcings over the period 2016-2017. Then, the MHWs detected in 2016-2017 are placed in a larger context and the possible consequences of the MHWs on fjord ecosystems are exposed in section 2.4. Finally, section 2.5 provides a summary of the main results of the study.

2.2.   Material and Methods

2.2.1. Study area

Chile, bordered to the West by the South Pacific Ocean and to the East by the Andean Cordillera, extends over more than 4300 km from 17° S to 56° S (Fig. 5). The Cordillera has a major role in Chilean hydrology as it regulates the climate by controlling precipitations due to the orographic effect (Viale and Garreaud, 2015; Aceituno et al., 2021). The climate and oceanic circulation off the southern part of Chile, the Patagonia (characterised by fjord ecosystems), are forced by large scale atmospheric systems. The two main ones are the Westerly Winds belt at midlatitudes and the basin-scale South Pacific Subtropical Anticyclone extending over the Southeast Pacific. The seasonal North-South migration of the two atmospheric systems is largely influencing the oceanic circulation by inducing the north-south migration of the South Pacific Current (Pérez-Santos et al., 2019; Strub et al., 2019). Thus, the wind-induced currents are also alternating from North to South direction with respectively equatorward currents in summer and poleward
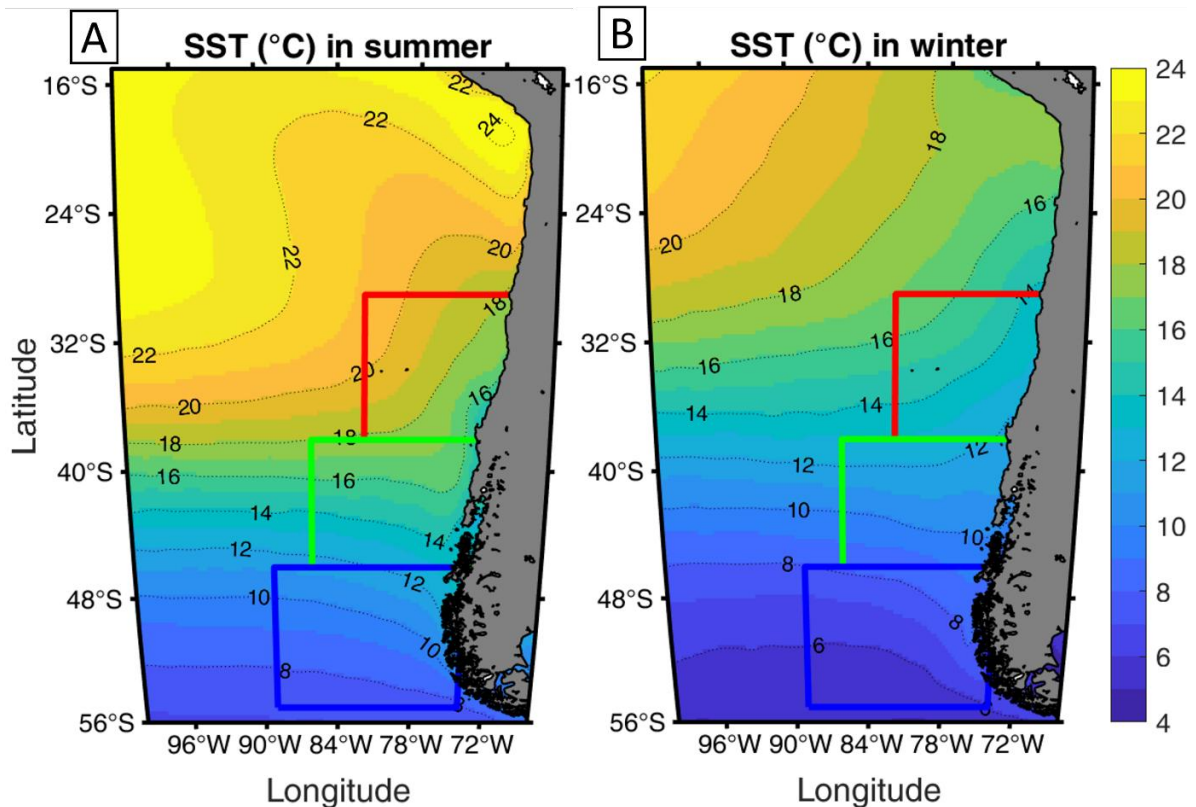
Figure 5: Mean sea surface temperature (SST; °C) in Southeast Pacific during summer (A) and winter (B). Seasonal averaged SST has been calculated over 1982-2020. Studied areas are indicated by the coloured squares: in red the Northern area (-82°E to -71°E and 38° S to 29° S); in green the Transition area (-86° E to -72° E and 46° S to 38° S); in blue the Southern area (-89° E to -74° E and 55° S to 46° S).

currents in winter along central coasts of Chile (Thiel et al., 2007; Strub et al., 2019). Consequently, along the coasts, currents are mostly equatorward north of 37° S (Sobarzo et al., 2007), North-South alternating between 37° S and 46° S, and mostly poleward south of 46° S (Strub et al., 2019). Our study region will therefore be separated in 3 areas according to the main currents circulation: as highlighted by (Strub et al., 2019), the region between 38° S to 46° S represents a "transition zone" where the currents are alternating from North to South. This zone, representing North Patagonia, will constitute our central study area, referred to as the "Transition area" in the study. The two other studied areas are North and South of the Transition one, the first one extending from 29° S to 38° S and corresponding to Central Chile, named in this study the "Northern area", and the second one being the South Patagonia, 46° S to 55° S, named in this study "Southern area". Longitudinally, the areas were delimited in order to have a similar oceanic surface: Northern area is limited from -82° E to -71° E; Transition area from -86° E to -72° E; Southern area from -89° E to -74° E.

2.2.2. Data

The SST was needed to first calculate the SST climatology and secondly to calculate the SST anomaly. The SST climatology was calculated using the reanalysed product Optimum Interpolated Sea Surface Temperature (OISSTv2) provided by NOAA (available at https://psl.noaa.gov/data/gridded/data.noaa.oisst.v2.highres.html) which has a daily resolution. OISSTv2 is one of the longest temporal global SST data available and makes available 39 years of daily data with a spatial resolution of 1/4 degree, from 1982 to 2020. This dataset was used for MHW detection as advised by (Hobday et al., 2016) and also to calculate SST long-term trends (described in section 2.2.4). To calculate the SST anomaly, we choose to use another dataset. Indeed, reanalysed products tend to be overly smooth (e.g. Subrahmanyam, 2015); we therefore preferred to create ourselves an L4 dataset instead of relying on existing ones to retain as much as possible SST variability. We decided to use the SST satellite dataset provided by the Advanced Microwave Scanning Radiometer 2 instrument (AMSR-2) onboard Global Change Observation Mission satellite, having a 1/4 degree resolution and being available at http://www.remss.com. Although our study focuses on the 2016-2017 MHWs, we downloaded the satellite data over the whole available period (2012-07-03 to 2020-12-31) for the whole Pacific Ocean. While microwaves do not interfere with clouds, they do interfere with rain; thus satellite data are still incomplete (36 % of missing data on average). Reconstruction of the satellite SST field was performed with DINEOF as described in section 2.2.3. SST anomalies were calculated by doing the difference between the reconstructed SST data and the daily climatology.

Sea level pressure and air temperature 2 meters above surface were downloaded from 1982 to 2020 using the European Centre for Medium-Range Weather Forecast (ECMWF) reanalysis data (ERA5) available at https://cds.climate.copernicus.eu/#!/home. They both have a spatial resolution of 1/4 degree and a daily temporal resolution. Daily and monthly average atmospheric temperature anomalies were calculated using the data described above doing respectively the difference between daily and monthly air temperature and long-term daily and monthly mean from 1982 to 2020. Same for daily and monthly sea level pressure anomalies.
Zonal and meridional winds components 10 meters above surface, also downloaded from the ECMWF, were analysed over the period 2012 to 2020 (hourly temporal resolution and a spatial resolution of 1/4 degree) and wind speed was calculated from u and v component (respectively eastward and northward components).

Time series of atmospheric temperature, sea level pressure, winds and anomalies for both atmospheric pressure and temperature were also calculated and a 3-months Gaussian filter was applied on each variable to remove variability inferior to the season.

The hourly heat fluxes were also downloaded from the ECMWF from 2012 to 2020 with a spatial

resolution of 1/4 degree. They are related as follows:

$$Qi = Qs - Qb - Qe - Qc$$

where Qi is the total net heat flux at the surface of the ocean, Qs the surface net solar radiation (also known as shortwave radiation) that reaches a horizontal plane at the surface of Earth minus what is reflected by Earth's surface (governed by the albedo); Qb is the surface net thermal radiation (also known as longwave radiation) which is the difference between downward and upward radiation received/emitted by Earth's surface; Qe is the surface latent heat flux representing the transfer of latent heat (e.g. heat transfer due to evaporation or condensation) between atmosphere and Earth's surface through turbulent motion; Qc is the sensible heat flux, i.e. the heat transfer between Earth's surface and atmosphere via turbulent motion but not taking into account heat transfer resulting from water phase change (e.g. evaporation and condensation). We have calculated a spatial average of the hourly heat fluxes between the ocean and the atmosphere within the 3 studied areas (Northern, Transition, Southern areas) to know the temporal evolution and applied a 3-month Gaussian filter to subtract variations inferior to the season. In addition, we calculated the anomaly of the total heat transfer from the ocean to the atmosphere ($Qbec$), which is the sum of Qb, Qe and Qc, by subtracting $Qbec$ monthly climatological mean (calculated based on 2012 to 2020 values) from monthly averaged $Qbec$ values. Within this study, we will consider that fluxes from ocean to the atmosphere are heat loss from the ocean, i.e. negative fluxes, whereas fluxes from the atmosphere to the ocean are heat gain for the ocean, i.e. positive fluxes.

Different remote forcings were evaluated. For El Niño Southern Oscillation (ENSO), we used the Oceanic Niño Index (ONI) provided by NOAA to monitor El Niño and La Niña phases. This index indicates the difference between the 3-month running mean SST and the 30-year climatology in the tropical Pacific between 120°-170° W (Niño3.4 region). El Niño (La Niña) phases are determined when the index is above (below) +0.5 (-0.5). For PDO, we used the ERSST PDO index provided by NOAA. It is the dominant year-round pattern of monthly SST anomalies in the Northern Pacific obtained via empirical orthogonal function analysis. For the Southern Annular Mode (SAM), we used the index calculated according to Marshall's method (2003) expressing the zonal pressure difference between 40° S and 60° S. All indexes were analysed from 1982 to 2020. We applied a 3-month Gaussian filter for PDO and SAM but not for ONI as it is already calculated as a 3-month average.

2.2.3. Reconstruction of the SST field

Data INterpolating Empirical Orthogonal Functions (DINEOF) was used to reconstruct the missing data in the SST field from AMSR-2. It is a tool developed by Beckers and Rixen (2003) and Alvera-Azcárate et al. (2005). It is based on an empirical orthogonal functions (EOF) calculation enabling to fill the missing data in large sets of data, especially satellite ones (Alvera-Azcárate et al., 2005). To fill the missing data, first, DINEOF removes a spatial and a temporal mean to the original dataset, and the missing data are set to zero. Then, a first EOF decomposition is performed with the first EOF for this field and the missing values are replaced by the values obtained by this EOF decomposition. In parallel, DINEOF calculates a cross-validation error. Then, the EOF decomposition and error calculation are repeated with 2 EOFs, then 3 EOFs, etc. The final number of EOFs retained corresponds to the minimal error obtained by the cross-validation. DINEOF has been applied year by year to fill the gaps in the microwave SST data in order to avoid working with too large data files. Indeed, multiyear reconstructions, if done all at once in DINEOF, can lead to overly smoothed reconstructions (as too much weight is given by the EOFs to long-term variations). Although the division of a long time series in separate years can lead to artificial changes between the years, it was not the case in this application. See example of reconstruction with DINEOF for the South Pacific Ocean in Figure 6.
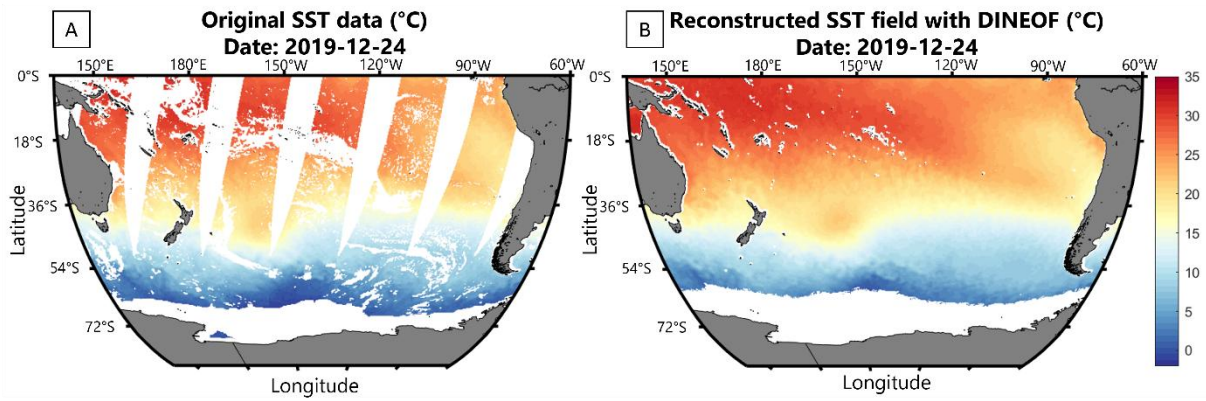
Figure 6: (A) AMSR-2 sea surface temperature (SST; °C). White parts indicate the missing data due to rain, ice and satellite limitations (swaths). (B) Reconstructed SST (°C) with DINEOF. Missing data are still present alongshore and everywhere water was covered at least one day by sea ice.

We reconstructed the whole South Pacific Ocean but decided that every portion of water covered at least one day by sea ice will not be part of the reconstruction, as we are not interested in high latitudes. For each year (2012-2020), the percentage of missing data in the original SST dataset for the whole South Pacific was between 35% and 37%. For the reconstruction, 50 EOF were calculated by DINEOF for each year, explaining in average 99.89% of the initial variance. To estimate the accuracy of DINEOF reconstruction, we calculate the bias, correlation and root mean square error (RMS) between the reconstructed field and in situ data from drifting buoys (shown in Table 2). We used 10 surface drifting buoys with hourly temporal resolution (allowing to select the same hour at which the satellite measures of the SST were done), all scattered offshore Central and South Chile between the coast and about 2 500 km offshore, with a complete temporal coverage from 2014 to 2020. In total, 4219 points were used to estimate the accuracy of our reconstruction (buoys' data are available at https://map.emodnet-physics.eu/). Results show a slight negative bias which indicates that the satellite and the reconstructed SST are lower than the in situ SST. The bias, the correlation and the RMS are very close for both sets of data, meaning that our reconstructed field is as accurate as the satellite data.

Table 2: Bias (°C), correlation and root mean square error (RMS, °C) calculated between original satellite SST and SST from in situ buoys and between the reconstructed SST field with DINEOF and the SST from the buoys. The number of points used for the reconstruction differs as there were gaps in the original satellite SST.

	Number of points	Bias (°C)	Correlation	RMS (°C)
Satellite data vs. buoys	3004	-0.06	0,98	0,55
Filled data vs. buoys	4219	-0.10	0,98	0,47

2.2.4. SST trends

We calculated the seasonal mean SST over the studied area by doing the long-term average (1982 to 2020) over austral summer, autumn, winter and spring. To calculate the SST long-term trends, as a first step we removed SST seasonal variation to our SST values through a low-pass filter in order to have only the annual SST trends and removed seasonal variations. Then, SST linear trends were calculated from 1982 to 2020, by using the OISSTv2 dataset. We choose p-value inferior to 0.05 as a significant trend. Secondly, trend calculation was performed again over ten-year periods, from 1982 to 1991, 1992 to 2001, 2002 to 2011 and 2012 to 2020.

2.2.5. Marine heatwaves

In this study, we used the MHW definition given by Hobday et al. (2016), which defines MHWs as continuous events of warm SST anomalies exceeding a threshold (90th percentile with respect to a 30-years climatology) during at least 5 days. Our marine heatwave detection is based on the HeatwaveR algorithms provided by Schlegel and Smit (2018) available at https://robwschlegel.github.io/heatwaveR/index.html. The SST is spatially averaged over a determined area (in our case Northern, Transition and Southern areas) and the algorithm determines when MHWs are occurring, calculating for each day a long-term climatology, a threshold according to this climatology (90th percentile), and find the periods during which SST exceed this threshold during at least 5 days with no more than 2 below-threshold consecutive days, based on a 11-days moving mean centred on each Julian day (in the case of time series SST data) or on each pixel (in the case of gridded data). In addition to the MHW calculation, the algorithm provides several metrics: number of events per year, duration of each event and maximal and mean intensity (the maximal intensity is the highest temperature anomaly value recorded during the MHW whereas the mean intensity is the mean temperature anomaly observed during the event).

To calculate the climatology, Hobday et al. (2016) recommend to have at least 30 years of SST data because multi-year cyclic events (e.g. ENSO) must be considered to calculate the MHWs. Here we used the same dataset as they did, that is to say the OISSTv2 dataset but over a longer period, from 1982 to 2020. The threshold we used to calculate MHWs is the 90th percentile. In addition, the algorithm also determines the long-term trends in MHW occurrence by first calculating the number of MHW in each pixel of the gridded data that has occurred, in our case between 1982 and 2020, and then applying a generalised linear model to each pixel. From the generalised linear model, slope and p-value (<0.05) are used to determine the long-term trends in MHW occurrence.

Hobday et al., (2018) have proposed a classification of the MHW events in order to have a better visualisation of the MHWs' real impact on ecosystems. This classification has 4 categories which depend on the maximal intensity reached by the MHW event (which in turn depends on the climatology). Categories are based on multiples of the local difference between the climatology and the threshold. Between 0 and 1 times the differences between the climatology and the threshold, no MHW is detected; between 1 and twice the difference it is a Category I MHW, between 2 and 3 times the difference it is a Category II MHW, Category III corresponds to 3 to 4 times the difference and a Category IV corresponds to more than 4 times the difference. This categorization is also given by the heatwave detection algorithm.

2.3. Results

2.3.1. Marine heatwaves in Central and South Chile: 39 years of data

To understand how MHWs have evolved within a 39-year period, we performed an analysis of the duration and intensity for each event and studied the number of MHWs occurring each year. MHWs were identified by doing the spatial average of the SST within the 3 studied areas and their metrics were identified using HeatwaveR code.

From 1982 to 2020, the Northern, Transition and Southern area experienced respectively a total of 75, 73 and 71 periods under MHW conditions from which 5, 6 and 9 MHW periods had a duration superior to one month. In the Northern and Transition areas, the highest number of MHWs was recorded during El Niño years, respectively 9 events in 1997 and 7 in 1998 (Fig. 7A, 3B). For the Southern area, in both 1987 and 2020, 6 MHWs were recorded of which 3 had a duration superior to 1 month (Fig. 7C). For the Transition area, alternance of years with and
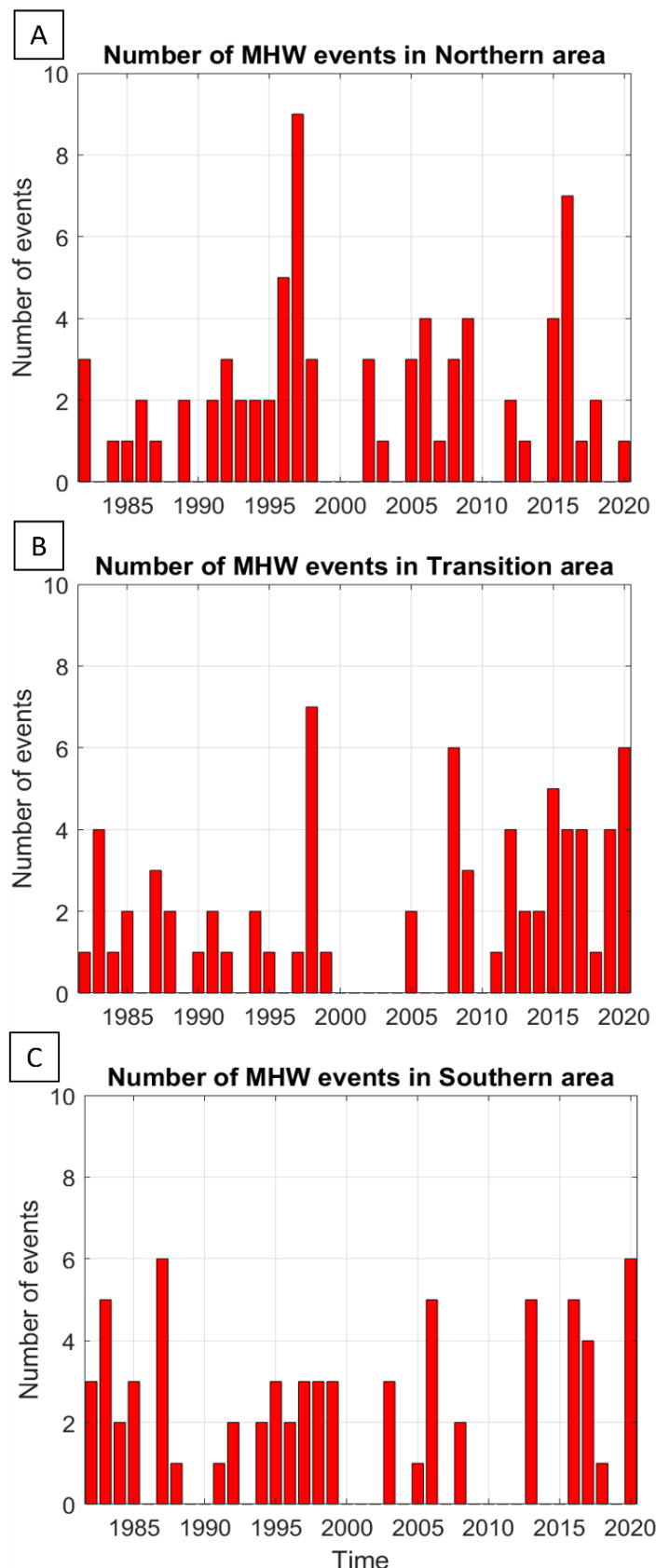
Figure 7: Number of marine heatwave events (MHW) that have occurred each year from 1982 to 2020 for Northern (A), Transition (B) and Southern (C) areas.

without MHWs was common until 2011 (Fig.7B). Nonetheless, from 2011 to 2020, MHWs were recorded every year totalling during that 10-year period 45% of all MHWs recorded for the area. The decade 2012-2020 was particularly active in terms of number of MHW events for the Transition area, totalling on average twice as many events than during the 1982-1991 decade and was 2.5 times superior to the number of events that have occurred during decades 1992-2001 and 2002-2011. It is notable that the early 21st century was MHWs-free for all 3 areas (this period was the longest in the Transition area).

For all 3 areas, the mean duration of MHWs for the 1982-1991 decade was about 10 days and was the lowest of the four decades (Fig. 8A), whereas mean duration during the 2012-2020 decade was the longest recorded, with 20 days, 19 days, 23 days for respectively Northern, Transition and Southern area (Fig. 8B). The mean duration was multiplied by 2.14, 1.9 and 2.3 respectively between the two decades. Between 1982-1991 and 2012-2020, the duration of the longest event has been multiplied by 8, 5 and 3 for respectively Northern, Transition and Southern areas. The longest event in the Northern area began in January 2017 and lasted for 137 days (4.5 months); in the Transition area, the longest event began in May 2016 and lasted for 148 days (almost 5 months), and in the Southern area, the longest event began in June 2016 and lasted for 119 days (almost 4 months).

Regarding the intensity over the decades, the mean intensity of the MHWs is the highest in the Northern area and the lowest in the Southern area (Fig. 8C). For the Northern area, the strongest event recorded was in 2017 with a maximal intensity of 2.3°C, classified as a Category III event. This strong event corresponds to the longest
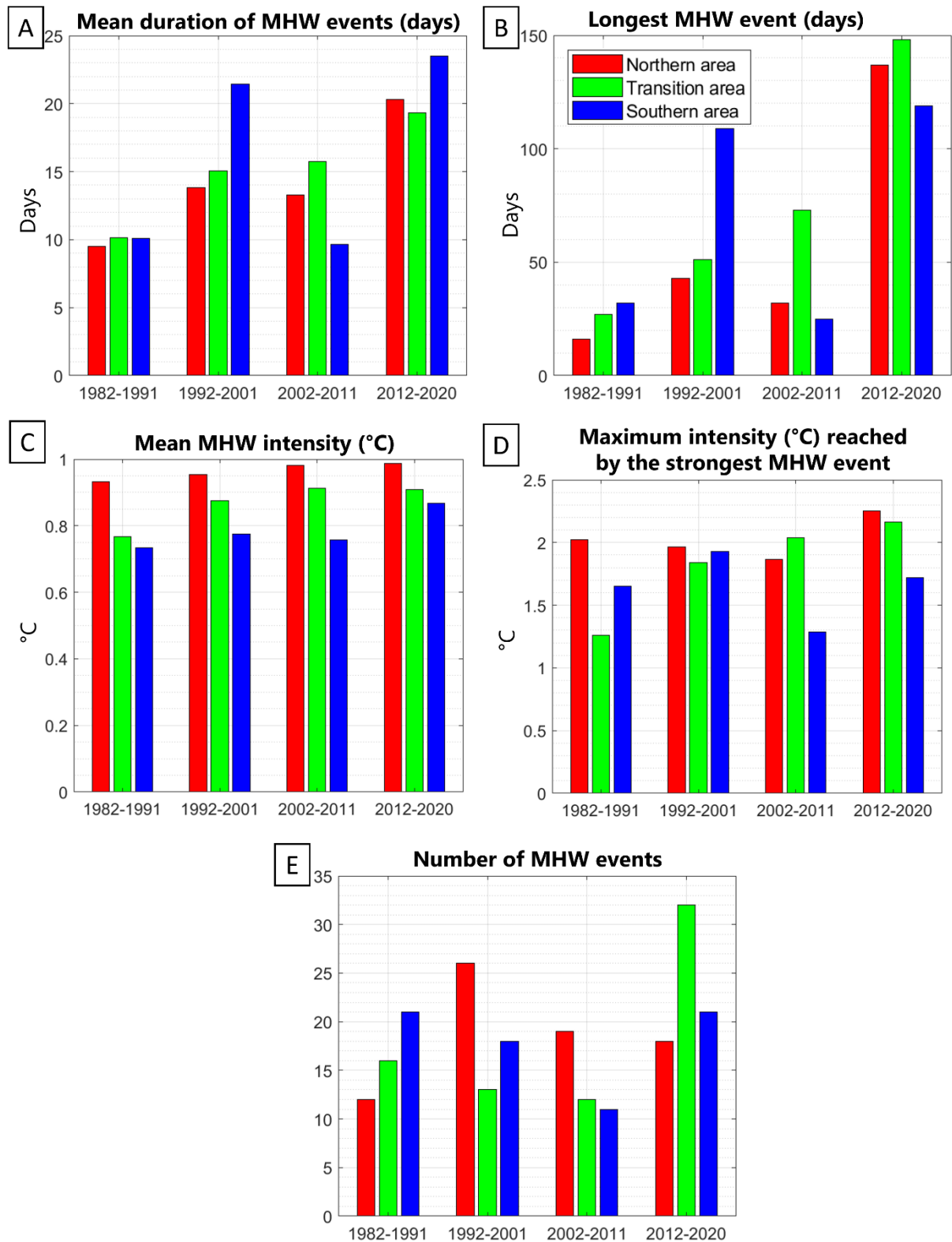
Figure 8: Decadal trends (1982-1991, 1992-2001, 2002-2012, 2012-2020) for Northern (red), Transition (green) and Southern (blue) areas (A, D, G: Northern area; B, E, F: Transition area; C, F, I: Southern area). Parameters analysed over the different decades are: (A) mean duration (days) of the events that have peaked during the decade, (B) duration (days) of the longest event of the decade, (C) mean intensity (°C) of all the events that have occurred during the decade, (D) maximal intensity (°C) reached by the strongest event of each decade, (E) number of MHW events that have occurred throughout the decades.
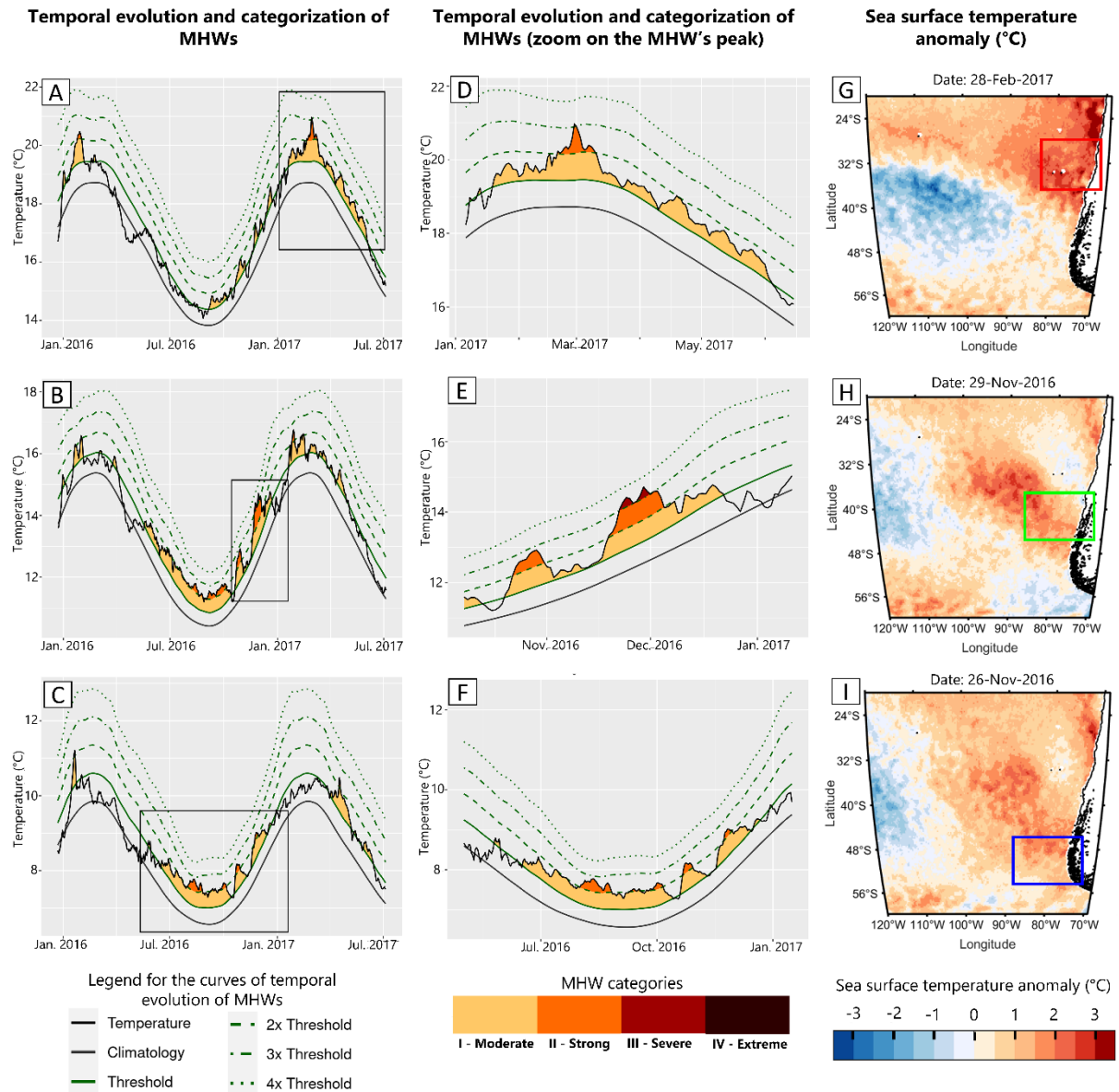
Figure 9: Temporal evolution of the marine heatwaves (MHWs) recorded between January 1st of 2016 and July 1st of 2017 (A, B, C). Those graphs are obtained by averaging the sea surface temperature (SST) over the corresponding area. (D, E, F) Represents a zoom over the strongest event recorded for each area over this period, highlighted by the black square in the left column. For both left and central columns, the lower line of the graph (black and bold) represents the long-term climatology. The irregular black line represents the daily SST temperature. The green bold line represents the threshold, the first green dashed line is 2 times the threshold, the second green dashed line represents 3 times the threshold and the final green dashed line represents 4 times the threshold. The MHWs categorization is represented by the colours with yellow, orange, red and dark purple corresponding respectively to Category I, II, III and IV. (G, H, I) Represents the SST anomaly on the day of the main peak of the strongest event. The areas are represented by the coloured squares. Upper line corresponds to the Northern area, middle one to the Transition area and bottom one to the Southern area.

one recorded in this area (137 days). For the Transition area, the highest intensity recorded was 2.2°C corresponding to a Category II MHW which started in October 2016 and lasted for 64 days. In the Southern area, the strongest event ever recorded was a Category II event in 1998. It occurred while a strong El Niño event was present and had a maximal intensity of 1.9°C with a duration of 99 days. It seems interesting to note that the strongest event recorded was during the last decade for both Northern and Transition areas. Indeed, 21%, 40% and 38% of the MHW events (respectively for Northern, Transition and Southern areas) that had a maximal intensity superior to 1°C occurred after 2011 whereas it represents only a fourth of the total period we studied. In the same way, 36%, 33% and 50% of the events (respectively for the Northern Transition and Southern areas) having a maximal intensity superior to 1.5°C occurred after 2011.

2.3.2. Development of the MHWs in 2016-2017

The years 2016 and 2017 were particularly hit by MHWs with, from May 2016 to May 2017, 219, 298 and 224 days under MHWs conditions for respectively Northern, Transition and Southern areas. More specifically, from May to December 2016 (that is to say a duration of 245 days), the Transition and Southern areas were under MHW conditions during respectively 212 and 216 days (and "only" 86 days for the Northern area). Those conditions were caused by a succession of
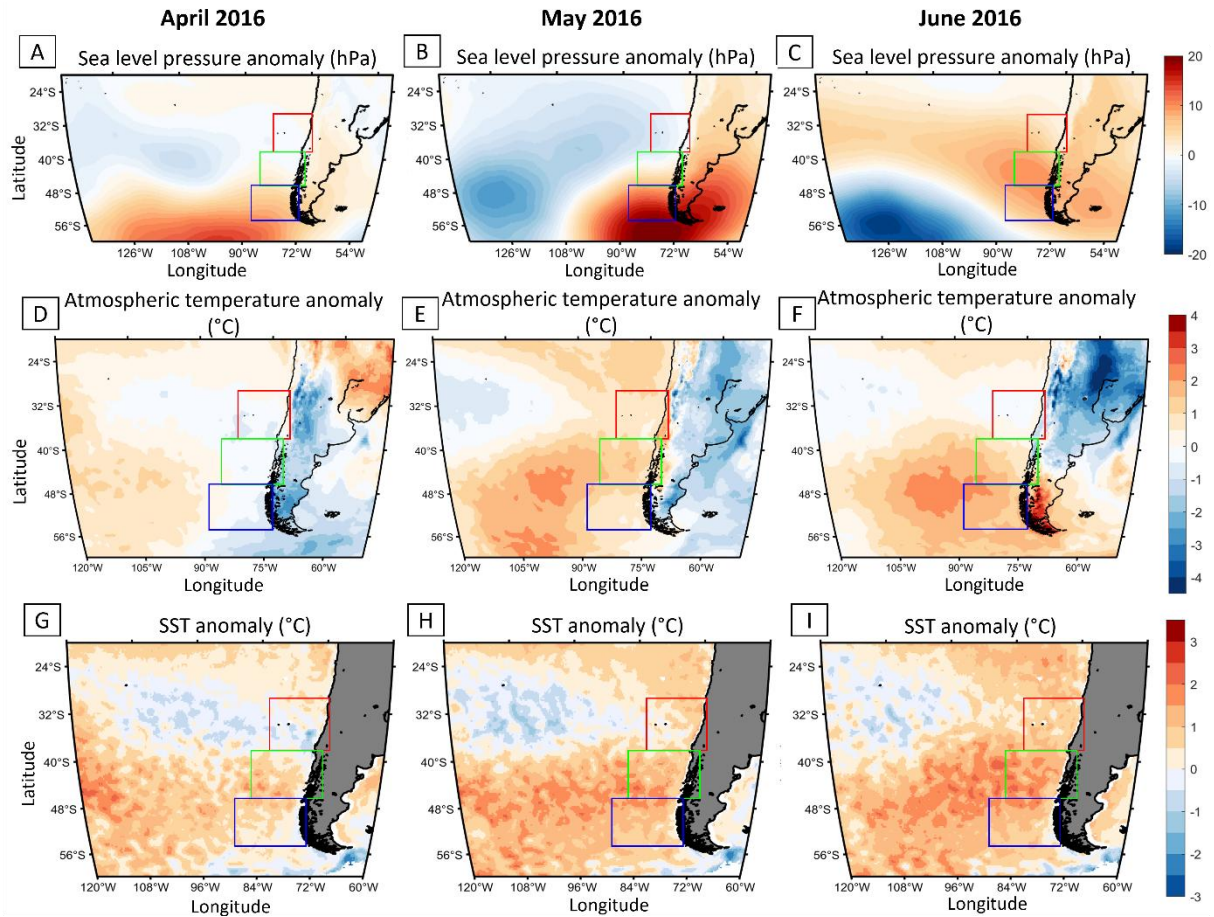
Figure 10: Monthly average sea level atmospheric pressure anomalies (A, B, C), atmospheric temperature anomalies (D, E, F) and sea surface temperature (SST) anomalies (G, H, I), expressed respectively in hPa, °C and °C, for the months of April 2016 (left column), May 2016 (central column) and June 2016 (right column). Colour scale is indicated on the right side of each line. Areas concerned are all located between 20° S and 50° S, and between 50°W and 140°W for pressure anomaly, between 60°W and 120°W for air temperature anomalies and between 60°W and 120°W for SST anomalies.

unusually long and strong MHWs that started on May 2016 (see details in Fig. 9).

On May 19th 2016 (austral fall) started MHW conditions in the Transition area and one month later, on June 17th, in the Southern area. The MHW peaked on June 29th (austral winter) in the Transition area with a maximal intensity of 1.4°C and on August 18th in the Southern area with a maximal intensity of 1.1°C. For both areas, the MHW was considered as a Category II event. On October 13th (austral spring), the MHW disappeared for both areas resulting in 148 days under MHW conditions for the Transition area and 119 days for the Southern area. However, only 7 days later, on October 20th, a new MHW started again in both areas. That time, the intensity of the MHW decreased quickly in early November, the MHW conditions almost disappeared for the Transition area and even disappeared in the Southern area on the 9th of November. Nevertheless, the MHW's intensity increased back by mid-November, provoking a new MHW for the Southern area with a maximal intensity of 1.2°C and for the Transition area the strongest intensity reached over the last 39 years with a value of 2.2°C on November 29th. The MHW then progressively disappeared by the end of December. Finally, MHW conditions totalled 64 days of uninterrupted MHW conditions in the Transition area and 55 days for the Southern area interrupted by 9 days without MHW conditions in November. The MHWs were Category III events for the Transition area and Category II for the Southern area. Concerning the Northern area, 4 relatively short (inferior to one month) and weak MHWs were recorded in austral spring 2016, from September to December. All were Category I events except the third one which was a Category II event with a maximum intensity on November 24th of 1.5°C. Then, on January 19th of 2017 began a Category III MHW which lasted for 137 days with a maximal intensity of 2.3°C on February 28th, being the longest event recorded for the Northern area and the
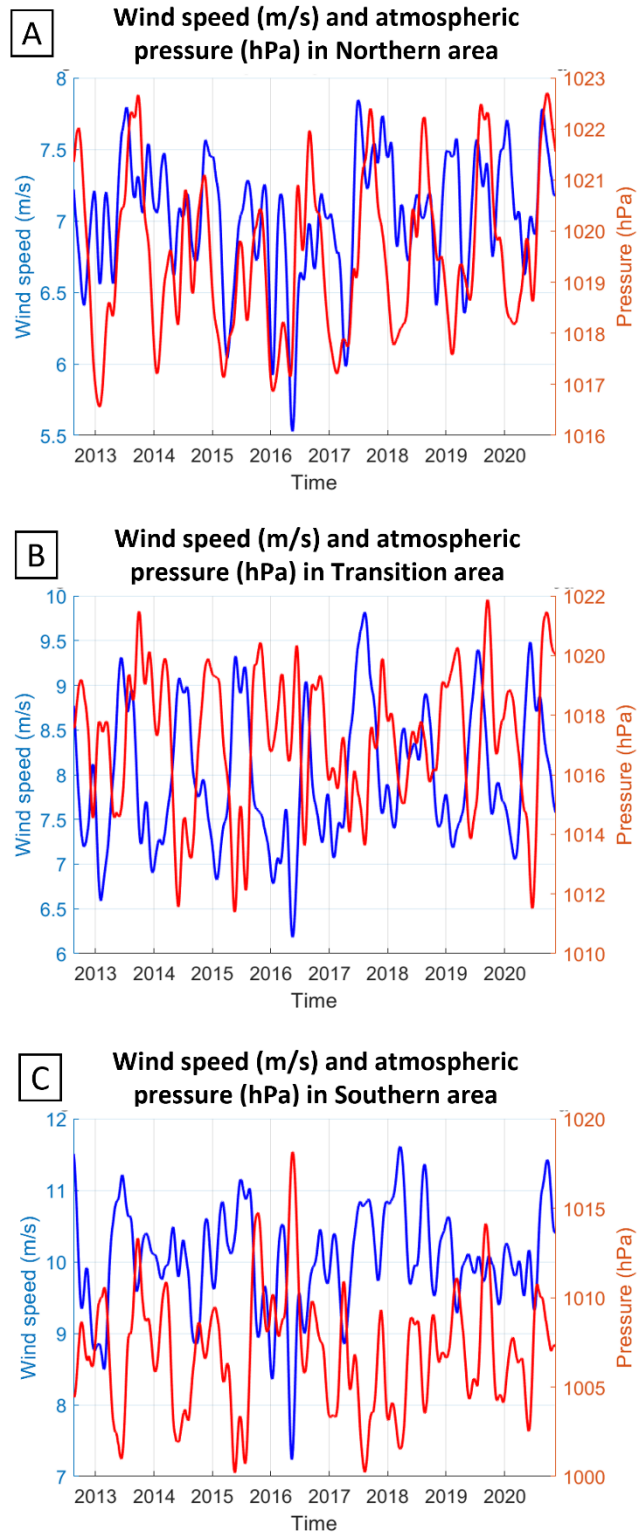
Figure 11: Wind speed (blue) and sea level atmospheric pressure (red) from 2012 to 2020 for Northern (A), Transition (B) and Southern (C) areas. A 3-month Gaussian filter was applied to the data. For a better visualisation of the variations, y-axis' scales differ.

strongest one of all areas combined. At the same period, the Transition area experienced discontinuous short (inferior to 1 month) and weak (all Category I events) MHWs from January to March 2017.

2.3.3. Atmospheric conditions in 2016-2017

In April 2016, a high-pressure system was present in the extreme South Pacific Ocean, reaching Chilean coasts up to 45° S (Fig. 10A). In May and June, the high-pressure system moved northward, encompassing the whole Patagonia and reaching the highest pressure ever recorded over the 2012-2020 period for both Transition and Southern areas (Fig. 10B, C). This resulted in very stable anticyclonic conditions over the Transition and Southern areas, leading to a low winds velocity, the lowest recorded over the 2012-2020 period for all 3 areas (Fig. 11A-C). Furthermore, in the Transition area, the east-component of the wind speed is fully eastward over the 2012-2020 period except in mid-May 2016, having a very low wind speed with a westward direction. During austral winter, the high-pressure system moved toward eastern Patagonia and disappeared in August.
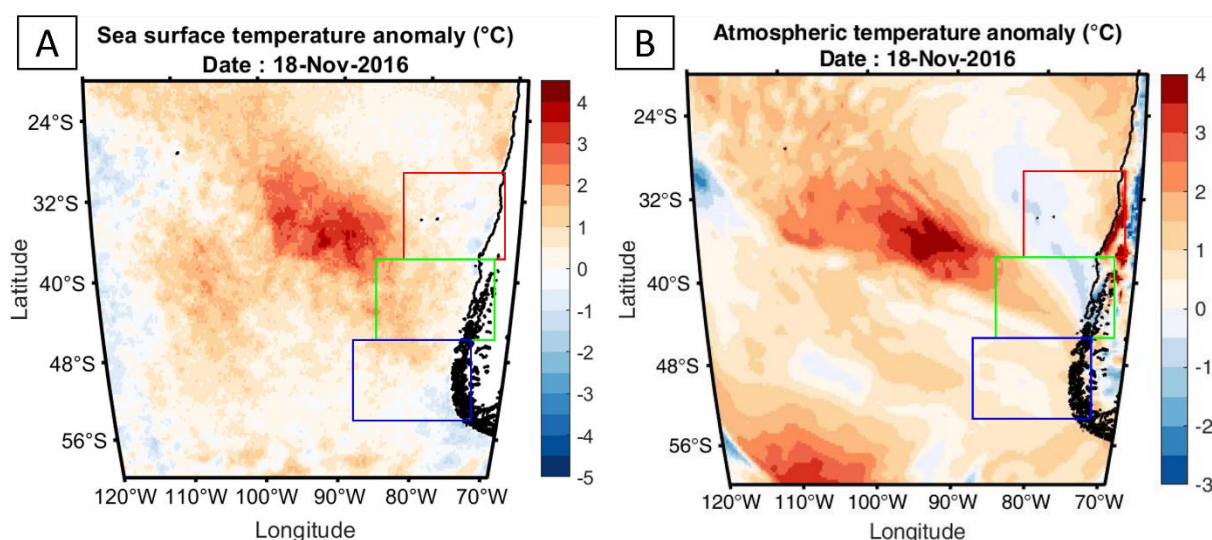
Figure 12: (A) Sea surface temperature anomaly and (B) air temperature anomaly (both in °C) on November 18th, 2016. A particularly warm patch is observable, centred on 90°W 35° S, with anomalies reaching locally 4.5°C for the SST and 4°C for the air temperature.

SST and air temperature were evolving in similar ways. In April 2016, at midlatitudes, a large patch of SST anomalies is present offshore Chile, affecting both Transition and Southern areas (Fig. 10G). A core of negative SST anomalies was observable between the mid-latitude warm patches and warm anomalies at tropical latitudes. The same pattern is observable for atmospheric temperature anomalies (Fig. 10D). In May, the SST patch moved eastward (Fig. 10H), bringing warm anomalies nearshore. Those anomalies were the highest in the Transition area with local anomalies between 2°C and 2.5°C. Alongshore, the warm anomalies merged with lower latitude anomalies, forming a continuous band of positive anomalies along Chilean coasts. Again, a similar distribution of warm atmospheric temperature anomalies is observed (Fig. 10E). In June, the patch of warm SST anomalies was still getting closer to Patagonian coasts. Although the SST anomalies persisted during austral winter, they were progressively diminishing until early spring. However, in October, a patch of warm air temperature anomalies formed in the tropical Pacific, moving progressively southeastward, reaching in November the Juan Fernández
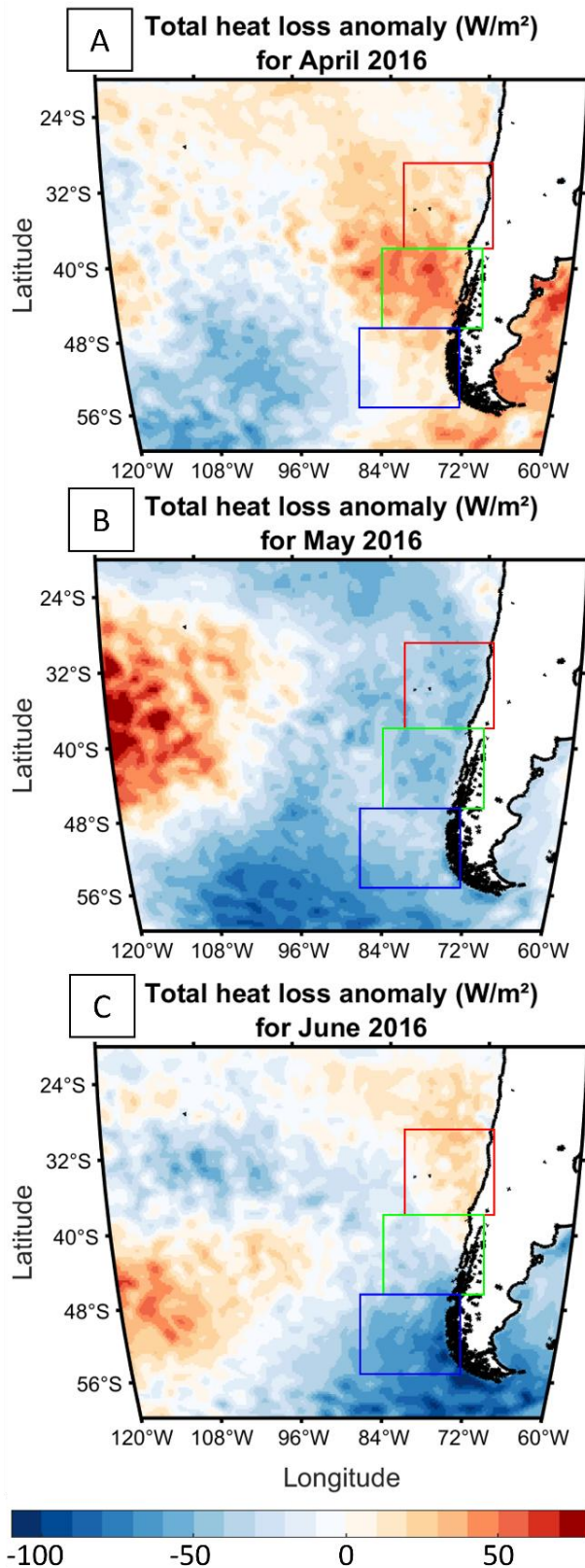
Figure 13: Monthly anomaly of total heat transfer (in W/m²) from the ocean to the atmosphere for (A) April, (B) May, and (C) June of 2016. The anomaly has been calculated according to the 2012 to 2020 average.

Archipelago. In early November, a very warm circular patch formed in the ocean, coinciding with the location of the warm air patch, centred approximately on 90° W and 35° S, West of Juan Fernández Archipelago. At this place, the temperature anomalies rose quickly, reaching on November 18th 4.5°C for the SST and 4°C for the air temperature (Fig. 12); no remarkable positive or negative pressure system was observed where the patches were present. Then, both warm SST and warm air patch migrated southeastward, losing in intensity, and reached coasts of the Transition area in late November. The warm SST patch progressively disappeared in December but pulsed again South-West of Juan Fernandez Archipelago in early 2017. The warm air patch was still present in January and February affecting at that time only the Northern area.

In addition to the atmospheric variables, we also analysed the mean heat transfer from the ocean to the atmosphere over the period 2012-2020 (Fig. 13). Indeed, during late fall and winter 2016, offshore Chilean coasts, the heat transfer from the ocean to the atmosphere was lower than usual, being reduced up to 100 W/m² in June in both Transition and Southern areas compared to the 2012-2020 average (Fig. 13C). This diminished heat transfer was caused by a lower latent and sensible heat transfer. Indeed, in the Transition area the latent heat was reduced by 1/4 in May and June, while in the Southern area it was reduced by ~1/3 from May to July. The sensible heat was reduced in the Transition area from May to September, being reduced up to 1/3 from June to August, whereas in the Southern area a reduction is observed from May to September being almost equal to zero in June and divided by 4 in July. By the end of austral spring, the heat transfer slightly recovers to normal values except in November when the warm SST and air patches were observed.

2.4. Discussion

SST satellite products covering the period of 1982-2020 were used in this manuscript to understand the forcing mechanisms involved in the formation of MHWs offshore central and south Chile. The data analysis showed an increase in MHWs events during the last decade, particularly offshore Northern Patagonia. On another side, the years of 2016-2017 were significant in MHWs occurrence, in terms of duration and intensity. Detailed descriptions of the main results are included in the following discussions sections.

2.4.1. SST and marine heatwaves trends

SST trends from 1982 to 2020 show that the Central South Pacific has been particularly hit by warming waters during the last 39 years (Fig. 14A). A very large patch from the Tropics to mid-latitudes suffered from positive trends, about 0.03°C per year within the patch's centre. The patch reaches South American coasts from 30° S to 47° S, except at 37° S where a cold trend is present. According to those trends, the Transition area is the only South American Pacific coast (South of 10° S) impacted by positive trends, ranging from 0.005 to 0.015°C per year. A closer look to the decadal trends confirms that Chilean coast did not suffer from warming trends during the three first decades (cooling trends are observed nearshore), although a tongue-shaped positive trend is observable in the open ocean centred approximately on 35° S (Fig. 14B-D). Nevertheless, the last decade shows a totally different pattern, with positive anomalies everywhere (except a horseshoe pattern of negative trends), particularly high along Patagonian coasts with trends of +0.05°C to +0.1°C per year (Fig. 14E). Note that the Central South Pacific has been badly hit during all 4 decades. The long-term trends are consistent with what was observed by Roemmich et al. (2016): a tongue-shaped warm patch, with a warm core between 30° S and 40° S getting closer to the coast between 38° S and 47° S. However, contrary to what we found, Roemmich et al. (2016) highlight cooling trends nearshore. The difference might be linked to the different time series used: their study has been realised from 1981 to 2015, whereas our study also encompassed the end of the last decade which was important in terms of warming. In addition, Gutiérrez et al. (2018) found that winter SST has been increasing from 2010 to 2016 in Northern Patagonian fjords, being maximal in 2016, the winter we observe the very long MHW in both Transition and Southern areas.

HeatwaveR algorithms can also provide the MHWs trends (Fig. 15A, B). Thus, we performed the analysis over a reduced portion of the Southeast Pacific Ocean from 1982 to 2020, focusing only on our 3 areas of interest. The results are the MHWs frequency trends within each pixel. An increase of the MHWs frequency is remarkable at mid-latitudes, especially at lower latitudes than 46° S. Along Transition area coasts, a positive trend is also present but not significant. Moreover, a negative trend is observable at 37° S, at the location of the Punta Lavapie upwelling system. The same distribution pattern of MHWs trends and SST trends can be explained by the fact that MHWs are highly related to increasing SST across the globe (Frölicher et al., 2018).

2.4.2. Formation and processes of the 2016-2017 MHWs

In autumn 2016 started a series of MHWs in the Southeast Pacific Ocean, offshore South Chilean coasts (Fig. 9). In April 2016, positive SST anomalies coming from the extratropical Pacific (~55° S, 130° W) started to be stronger in the Transition area, accompanied with diminishing winds (Fig. 10G). This warm patch observed in the extratropical South bringing positive SST anomalies to Patagonia through the Pacific Gyre could be part of the South Pacific Ocean Dipole. This dipole is composed of an extratropical positive SST anomalies patch (which would corresponds to the one we highlighted) centred on about 58° S, 125° W and a subtropical negative SST anomalies
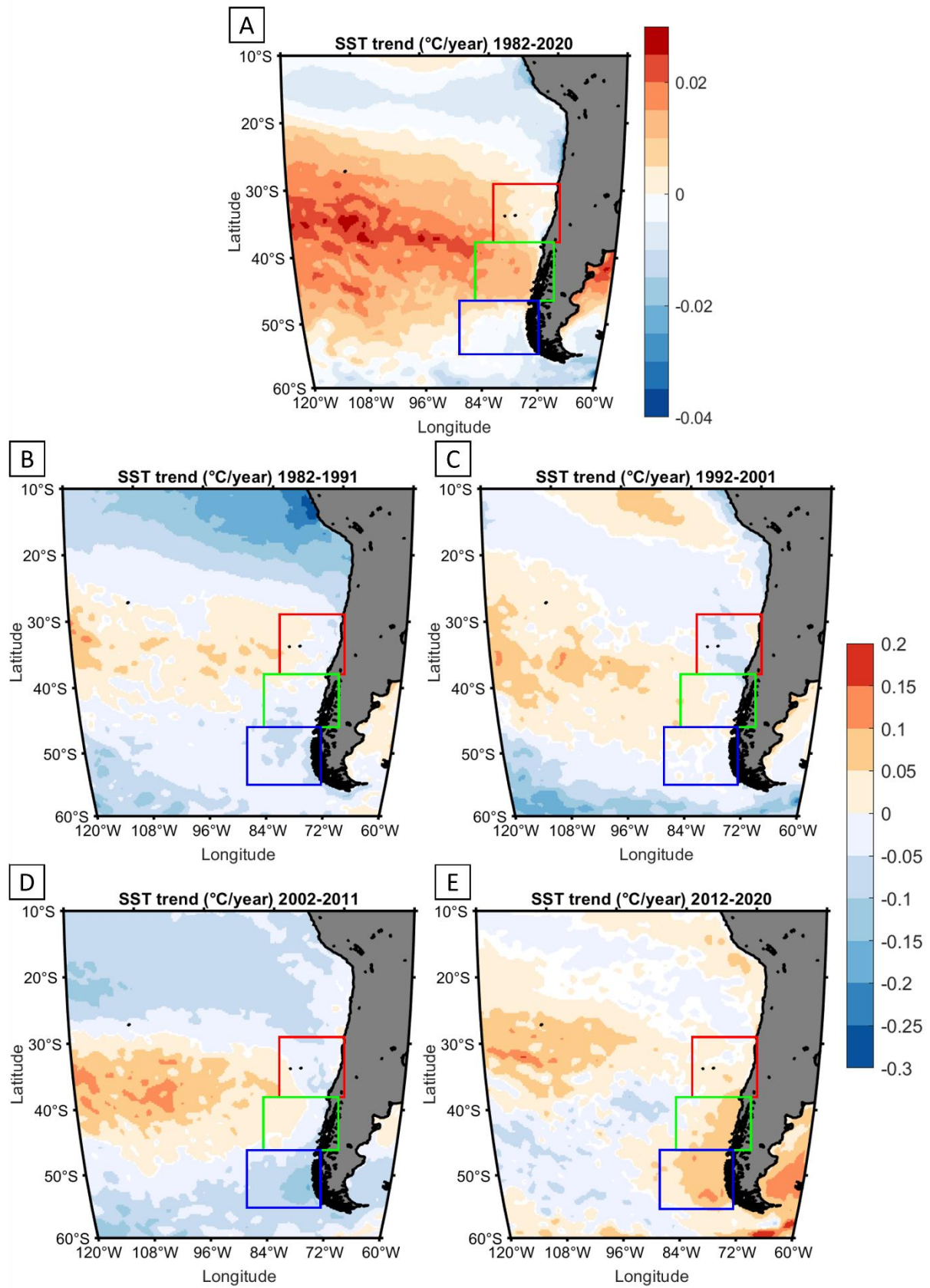
Figure 14: Significant sea surface temperature (SST) trends (according to pvalue<0.05) in °C per year for (A) 1982-2020, (B) 1982-1991, (C) 1992-2001, (D) 2002-2011 and (E) 2012-2020. Areas where no significant trends were observed are shown in white.

patch centred on the eastern coast of New-Zealand (Saurral et al., 2020). The main variability of the dipole is explained by ENSO (Li et al., 2012; Chatterjee et al., 2017): the warm anomalies in the extratropical dipole are enhanced when positive phases of ENSO are occurring. Strong El Niño conditions were present in austral summer 2015-2016 (Fig. 16A), probably strengthening the dipole's warm anomalies. In addition, dipole's SST anomalies are subject to eastward propagation (Li et al., 2012) explaining why they reached Patagonia. In May 2016, the wind speed reached its lowest value over the 2012-2020 period for both Northern and Southern areas (Fig. 11), and the Transition area experienced unusual westward winds. The combination of unusually weak winds due to a persisting high-pressure system (the highest recorded for the Southern area over the period 2012-2020) reducing the heat loss from the ocean (sensible and latent heat; Fig. 13) and the presence of anomalously warm waters triggered MHW conditions in the Transition area in mid-May. In June, the SST anomaly, still coming from the extratropical ocean (Fig. 10I), got stronger in the Southern area, allowing to trigger MHW conditions in that area by the end of the month (Fig. 9F). We did not perform a comparison between 2016 wind speed and long-term wind speed, but Garreaud (2018) did it off Chiloe Island (42.5° S, 74.3° W, located in the Transition area) and shown that winds were about twice inferior to the long term average from late-May to mid-June. In winter, the wind gets back to usual values, and the heat transfer from the ocean to the atmosphere progressively gets back to normal by early spring. In spring, SST anomalies were present but were getting lower than during previous months, barely maintaining MHW conditions. The MHWs conditions stopped by mid-October in both Transition and Southern areas, totalling 148 days under MHWs conditions in the first area and 119 in the second one (Fig. 6). The Northern area has not been affected by this MHW, except in the form of short heat peaks during winter. However, advection of warm waters coming from extratropical South Pacific triggered new MHWs in all 3 areas in mid-October but were not high enough to maintain the MHW conditions resulting in early November in a break within the MHW period in Northern and Southern areas and to its almost disappearance in the Transition area. Meanwhile, a warm patch formed very quickly in both ocean and atmosphere West of Juan Fernández Islands in early November 2016 (Fig. 12), with an SST anomaly increase of 2.5°C in only 12 days. Both
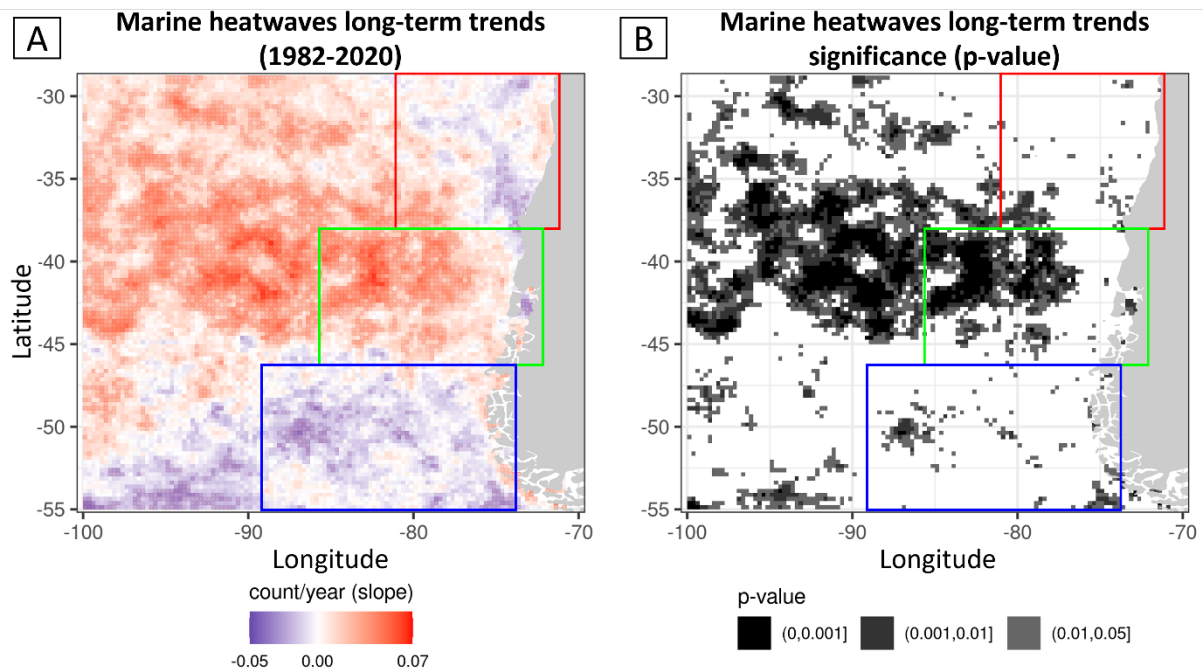
Figure 15: (A) Marine heatwaves (MHWs) trends and (B) significance of the trends according to the p-value. The trend is calculated according to the number of MHWs that have occurred in each pixel from 1982 to 2020. Consequently, a positive (negative) trend significant that the number of MHWs is increasing (decreasing) with time.

atmospheric and oceanic warm patches moved southeastward and reached the coasts in late November, encompassing the three areas and coinciding with the new apparition of MHW conditions in Northern and Southern area and to the strengthening of the MHW in the Transition area. In the Transition area, this MHW corresponds to the most intense one recorded over the 1982-2020 period. In the Northern area, the MHW was not that strong because of the presence of a coastal negative anomaly signal at approximately 37° S, corresponding to Punta Lavapie, an area where upwelling favourable winds are predominant from September to February (Letelier et al., 2009), explaining the negative SST anomalies often observed in this area. However, the positive anomalies patches got cooler while moving northeastward in mid-December and the anomalies were decreasing. Nevertheless, in late January 2017, both SST and atmospheric temperature anomalies patch increased back, provoking the 137 days (4 and a half months) MHW in the Northern area (which was, by the way, the strongest event ever recorded along Chile) and to short pulses in Transition and Southern areas.

It is important to note that in the part of the world we are interested in, SST is generally higher than the air temperature. To understand how SST and air temperatures are related, we spatially averaged SST anomalies and air temperature anomalies (and applied a 3-months Gaussian filter on both) over the period 2012-2020 for the 3 areas and calculate their correlation to know how they are related. Over the period 2012-2020, the correlation between air temperature anomalies and SST anomalies was the highest with a 10, 1 and 3-days lag respectively for Northern, Transition and Southern areas. The correlation was therefore 0.9291, 0.8748 and 0.8711 respectively. However, having a more specific look to the year 2016 only, air temperature and SST anomalies were occurring with no lag for both Northern and Transition areas, whereas for the Southern area, SST anomalies were leading air temperature anomalies by 9 days; correlation between the two parameters for all 3 areas being higher than 0.94 for the year 2016. Consequently, as the SST is higher than the air temperature and as SST variations precede or occurred at the same time as air temperature variations, this would signify that the autumn-winter-spring MHWs in 2016 were not led by the air temperature. However, the global
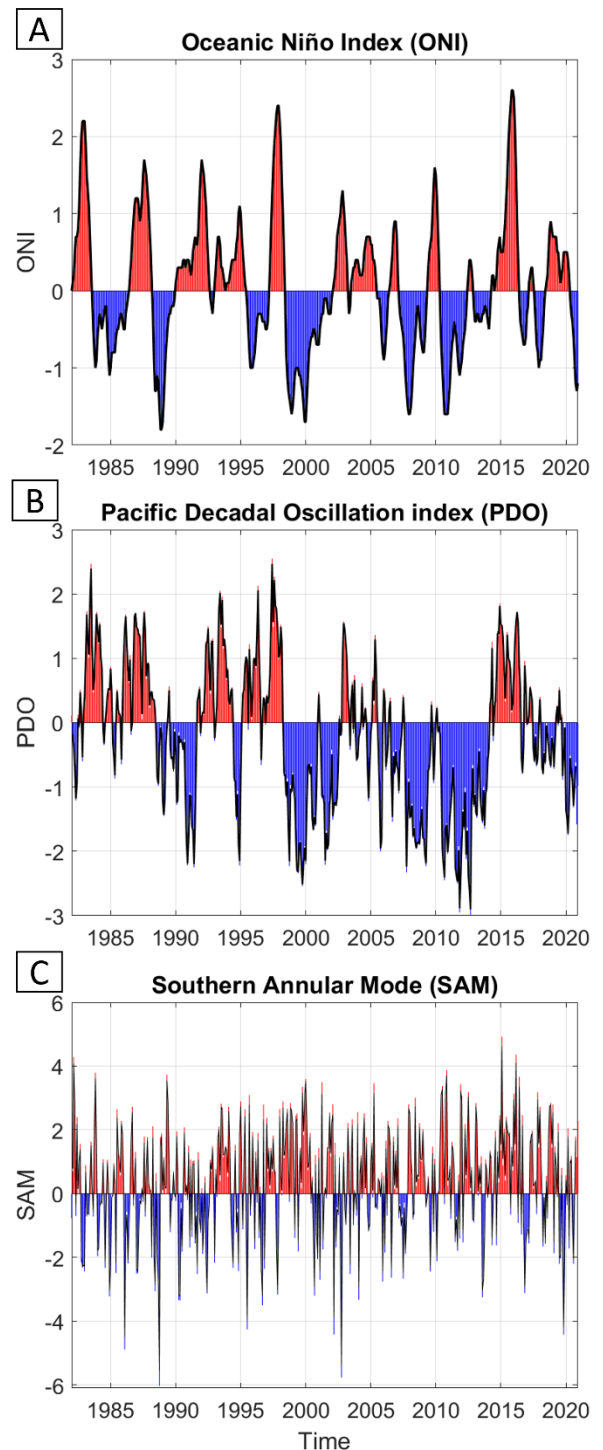
Figure 16: Different remotes forcings expressed by their index. (A) Oceanic Niño Index for ENSO monitoring (ONI), (B) Pacific Decadal Oscillation (PDO) index, (C) Southern Annular Mode (SAM) index. Red indicates a positive period and blue a negative period. PDO and SAM index are expressed with a 3-month Gauss filter, represented by the black bold line. ONI calculation is already based on a 3-month average. The scale differs according to the index.

atmospheric conditions (lower winds associated with high-pressure system, thus reducing heat loss from the ocean) contribute to enhance the SST anomalies, preventing waters to cool during winter, in addition to the warm waters advected from the South-Central Pacific Ocean. That combination of oceanic and atmospheric factors, i.e. advected warm waters, high pressure system inducing reduced winds and in return a decrease in the sea-air fluxes, having led to MHW formation has already been observed in the past, for instance in the Pacific Ocean when a MHW lasted from 2013 to 2015 (Bond et al., 2015) or in 2011 in Western Australia (Pearce and Feng, 2013).
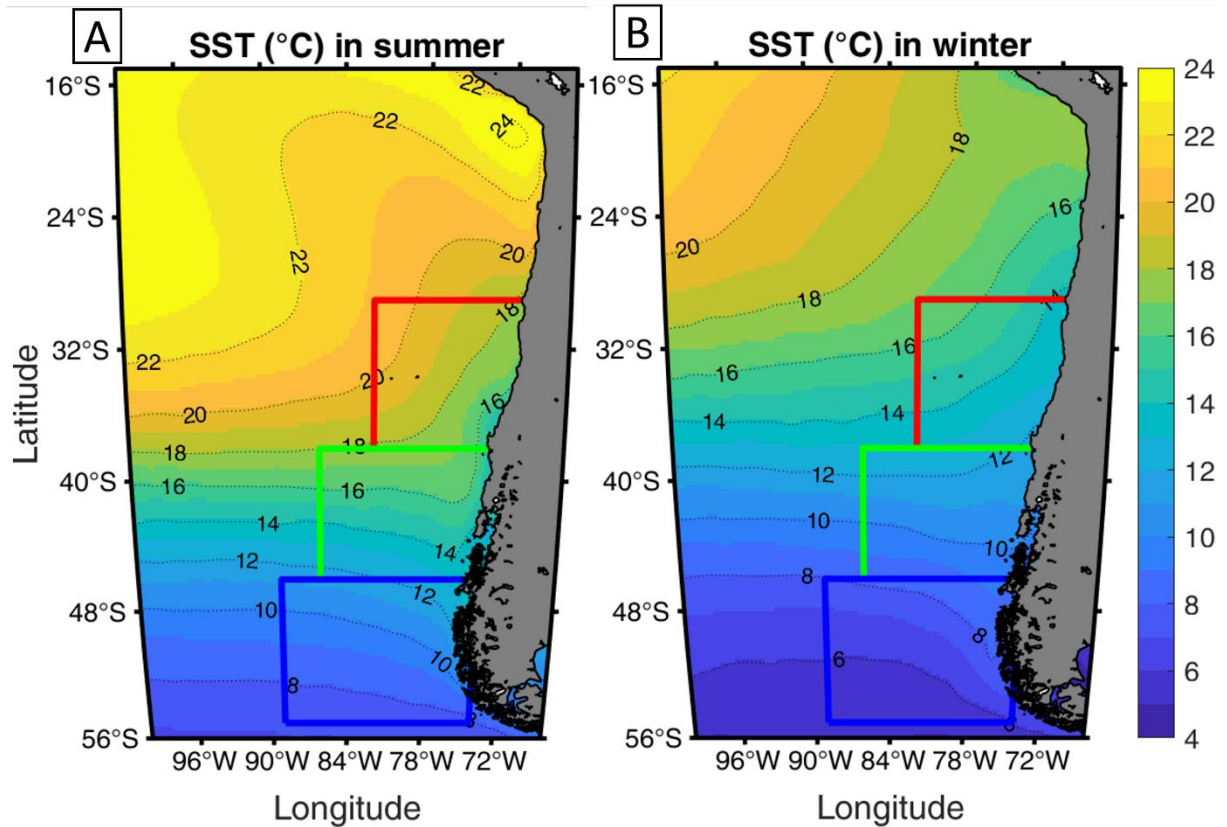
Figure 17: (A) Sea surface temperature (°C) long-term monthly averaged over 1982 to 2020 period for February and (B) monthly average for February 2017.

Besides the oceanic and atmospheric forcings, remote forcings could have played a role within the longevity and intensity of the MHWs events during 2016 and 2017. Indeed, in 2014, ENSO switched to a positive phase until mid-2016, being one of the three strongest El Niño events ever recorded with the 1982-1983 and 1997-1998 ones (Fig. 16A). Because of its importance, it has been popularly named "Godzilla El Niño". Garreaud (2018) has shown that the Godzilla El Niño event, was associated with strong positive sea level atmospheric pressure anomalies (>5 hPa) at extratropical latitudes during austral summer 2016. In our study, we found that during austral autumn (March-April-May), the atmospheric pressure anomalies were also high, with seasonal average up to 10 hPa. In addition, the warm patch we described West of Juan Fernández Archipelago that formed in November 2016 and strengthened in January 2017 was probably linked to a "coastal El Niño" (Garreaud, 2018a; Rodríguez-Morata et al., 2019; Smith et al., 2021), whose characteristics were a strong and rapid warming of the easternmost Equatorial Pacific in January 2017 followed by other warm pulses in February and March, associated with very weak Tradewinds from January to April 2017 (Garreaud, 2018a). In fact, the whole Central Pacific experienced a very strong El Niño in 2015-2016 and the easternmost Central Pacific experienced a coastal El Niño in summer 2016-2017 (Garreaud, 2018a). In its study, (Garreaud, 2018a) highlights a tongue-shaped warm SST coming from Equatorial Pacific and extending southeastward to the coasts of our Northern area, in accordance with what we described. This warm patch resulted in

the formation of the most intense MHW in the Northern area, which lasted from January 19th to June 4th 2017. In addition to the El Niño event, a positive phase of PDO also occurred from 2014 to 2017 (Fig. 16B). PDO has already been correlated with positive sea surface temperature for the period 2014-2017 in previous study (Narváez et al., 2019). Indeed, when its positive phase occurs together with ENSO's positive phase, their consequences can cumulate and cause lower winds and warmer conditions at mid-latitudes (Garreaud et al., 2009; Ancapichun and Garcés-Vargas, 2015; Yáñez et al., 2017a). Besides the El Niño and PDO events, a strongly positive phase of SAM also occurred in 2016 (Fig. 16C). Nevertheless, usually ENSO and SAM have negative correlation (Gong et al., 2010), thus the synchronisation of very strong positive events of both phenomena seems confusing. However, as the two phenomena have the same consequences over Chilean Patagonia, meaning high pressure systems South of Patagonia, reduced Westerly winds at mid-latitude and higher temperatures, their combined effects might exacerbate their consequences. And effectively, the drop in wind speed we observed in late autumn 2016 and the high pressure associated were the highest ever recorded at least over the period 2012-2020. Although SAM has been cited in a few studies as a factor maintaining or initiating environmental conditions for MHW formation (e.g. Perkins-Kirkpatrick et al., 2019; Salinger et al., 2019); Su et al. 2021), its implication within the formation of MHWs, particularly in the Southeast Pacific Ocean, needs to be in-depth investigated.

2.4.3. Marine heatwaves consequences on fjords ecosystems

Although Patagonian ecosystems are extremely vulnerable to global warming (Yáñez et al., 2017a) and even if fjords are considered as aquatic critical zones (Bianchi et al., 2020), only few studies have been realised on MHWs' consequences on fjords ecosystems and none on Patagonian fjords. Here, we suggest that numerous typical impacts of MHWs could be considered according to what has been observed in other parts of the world. For instance, a HAB occurred in North Patagonia inner seas from February to May 2016 (Armijo et al., 2020; Garreaud, 2018b; León-Muñoz et al., 2018)resulting in economic losses of several hundred million dollars (e.g. Díaz et al., 2019). HABs are often described as a consequence of MHWs (e.g. NOAA Climate, 2015; Roberts et al., 2019), but this one occurred shortly before the MHW we detected in the Transition area. That temporal mismatch could be due to the coarse spatial resolution of the SST data we used to perform our MHWs detection, preventing us to know if the inner seas experienced more numerous or longer MHWs than the open ocean did and if the HAB coincided with a MHW event. Another type of consequences of MHWs on Patagonian fjords could be the diminution of oxygen concentration. Indeed, Patagonian fjords are already experiencing hypoxic conditions due to fjord alimentation by low-oxygenated Equatorial Subsurface water mass filling the deep micro-basins (Silva and Vargas, 2014; Pérez-Santos et al., 2018), a strong stratification which prevents deep waters to be re-oxygenated by vertical mixing (Silva and Vargas, 2014) and anthropogenic activities (Silva and Vargas, 2014). The presence of a long-lasting and severe MHW as the one we observed during winter 2016 could worsen the hypoxic conditions by increasing thermal stratification and reducing oxygen dissolution (Breitburg et al., 2018), as it has already been observed in Norwegian deep-fjords where hypoxic conditions were exacerbated by deep waters warming, then affecting benthic communities (Aksnes et al., 2019). In addition, Patagonia is also a place for large aquaculture development, particularly salmon farming as the environmental conditions are optimal with average temperatures up to 15°C in summer for Northern Patagonia (Fig. 17A). However, in February 2017, the strongest ever MHW event was recorded and SST nearshore was nearly 2°C higher than average, reaching 17°C (Fig. 17B) in northernmost Patagonia, being close to the upper limit of optimal temperature growth for Atlantic salmons (Elliott and Elliott, 2010). Finally, decreases in microbial richness have already been observed in Patagonian fjords, associated with seasonal increase of sea temperatures, particularly in winter (Gutiérrez et al., 2018). This would probably be exacerbated as MHWs are projected to be more numerous, as we saw in section 2.4.2.

2.5. Conclusion

This study presents, to the best of our knowledge, the first assessment of the marine heatwaves (MHWs) that have occurred along Central and South Chile (29° S-55° S) from 1982 to 2020. We found that, although MHWs were already present in the 1980s, their intensity and their duration have increased, particularly over the period 2012-2020 with record-breaking events. The central studied area (North Patagonia) located between 38° S-46° S is the only Chilean coastal area where a long-term positive trend of MHWs frequency is present, probably related to the SST long-term warming trends. Indeed, that area totals 45% of the MHW events and 40% of the events that had an intensity superior to 1°C during the 2012-2020 period, showing how badly the area has been hit during the last decade. More particularly, the period from austral fall 2016 to summer 2017 suffered a succession of unusually long and strong MHWs. From May 2016 to May 2017, North Patagonia suffered about 300 days under MHW conditions. We found that in fall and winter 2016, warm waters were advected from the extratropical Pacific Ocean to the Patagonian coasts, contributing to the MHWs triggered and that atmospheric conditions were optimal for MHW development. Indeed, in May and June 2016, winds were abnormally low contributing to the diminution of the heat lost by the ocean. The MHW conditions persisted until spring 2016 and progressively disappeared. However, in November, new MHW conditions started causing the strongest MHW we recorded which lasted until early June 2017 in Central Chile, probably linked to a coastal El Niño. In addition, in early 2016, very strong El Niño conditions were reported and were associated with positive phases of SAM, probably having influenced the environmental conditions that have led to very intense and long MHW events.

In this study we analysed the surface development of the MHWs. However, the evolution of the detected MHWs off the coast of Chile, with several MHWs happening sequentially with only a few days between them, indicates that the subsurface temperatures might stay high during longer periods of time, favouring the development of new MHWs in the surface more easily. Therefore, further works should be dedicated to the subsurface development of the MHWs which is also primordial as it will define the depth at which species will be affected by the warming. Additionally, further studies should assess how the inner seas of Patagonia are affected by MHWs. Indeed, MHWs consequences add to the already existing hypoxia and to global warming might severely damage fjords ecosystems and aquaculture production.

CHAPTER 3. HIGH-RESOLUTION DETECTION OF MHWS AND MCSS IN NORTHERN PATAGONIA

Foreword

The previous chapter provided a first large-scale assessment of MHWs along the coasts of Central and Southern Chile using coarse-resolution reanalysis data. This approach allowed to identify broad spatial and temporal patterns, revealing that Northern Patagonia stands out at the most impacted of the three regions examined. Over the last decade in particular, this region experienced a marked increase on the frequency, duration and intensity of MHWs, including several prolonged and extreme events. While Central Chile also showed a slight positive trend in frequency and southern Patagonia exhibited overall negative trends, Northern Patagonia emerged as a clear hotspot of change.

These findings raise important questions about how extreme events develop and persist within the high intricate Inner Sea of Northern Patagonia. The coarse-resolution OISSTv2 dataset used previously is not capable of resolving the complex fjords and channels of this region, and even available satellite observations lack the spatial and temporal detail required to adequately detect and characterise these events and their spatial variability. This necessitated the development of a high-resolution (<1 km) methodology specifically designed to detect both MHWs and MCSs in these confined coastal environments.

The next chapter introduces this new methodology, which forms a key part of this thesis. It provides a compact study that was initially planned as two separated chapters, one focusing on the methodology for climatology calculation and extreme events detection, and the other dedicated to the application of this methodology, with case studies and driver analyses. However, it was preferred to combine both aspects to provide a single complete work. This chapter therefore presents the methodology developed to achieve the detection of MHWs and MCSs in such complex environment, and presents the overall metrics of MHWs and MCSs in Northern Patagonia, and highlights their spatial variability. It also includes detailed case studies that explore the mechanisms triggering and sustaining these extreme events.

This extensive work was submitted to the review *Ocean Science* in March 2025 and is currently still under review.

Pujol, C., Barth, A., Pérez-Santos, I., Muñoz-Linford, P., and Alvera-Azcárate, A.: Overcoming Challenges in Coastal Marine Heatwave Detection: Integrating In Situ and Satellite Data in Complex Coastal Environment, EGUsphere [preprint], https://doi.org/10.5194/egusphere-2025-1421, 2025.

Data availability

The monthly and daily-derived climatologies described in Sections 3.2.2 and 3.3.3 are available on Zenodo (DOI: https://doi.org/10.5281/zenodo.14845077) and can be freely used for any purpose. The threshold dataset described in Sections 3.2.3 and 3.3.3 and the SST dataset described in Sections 3.2.3 and 3.3.4 are also available on the same page; however we recommend to use it for the detection of MHWs and MCSs, in addition to the daily-derived climatology.

The list, description and sources/DOIs of all the in situ data used for the construction of the climatologies (Section 3.2.2) are also available in the Annexes.

Annexes

Figures fully describing the monthly climatology at every depth are available in the Annexes at the end of this manuscript (for digital version of the manuscript only).

3.1. Introduction

Marine heatwaves (MHWs) and marine cold spells (MCSs) are phenomena characterized by anomalously warm or cold water events that persist for at least 5 days to several months, as defined by Hobday et al. (2016) and Schlegel et al. (2021). MHWs have been increasingly observed worldwide, with rising intensity and duration linked to global warming (Oliver et al., 2018a; Laufkötter et al., 2020; Cheng et al., 2023; Capotondi et al., 2024), while MCSs, although much less studied, are generally declining (Yao et al., 2022).

MHWs are responsible for increasing ocean stratification (Holbrook et al., 2020b), decreasing oxygen concentration (Brauko et al., 2020; Gruber et al., 2021; Shunk et al., 2024) and increasing ocean acidification (Gruber et al., 2021; Burger et al., 2022; Mignot et al., 2022). They are also responsible for numerous impacts on biodiversity (Smith et al., 2023b), among others, coral bleaching (Dalton et al., 2020; Soares et al., 2023; Huang et al., 2024), habitat loss (Arafeh-Dalmau et al., 2019; Filbee-Dexter et al., 2020), mass mortality (Garrabou et al., 2022), and favouring conditions for harmful algal blooms proliferation (Kuroda et al., 2021; McCabe et al., 2016; Takagi et al., 2022), with economic repercussions on aquaculture, fisheries and tourism (Barbeaux et al., 2020; Cheung and Frölicher, 2020; Maulu et al., 2021; Smith et al., 2023b). Similar observations can be made for MCSs (Schlegel et al., 2021).

MHWs and MCSs are identified by comparing daily sea temperature against a long-term climatology. Hobday et al. (2016) recommend to use at least 30 years of temperature data to study MHWs, as this duration captures decadal trends such as El Niño Southern Oscillation and includes periods that were less impacted by the global warming than present day. The 90th (10th) percentile typically marks MHWs (MCSs) threshold, though some studies adopt higher percentile to focus exclusively on the most extreme events, thereby excluding what might be considered as "normal" extreme events (e.g. Frölicher et al., 2018; Holbrook et al., 2019; Laufkötter et al., 2020).

The primary method for detecting and tracking MHWs and MCSs relies on global satellite products, notably NOAA's Optimum Interpolation Sea Surface Temperature product (OISST; (Huang et al., 2021a), which has a resolution of 1/4°. This product has been popularly used to track MHWs at global, regional and basin scale all around the globe since the beginning of MHW research. Other studies are using models to investigate MHWs at both surface and subsurface (e.g. Guo et al., 2022; Wang et al., 2022; Pontoppidan et al., 2023), while studies based in in situ data remain scarce due to limited deployment of long-term monitoring equipment (e.g. Cook et al., 2022; Magel et al., 2022; Mazzini and Pianca, 2022).

Although MHWs in the open ocean have been well-documented, their occurrence and dynamics within coastal environments remain poorly understood. While global low and high-resolution sea surface temperature (SST) datasets derived from satellites have been used in coastal MHW research (e.g. Marin et al., 2021; Dabulevičienė and Servaitė, 2024; Xie et al., 2024), they might be suboptimal for highly complex areas such as semi or fully-enclosed seas, or seas that comport a lot of channels, gulfs, islands or fjords.

Indeed, although fjords are present in regions of the world where MHWs have been investigated, such as New Zealand (Shi et al., 2020), Norway (Bayoumy et al., 2022; Jordà-Molina et al., 2023), Canada (Jackson et al., 2018; Khangaonkar et al., 2021), Chile (Pujol et al., 2022) or the Kerguelen Islands (Su et al., 2021a), very few studies have been conducted to understand how MHWs interact with fjords. It is largely due to the observational challenges these regions present, particularly for satellites which are compromised by land interferences and typically rainy and/or cloudy climate

associated with fjords, which results in data loss. Nevertheless, a few studies have been conducted on MHWs in fjords using satellite data and models (Khangaonkar et al., 2021) and in situ data (Aksnes et al., 2019; Jackson et al., 2018, 2021; Jordà-Molina et al., 2023), providing insights on how fjord characteristics influence MHWs' dynamics. While precise data are unavailable, fjords ecosystems contribute significantly to the global aquaculture production, particularly Norwegian and Chilean fjord systems. MHWs could directly impact this production through thermal stress, and by favouring the development of fish-killing algae, or by increasing oxygen depletion (Díaz et al., 2023b).

In this study, we are focusing on the Northern Patagonian Fjords, in southern Chile (Fig. 18). This region is particularly narrow, averaging about 50 km wide, and characterised by the presence of fjords, numerous islands and intricate channels, restricting the water exchanges with the Pacific Ocean and shielding the Inner Sea. Actually, most of the fjords and channels have a wide inferior to 5 km. This complex geography presents considerable challenges for observation and analysis. Standard satellite products and global models, often limited by coarse spatial resolution, typically fail to resolve fjords ands channels, and cannot capture the finer scale processes occurring in the most confined areas. Although high-resolution satellite products do resolve most the fjords and channels, their temporal coverage and temporal resolution is not sufficient to calculate a long-term baseline, which should be based on at least 30 years data according to Hobday et al. (2016) and WMO (2023). In addition, the region is particularly cloudy and rainy, further limiting the availability of remote sensing data.

We propose a novel method for detecting MHWs and MCSs in coastal areas with complex features, which, to our knowledge, has never been used before, consisting in combining in situ and satellite data. We used in situ data to build a climatology with a daily temporal resolution and satellite data to set thresholds and provide daily SST. This approach allows the detection of MHWs with a resolution of 0.008° (~900m), effectively capturing all the fjords and narrow channels of Northern Patagonia. Finally, we described the MHWs and MCSs characteristics and trends observed for the period 2003-2023 and examined case studies using the method described in the following section.

3.2. Material and Method

3.2.1. Study area

The Northern Patagonian Fjords is located in the south of Chile and represents the northernmost part of Chilean Patagonia (41°-56° S). It spans from 41.4° S to 46.7°S and from 72°W to 74°W (Fig. 18). It is delimited to the east by the continent, to the north-west by the Island of Chiloé, and to the south-west by the Chonos Archipelago composed of more than a thousand islands and playing a crucial role in reducing the wind stress and mitigating the waves intensity before they reach the mainland (Pinilla et al., 2019). To the west of the sea, the continental shelf drops sharply, with depths increasing rapidly to over 2000 m due to the presence of the Peru-Chile Trench. The Northern Patagonian Fjords encompasses diverse basins, channels and fjords. From north to south, the key areas include the large semi-enclosed gulf Reloncaví Sound and the Reloncaví Fjord, which flows into the sound. To the south of Reloncaví Sound, lies the Ancud Gulf and the Corcovado Gulf, separated by the Desertores Islands, forming a natural barrier separating the deeper waters of the Reloncaví Sound and Ancud Gulf from the shallower Corcovado Gulf. Ancud and Corcovado Gulf are regions more influenced by oceanic waters entering through the Guafo
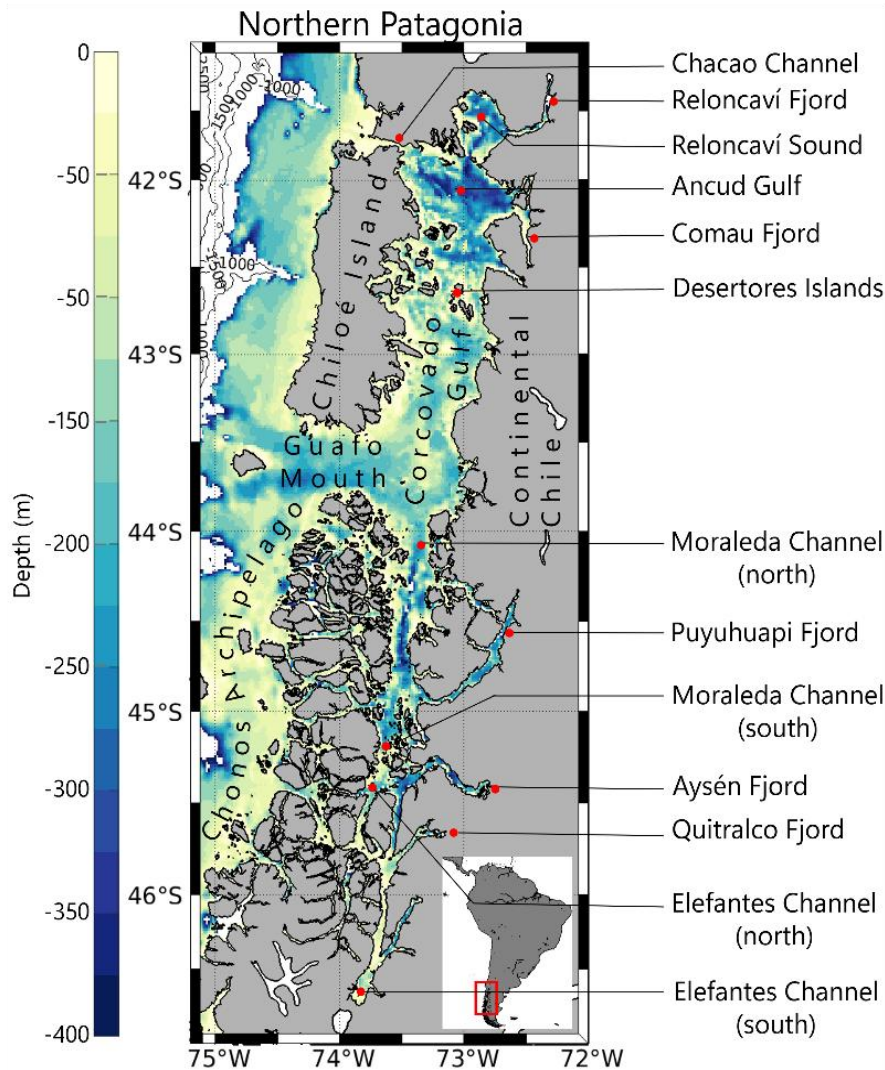
Figure 18: Map of the study area with depth. The level lines are indicating the depth every 500m.

Mouth (Calvete and Sobarzo, 2011; Pérez-Santos et al., 2014; Linford et al., 2023), with some fjords extending eastward into the continent. South of the Corcovado Gulf, lies the narrow canal of Moraleda, which transitions into the Elefantes Channel, forming an extensive and complex network of channels and fjords (Soto-Riquelme et al., 2023; Linford et al., 2024). The bathymetry in the Northern Patagonian Fjords is very complex due to its numerous microbasins and islands. Although the bathymetry is mainly lower than 400m, certain microbasins can be exceptionally deep, reaching for example the Jacaf channel with 600m depth (Schneider et al., 2014; Pinilla et al., 2020).

3.2.2. Construction of the climatology

MHWs and MCSs detection requires a long-term temperature climatology, typically based on at least 30 years of data, to compare with daily local SST (Hobday et al., 2016). This climatology is generally derived from long-term satellite data, with the NOAA OISST dataset (Huang et al., 2021a) being the most commonly used (e.g. Hobday et al., 2016; Frölicher et al., 2018; Holbrook et al., 2019). However, long-term global satellite products often have a coarse resolution; for instance, the OISST product has a resolution of 1/4°. Unfortunately, the Northern Patagonian is not suitable for

49

the use of long-term satellite data: it is a quite narrow sea of fifty kilometres wide on average, composed of various fjords and channels that cannot be adequately resolved by satellite data with a resolution of 1/4°. In addition, the weather in the study area is often rainy and cloudy (Garreaud and Aceituno, 2007), obscuring the view of the satellite sensors. Consequently, satellite data is not the preferred choice for this region. Fortunately, the Northern Patagonian has been extensively sampled over the last decades, resulting in a multitude of in situ data, totalling more than 3 million observations across all depths from 5880 unique sampling stations. We therefore decided to take benefits from the amount of in situ data to build the climatology.

To construct the climatology, we gathered all available in situ data to have the largest dataset possible. The data come from various online platforms and direct in situ measurements (see Annexes for details and DOIs of the in situ data). Only samples within the study area (-75.1°E, -72.0°E and -41.4°N, -46.7°N) were retained, encompassing both surface and depth. The entire dataset spans the period from 1948 to September 2022, although spatial and temporal coverage are sparse (Fig. 19A-C). Vertically, they range from surface to 400 m, but 70% of the total amount of observations is present within the first 25 m (Fig. 19D).

Data selection involves using only valid flagged data when such indicators were available, and excluding "obviously" wrong data (such as temperatures superior to 30°C). Duplicates were eliminated if they met the following conditions: they were horizontally separated by less than 0.01° (about 1km), by less than 10 cm depth, sampled with no more than one day apart (considering that a significant part of the samples have a daily-precision and not a hourly one), and had a temperature differing by no more than +/- 0.1°C. In total, 3.3 million data samples were used for the climatology construction, representing 5880 unique stations (Fig. 19). Given that the climatology forms the core of our analysis, it was essential to use a reliable and representative dataset. The extensive spatial and temporal distribution of in situ measurements makes them well-suited for this purpose.

Due to the sparse and discrete nature of the in situ data, it was necessary to interpolate these observations to create a continuous field. For this purpose, we employed DIVAnd (Data-Interpolating Variational Analysis in n dimensions), spatio-temporal interpolation tool for geophysical variables that utilises scattered, spatially and temporally irregularly distributed data to create a continuous field via variational interpolation, taking the bathymetry into account (Troupin et al., 2010; Barth et al., 2014). This tool is particularly well-suited for our study area since it can handle both spatial and temporal dimensions, allowing for the interpolation of data across 2D (longitude x latitude), 3D (time or depth) or 4D (time and depth). The input to provide is a field of potentially irregularly distributed data with associated coordinates (longitude and latitude) and date, and adjust specific parameters such as the expected error variance of the data, the resolution of the final grid or the smoothness of the interpolation. The variable to interpolate in this study was the temperature, with the objective to build a 4D climatology.

To generate a fine-scale spatio-temporal climatology from in situ surface and subsurface data, we first calculated a background with seasonal temporal resolution by grouping the months into standard seasons (January-February-March, April-May-June, July-August-September, October-November-December). For each season, only the in situ observations corresponding to the relevant months were used. This approach addresses the lack of in situ data in some areas of the sea and the absence of samplings during certain periods, and produces a representative average seasonal state of the temperature that captures the main patterns of variability at the seasonal scale. The final product is an average representation of the study area with a seasonal temporal resolution.
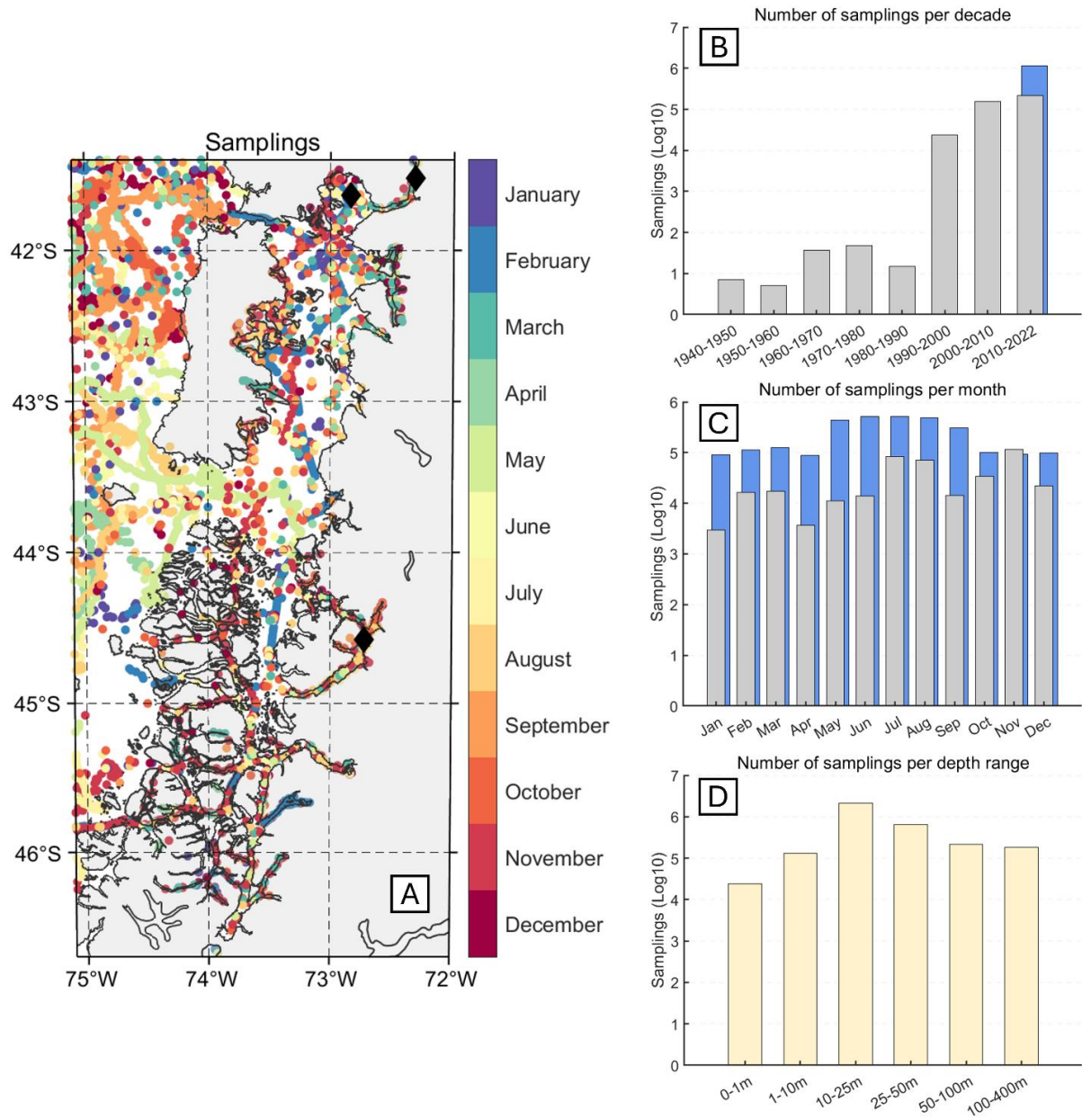
Figure 19: Spatial distribution of the in situ observations (0-400m depth), and the month during which it has been collected (A). The three black rhombus in Reloncaví Sound, Reloncaví Fjord and Puyuhuapi Fjord represent the localisation of the three moorings. Temporal distribution (B-C) of the in situ observation over decades (B) and over months (C). Vertical distribution (D) over certain depth ranges is shown. For (B) and (C), grey bars represent the non-mooring data, while blue bars represent the mooring data, and for (D) both mooring and non-mooring data are merged.

Then, a monthly climatology was performed by refining the seasonal field. For each month, the corresponding seasonal grid was used as a background field, and added all available in situ data for the specific month to increase spatial and temporal variability. This two-steps approach ensured that the monthly climatology remains physically consistent with the larger seasonal patterns while capturing the finer monthly variability. The outcome of this step is a set of twelve monthly climatology fields (monthly temporal resolution), each providing a mean state for every pixel of the study area. For both seasonal background and monthly climatology, vertical and horizontal resolution are the same, and data processing is equal.

To calculate both seasonal background and monthly climatology with DIVAnd, bathymetry data was sourced from the GEBCO dataset with a resolution of 30 seconds (https://www.gebco.net/data_and_products/gridded_bathymetry_data/). Temperature was interpolated over 32 different depth levels, irregularly distributed from the surface to a depth of 400m, with higher resolution at the surface (0m, 2.5m, 5m, 7.5m, 10m, 12.5m, 15m, 17.5m, 20m, 25m, 30m, 35m, 40m, 45m, 50m, 60m, 70m, 80m, 90m, 100m, 125m, 150m, 175m, 200m, 225m, 250m, 275m, 300m, 325m, 350m, 375m, 400m). The DIVAnd weight function was performed to reduce the influence of clustered data during the interpolation, with 0.1° (~10km) set as the threshold for identifying the clustered data. The interpolation smoothness was calibrated using a correlation length, defining the distance over which observations influence the interpolation, of 50 km horizontally and 50 m vertically and by setting an error variance of the observations that represents the level of confidence in the data multiplied by the weight attributed previously. The parameters were chosen to optimise metrics calculated for the validation of the climatology. The final grid resolution was set at 0.008°, which corresponds approximately to 900m, covering the Northern Patagonian Fjords from -75,1°E to -72°E and -47°N to -41°N.

To validate the monthly climatology, 5% of the data was put aside from the reconstruction process (see Table Sup. 1 for details on the in situ data used for validation). This data was subsequently used to conduct statistical tests and calculate different metrics comparing the monthly climatology to the data kept apart, including the correlation, the bias, the root mean square error (RMS), the centred root mean squared error (CRMS), and the standard deviation. The DIVA interpolation results in a monthly climatology at 32 different depths with a resolution of approximately 900 m, effectively resolving all fjords and channels from the northern Patagonia.

MHW detection requires a climatology at a daily time resolution, to compare with daily temperature data in order to follow on a daily-basis the evolution of the MHW. To convert this monthly climatology into a climatology with a daily time scale resolution, each monthly field was expanded over the corresponding number of days for each month (for instance, the January values were repeated 31 times, February 29 times, March 31 times, etc.) This produces a continuous sequence of 366 daily values for each grid point. Finally, to smooth the resulting daily time series, and to ensure a realistic and gradual transition between months, a 90-day moving average was applied. This temporal filter reduces abrupt changes at the boundaries between months and provides a smoothed daily-derived climatology, yielding one representative value per day of the year. This methodology provides a consistent and realistic daily-derived climatological dataset, which can be used for comparison with daily temperature products. This climatology will be later in the manuscript referred as "daily-derived climatology".

3.2.3. Calculation of the thresholds

Thresholds for MHW (MCS) detection are based on the 90th (10th) percentile of the same temperature dataset used to construct the climatology (Hobday et al., 2016). However, we did not use satellite data for the climatology but relied instead on in situ data. While being adequate for constructing the climatology, the inhomogeneity of in situ data in space and time, and their limited availability in some places limits their direct use for threshold calculations. Some areas have been sparsely sampled or remain unsampled during some months of the year, making the determination of the 90th (10th) percentile from such sparse data meaningless.

The use of a zonal threshold based on in situ data was considered, i.e. pooling all the in situ data in one specific basin or fjord to define a single threshold for that area. However, this approach

would have resulted in an insufficiently detailed representation of the dynamics of the sea.

Hence, we opted for satellite data for the surface threshold determination. Specifically, we used MODIS AQUA, providing sea surface temperature data (SST) with a daily temporal resolution from 2003 to June 2023 and a spatial resolution of 4 km, over the area -100°E to -70°E and -29°N to -55°N (https://podaac.jpl.nasa.gov/dataset/MODIS_AQUA_L3_SST_MID-IR_8DAY_4KM_NIGHTTIME_V2019.0#; NASA OBPG, 2020). However, this dataset is a level 3 product (L3) and contains gaps due to cloud cover, which is suboptimal for MHWs (MCSs) detection because it limits or prevents their tracking and their estimation of their spatial and temporal extensions which are criterions for their identification. Consequently, it was necessary to reconstruct the dataset to produce a gap-free field.

For this purpose, we used the interpolation tool DINEOF (Data INterpolating Empirical Orthogonal Functions) DINEOF aims to reconstruct spatial datasets by calculating empirical orthogonal functions (EOFs) to identify the dataset's main patterns of variability. DINEOF is particularly relevant for satellite geophysical datasets that contain gaps due to cloud cover or precipitation (Alvera-Azcárate et al., 2005, 2011). To fill-in the missing data, DINEOF first removes a spatial and temporal mean from the original dataset, with missing data initially set to zero. Then, a first EOF decomposition is performed and the missing values are replaced with those estimated through the EOF decomposition. Some randomly chosen data is set aside and not used for the reconstruction to simultaneously calculate a cross-validation error. Then, the EOF decomposition and error calculation are repeated with 2 EOFs, then 3 EOFs, and so on, and the final number of EOFs retained corresponds to the minimal error obtained by the cross-validation. To optimise computation and avoid errors associated with handling large files, we applied DINEOF to the MODIS temperature dataset on a year-by-year basis. To address the limitations of DINEOF when applied over extended time periods (notably the fact that it tends to emphasize the persistent large-scale patterns such as annual cycles), we implemented the method separately for each year. This year-by-year approach allows to adapt the number of optimal EOFs to the specific spatio-temporal characteristics of each individual year, improving the reconstruction of the dominant patterns of variability, and better capture interannual variability (Alvera-Azcárate et al., 2021).
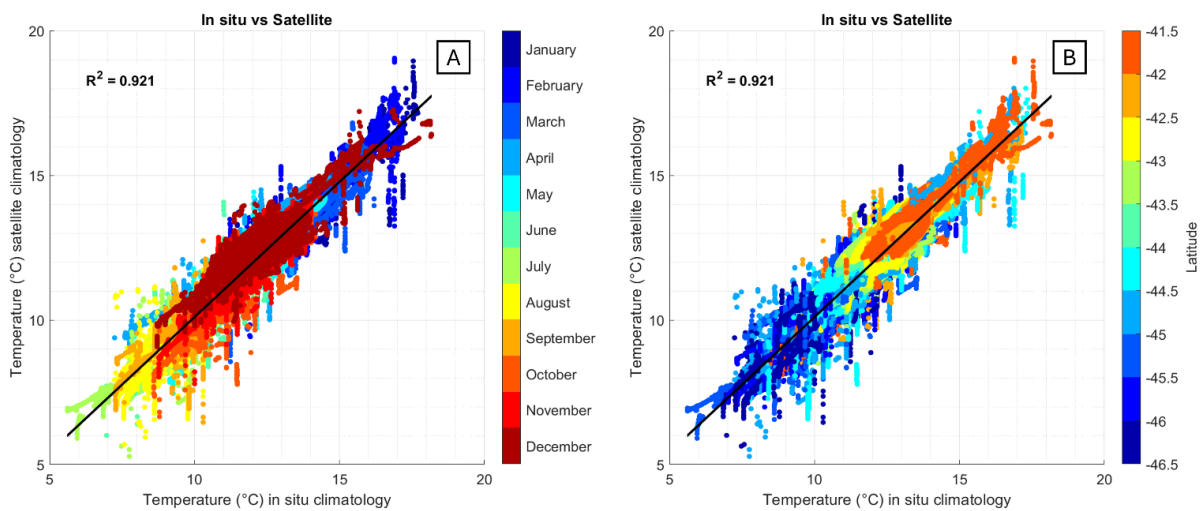
Figure 20: Comparison of the temperature given by the monthly in situ-based climatology (x-axis) and the monthly satellite-based climatology (y-axis), with associated linear regression and R^2. Colours stand for the month during which the observations have been sampled (A) and for the latitude corresponding to the observation (B).

After reconstructing the MODIS dataset, a horizontal bilinear interpolation was performed to match the spatial resolution and grid of the DIVA climatology. Once the satellite dataset was adapted (gap-filled and interpolated to match DIVA climatology's grid), monthly averages were calculated to match the monthly climatology, and we extracted the 10th and 90th percentiles. As for the climatology calculation, a 90-day moving average was applied to ensure a smooth threshold. This process resulted in a daily threshold for each pixel of the study area, which could not have been feasible using only in situ data. The same dataset was used as daily SST for MHWs and MCSs detection.

To compare satellite data with the in situ climatology, we calculated the bias between the two datasets. Specifically, we calculated the difference between the monthly in situ climatology and the monthly satellite-derived threshold. This monthly difference was smoothed using a 90-days moving average to produce a daily bias correction, which was subtracted from the daily satellite dataset. Figure 20A shows a comparison between the monthly in situ-based climatology and the monthly satellite-based climatology before bias calculation, along with the corresponding linear regression. The strong agreement between the tow datasets demonstrates their overall coherence. Additional analyses (Fig. 20B), using longitudinal and latitudinal gradients instead of month as the third dimension, suggest that the satellite climatology captures greater variability in fjords and channels than in the in situ climatology, particularly in Chonos Archipelago, likely due to land contamination effects in coastal regions.

3.2.4. MHWs and MCSs detection

The detection of MHWs and MCSs is based on the comparison between daily-derived climatology and daily temperature exceeding a threshold derived from the climatology (Hobday et al., 2016). Here, the climatology was calculated using in situ data, while the threshold and daily temperature were derived from satellite dataset, as explained in the previous section. The threshold corresponds respectively to the 90th and 10th percentile for MHWs and MCSs. Satellite and in situ datasets are not merged but rather used in a complementary manner. The daily-derived climatology is derived from over 30 years of in situ data to ensure spatial accuracy and long-term reliability in the complex study area, while satellite data, with its consistent daily coverage, is employed to determine the threshold for MHW detection. This methodology thereby combines a robust baseline with high temporal resolution for effective event detection. Additionally, MHWs and MCSs were categorised following the definition of Hobday et al. (2018). It implies that category I event is encompassed between 1 and 2 times the difference between the climatology and the threshold, category II is between 2 and 3 times the difference, category III is between 3 and 4 times the difference, and category IV is superior to 4 times the difference. Different metrics were studied: the mean and maximal intensity of the different events (°C), their frequency (event/year), their duration (days), and cumulative intensity which corresponds to the sum of the temperature anomalies accumulated during the event (°C.day). The seasonality of MHWs and MCSs as well as their long-term trends were also analysed.

The SST anomalies were calculating by subtracting from the daily-derived climatology (in situ-based product) the daily SST (de-biased satellite-based product). The SST anomalies is the only dataset that really merges in situ-based climatology and the daily satellite-based SST.

The detection process was realised using the m_mhw Matlab toolbox developed by Zhao and Marin (2019) following the definition of MHWs given by Hobday et al. (2016).

3.2.5. Atmospheric data

To understand regional atmospheric conditions before and during MHW/MCS events, we analysed different atmospheric parameters including the heat fluxes: the surface latent and sensible heat flux (respectively Qe and Qc), the net solar radiation that reaches the Earth surface (Qs), the surface net thermal radiation (Qb) which represents the difference between the downward and upward radiation received and emitted by the Earth's surface. The total net heat flux (Qi) was calculated as the difference between the incoming solar radiation (Qs) and the other parameters (Qb, Qe, Qc). Q_B, Q_E and Q_C are negative when the ocean is losing heat to the atmosphere. In other words, it represents the net solar radiation minus the heat reflected or lost by Earth's surface, following Eq. (1):

$$Qi = Qs + Qb + Qe + Qc$$

Additionally, we examined u and v wind components at 10m, atmospheric temperature at 2m, surface pressure, low and total cloud cover, total precipitation and evaporation. Those parameters were taken from ERA5 reanalysis data provided by the European Centre for Medium-Range Weather Forecast (ECMWF, Hersbach et al., 2023), available at https://cds.climate.copernicus.eu/cdsapp#!/dataset/reanalysis-era5-single-levels?tab=form. This data has an hourly resolution and a spatial resolution of 1/4°. Data was downloaded over the region between 30°S to 55°S and 65°W to 90°W, spanning the years 1993 to 2023. Since the ERA dataset has an hourly resolution, a daily average was calculated to match with the daily-derived climatology that also has a daily resolution. The anomaly of every parameter was calculated by subtracting the daily values from a climatology realised with the 30-years data.

3.3. Results and discussion

3.3.1. Validation of the climatology

To validate the monthly climatology, 5% of the total in situ data was set aside and excluded from the reconstruction process (see Methods and Appendix). This reserved data was then used to evaluate the accuracy of the monthly climatology through statistical comparisons. The root mean square error (RMSE) is the lowest during the winter months (May to September), which coincides with the months of lower standard deviation (Table 3). Overall, the RMSE and bias are quite low, while the correlation is notably high, indicating that the monthly climatology is very close to the in situ observations. Since the RMSE is based on the difference between the monthly climatology and instantaneous measurements, it also includes the sub-seasonal variability and interannual variability. Even a perfect climatology derived from an unlimited number of observations would not achieve zero RMS error and a perfect correlation of one. January and April exhibit the lowest correlations, which aligns with these months having the least available data. On average, 485 samples (not coming from moorings) are available per month, however, for January and April, only 99 and 161 are available respectively. The comparison between in situ data and in-situ data based monthly climatology shows a greater variability in summer than in winter, consistent with a larger standard deviation in summer than in winter as shown in Table 3. The climatology is available on https://doi.org/10.5281/zenodo.14845077.

Table 3: Statistic metrics for the validation of the monthly climatology at the surface level only (between 0 and 1m) for every month: Correlation, Bias (°C), Root mean square error (RMSE, °C), Centred root mean square error (CRMS, °C), the average Standard deviation (SD, °C) across the entire study area for the climatology, the average Standard deviation (°C) across the entire study area for the entire in situ dataset.

Month	Correlation	Bias (°C)	RMSE (°C)	CRMS (°C)	SD climatology	SD in situ data
Jan	0,159	0,214	1,847	1,834	1,160	1,974
Feb	0,709	0,039	1,433	1,433	1,274	2,054
Mar	0,320	0,112	1,141	1,135	1,019	1,685
Apr	0,171	-0,068	1,006	1,004	0,910	0,830
May	0,558	-0,082	0,783	0,779	0,937	0,774
Jun	0,810	-0,083	0,709	0,705	1,002	0,458
Jul	0,806	0,062	0,872	0,870	0,811	0,594
Aug	0,821	-0,139	0,707	0,693	0,536	0,580
Sep	0,748	0,010	0,731	0,731	0,608	0,511
Oct	0,396	0,202	0,952	0,930	0,672	0,817
Nov	0,410	0,086	1,232	1,229	0,738	1,234
Dec	0,446	0,105	1,421	1,417	1,081	2,184

3.3.2. Climatology

By processing the in situ data with DIVA, we produced a monthly climatology at 32 different depths from the surface to 400m (Fig. 21, 22, 23). Full results are presented in the Annexes. At the surface (Fig. 21), summer months (Jan-Feb-Mar) are characterised by a strong west-east gradient in the open Pacific and another strong gradient in the Northern Patagonia, in Reloncaví Sound and Ancud Gulf. The other parts of the study area record temperatures between 12°C and 14°C, with maximums in February of about 18°C in Puyuhuapi Fjord, 17°C in Reloncaví Sound and Fjord, 16°C in Comau Fjord, (also observed by Castillo et al., 2016; León-Muñoz et al., 2013; Saldías et al., 2021; Linford et al., 2024) and in the north-western part of the domain, in the open Pacific. Although located only 50 km south of Puyuhuapi Fjord, Aysén Fjord only reaches 13°C in February, linked to a higher input of freshwater from the Andean melting in Aysén than in Puyuhuapi Fjord (Calvete and Sobarzo, 2011; Pinilla et al., 2019).

The Chacao Channel and south of Desertores Islands stand out as particularly cold regions, especially in February, also highlighted in the study Narváez et al. (2019). This same study suggested that the differences in temperature amplitudes in the Inner Sea of Chiloé might be linked to different influences of tides, water time residences and winds. During autumn (Apr-May-Jun), the monthly climatology shows a general decline in temperatures, although a gradient persists in the northwest of the domain but much less intense than in summer. In June, a North-
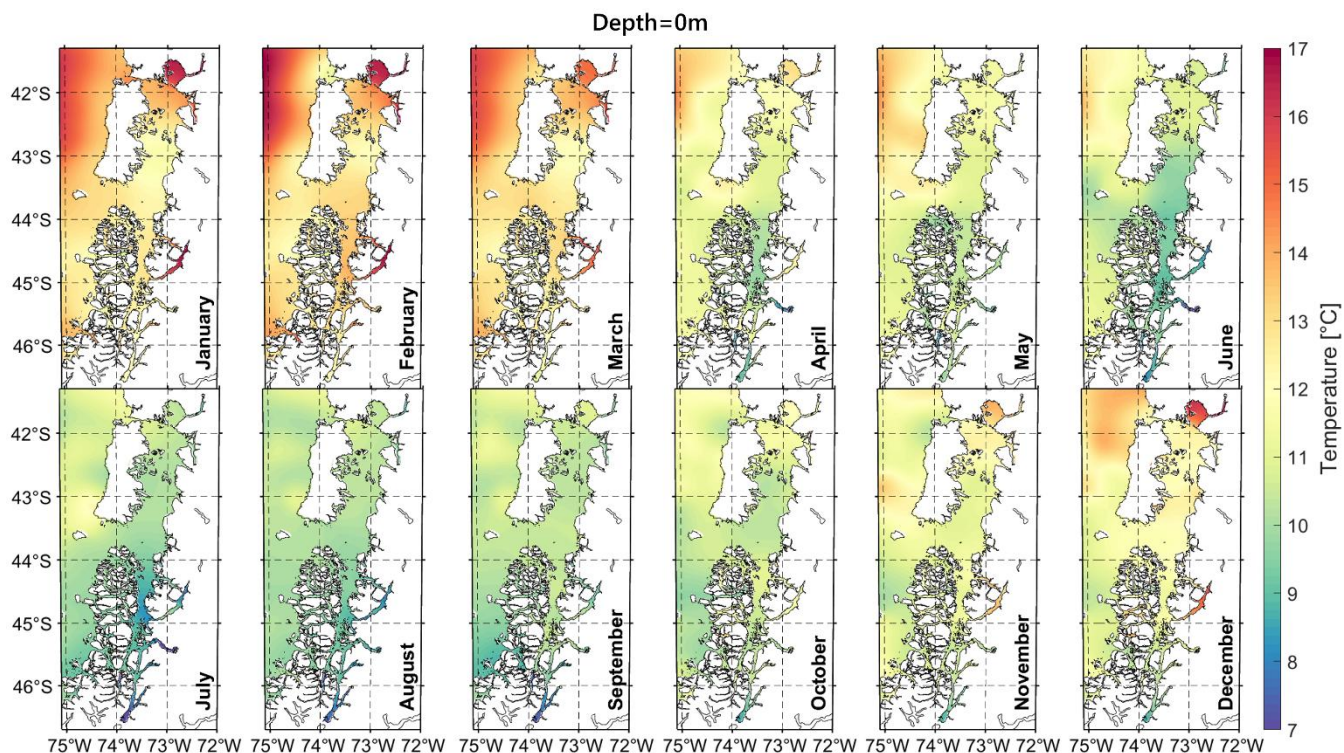
Figure 21: Monthly climatology of the sea temperature at the surface.

South temperature gradient in the study area appears, with values between 10°C and 11°C in Reloncaví Sound and 8°C at the extreme south (Fig. 21; Saldías et al., 2021; Linford et al., 2024). In winter (Jul-Aug-Sep), the surface temperatures are relatively uniform and show little variation. The temperature is the lowest in Elefantes Channel and Aysén Fjord, reaching 7°C, while most areas remain around 10°C. Notable exceptions include the slightly cooler Puyuhuapi Fjord (Pérez-Santos, 2017; Schneider et al., 2014) and a potential warm anomaly southwest of Chiloé in July, possibly due to an anomalously warm measurement and inhomogeneous sampling in time.

The temperature in October is very similar to September, slightly warmer, reaching around 12°C in the north and in Puyuhuapi Fjord. Spring (Oct-Nov-Dec) sees gradual warming, with pre-summer conditions in December: 15°C to 17°C in Puyuhuapi Fjord and Reloncaví Sound, and the progressive development of a gradient in the open ocean. However, relatively cold temperatures are still present in the southern parts of the Northern Patagonia and west of Chonos Archipelagos, with overall temperatures below 11°C, and even dropping to 9°C in Elefantes Channel.

The surface monthly climatology aligns with Saldías et al. (2021), who observed similar seasonal patterns from 2003-2019 satellite data: a strong gradient in summer in both the open ocean and the Northern Patagonian progressively fading away in autumn, a relatively homogeneous pattern in winter between 9°C and 12°C, and warming in spring.

Temperature fluctuations are more pronounced in enclosed areas: Reloncaví Sound varies from 10°C in winter to 17°C in summer, Puyuhuapi Fjord's head has a temperature that falls to 8°C in winter and rises to 18°C in summer, while in its central region it varies between 9°C and 16°C, coherent with Schneider et al. (2014), Pinilla et al. (2020) and Pérez-Santos et al. (2021)'s results. Aysén fjord shows a seasonal range between 6°C and 13°C at its head and between 9°C and 13°C at its mouth. Saldías et al. (2021) also illustrate that the standard deviation of the SST is much higher in enclosed fjords than in the more exposed basins, confirming that our interpolation reflects know physical processes. In contrast, open areas experience slighter variations. Corcovado Gulf varies

57
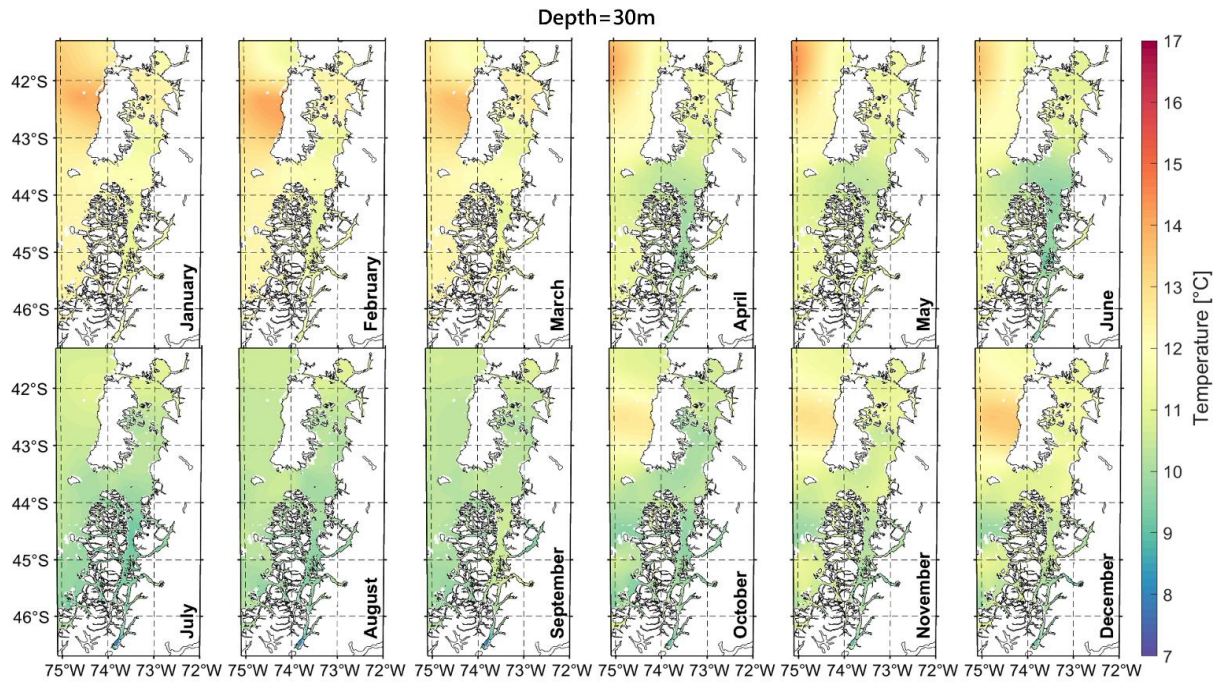
Figure 22: Monthly climatology of the sea temperature at 30m depth.
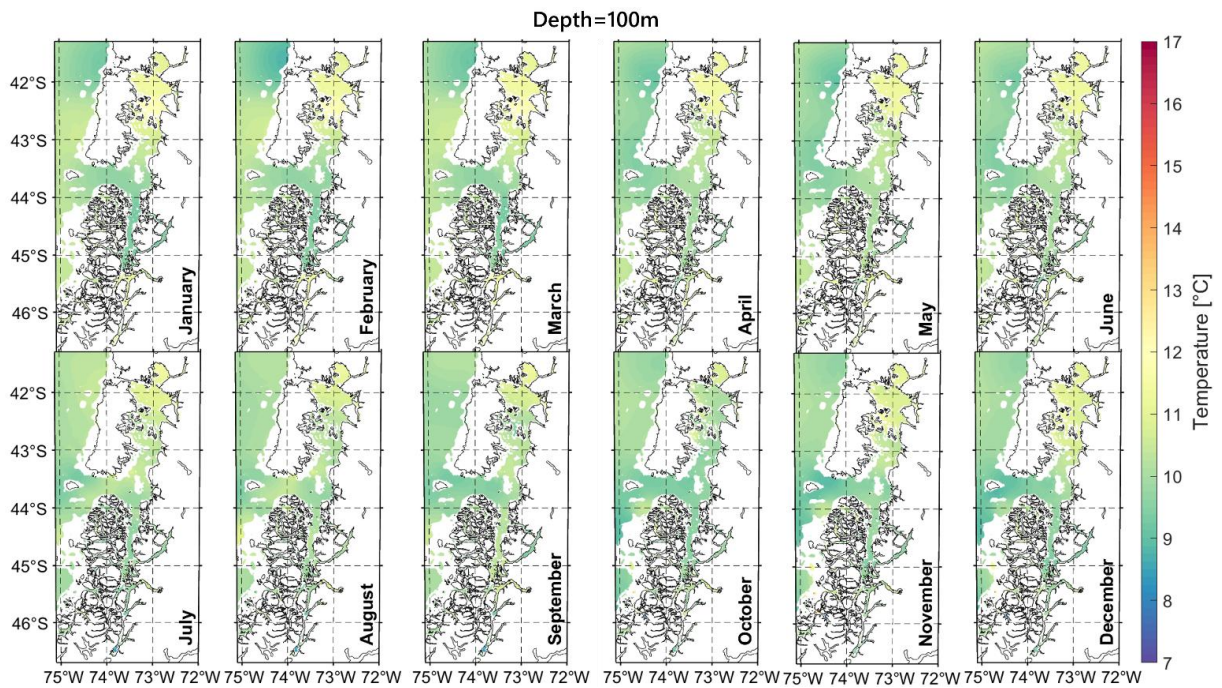
Figure 23: Monthly climatology of the sea temperature at 100m depth.

little throughout the year, ranging from 10ºC in winter to 13ºC in summer, as also reported by Buchan et al. (2021), Moraleda Channel vary from 9ºC in winter to 13ºC in summer, while Ancud Gulf varies from 11ºC to 14ºC. An exception is the open Pacific west of Chiloé, where temperatures vary significantly from 10ºC to 17ºC. However, west of Chonos Archipelago, variations are more modest, between 9ºC and 13ºC. Narváez et al. (2019) suggested that the greater warming in the northern half of the Northern Patagonia could be due to the Desertores Islands, which reduce winds and current velocities, allowing a greater warming of the sea surface.

Below the surface, the temperature decreases as expected and spatial temperature gradients are

smoother, particularly in summer. For instance, at 30m depth, temperatures are almost homogeneous in winter (as observed in Pérez-Santos et al., 2021), while in summer they vary from 14°C west of Chiloé Island to 10°C in the southern part of the study area (Fig. 22).

When reaching 100m depth (Fig. 23), temperature patterns remain consistent year-round, at round 10°C, aligning with Pinilla et al. (2021). Ancud Gulf, Reloncaví Sound and their associated fjords remain, slightly warmer with temperatures of 11°C in winter and 12°C in summer. At 200 meters depth, all year long, the temperature remains warmer in Ancud Gulf and Reloncaví Sound (10 to 11°C) than elsewhere (8 to 9°C), likely due to the Desertores Islands acting like a barrier, trapping warmer waters to the north (Pérez-Santos et al., 2021; Linford et al., 2024). At 400m depth, temperatures stabilise around 7°C in the entire study area and all year long, except in Aysén Fjord, where they fluctuate between 10°C (July to December) and 8.5°C (January-June). This particularity, consistent with the in situ samples that have been conducted over different years, maybe linked to Aysén Fjord's long water residency time (120 days, Linford et al., 2024) inducing slower temperature changes.
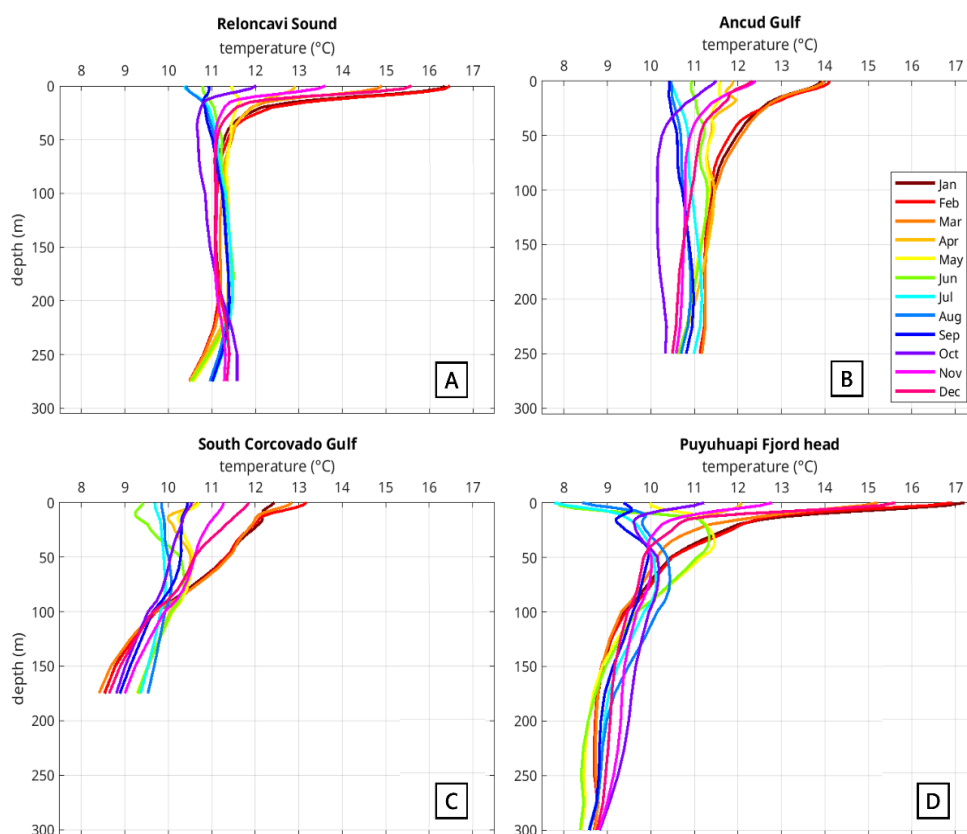
Figure 24: Profile plots of the monthly climatology in different basins of the study area: A: Reloncaví Sound, B: Ancud Gulf, C: South of the Corcovado Gulf, D: the head of Puyuhuapi Fjord. Each colour represents the monthly climatology for a specific month of the year. The profile terminates according to the local bathymetry.

In most basins, the thermocline typically lies between surface and 20 meters, strengthening in summer, as observed for instance in the Reloncaví Sound (Fig. 24A). However, the thermocline can extend deeper (up to 50m) as seen for instance west of Chiloé Island during summer, or in Aysén and Puyuhuapi Fjords (Fig. 24D). In Guafo Mouth and Corcovado Gulf, the thermocline can extend even further, ranging from 10 to 100m (Fig. 24C), reflecting the region's well-mixed nature (Calvete and Sobarzo, 2011). In winter, the entire water column is homogeneous, particularly

around Chacao Channel, the northern half of Corcovado Gulf, and Ancud Gulf regions (Fig. 24B). The surface mixed layer is shallow in summer, usually under 10m, with strong surface stratification in fjords and enclosed basins (Fig. 24A and D), similar to observations in Finnish (Merkouriadi and Leppäranta, 2015) and Norwegian fjords (Skogseth et al., 2020). In the fjords, the stratification is higher at their heads than at their mouths, as regularly observed in other fjords, such as in south Patagonian fjords (e.g. Maturana-Martínez et al., 2021) or in Arctic fjords (e.g. Szeligowska et al., 2020).

3.3.3. Thresholds

The thresholds for detecting MHWs and MCSs (respectively the 90th and 10th percentile) were calculated using satellite data and by applying a temporal moving average to smooth it (see Methods). This approach ensures a consistent and coherent threshold for every place in the study area.

The results show that for every location, there is a difference of the thresholds' amplitude between summer and winter. While this difference is about a few decimals of a degree in most of the basins, the most pronounced variations are observed in the Reloncaví Sound with a threshold about 1.6°C above (below, for the 10th percentile) the daily-derived climatology in summer and 0.6°C in winter. Similarly, in the Puyuhuapi Fjord, the thresholds are 1.9°C above (below) the daily-derived climatology in summer and 0.8°C in winter. It can be noted that the locations with the highest threshold amplitudes also show the highest seasonal temperature amplitude. For the northern half of the

Figure 25: MODIS-AQUA satellite data (A, C) on the 7th of February 2019, and its reconstruction with DINEOF (B, D) over the entire domain (up) and with a zoom on the Inner Sea of Chiloé (bottom).

domain, the high temperature amplitude has also been shown in Narváez et al. (2019) and Saldías et al. (2021).

3.3.4. DINEOF

To detect MHWs/MCSs, we used daytime L3 level satellite SST data from MODIS AQUA. However, this kind of data contains gaps due to cloud coverage or land contamination. It was therefore necessary to fill these gaps to enable the tracking of MHWs and MCSs. For this purpose, DINEOF
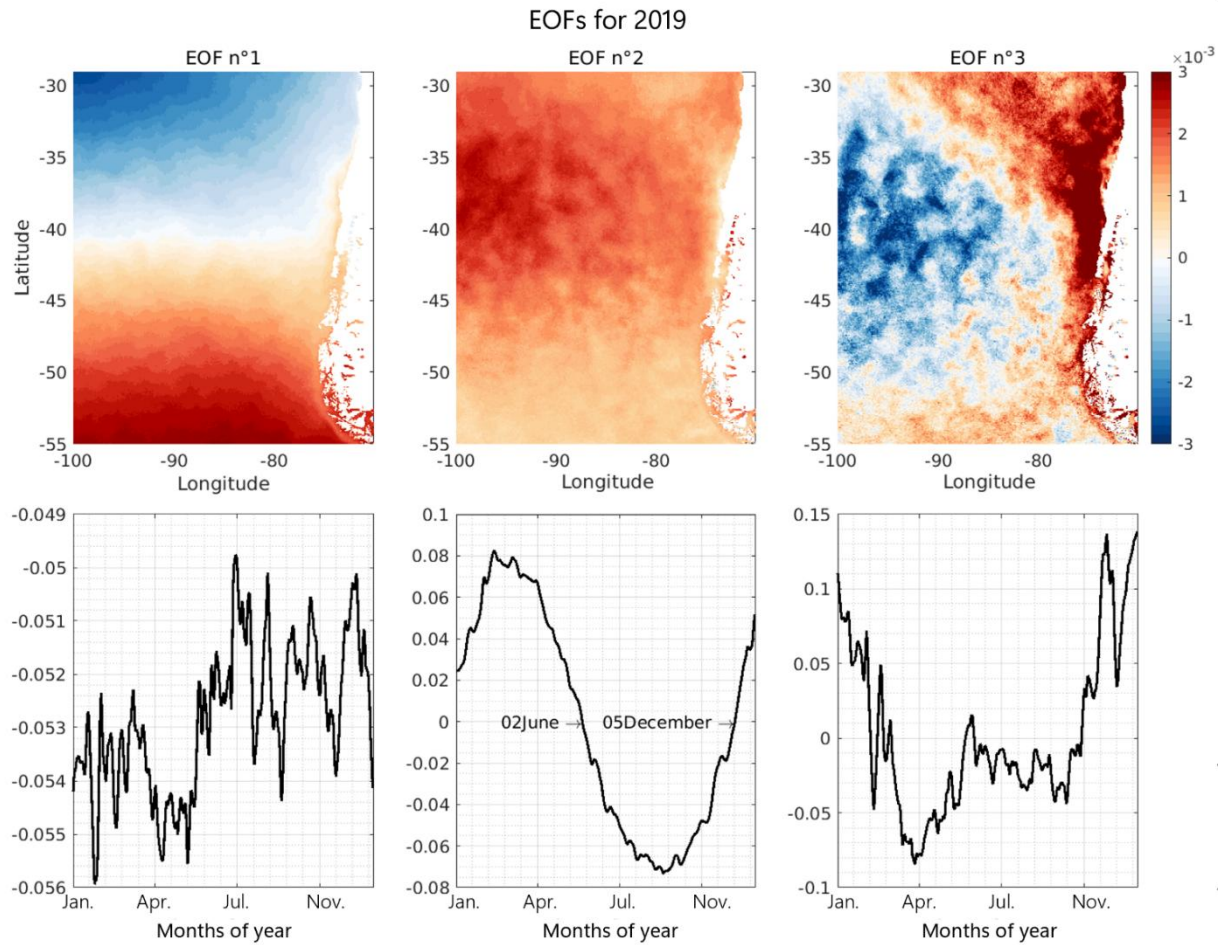
Figure 26: First 3 EOFs for the year 2019. Top: spatial EOF, Bottom: temporal variation. For the second EOF, there is a state switch that happens on the 2nd of June and on the 5th of December.

was applied (see Methods) across a large area, from 29°S to 55°S and -100°W to -70°E. The reconstruction with DINEOF was conducted year by year from 2003 to 2023. Overall, over the entire domain, 78% of the data is missing. An example of the reconstruction is shown in Fig. 25.

DINEOF determines the optimal number of EOFs for each year using cross-validation, with an upper limit of 50 (see Fig. 26 for a typical year). On average, for each individual year from 2003 to 2023, 10 EOFs were selected as optimal. Typically, the first EOF represents 85.1% of the explained variance, the second one 14% and the third one 0.3%. Since we conducted the analysis year by year, we choose here to show the year 2019 which is representative of the other years. The first EOF, representing 84.7% of the explained variance, reveals a north-south gradient at about 40°S, likely due to the different atmospheric systems: a permanent anticyclone system along the coast of North Chile, and a cyclonic-dominated system to the south (Aguirre et al., 2012; Ancapichún and Garcés-Vargas, 2015). The second EOF (15% of the explained variance) shows a uniform pattern that switches state every year between the end of May and the beginning of June and between the end of November and the beginning of December. This EOF is probably associated with seasonal changes. The third EOF (0.3% of the explained variance) exhibits more small-scale variations and changes from year to year. However, a spatial pattern can be observed, with a coastal pattern present almost every year and an oceanic patch dissociated from the coastal pattern. No more than 3 EOFs were described as they represent for every year more than 99.4% of the total variance of the SST. Saldías et al. (2024) calculated salinity EOFs over the last decade, and found very similar patterns as presented in this work: the first one shows a

north-south separation, the second one shows that the entire area varies together, and the third one a east-west separation.

3.3.5. MHWs and MCSs from 2003 to 2023

In this section, we used the daily-derived climatology to detect, track and characterise surface MHWs and MCSs.

MHWs frequency is around 2 events per year in most of the domain: in the southern part of Corcovado Gulf, Guafo Mouth, Moraleda Channel, the west part of Ancud Gulf, Comau Fjord, and outside of the Northern Patagonian in the open ocean (Fig. 27A). Nevertheless, Reloncaví Sound, surroundings of Desertores Islands, Chonos Archipelago and the very south of the study area experience fewer events per year. For MCSs, Ancud Gulf and Reloncaví Sound stand out with an average frequency exceeding 2.5 events per year (Fig. 27E). In the south and west coast of Corcovado Gulf and in Moraleda Channel, the frequency is about 2 to 2.5 events a year, as well as along the west coast of Chiloé Island. Offshore Chiloé and on the west side of Corcovado Gulf, the frequency of MCSs drops below 1.5 events per year. Overall, all areas in the study region experienced at least one MHW or MCS annually. These results are consistent with Pujol et al. (2022), who reported an average of 1.8 MHW events per year from the 1980s to 2020s.

The mean intensity over the last 20 years has varied depending on the basin for both MHWs and MCSs (Fig. 27B, F). The highest MHW intensities can be seen in the most enclosed areas: Reloncaví Sound with a mean intensity of 2°C (with a west-east gradient), in Aysén Fjord with a higher intensity at its head (more than 2°C), and the highest intensity is found in Puyuhuapi Fjord with an average intensity of 2.5°C in its centre. A coastal zone along the western coast of Chiloé, excluding Chacao Channel, is also highlighted. These regions are also the most stratified and show the highest seasonal temperature amplitude, especially during summer months (Fig. 24A, D), and are also the regions showing the highest salinity variations due to large freshwater inputs (Vásquez et al., 2021). In contrast, the lowest intensities are found in the regions of generally low stratification and low thermal amplitude, such as Corcovado Gulf (which has particularly homogeneous water column) and in the Chonos Archipelago, with values below 0.5°C. When looking at the average maximum intensity of MHWs, similar patterns emerge (Fig. 27C): maximum intensities are found in enclosed areas with strong stratification, reaching up to 5°C in Aysén and Puyuhuapi Fjords and 4°C in Reloncaví Sound. Within the fjords, intensity tends to be higher at their heads, where freshwater inputs and stratification are strongest, and gradually decreases toward their mouths, as the stratification and temperature seasonal amplitude diminishes. For instance, at Puyuhuapi's head, the temperature varies from 17°C to 12°C from the surface to 20m depths in summer, whereas in its centre, the temperature varies from 16°C to 12.5°C from surface to 20m depth, explaining that MHW could be more intense at its head than at its mouth (Fig. 24D; Gröger et al., 2024). Similarly, the freshwater layer in fjords is quite thin, ranging from 5 to 15m (Calvete and Sobarzo, 2011). This high stratification facilitated the rapid warming of the upper layer in case of intense solar radiation (Gröger et al., 2024). The lowest maximal intensities, below 2°C, occur in Corcovado Gulf and Chonos Archipelago. When looking at the MCSs (Fig. 27F), the intensity patterns are comparable. Intensities remain relatively mild in the Inner Sea of Chiloé and Chonos Archipelago (above -1°C), and stronger in the Reloncaví Sound (between -1.5°C and -1 °C), Comau, Puyuhuapi and Aysén Fjords (about -1.5°C and reaching -2.5°C at Puyuhuapi's head). The regions experiencing the strongest MCSs are also the regions with the highest temperature amplitude and the highest stratification considering temperature, freshwater inputs and salinity. For the maximum intensity (Fig. 27G), again, a similar

pattern can be observed as for MHWs with a maximum intensity peaking at -5°C in Puyuhuapi Fjord and Reloncaví Sound, while most of the other parts of the study area experience maximum intensities above -2°C. The spatial distribution of MHWs and MCSs intensity well reflects the high spatial variability of the region: stronger in stratified enclosed areas (fjords, Reloncaví and Ancud Gulfs) than in open regions where the water column shows higher mixing such as Corcovado Gulf (Narváez et al., 2019; Saldías et al., 2021; Vásquez et al., 2021).

Regarding duration (Fig. 27D), the area around Desertores Islands is particularly impacted, with average duration of 20 to 25 days. The extreme South of the Inner Sea of Chiloé, the Elefantes channel and some channels of the Western part of Chonos Archipelago, also experience prolonged MHWs. Notably, the northwest of Chiloé Island is similarly affected. In the open-ocean, MHWs typically last over 15 days, whereas shorter durations, under 15 days, are recorded in south Corcovado Gulf, Moraleda Channel, Comau Fjord and Reloncaví Gulf. For the MCSs, a
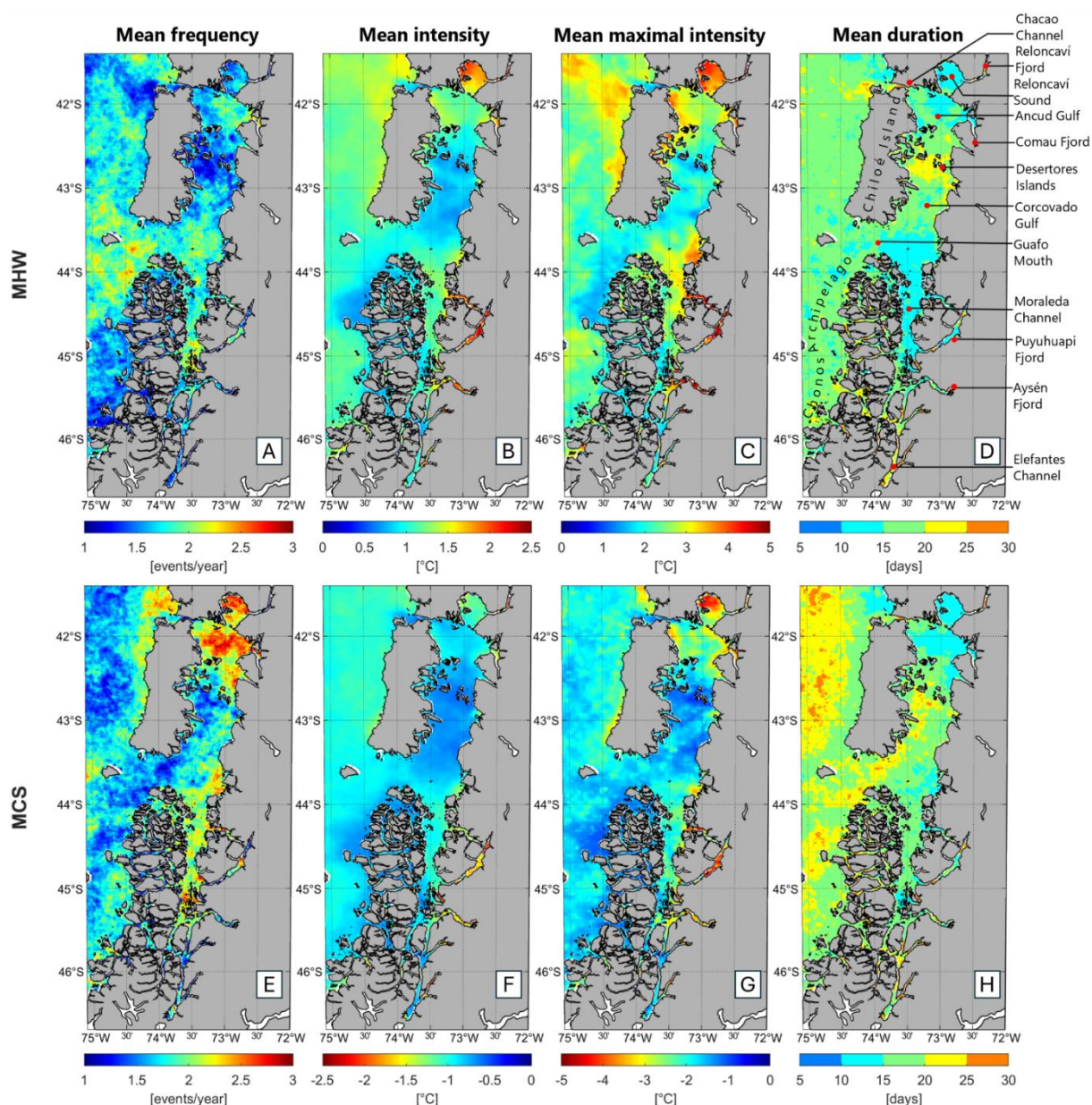
Figure 27: Spatial representation of the average Frequency (A, E), Mean Intensity (B, F), Mean Maximal Intensity (C, G), Duration (D, H) for MHW (top) and MCS (bottom) on the period 2003-2023. Main regions are highlighted in (D).

clear distinction is visible between the open ocean and coastal environments: the average duration reaches 30 days in the open ocean, but decreases to less than 20 days along Chiloé shores (Fig. 27H). Within the Inner Sea of Chiloé, MCS length is generally shorter than 20 days, with the lowest length being in Reloncaví Sound and Ancud Gulf (between 10 and 15 days). However, along Chiloé's east coast, from Desertores Islands to further south, MCS lengths are significantly higher, averaging around 25 days. That pattern matches the overall circulation inside of the sea, with surface waters entering by the Boca del Guafo and following along the East coast of Chiloé up to Desertores Islands (Linford et al., 2023, 2024). On the other hand, upwelling intensification in the adjacent oceanic water to the west coast of Chiloé and Guafo Mouth could contribute to the MCS's duration (Aguirre et al., 2019; Narváez et al., 2019; Pérez-Santos et al., 2019).

Examining cumulative intensity (not shown), the Inner Sea of Chiloé and the southern part of the study area record relatively low averages, below 20°C.day, except for Puyuhuapi Fjord which reaches up to 50°C.day. West of Chiloé, cumulative intensities are slightly higher, ranging between 20 and 30°C.day. For MCSs, a similar pattern is observed, with higher values in the open ocean and Puyuhuapi and Aysén Fjords (-30 to -20°C.day) and lower values in the Inner Sea and Chonos Archipelago (-15 to -10°C.day).
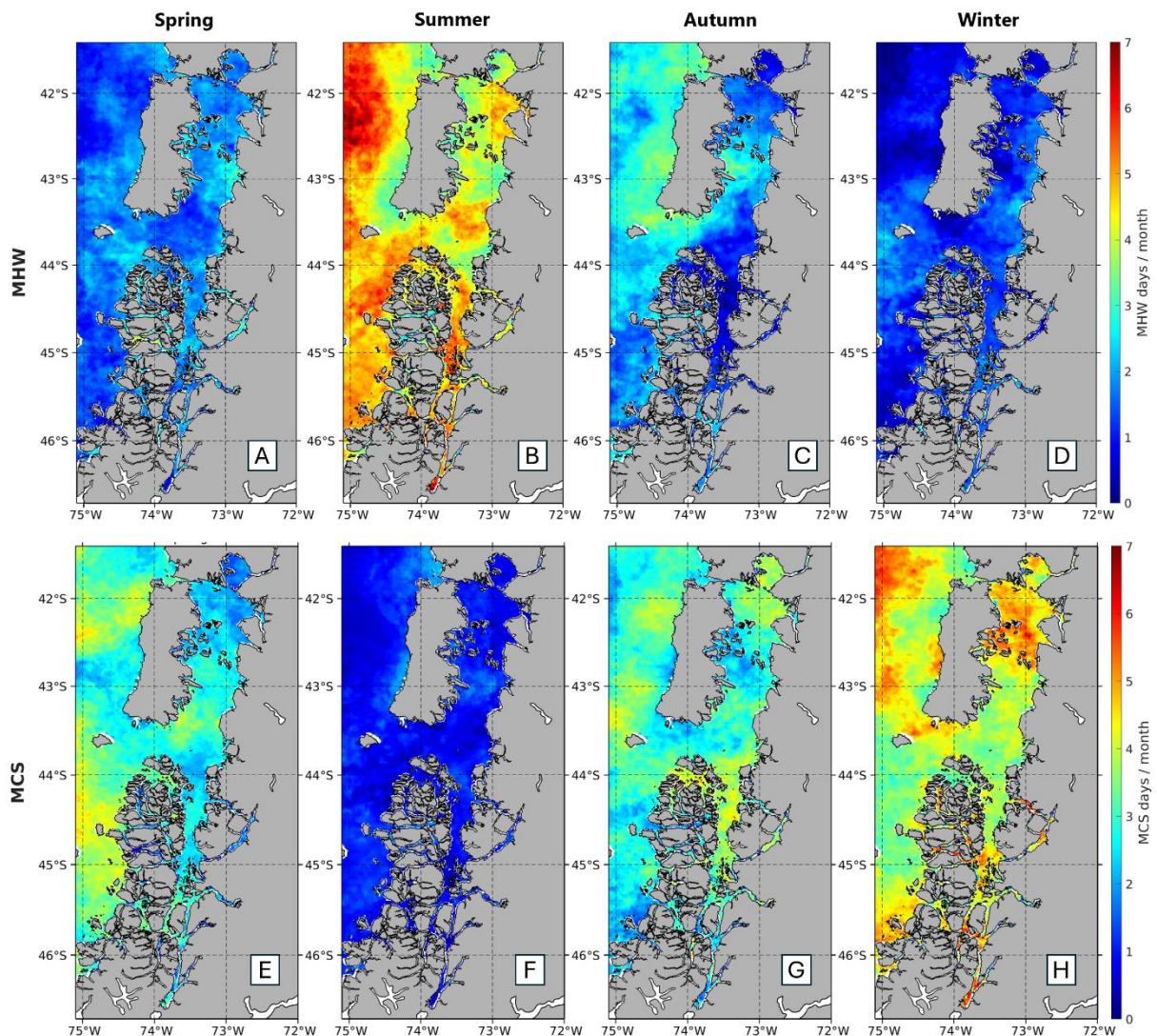
Figure 28: Seasonal occurrence of MHWs (top) and MCSs (bottom): Spring (A, E), Summer (B, F), Autumn (C, G), Winter (D, H). It represents the number of days under MHW/MCS condition per month for each season. Representation for the period 2003-2023.

3.3.6. MHWs and MCSs seasonality

The seasonality of MHWs and MCSs is clearly marked across the study area. Indeed, on average, during summer (2003-2023), there are at least 3 days of MHWs per month, up to 5 days in the East of Ancud and South of Corcovado Gulfs and up to 6 days in Moraleda Channel (Fig. 28B). In the open ocean, occurrences can reach up to 7 days per month. Conversely, almost no MHWs are registered in winter (fewer than 1 day per month; Fig 28D). Spring (Fig 26A) and autumn (Fig. 28C) lie in between, although in autumn MHWs are above all present in the open ocean, up to 4 days per month around Chiloé Island. On the contrary, MCSs are far more frequent during winter (Fig. 28H), with a minimal occurrence of 3 days per month, and up to 6 days per month in Ancud Gulf and the open ocean. In summer, less than 1 event per month is registered (Fig. 28F). However, MCSs tend to occur more often during spring and autumn than MHWs, occurring more frequently outside Northern Patagonia in spring (Fig. 28E) and inside in autumn (Fig. 28G). The preferred occurrence of MHWs in summer and MCSs in winter is well known in literature and follows here what is commonly observed (Schlegel et al., 2021; Wang and Zhou, 2024).
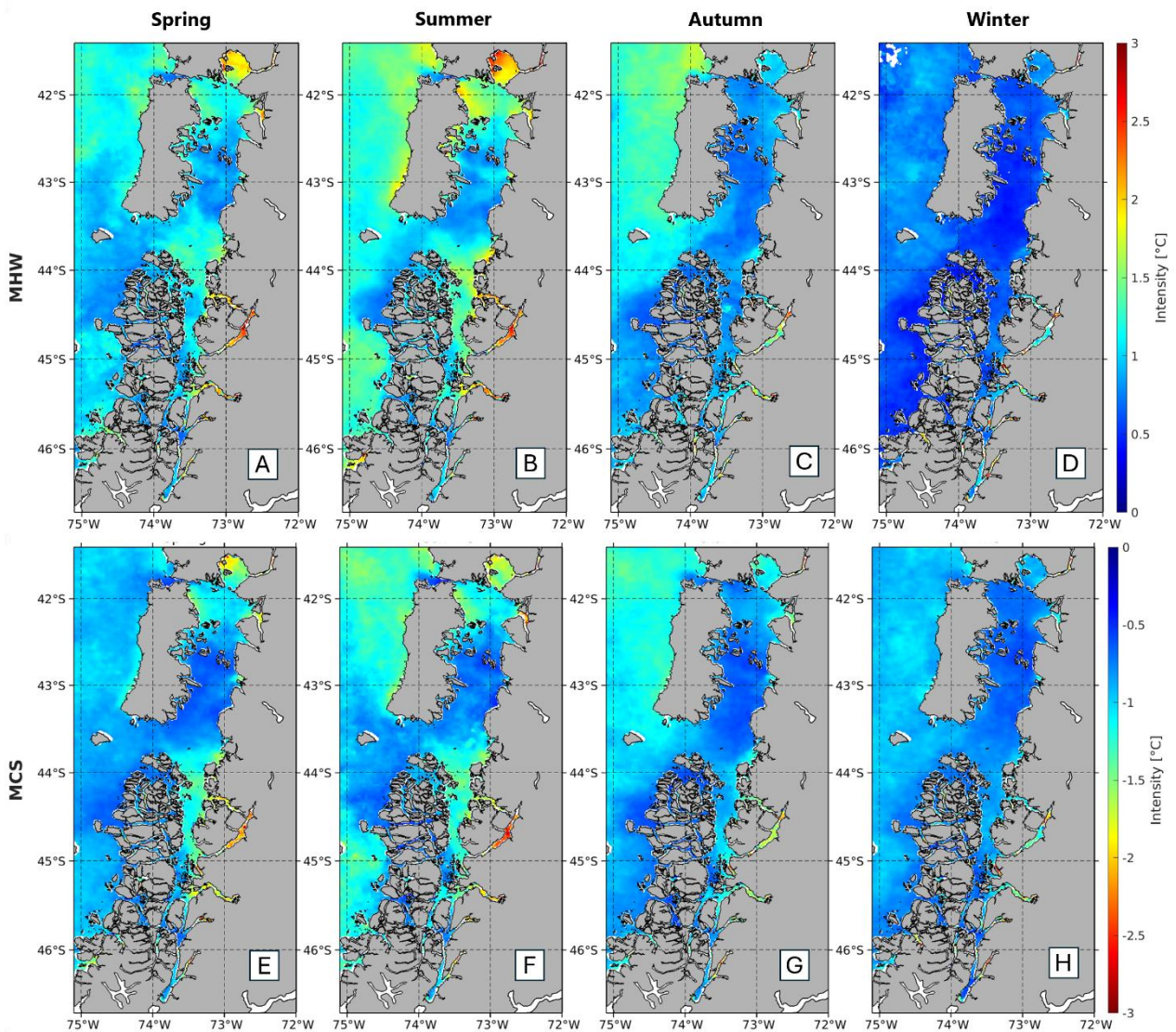
Figure 29: Mean intensity of MHWs (top) and MCSs (bottom) for each season: Spring (A, E), Summer (B, F), Autumn (C, G), Winter (D, H). Representation for the period 2003-2023.

When looking at the seasonal intensity of MHWs and MCSs, the patterns and intensities are remarkably similar. Indeed, in both cases, the least intense events are occurring in winter, with MCSs exhibiting a uniform distribution (Fig. 29H), and MHWs being slightly more intense in the open ocean than in the Northern Patagonian Fjords (Fig. 29D). However, in both cases, the intensity is higher in the fjords, e.g., Puyuhuapi, Aysén, and Comau Fjords. The most intense events occur in summer, with the highest being in Puyuhuapi Fjord for both MHWs and MCS reaching 2,5°C and -2,5°C respectively (Fig. 29B, F). Reloncaví Sound, however, experiences more intense MHWs (up to 2.5°C) than MCSs (nearly -2°C). During spring (Fig. 29A and Fig. 27E), the Ancud Gulf and the southern part of the Inner Sea of Chiloé are more impacted for both MHWs and MCSs, the Puyuhuapi Fjord being again the region with the highest and lowest values (respectively 2,5°C and -2°C). Summer and spring are actually the seasons with the highest stratification, summer due to higher surface temperature (Fig. 21 and Fig. 24) and spring due to higher river discharge (Calvete and Sobarzo, 2011). Enhanced stratification can accelerate under higher solar radiation, particularly in strongly stratified coastal areas as Patagonian Fjords (Gröger et al., 2024). In autumn the fjords remain the regions of highest intensity, along with the open ocean west of Chiloé Island (Fig. 29C, G). The MCS intensity being more intense in summer is quite opposite to what is found in literature. Indeed, MCSs tend to occur more frequently in winter, and are generally less destructive when happening in summer (Schlegel et al., 2021).

3.3.7. MHWs and MCSs trends

Trend for MHW and MCS metrics were calculated over the period 2003-2023.

The trend of MHW frequency is quite heterogeneous, with positive trends in most of the region, except in Corcovado Gulf, Guafo Mouth and along the west side of Chiloé Island (Fig. 30A). In the northernmost part of Northern Patagonia, Reloncaví Sound and Ancud Gulf, the frequency is yearly increasing by 0.1 events per year, a trend also observed in Moraleda Channel, which is coherent with what was found by Pujol et al. (2022). More pronounced increases are observed in Puyuhuapi and Aysén Fjords, with frequency rising by 0.1 to 0.2 events per year. Outside Northern Patagonia, a similar trend is observed with an increase in frequency of approximately 0.1 events per year. In contrast, Corcovado Gulf and the west coast of Chiloé show a negative trend, indicating a decrease in MHW frequency over the years, also observed in Pujol et al. (2022). Looking at the MCSs, the trend is more consistent in Northern Patagonia: it is negative everywhere with a decrease of between 0.1 and 0.2 events per year (Fig. 30E). A similar pattern is observed west of Chonos Archipelago. West of Chiloé Island, the MCSs tend to increase by about 0.1 events per year.

The trends in MHW mean and maximal intensity display similar patterns (Fig. 30B, C). Indeed, the intensity tends to increase in the open ocean west of Chiloé, but not West of Chonos Archipelago and in the southern part of the Inner Sea, from Moraleda Channel to further South, where a decrease is observed. An increasing trend is also evident in Reloncaví Sound, particularly near the mouth and north of Reloncaví Fjord, as well as in the Comau Fjord. Other parts of the study area, i.e. the Ancud and Corcovado Gulfs, Chonos Archipelago and its adjacent waters show a decreasing trend, with the declines observed in the northern Chonos Archipelago and the western Ancud Gulf, at about -0.03°C per year. A distinct demarcation is evident at Guafo Mouth, where a clear separation in trends at its centre. For MCSs, the trends are more uniform: intensity is increasing everywhere across the study area (Fig. 30F, G). This increase is higher inside the Sea of Chiloé, especially in some fjords such as Comau, Aysén and Jacaff Channel, as well at their mouths with maximum intensity rising by 0.06°C per year. Globally, fjords are experiencing

warming sea temperature (Pavlov et al., 2013; Aksnes et al., 2019; Skogseth et al., 2020; Bloshkina et al., 2021) as well as Northern Patagonia especially during the last decade (Pujol et al., 2022). Those elements are coherent with an increase in the intensity of MHWs in our study area.
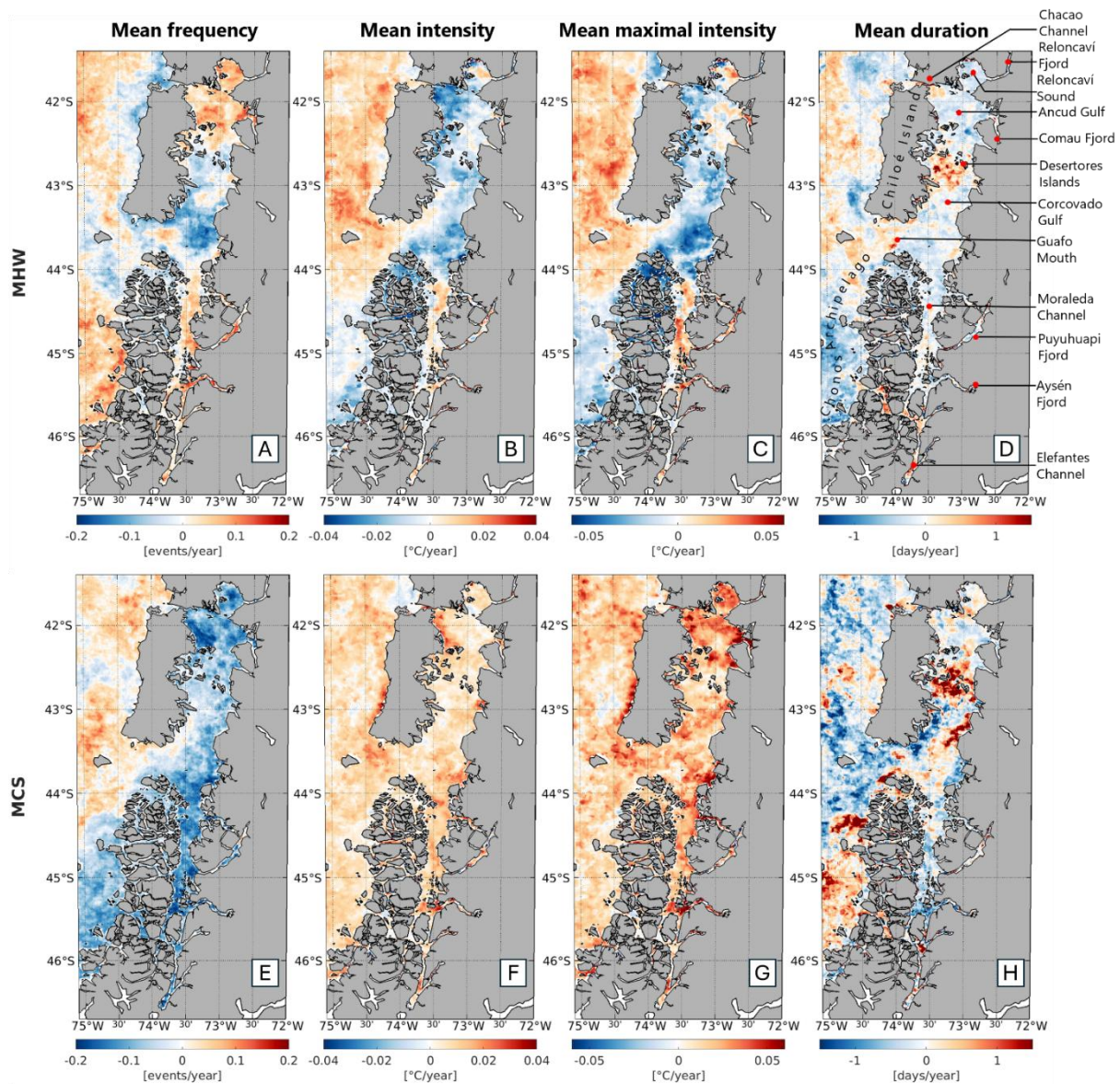
Figure 30: Annual trend for MHWs (top) and MCS (bottom) for different metrics: Frequency (A, E), Mean Intensity (B, F), Mean Maximal Intensity (C, G), Duration (D, H). The trend is expressed in unit per year, which means that for instance in the Reloncaví Sound, the mean intensity of the MCS is increasing by 0.01°C per year. Period: 2003-2023.

The duration trend of MHWs (Fig. 30D) is overall neutral or slightly decreasing within the Northern Patagonian Fjords, except south of Desertores Islands where is observed a positive trend of more than one day per year, as well as in the southernmost areas of the sea, such as Elefantes Channel and several channels in the Chonos Archipelago. In the open ocean, no clear pattern is apparent, although much of the western coast of Chiloé shows an increasing trend, occasionally reaching up to 1 day per year. For MCSs (Fig. 30H), a similar patch of increased duration is evidenced around Desertores Islands, with a rise of 1.5 days per year. West of Chonos Archipelago, an increase of 1 day per year can also be observed. Elsewhere, the trend is more likely in favour of a decrease in the duration by about 1 day per year.

67

3.3.8. Examples of remarkable events

3.3.8.1. Succession of MCSs and MHWs: 2007-2008

Among the different events observed during the last 20 years, some were remarkable by their length, intensity or by the succession of MCSs and MHWs. It is for example the case for the years 2007-2008.

Between 2007 and 2008, the region experienced successive MCSs and MHWs with brief intervals between events. In May 2007, following an atmospheric cold spell, a MCS began around Guafo Mouth, Chonos Archipelago and Moraleda Channel, with temperature anomalies between -0.5°C and -1°C. The MCS continued to spread and by the month of July, most of the study area was affected (Fig. 31A) due to a low-pressure system causing very strong eastward winds and substantial heat loss in the ocean surface, with SST anomalies of -1.5°C. The MCS persisted throughout the austral winter and most of spring, fading in late December. At that time, positive sea temperature anomalies dominated the study area, though negative sea anomalies (-1.5°C) persisted along Chiloé Island until January 2008, influenced by a La Niña event which cooled the region and intensified upwelling systems (Muñoz et al., 2023).
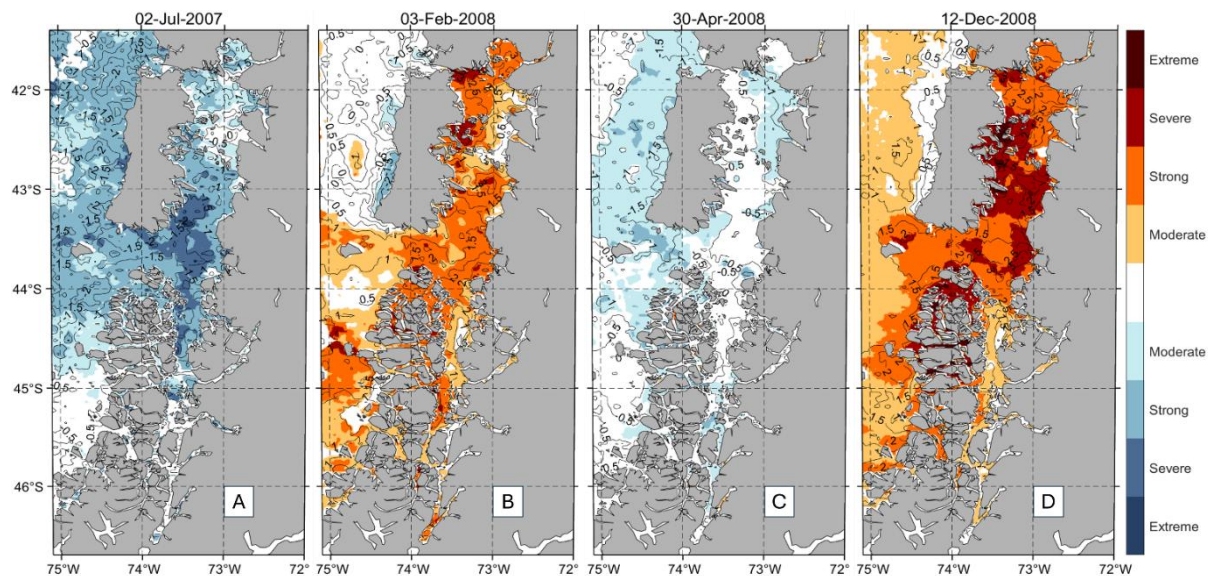
Figure 31: MHWs and MCS categories (respectively shades of reds and blues) on the peak day and the corresponding SST anomalies indicated by the thin black lines.

On the 22nd of January 2008, a very strong MHW started in Northern Patagonia, driven by increased solar radiation (due to low cloud cover) leading to positive heat flux anomaly. SST anomalies peaked on the 3rd of February with positive anomalies everywhere except along the West coast of Chiloé Island, with +3.5°C in Reloncaví Sound, +3°C west of Ancud Gulf, and exceeded +1.5°C from Reloncaví Sound to the Moraleda Channel (Fig. 31B). This MHW was a category II event in most of the Inner Sea of Chiloé and Southern part of the study area, and reached in localised areas category III (Fig. 31B). The event coincided with an atmospheric heatwave (+3°C on average over the sea) and increased solar radiation (low cloud cover), contributing to a positive heat flux anomaly. It dissipated very quickly in the Inner Sea, due to a low-pressure system in mid-February, bringing some clouds and strong southward winds, dispersing the atmospheric heatwave.

In April, strong eastward winds associated to negative latent heat anomalies (superior

to -100 W/m^2) triggered negative sea temperature anomalies as low as -1.5°C west of Chiloé Island, inducing a MCS across most of the study area (Fig. 31C & Fig. Sup. 1). Although this MCS remained relatively weak and largely confined to the Inner Sea, it persisted during the entire winter.

After a period of weaker winds and positive total net heat flux anomalies, a weak MHW emerged in September 2008 in the open ocean and Guafo Mouth, intermittently persisting and intensifying in December, encompassing almost the entire study area on the 12th of December (Fig. 31D). SST anomalies exceeded +1°C across the entire domain, and reached +4°C in the Reloncaví Sound, +3°C on the west side of Ancud Gulf and in the coastal part of the south of Corcovado Gulf. It was classified as category II event in the half North of the Inner Sea and category III around Desertores Islands, Corcovado Gulf and Chonos Archipelago (Fig. 31D). This MHW was linked to a high solar radiation and atmospheric heatwave, resulting in most of the time a positive total heat flux for the ocean. On the 12th of December, the air temperature anomaly above the ocean was +4°C across the entire study area. The MHW dissipated by mid-January as cloud cover increased, reducing solar radiation and air temperature, resulting in negative total heat flux anomalies.

Overall, these events were closely linked to atmospheric conditions, including La Niña, low-pressure systems and atmospheric heatwaves, driving significant SST anomalies in the region.

3.3.8.2. Strong MHW: 2013

Another notable event was a very strong MHW that occurred during summer 2013. It began by mid-January in the Inner Sea of Chiloé and quickly spread to the open sea, reaching its peak between the 7th and 10th of February, with temperature anomalies of 4°C in Reloncaví Sound, Puyuhuapi and Aysén Fjords, 3°C in the north of the Gulf of Ancud, Comau Fjord and Moraleda Channel, and superior to 1°C in the remaining parts of the Northern Patagonia (Fig. 32A). It was classified as a category II in most areas, with localised category III (Fig. 32A). Notably, the west shore of Chiloé Island remained unaffected likely due to upwellings (Narváez et al., 2019; Pérez-Santos et al., 2019). The event then vanished in about 10 days but persisted west of Chonos Archipelago until May.

This MHW coincided with a very intense atmospheric heatwave that started a few days before the MHW, with temperature anomalies exceeding +10°C over the continent, +5°C over parts of the Inner Sea and +3°C over the open ocean. Both marine and atmospheric heatwaves were accompanied by an unusually low cloud cover, increasing solar radiation, leading to positive total net heat fluxes (Fig. Sup. 2). Wind speed showed no distinct pattern that might have contributed to the MHW; in fact, they were stronger than usual and directed northward when the event began.

3.3.8.3. Long lasting period of MHWs: 2016-2017

The years 2016-2017 experienced prolonged MHW conditions, with events spanning from late December 2015 to early Arpil 2016 and mid-May 2016 to late July 2017, interrupted by just one month without MHW activity during austral summer.

The first MHW began west of Chiloé Island in late 2015, quickly spreading to the Inner Sea by January 2016, driven by strong positive solar radiation anomalies (>+180W/m^2 on the 7th of January 2016) and exceptionally low cloud cover, leading to positive total heat fluxes of about 100 W/m^2 centred on Northern Patagonia, and positive air temperature anomalies on both land and ocean (Fig. Sup. 3). By the 20th of January, the entire area was experiencing MHW with SST anomalies of +1.5°C to +2°C, peaking at +3°C in Puyuhuapi and Aysén Fjords (Fig. 32B). Strong

winds in February induced negative heat flux, weakening the MHW which fully dissipated by late February, except south of Desertores Islands where it lasted until early April.

March and April were hit by various events of strong winds and strongly negative total net heat flux anomalies. However, by mid-May, weakened winds led to positive heat flux, triggering another MHW near Desertores Islands, gradually spreading north, west and south by June. Anticyclonic conditions accompanied the MHW, but declined in July with the arrival of a low-pressure system. Summer and spring 2016 were marked by toxic algal blooms attributed to the atmospheric heatwave and reduced rainfall (Garreaud, 2018b; León-Muñoz et al., 2018; Díaz and Figueroa, 2023) and causing strong economic losses in aquaculture farms (León-Muñoz et al., 2018), coinciding with the MHWs observed here.
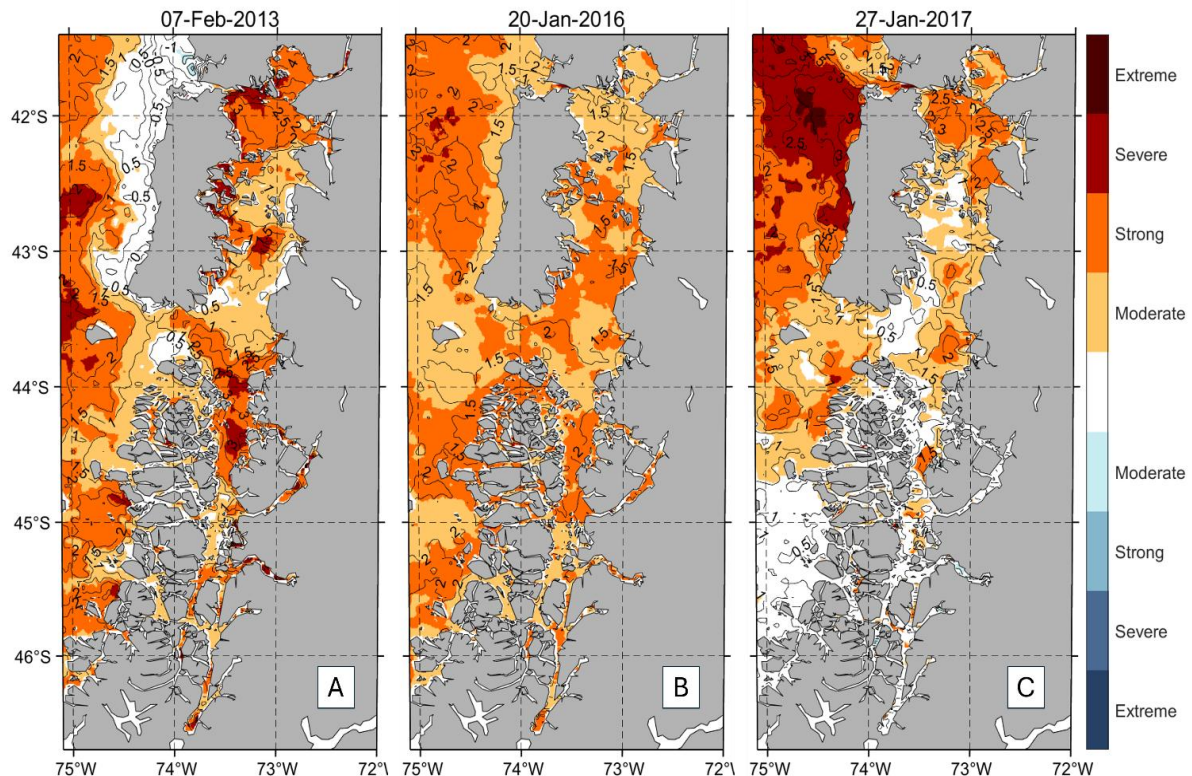
Figure 32: MHWs and MCS categories (respectively shades of reds and blues) on the peak day and the corresponding SST anomalies indicated by the thin black lines.

Throughout winter and spring 2016, the MHW persisted intermittently along the continental east coast of the Inner Sea, with SST anomalies around +0.5°C. It pulsed sporadically across the Inner Sea until almost vanishing in December. However, a new intense MHW emerged west of Chiloé Island at the end of December, classified as category IV. The MHW spread to the northern half of the study area, and peaked on the 27th of January 2017 with SST anomalies of +3°C at its centre (Fig. 32C). Similar anomalies appeared in Ancud Gulf and Reloncaví Sound but were classified only as category II events due to the greater temperature variability in these areas in summer.

The intense 2017 event was linked to positive heat flux and atmospheric heatwave, though these conditions alone could not fully explain its strength compared to previous events in 2008 and 2013. The 2016-2017 MHWs align with those described by Pujol et al. (2022), noting winter 2016 and particularly intense ones west of Northern Patagonia in summer 2017. The MHW shrank but pulsed again in the southern Inner Sea in late February, continuing intermittently in March, April and May around the Chonos Archipelago and Desertores Islands before fully dissipating by the end of July. The years 2016 and 2017 were impacted by a particularly strong El Niño event, linked

to reduced precipitations, atmospheric heatwaves and harmful algal blooms (Garreaud, 2018a, b), but also registered as being part of MHW triggering around Chilean Patagonia (Pujol et al., 2022).

3.4. Conclusion

In this study, we presented a new methodology for detecting MHWs and MCSs. It involves basing the climatology on long-term in situ data (1948-2022) while calculating the threshold and the daily temperature using satellite data over the study period of 2003 to 2023.

A key issue in MHW and MCS detection is that the climatology should be based on long-term data to take into account multi-decadal temperature trends. Although the climatology is generally calculated using satellite data, this was not feasible for our study area, the Chilean Northern Patagonia. Indeed, long-term satellite data lack the spatial resolution required to resolve intricate fjords, gulfs and channels of Northern Patagonia. Consequently, we decided to use in situ data to build the climatology, incorporating over 3 million sparse samples. These data were interpolated spatially and temporally to produce a monthly and daily-derived climatology of the sea temperature of the Northern Patagonia with a spatial resolution of 900m at 32 different depths. This daily-derived climatology was then used to detect MHWs and MCSs at high resolution, appearing consistent with the available literature.

This methodology enabled us to detect surface MHWs and MCSs individually and to analyse their different metrics. We found that every location experiences MHW and MCS at least once a year, and that they do not show similar or opposite spatial patterns. MCSs are particularly frequent in the northern part of Northern Patagonia, more precisely in Ancud and Reloncaví Gulfs, as well as Comau fjord, whereas MHWs are more frequent in the southern part of Northern Patagonia. Regarding the mean intensity, both MHWs and MCSs are significantly more intense in the most enclosed basins, such as Reloncaví Sound, Comau, Aysén and Puyuhuapi Fjords. The higher intensities of MHWs and MCSs in these regions reflects the water column structure: these regions are the most stratified, receiving high freshwater inputs, and forming a shallow surface layer more prone to rapid warming. MCS duration is also generally longer (between 10 and 25 days) than MHWs (10 to 20 days).

Seasonal patterns reveal that MHWs are more frequent in summer, when water column stratification is higher, and absent in winter, while MCSs are more frequent in winter and absent in summer. When looking at the intensity, both phenomena exhibit similar seasonal patterns, tending to be more intense during summer months.

By analysing several case studies, we observed that in Northern Patagonia, MHWs can be triggered and/or accompanied by atmospheric heatwaves, reduced winds, reduced cloud cover and positive El Niño Southern Oscillation phase. Conversely, MCSs are triggered by low-pressure systems, stronger winds and negative phase of El Niño Southern Oscillation (La Niña).

Trends over the 2003-2023 period indicate that MCSs are becoming less frequent but more intense, whereas MHWs are becoming more frequent (except in Corcovado Gulf) but less intense. The intensity trend of MCSs is positive everywhere and particularly homogeneous, in contrast to the MHW trend which shows more basin-specific variability, both positive and negative. Regarding duration, MCSs are becoming longer around Desertores Islands and Chonos Archipelago, whereas MHWs are very slightly becoming shorter overall except around Desertores Islands where they also tend to be longer.

This study highlights the importance of examining MHWs and MCSs at high resolution in coastal environment: these events are far from homogeneous across the Northern Patagonia, as is likely the case for other complex coastal regions. Enclosed basins such as Reloncaví Sound, Puyuhuapi and Comau Fjords, are more likely to be prone to intense events, whereas Corcovado Gulf appears relatively resilient, with low intensity events. High-resolution detection of these events is crucial for gaining a comprehensive understanding of MHWs and MCSs dynamics in coastal areas, enabling better analysis of their consequences on ecosystems and assisting local stakeholders in mitigating such events.

CHAPTER 4.   SUBSURFACE MHWS AND MCSS

Foreword

The two previous chapters established how surface MHWs and MCSs develop along the Chilean coats, from large-scale offshore patterns (Chapter 2) to finer-scale dynamics within the fjords and channels of Northern Patagonia (Chapter 3). Together, these chapters provided new insights into the surface expression of extreme events and highlighted the atmospheric drivers that sustain them.

However, these analyses were limited to the surface layer. Understanding the vertical structure and development of extreme events is particularly important, especially in Northern Patagonia which is composed of different basins where, as we saw in Chapter 3, the spatial variability of extreme temperature events is principally linked to the stratification and topography.

This chapter therefore complements the surface-based approach by providing the first overview of subsurface MHWs and MCSs in Northern Chilean Patagonia over the last 30 years, based on a hydrodynamic model. It investigates the vertical and temporal extension of these events, their links between surface and subsurface events, temperature, salinity, and water masses, and considers how their occurrence might affect ecosystems and aquaculture.

This chapter has not been submitted to publication as the content is not sufficient to constitute a standalone paper.

4.1. Introduction

Marine heatwaves (MHWs) and marine cold spells (MCSs) are extreme sea temperature events, defined as periods of anomalously warm or cold conditions that exceed a threshold for at least five consecutive days (Hobday et al., 2016; Schlegel et al., 2021). They have been detected and studied in every ocean and at any depth, from surface to seafloor (Amaya et al., 2023b; Elzahaby and Schaeffer, 2019; Hu et al., 2021; Lien et al., 2024; Zhang et al., 2023).

While MHWs have received considerable scientific attention over the past decade, MCSs remain comparatively much less studied, particularly at depth (He et al., 2024; Schlegel et al., 2021; Sun et al., 2024b). Most studies have focused on surface MHWs, largely because they can be effectively monitored using high or low spatial resolution satellite data, reanalysis products or models (Dzwonkowski et al., 2020; Gupta et al., 2024; Marin et al., 2021; Pilo et al., 2019; Wang et al., 2022b). In contrast, subsurface events are more challenging to assess, particularly in coastal areas, as they often require high resolution datasets or long-term in situ data (Dalsin et al., 2023; Elzahaby and Schaeffer, 2019; Guo et al., 2022; Hayashida et al., 2020b; He et al., 2024; Li and Donner, 2022; Scannell et al., 2020). Subsurface MHWs and MCSs are often examined using monthly temperature data, as subsurface dynamics tend to evolve more slowly than at the surface (Amaya et al., 2023b; Scannell et al., 2020; Zhang et al., 2025).

Subsurface extremes may be even more consequential than their surface counterparts: their last longer and can be more intense than at the surface (Amaya et al., 2023b; Xu et al., 2024), and their impacts can directly affect benthic, demersal and pelagic communities. For example, bottom water temperature anomalies have been linked to population decline in Pacific cod in the Gulf of Alaska (Barbeaux et al., 2020), spatial redistribution of lionfish in the southeast of United States (Fogarty et al., 2008), massive coral bleaching (Bell et al., 2024; Fordyce et al., 2019) and decrease in abundance and biomass of many benthic invertebrates (Pansch et al., 2018).

Yet, in Chile, although surface events have been recently assessed (Carrasco et al., 2023; Pujol et al., 2022, 2025), subsurface extremes remain almost entirely unstudied, despite the presence of one of the world's most important upwelling system (Chavez et al., 2008; Cooley et al., 2022; Pietri et al., 2021). This represents a major knowledge gap, especially given the potential for strong interactions between local hydrography, climate variability and extreme events (Carrasco et al., 2023; Garreaud et al., 2013a; Garreaud and Aceituno, 2007; Pujol et al., 2025).

Northern Chilean Patagonia provides a particularly interesting setting to investigate subsurface events. Located on the western side of southern South America, it is characterised by a highly complex topography, with a central Inner Sea connected to an intricate network of fjords and channels. Oceanographic circulation is strongly influenced by buoyancy forcing, as large freshwater inputs from rivers, rainfall and glacial melt reduce surface salinity (León-Muñoz et al., 2024; Pérez-Santos et al., 2014; Sievers and Silva, 2008; Valle-Levinson et al., 2007). Each of these water mass entering Northern Patagonia can be identify from its salinity signature, with the least saline at the surface and the most saline at the bottom (Linford et al., 2024; Sievers and Silva, 2008; Silva et al., 2009). The upper layer, known as Estuarine Waters (EW), is typically 20 to 30 m thick (Pérez-Santos et al., 2014; Sievers, 2008; Sievers and Silva, 2008), exhibits low salinity, and responds rapidly to solar radiation, vertical mixing and freshwater discharge (Pérez-Santos et al., 2014; Sievers, 2008; Sievers and Silva, 2008). Below, lies the Subantarctic Water (SAAW), an oxygen-rich layer generally extending to about 150 m depth (Pérez-Santos et al., 2014; Sievers and Silva, 2008). It plays a key role in renewing deep waters in the different fjords (Pérez-Santos, 2017; Sievers and Silva, 2008). This layer

eventually mixes with the estuarine one to form Modified SubAntarctic Water (MSAAW) that has an intermediate salinity (Sievers and Silva, 2008; Silva, 2008). The deepest water mass is named the Equatorial Subsurface Water (ESSW). It originates from the Equatorial Pacific Oxygen Minimum Zone, bringing dense low-oxygenated waters to Northern Patagonia (Linford et al., 2023; Palma and Silva, 2004). It is constrained by the topography and therefore fills only the deepest basins and fjords of Northern Patagonia (Sievers and Silva, 2008).

This study provides the first assessment of subsurface MHWs and MCSs in Northern Chilean Patagonia. The main objectives are to characterise the occurrence and development of subsurface events in a region of complex topography and strong freshwater influence, and to understand their interactions with salinity and water masses. To achieve this, we used the global model GLORYS12V1 which has a spatial resolution of about 8 km (European Union-Copernicus Marine Service, 2018). We characterised the spatiotemporal variability of temperature and salinity anomalies across the different subregions of Northern Patagonia, and their implications for MHWs and MCSs development.

4.2. Material and Methods

4.2.1. Data and study area

To investigate subsurface temperature variability and development of warm and cold anomalies in Northern Patagonia, we used the outputs from the Global Ocean Reanalysis and Simulations GLORYS12V1 product. This eddy-resolving product is based on the NEMO ocean model, and is distributed by the Copernicus Marine Service Environment Monitoring Service (CMEMS, European Union-Copernicus Marine Service, 2018). The dataset provides ocean physical parameters, including the sea water potential temperature, salinity, and mixed-layer depth, with a spatial resolution of 1/12° (~8 km), and 50 vertical levels, making it well-suited for exploring mesoscale oceanographic variability and subsurface processes (Amaya et al., 2023a).

However, the spatial resolution of GLORYS12V1 presents some limitations in the context of Northern Patagonia's complex coastal region (Fig. 33). While Reloncaví, Ancud, Corcovado, Moraleda and Elefantes Channel are resolved, many smaller-scale features are not. For example, Chonos Archipelago appears as a single landmass, Desertores Islands are not represented and the Chacao Channel is missing resulting in an artificial connection between Chiloé Island and the mainland. Furthermore, no fjords are resolved. Despite these limitations, the product remains valuable for providing a regional overview of how temperature anomalies develop and propagate across the broader Northern Patagonia domain.

We used the daily sea potential temperature, salinity and mixed layer depth fields from January 1993 to December 2024 that we monthly averaged in order to capture only the most persistent and intense warming or cooling periods. The study domain covers the Northern Patagonia region, from 41°S to 47°S and 72°W to 76°W, encompassing both the inner sea of Northern Patagonia and adjacent sectors of the Southeast Pacific Ocean. For the vertical dimension, we selected the upper 30 levels available in the dataset, corresponding approximately to the 0 to 380 m depth, capturing most of all the deepest basins of Northern Patagonia.

Monthly temperature anomalies were calculated for each level depth by subtracting the long-term monthly climatology (based on the full 1993-2024 period) from the original temperature time series. Same was realised to calculate salinity anomalies. To explore vertical an temporal
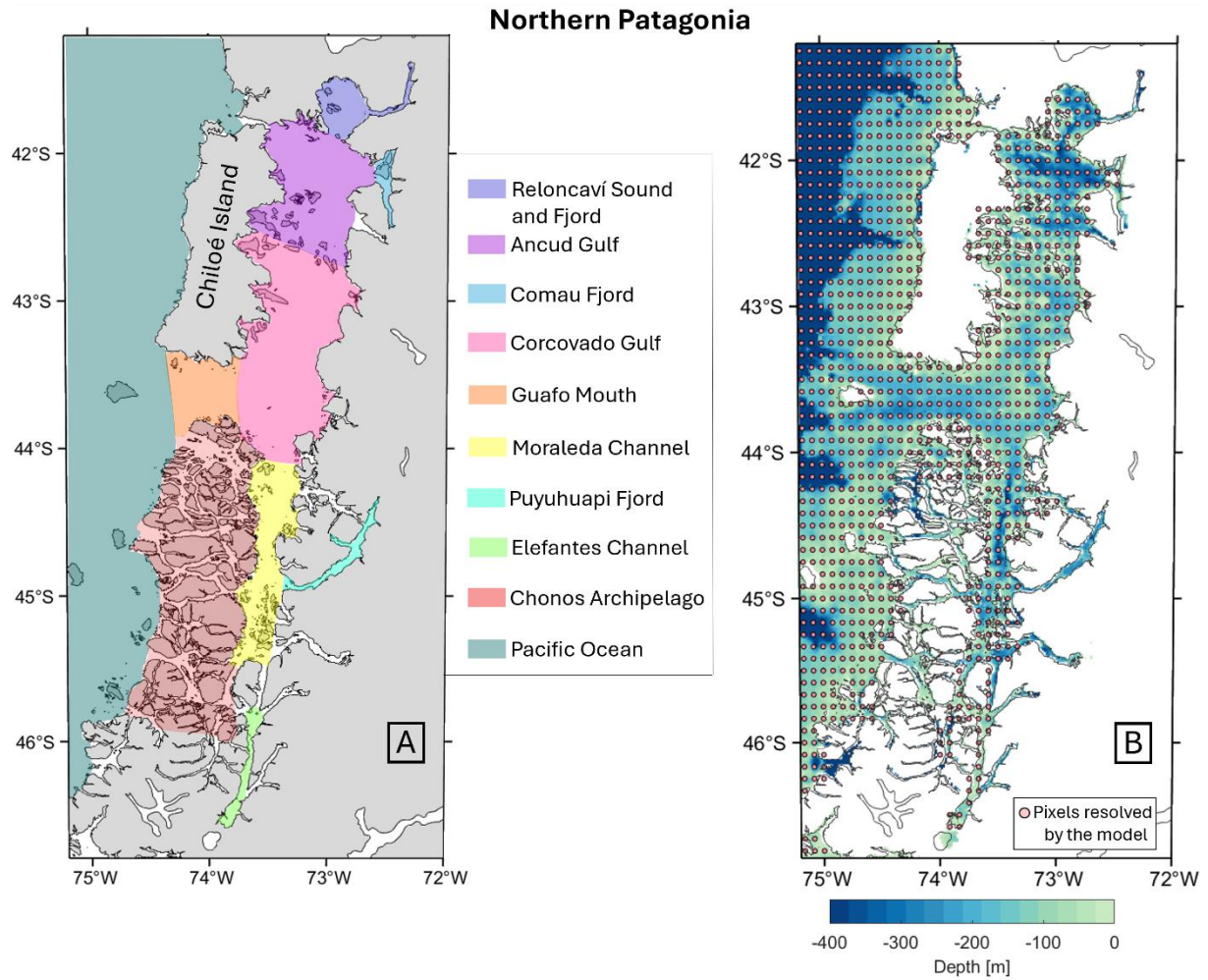
Figure 33: (A) Key basins of Northern Patagonia. (B) Bathymetry of Northern Patagonia, limited to 400 m. The pink dots represent all the areas resolved by the model GLORYS12V1, highlighting that only the largest basins are resolved.

dynamics, anomalies were analysed both at individual depth levels and across aggregated depth layers, defined as: ([0-10m], [10-20m], [20-30m], [30-40m], [40-50m], [50-75m], [75-100m], [100-150m], [150-200m], [200-300m], [300-400m]). The aggregated depth layers were used to calculate the depth range at which the temperature anomalies are the strongest and to estimate their duration.

4.2.2. Water masses

Four principal water masses can be identified in Northern Patagonia on the basis of their salinity characteristics (Linford et al., 2024; Sievers and Silva, 2008; Silva et al., 2009). At the surface, the Estuarine Waters (EW) form generally a thin layer (20 to 30 m) that is defined by salinities below 31, reflecting strong influences from freshwater inputs. Beneath this, the Modified SubAntarctic Waters (MSAAW) appears as a transitional layer in which the salinity of the SubAntarctic Waters has been reduced through mixing with overlying estuarine waters, resulting in intermediate values between 31 and 33. The SubAntarctic Waters (SAAW) proper occupy the next depth range and are characterised by salinities from 33 up to 34.3, representing a relatively stable intermediate mass that isolates surface layers. Finally, at greater depths, the Equatorial Subsurface Waters (ESSW) are present, distinguishable by their comparatively high salinity and

are generally associated with lower oxygen concentrations in comparison to the upper layers. The ESSW has been defined with different salinity signature according to how far in Northern Patagonia the water mass has entered. (Linford et al., 2023) define it for instance as a water mass of salinity superior to 33.8 in Puyuhuapi Fjord due to the high freshwater influences, therefore restricting the SAAW to salinities between 33 and 33.8. We will however consider that the ESSW is defined in the entire domain by the salinity it has while entering Guafo Mouth, which means 34.3 (Silva et al., 2009).

4.2.3. Definition of MHW and MCS

MHWs and MCSs were identified following the definition proposed by (Hobday et al., 2016) and extended by (Schlegel et al., 2021). These events are defined as prolonged periods of anomalously warm or cold water temperature, during which the temperature exceeds a predefined threshold for at least 5 consecutive days. Typically, the threshold for MHWs is set as the 90th percentile of a historical temperature baseline, while the MCS threshold is set as the 10th percentile of the same historical temperature baseline.

In this study, we applied this approach using the temperature, temperature anomaly, and thresholds calculated from the monthly dataset of GLORY12V1 ocean reanalysis product from CMEMS. The monthly temporal resolution is used to detect only the most persistent and large-scale events, more specifically those lasting at least for 1 month. This method does not capture the occurrence of shorter events occurring on daily to weekly timescales as they cannot be resolve with this approach.

To detect the MHWs and MCSs, we first calculated the monthly climatological mean and the corresponding 90th and 10th percentiles threshold over the period 1993 to 2024 for each grid cell and depth level. A MHW (or MCS) was identified when the monthly temperature exceeded (or fell below) the respective threshold for at least one month. Events detection was performed independently at each depth level, allowing the capture of the vertical structure of each event. In addition, the average duration and frequency of MHWs and MCSs across the full time period were analysed, but over averaged aggregated depths, as for temperature anomalies: [0-10m], [10-20m], [20-30m], [30-40m], [40-50m], [50-75m], [75-100m], [100-150m], [150-200m], [200-300m], [300-400m].

4.3. Results

4.3.1. Temperature

From 1993 to 2020, the region experienced a sequence of alternating thermal phases (Fig. 34). Warmer conditions predominated between 1993 and 1998, followed by a colder phase from 1999 to 2002. A return to warmer conditions was observed from 2003 to 2006, succeeded by a prolonged cold period from 2007 to 2014. Another warm phase extended from 2015 to at least 2018. While this alternation is evident across most of the study area, the regions north of Desertores Islands, more precisely Ancud and Reloncaví Gulfs, display a clear disconnection between surface and subsurface events. In Ancud, subsurface temperature anomalies remained slightly positive (below 0.5°C) from 1994 to 2007, shifted to negative values between 2008 and 2016-17 (always superior to -0.5°C), and turned positive again after that (Fig. 34E). A similar trend occurred in Reloncaví Sound, where positive temperature anomalies were present from 1995 to 2012, followed by a negative phase until 2024 (Fig. 34F). Interestingly, below approximatively

Temperature anomaly in different basins

Figure 34: Sea temperature anomalies spatially averaged over west of Chiloé Island (A), Guafo Mouth (B), Corcovado Gulf (C), Moraleda Channel (D), Ancud Gulf (E) and Reloncaví Sound (F), from 1993-2024.

Figure 35: Sea temperature spatially averaged over west of Chiloé Island (A), Guafo Mouth (B), Corcovado Gulf (C), Moraleda Channel (D), Ancud Gulf (E) and Reloncaví Sound (F).

100 m depth, temperature fluctuations are minimal ([Fig. 35F](#)), suggesting that except exceptional event, surface conditions in these gulfs may not have sufficient influence to affect deeper layers. Nevertheless, particularly in Ancud, the timing of subsurface warming and cooling corresponds to strong thermal events at the surface that seemed to have been strong enough to propagate at depth.

Among the observed events, the 1997-1998 warming stands out as the most intense. During this period, positive temperature anomalies affected the entire water column across the entire study area. In Guafo Mouth, between May 1997 and December 1998, the water column throughout the region exhibited persistent warming, with temperature anomalies exceeding 0.5°C from June 1997 to September 1998. In winter 1998, anomalies above 1.5°C were observed from the surface to 100 m, reaching temperature superior to 11°C at 100 m depth ([Fig. 35B](#) & [Fig. 36](#)). This exceptional warming extended beyond Guafo Mouth. In Corcovado Gulf, warming greater than 1°C was recorded between February and August 1998, reaching as deep as 220 m. Below 125 m depth, the anomalies registered in Guafo Mouth and Corcovado Gulf corresponded to a temperature of 10°C ([Fig. 35](#)). Moraleda Channel also showed strong warming, with anomalies exceeding 0.5°C from February 1998 to November at 250 m depth, and values over 1°C in the upper 175 m. The most pronounced warming in this channel occurred between surface and 180 m, with anomalies superior to 1°C. Similarly, Elefantes Channel experienced widespread warming throughout the water column during autumn-winter 1998, with values greater than 1°C. North of Desertores Islands, in Ancud and Reloncaví Sound, the warming also extended throughout the water column, although the strongest anomalies were generally limited to the upper 100 m. At the surface, the warming corresponded to a temperature of 15°C and 16°C in Ancud Gulf and Reloncaví Sound ([Fig. 35E-F](#)). Overall, the 1997-1998 event was remarkable for its magnitude, duration and vertical extent, making it the most significant warming phase of the observed period. Another notable warm event occurred between 2015 and 2017. It initiated between autumn and winter 2015 and encompassed the entire water column everywhere except north of Desertores Islands. Along the west coast of Chiloé Island, temperature anomalies superior to 2°C were observed from surface to 30 m depth. In Corcovado Gulf, the temperature anomalies at depth persisted from June 2015 to October 2017, a duration of nearly 2 years and 4 months. At depth, the most intense phase occurred between February and May 2016, when subsurface anomalies ranged between 0.5 and 1°C. At the surface, the warming fluctuated but intensified during autumn 2016, reaching over 1.5°C in summer 2017 near the surface in Corcovado Gulf and Moraleda Channel ([Fig. 36](#)). In Ancud and Reloncaví the warming was different than in the other regions. In Ancud, the warming was primarily in the upper layers, and slowly propagated to depth, reaching the deepest layers in 2018, while the surface layer was experiencing cold event. In Reloncaví Sound, the warming occurred only in the first 100 m, but was as intense at the surface as in the other regions. Overall, from Guafo Mouth to Reloncaví Sound, temperature was between 16°C and 17°C during summer 2017 at the surface and up to 25 m depth in some regions ([Fig. 35](#)).

In contrast, a major cold episode occurred in 2007-2008. This event propagated through the entire water column everywhere, except in Reloncaví Sound, where it remained confined to the upper 100 m. In Ancud Gulf, the event at depth was delayed by one year, starting only at the beginning of 2008. The strongest negative anomalies reached -1.5°C outside of Northern Patagonia, in Guafo Mouth and Corcovado Gulf during summer 2008, corresponding to a temperature of 7°C ([Fig. 35C](#)). In Reloncaví Sound, although the temperature anomalies were between -0.5 and -1°C in the upper layer, they did not penetrate to the lower layers, remaining above 100 m depth, indicating differences in vertical penetration of the cold anomaly across the regions. Between
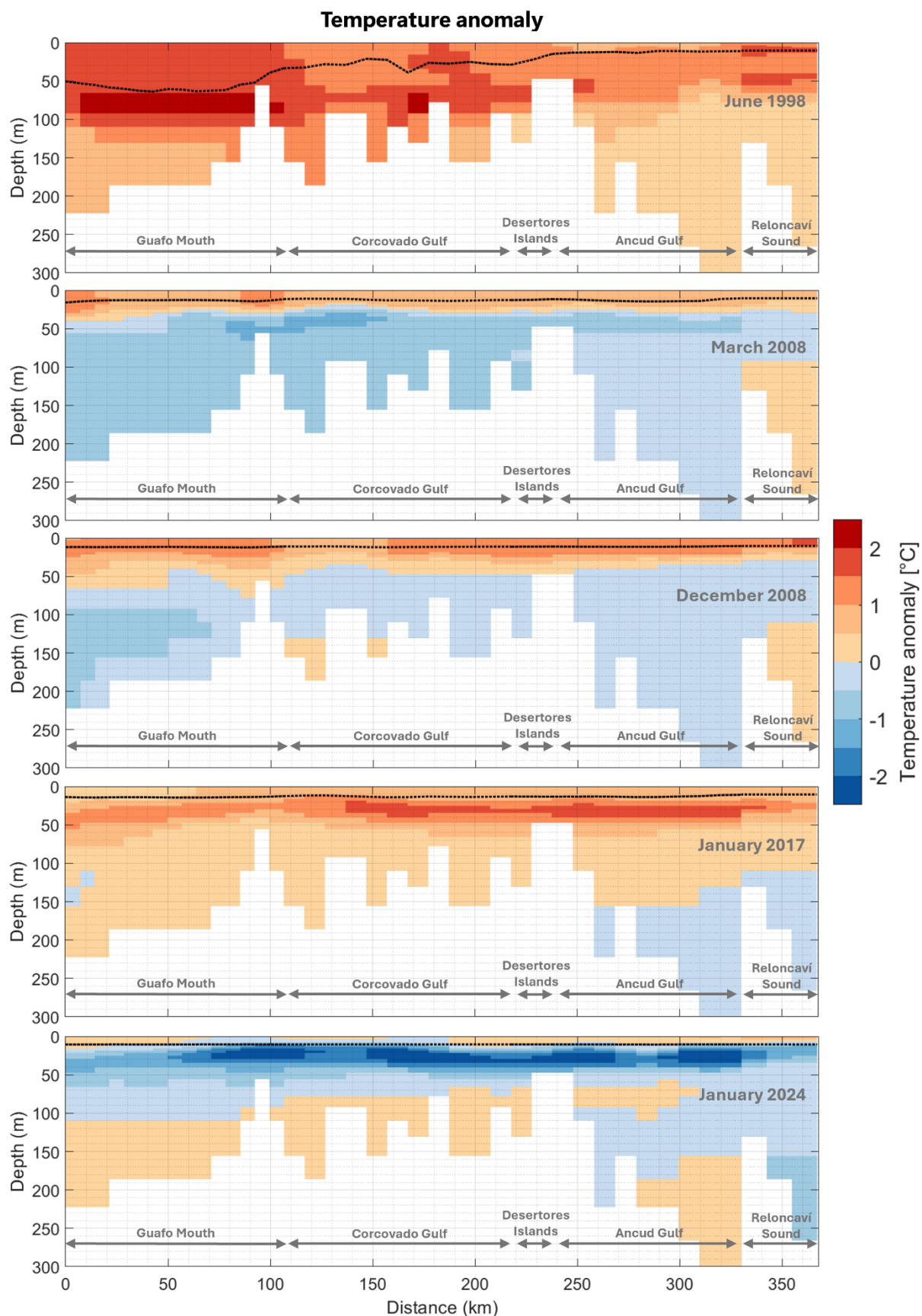
Figure 36: Transects through Guafo Mouth to Reloncaví Sound of the temperature anomalies during different periods corresponding to: MHW during June 1998, surface MHW and subsurface MCS in March 2008 and December 2008, MHW in January 2017, MCS in January 2024. Dotted lines indicate the mixed-layer depth.

January and April 2008 however, the surface (up to 30 m depth) switch to positive anomalies, everywhere in Northern Patagonia (Fig. 36). From 2019 to 2024, some successive short but cold event with anomalies above -2°C occurred between 10 and 60 m depth in different regions of Northern Patagonia, and were particularly pronounced in Ancud Gulf. In Moraleda, this period was also marked by a relatively stable mixed layer, whereas this region usually experiences strong changes between summer and winter.

The vertical distribution of temperature anomalies across Northern Patagonia reveals that the most pronounced anomalies (both warm and cold) generally occur in the subsurface, rather than at the surface (Fig. 37). On average, over the entire study area, the strongest positive temperature anomalies are found between 30 and 50 m depth (except for Elefantes Channels that is deeper) with mean values around +0.47°C. Negative anomalies also peak between 30 and 40 m with an average intensity of -0.50°C. When individual subregions are considered, all areas except Elefantes Channels display maximum positive anomalies between 20 and 50 m. In contrast, Elefantes Channel exhibits its strongest warming at the bottom. The most intense average positive anomalies range from +0.40°C in Reloncaví Sound to +0.50°C in Ancud Gulf (Fig. 37B). Even stronger anomalies are observed outside Northern Patagonia, west of Chiloé Island, where maximal anomalies reach +0.54°C between 40 and 50 m depth. For cold anomalies, a similar patter emerges, with the strongest cooling typically observed between 20 and 50 m depth (Fig. 37A). Minimal average negative anomalies are found in Reloncaví Sound with -0.36°C, while the most extreme is found in Elefantes Channel, with -0.56°C. As with warm anomalies, the open ocean also shows quite pronounced anomalies, reaching -0.51°C between 30 and 40 m depth.

Overall, the strongest thermal anomalies in Northern Patagonia are consistently observed in the subsurface layers, from 20 to 50 m depth, rather than at the surface. The deepest layers, particularly below 100 m remain the most stable, experiencing the least intense changes in temperature.
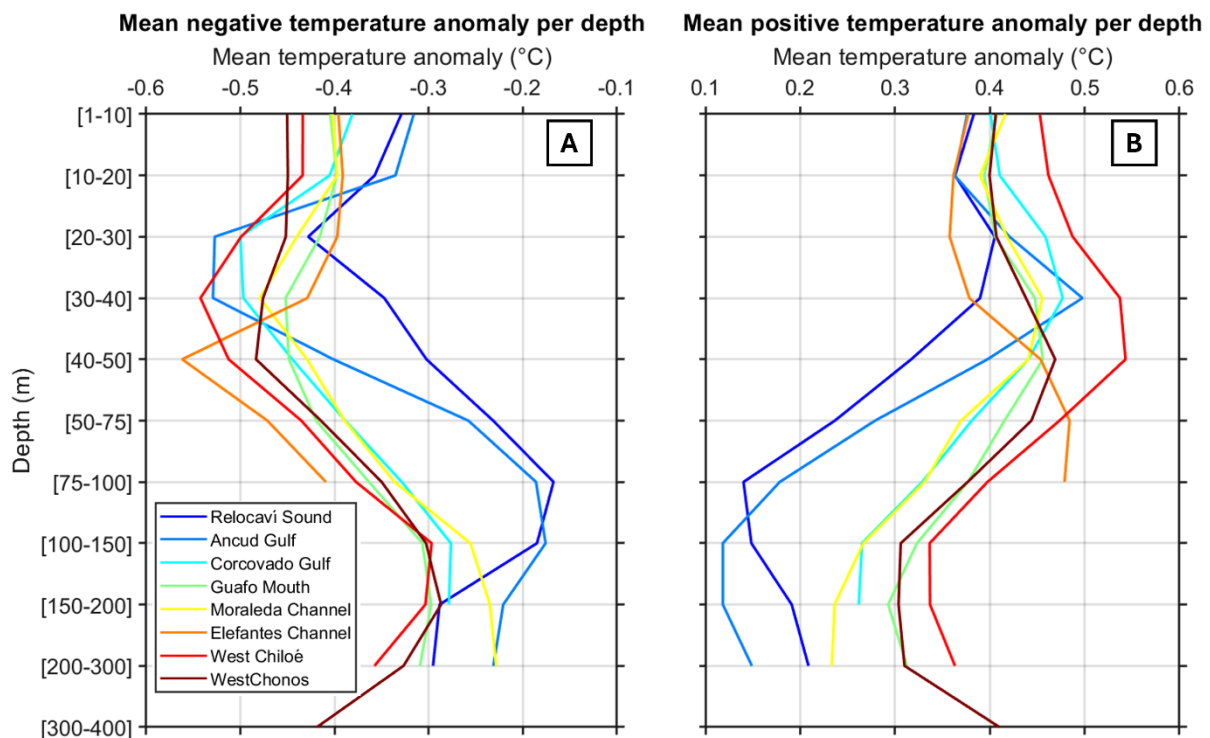
Figure 37: Mean temperature anomaly for (A) only negative anomalies and (B) only positive anomalies.

4.3.2. Salinity and water masses

Salinity distributions reveal the presence and variability of distinct water masses across Northern Patagonia. Offshore, SAAW typically extend from the surface to about 100 m depth, while ESSW dominate below this depth (Fig. 38A). A similar structure is observed at Guafo Mouth, although during winter SAAW often occupies the entire water column, with occasional incursions of MSAAW, particularly during the periods 1993-1997, 2007-2010 and 2017-2024 (Fig. 38B).

In Corcovado Gulf and Moraleda Channel, SAAW generally spans the full depth range but they are regularly incursions of ESSW. At the surface, MSAAW is frequently detected, with an almost continuous presence between 0 and about 50 m depth from 2016 to 2014 (Fig. 38C, D). This feature was especially pronounced in Moraleda Channel, where even estuarine waters (salinity inferior to 31) were observed. During this period, SAAW did not reached the bottom layers of the Moraleda Channel.

In Ancud Gulf and Reloncaví Sound, SAAW predominates throughout the water column, though exceptional intrusions of high salinity waters (superior to 34.3) were recorded, but they were not synchronised across the two basins (Fig. 39E,F). In Ancud Gulf, MSAAW was mostly present from autumn to spring, with reduced occurrence in summer, although from 2016 to 2024 extended periods with salinities below 31 were observed. In Reloncaví Sound, a clear estuarine surface layer (0-20m) is constantly present, with a relatively thin but persistent MSAAW underneath. Beneath, SAAW occupies the water column from about 30 m to depth, producing a distinct three-layer structure.

Salinity anomalies further highlight spatial and temporal variability. Offshore Northern Patagonia and Guafo Mouth display little interannual variation, whereas the inner basins exhibit much stronger anomalies due to their proximity to fjords and river inputs (Fig. 39). Between 2019 and 2024, particularly strong negative salinity anomalies were recorded, most markedly in Moraleda Channel where values reached -2 (Fig. 39D). These anomalies were confined to the MSAAW and EW, extending from surface to depths superior to 50 m in Moraleda Channel and to about 10 m in Reloncaví Sound. This represents the lowest salinity recorded during the entire study period, with in Moraleda Channel values dropping below 31 compared with an average of 33.

By contrast, positive salinity anomalies were observed during the periods 1998-2006 and 2012-2016 in Moraleda Channel and, to a lesser extent, in Corcovado Gulf and Ancud Gulf. In Reloncaví Sound, while surface waters exhibited strong freshening during the 2019-2024 event, the MSAAW layer simultaneously showed positive anomalies of up to +1 (Fig. 40F). The warm episode of 1998-1999 was also accompanied by strong positive anomalies, superior to +0.5 across much of Northern Patagonia, extending down to 30-50 m and corresponding to the saltiest conditions observed over the entire period studied.

4.3.3. MHWs and MCSs

The strongest temperature anomalies observed during 1997-1998 led to the development of a MHW that extended throughout the entire water column in the open Pacific, Guafo Mouth, Corcovado Gulf, Moraleda and Elefantes Channels. In Corcovado Gulf, below 100 m, the MHW lasted from December 1997 to October 1998, while in Moraleda Channel, it lasted from November 1997 to December 1999 (Fig. 40C, D). In Guafo Mouth, the mixed layer during winter 1998 was deeper than it used to be, reaching 75 m depth (Fig. 36). In Ancud Gulf, the MHW began by the end of 1997 and initially reached down to approximately 150 m. It only extended into the
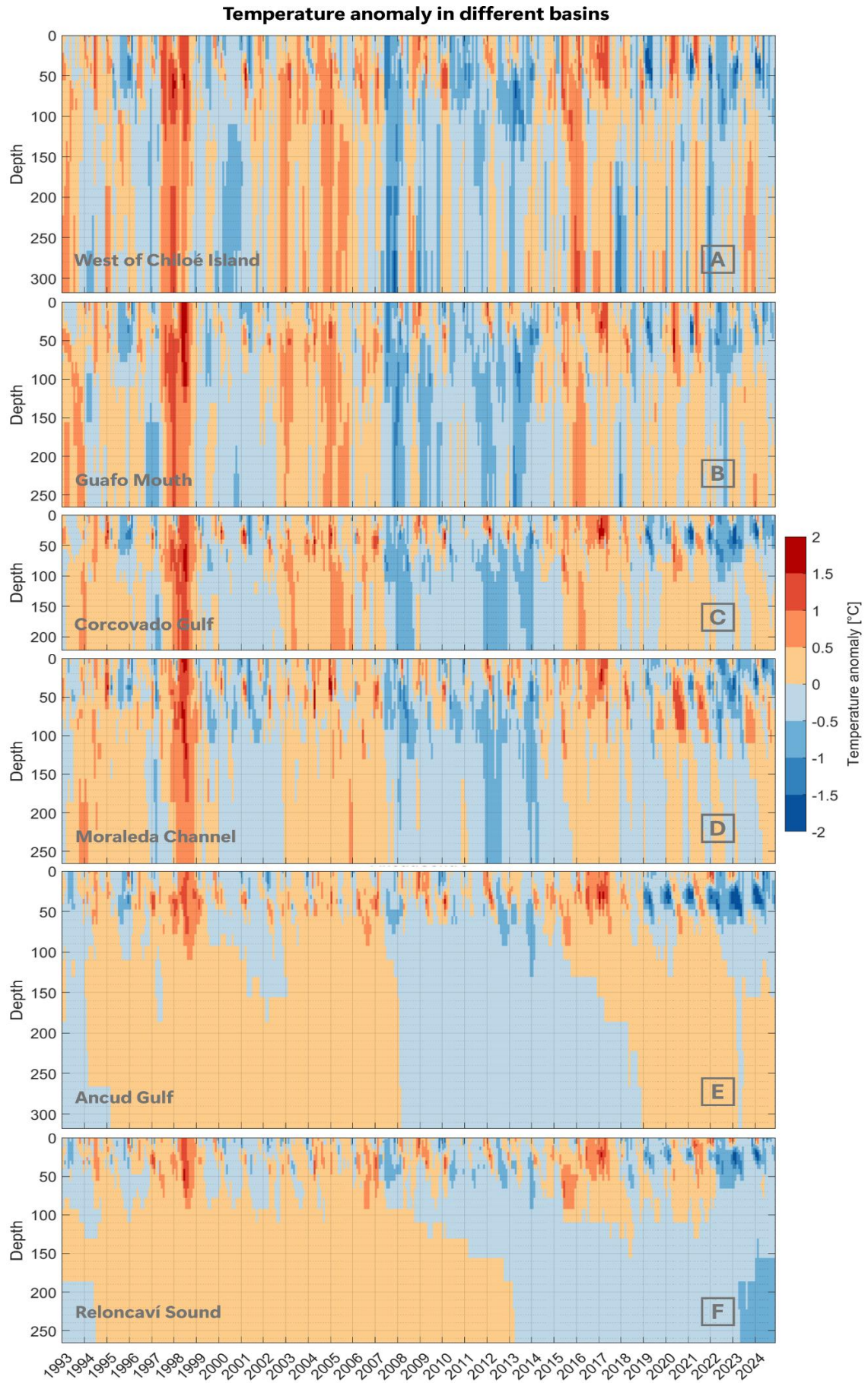
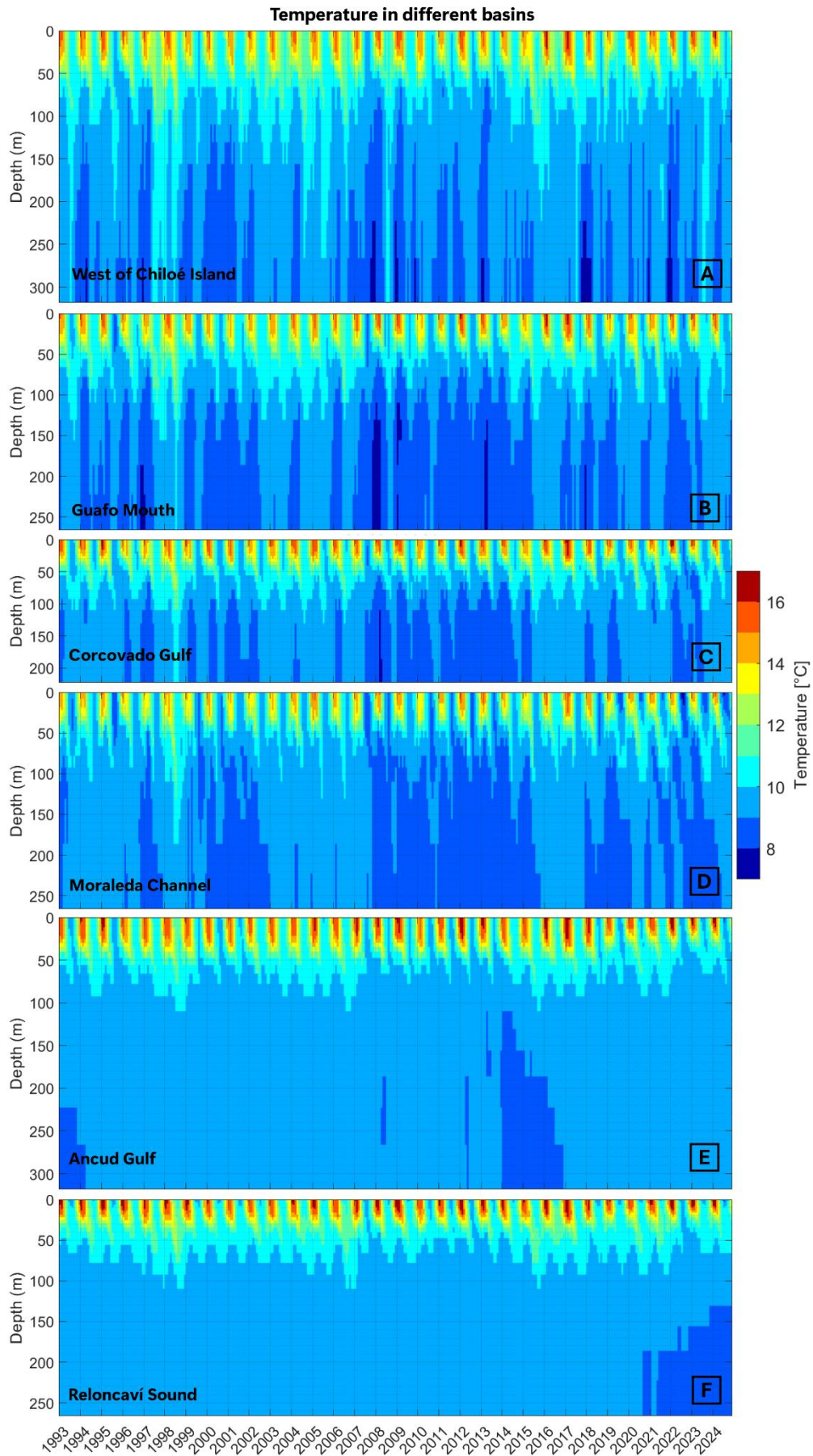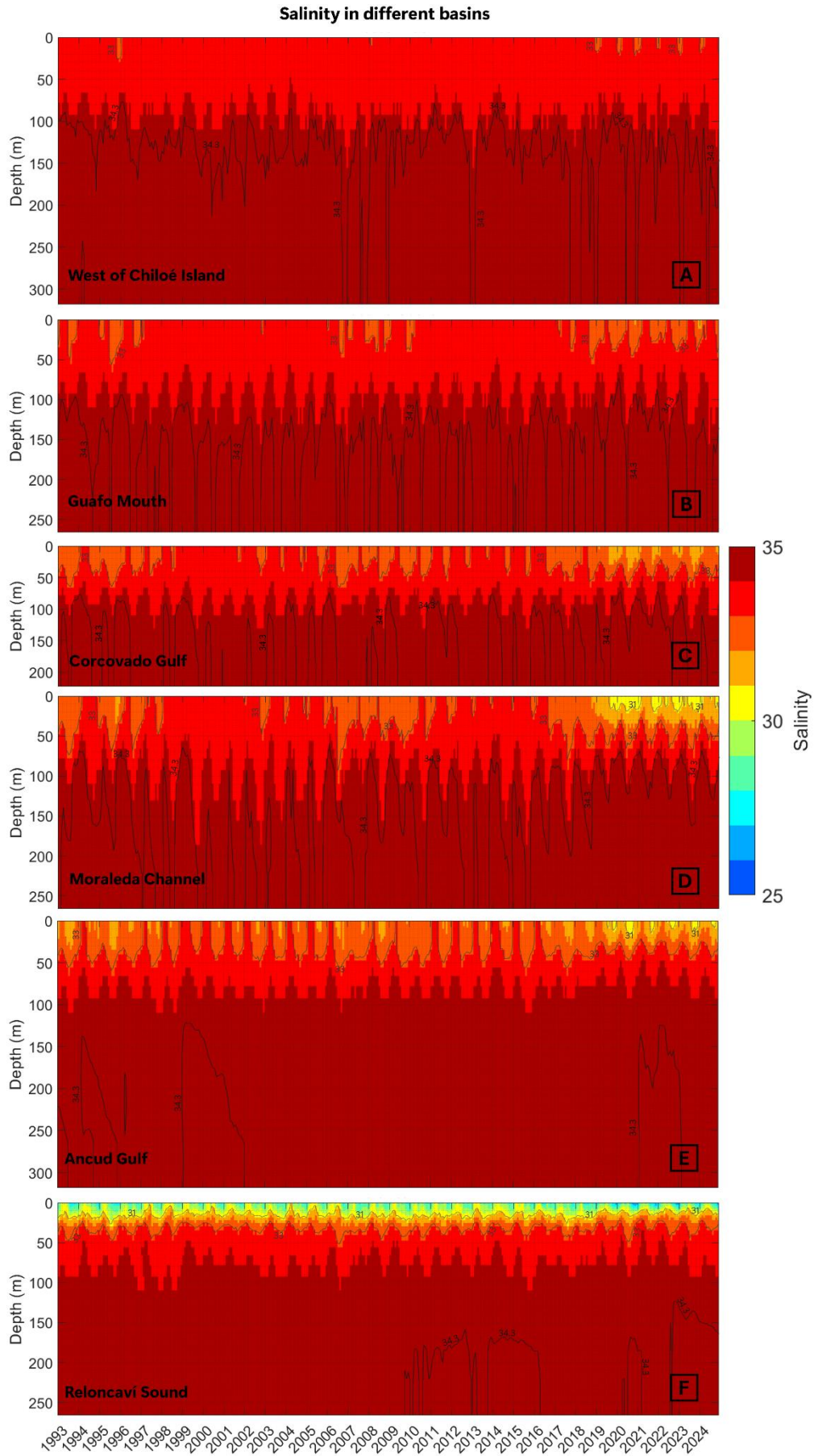*Figure 38: Salinity spatially averaged over west of Chiloé Island (A), Guafo Mouth (B), Corcovado Gulf (C), Moraleda Channel (D), Ancud Gulf (E) and Reloncaví Sound (F). The thin lines delimitate the salinity that define the different water masses: Estuarine Waters (0-31), Modified SubAntarctic Waters (31-33), SubAntarctic Waters (33-34.3), and Equatorial Subsurface Waters (>34.3).*
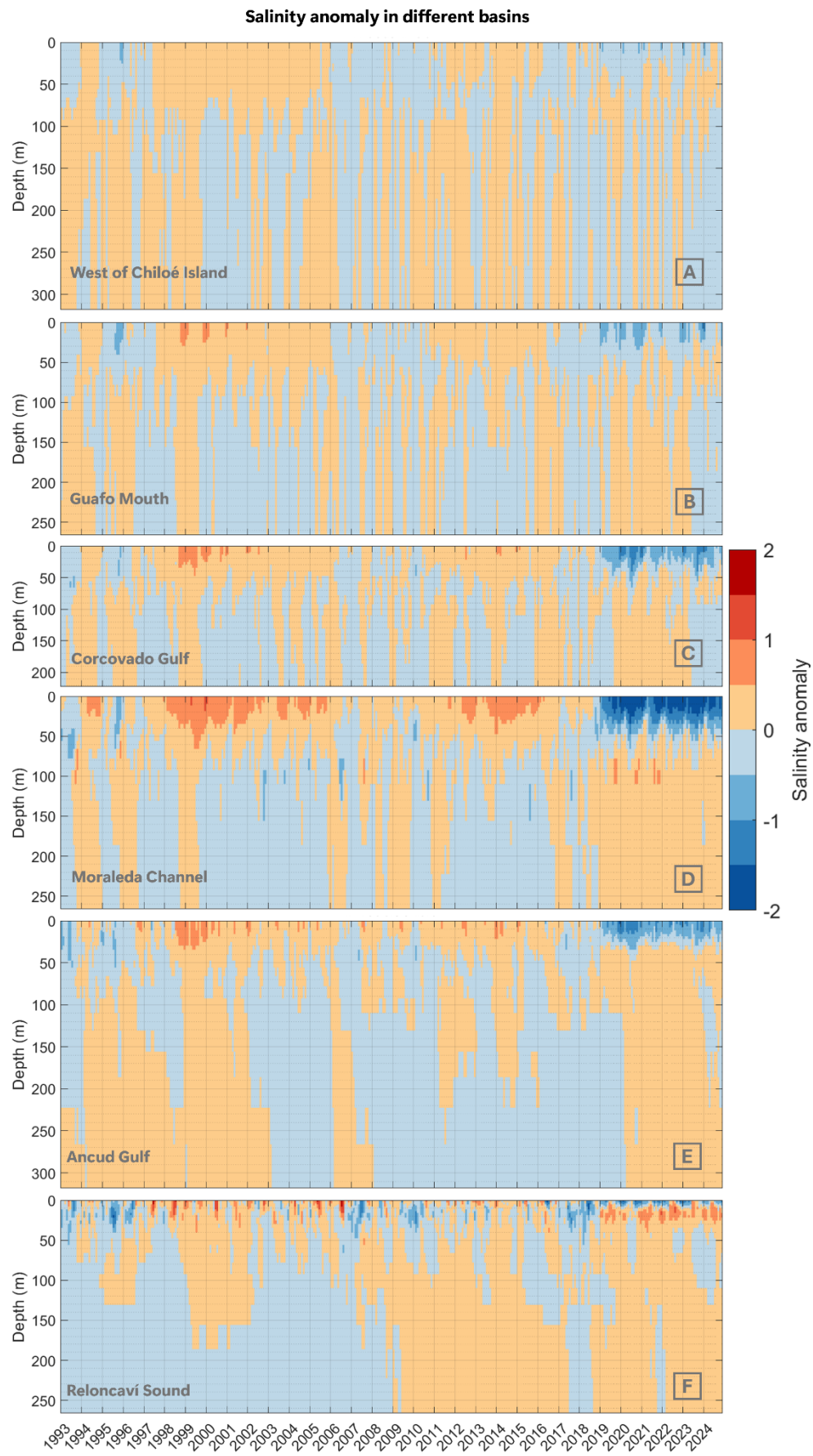
Figure 39: Salinity anomaly spatially averaged over west of Chiloé Island (A), Guafo Mouth (B), Corcovado Gulf (C), Moraleda Channel (D), Ancud Gulf (E) and Reloncaví Sound (F).
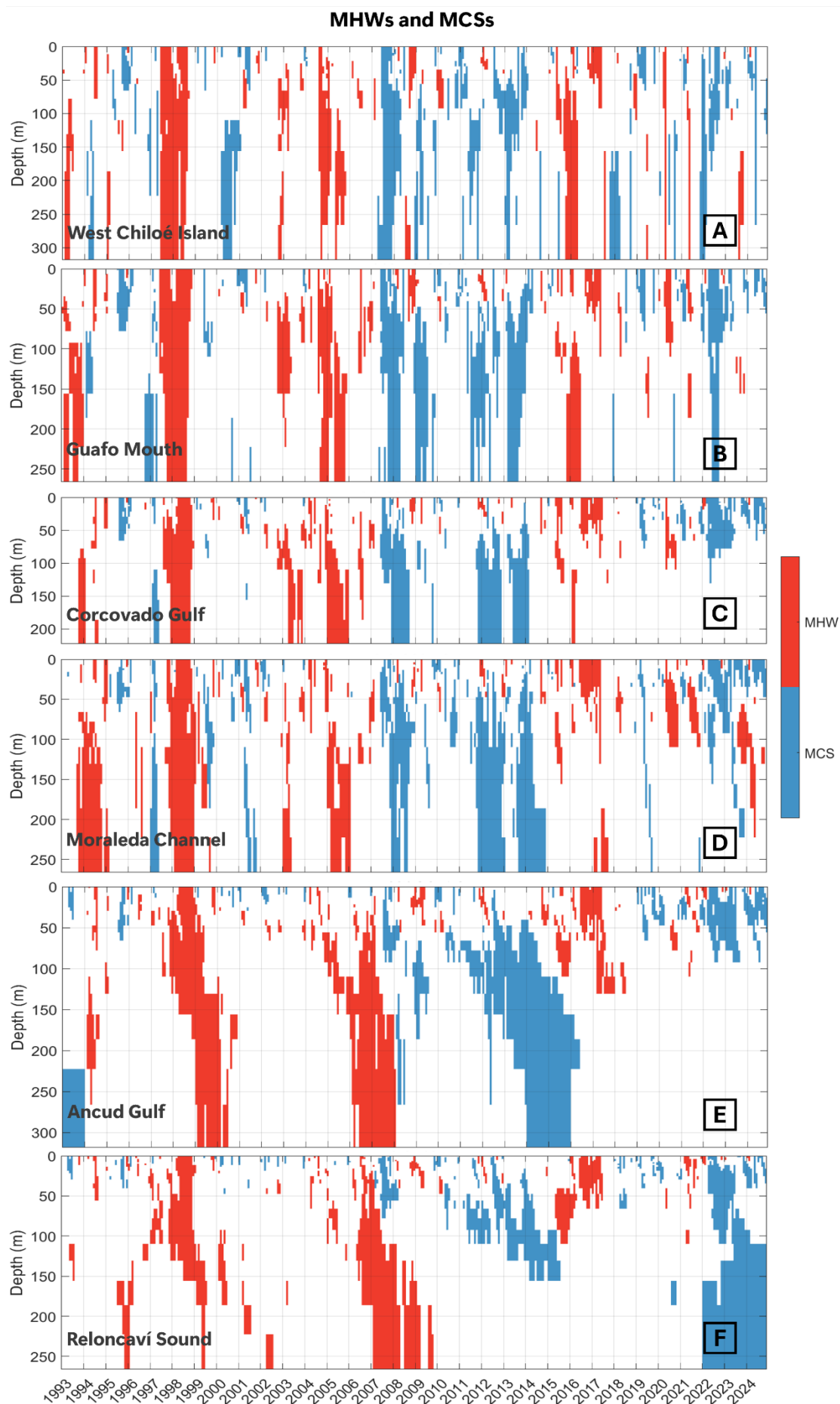
Figure 40: Vertical development of MHWs (red) and MCSs (blue) over time in west of Chiloé Island (A), Guafo Mouth (B), Corcovado Gulf (C), Moraleda Channel (D), Ancud Gulf (E) and Reloncaví Sound (F).

deeper layers towards the very end of that year. Below 150 m, the warming persisted from January 1999 until March 2000, indicating a delayed but prolonged subsurface response (Fig. 40E).

Other extended MHWs were also detected at subsurface in both Ancud and Reloncaví. For example, in Ancud Gulf, a prolonged warm event lasted from November 2005 to January 2008, while in Reloncaví, this event was delayed and started in May 2006 at the subsurface and lasted until April 2008. Another significant episode occurred between 2015 and 2017. Initially, this warm event was mostly confined to the subsurface in Guafo Mouth and pulsed at the surface by mid-2016. At the surface, it lasted from June 2016 until May 2017, and was mainly confined to the upper 50 m. It was at the surface and more generally in the upper layer, the longest MHW recorded (1 year), follow by the 1997-1998 event.

A contrasting cold phase occurred in 2007, with negative temperature anomalies giving rise to a significant MCS. This event encompassed the entire water column in offshore regions, as well as in Guafo Mouth, Corcovado Gulf and Moraleda Channel, starting in June 2007 and vanishing during the second half of 2008 according to the region (Fig. 40). In contrast, in Ancud Gulf and Reloncaví Sound, the negative anomalies remained largely restricted to the upper layers, and the resulting MCSs were limited to the upper 100 m. Other notable and persistent subsurface MCSs occurred during the years 2011 to 2014, only in the subsurface. In Corcovado Gulf, the events lasted from June 2011 to November 2012, and from March 2013 to February 2014. In Ancud Gulf, a particularly long-lasting MCSs developed in the subsurface, persisting for over two years between February 2013 and February 2016 at 175 m depth. The event progressively deepened over time, reaching the bottom layer in January 2014. At depths below 200 m, this cold anomaly continued from January 2014 to December 2015. A similar sequence of events was recorded in Reloncaví Sound, where disconnected MCSs were observed from surface to 150 m, showing partial resemblance to the patterns identified in Ancud. Another particularly long MCS was recorded in Reloncaví Sound, lasting for 3 years and maybe more as it reached our time limit, from January 2022 to December 2024, from 150 m to bottom. The MCS reached the surface as well sporadically but always very briefly. Winter 2022 shown the lowest temperatures recorded: 7°C in July and August from surface to 15 m depth in Moraleda Channel (Fig. 35). In the upper layers, mainly below the surface, sequences of MCS occurred between 2022 and 2024 in the entire Northern Patagonia, due to cold successive temperature anomalies.

Overall, both MHWs and MCSs are observed less frequently at depth compared to the surface. Nevertheless, while surface events tend to be shorter in duration, subsurface events tend are much longer, often persisting for several months of even years (Fig. 41). Quantitatively, the mean duration of both MHWs and MCSs remains relatively consistent in the upper 50 m, ranging between two and three months across all regions. Below 50 m depth, the duration of the events increases, particularly for MHWs. The longest MHW events are registered in Ancud Gulf where they last on average for more than 10 months between 200 and 300 m. It is notably due to the fact that deep MHWs were rare but particularly long. A similar pattern is seen for MCSs, with Reloncaví Sound registering the longest events at depth, with 36 months in duration. As in Ancud, this results from a unique very long event of prolonged MCSs rather than a high frequency of shorter events. Overall, it is possible to observe a disconnection between the first upper 50 m where the extreme events are 1.7 time more frequent than in the below layers. Events are on average two times longer below 50 m depth.
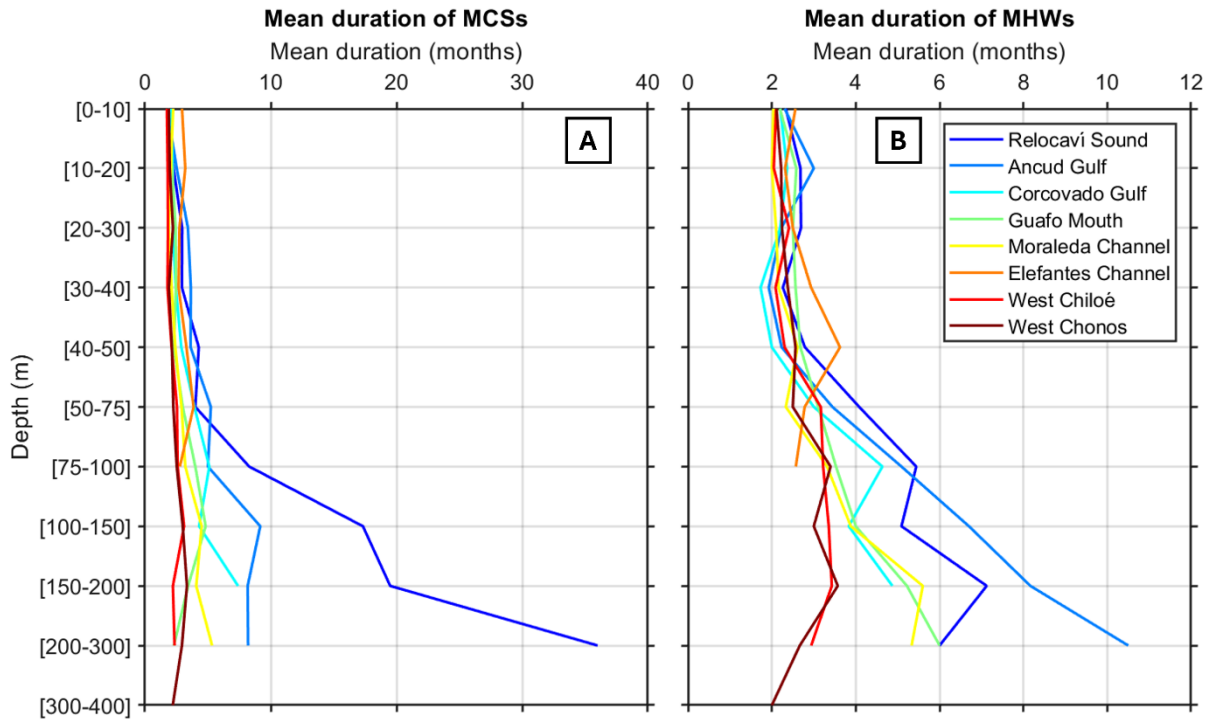
Figure 41: Average duration of MCSs (A) and MHWs (B) over certain depth ranges.

4.4. Discussion

4.4.1. Model

The results presented in this chapter are based on the CMEMS GLORYS12V1 reanalysis product, a global ocean model with a horizontal resolution of 1/12° (~8 km). While this dataset provides valuable insights into large-scale oceanographic variability, the interpretations of our findings depend on the inherent limitations of this dataset, particularly with regards of unique characteristics of Northern Patagonia.

One of the primary limitations is the model's spatial resolution, which is insufficient to resolve the intricate network of fjords and channels that define Patagonian Inner Seas. Although the model adequately captures the broader structure of the main basin, it cannot represent the smallest hydrographic features and fine-scale circulation patterns that are crucial for understanding the region's high spatial and temporal variability. These limitations are especially important in coastal and estuarine areas, where complex interactions between oceanic and freshwater processes occur. Although previous studies have demonstrated the performance of GLORYS12V1 in coastal environment (Amaya et al., 2023a), caution mut be exercised when applying the dataset to intricate regions. For example, although the product does incorporate net surface freshwater inputs (European Union-Copernicus Marine Service, 2018), it remains uncertain how accurately it captures the spatial and temporal variability of freshwater discharge in Northern Patagonia. Riverine inputs in this regions plays a critical role in shaping the upper water column through the formation of a distinct low-salinity surface layer known as the Estuarine Waters, that extends from several meters to a few tens of meters, having a strong impact on vertical stratification, mixing processes and the surface heat budget, and therefore affect the estimation of the temperature (Pérez-Santos et al., 2014; Sievers, 2008; Sievers and Silva, 2008). For example, (León-Muñoz et al., 2024) found a good correlation between GLORYS12V1 salinity and in situ observations in the northern sector of Northern Patagonia (Ancud and Reloncaví Sound), but

the model showed a reduced correlation and a tendency to overestimate salinity in the more intricate southern region (Moraleda and Elefantes Channels), which means that it underestimates the freshwater inputs of this region. In addition, some studies have highlighted the fact that GLORYS12V1 tends overestimate long-term warming trends (Lellouche et al., 2021), which in return might influence the intensity and duration of MHWs and MCSs. For example, (Sun et al., 2023b) shown that GLORYS12V1 overestimates surface MHWs while underestimating subsurface events in comparison to other models such as HYCOM which identify a greater number of subsurface events.

Another methodological consideration is the use of monthly averaged temperature data to calculate MHWs and MCSs. This approach highlights only the most persistent thermal anomalies and is therefore likely to miss shorter-lived events, which can still have ecological impacts (Jacox et al., 2020; Tanaka and Van Houtan, 2022). This lead for instance to an average duration of MHW and MCS events of 2 months at the surface, while Pujol et al. (2025) found that they last for 10 to 25 days on average, due to the fact that MHWs shorter than 1 month are not taken into account. Despite using a coarser temporal resolution, this approach is considered appropriate for characterising major basin-scale MHWs and MCSs, particularly in the subsurface, where temperature anomalies tend to develop and persist over longer timescales than surface (Cervantes et al., 2024; Jackson et al., 2018).

4.4.2. Large-scale climate modes

The occurrence of MHWs and MCSs in Northern Patagonia appear to be closely related to large-scale climate variability, particularly the ENSO. The strongest and most spatially extensive warming event in Northern Patagonia occurred during the 1997-1998 El Niño, which was in the top three of the most intense ever recorded (Huang et al., 2016). In Northern Patagonia, it triggered anomalous warming that extended trough the entire water column during at least 1.5 year in some regions, and a MHW that lasted for 1 year at depth (Fig. 34 and Fig. 40). Similarly, the 2015-2017 period, also associated with a very strong El Niño event (Huang et al., 2016; Santoso et al., 2017), gave rise to the longest-lasting surface MHW recorded over the period 1993-2024. While the warming at depth was generally less pronounced than for the 1997-1998 event, it nonetheless marked a prolonged period of surface ocean warming, and a surface MHW that lasted for one year. These results are consistent with broader patterns reported across the southeast Pacific Ocean, where positive ENSO phases are typically associated with enhanced ocean warming, driven by large-scale changes in wind regimes, reduced precipitations and weaker upwellings (Ancapichún and Garcés-Vargas, 2015; Garreaud, 2018b; Pujol et al., 2022).

In contrast, periods of strong negative temperature anomalies and MCSs in Northern Patagonia have coincided with La Niña events. For instance, the periods 2007-2008, 2010-2012 and 2020-2023 were characterised by both prolonged and intense MCS and some of the most intense La Niña events that occurred during the past decades (Boening et al., 2012; Hu et al., 2014; Li et al., 2023). These episodes led to significant MCSs, in some cases extending over the entire water column, as observed during the 2007-2008 MCS that lasted for 7 months below 150 m. The consecutive cold anomalies recorded between 2020 and 2024 in our study are very likely to be linked to different La Niña events, including the exceptional triple La Niña that occurred between 2020 and 2023 (Li et al., 2023). During La Niña phases, winds are enhanced, coastal upwellings are stronger, and precipitations are increased, all factors that can promote the vertical mixing and contribute to cool waters of Northern Patagonia (Ancapichún and Garcés-Vargas, 2015; Montecinos and Gomez, 2010; Rind et al., 2001).

4.4.3. Surface and Subsurface events

While it might be expected that the ocean surface would experience the most intense warmings and coolings, our results show that the strongest average temperature anomalies were actually found below the surface, particularly between 20 and 50 m depth. This findings aligns with recent research suggesting that subsurface MHWs can be stronger than their surface counterparts (Amaya et al., 2023b; Elzahaby and Schaeffer, 2019; Hu et al., 2021; Zhang et al., 2023).

Another key observation is the disconnection between surface and subsurface events. Surface MHWs and MCSs were generally more frequent and shorter than the other events below 50 m depth. This may correspond to the presence of Estuarine Waters, a buoyant, low-salinity surface layer that forms due to freshwater inputs. Due to its distinct density and stratification, this layer tends to limit vertical exchanges with underlying water masses, making it more sensitive to rapid atmospheric forcings such as winds, solar radiation and precipitations. Consequently, surface layer is more prone to short-duration thermal anomalies, whereas subsurface waters exhibit greater thermal stability.

Topography also plays an important role in shaping the distribution and development of extreme temperature anomalies in Northern Patagonia. For example, Desertores Islands act as a natural barrier, impeding the horizontal propagation of temperature anomalies at depth, limiting subsurface exchanges between the Pacific and the deeper parts of Ancud Gulf (Pinilla et al., 2021). Similarly, Reloncaví Sound has limited exchanges with Ancud Gulf, further restricting water exchanges. In contrast, some regions such as the open Pacific (west of Chiloé Island and Chonos Archipelago), Guafo Mouth, Corcovado Gulf and Moraleda Channel are very well connected and not separated by topographical features (Pinilla et al., 2019, 2021). This permits a facilitated water exchanges, leading to greater similarities and continuity in temperature anomalies and extreme events across these regions.

Greater persistence of MHWs and MCSs at depth underscores the thermal inertia of subsurface layers, reinforcing the importance of subsurface monitoring when evaluating the full extent and ecological impact of extreme thermal events (Cervantes et al., 2024; Jackson et al., 2018). This is particularly relevant in regions with complex stratification, such as Northern Patagonia, where the strongest anomalies are located just below the surface. Although the anomalous layers observed in this study was much thinner than in deeper oceanic regions (Elzahaby and Schaeffer, 2019), it holds significant implications for biological processes and for aquaculture.

Several MHWs and MCSs identified in this work correspond to events previously described in Pujol et al. (2022 and 2025). In particular, the years 1997 and 1998 were described by Pujol et al. (2022) as having the highest frequency of surface MHWs over the last 40 years, consistent with our results that show intense and widespread positive temperature anomalies during this period.

The MCSs of 2007 and 2008 were also recorded at the surface by Pujol et al. (2025) who described this period as a sequence of alternating cold and warm events: a MCS from May to December 2007, followed by a MHW in January-February 2008, another MCS from April through winter 2008, and then a second MHW from September 2008 to January 2009. Our analysis confirms this sequence and further reveals that the MCS events impacted most of the water column, lasting for one year at 75 m depth, with the exception of deeper layers in Ancud and Reloncaví Gulfs, where positive anomalies persisted below 100 m. The first MHW of early 2008 was also detected in our data but was confined to the upper 30 m (Fig. 36), consistent with the interpretation of (Pujol et al., 2025) who attributed the warming to increased solar radiation during a MCS dominant period. The shallowness of this event delimited by negative underlying anomalies probably contributed to its

rapid dissipation, quickly giving way to a new MCS, as suggested by both our data and (Pujol et al., 2025). The quick return of surface MCS conditions might be explained by the fact that the underlying negative anomalies never disappeared, and that increased winds have helped to the dissipation of the warm anomalies (Pujol et al., 2025). The second MHW, that peaked in December 2008, was likewise confined to the upper water column, between 30 m in the northern part and 70 m in the Guafo Mouth area. During this time, the mixed layer depth across Northern Patagonia was approximately 10 m, which may have favoured the development of intense but shallow warming, and why it was able to dissipate so rapidly.

The 2016 MHW event, also described by Pujol et al. (2022, 2025), was characterised as a particularly long-lasting event. Our results show that positive temperature anomalies were present almost continuously throughout the entire water column, except in the deeper layers of Ancud and Reloncaví Gulfs, where negative anomalies persisted. The extensive vertical reach of the warming likely contributed to the longevity of this MHW at the surface, acting as a thermal reservoir. However, the MHW itself remained confined to the upper layers and did not spread vertically as much as the 1997-98 event. This MHW was particularly important for Northern Patagonia as is was accompanied by drought, atmospheric heatwaves and harmful algal blooms (Garreaud, 2018b; León-Muñoz et al., 2018; Pujol et al., 2025).

By contrast, the brief but intense summer MHW of 2013, although reported by Pujol et al. (2025), was too short to be captured in our analysis, which is based on monthly averaged temperature data. Nonetheless, we did detect positive anomalies below 1°C in February 2013, mainly confined to the upper 30 m in most regions. This limited vertical extent and shallow development likely explain why the event was so short-lived and quickly dissipated.

In addition, particularly strong temperature anomalies were registered along the west coast of Chiloé Island during summer 2017. These anomalies may reflect a weakening of the upwelling system that typically develops in this area during austral summer (Narváez et al., 2019), therefore contributing to the MHW. This could help explain why the MHW reported by Pujol et al. (2022, 2025) reaching such intensity and extended so close to the coast of Chiloé Island. Conversely, in April 2008, a MCS was detected at both surface and subsurface, being particularly strong off Chiloé Island. This event coincided with strong northward winds (Fig. Sup. 1; Pujol et al., 2025), favourable to upwelling formation. The anomalies observed both at the surface and depth along Chiloé Island are therefore consistent with an intensification -or onset- of upwelling during a period that would normally be characterised by downwelling (Narváez et al., 2019).

4.4.4. Potential impacts on bottom ecosystems

MHWs pose a significant threat to both natural ecosystems and aquaculture in Northern Patagonia, particularly due to their increasing frequency, intensity and persistence in surface and subsurface (Pujol et al., 2025).

In aquaculture, salmon farming is especially vulnerable, as salmon cages typically extend from surface to 60 m (Ministerio de Economía, Fomento y Reconstrucción and Subsecretaría de Pesca, 2009), which coincides with the depth range where the most pronounced thermal anomalies are observed (Fig. 39). Atlantic salmon (*Salmo salar*), a key species in regional aquaculture (SUBPESCA, 2025), has a relatively narrow optimal growth temperature range of 12 to 18°C (Elliott and Elliott, 2010). Exposure beyond this range can lead to physiological stress, reduced growth rates, and increases susceptibility to diseases and pathogens (Calado et al., 2021; Hevrøy et al., 2012; Meng et al., 2022; Wade et al., 2019; Yáñez et al., 2017a). In recent years, innovative submersible

cage technologies have been tested in Chile, allowing the salmons to be relocated to deeper, cooler and more oxygenated waters during adverse conditions such as algal blooms or surface-confined MHWs (Glaropoulos et al., 2019; Salmonexpert, 2020b). Such adaptive systems may provide an effective mitigation strategy against the surface impact of MHWs and their associated consequences (Glaropoulos et al., 2019; Warren-Myers et al., 2024). Another species of aquacultural important, the native mussel *Mytilus chilensis*, is typically found in the subtidal zone, down to depths around 15 m (Molinet Flores et al., 2015; SUBPESCA, 2025). Although it is less directly affected by thermal temperature increases, the combined effects of warming and ocean acidification can affect their shell dissolution and their larval staged (Duarte et al., 2014; Navarro et al., 2016).

Chilean Patagonia supports over 1650 benthic species, with molluscs, cnidarians, annelids and sponges representing the groups with the highest biomass (Haüssermann and Försterra, 2009). Subsurface MHWs have the potential to severely affect benthic ecosystems, including cold-water coral communities. For instance, the cold-water coral *Desmophyllum dianthus,* distributed from shallow (7m) to deep waters (225m), has a thermal tolerance range of 4 to 17.5°C (Försterra et al., 2014; Jantzen et al., 2013; Naumann et al., 2013). In Comau Fjord's mouth, monthly averaged temperatures in the first 20 m reached 17°C during summers MWHs in 2017 and 2022, approaching the upper thermal tolerance of this species. Within the fjord which is naturally warmer than its mouth (Linford et al., 2024; Pujol et al., 2025), localised temperature spikes may have exceeded 18°C during intense short-lived events, posing a serious threat to survival. Elevated temperatures can increase coral metabolic rates while simultaneously depleting energy reserves, meaning that sustained warming could critically undermine their resilience and long-term viability (Beck et al., 2024; Chapron et al., 2021; Gómez et al., 2022).

Macroalgal forest, dominated in Northern Patagonia by the giant kelp *Macrocystis pyrifera,* also face increasing vulnerability. This foundation species, essential for coastal biodiversity and ecosystem structure (Almanza and Buschmann, 2013), lives in an optimal temperature range of 12 to 17°C. MHWs-induced temperature above these thresholds can affect the kelp's reproduction (Hollarsmith et al., 2020). Its upper thermal tolerance lies between 18°C and 25°C depending on local acclimatisation (Ladah and Zertuche-González, 2007; Le et al., 2022; Peters and Breeman, 1993; Solas et al., 2024).

The development of surface harmful algal blooms should also be feared, since MHWs are particularly favourable to their development and because Northern Patagonia is a harmful algal bloom hot spot (Díaz et al., 2019; León-Muñoz et al., 2018; Smith et al., 2021, 2023b). Indeed, blooms frequently occur during or shortly after MHWs, as for example in 1997, 1998, 2009, 2016 and 2017 (Chap. 5; Aguilera-Belmonte et al., 2013; Barría et al., 2022; León-Muñoz et al., 2018). In Northern Patagonia, harmful algal blooms can affect both shellfish and fishes, including *Mytilus chilensis* and the Atlantic salmon, two important species of Chilean aquaculture, having repercussions for human health in the form of intoxications and even death (Díaz et al., 2019; Yáñez et al., 2017a). This MHWs-harmful algal blooms compound have also lead to particularly important economic losses leading for instance in summer 2016 to the death of 24 million salmons, resulting in loss of US$800 million, closure of shellfish harvesting, and 4000 unemployed persons (Barría et al., 2022; Díaz et al., 2019; Yáñez et al., 2017a).

4.5. Conclusion

This study highlights the complex interplay between large-scale climate variability, local oceanographic dynamics, and the vertical structure of extreme thermal events in Northern Patagonia. ENSO-related variability seems to play a central role in modulating the most extreme events, by amplifying the duration, intensity and depth penetration of MHWs and MCSs. El Niño conditions tend to favour prolonged and widespread MHWs while La Niña phases are often linked to deep, persistent cooling events. Interestingly, the northern basins (Ancud and Reloncaví Gulfs) seem to be less affected by ENSO, suggesting a stronger influence of local processes in shaping their thermal extremes.

The vertical study of the development of MHWs and MCSs offers valuable insights beyond those obtained from surface-based analyses. Events that penetrate deeply into the water column tend to persist for months or even years, whereas those confined to the upper layers can develop rapidly, reach high intensities but generally dissipate quickly. This vertical structure not only controls the longevity and stability of surface anomalies but also has profound implications for ecosystem responses.

Along Chiloé Island, upwelling regime appears to play an important role in the formation of MHWs and MCSs. However, further research is needed to better understand how variations of upwelling influence the development and intensity of such extreme temperature events in that region.

Given the limitations of the CMEMS GLORYS12V1 global product used in this study (more particularly its inability to resolve the fjords, narrow channels and islands of the region), future research should focus on the development and use of higher-resolution regional models, capable of capturing the fine-scale processes unique to Northern Patagonia. This would allow to better represent the impacts of river discharge on local circulation, estuarine dynamics and complex bathymetry, in order to improve our capacity to understand and mitigate the impacts of extreme thermal events in this sensitive coastal environment, and improve the sustainability of aquaculture in Northern Patagonia. Indeed, in a context of increasing MHWs trends, local species and ecosystems are being more and more threaten by extreme thermal events, reaching for some species their upper thermal limits. Aquaculture production could also be threatened, as decreases in productivity could be expected due to the higher temperature.

CHAPTER 5.   MHWS AND *ALEXANDRIUM CATENELLA* BLOOM FORMATION

Foreword

The previous chapters introduce a novel high-resolution methodology designed to detect MHWs and MCSs at high resolution in the complex coastal environment of Northern Patagonia. This approach provided for the first time a detailed characterisation of the spatial and temporal dynamics of extreme thermal events within the intricate fjords and channels of the region, overcoming the limitations of coarse reanalysis data and satellite observations.

Building on this methodological framework, the present chapter examines how such extreme events can influence ocean properties and, in turn, affect ecosystems and human activities. A key parameter directly linked to ecosystem functioning is phytoplankton biomass. Although phytoplankton forms the base of the marine food web, some species can produce toxins, and when proliferating, leading to the formation of HABs. These events can disrupt marine biodiversity and have severe socio-economic consequences, particularly for aquaculture, which is a major activity in Northern Patagonia.

By applying the high-resolution detection of MHW, this chapter investigates the relationship between sea temperature anomalies, the occurrence of MHWs and the development of the dinoflagellate *Alexandrium catenella* in this highly dynamic coastal environment. The general objective is to improve our understanding of how MHWs can shape the occurrence of *Alexandrium catenella* blooms in such intricate ecosystems, providing crucial insights for the monitoring and management of the phenomena in the context of intense aquaculture.

This chapter was submitted to *Marine Pollution Bulletin* in September 2025.

5.1. Introduction

The Patagonian Fjord System has been identified as global "hotspot" of HAB events, among then species of the genus *Alexandrium*, *Dinophysis* and *Pseuso-nitzschia* (Díaz and Figueroa, 2023; Mardones, 2021). *Alexandrium* is one of the most important Harmful Algal Bloom (HAB) producing genera in the world, in terms of diversity, distribution and socio-economic and human health impacts (Anderson et al., 2012). In southern Chile, HABs of *Alexandrium catenella* -associated with Paralytic Shellfish Poisoning (PSP) due to the saxitoxins (STX) production- have been a recurrent problem since 1972, when the first episode of this species was recorded in the Magallanes region (Gúzman and Lembeye, 1975). In the Aysén region (44°S), Northwest (NW) Patagonia, the first records date back to 1992, generating important episodes from 1995 onwards, even reaching the Los Lagos (41°S) region during 2002 (Molinet et al., 2003) and Los Ríos region (39°45'S) in 2016 (Álvarez et al., 2019; Díaz et al., 2024; Hernández et al., 2016). Recently, vegetative cells in the water column and resting cysts in sediments of this toxic dinoflagellate were detected in the Bío-Bío region (37°S) confirming the rapid and worrying towards the north of Chile (Paredes-Mella et al., 2021; Rodríguez-Villegas et al., 2024).

PSP events have varied interannually, alternating years with little or rare occurrence to years with more than 1×10^6 cells L^{-1} of *A. catenella* and toxin concentrations of up to 30×10^3 µg STX eq. 100 g^{-1} flesh recorded in filter-feeders natural beds (Molinet et al., 2003). The high concentrations of PSP recorded in this area with a maximum toxicity in mussels *Mytilus chilensis* of 143×10^3 µg STX eq. 100^{-1} g in 2018 (Díaz et al., 2019), have caused serious effects on human health, resulting in the severe intoxication of >500 people, 37 of them with fatal consequences as of December 2024, in addition to significant economic losses (Barría et al., 2022; Díaz et al., 2019). Some authors suggest that such inter-annual trends in shellfish toxicity are associated with large-scale climate variability (Moore et al., 2009). In Chile Guzmán et al. (2002) and Molinet et al. (2003) suggested that events such as El Niño and the Antarctic Circumpolar Wave, respectively, could modulate the variation of HABs.

Marine heatwaves (MHW) are anomalously warm event observe in every ocean, lasting from at least 5 days to several weeks, sometimes months (Hobday et al., 2016). Their frequency and intensity have increased during the last decades, in relation to the global warming (Capotondi et al., 2024; Frölicher and Laufkötter, 2018). They alter environmental conditions by directly raising the temperature and enhancing stratification, causing severe impacts on the marine ecosystems (Holbrook et al., 2019). The impacts include mass mortality events, habitat loss following the die-off of key species such as kelp forests and coral reefs, shifts in species distribution, and economic repercussions for fisheries and aquaculture industries (Smith et al., 2023b).

By altering the environmental conditions, MHWs can also create favourable conditions for the onset and proliferation of HAB, which thrive in warm, stratified waters (Gobler, 2020; Trainer et al., 2020). The co-occurrence of MHWs and HABs have been recorded in different regions of the world (e.g., (Kuroda et al., 2021; Lim et al., 2021; McCabe et al., 2016), but not in Chile, although HABs and MHWs have been frequently reported independently (Díaz et al., 2024; Garreaud, 2018b; León-Muñoz et al., 2018; Pujol et al., 2022, 2025). These HAB events have devastating consequences, including the death of ~25 million aquaculture salmon with a total biomass of 40,000 tons, resulting in an estimated economic loss of 800 million US$ (Buschmann et al., 2016; León-Muñoz et al., 2018; Mardones, 2021).

The co-occurrence of MHWs and HABs have never been specifically studied in Northern

Patagonia. Although this region supports an important aquaculture industry of fishes (especially salmons) and shellfish (mussels), that are particularly sensitive to HABs (Díaz et al., 2019; Díaz and ueroa, 2023). This paper analyses the interannual trends in the occurrence and intensity of *A. catenella* events recorded in the NW Patagonia (Aysén and Los Lagos regions) between 2003 and 2023 and their relationship with hydroclimate anomalies, more particularly MHWs. Thus, warmer temperatures for longer time periods caused by climate change favour some HAB taxa and may be improving their competitive fitness over other non-harmful algal taxa (Gobler et al., 2017).

5.2. Material and methods

5.2.1. Study area

The fjord and channel system of the Northwest Patagonia is characterized by complex coastal morphology, including large bathymetric gradients and an irregular shoreline, that influence the circulation of oceanic water (Pickard, 1971). The water column stratification is determined by runoff from ice-melt in late spring (November–December), and by persistent rainfall (>3000mm/year) (Sauter, 2020). Rainfall is largely produced by synoptic systems (Pérez-Santos et al., 2019) and atmospheric rivers (Díaz et al., 2023a) embedded in the westerly wind belt that impinges upon southern Chile year-round (Aguirre et al., 2012; Saldías et al., 2019). On interannual time scales, climate in NW Patagonia is modulated by the El Niño Southern Oscillation (ENSO) and the Southern Annular mode (SAM) (Garreaud et al., 2013a).

Northern Patagonia is administratively divided into two regions: the region of Los Lagos from Reloncaví Sound to the south of Corcovado Gulf, and the region of Aysén from Moraleda Channel and top of Chonos Archipelago to the south of the study area (Fig. 42). At the northern section of Northern Patagonia, the Desertores Islands are one of the main geographic features that contribute to the transport and exchange of water masses within the Chiloé Inland Sea, in particular the exchange of freshwater between Gulf of Ancud and the Gulf of Corcovado (Strub et al., 2019). Meanwhile, in the southern section, the Moraleda Channel divides a highly stratified zone to the east, where the fjords (e.g., Pitipalena, Puyuhuapi, Aysen) are located, and a zone with high oceanic influence on the west, where the Los Chonos Archipelago is located. The entirety of the Northern Patagonia Inland Sea system is dominated by semidiurnal tides with amplitudes increasing from south to north, reaching up to 7 m in the Reloncaví Sound during spring tides. In contrast, the tidal range in the Guafo Mouth –the main connection of the fjords and channels of Patagonia to the Pacific Ocean– is approximately 2 m (Aiken, 2008).

5.2.2. Alexandrium catenella databases

Data on *Alexandrium catenella* cell densities at 234 sampling stations from inner sea of Northern Patagonia (Fig. Sup. 4) were obtained from monthly reports of phytoplankton distribution from the Fisheries Development Institute (IFOP) HABs Monitoring Programme. Under the framework of this program, integrated water-column samples for quantitative analyses of phytoplankton are collected with a dividable hose sampler from 0 to 10 and 10 to 20 m (Lindhal, 1986) and immediately fixed with acidic Lugol's solution (Lovegrove, 1960). For quantitative analyses of phytoplankton, 10 mL of the hose-samples are left to sediment overnight and analysed under an inverted microscope (Olympus CKX41) using the method described in Utermöhl (1958). To enumerate large but less abundant species, such as *A. catenella*, the whole surface of the chamber is scanned at a magnification of ×100, so that the detection limit is 100 cells L^{-1}. Monthly
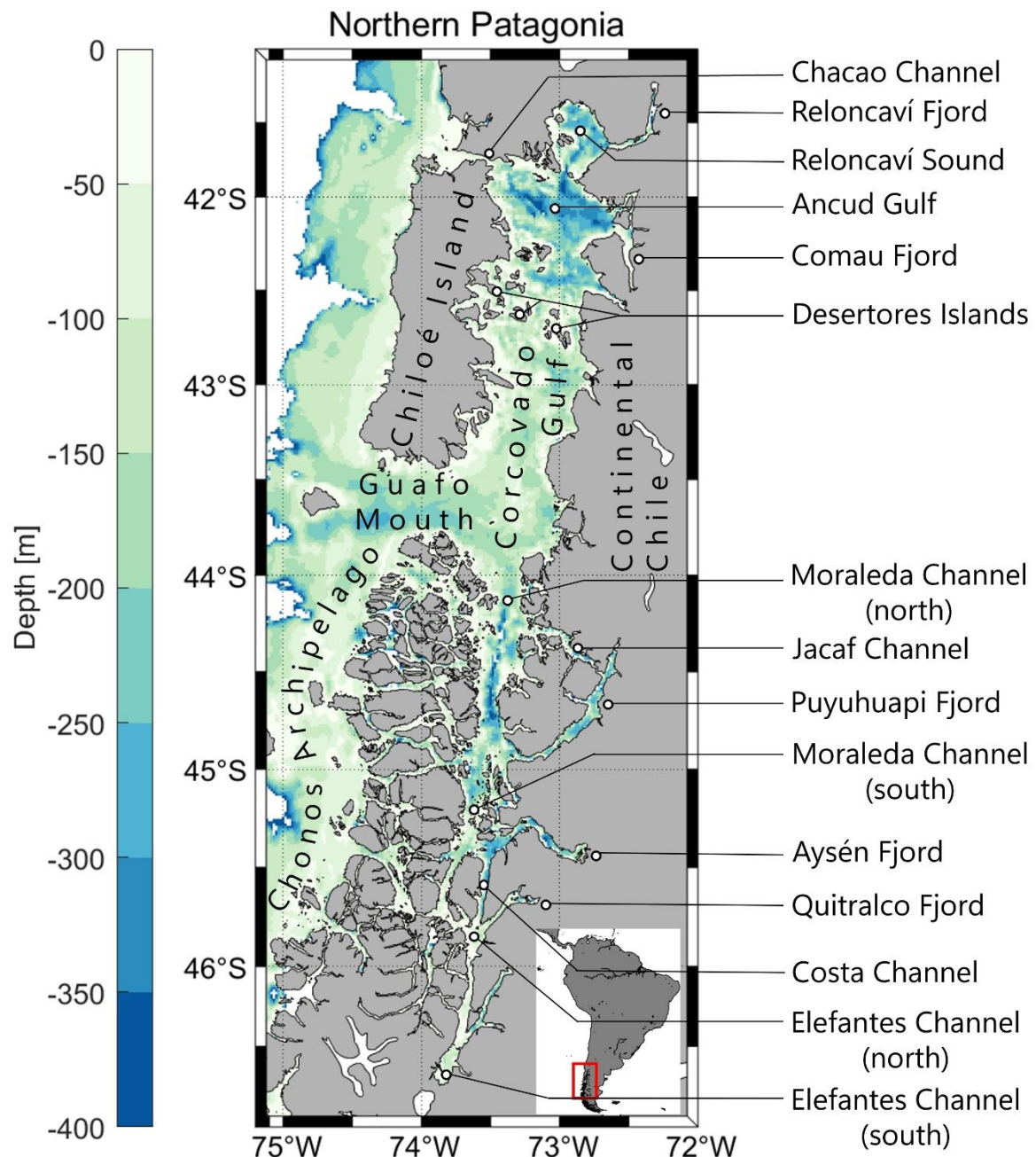
Figure 42: Map of the study area in the NW Patagonia. The scale bar shows the bathymetry. The main names sector used in the text were included.

A. catenella cell densities were analysed for every summer period (November to March) from the beginning of the monitoring program in 2006 to summer 2023.

To obtain better temporal resolution during *A. catenella* events, cell densities of this dinoflagellate collected at several sampling stations positioned within salmon farms along the coast of the inner sea of the Los Lagos and Aysén region (Fig. Sup. 4) were obtained from the Phytoplankton Monitoring Program (PROMOFI: Programa de Monitoreo de Fitoplancton) from January 2003 to December 2023. Under the framework of this program, Niskin bottles (2 L) were used to collect water samples from four depths (0, 5, 10, 15 m) for quantitative analyses of fish-killer species, including *A. catenella*. The preservation and analysis of the samples is identical to that described above.

5.2.3. Marine Heatwaves (MHWs) detection

MHWs are defined by Hobday et al. (2016) as anomalously warm events that persist for at least 5 days. An anomalously warm event occurs when the local sea temperature exceeds a threshold, typically the 90th percentile of a temperature dataset, for at least 5 consecutive days, with no more than two consecutive below-threshold days. The concept involves comparing local Sea Surface Temperature (SST) to a long-term climatology (Fig. 43).
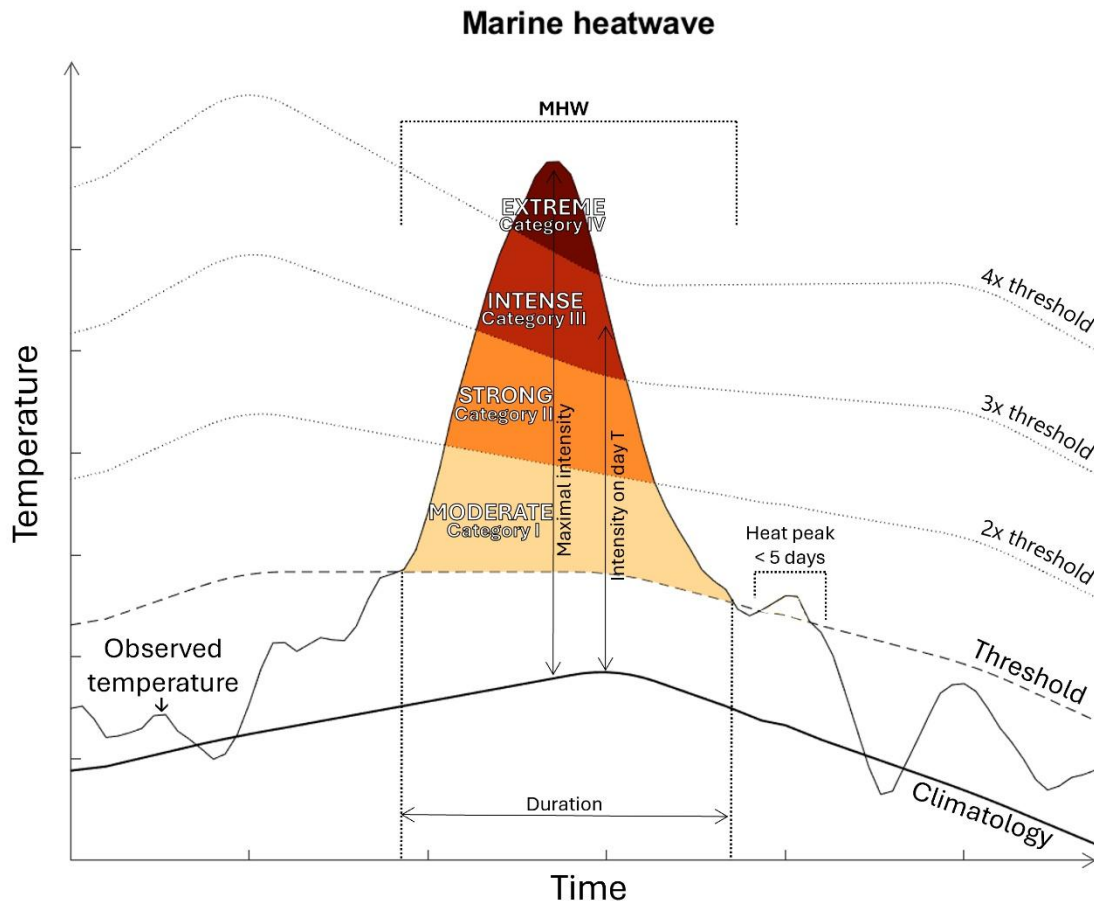
Figure 43: Description of a MHW and its principal metrics (duration, intensity and maximal intensity). Dash line represents the threshold, and bold line the climatology. The dotted lines represent multiples of the difference between the threshold and the climatology. The shades represent MHWs classification: moderate for category I, strong for category II, intense for category III and extreme for category IV.

MHWs are commonly characterised by several metrics: frequency (event/year), mean and maximal intensity (°C) and duration (days). In addition, MHWs are classified into category based on their intensity: a Category I (moderate) event has an intensity between 1 and 2 times the difference between the threshold and the climatology, Category II (strong) corresponds to 2 to 3 times the difference, Category III (intense) to 3 to 4 times, and Category IV (extreme) to 4 times and more (Fig. 43) (Hobday et al., 2018a).

The detection of MHWs generally relies on long-term satellite data Hobday et al. (2016), in order to capture long-term trend and decadal modes affecting sea temperature. Given the geographical complexity of Northern Patagonia, spatial high-resolution data are necessary to detect MHWs in the region's narrow channels and fjords. However, satellite products may be compromised by land-sea interferences and by the high precipitation associated with this region. Therefore, we

adopted the method described in Pujol et al. (2025) which involves using in situ data to calculate a long-term climatology at a suitable resolution for fjord environment, and to use satellite data to calculate the threshold.

We used the datasets for MHWs detection available on https://doi.org/10.5281/zenodo.14845077. Their climatology is based on *in situ* data collected between 1948 and 2022 and spanning -75.1°E to -72.0°E and -41.4°N to -46.7°N. They interpolated spatially and temporally these data using DIVAnd (Data-Interpolating Variational Analysis in n dimensions), a tool designed to interpolate sparse and inhomogeneous data into a continuous field, typically for generating climatologies (Barth et al., 2014; Troupin et al., 2010). The MHW threshold is based on the 90th percentile of daily temperature MODIS-AQUA satellite data, calculated over the period 2003-2023. Daily SST values used for comparison with the climatology were obtained from the same satellite dataset as the threshold. The SST anomaly (SSTa) was calculated by subtracting the climatology to the daily SST. All datasets have a resolution of approximately 900m, and we conducted the MHW detection at the sea surface from January 2003 to May 2023.

The MHWs detection was realised using the m_mhw Matlab toolbox developed by Zhao and Marin (2019). To represent the spatial extent of MHWs, we choose to illustrate the monthly maximal extent, and the highest category reached during each MHW event. This approach allows for a better comparison with the monthly phytoplanktonic distribution data. Therefore, this representation does not correspond to a single day's extent, nor does it reflect an average over the month, but well captures all pixels that were affected by a MHW during any moment of the month and assign every pixel the maximum category that occurred during that period.

5.3. Results

5.3.1. Temperature anomalies

The temperature anomalies in Northern Patagonia highlight relatively warm summers during the periods 2004 to 2009, 2013, 2016 to 2018, and 2022 (. 3). Notably, warm years include the year 2004 which experienced exclusively positive temperature anomalies, with 9 months showing anomalies exceeding +0.25°C. The years 2015 and 2016 also stand out, with 11 months of positive anomalies each; in 2016, 6 of those months recorded anomalies superior to +0.5°C. In 2020, 10 months exhibited positive anomalies, while the years 2003, 2017 and 2021 shown 9 months with positive anomalies. Conversely, the data also highlights particularly cold periods, including the particularly cold winter and spring of 2007, as well as the winters and springs from 2009 to 2013 and 2018. The winter of 2022 was the coldest, with temperature anomalies falling below -0.75°C for seven consecutive months. When examining the Los Lagos and Aysén regions separately, similar patterns emerge, with the same with the same cold and warm years standing out (Fig. 44).

5.3.2. Twenty years of marine heatwaves

Over the period 2003-2023, MHWs in Northern Patagonia exhibit subtle yet distinct regional patterns in terms of duration, frequency, and intensity. On average, these events persisted for 16 days. They tend to last longer in the Aysén region, with a mean duration of 18 days, compared to 15 days in the region of Los Lagos, suggesting a potential influence of regional oceanographic and/or climatic conditions that modulate MHWs persistence (Fig. 45). Despite their shorter duration, Los Lagos registered a higher mean frequency of events, with 1.7 event per year, while

Aysén region experienced an average of 1.4 event per year. Across Northern Patagonia as a whole, MHWs frequency is 1.5 event per year. In terms of intensity, MHWs' mean and maximal intensity was relatively consistent between the two regions. Aysén recorded the highest values, with a mean intensity of 1.06°C and a maximal intensity of 1.52°C, whereas Los Lagos registered a mean of 1.03°C and a maximal intensity of 1.47°C. Overall, MHWs in Northern Patagonia had a mean intensity of 1.05°C and a maximal intensity of 1.5°C.

When examining MHWs annual variability, certain years emerge as particularly significant in terms of frequency, duration and intensity. Overall, the year 2016 recorded the highest frequency of MHWs, with an average of 4.5 events, peaking at nearly 6 events in Los Lagos and 3.5 in Aysén (Fig. 45A). This was followed by 2004 with an average of 3 events and then 2017 and 2008 with 2.5 events each. In terms of duration, 2016 again stood out, with MHWs lasting an average of 29 days in NW Patagonia (Fig. 45B). The years 2017 (25 days), 2008 (21 days) and 2013 (20 days) followed. Notably, the average number of days under MHWs varied significantly between the regions of Los Lagos and Aysén, with Los Lagos experiencing far more prolonged events than Aysén (Fig. 45C). In 2016, the regional disparity was particularly stark: Los Lagos endured MHWs for an average of 60 days, compared with just 15 days in Aysén, resulting in an overall average of 35 days. The next most affected years were 2017 (17 days on average, 33 in Los Lagos and 7 days in Aysén), 2008
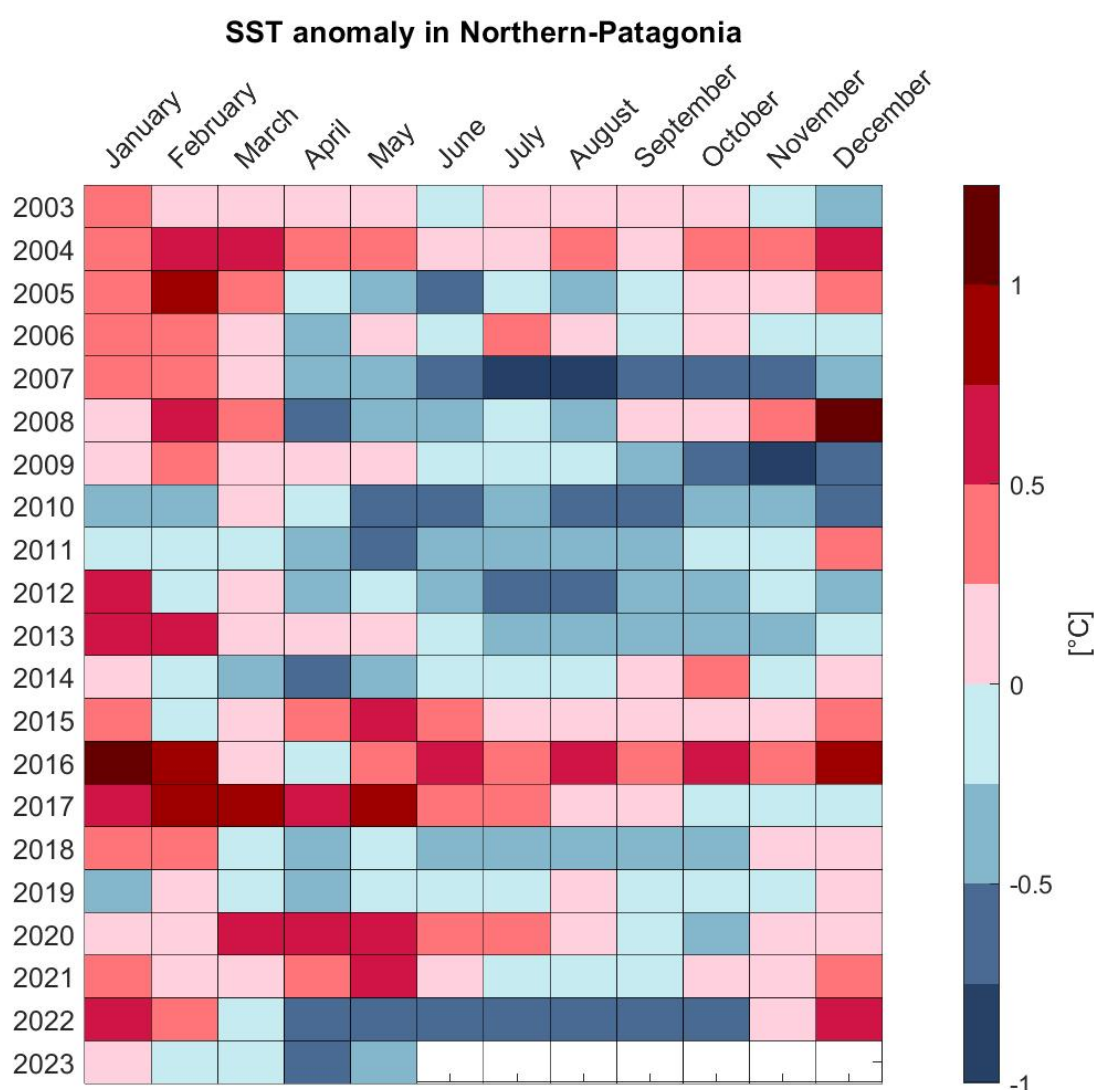
Figure 44: Monthly average SST anomaly (°C) for Northern Patagonia from 2003 to May 2023.

(15 days), and 2005 (10 days). Regarding intensity, 2008 was the most notable year, with an average MHW intensity of 1.3°C (Fig. 45D). This was followed by 2005, 2012, 2013 and 2023, all of which recorded mean intensities of around 1.2°C. By contrast, 2016 was not among the most intense years, averaging just 0.9°C. When examining maximal intensities, 2008 remained the most severe, with an average maximum of 2°C, ahead of 2005 (1.9°C), and then 2012, 2013 and 2016, all at 1.7°C (Fig. 45E). The maximal intensities reached by the strongest MHW observed are shown in Fig. Sup. 5.

When looking at MHWs spatial extent in Northern Patagonia, February was the month during which the greatest coverage, affecting on average of 41% of the region. This is followed by the month of January, during which on average 38% of Northern Patagonia is covered by MHWs, March (24%), December (22%) and November (11%). Independently, Los Lagos and Aysén Regions show similar patterns, with relatively comparable percentages.

To assess the broader regional impact of MHWs, their spatial extent was analysed monthly over the 245-months period from January 2003 to May 2023. This perspective highlights how widespread MHWs were across Northern Patagonia during each month (Table 4). Overall, MHWs exhibited limited spatial extent across most of the study period. In more than 150 months, MHWs -when present- affected less than 10% of Northern Patagonia. Notably, in 90 of these months, the spatial coverage was below 1%, indicating near-total absence of MHWs. By contrast, months in which MHWs reached a broader spatial extent were far less frequent. If a threshold of 10% spatial coverage is used to define a region-wide MHW, then Northern Patagonia experienced MHWs for 95 months out of the 245 analysed. However, only 32 months saw MHWs affecting more than half of the
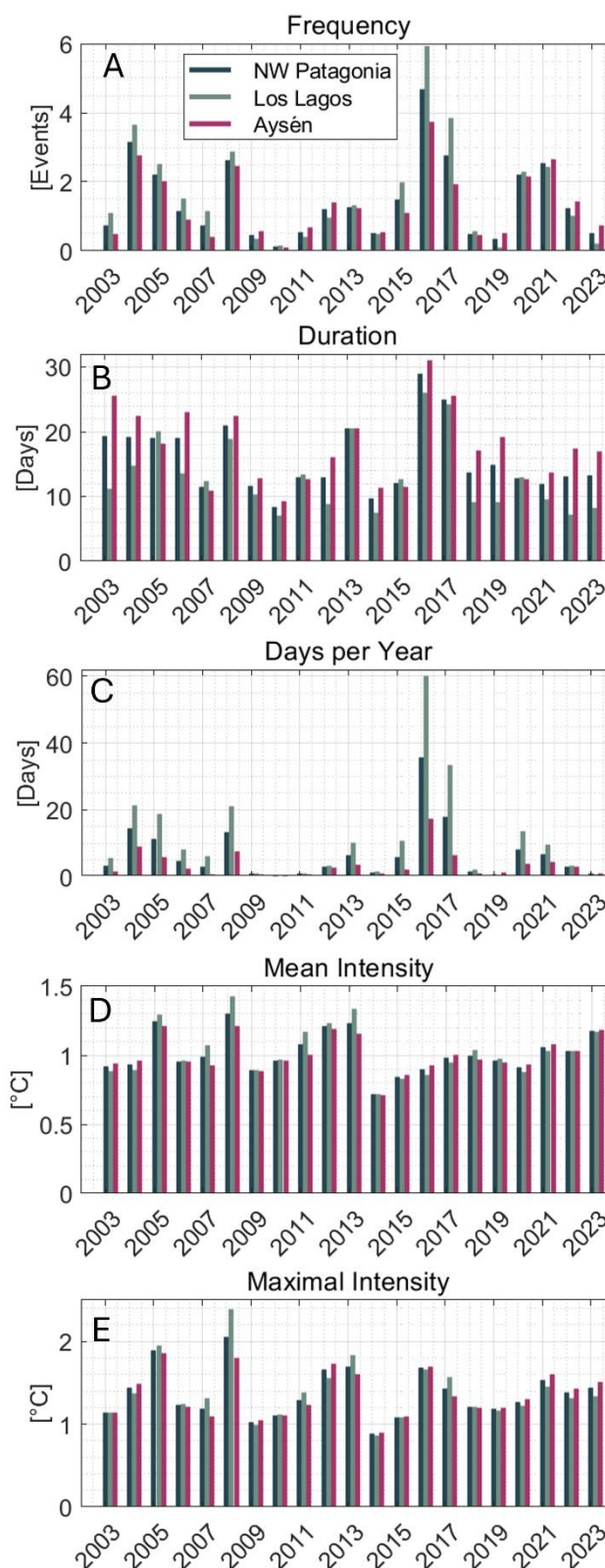
Figure 45: MHWs' average metrics for each year: Frequency (A), Duration (B), Days per year (C), Mean Intensity (D), Maximal Intensity (E). The regions analysed are represented in different colours: Northwestern Patagonia (black), Los Lagos Region (green), and Aysén Region (red).

region, and just 6 months recorded extreme events with over 90% spatial coverage. These findings suggest that, although MHWs occur regularly in Northern Patagonia, their spatial footprint is usually limited. Widespread events remain relatively rare over the two-decade period.

Table 4: Monthly spatial coverage (%) of MHWs in Northwest Patagonia over the 245-months period from January 2003 to May 2023. No data are available in December 2022. Values greater than 50% are highlighted in bold.

Year	Jan	Feb	Mar	Apr	May	Jun	Jul	Aug	Sep	Oct	Nov	Dec	Average (monthly)
2003	37.99	24.15	15.85	3.57	0.27	0.55	0.94	9.89	4.27	5.76	1.33	0.28	8.74
2004	28.75	**91.17**	**59.98**	23.97	17.8	29.6	0.72	21.4	12.96	45.87	29.09	43.03	33.7
2005	25.43	**94.74**	**71.34**	1.73	0.85	0.93	0.37	0.32	1.65	7.6	23.97	**76.66**	25.47
2006	**53.18**	**55**	5.67	0.16	0.59	1.84	9.58	9.07	1.32	3.98	0.87	5.39	12.22
2007	**57.16**	41.04	7.93	0.45	0.86	0.04	0.04	0.01	0.04	0	0	8.59	9.68
2008	**89.11**	**91.3**	47.59	1.24	0.77	0.82	1.12	1	21.79	22.07	33.18	**92.07**	33.51
2009	8.89	18.17	10.45	2.13	1.86	1.43	0.61	0.2	0.19	0.2	0.12	0.24	3.71
2010	7.3	1.44	2.01	0.1	0	0.01	0.02	0.09	0.2	0.77	0.59	2.16	1.22
2011	4.69	8.65	11.58	0.05	0.12	0.15	0.28	0.32	0.28	0.52	0.46	25.24	4.36
2012	**73.36**	1.79	3.12	0.29	0.31	0.33	0.02	0	0.02	0.66	0.19	0.64	6.73
2013	**78.07**	**87.31**	8.87	6.53	4.55	0.63	0.07	0.08	0.11	0.46	0.2	18.79	17.14
2014	4.35	4.76	3.3	0.01	0.03	0.11	0.39	1.46	26.44	18.99	0.07	0.51	5.04
2015	29.49	14.68	6.76	2.83	20.88	32.03	6.45	35.87	27.96	5.44	34.85	25.38	20.22
2016	**96.1**	**95.78**	27.28	10.7	**56.21**	**74.24**	36.46	**85.62**	**72.5**	**84.56**	**62.92**	46.67	62.42
2017	**59.64**	**72.57**	**89.74**	**87.77**	**61.76**	41.14	19.32	27.46	2.2	1.41	1.38	3.91	39.03
2018	31.78	17.74	12.69	0.26	0.53	3.96	0.44	0.22	0.21	0.3	1.82	4.74	6.22
2019	0.69	11.11	0.39	0.31	0.69	1.31	1.03	1.75	2.72	0.84	0.99	1.47	1.94
2020	21.98	3.87	**53.9**	**51.92**	31.82	15.45	27.3	26.85	0.61	0.11	11.73	26.3	22.65
2021	34.19	**57.85**	19.29	19.96	20.03	16	0.61	20.54	0.83	18.69	6.18	**71.18**	23.78
2022	33.32	**58.88**	49.01	0.05	0.25	0.36	0.33	0.1	0.12	0.16	15.38		13.16
2023	25.01	6.75	3.54	0.7	2.67								7.73
Average (2003-2023)	38.12	40.89	24.3	10.23	10.61	11.05	5.31	12.11	8.82	10.92	11.27	22.66	17.1

When examining the Los Lagos and Aysén regions separately, similar patterns are observed; however, Los Lagos shows a tendency toward more extreme coverage. In Los Lagos, MHWs affecting more than 90% of the region occurred during 11 of the 245 months analysed, compared to only 4 months in Aysén. Likewise, extreme absence of MHWs (defined as spatial coverage below 1%) was more common in Los Lagos, occurring 113 months, whereas Aysén recorded 72 such months. Moderate spatial extent was typical in both regions: MHWs covered less than 10% of the region in 150 months in Los Lagos and 149 months in Aysén. Conversely, more extensive events where MHWs affected more than 50% of the region were recorded in 34 months in Los Lagos and 29 months in Aysén. Coverage exceeding 70% occurred during 21 months in Los Lagos and 19 months in Aysén.

5.3.3. MHWs and Alexandrium catenella

The analysis of co-occurrence between MHWs and the proliferation of *A. catenella* generally reveals a positive correlation. During summers 2008, 2009, 2016 and 2017, an increase in cell density was observed during or shortly after a MHW. Conversely, in summers 2014, 2015 and 2018, cell density increased in the absence of major MHW but coincided with positive anomaly of Sea Surface Temperature (SSTa). Minor MHWs were however detected in Aysén region during those summers before the development of the blooms. These observations suggest that surface temperature plays a major role in blooms dynamics, and that MHWs may contribute to the

Figure 46: Range of cell density (cell L-1) of Alexandrium catenella (A-E) and maximal extension and category of MHW (F-J) for the months of November (A, F) and December (B, G) 2008, January (C, H), February (D, I), and March (E, J) 2009.

initiation or intensification of *A. catenella* blooms.

In contrast, years without MHWs did logically not exhibit any notable increase of cell density, as for summers 2010, 2019 and 2020. This supports the idea that the absence of significant thermal stress is generally associated with lack of proliferation. However, this correlation is not consistent across all years. For instance, MHWs were recorded in summers 2012, 2013, 2022 and 2023, but no increase of *A. catenella* cell density was detected. This indicates that MHWs alone are not sufficient to trigger blooms, and that other environmental factors likely influence bloom development.

The year 2007 is particular as high cell densities were registered as early as November (superior to 5,000 cells L^{-1}, and locally superior to 50,000 cells L^{-1}). Due to insufficient *A. catenella* data, no reliable analysis can be conducted for summers 2011 and 2021.

It is also worth noting that no *A. catenella* blooms were reported during summers dominated by negative SSTa. The most intense blooms (2008, 2009, 2018) were associated with either significant MHWs or short periods of strong positive SSTa resulting in brief MHWs. These results highlight the complexity of environmental drivers behind *A. catenella* blooms, and in particular the importance of considering both SST, SSTa and MHWs for a better understanding of bloom dynamics.

The following sections examine selected key years in more details, focusing on the co-evolution of SSTa, MHWs and the presence or absence of *A. catenella* blooms.

5.3.4. Bloom occurrence following MHW events

To better understand the mechanisms underlying the co-occurrence of MHWs and *A. catenella* blooms, the following section focuses on the years 2009 and 2016 where a bloom clearly followed the development of a MHW.

Summer 2009 experienced very strong bloom of *A. catenella* (Fig. 46). The microalgae were already present in the entire Aysén Region in December 2008 in relatively low cell densities, generally below 500 cells L^{-1} and occasionally between 501 and 5,000 cells L^{-1}. By February, *A. catenella* had proliferated significantly, particularly in the southern part of Aysén Region, with cell densities between 50,000 and 500,000 cells L^{-1}, and exceeding 500,000 cells L^{-1} at one station located close Costa Channel (Fig. 46D). These high cell densities persisted through March in Elefantes, Costa and Moraleda Channels, as well as in Chonos Archipelago. *Alexandrium catenella* was also detected in the Puyuhuapi Fjord and Jacaf Channel but the cell densities were below 5,000 cells L^{-1}. No presence of *A. catenella* was detected in Los Lagos Region. Unfortunately, IFOP monitoring program during summer 2009 was inconsistent: November 2008 was not sampled at all, Aysén Region was not sampled in January 2009, and in February data availability was limited in the entire study area. However, PROMIFI monitoring programme recorded *A. catenella* cell densities at higher frequency (Fig. 47). The first report from these monitoring programmes was on 15 January, and an exponential growth started on 26 February. The maximal cell density was recorded on 9 March, reaching 3,402 × 10^3 cells L^{-1}. Subsequently, cell densities declined progressively until the end of March (Fig. 47A).

Summer 2009 also witnessed early MHW activity (Fig. 46), which began in November 2008 in some channels of Chonos Archipelago, where it immediately reached category III status, and around Desertores Islands. By the end of the month, the MHW had spread across the entire study area, intensifying to category II and III in Los Lagos Region and Chonos Archipelago. It reached

peak intensity by mid-December ([Fig. S5](#)), with SSTa of at least +1.5°C everywhere (corresponding to an absolute temperature of 13°C in Moraleda Channel), exceeding 2.5°C in southern Ancud and Corcovado Gulf, and Puyuhuapi Fjord, and surpassing +3°C in western Ancud Gulf and Reloncaví Sound (respectively a temperature of 14°C and 17°C). The average SST in Aysén Region was between 12.5°C and 13°C ([Fig. Sup. 6](#)). In December, the MHW was covering 91% of Northern Patagonia ([Table 4](#)). The MHW progressively faded, except in Chonos archipelago and around Desertores Islands where it subsisted until end of December. From January to March, positive temperature anomalies continued in Chonos Archipelago, Moraleda Channel, Jacaf Channel and Puyuhuapi Fjord, reaching +1°C in the different channels and fjords east of Chonos Archipelago. Nonetheless, the few MHWs present in February and March were limited in extend and duration, and sporadic in occurrence.
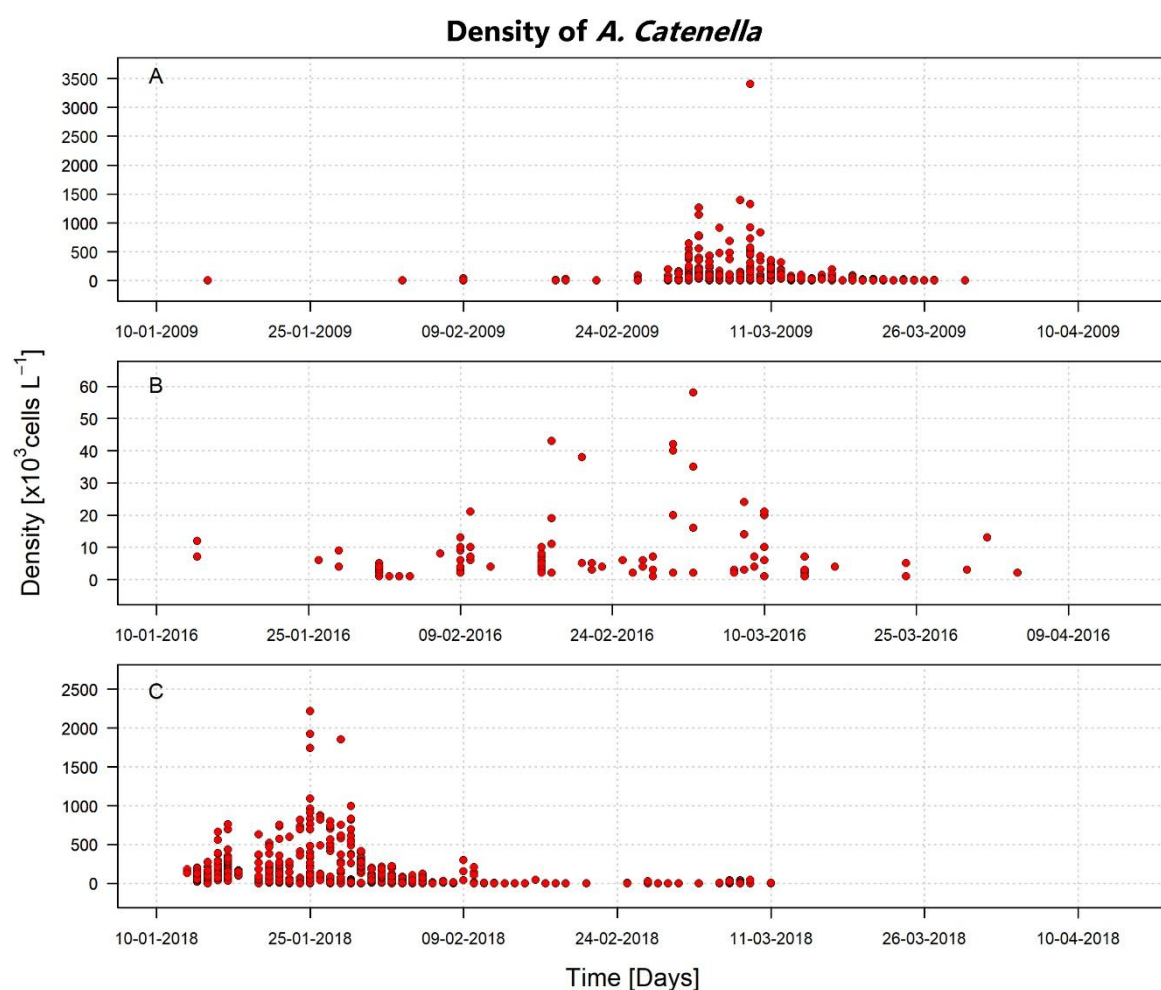
Figure 47: Reported presence of Alexandrium catenella in cell density (x10³ cell L-1) in different stations of Northwestern Patagonia for summers 2009 (A), 2016 (B) and 2018 (C).

Summer 2016 was also marked by an intense *A. catenella* bloom ([Fig. 48](#)). Early presence of the microalgae was recorded by November 2015 in Aysén Region only, with low cell densities (below 500 cells L^{-1}). Cell density gradually increased over summer, reaching in January values between 500 and 5,000 cells L^{-1} in northern Chonos Archipelago, Moraleda Channel and Puyuhuapi Fjord; higher cell densities in Jacaf Channel ranged between 5,000 and 50,000 cell L^{-1}, while the head of Puyuhuapi Fjord peaked between 50,000 and 500,000 cell L^{-1}. In February, the bloom extended northward, reaching the southern coasts of Chiloé Island. Almost every station in Aysén reported cell densities exceeding 500 cell L^{-1}. By March, cell densities have declined, falling below 5,000

cell L^{-1} everywhere except at two stations, one in western Chono Archipelago and the second at the entrance of Jacaf Channel.

When looking at the development of the bloom at higher temporal resolution, event showed an increase in cell densities from 26 January to 3 March, with a peak on that day of 5,800 cells L^{-1} followed by a gradual decline (Fig. 47B).
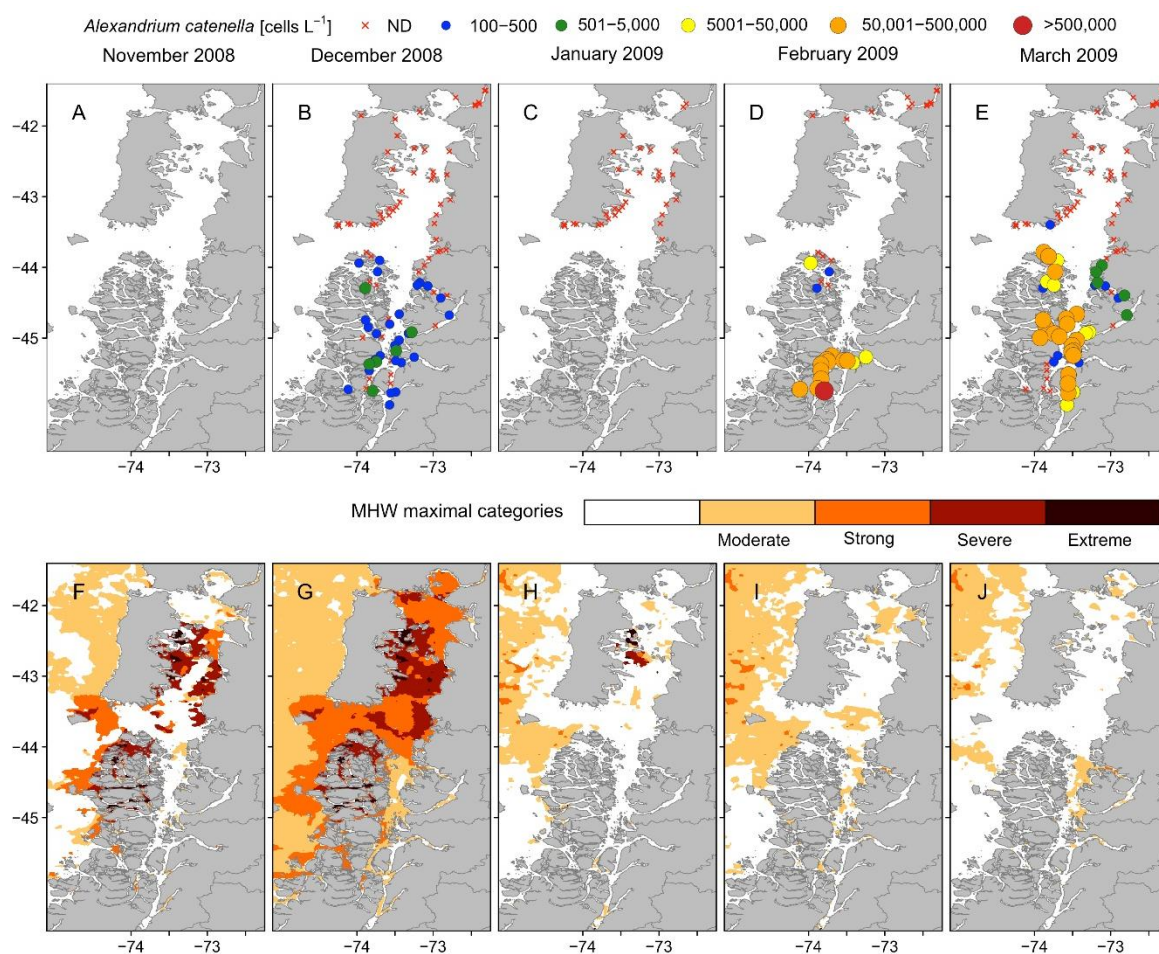

Figure 48: Range of cell density (cell L-1) of Alexandrium catenella (A-E) and maximal extension and category of MHW (F-J) for the months of November (A, F) and December (B, G) 2015, January (C, H), February (D, I), and March (E, J) 2016.

In summer 2016, MHW activity was already evident by November 2015 around Desertores Islands, Chonos Archipelago, Moraleda Channel, and Puyuhuapi and Aysén Fjords. Although it weakened in December, it persisted in some channels of Chonos Archipelago (Fig. 48F). In November and December, temperature anomalies were positive almost all the time. The MHW pulsed again in January 2016 around Desertores Islands and in Chonos Archipelago (category II), expanding to cover entirely the study area from mid-January to February. On average, the MHW covered 96% of the region in January and 95% in February (Table 4). During this peak phase, temperature anomalies exceeded +1°C everywhere, and +1.5°C around Desertores Islands, Reloncaví Sound, Chonos, Moraleda and Jacaf Channels, and the Comau, Puyuhuapi and Aysén Fjords (Fig. S5). Anomalies above +1.5°C were also recorded offshore in the open ocean. It corresponds for instance to a SST of 12°C in Chono Archipelago, 13°C in Moraleda Channel and 16°C in Puyuhuapi Fjord (Fig. Sup. 6). The average temperature in Aysén Region in January, was for instance of 13.5°C. By late February, the event started to recede, though it persisted into mid-

March in northern Chonos and southern Desertores, and until early April in King Channel (Chonos Archipelago).

5.3.5. Strong bloom, minor MHWs

In some years, *A. catenella* blooms have occurred despite the absence of major MHW, suggesting that positive SSTa alone may be sufficient to initiate bloom events. The following section examines such a case in detail.

Summer 2018 was also notably affected by the development of an intense *A. catenella* bloom in Aysén Region (Fig. 49). The bloom developed progressively, with in November no or low presence of *A. catenella*, increasing in December reaching between 5,000 and 50,000 cells L^{-1} in Puyuhuapi Fjord and Jacaf Channel. In January, *A. catenella* had bloomed in the entire region, even spreading to the southern coast of Chiloé Island. The entire southern part of Aysén Region recorded cell densities between 50,000 and 500,000 cells L^{-1} (Fig. 49C). In the northern part of Aysén Region, cell densities varied between 5,000 and 50,000 cells L^{-1}. One station in the southern Chonos Archipelago registered values superior to 500,000 cells L^{-1}. Cell densities then decreased progressively in February, with the highest values observed in Moraleda Channel. By March, cell densities had dropped to bellow 5,000 cell L^{-1} across the entire region. Data from the PROMOFI monitoring programme evidenced *A. catenella* high cell densities from 16 January, with a sharp

Figure 49: Range of cell density (cell L-1) of Alexandrium catenella (A-E) and maximal extension and category of MHW (F-J) for the months of November (A, F) and December (B, G) 2017, January (C, H), February (D, I), and March (E, J) 2018.

rise to a maximum of $2{,}216 \times 10^3$ cells L^{-1} on 25 January ([Fig. 47C](#)). After this peak, cell densities dropped below the levels recorded on 16 January and remained low until 11 March ([Fig. 47C](#)).

November 2017 shown mostly negative temperature anomalies, and reverse in December, being superior to 0.5°C in Moraleda Channel, and superior to 1°C in Puyuhuapi and Aysén Fjords, as well as in Jacaf Channel. SSTa are higher in early January, being superior to 1.5°C in Moraleda Channel. The temperature anomaly, although lower, maintained during January and February and finally become newly negative in March. In January, when the bloom peak was observed, average SST was around 12°C ([Fig. Sup. 6](#)). Although the presence of positive anomalies, MHWs were still minor and localised in certain channels and Fjords ([Fig. 49F-J](#)). They started to pulse in some Channels of Chonos Archipelago (where the highest *A. catenella* values will be found later), Puyuhuapi and Aysén Fjords in December, and another MHW developed in January between Desertores Islands and Moraleda Channel. It however was relatively short, except in the southern part of Moraleda Channel where the MHW maintained until March.
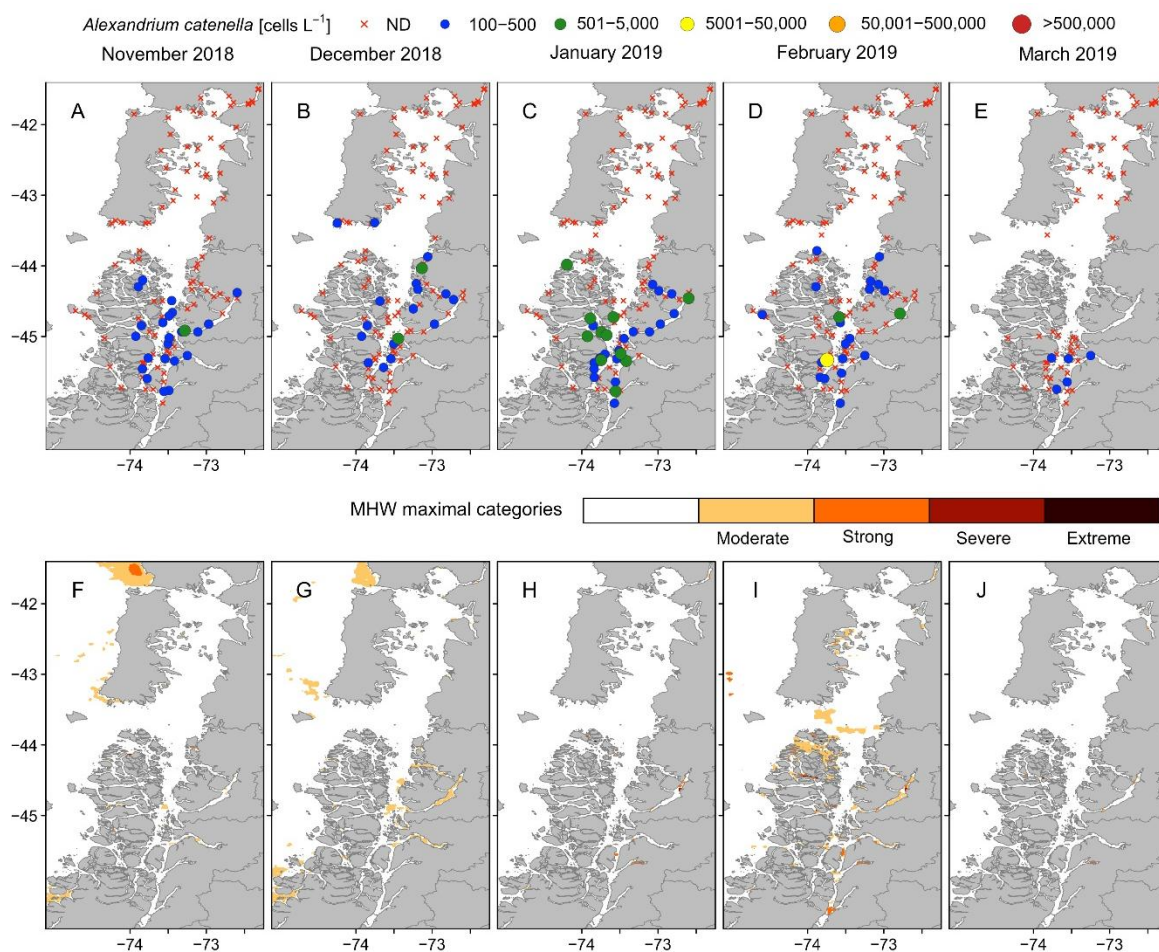
Figure 50: Range of cell density (cell L-1) of Alexandrium catenella (A-E) and maximal extension and category of MHW (F-J) for the months of November (A, F) and December (B, G) 2018, January (C, H), February (D, I), and March (E, J) 2019.

5.3.6. Absence of blooms in the absence of MHWs

Not all years were marked by bloom activity or thermal extremes. This section focuses on those quieter periods, where lack of MHWs coincided with the absence of *A. catenella* proliferation.

Summer 2019 experience a continuous weak cell densities of *A. catenella* in the Aysén Region,

with values generally remaining bellow 500 cells L^{-1} (. 9A-E). While localised areas did experience densities exceeding 500 cells L^{-1}, the conditions insufficient to classify the event as a bloom. By March, *A. catenella* was absent from the whole region, except for Costa Channel, the entrance of Aysén Fjord and at the far southern of Moraleda Channel.

After summer, the year 2018 did not experience any major MHW. In fact, temperature anomalies were predominantly negative. In December 2018, weak and sporadic MHWs appeared in Moraleda and Jacaf Channels, as well as in Puyuhuapi and Aysén Fjords (Fig. 50G). These events were associated with temperature anomalies of 0.5°C to 1°C in Moraleda Channel and up to 3°C in Puyuhuapi Fjord and lasted only a few days. January 2019 experienced mostly negative temperature anomalies, although some sparse and week MHWs occurred in Elefantes and Costa Channels, in northern Chonos Archipelago, and in Puyuhuapi, Aysén and Quitralco fjords (Fig. 50H). Although some of these events persisted locally for up to two weeks, they remained highly confined and did not extend beyond the channels or enclosed areas in which they originated. Overall, the months of December, January and March were free of MHW in Northern Patagonia.

Summer 2020 was characterised by the almost entire absence of *A. catenella* (Fig. 51). Indeed, most of Northern Patagonia did not register its presence, except in a few locations within the Aysén Region, where values remained below 500 cells L^{-1} from November to February (note that
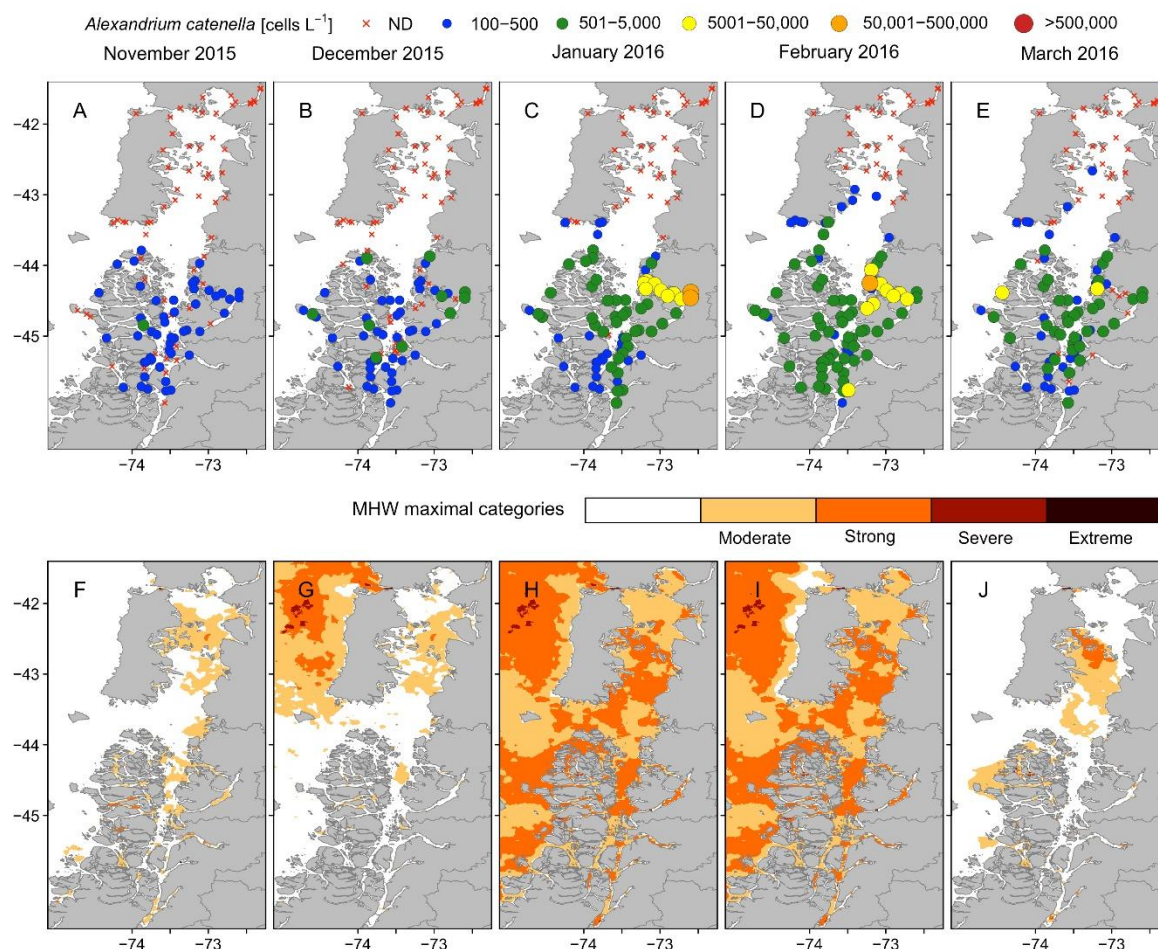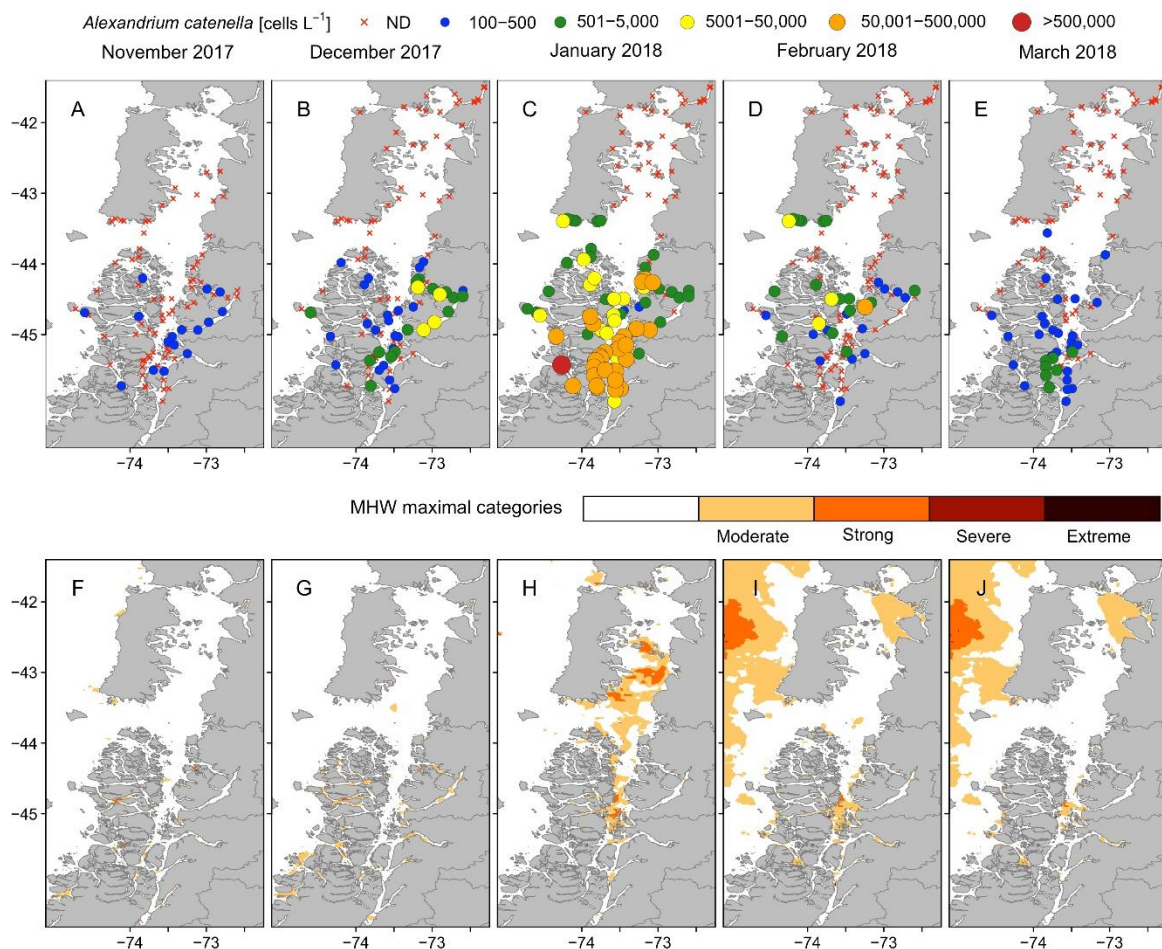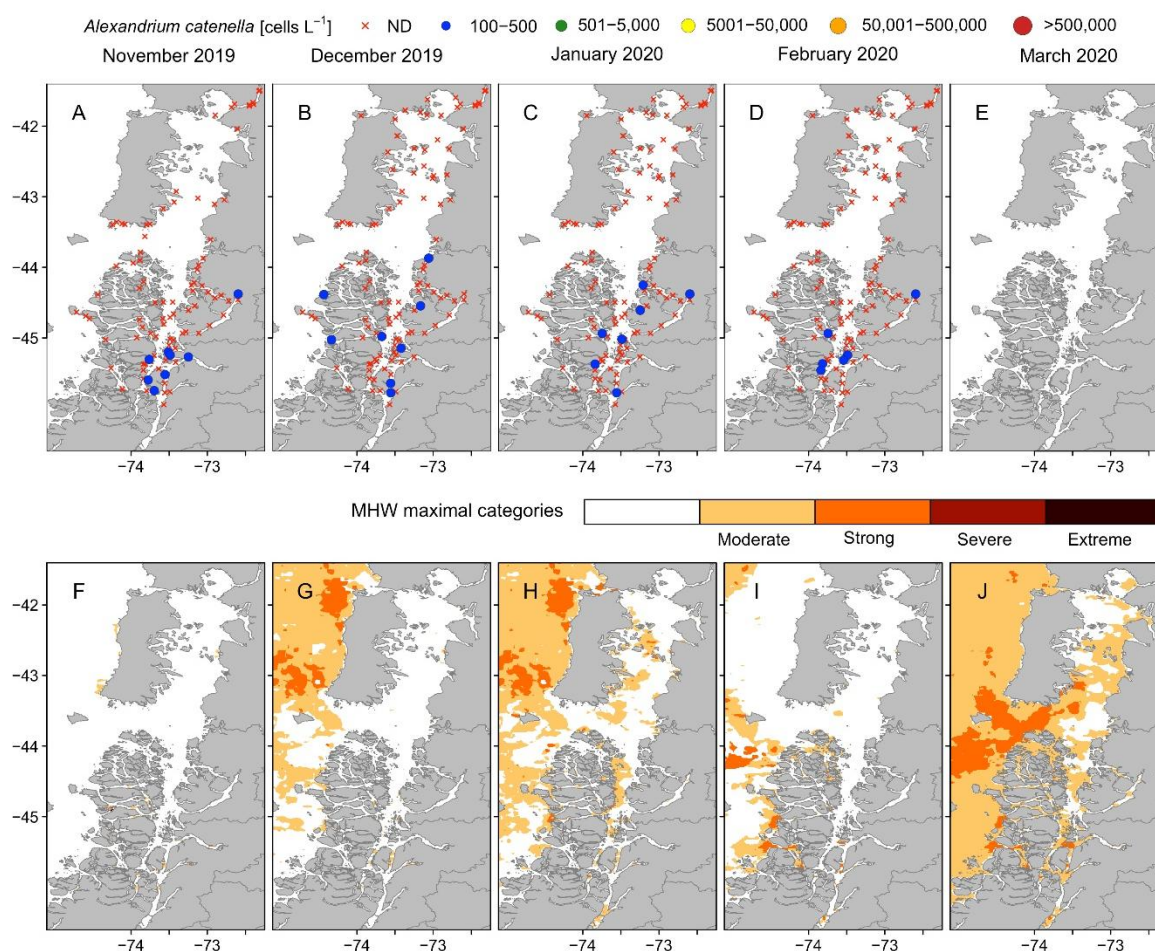

Figure 51: Range of cell density (cell L-1) of Alexandrium catenella (A-E) and maximal extension and category of MHW (F-J) for the months of November (A, F) and December (B, G) 2019, January (C, H), February (D, I), and March (E, J) 2020.

no sampling campaigns were conducted in March).

At the very end of December 2019, a MHW in the Pacific Ocean and briefly extended into Northern Patagonia, affecting the southern coast of Chiloé Island and Aysén Channels for only 5 days in January 2020 (the minimum duration required to be classified as a MHW) before dissipating (Fig. 51G). By late February started a MHW offshore and within the Chonos Archipelago. It spread sporadically through various channels of Aysén Region and, by the end of March, reach Corcovado Gulf (Fig. 51I). In some southern channels of Chonos Archipelago as well as west of the archipelago, and in Guafo Mouth, the MHW persisted the entire month of March. However, in most other parts of Aysén Region, it lasted for less than 10 days (Fig. 51J). Temperature anomalies were predominantly negative in November and December, before becoming positive by late December and early January, when occurred the small MHW.

5.4. Discussion

Among the environmental factors involved in the formation, maintenance, and decline of HAB-forming microalgae populations, temperature has been identified as a key variable (Gobler, 2020; Wells et al., 2015, 2020). Recently, Díaz and Figueroa (2023) reviewed the recurrence of toxic algal blooms in the Chilean Patagonian Fjords system suggesting the processes that may be affected by temperature changes in a dinoflagellate life cycle. These authors describe that in species that present resistance stages, such as *A. catenella*, changes in ambient temperature affect the following processes: i) division cell; ii) gamete fusion; iii) excystment; iv) long-term encystment.

Our study shows for the first time the positive association between *A. catenella* blooms and MHWs in NW Patagonia, a toxic algal bloom "hot spot". A general positive correlation between SSTa and *A. catenella* blooms, with increased cell density often occurring during summers of positive SSTa (i.e. in 2008, 2009, 2014, 2015, 2016, 2017, 2018). All those years were associated with at least short period of MHWs, and 4 of them with particularly intense and long MHWs (i.e. 2008, 2009, 2016, 2017). In contrast, years without MHWs or with negative SSTa in Aysén Region shown little to no bloom activity (i.e. 2010, 2019, 2020). Still, the correlation is not consistent, since some years with MHWs did not show any bloom development (i.e. 2012, 2013, 2022, 2023).

5.4.1. MHWs facilitating *A. catenella* proliferation

Our analysis shows that large *Alexandrium catenella* blooms in NW Patagonia are frequently associated with marine heatwaves (MHWs), yet these events alone are not sufficient to explain bloom development. Instead, MHWs appear to act as catalysts whose effects depend on hydrographic and climatic context.

The summers of 2009 and 2016 demonstrate this pattern. In both years, intense and long-lasting MHWs preceded extensive *A. catenella* proliferation, with cell densities reaching exceptional levels (Mardones et al., 2010). The warm average SST in the Aysén Region during 2009 ranged between 12.5 and 13°C, which corresponds to the optimal thermal window for *A. catenella* growth (Aguilera-Belmonte et al., 2013). In addition, salinity values above 30 psu were recorded where the bloom was strongest, matching known growth optima (Aguilera-Belmonte et al., 2013; Avila et al., 2015). In addition, during summer 2009, higher concentrations of silicic acid, promoting phytoplanktonic blooms, were measured associated with inputs of low-salinity waters (Montero et al., 2017). In comparison, summer 2008 also shown the development of MHWs but no bloom, was associated with lower concentration of silicic acid (Montero et al., 2017).

A similar combination of drivers occurred in 2016, when the bloom coincided with a widespread MHW that started in November 2015 and intensified through summer. This event happened in the context of a positive ENSO phase, with elevated SST, weaker winds, reduced precipitations, and weaker vertical stratification (Díaz et al., 2024; Hernández et al., 2016; León-Muñoz et al., 2018). Reductions in freshwater inputs weakened the stratification of the upper layer enabling the upward advection of saline, nutrient rich waters which, combined with higher insolation, favoured *A. catenella* proliferation (Aguilera-Belmonte et al., 2013; León-Muñoz et al., 2018). Both 2009 and 2016 blooms spread beyond NW Patagonia and had severe consequences, including salmon mortality a several human intoxications (Álvarez et al., 2019; Armijo et al., 2020; Barría et al., 2022; Díaz et al., 2024; Hernández et al., 2016).

Blooms in 2018 followed a similar but weaker pattern in terms of MHWs. SST anomalies were positive from December to February, reaching +1.5°C locally, yet MHWs were shorter and more spatially restricted than the 2009 and 2016 events. *A. catenella* reached high densities earlier in the summer, and as for the events described previously, this bloom also caused aquaculture losses (Barría et al., 2022; Díaz et al., 2019).

Conversely, summers with unstable or negative SST anomalies (therefore not leading to MHWs) did not sustain blooms. In 2019 and 2020, *A. catenella* cell densities remained low despite presence of short-lived anomalies. Both years were characterised by an alternating positive and negative SSTa, as well as lower salinity linked to increase precipitations, creating less favourable conditions for bloom development by decreasing exchanges with nutrient-rich lower layers (Crawford et al., 2021; Saldías et al., 2024). This pattern is consistent with observations that surface layers in Patagonian fjords are often nitrate-limited unless vertical mixing or intrusions of deeper more saline waters occur (Iriarte et al., 2010). These cases highlight that prolonged and stable warming, rather than transient anomalies, is required to sustain bloom proliferation.

However, some years (e.g. 2012, 2013, 2022, 2023) illustrate that even strong MHWs do not always translate into blooms. This suggests that temperature is not the sole determinant of *A. catenella* dynamics. Instead, MHWs likely amplify pre-existing environmental conditions. For example, Cuevas et al. (2019) and Martínez et al. (2015) showed that where oceanic nutrient intrude, rather than river-dominated inputs, and if the nutrient ratio is favourable, warm periods are more likely to translate into productive blooms. This supports the idea that MHWs act as catalysts with nutrients acting as gatekeepers. In addition, recent hydroclimatic changes alter the nutrient balance: changes in the stratification and in nutrient delivery have been observed following changes in quantity and timing in freshwater inputs, creating years where SST is high but surface nutrients remain too low to sustain blooms (León-Muñoz et al., 2021, 2024). Hayashida et al. (2020) demonstrated that bloom response to MHWs depend strongly on nutrient availability: nutrient-poor regions tend to exhibit weak or no MHWs-related blooms, whereas nutrient-rich waters are more likely to experience strong proliferations. Other factors such as water column stratification and freshwater inputs also precondition the system (Aguayo et al., 2019). The 2016 bloom, for example, has been linked to reduced freshwater discharge, higher salinity and nutriments, and increased stratification where estuarine influence are lowers, all favourable to *A. catenella* (Garreaud, 2018b; León-Muñoz et al., 2018; Mardones et al., 2010).

In this study, we followed the definition from Hobday et al. (2016), detecting MHWs using a moving threshold whereby the SST must exceed the 90th percentile of a long-term climatology for at least 5 consecutive days. This moving threshold is calculated independently for each day of the year, considering seasonal cycles. An alternative approach could have been to use a fixed threshold, based on a constant temperature reflecting the thermal physiology of *A. catenella*. However, the

onset of a bloom does not depend solely on sea temperature but also on environmental factors such as nutrient availability and stratification (Glibert and Burford, 2017; Glibert, 2020). For example, between December 2008 and February 2009, the average temperature in Aysén Region ranged from 12.5°C to 13°C, yet the bloom did not begin until end of February, despite similar temperatures in the preceding months (Fig. Sup. 6). Aguilera-Belmonte et al. (2013), using *A. catenella* strain isolated from the outbreak occurring in 2009, evaluated the combined effect of salinity and temperature on the growth and toxin content of this species. These authors evidenced that growth parameters (growth rates and maximum cell densities) were higher at a salinity of 35 psu and a temperature of 15°C, supporting the idea that temperature alone is an insufficient predictor.

Taken together, these findings suggest that MHWs are important but not deterministic in shaping *A. catenella* dynamics. Blooms arise when warming coincides with optimal environmental factors. This has critical implications under climate change, as MHWs are projected to become more frequent and intense (Oliver et al., 2018a; Pujol et al., 2025).

5.4.2. Future perspectives in a Patagonian climate scenario

Climate change is fundamentally altering key oceanic properties, including enhanced stratification (Li et al., 2020), shallower and warmer mixed layer (Richards et al., 2021), increased heat content (Yao et al., 2022) and reduced sea ice (Deser et al., 2024). The physical changes significantly influence MHWs drivers, thereby changing their characteristics and behaviour (Capotondi et al., 2024). In response to these changes, MHWs are projected to intensify in future climate scenarios (Deser et al., 2024), and occur with increasing frequency (Frölicher et al., 2018; Oliver, 2019).

Chile and in particular NW Patagonia is highly vulnerable to the impacts of climate change (Marquet et al., 2023). During the past decade, Chile has been exposed to droughts, wildfires, a glacial retreat, and extreme weather conditions (Garreaud, 2018b). Global climate models for Patagonia project that by 2070, and assuming a scenario of moderate change in greenhouse gas concentrations (RCP 4.5), average temperature will increase from 0, 9 to 1.4 °C and precipitation will decrease between 5.5 and 116 mm on average (Marquet et al., 2023). A decade ago, Wells et al. (2015) proposed a conceptual model of how environmental change may affect different HAB types. The selected climate change stressors, included the increasing temperature, predicted a positive response in toxic flagellates such as *Alexandrium catenella*. Likewise, (Moore et al., 2009) predicted the window of opportunity for *A. catenella* development in Puget Sound, USA, under future climate scenarios. These authors demonstrated that the period that *A. catenella* occur annually may also expand because of climate change and specifically by an increase in SST.

The climate trend and projections for the coming decades suggest that the northern Patagonian fjord system will continue to be the scene of intense blooms of toxic dinoflagellates, including *A. catenella*.

5.5. Conclusions

This study highlights the complex interplay of environmental factors in the development of HABs, specifically the dinoflagellate *Alexandrium catenella* blooms in NW Patagonia, a region prone to such events, where MHWs act as a catalyst. This study is the first to show a positive association between *A. catenella* blooms and MHWs in NW Patagonia, and the key role of sea temperature in the development and the intensification of *A. catenella* blooms. Summers with stable positive SST anomalies generally coincided with significant *A. catenella* blooms, particularly in years with strong and prolonged MHWs (summers 2008, 2009, 2016, 2017), which exhibited very high cell density (3,402× 10^3 cell L^{-1} in 2009). Conversely, years with unstable temperature conditions, resulting in no MHW or weak and short MHWs (summers 2010, 2019, 2020), shown no bloom activity, though low-density early presence *A. catanella* was recorded. However, some exceptions were observed (summers 2012, 2013, 2022, 2023), where MHWs occurred without subsequent bloom development. This inconsistency suggests that while temperature acts as a catalyst, other environmental conditions are crucial for bloom development, particularly the nutrient availability. Thus, while sea temperature and MHWs strongly promote *A. catenella* blooms, they are not the sole drivers, as bloom initiation and progression depend on their interactions with other environmental factors, such as salinity and nutrient availability and biological interactions.

CHAPTER 6.   GENERAL DISCUSSION

6.1. Main results

This thesis provides the first assessment of MHWs and MCSs in Central and Southern Chile, with particular emphasis on Northern Patagonia.

The first part of the work focused on a large-scale analysis of surface MHWs using the OISSTv2 satellite data (Huang et al., 2021a), the most widely employed product for MHWs detection (Dowd et al., 2025; Hobday et al., 2016; Holbrook et al., 2019; Peal et al., 2023; Schlegel et al., 2021; Smith et al., 2024). We carried out the first systematic assessment of warm events over the period 1982-2020 from 29°S to 55°S, dividing the region into three sub-areas: central Chile, Northern Patagonia and Southern Patagonia. The aim was to identify MHWs characteristics in each of the three areas. The results revealed marked regional contrasts: MHWs in Southern Patagonia are on average the longest but the least intense, while those in Central Chile are the most intense but also the shortest in duration. Certain years were particularly affected by MHWs such as 1998, 2008 and 2016, although the regional responses varied and a single year did not impact all areas the same way. Importantly, we also identified a progressive increase in both duration and intensity of MHWs across all three regions during the study period. A special focus was placed on 2016-2017 period to examine the mechanisms driving the development of exceptionally long and intense MHWs. Finally, trends in SST and MHW frequency were evaluated, revealing a clear increase, particularly in Northern Patagonia.

Building on these large-scale patterns, the second part of the thesis focused specifically on Northern Patagonia, in order to explore the limitations of coarse-resolution data. While the first analysis provided an essential regional overview, it could not resolve the fine-scale variability inherent to coastal systems, particularly in fjords and channels. To address this, a new methodology combining in situ and satellite observations was developed to detect MHWs and MCSs at very high resolution, allowing to capture the spatial variability within the Inner Sea and across individual fjords and channels. The results demonstrate that MHWs do not follow a uniform pattern, but instead respond strongly to local topography and basin dynamics. Even within a single fjord or basin, events were found to be highly heterogeneous. The trend identified were broadly consistent with those obtained from coarser resolution datasets, but the high resolution approach provided crucial insights into localised dynamics. Key events and their drivers were described in detail, including the major 2016-2017 MHWs, which display a similar large-scale development to what was observed in the low-resolution data, but for which high-resolution analysis revealed much greater complexity and variability that were invisible at lower resolution.

Having characterised the spatial heterogeneity of surface events, the third part of the thesis extended the analysis to the subsurface, using the GLORYS12V1 reanalysis product at an intermediate resolution of 8 km (European Union-Copernicus Marine Service, 2018). This step was motivated by the recognition that surface anomalies only provide a partial view of thermal extremes, and that the underlying vertical structure may have distinct dynamics. The objective was therefore to investigate how surface-detected MHWs and MCSs propagate with depth. The results show a partial decoupling between surface and subsurface events, with only exceptional climatic conditions such as ENSO, producing events that extend throughout the entire water column. In contrast to surface MHWs, subsurface events are lasting for much longer, and their maximal intensity is typically observed below the surface layer rather than at the surface itself. Topography was also shown to play a key role in constraining the spatial extent of subsurface anomalies.

Finally, the fifth chapter connected these physical findings with ecological implications by examining the influence of MHWs on the development of the toxic dinoflagellate *Alexandrium catenella*. This analysis represents a logical extension of the previous chapters, moving from the characterisation of physical processes to their biological consequences. We found that while this species is favoured by the thermal preconditioning associated with MHWs, and often proliferate during of shortly after such events, MHWs alone cannot explain bloom dynamics. The interactions of temperature with other environmental factors such as salinity and nutrient availability can modulate or limit bloom development.

Taken together, these chapters provide a coherent framework linking large-scale patters, local dynamics subsurface processes and ecological consequences, demonstrating the complexity of extreme events dynamics in Chilean waters. The following sections discuss the methodological approach, compare the findings with broader studies, critically assess the limitations of the methods, propose further reflexions, and finally consider how such events may affect ecosystems and key species.

6.2.   Trends and changes in extremes

The thesis demonstrates that Northern Patagonia is undergoing notable changes in SST trends and in the occurrence of MHWs and MCSs. Long-term analysis revealed a significant warming trend of approximately +0.1°C per decade over the period 1982-2020 (Chapter 2), leading to positive trends in MHWs occurrence, consistent with global ocean warming patterns (Capotondi et al., 2024; Frölicher et al., 2018; Oliver et al., 2018a; Peal et al., 2023; Wang et al., 2022c).

By complementing low-resolution satellite-based analysis with high-resolution fjord-scale analysis (Pujol et al., 2022, 2025), we confirmed that offshore Northern Patagonia exhibits a consistent increase in both SST and MHW frequency over similar periods. This coherence across scales validates the methodology developed in Chapter 3 and highlights its ability to capture large-scale changes while resolving fine-scale variability. Within Northern Patagonia however, the response is more heterogeneous. MCS frequency is declining across most of the Inner Sea, with losses of up to -2 events per decade in the Aysén Region and Ancud Gulf. Conversely, MHW frequency is rising by approximately +1 event per decade in many areas, although exceptions exist: for instance, Corcovado Gulf exhibits a decrease of nearly -1 event per decade. Trends in intensity further illustrate this complexity. While MCS are becoming less frequent, they tend to be more intense when they occur. MHWs by contrast, are more frequent but show a tendency

towards weaker intensity across much of Northern Patagonia. These results suggest that fjord systems do not simply mirror the global signal of intensifying MHWs (Oliver et al., 2018a), but instead respond in ways that reflect their unique hydrography, freshwater inputs and local circulation.

6.3. Methodological advances and strengths

We choose to focus on Northern Patagonia, characterised by a highly complex bathymetry, strong freshwater inputs, and intricate fjord networks (Pantoja et al., 2011; Rodrigo, 2008; Strub et al., 2019), to study MHWs and MCSs more in details. We developed a methodology relying on in situ and satellite data to detect MHWs and MCSs at very-high resolution in Northern Patagonia. Derived from more than 30 years of data and with a horizontal resolution of ~900 m, the approach reproduced the climatology of the temperature of Northern Patagonia, the temperature anomaly and the detection of extreme events at the surface with high accuracy in a region where fjords and channels are particularly intricate. It represents the first of its kind for this region. Since each region of Northern Patagonia exhibits a unique response to external forcings and topographic influences (such as winds, freshwater inputs, water residency time, or temperature), it was therefore essential to accurately represent local variations in sea temperature in order to better characterise MHWs and MCSs (Kilpeläinen et al., 2011; Pinilla et al., 2019, 2021; Soto et al., 2019). This represents a major advance compared with previous studies that rely on coarser products that tend to homogenize the fjords region and miss the variability of enclosed basins (León-Muñoz et al., 2024; Saldías et al., 2019; Strub et al., 2019). In contrast, the high-resolution methodology applied here revealed local patterns of intensity, frequency and duration, including events trapped within specific fjords or separated topographic features such as sills and islands. Seasonal or annual climatologies of the sea surface temperature of Northern Patagonia have been produced previously, but were based on shorter time period (Saldías et al., 2021; Strub et al., 2019).

By resolving the fjord-scale variability, our methodology demonstrates that MHWs and MCSs cannot be considered as uniform regional events. Instead, they are shaped by fine-scale hydrodynamics, freshwater inputs and bathymetric constraints. This level of resolution also highlights contrasts between adjacent fjords: although Puyuhuapi and Aysén Fjords are separated by only 50 km, they show markedly different climatologies and extreme event characteristics, with Aysén Fjord remaining significantly cooler in summer due to higher snowmelt influence (León-Muñoz et al., 2024). Even within individual basins, high-resolution detection captures fine-scale variability: Reloncaví Sound, only about 40 km wide displays differences of 0.6°C in mean intensity and a doubling in MHW density between its northwest and southeast coasts. The Reloncaví Sound is indeed strongly influence at its southeast by the Reloncaví Fjord and the connections with Ancud Gulf, and dominant winds tend to accumulate waters on the northwest side of the gulf (Soto-Mardones et al., 2009). Similarly, in Puyuhuapi Fjord, mean MHW intensities reach about 2.5°C in the head and centre compared with only 1.25°C at the mouth. Fjords in general exhibit different characteristics between their head and their mouth due to local topographic effects (Kilpeläinen et al., 2011). Puyuhuapi Fjord follows this global pattern with distinct influences of freshwater inputs and winds along its length (Schneider et al., 2014), explaining why such variations of temperature are observed. Stratification plays a central role in modulating MHWs and MCSs: the fjords with the most complex hydrography and highest freshwater inputs, such as Puyuhuapi, Reloncaví, Aysén and Comau (Castillo et al., 2012; Schneider et al., 2014; Valle-Levinson et al., 2007), consistently show the strongest variability in intensity of

extreme events. These examples underline the critical importance of working at very high resolution scale, when analysing extremes in fjord systems, as all of these features would be invisible at coarser resolution. Although the main MHW were initially identified using coarse resolution satellite data in Chapter 2, the high resolution developed in Chapter 3 revealed much greater spatial variability, including features that were entirely absent at coarser scales. This demonstrates the value of multi-resolution approaches to fully capture the structure of extreme events.

In addition to the surface detection, we used the GLORYS12V1 reanalysis product to investigate subsurface development of the extreme events. This dataset has a resolution of about 8 km, it covers only the main Inner Sea and does not resolve the fjords and channels. The results reveal Northern Patagonia as a region of pronounced spatial and vertical variability in the occurrence of MHW and MCS. Subsurface events are also basin-dependant, developing at different times and progressively extending towards the bottom. Among them, the 1997-1998 MHW was probably the most remarkable as it was lasted for more than 1.5 year, and spread almost immediately though the entire water column in several regions, although a lag was observed in Ancud Gulf, likely due to topographic constraints (Pinilla et al., 2021). This period has also been widely reported in other parts of the world as one of exceptional intensity, both at the surface and in the subsurface (Holbrook et al., 2020a; Zhang et al., 2025). In the case of MCSs, the 2015-2016 event was particularly noteworthy. It evolved differently across basins: it was almost absent outside Northern Patagonia, it appeared as two separate events in Corcovado Gulf and Moraleda Channel, it was exceptionally long in Ancud Gulf, where it spread progressively to depth and persisted for nearly three years in some layers, and was finally weak and confined to the upper half of the water column in Reloncaví Sound. These differences demonstrate that, even at depth and in the largest basins, temperature anomalies do not propagate uniformly but remain strongly dependant on local dynamics and topography. The general tendency for longer-lasting warming and cooling at depth is consistent with previous observations, including in fjord systems where prolonged cold or warm anomalies are often associated with restricted circulation and topographic barriers that limit water mass renewal (Amaya et al., 2023b; Bianucci et al., 2024; Fragkopoulou et al., 2023; Jackson et al., 2018; Scannell et al., 2020; Yao and Wang, 2024).

The vertical patterns further show a disconnection between surface and subsurface events, a phenomenon frequently reported worldwide (Amaya et al., 2023b; Li et al., 2025; Zhang et al., 2023). While surface MHWs and MCSs are generally short-lived, lasting on average 10 to 25 days according to the results in Chapter 3, subsurface extremes can persist for months, sometimes years. This decoupling typically emerges at around 50 m depth, corresponding to the transition between estuarine-influenced surface waters and (Modified) Subsurface Antarctic Waters (Pérez-Santos et al., 2014; Sievers, 2008; Sievers and Silva, 2008). To fully investigate the origins of these anomalies would require higher temporal resolution data, capable of distinguish water masses and tracking the vertical propagation of signals. Our analysis also highlighted the role of the topography in constraining spatial propagation. For example, the Desertores Islands act as a barrier that separates the Corcovado and Ancud basins, preventing the development of extreme events below the sill formed by the island chain (Bao and Moffat, 2024; Pinilla et al., 2021; Sievers and Silva, 2008). These findings again underscore the complexity of Northern Patagonia and fjord systems more generally, where the development of MHWs and MCSs, both at the surface and subsurface, is shaped by a combination of local dynamics and topography.

The analyse of salinity and water masses also revealed a distinct pattern since the year 2016, characterised with lower salinities, creating a change in water structure. Linford et al. (2023)

reported an intensification Equatorial Subsurface Waters (ESSW) in Northern Patagonia between 2016 and 2022, which we also detected in Moraleda Channel, where it reinforced the stratification. They further linked this process to the observed deoxygenation of Northern Patagonia. In addition, they documented a marked decline in salinity at Guafo Mouth during winter and spring 2020, which we also noticed. Saldías et al. (2024) also identified particularly low salinity levels offshore Northern Patagonia around summer 2019, coinciding with the onset of strong anomalies within the Inner Sea (Chap. 3). Their EOF analysis also confirmed a sustained shift towards less saline conditions from 2016 onwards. Despite these convergent findings, we did not identify any study that might explain this change over this period. One plausible mechanism could be an increase in precipitations, however local studies indicate a general tendency towards declining rainfall (Castro and Gironás, 2021; León-Muñoz et al., 2024; Saldías et al., 2024), consistent with the more positive state of the SAM which alters the large-scale climate patterns (León-Muñoz et al., 2021). The coincidence of positive SAM and El Niño event has been shown to amplify the droughts phenomenon, especially during the years 1998 and 2016 (Garreaud, 2018b; León-Muñoz et al., 2021). Another hypothesis could be the accelerating glacier melting due to poleward shifts of subtropical high-pressure systems. Such phenomena could over short timescales enhance freshwater discharge into Northern Patagonia's fjords (Noël et al., 2025).

6.4. Limitations and knowledge gaps

The development of a new methodology for high-resolution detection of MHWs and MCSs (Chap. 3) represents a significant advance. This approach is particularly valuable in regions where satellite observations alone are insufficient. It establishes a solid foundation for future research in an area that is inherently complex, even for well-studied and apparently straightforward variables such as temperature (Pinilla et al., 2019, 2021; Soto et al., 2019). Future work could, for instance, focus on further increasing the spatial resolution beyond the ~900 m used here, which was constrained by computational performance. Although most of the region is resolved and much of the fjord-scale variability is captured, finer resolution would allow better representation of the most intricate systems, such as the narrowest channels of the Chonos Archipelago, and clarify the connections currently unresolved between Reloncaví Fjord and Sound, or between Jacaf Channel and Puyuhuapi Fjord.

In addition to the surface climatology developed in Chapter 3 and used for the detection of surface MHWs and MCSs, equivalent climatologies were also computed at 31 additional depth levels, extending down to 400 m. These multi-depth climatologies have been made available online (https://doi.org/10.5281/zenodo.14845077), but they were not integrated into the core analysis presented in this thesis. The initial plan was to develop and run a fjord-resolving hydrodynamic model for Northern Patagonia over selected periods corresponding to major MHWs or MCSs. Model outputs could then have been compared with the multi-depth climatologies in order to estimate temperature anomalies and identify subsurface extreme events with greater precision. However, due to time constraints, this approach could not be fully implemented. Instead, we relied on outputs from the existing GLORYS12V1 product, which, while offering global coverage, operates at a much coarser spatial resolution and is therefore less suited to resolving the fine scale hydrography of fjords and channels.

The GLORYS12V1 reanalysis product used for subsurface analysis, although valuable, also imposed notable limitations. Its spatial resolution too coarse to resolve the narrow fjords and channels that characterise Northern Patagonia, while the monthly temporal resolution limited

the characteristics of the event, by first smoothing their intensity and limiting the detection only to event of at least one month. Developing dedicated hydrological models in specific fjords such as Puyuhuapi, Comau or Reloncaví could therefore provide more accurate insight dynamics of subsurface anomalies. Identify the role of water masses in fjords would also help to quantify the influence of bathymetric sills and complex circulation patterns in trapping or dispersing anomalies.

Different drivers were identified as contributing to the formation and development of MHWs and MCSs, including large-scale atmospheric anticyclones and low-pressure systems, water masses advection, changes in cloud cover and solar radiation, reduced or increased winds and changes in heat budget (Pujol et al., 2022, 2025). For that purpose, we used ERA5 reanalysis data to identify the drivers involved in MHW and MCS development. Its coarse resolution (~25 km) is unable to capture fjord-specific dynamics, and allow an understanding of atmospheric drivers at regional scale only. Fjords, however, represent particularly complex systems where local processes play a decisive role. Among the different local drivers, there is the topography that modulates synoptic winds intensity and direction (Sundfjord et al., 2017), katabatic winds (Gierens et al., 2020), freshwater that vary according to the different rivers discharge into each fjord and influence the density gradient, and in return the local circulation (León-Muñoz et al., 2024; Soto-Riquelme et al., 2023; Sundfjord et al., 2017), the different oceanic influences (Cisek et al., 2017), or the cloud and precipitation formation due to orography (Gierens et al., 2020; Lenaerts et al., 2014). On-site observation of atmospheric data remain scarce in Northern Patagonia, limiting the ability to interpret the detected events with local in situ data. Atmospheric data with higher resolution could allow to have better results and maybe more basin-specific interpretations. Finally, large-scale climate modes act as additional modulators of variability. Teleconnections such as ENSO strongly influenced the duration and intensity of MHWs, with notable events in 1998 and 2016 (Holbrook et al., 2020a; Huang et al., 2016). SAM also played a role by creating favourable conditions, particularly through weakened Westerly Winds, that promoted MHW development, a mechanism consistent with findings across the southern hemisphere (Gurumoorthi and Luis, 2025; Su et al., 2021a). Overall, fjords are influenced by drivers operating at different scales, leading to unique climatic conditions in each fjords (Crosswell et al., 2022; Iriarte et al., 2014). Taken together, these results emphasise that while local stratification and topography govern the fine-scale manifestation of extremes within fjords, regional to basin-scale climate drivers provide the background conditions that modulate or supress their development.

The methodology developed in Chapter 3 relies exclusively on in situ data freely accessible online, the majority of which originates from local monitoring campaigns funded by public institutions. However, considerable amounts of high-resolution data are also collected by private companies whose activities depend on marine environment. Aquaculture farms, for example, continuously record key parameters such as temperature, salinity and oxygen concentration at multiple depths, often at hourly or sub-hourly frequency. Despite the fact that such measurements would not reveal commercially sensitive information, they are rarely made publicly available. Greater collaboration and data sharing between the private sector and the scientific community would provide substantial mutual benefits advancing public research while also offering private stakeholders improved environmental knowledge, forecasting capacity and long-term sustainability strategies.

6.5. Extreme events on ecosystems and aquaculture production

The fragile ecosystems of Northern Patagonia are expected to be strongly affected by climate change (Häussermann et al., 2023), and could be an important natural laboratory for studying the impacts of global warming on benthic organisms (Betti et al., 2021). Chilean Patagonia host 1650 benthic species, among which molluscs, cnidarians, sponges and annelids representing the most biodiverse groups (Haüssermann and Försterra, 2009). At the same time, this region developed an important aquaculture industry, particularly in salmon farming (SUBPESCA, 2025), which coexists with the rich natural ecosystems and is equally vulnerable to the environmental changes (Iriarte et al., 2010; Soto et al., 2019; Yáñez et al., 2017a). This section explores the potential impacts of MHWs and MCSs on both native biodiversity and species cultivated for aquaculture purposes, with a particular focus of some emblematic species that are central to the ecosystem functioning of very important from an economic point of view.

6.5.1. Algae

Marine macroalgae often dominate shallow-water ecosystems, where they form extensive marine forests that provide habitat and shelter for entire ecosystems (Macreadie et al., 2017; Steneck and Johnson, 2013; Wernberg and Filbee-Dexter, 2019). The effects of global change and MHWs on these systems are varied and species-specific, with kelp forests, extensive systems dominated by large laminarian seaweeds (Steneck and Johnson, 2013; Wernberg and Filbee-Dexter, 2019), being particularly sensitive (Pecuchet et al., 2025; Straub et al., 2019). A common observed trend is the shift from kelp-dominated ecosystems to turf-dominated systems (Gao et al., 2021; Straub et al., 2019). Documented consequences include reduced biomass, impaired reproduction, dieback of meadows and forests, and changes in distribution and abundance (Filbee-Dexter et al., 2020; Liu et al., 2025; Smale et al., 2019; Wernberg et al., 2016). These changes cascade to the wider ecosystems, altering species interactions, competition, grazing dynamics, and other ecological processes (Arafeh-Dalmau et al., 2019; Ferreira et al., 2025; Franco et al., 2015; Smale et al., 2019; Wernberg et al., 2016). The severity of MHW impacts depends on multiple factors, including the resilience, recovery, and recolonisation capacity of the affected macroalgae, its position relative to thermal safety margin, interaction with external stressors such as eutrophication, grazing pressure, and the characteristics of the MHW itself (Straub et al., 2019). In Chile, marine macroalgae play a fundamental ecological and economic role, with diverse species forming extensive coastal forests that are increasingly exposed to the impacts of climate change.

Macrocystis pyrifera is a giant kelp naturally distributed along the entire coast of Chile, with highest densities in southern Chile (Graham et al., 2007; Thompson-Saud et al., 2024). It is the largest algae and benthic organism, reaching lengths of more than 40 m, and forming dense underwater forests (Graham et al., 2007; Thompson-Saud et al., 2024). It plays a particularly important ecological role, serving as engineer species offering food resources, habitat, shelter and other services to a myriad of organisms (Thompson-Saud et al., 2024). It has also a considerable economic value: harvested mainly by small-scale fisheries from natural beds, it supports coastal communities and is used in aquaculture for the agro-food industry and pharmaceutical applications (Márquez Porras, 2019; Purcell-Meyerink et al., 2021). This giant kelp has a complex life cycle, with an anchored thallus and reproductive parts that may detach and survive drifting at the surface of the ocean for up to three months, allowing long-distance dispersal of over 2 000 km via currents and winds (Bernardes Batista et al., 2018; Graham et al., 2007). Laboratory studies have shown optimal growth between 12 and 17°C, while growth slows above 20°C, and increased irradiance may exacerbate

thermal stress, leading to detachment and mortality. In the case of already detached individuals, more rapid disintegration was observed (Ladah and Zertuche-González, 2007; Peters and Breeman, 1993; Rothäusler et al., 2009; Solas et al., 2024). In Central Chile, summer conditions of high temperature and solar radiation have caused reproductive tissues to die, severely limiting reproductive capacity (Rothäusler et al., 2009). Such kind of environmental conditions were for example reached during the summer 2017 MHW, detailed in Pujol et al. (2022). Similarly, at temperatures superior to 20°C, the floating algae disintegrated at faster rates than algae present in cooler waters (Rothäusler et al., 2009). Observations in New-Zealand further suggest a thermal threshold for *M. pyrifera* distribution, as it is found only where waters never exceed 18°C (Hay, 1990). Increasing ocean warming and frequency and intensity of MHW could therefore remap *M. pyrifera*'s distribution in Chile, and maybe cause physical damages and reduced its geographical through rafting during the strongest MHW events. In Mexico, alteration in *M. pyrifera*'s associated communities was observed after ENSO-associated MHWs, as well as mortality of the kelp (Arafeh-Dalmau et al., 2019), which could also be expected to happen in Chile. Some emblematic species and the risks they might face during MHWs and MCSs are described below. Another species, *Macrocystis integrifolia*, present in Northern Chile, appears to benefit from MCSs associated with intensified upwellings, which provide cooler temperatures and higher nutrient concentrations, creating favourable condition for its growth, which could also be suggested for *M. pyrifera* (Alonso Vega et al., 2005; Gonzalez-Aragon et al., 2024).

Another large brown algae, the bull-kelp *Durvillaea antarctica* (locally called Cochayuyo), occupies the low intertidal zone of wave-exposed coasts (Velásquez et al., 2020), ranging from 30°S to the extreme south of Chile, and even subantarctic regions (Mansilla et al., 2017; Tala et al., 2013). It plays both an important ecological and economic role: its strandings can sustain up to 89 associated species in central Chile (López et al. 2018), and it is the most heavily harvested alga in the country, with nearly 10 000 tonnes collected in 2015 (Velásquez et al., 2020). Historically consumed by coastal populations since centuries, it is now also used in agro-food industries, with emerging applications in biotextiles (European Food Safety Authority (EFSA) et al., 2025; Figueroa et al., 2023; Parra Núñez, 2024; Velásquez et al., 2020). Like *M. pyrifera,* it reproduces via anchored thalli and detached parts that drift and disperse spores, with floating specimens remaining viable for over a month in moderate seasons (Graiff et al., 2013; Velásquez et al., 2020). However, high temperatures and solar radiation reduce the persistence of rafts, accelerating biomass loss, disintegration, and sinking, thereby limiting dispersal capacity (Graiff et al., 2013; Tala et al., 2016, 2019). Warm conditions also generally induce metabolic deficiencies and tissue degradation (Graiff et al., 2013). More frequent, intense and prolonged surface MHWs, often driven by increased solar radiation (Pujol et al., 2025), are therefore expected to exacerbate damage to *D. antactica*. Severe impacts have already been documented in New Zealand, where a 23°C MHW event caused the local extinction of populations with no recovery after five years (Montie, 2023; Montie et al., 2024; Salinger et al., 2019; Thomsen et al., 2019). Although such extreme temperatures have not yet been reached in Chilean Patagonia, they may occur under future warming. Laboratory experiments further show that even short-term exposure to 20°C, already recorded during MHWs in central Chile (Pujol et al., 2022), could exacerbates the detrimental effects of solar radiations on the algae and induces physiological reactions due to the thermal and oxidative stress, even after short-term exposure of a few hours (Cruces et al., 2013).

In Northern Patagonia, both *D. antarctica* and *M. pyrifera* reproduce mainly during winter with little activity in summer (Tala et al., 2016, 2019). This makes winter prolonged MHWs, such as those observed during the years 1997-1999 or 2016-2017, a potential threat to reproductive success. In addiction, to thermal stress, grazing pressure (sometimes increased during warm temperatures)

may further compromise their resilience under climate change (Rothäusler et al., 2009).

Beyond individual stressors, the increasing frequency of compound events such as simultaneous atmospheric and marine heatwaves or MHW and extreme ocean acidification event poses and even greater risk for intertidal organisms. The absence of recovery or "cooling" periods during such events can cause mass mortality and accelerate biogeographic redistributions across stress gradients (Salinger et al., 2019; Thomsen et al., 2019; Weitzman et al., 2021; Whalen et al., 2023). This highlights the importance of considering compound climate extremes, rather than single drivers, when assessing the vulnerability of Patagonian ecosystems.

Patagonia and central Chile also support aquaculture of the native red seaweed *Agarophyton chilensis* (formerly named *Gracilaria chilensis*), primarily cultivated for agar extraction (Buschmann et al., 2017). Domestication of this species began only a few decades ago, yet genetic and phenotypic differences between farmed and wild populations are already evident (Guillemin et al., 2008). *A. Chilensis* is naturally distributed along Chilean coasts between 30°S and 45°S, even if farmed populations extend up to the extreme north of the country (Guillemin et al., 2008). Although human selection have led to a loss of genotypic diversity in farmed populations, the general-purpose genotypes selection have generated the non-anticipated selection of organisms more resistant to warm temperatures compared to wild individuals (Usandizaga et al., 2019). This particularity could greatly help this seaweed to resist to future MHWs and climate change. Nevertheless, structured breeding programs and cultivar selection strategies to strengthen resilience under global change have not yet been implemented in Chile, and long-term management plans are therefore urgently required to ensure sustainability use of *A. chilensis* under warming conditions (Usandizaga et al., 2019).

6.5.2. Molluscs and crustaceans

Marine benthic invertebrates are also highly sensitive to MHWs, being affected by both direct and indirect impacts (Michaud et al., 2022). Their vulnerability is largely due to their limited or non-existence capacity for migration and their dependence on key habitat-forming species such as kelp forest (Michaud et al., 2022). The consequences of MHWs in these systems include shifts in invertebrate community structure, species invasions, declines in richness and abundance, and habitat loss (Caputi et al., 2019; Michaud et al., 2022). Among molluscs and crustaceans, MHWs have been associated with increased mortality, stock reductions, recruitment failure, heat stress, and spawning collapse (Caputi et al., 2016, 2019; Chandrapavan et al., 2019; Ishida et al., 2023; Marochi et al., 2022; Shanks et al., 2020). Nevertheless, some species appear to benefit from these conditions: for instance, invasive gastropods that either tolerate higher temperatures or outcompete native fauna have shown marked proliferation under MHW (Ishida et al., 2023; Michaud et al., 2022).

In Chile, beyond algae, molluscs and crustacean are also particularly important for the economy, yet they are threatened by increasing temperature. *Mytilus chilensis*, a mussel species naturally present in the intertidal zone of Northern Patagonia at depths of 3 to 20 m (Molinet Flores et al., 2015), is the most widely cultivated mollusc in Chilean aquaculture (SUBPESCA, 2025). This mussel typically prospers in fjords, where the freshwater inputs imply reduced salinity, giving it a competitive advantage over other species (León-Muñoz et al., 2024). For aquaculture purposes, mussel's larvae are captured from natural beds in the Reloncaví and Comau Fjords using long-line systems, before being transported to distinct areas, mostly Chiloé Island, for fattening process (Jahnsen-Guzmán et al., 2021; León-Muñoz et al., 2024; Molinet et al., 2021). These fjords

therefore act as natural hatcheries for the aquaculture industry (León-Muñoz et al., 2024). However, declining freshwater inputs observed in Northern Patagonia (León-Muñoz et al., 2024; Molinet et al., 2025) may reduce the competitiveness of *M. chilensis*, allowing the more resilient mussel *Aulacomya atra* to dominate (Molinet et al., 2025). Compound event of reduced freshwater inputs and MHWs, which often co-occur, could place particular stress on *M. chilensis* larvae. Over longer time-scales, the combined trends of increasing MHWs and decreasing freshwater inflows could drive shifts in the habitat and distribution of this species (León-Muñoz et al., 2024; Molinet et al., 2025; Molinet Flores et al., 2015; Pujol et al., 2025). In addition to the direct thermal stress caused by the increased temperatures, the combined effects of MHWs and ocean acidification may further weaken *M. chilensis*, with increased dissolution of shell compromising growth and survival (Duarte et al., 2014).

Other bivalves in Chile also exhibit vulnerabilities. Urban (1994) investigated the effects of rapid warming during ENSO events, often considered to analogous to MHWs, on molluscs distributed along the coasts of Peru and Chile. The study found that the bivalve *Gari solida* exhibited mortality rates of around 10% at temperatures of 20°C. More recently, Martel et al. (2022) examined the interactive effects of elevated pCO2 and temperature on the clam *Ameghinomya antiqua*, another species naturally distributed along the coasts of Chile. While temperature alone did not directly impact survival, in combination with increased pCO2, it is the temperature that determines the amount of shell loss by decalcification, potentially raising concerns for the sustainability of this important artisanal fishery resource (Martel et al., 2022). The sea snail *Trophon geversianus*, present in the entire Patagonia, has also shown alteration of its shell at 18°C, associated with mortality (Vilela et al., 2024).

The southern king crab, *Lithodes Santolla,* is a cold-eurythermal species, present in Chile from 41°S to 55°S (Anger et al., 2004; Molinet et al., 2020). It is the most exploited king crab in South America, with about 67% of the catches occurring in Chilean waters (Molinet et al., 2020). In the oceanic zone between 41°S and 46°S, *L. Santolla* is most abundant at 150-200 m depth, where temperature remain around 8 to 9°C (Molinet et al., 2020). Conversely, in Northern Patagonia, most catches are concentrated between 15 and 50 m depth (Molinet et al., 2020), although the species is also caught as deep as 200 m in Puyuhuapi Fjord (Figueroa-Muñoz et al., 2021). They effectuate seasonal reproductive migrations toward shallow waters, and their recruitment occurs above 40 m, being closely related to the distribution of the giant kelp *Macrocystis pyrifera* (Tapella and Lovrich, 2006). It has been shown that thermal tolerance of *L. Santolla* varies considerably with age (Paschke et al., 2013). Its lower tolerance has been reported between 1°C and 4.2°C (Anger et al., 2004; Paschke et al., 2013), which is well below the temperature currently observed in Northern Patagonia, even during the strongest MCSs ([Chap. 4](#)), although cold extremes in Southern Patagonia may approach these values (Iriarte et al., 2014; Landaeta et al., 2011). By contrast, warming during MHWs may present greater risks: while development rates increase at higher temperatures, survival rates declines with mortality observed at 15°C during moulting period, and complete larval mortality at 18°C (Anger et al., 2004; Calcagno et al., 2005). Such values are reached in the upper layers during MHWs ([Chap. 4](#); Pujol et al., 2025). Reproductive processes also appear vulnerable: in the Reloncaví Sound, seminal recovery of males is significantly faster at 9°C than at 12°C, suggesting that warming may aggravate the risk of seminal depletion, particularly under conditions of intense fishing pressure on male individuals (Pretterebner et al., 2019). MHWs could therefore affect various life stages of *L. Santolla* when present in shallow waters. Vertical migration to deeper cooler waters may provide refuge during MHWs as suggested by similar behavioural responses in others *Lithodes* species of Northern Pacific to escape heat (Figueroa-Muñoz et al., 2021; Hall and Thatje, 2009). However, such shifts could reduce catchability in artisanal

fisheries, which largely operate in the upper layers of Northern Patagonia (Molinet et al., 2020).

In contrast, recent experiments on the Chilean crab *Metacarcinus edwardsii* (locally called jaiba marmola) conducted in the Valdivia estuary (~40°S) revealed more nuanced responses to MHWs (Bruning et al., 2024). *M. edwardsii* is the most important crab species in Chilean artisanal fisheries, representing about 70% of national landings (Rojas-Hernandez et al., 2016). This species undertakes spatial migrations between estuaries, where it completes its larval stages, and oceanic coastal waters as adults, performing vertical migrations, and being found mostly above 50 m depth (Figueroa-Muñoz et al., 2021; Pardo et al., 2020). Experimental exposure of larvae to typical Valdivian MHWs (14°C) shown that the timing of warming within the moulting cycle was critical: early MHW increased survival and accelerate development, whereas latter exposure reduced survival and prolonged development (Bruning et al., 2024). These results suggest that moderate warming above the average ambient temperature may enhance larval performance under certain circumstances. However, as elevated temperatures increase energetic demands (Ren et al., 2021), it has been suggested that MHWs may exacerbate food requirements, creating a risk of energetic deficiency and unsuccessful moulting if food is limited (Bruning et al., 2024).

6.5.3. Cold-water corals

Corals have been widely impacted by MHWs, causing bleaching and mortality by reducing calcification, causing the loss of their symbiotic zooxanthella, and promoting the emergence of diseases (Leggat et al., 2019; Marzonie et al., 2023; Sully et al., 2019; Yao and Wang, 2022). Continental Chile does not host tropical corals due to the low sea temperature of its coasts. However, Northern Patagonia is host to cold-water corals, which, unlike their tropical counterparts, thrive in cold conditions, either at depth or in naturally temperate environments (Cordes and Mienis, 2023; Häussermann et al., 2023). In 2007, 63 species of cold-water corals were described in Chilean Patagonia, including gorgonians (Häussermann and Försterra, 2007). Although few studies have been conducted, current evidences suggest that they are also likely to be affected by climate change, with different responses between species (Chapron et al., 2021; Dodds et al., 2007; Jantzen et al., 2013; Rodolfo-Metalpa et al., 2015). Higher temperature can alter their behaviour, reduce energy reserves and skeletal growth, disrupt bacterial associations, lower physiological activity, and lead to mortality (Chapron et al., 2021; Dodds et al., 2007; Gori et al., 2016).

Among the species present in Northern Patagonia, *Desmophyllum dianthus*, is probably one of the most studied. It has been recorded in Comau Fjord from 7 to 225 m depth (Försterra et al., 2014; Jantzen et al., 2013), and has a thermal tolerance ranges between 4 and 17.5°C (Naumann et al., 2013). However, according to findings in Chapter 4 with GLORYS12V1 reanalysis data, temperature at the mouth of Comau Fjord was of 17°C in 2017 from surface to 20 m depth, and according to non-shown data from Chapter 3, sea surface temperature was above 17°C inside the fjord, and above 18°C in February 2008 during another MHW, already approaching the species' upper thermal limit. In 2013 and 2022, very short but intense surface MHWs lead to temperatures exceeding 19°C. Yet, it has been observed that *D. dianthus* shows lower calcification rates at temperatures of 15°C, and that thermal stress can impact them even more than ocean acidification (Gori et al., 2016). In addition, elevated temperatures are known to increase corals' metabolic activities and to decrease their energy reserves (Dodds et al., 2009; Dorey et al., 2020; Gómez et al., 2022). As a result, during MHWs, cold water coral populations might face challenges in accumulating sufficient energy reserves and resisting future changing environmental conditions (Anthony et al., 2009).

Another important representative cold-water coral in Northern Patagonia is *Caryophyllia huinayensis*. This species is distributed along the Chilean coast from 37°S to the southern Patagonia (Rossi et al., 2017). In Comau Fjord, it is present between 11 m and at least 265 m depth, while on the continental slope has been found between 740 and 870 m (Sellanes et al., 2008). Laboratory experiments indicate that elevated temperatures (~15°C) have strong negative effects on its metabolism and health, leading to moribund or dead corals after three months of exposure (Beck et al., 2023). The three month delay was attributed to the time required for the corals to deplete their energy reserves. Adults appear to be less resilient than juveniles in these conditions (Beck et al., 2023). Moreover, high temperature were shown to reduce juvenile calcification more severely than food limitation (Beck et al., 2023). (Beck et al., 2023) suggest that *C. huinayensis* can tolerate 15°C up to 3 months maximum, especially if warm temperatures are coupled with other stress factor. In Comau Fjord, surface temperatures exceed 15°C during summer, and temperature superior to 15°C can be observed up to 30 m depth for a couple of months. In this context, prolonged recurrent MHWs could represent a major threat to *C. huinayensis,* as they may push environmental temperatures beyond the species' tolerance limits for extended periods. The persistence of *C. huinayensis* in shallow regions could therefore suggest that some degree of thermal acclimatization may occur in these populations, which is used to experience much more variable conditions compared to deeper habitats (Beck et al., 2023; Heran et al., 2023). However, the increasing trends of MHWs' frequency and intensity in Comau Fjord (Pujol et al., 2025) could exceed its capacity, ultimately compromising the persistence of local populations. At the mouth of Comau Fjord, with the reanalysis GLORYS12V1 data, even during MHWs, we never registered temperatures superior to 14°C below 80 m depth. This could suggest that individuals located at higher depths could be protected from MHWs influence.

6.5.4. Cetaceans, plankton, fishes and other pelagic species

Pelagic species are also affected by MHWs, although generally less severely than sessile organisms because of their ability to migrate to avoid thermal stress, either horizontally (longitudinally or latitudinally) or vertically toward deeper layers (Deutsch et al., 2015; Freitas et al., 2016; Rutterford et al., 2015; Smith et al., 2023b). When migration is not possible, as in the case of planktonic species, adaptative strategies may be employed, such as reducing reproductive investment or increasing feeding effort to compensate for higher energy demand associated with thermal stress (Barbeaux et al., 2020; Caputi et al., 2016; Gunderson and Leal, 2016).

About half of the cetacean species worldwide have been registered in Chilean waters (Lobo et al., 1998). Northern Patagonia seasonally hosts many cetaceans species (Viddi et al., 2010), including blue and humpback whales, killer whales, and several species of dolphins, some of which can be found in fjords and channels (Viddi et al., 2010). In many regions of the world, different whales species have changed their behaviour during MHWs, either by attempting to avoid elevated temperatures or by migrating following lower food availability due to changes in phytoplankton biomass (Barlow et al., 2023; Kohlman et al., 2024; Pecuchet et al., 2025; Santora et al., 2020). Similar conditions in Northern Patagonia could cause comparable impacts, as this region serves as an important nursing and feeding ground (Galletti Vernazzani et al., 2017; Hucke-Gaete et al., 2004; Hucke-Gaete et al., 2013; Seguel and Pavés, 2018). While yet no evidence exists of MHW-driven delay or disruptions in their migrations in Chile, unusual mass strandings were reported during the 2015-16 El Niño event, linked to HABs (Alvarado-Rybak et al., 2020; Häussermann et al., 2017). As MHWs have been associated with enhanced HAB formation (Chap. 5; Trainer et al., 2020), the risk of mass strandings in Patagonia could increase under warming conditions.

At the planktonic level, MHWs often lead to reduction in taxonomic richness, as observed in the Gulf of Alaska (Batten et al., 2022), and to restructuring of the ecosystems by altering the food-chain (Gomes et al., 2024). In some cases, increased zooplankton abundance has been reported, though largely as a consequence of reduced predation rather than population growth (Batten et al., 2022; Piatt et al., 2020). In the South Pacific, MHWs have been linked to changes in plankton dynamics (Morato et al., 2020), and rapid winter warming off central Chile has been associated with jellyfish blooms (Castro et al., 2000). Although planktonic dynamics changes are less well documented along the Patagonian coast, the risk of altered plankton regimes remains.

Forage fishes, linking plankton to higher trophic level, play a crucial role in sustaining marine food webs (Nissar et al., 2023; Pikitch et al., 2014). However, declines in forage fish populations have been documented during MHWs, often linked to reductions in zooplankton availability (Arimitsu et al., 2021). In Chile, the jack mackerel (*Trachurus murphyi*), locally known as jurel, extends from Peru to southern Chile and is typically associated with waters below 15°C influenced by the Peru-Chile upwelling (Bertrand et al., 2016; Rollins, 1988). During the 1997-1998 El Niño, its distribution shifted southward, with nurseries displaced beyond 40°S, adults forced to coastal areas where the upwelling was stronger, and modified migratory routes (Arcos et al., 2001). During the MHW, juveniles predominated offshore south Chile, while adults were largely absent, delaying their return to feeding zones of the northern upwelling system and causing reduced catches (Arcos et al., 2001). The Peruvian anchovy, *Engraulis ringens*, named in Chile anchoveta, is another key forage species distributed from Peru to Northern Patagonia (Silva et al., 2016; Valdivia et al., 2007). Its life cycle is closely tied to upwelling areas, where productivity is high (Cubillos, 2001). Anchoveta typically reproduces in cooler waters offshore of Central Chile (Valdivia et al., 2007), but warming has already driven poleward shifts during their reproduction period (Bustos et al., 2008). Future declines are projected in Central Chile, particularly during winter, due to elevated temperatures (Silva et al., 2016). Long-lasting winter MHWs such as in 2016 (Pujol et al., 2022) may exacerbate these trends, pushing anchoveta populations further into Northern Patagonia. Moreover, jellyfish proliferation triggered by warming can increase predation pressure on anchoveta larvae (Castro et al., 2000). Conversely, MCSs linked to La Niña events appear to favour anchoveta abundance (Lazo-Andrade et al., 2024). In the case of the common sardine (*Strangomera bentincki*), abundance and recruitment are closely associated with cooler conditions and increased upwelling (Cubillos and Arcos, 2002; Gomez et al., 2012). During El Niño-driven MHWs, reduced upwelling and warmer waters led to lower recruitment (Gomez et al., 2012). Given annual catches of up to 840 000 tonnes, (Silva et al., 2015), MHWs may have particularly detrimental consequences for sardine fisheries, whereas MCSs could have positive impacts.

Other pelagic species also display vulnerabilities. The South Pacific endemic Ge*nypterus maculatus* (congrio negro), important for fisheries and aquaculture, experiences thermal stress and altered gill immune responses under MHWs exposure (Becerra et al., 2025). The swordfish *Xiphias gladius*, harvested in Chile by both artisanal and industrial fleets (3000 to 6000 tonnes annually; Silva et al., 2015), also shows indirect sensitivity to MHWs and MCSs. In the northeast Pacific, swordfish modified their diet during the 2014-2016 MHW in response to prey availability (Preti et al., 2025). Similar consequences have been observed in central Chile, where swordfish shifted diet composition between the 2015-2016 El Niño MHW and the cooler La Niña year of 2017 (Lazo-Andrade et al., 2024). During cold anomalies, the anchoveta *E. ringens* contributed more significantly to swordfish diets, consistent with its La Niña-driven abundance of this forage fish (Lazo-Andrade et al., 2024). The southernmost distribution of the swordfish in Chile also corresponds to the southern distribution of the anchoveta (Espíndola et al., 2009); the southward displacement of anchoveta may in turn drive shifts in swordfish distribution.

126

Overall, MHWs and MCSs have the potential to reshape pelagic ecosystems in Northern Patagonia and Central Chile, altering plankton communities, shifting in forage fish distribution and cascading upwards to predators such as swordfish and cetaceans. While the mobility of pelagic species offers some resilience, the dependence of fisheries on a few key species means that even moderate changes in abundance, recruitment or distribution could have substantial ecological and socio-economic consequences (SUBPESCA, 2025). Indeed, the jack mackerel, anchoveta and common sardine are the three most harvested species in Chile, representing 1.5 millions of tonnes of biomass in 2024, with the jack mackerel alone valued to 513 millions US$ in exportations (SUBPESCA, 2025).

6.5.5. Salmon industry

Atlantic salmon (*Salmo salar*) is not native to Chilean Patagonia, having been introduced for farming purposes in the 1970s (Ceballos-Concha et al., 2025). This cold-temperate water species spends its early life in freshwater environments before migrating to the open ocean (Birnie-Gauvin et al., 2019; Hansen and Quinn, 1998). Northern Patagonia provides particularly favourable conditions for salmon aquaculture, with extensive fjords and rivers systems, and average temperatures that closely match the species' developmental requirements (Korus et al., 2024; Salgado et al., 2015).

Despite this suitability, salmon farming in the region is increasingly affected by climate change. Salmons are vulnerable to different stressors that are exacerbated by warming, including direct increase of temperature, HABs, low water oxygen levels, or diseases and parasites (Nuic et al., 2025; Sajid et al., 2024). An example is for instance Newfoundland in 2020, where approximately 450 000 farmed salmons died following sustained high water temperatures combined with hypoxia and sea lice infestation, species of copepods parasite of salmons (Burt et al., 2013). Elsewhere, mass mortality events of both wild and farmed salmons have been associated with MHWs in Canada, Tasmania, New-Zealand and Alaska (Calado et al., 2021; Cook et al., 2025; Wade et al., 2019; Westley, 2020).

The direct impact of temperature on salmon survival has been extensively studied. Although showing signs of stress and reduced performance and growth at temperature above 18°C (Soto et al., 2019), salmons can be able to resist to temperature above 22°C over long-term period and 26°C over short periods (Benfey et al., 2024; Gamperl et al., 2020, 2021; Ignatz et al., 2023). However, some mortality has been observed at 21-22°C and sustained exposure to temperatures above 18°C in combination with hypoxia or parasitic infection can lead to large-scale death (Gamperl et al., 2020; Godwin et al., 2020; Sajid et al., 2024). Behavioural response has been observed to such conditions, with salmons tending to move deeper within their cages during warm periods (Gamperl et al., 2021). For the moment, water temperatures exceeding 18°C remain rare in Northern Patagonia. However, temperatures exceeding 19°C can be observed in summer in Reloncaví Sound, Reloncaví Fjord, Comau Fjord, Puyuhuapi Ford and Jacaf Channel. Temperatures exceeding 21°C is extraordinarily rare, but occurred during certain MHWs in Reloncaví Sound, Reloncaví Fjord and Puyuhuapi Fjord, as during the 2013 summer MHW (Chap. 3 not shown). Nonetheless, such extremes are exceptional and last only for a few days, although Reloncaví Fjord can show longer-lasting very high temperatures, and affect only precise regions of Northern Patagonia, remaining confined. The main concern, therefore, lies in the interaction of moderate warming with other stressors such as HABs and hypoxia.

In Chile, mass mortalities of salmons have been most often associated with HABs and decrease

in oxygen concentration. The most catastrophic event occurred in summer 2016, when a severe drought coincided with atmospheric and marine heatwaves, triggering a bloom of *Pseudochattonella sp.*. This resulted in the death of 25 million fishes, 94% of them were Atlantic salmon, representing 40 000 tonnes of biomass and involving half of the aquaculture companies (Armijo et al., 2020; Garreaud, 2018b; Pujol et al., 2025; Souto Cavalli et al., 2023). Other major losses have since followed in Northern Patagonia. In 2019, another bloom of *Pseudochattonella* caused 123 tonnes of mortalities (SERNAPESCA, 2019; Souto Cavalli et al., 2023). In 2020, several toxic algal outbreaks, including *Cochlodinium sp.*, some of them associated to low-oxygen conditions, lead to further deaths totalling 40 tonnes (Salmonexpert, 2020a; SERNAPESCA, 2020; Souto Cavalli et al., 2023). In 2021, four mass mortality events were recorded: *Lepidodinium chlorophorum* caused the death of 162 000 fishes (600 tonnes) with an estimated loss of US$3.5 million); *Heterosigma akashiwo* killed 1 300 tonnes of fish; and two further HABs, including multi-species blooms, caused losses of more than 6 000 tonnes combined (FishfarmingExpert, 2021a, b; SERNAPESCA, 2021a, b, d, c; Souto Cavalli et al., 2023). The year 2022 was also particularly severe, with almost 5 000 tonnes of mortality linked to several species of toxic algae and decrease in dissolved oxygen (SERNAPESCA, 2022a, b, c). More recently, in summer 2024, another *Pseudochatonella sp.* outbreak resulted in the loss of approximately 3 800 tonnes of Atlantic and coho salmon (Gairn, 2024). The 2016 crisis was clearly associated with a prolonged MHW that lasted during the whole summer and parts of autumn and winter, facilitating the development of the HAB and probably reducing salmon resilience (Pujol et al., 2022, 2025; Chap. 5). More recent events also occurred in similar conditions; for example the 2022 toxic blooms coincided with MHWs the Aysén Region, while in 2021, blooms developed during warm temperature anomalies corresponding to MHWs in several areas (Chap. 4; Chap. 5; not shown data from Chap. 3).

Cold water events have also caused severe mortality in Atlantic salmon aquaculture. In eastern Canada, large-scale losses were reported in 2014, 2015, 2019 and 2020 (Vadboncoeur, 2023). When temperatures reach 6°C, a diminution of the food intake is observed in salmon populations, metabolisms changes at 4-5°C, and short-term cold shocks (0-3°C) cause complete cease of food intake and alter metabolism but do not cause significant mortality if lasting for no more than one day (Vadboncoeur, 2023). According to our results, such conditions are not reached during MCSs in Northern Patagonia (Pujol et al., 2025). However, prolonged exposure to temperature below 8°C has been linked to moribund and dead fishes (Vadboncoeur, 2023). Temperatures below 8°C can eventually be reached in Aysén Region of Northern Patagonia in winter in Moraleda Channel, Puyuhuapi and Aysén Fjords, and sometimes even lower temperatures, dropping to 6°C in the cold Elefantes Channel and Quitralco Fjord (Pujol et al., 2025). For example, during winter 2022, a MCS caused surface to 15 m temperature in Moraleda Channel to drop to 7°C between July and August, and at the surface, temperatures in Puyuhuapi, Aysén and Elefantes Channel also dropped to 7°C (Chap. 3; Chap. 4). Prolonged MCS in these fjords and channels could therefore strongly impact the health and salmons production.

In addition, disease outbreaks add another layer of vulnerability for salmons. In 2007-2008, Chile experienced a severe outbreak of Infectious Salmon Anaemia (ISA) virus, which reduces red blood cell counts, leading to anaemia, diminishing oxygen transport (Falk and Aamelfot, 2017; SERNAPESCA, 2008). Besides, it is known that ISA virus spread more effectively at low temperatures (Groves et al., 2023; Tunsjø et al., 2007). The outbreak began in June 2007, coinciding with the onset of a MCS that caused temperatures of 7°C in some parts of Aysén Region, spread exponentially during another MCS in autumn 2008, and peaked in December 2008 during a strong MHW (Chap. 4; Godoy et al., 2013; Pujol et al., 2025; SERNAPESCA, 2008). The most severely aquaculture centres were in central and southern Chiloé Island, which corresponded to the

regions where the 2007 MCS and the 2008 MCS and MHW were the strongest (Pujol et al., 2025; SERNAPESCA, 2008). This sequence suggests a strong link between extreme temperature events (both warm and cold) and increased disease vulnerability, with MCSs and MHWs likely exacerbating the spread and lethality of pathogens such as ISA virus.

6.5.6. Invasive species

Chilean Patagonia may face increased risk of non-indigenous species introductions and proliferation following MHWs and, more broadly, as a consequence of rising temperatures. Chilean coasts are already subject to non-indigenous species colonisation and pressure (Castilla et al., 2005; Stowhas Salinas et al., 2023; Valiñas et al., 2022), some of them via boat hull fouling facilitating the transport of both native and non-native species, including cold-water species well adapted to Chilean waters (Oyarzún et al., 2024; Pinochet et al., 2023). Although biogeographic boundaries such as upwellings, sea temperature, salinity and interspecies competition might act as partial barriers (Galván et al., 2022; Oyarzún et al., 2024), the increasing temperature and occurrence of MHW might facilitate the implantation and proliferation of alien species (Atkinson et al., 2020; Félix-Loaiza et al., 2022). In addition to the risk of non-native species invasions, Chilean Patagonia may also face the spatial expansion of native species from other regions of Chile, facilitated by the rising temperatures, as already observed in Argentinian Patagonia and in other regions of the world such as New-Zealand and North America (Galván et al., 2022; Lonhart et al., 2019; Spyksma et al., 2024). This process, known as the tropicalisation of temperate environment (Galván et al., 2022), has parallels in Arctic fjords, where warming processes have been linked to the "borealisation" of ecosystems, with boreal species expanding poleward and outcompeting native assemblages (Fossheim et al., 2015; Gorska et al., 2023). These dynamics suggest potential analogues for the fjord ecosystems of Southern Chile. Furthermore, in Chilean Patagonia, invasive species are already threatening indigenous species, and, in some cases, causing economic impacts on commercially important species, as for the urchin *Loxechinus albus*, outcompeted by an alien anemone (Stowhas Salinas et al., 2023). However, interactions between native and introduced species remain highly complex and can in some cases not be completely negative (Valiñas et al., 2022).

6.5.7. Oxygen and MCSs/MHWs

MHWs and MCSs are key modulators of biogeochemical processes, with significant implications for dissolved oxygen concentrations. Elevated temperatures during MHWs can exacerbate hypoxic conditions through several mechanisms: reducing oxygen solubility, enhancing metabolic oxygen demand across trophic levels and strengthening water column stratification, thereby restricting vertical mixing and oxygen renewal (Brauko et al., 2020; Fan et al., 2025; Gruber et al., 2021; Keeling et al., 2010). In addition, Fan et al. (2025) shown that deoxygenation is more probable to occur during MHWs than during a temperature warming that does not imply a MHW. Conversely, MCSs may temporarily enhance oxygen availability by cooling the surrounding waters and increasing their solubility (Walter et al., 2024). In Northern Patagonia, the deoxygenation risk is higher in the most enclosed areas, such as Reloncaví Sound and Fjord, Moraleda Channel and Jacaf and Puyuhuapi Fjord, where water renewal is very low (Linford et al., 2023; Quiñones et al., 2019).

Observations from Patagonia highlight the interplay between temperature and oxygen availability. Between, mid-May and late June 2015, dissolved oxygen concentrations at 122 m depth in Puyuhuapi Fjord shifted from hypoxic conditions (~1.5 mL/L) to oxic conditions (~2.8 mL/L) within

a short period, before returning to hypoxic conditions in July (Pérez-Santos, 2017). This fjord is known for its low oxygen conditions, being most of the time an hypoxic fjord (Schneider et al., 2014). Our analysis of the temperature outputs from the reanalysis GLORYS12V1 in Chapter 4 indicates that this event coincided with positive temperature anomalies between Guafo Mouth and Elefantes Channel, associated with a MHW. At Puyuhuapi's mouth, warming first appeared in April, extending from surface to 60 m depth. By May, the warming had intensified and reached 130 m with sea surface temperature anomalies of 0.5°C. In June, warming propagated to 185 m depth and maximum anomalies of +1°C were observed between 75 and 110 m. Although the water column cooled in August, positive anomalies persisted around Puyuhuapi's mouth. During the warming period, the mixed layer deepened from 30 m to 70 m and a MHW was identified between May and August at depth of 65 to 155 m. These changes in the water column structure were attributed to variations in the Modified Subantarctic Waters (MSAAW) which deepened, creating a ventilation event (Pérez-Santos, 2017). Interestingly, this intrusion coincided with both a MHW and higher concentrations in oxygen, contrary to the commonly held assumption that warming necessarily promotes lower oxygen concentrations. It underlines the complexity of interactions between thermal anomalies, water mass dynamics, and oxygen availability in Patagonian Fjords, and would require a more in depth analyse to understand how temperature anomalies developed inside Puyuhuapi Fjord.

In addition, in Northern Patagonia, the high solar radiation often associated with surface MHWs (Pujol et al., 2025), coupled to increased temperatures and enhanced stratification, can lead to more frequent and widespread phytoplankton blooms (Chap. 5; Díaz et al., 2023b; Garreaud, 2018b; León-Muñoz et al., 2018; Marquet et al., 2023). When the bloom vanishes, the sinking microalgae are decomposed by bacteria, a process that consumes oxygen and that can trigger hypoxic events, leading to stress of marine organisms and potentially in mortalities (Mayr et al., 2014; Pérez-Santos et al., 2018).

Several species are particularly vulnerable to the combined effects of warming and oxygen depletion. For example, salmon experience physiological stress under elevated temperatures when oxygen is reduced, whereas temperature alone would not have induced thermal stress, making them less able to tolerate additional environmental stressors (Gamperl et al., 2020, 2021; Sajid et al., 2024). Similarly, cold-water corals are sensitive to oxygen depletion. Studies on the emblematic cold-water coral *Lophelia pertusa* (although not present in Chilean Patagonia) suggest that oxygen availability is a major factor limiting the distribution of cold-water corals in general (Dodds et al., 2007). Increasing temperatures combined with hypoxia or anoxia are expected to pose severe threats to these organisms, possibly exceeding the risks associated with ocean acidification (Jantzen et al., 2013).

6.6. Management

Mitigating the impacts of MHWs on ecosystems and aquaculture in a warming world is becoming more and more necessary, before economic and ecological losses become too important.

Some studies suggest that the establishment of marine protected areas may buffer the effects of MHWs on native species, supporting faster recovery following such event (Kumagai et al., 2024; Ziegler et al., 2023). Although marine protected areas do not shield species from the occurrence of MHWs, they can facilitate post-disturbance recovery (Kumagai et al., 2024; Ziegler et al., 2023), even if this effect is not observed systematically across systems (Freedman et al., 2020; Smith et al.,

2023a). Chile hosts several marine protected areas and marine parks where human activities are restricted, including in the regions of Los Lagos, Aysén and Magallanes (Ministerio de Economía et al., 2004). In Patagonia, marine protected areas cover 6% of coastal marine zone, and National Protected Areas System cover 35% of the coastal zone (Tecklin et al., 2023). Evaluating the ecological state of these protected areas following MHW events could provide valuable insights into their potential role in enhancing ecosystems resilience. If a buffering effect is confirmed, this would further strengthen the need of expanding protected areas in the region. In addition, restrictions on extraction following MHWs have also been shown to promote stronger recovery from heatwave-induced damage (Caputi et al., 2016). Implementing such measures in Northern Patagonia could help alleviate pressure on native populations.

In the case of aquaculture, different methodologies and technologies have been developed in the recent years to counter warming effects. For mussel farming, transplanting individuals between aquaculture lines at different depth has shown positive results, likely due to the thermal buffering provided by deeper waters (Jahnsen-Guzmán et al., 2021). A similar approach in salmon aquaculture could involve the use of deeper cages, which could reduce thermal stress by allowing natural vertical migration to enable the fishes to avoid the warmer and less oxygenated surface waters (Gamperl et al., 2021). Recently, new technologies have been developed in Chile, including submersible salmon cages that can be lowered to deeper layers during HAB, extreme weather or low-oxygen events, thereby offering an adaptative response to surface MHWs (Salmonexpert, 2020b, 2021).

At the farm-management level, practices that enhance water quality and reduce stress are critical. Lowering stocking densities within cages can decrease overall oxygen consumption (Berntsson et al., 2025; Poston and Williams, 1988), reduce pathogen transmission (Jones et al., 2015), and allow individuals more freedom to migrate vertically in response to surface warming (Gamperl et al., 2021). In addition, maintaining high water quality through regular net cleaning to improve water flow, installing farms in areas with strong water flow if tolerated by the species and low susceptibility to hypoxia and HAB development, and relocating sites if environmental risks are detected can reduce environmental stress. Supplemental oxygenation within cages during hypoxia or elevated surface temperature has also been successfully applied (Sajid et al., 2024).

Disease prevention remains another key challenge, particularly under warmer temperatures, as pathogens tend go better propagate under such conditions (Cascarano et al., 2021; Combe et al., 2023). Selective breeding and genetic selection of individuals more tolerant to elevated temperatures of high pCO2 could be another approach to deal with warming temperatures, as it has for example been observed with the seaweed *Agarophyton chilensis* (Benfey et al., 2024; Ignatz et al., 2023; Usandizaga et al., 2019). However, care must be taken to avoid reducing genetic diversity, as this can compromise the population's resistance to pathogens and other stress factors, and limit future adaptive potential (Robinson et al., 2013).

Finally, large-scale spatial strategies, such as shifting farms to higher latitudes could provide long-term protection by exploiting cooler waters that are less exposed to extreme heat events (Pujol et al., 2022). However, such relocation must account for regional constraints, as for example the cultivation of *Mytilus chilensis* is regularly prohibited in the Aysén Region due to the high risk of paralytic shellfish poisoning (Ministerio de Salud and Secretaría Regional Ministerial Región de Los Lagos, 2024; Ministerio de Salud and Subsecretaría de Salud Pública, 2022). Together, these measures (ranging from technological innovations and improved farm management to genetic strategies and spatial planning) offer a multi-layered approach to mitigate the growing threat of MHWs to aquaculture under climate change.

CHAPTER 7.   SUMMARY, CONCLUSIONS, FUTURE DIRECTIONS AND IMPLICATIONS

This thesis presents the first assessment of marine heatwaves (MHWs) and marine cold spells (MCSs) across Central Chile and Chilean Patagonia (29°S-55°S) over the period 1982 to 2024, with a particular emphasis on Northern Chilean Patagonia. The key strength of this work lies in its multi-scale approach, combining datasets of different origins and resolutions to characterise events of varying importance.

At larger scale, satellite data reveals that Central Chile, Northern Patagonia and Southern Patagonia respond differently to MHWs, shaped by distinct atmospheric drivers acting at different time, creating a regional variability. In both Central Chile and Northern Patagonia, the past decade experienced the most severe conditions. Among the three regions, Northern Patagonia emerges as the most vulnerable, showing the strongest trends of SST warming and the greatest increase in MHWs occurrence.

Focusing on Northern Patagonia, this thesis provides the first detailed characterisation of MHW and MCS dynamics in a region that is both ecologically sensitive and economically important due to its aquaculture and fisheries. Despite this economic significance, its exposure to MHWs and MCSs had not previously been quantified. To address this gap, a novel methodology was developed to detect thermal extremes in highly coastal systems, combining in situ and satellite data resulting in an analysis at a spatial resolution of 900 m for surface events. The results reveal pronounced spatial variability in the occurrence, intensity and duration of MHWs and MCSs, even between adjacent fjords such as Puyuhuapi and Aysén. This variability is driven by a combination of global and local atmospheric, oceanic and remote forcings, strongly influenced by the topography. To our knowledge, this is the first study to highlight such fine-scale variability of MHWs and MCSs across a same region.

Overall, in Northern Patagonia, the findings point to a general decrease in MCSs and an increase in MHWs, though variations are observed across basins, with for example Corcovado Gulf and experiencing negative trends for both events. Fjords and semi-enclosed areas as Reloncaví Sound are particularly prone to stronger anomalies due to local circulation and stratification process. Subsurface analyses further reveal that MHWs and MCS can be more intense below the surface layer and persist much longer in the subsurface, such as the three-year long MCS in Reloncaví Sound from 2022 to 2024 and the two-year long MHW in Ancud Gulf from 2006 to 2008. Historical extremes illustrate the complex dynamics: the 1997-1999 ENSO-related MHW event was particularly strong, and penetrated rapidly to bottom layers in homogeneous basins, while it extended to the deep layers months later in Ancud and Reloncaví Gulfs due to topographic

constrains. On the contrary, whereas the ENSO-related 2016-2017 MHW was particularly long and intense, especially in the Inner Sea, it remained confined to the upper 50 m.

These findings underline both the limitations of global-scale models in capturing local dynamics and the necessity of regional approaches to understand the formation, drivers and impacts of marine thermal extremes in coastal systems. The results also highlight the indispensable contribution of in situ measurements for identifying MHWs in highly complex environment, including fjords areas, where satellite data and hydrodynamic models can be unreliable or insufficient. Although large-scale detection of MHWs and MCSs provides valuable insights into global dynamics, this thesis shows the importance of adequately resolving these processes, which display particularly high variability in coastal areas, and demonstrates the value of high-resolution approaches in complex coastal systems. The methodology developed here not only advances the detection of MHWs and MCSs in Northern Patagonia but can also be applied to other fjords and coastal regions worldwide, when in situ data are available. By revealing the heterogeneity of thermal extremes, such approaches provide valuable tools for aquaculture and fisheries management, as well for conservation planning. Identifying hotspots of extreme variability, alongside potential refugia where conditions remain comparatively stable, is essential for designing adaptation strategies in a world of changing climate.

These changes in MHWs carry significant implications for Patagonia's fragile ecosystems, where even small temperature anomalies may alter community structure, oxygen, oceanic dynamics, harmful algal blooms (HAB) formation and trophic stability. Increasing exposure to MHWs may also facilitate the spread of invasive species better adapted to warmer conditions, while cold-water native species and commercially important resources may experience growing stress. The consequences of MCSs on local species and ecosystems remain quite limited, as most native species are cold-water organisms already adapted to cooler conditions in a warming world. Overall, the vulnerability of Patagonian benthic, pelagic and coastal organisms to climate change cannot be understood solely in terms of temperature rise. For many species, it is the combination of warming with other stressors (such as reduced freshwater inputs, ocean acidification, or declining oxygen availability) that drives the strongest biological impacts. These compound events often exacerbate physiological stress, reduce survival or reproductive success and may accelerate shifts in species distributions. Importantly, while the upper thermal tolerance of several organisms may soon be exceeded in Northern Patagonia, the lower thermal limits of most species remain well below the temperatures typically reached during MCSs. This contrast suggests that Southern Patagonia, where oceanic conditions are colder even during MHWs, could act as a critical refuge for species displaced from northern habitats. For fisheries and aquaculture, this highlights the urgent need for diversification strategies and for research focused on species-specific thermal sensitivities at different life stages. Protecting these ecosystems, while also developing adaptive strategies for aquaculture and fisheries, will be essential to maintain biodiversity and sustain human livelihoods strongly dependant of the marine resources. Importantly, this study did not present single temperature threshold to characterise ecological or economic risk, as vulnerability differs across basins, ecosystems and species. A summary of this thesis is available in Figure 52.

Finally, while this work focused on Northern Patagonia, the methodology developed here can be extended to Central Chile, Southern Patagonia, and any other coastal region worldwide where sufficient in situ data are available. Future studies should address the cascading ecological effects of MHWs, particularly their interactions with oxygen availability and trophic dynamics, in order to anticipate long-term impacts on ecosystems stability and socio-economic activities.
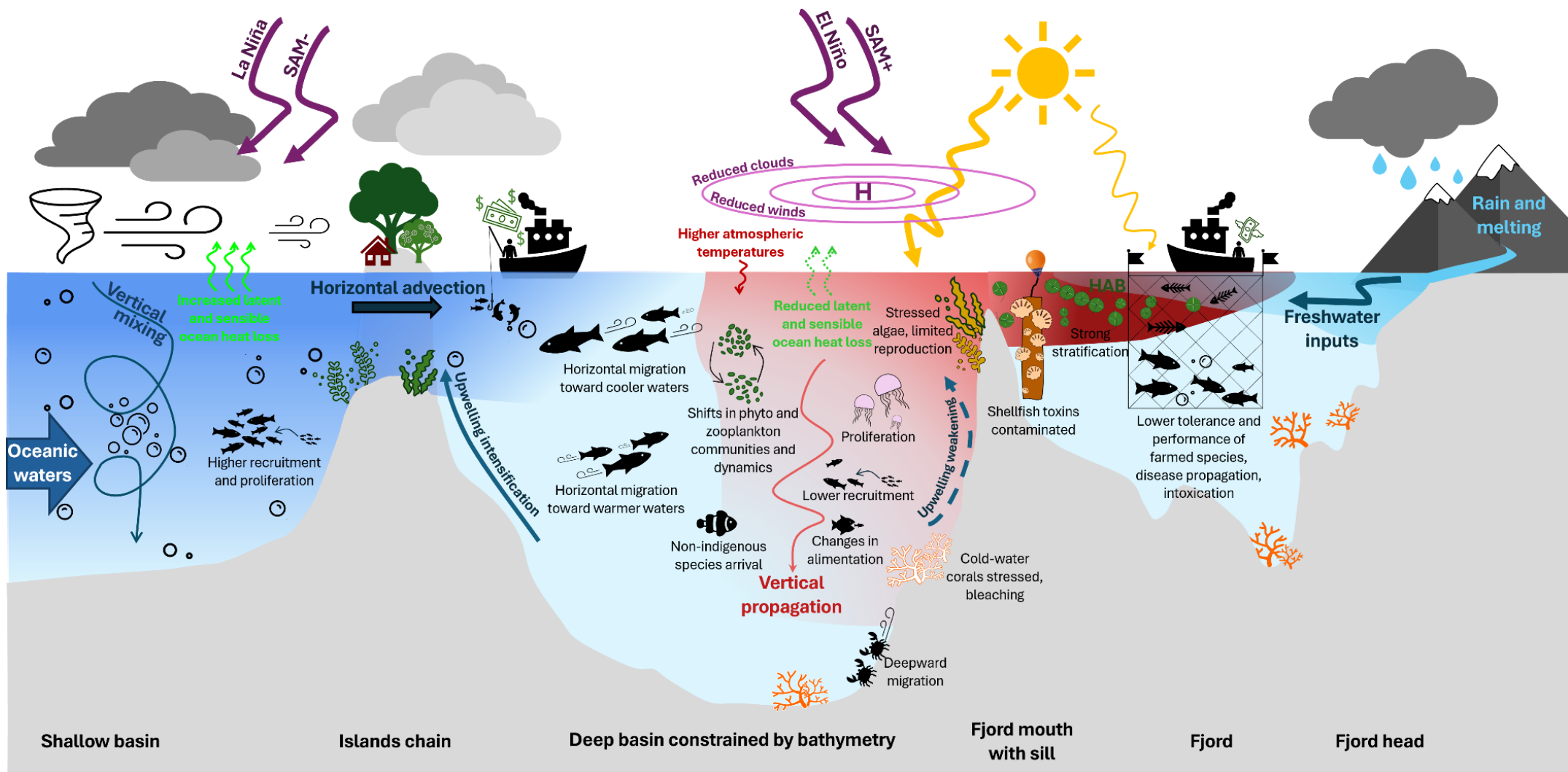
Figure 52: Summary figure of marine heatwaves (MHWs, red) and marine cold spells (MCSs, dark blue) in a typical fjord system, such as Northern Patagonia. In our case, the shallow basin is comparable to Corcovado Gulf, the islands chain to the Desertores Islands, the deep basin to Ancud Gulf, and the fjord to Comau Fjord. Extreme events can propagate horizontally through advection (restricted to the upper layers when passing through a shallow physical barrier), and can penetrate deeper layers through vertical heat transfer or mixing. MHWs are favoured by increased solar radiation and reduced winds, which reduce the heat transfer from the ocean to the atmosphere, conditions that often occur under high-pressure system (H), and are further intensified during positive phases of ENSO (El Niño) or SAM, and may also develop when upwelling weakens. MHWs increase stratification, can trigger harmful algal blooms (HABs) and toxicity, reduce oxygen levels, and affect marine organisms by altering plankton dynamics, causing vertical or horizontal migrations, facilitating species shifts and proliferation, impairing reproduction and recruitment, enhancing disease spread and generally causing physiological stress. In contrast, MCSs are driven by wind-induced mixing, often under low-pressure systems, which enhance vertical mixing and heat transfer from the ocean to the atmosphere, and are typically intensified during negative ENSO (La Niña) or SAM, and may also arise from intensified upwelling. Their ecological impacts on the cold-water ecosystems, such as those of Northern Patagonia, are generally more limited, although they can favour the development of certain species.
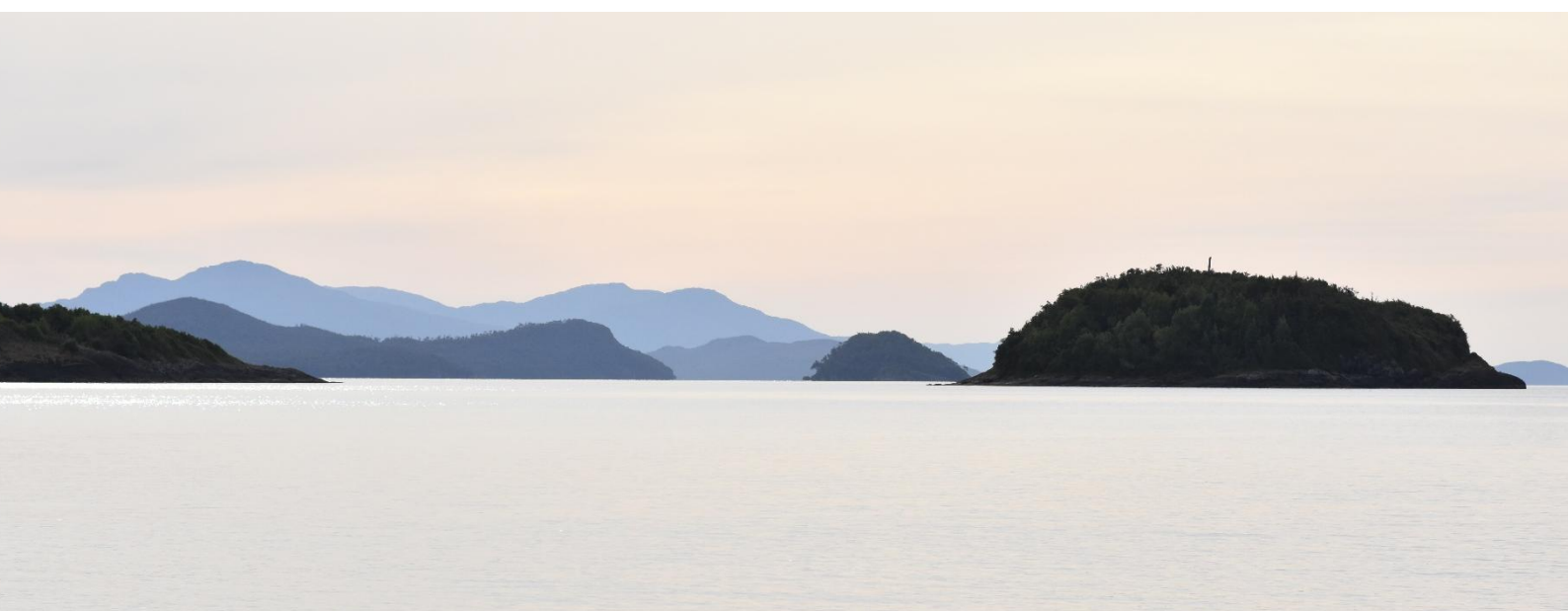
CHAPTER 8.   SUPPLEMENTARY MATERIALS

Table Supplementary 1: Total number of samples collected at the sea surface (0-1m depth), separated into mooring and non-mooring sources, along with the 5% of each group set aside for validation.

Month	Total samples	Mooring samples	Mooring validation	Non-mooring samples	Non-mooring validation
Jan	8792	8693	435	99	5
Fev	14680	13685	684	995	50
Mar	13921	13711	686	210	11
Apr	8534	8373	419	161	8
May	10081	9478	474	603	30
Jun	9409	9077	454	332	17
Jul	9825	9331	467	494	25
Aug	9022	8557	428	465	23
Sep	10289	9540	477	749	37
Oct	9659	9174	459	485	24
Nov	8712	7701	385	1011	51
Dec	9238	9020	451	218	11
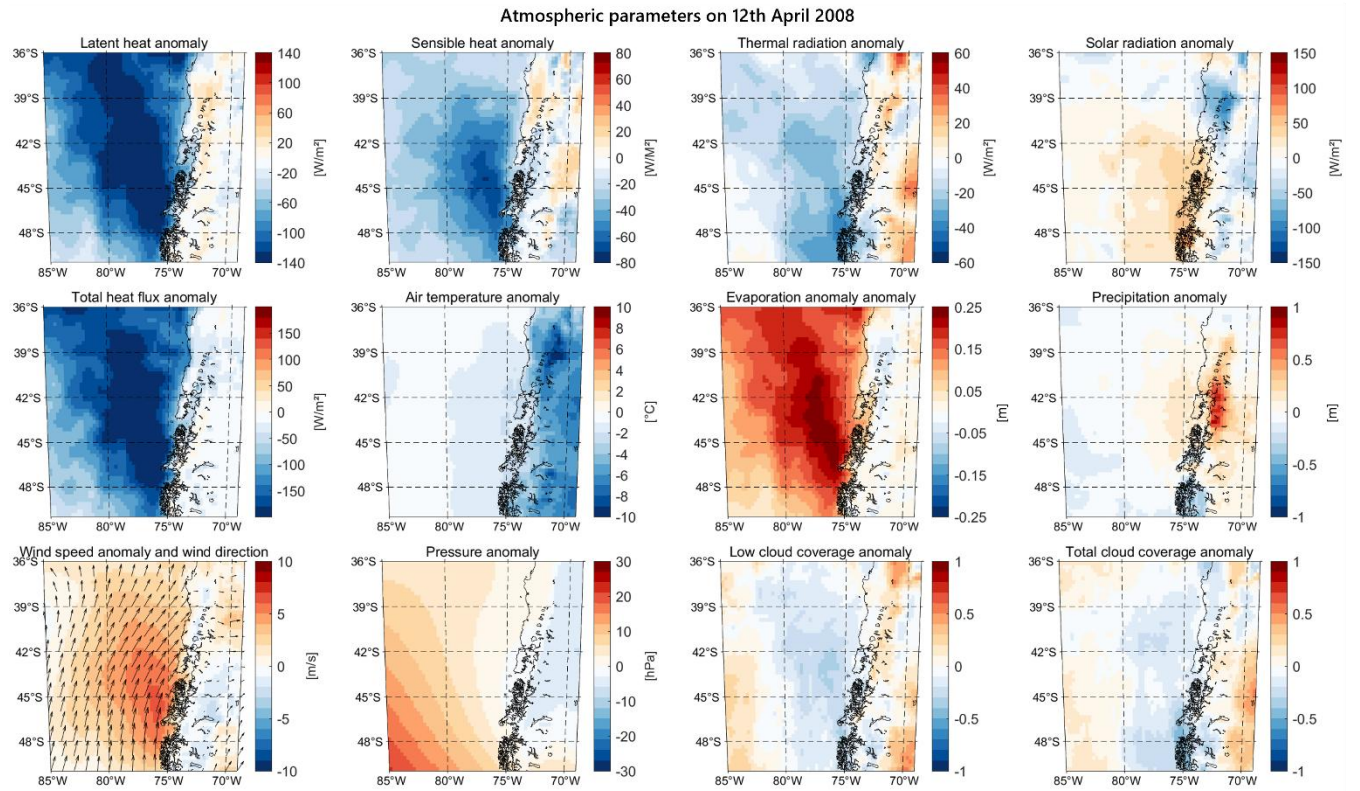
Figure Supplementary 1: Atmospheric parameters anomalies (calculated over the period 1993-2023) preceding the onset of a MCS. Low and total cloud coverage are dimensionless, representing from 0 to 1 the proportion of the pixel covered by clouds.
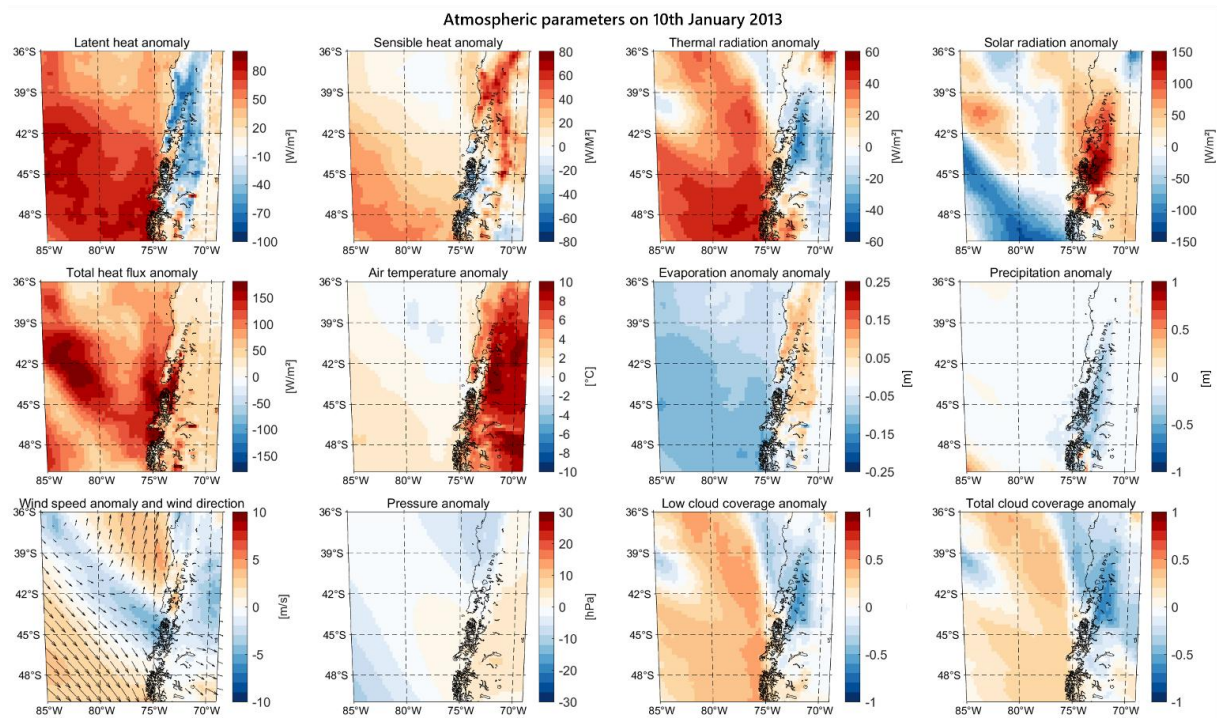
Figure Supplementary 2: Atmospheric parameters anomalies (calculated over the period 1993-2023) preceding the onset of a MHW. Low and total cloud coverage are dimensionless, representing from 0 to 1 the proportion of the pixel covered by clouds.
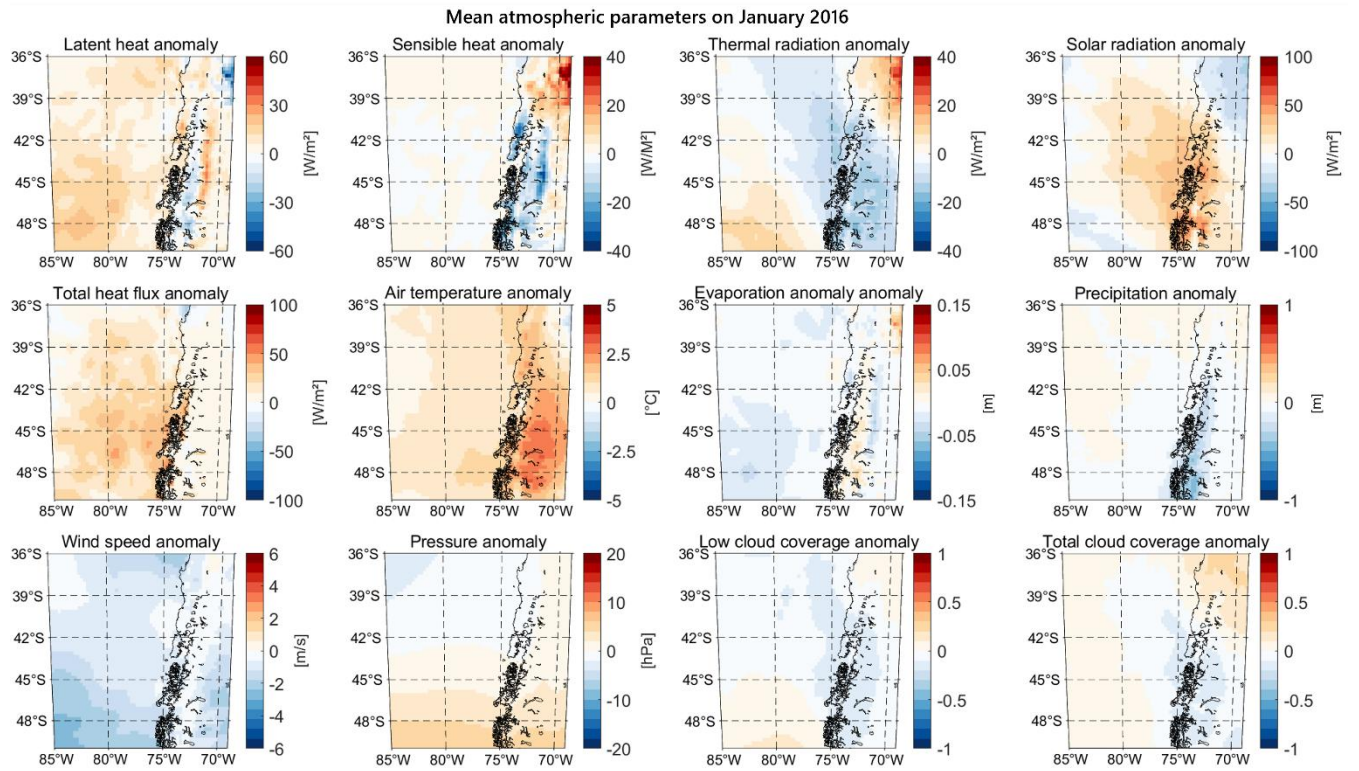
Figure Supplementary 3: Monthly average atmospheric parameters anomalies (calculated over the period 1993-2023) during the MHW. Low and total cloud coverage are dimensionless, representing from 0 to 1 the proportion of the pixel covered by clouds.
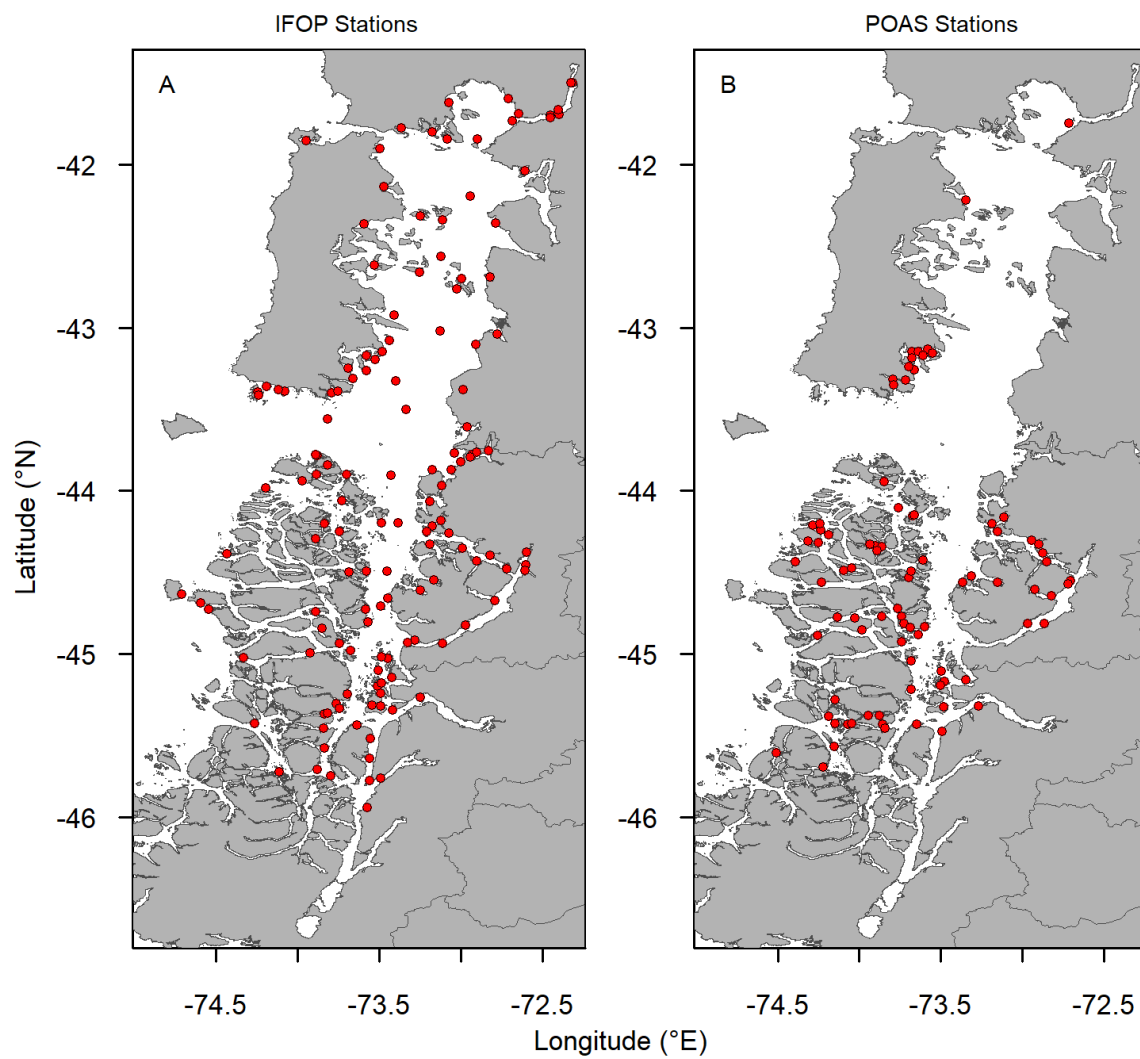
Figure Supplementary 4: Location of the different monitoring stations of Alexandrium catenella from the IFOP monitoring system (A) and PROMOFI (B).

Figure Supplementary 5: Representation of MHWs on the day of their maximal intensity reached (colours) and the associated temperature anomaly on that day (thin lines).

Figure Supplementary 6: Monthly average of SST (°C) for Aysén Region from January 2003 to May 2023.

CHAPTER 9.   LIST OF PUBLICATIONS

Published papers

Pujol C., Pérez-Santos I., Barth A. & Alvera-Azcárate A. (2022). **Marine Heatwaves Offshore Central and South Chile : Understanding Forcing Mechanisms During the Years 2016-2017**. Frontiers in Marine Science, 9, 800325. https://doi.org/10.3389/fmars.2022.800325

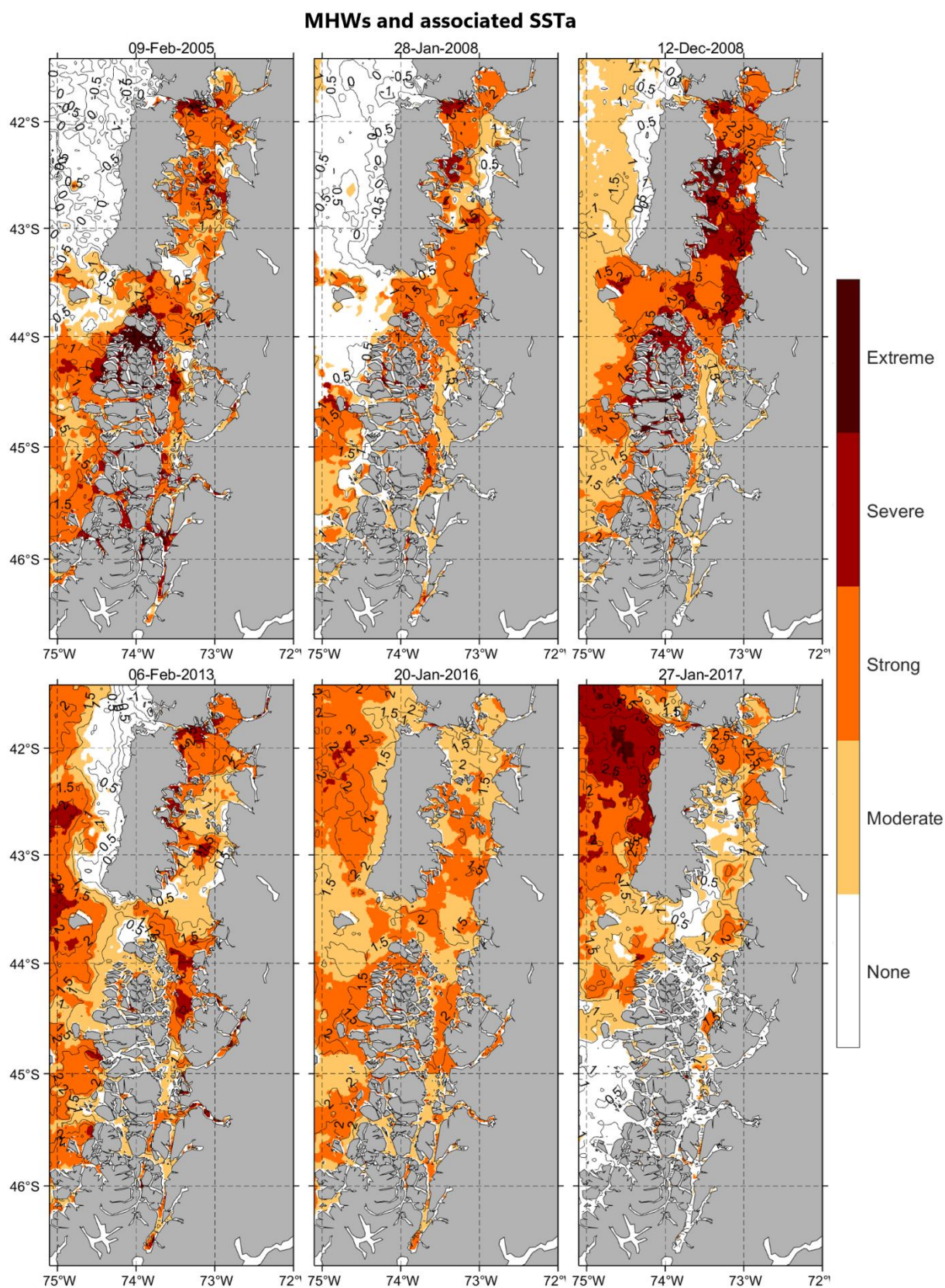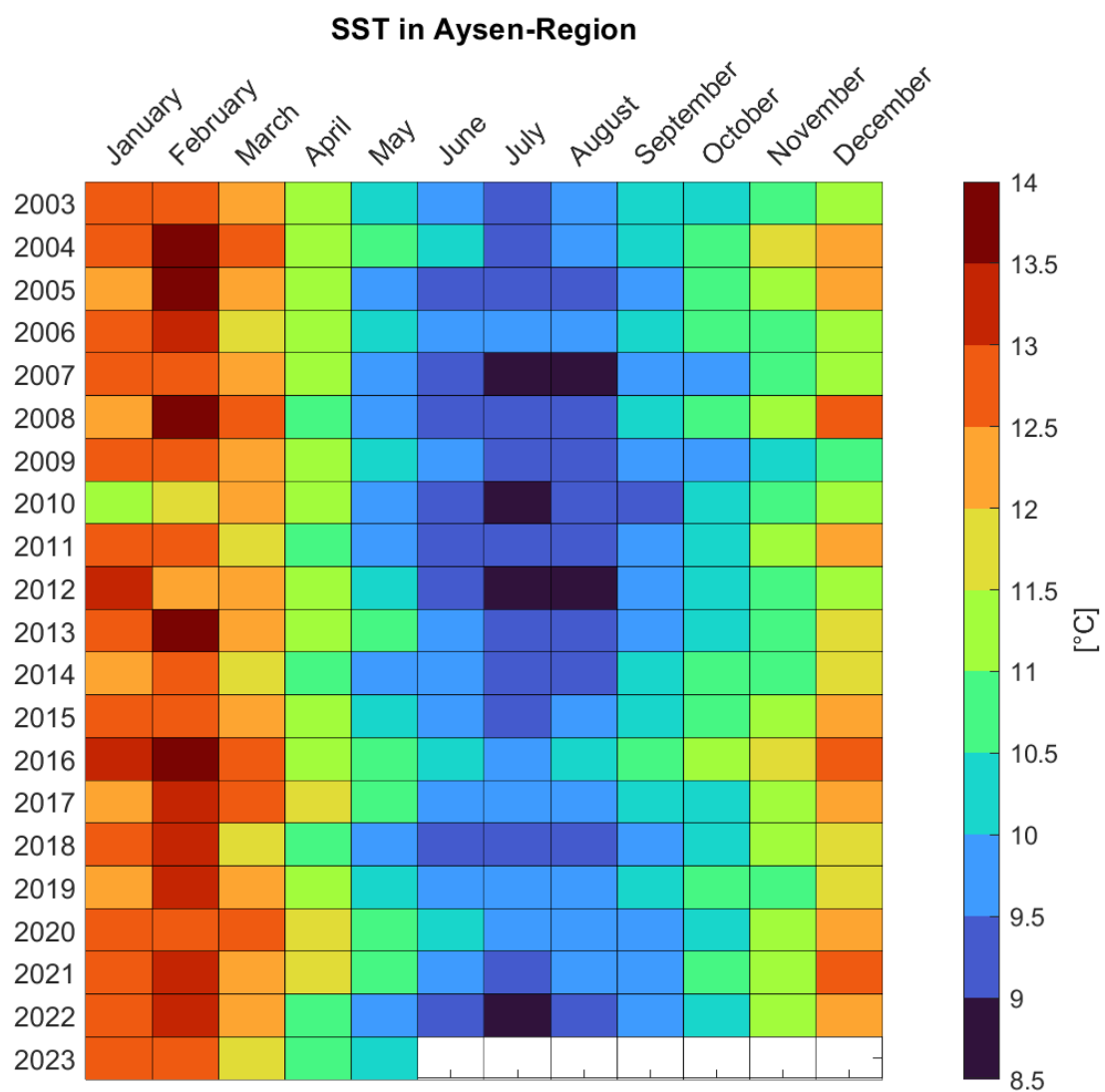Linford P., Pérez-Santos I., Montero P., Díaz P. A., Aracena C., Pinilla E., Barrera F., Castillo M., Alvera-Azcárate A., Alvarado M., Soto G., **Pujol C.**, Schwerter C., Arenas-Uribe S., Navarro P., Mancilla-Gutiérrez G., Altamirano R., San Martín J., & Soto-Riquelme C. (2024). Oceanographic processes driving low-oxygen conditions inside Patagonian fjords. Biogeosciences, 21(6), 1433-1459. https://doi.org/10.5194/bg-21-1433-2024

Mancilla-Gutiérrez G., Díaz P. A., Pérez-Santos I., **Pujol C.**, Schwerter C., Altamirano R., Arenas-Uribe S., Navarro P., & Saldías G. S. (2022). High-Biomass Harmful Algal Blooms (HB-HAB) in the Chilean Fjords System : Lepidodinium chlorophorum. Harmful Algae News, 71, 5-6. https://doi.org/10.5281/zenodo.7383099

Papers under review/submitted

Pujol C., Barth A., Pérez-Santos I., Muñoz-Linford P., and Alvera-Azcárate A.: **Overcoming Challenges in Coastal Marine Heatwave Detection: Integrating In Situ and Satellite Data in Complex Coastal Environment**, *EGUsphere [preprint],* https://doi.org/10.5194/egusphere-2025-1421 , 2025.

Pujol C., Díaz P., Mancilla-Gutiérrez G., Tucca F., Barth A., Alvera-Azcárate A.: **Alexandrium catenella blooms and Marine Heatwaves in Northwestern Patagonia**, *Submitted to Marine Pollution Bulletin*

On-going papers

Julio Salcedo-Castro, Neil Holbrook, Thomas Wernberg, Alistair Hobday, Pip Moore, Dan Smale, Bronwyn Cahill, Specer Tassone, Andrea Piñones, Antonio Olita, Hans Burchard, Christopher Harley, Piero Mazzini, **Pujol Cécile**, Ryan K. Walter, David Carrasco, Murilo Marochi, Romain Le Gendre, Serge Andrefouet, Sophie Cravatte, Alex Sen Gupta, Neil Malan, Michael Burrows, Karen Filbee-Dexter, Eric Oliver, Mads Thomsen, Kathryn Smith. **Review article on coastal marine heatwaves**. Targeted review: *Nature Reviews Earth & Environment*

Eisbrenner Ezra, Manay Roger, **Pujol Cécile**, Shi Jiaxin, Zhang Shujing, Villani Mattias, Smith Kathryn E., Rodrigues Regina R.. **Marine heatwaves and coral bleaching in the Caribbean Sea**. Targeted review: *Communications 0Earth & Environment*

CHAPTER 10.   REFERENCES

Aceituno, P., Boisier, J. P., Garreaud, R., Rondanelli, R., and Rutllant, J. A.: Climate and Weather in Chile, in: Water Resources of Chile, vol. 8, edited by: Fernández, B. and Gironás, J., Springer International Publishing, Cham, 7–29, https://doi.org/10.1007/978-3-030-56901-3_2, 2021.

Aguayo, R., León-Muñoz, J., Vargas-Baecheler, J., Montecinos, A., Garreaud, R., Urbina, M., Soto, D., and Iriarte, J. L.: The glass half-empty: climate change drives lower freshwater input in the coastal system of the Chilean Northern Patagonia, Climatic Change, 155, 417–435, https://doi.org/10.1007/s10584-019-02495-6, 2019.

Aguayo, R., León-Muñoz, J., Garreaud, R., and Montecinos, A.: Hydrological droughts in the southern Andes (40–45°S) from an ensemble experiment using CMIP5 and CMIP6 models, Sci Rep, 11, 5530, https://doi.org/10.1038/s41598-021-84807-4, 2021.

Aguilera-Belmonte, A., Inostroza, I., Carrillo, K. S., Franco, J. M., Riobó, P., and Gómez, P. I.: The combined effect of salinity and temperature on the growth and toxin content of four Chilean strains of Alexandrium catenella (Whedon and Kofoid) Balech 1985 (Dinophyceae) isolated from an outbreak occurring in southern Chile in 2009, Harmful Algae, 23, 55–59, https://doi.org/10.1016/j.hal.2012.12.006, 2013.

Aguirre, C., Pizarro, Ó., Strub, P. T., Garreaud, R., and Barth, J. A.: Seasonal dynamics of the near-surface alongshore flow off central Chile, J. Geophys. Res., 117, 2011JC007379, https://doi.org/10.1029/2011JC007379, 2012.

Aguirre, C., García-Loyola, S., Testa, G., Silva, D., and Farías, L.: Insight into anthropogenic forcing on coastal upwelling off south-central Chile, Elementa: Science of the Anthropocene, 6, 59, https://doi.org/10.1525/elementa.314, 2018.

Aguirre, C., Rojas, M., Garreaud, R. D., and Rahn, D. A.: Role of synoptic activity on projected changes in upwelling-favourable winds at the ocean's eastern boundaries, npj Clim Atmos Sci, 2, 44, https://doi.org/10.1038/s41612-019-0101-9, 2019.

Aiken, C. M.: Barotropic tides of the Chilean Inland Sea and their sensitivity to basin geometry, J. Geophys. Res., 113, 2007JC004593, https://doi.org/10.1029/2007JC004593, 2008.

Aksnes, D. L., Aure, J., Johansen, P.-O., Johnsen, G. H., and Vea Salvanes, A. G.: Multi-decadal warming of Atlantic water and associated decline of dissolved oxygen in a deep fjord, Estuarine, Coastal and Shelf Science, 228, 106392, https://doi.org/10.1016/j.ecss.2019.106392, 2019.

Almanza, V. and Buschmann, A. H.: The ecological importance of Macrocystis pyrifera (Phaeophyta) forests towards a sustainable management and exploitation of Chilean coastal benthic co-management areas, IJESD, 12, 341, https://doi.org/10.1504/IJESD.2013.056331, 2013.

Alonso Vega, J. M., Vásquez, J. A., and Buschmann, A. H.: Population biology of the subtidal kelps Macrocystis integrifolia and Lessonia trabeculata (Laminariales, Phaeophyceae) in an upwelling ecosystem of northern Chile: interannual variability and El Niño 1997-1998, Rev. chil. hist. nat., 78, https://doi.org/10.4067/S0716-078X2005000100004, 2005.

Alvarado-Rybak, M., Toro, F., Escobar-Dodero, J., Kinsley, A. C., Sepúlveda, M. A., Capella, J., Azat, C., Cortés-Hinojosa, G., Zimin-Veselkoff, N., and Mardones, F. O.: 50 Years of Cetacean Strandings Reveal a Concerning Rise in Chilean Patagonia, Sci Rep, 10, 9511, https://doi.org/10.1038/s41598-020-66484-x, 2020.

Álvarez, G., Díaz, P. A., Godoy, M., Araya, M., Ganuza, I., Pino, R., Álvarez, F., Rengel, J., Hernández, C., Uribe, E., and Blanco, J.: Paralytic Shellfish Toxins in Surf Clams Mesodesma donacium during a Large Bloom of Alexandrium catenella Dinoflagellates Associated to an Intense Shellfish Mass Mortality, Toxins, 11, 188, https://doi.org/10.3390/toxins11040188, 2019.

Alvera-Azcárate, A., Barth, A., Rixen, M., and Beckers, J. M.: Reconstruction of incomplete oceanographic data sets using empirical orthogonal functions: application to the Adriatic Sea surface temperature, Ocean Modelling, 9, 325–346, https://doi.org/10.1016/j.ocemod.2004.08.001, 2005.

Alvera-Azcárate, A., Barth, A., Sirjacobs, D., Lenartz, F., and Beckers, J. M.: Data Interpolating Empirical Orthogonal Functions (DINEOF): a tool for geophysical data analyses, Medit. Mar. Sci., 12, 5, https://doi.org/10.12681/mms.64, 2011.

Alvera-Azcárate, A., Van Der Zande, D., Barth, A., Troupin, C., Martin, S., and Beckers, J.-M.: Analysis of 23 Years of Daily Cloud-Free Chlorophyll and Suspended Particulate Matter in the Greater North Sea, Front. Mar. Sci., 8, https://doi.org/10.3389/fmars.2021.707632, 2021.

Amaya, D. J., Alexander, M. A., Scott, J. D., and Jacox, M. G.: An evaluation of high-resolution ocean reanalyses in the California current system, Progress in Oceanography, 210, 102951, https://doi.org/10.1016/j.pocean.2022.102951, 2023a.

Amaya, D. J., Jacox, M. G., Alexander, M. A., Scott, J. D., Deser, C., Capotondi, A., and Phillips, A. S.: Bottom marine heatwaves along the continental shelves of North America, Nat Commun, 14, 1038, https://doi.org/10.1038/s41467-023-36567-0, 2023b.

Ancapichún, S. and Garcés-Vargas, J.: Variability of the Southeast Pacific Subtropical Anticyclone and its impact on sea surface temperature off north-central Chile, Cienc. Mar., 41, 1–20, https://doi.org/10.7773/cm.v41i1.2338, 2015.

Ancapichun, S. and Garcés-Vargas, J.: Variability of the Southeast Pacific Subtropical Anticyclone and its impact on sea surface temperature off north-central Chile, Cienc Mar, 41, 1–20, https://doi.org/10.7773/cm.v41i1.2338, 2015.

Anderson, D. M., Alpermann, T. J., Cembella, A. D., Collos, Y., Masseret, E., and Montresor, M.: The globally distributed genus Alexandrium: Multifaceted roles in marine ecosystems and impacts on human health, Harmful Algae, 14, 10–35, https://doi.org/10.1016/j.hal.2011.10.012, 2012.

Androulidakis, Y. and Pytharoulis, I.: Variability of marine heatwaves and atmospheric cyclones in the Mediterranean Sea during the last four decades, Environ. Res. Lett., 20, 034031, https://doi.org/10.1088/1748-9326/adb505, 2025.

Anger, K., Lovrich, G. A., Thatje, S., and Calcagno, J. A.: Larval and early juvenile development of Lithodes santolla (Molina, 1782) (Decapoda: Anomura: Lithodidae) reared at different temperatures in the laboratory, Journal of Experimental Marine Biology and Ecology, 306, 217–230, https://doi.org/10.1016/j.jembe.2004.01.010, 2004.

Anthony, K. R. N., Hoogenboom, M. O., Maynard, J. A., Grottoli, A. G., and Middlebrook, R.: Energetics approach to predicting mortality risk from environmental stress: a case study of coral bleaching, Functional Ecology, 23, 539–550, https://doi.org/10.1111/j.1365-2435.2008.01531.x, 2009.

Arafeh-Dalmau, N., Montaño-Moctezuma, G., Martínez, J. A., Beas-Luna, R., Schoeman, D. S., and Torres-Moye, G.: Extreme Marine Heatwaves Alter Kelp Forest Community Near Its Equatorward Distribution Limit, Front. Mar. Sci., 6, 499, https://doi.org/10.3389/fmars.2019.00499, 2019.

Arcos, D. F., Cubillos, L. A., and P. Núñez, S.: The jack mackerel fishery and El Niño 1997–98 effects off Chile, Progress in Oceanography, 49, 597–617, https://doi.org/10.1016/S0079-6611(01)00043-X, 2001.

Arias-Ortiz, A., Serrano, O., Masqué, P., Lavery, P. S., Mueller, U., Kendrick, G. A., Rozaimi, M., Esteban, A., Fourqurean, J. W., Marbà, N., Mateo, M. A., Murray, K., Rule, M. J., and Duarte, C. M.: A marine heatwave drives massive losses from the world's largest seagrass carbon stocks, Nature Clim Change, 8, 338–344, https://doi.org/10.1038/s41558-018-0096-y, 2018.

Arimitsu, M. L., Piatt, J. F., Hatch, S., Suryan, R. M., Batten, S., Bishop, M. A., Campbell, R. W., Coletti, H., Cushing, D., Gorman, K., Hopcroft, R. R., Kuletz, K. J., Marsteller, C., McKinstry, C., McGowan, D., Moran, J., Pegau, S., Schaefer, A., Schoen, S., Straley, J., and Von Biela, V. R.: Heatwave-induced synchrony within forage fish portfolio disrupts energy flow to top pelagic predators, Global Change Biology, 27, 1859–1878, https://doi.org/10.1111/gcb.15556, 2021.

Armijo, J., Oerder, V., Auger, P.-A., Bravo, A., and Molina, E.: The 2016 red tide crisis in southern Chile: Possible influence of the mass oceanic dumping of dead salmons, Marine Pollution Bulletin, 150, 110603, https://doi.org/10.1016/j.marpolbul.2019.110603, 2020.

Athanase, M., Sánchez-Benítez, A., Goessling, H. F., Pithan, F., and Jung, T.: Projected amplification of summer marine heatwaves in a warming Northeast Pacific Ocean, Commun Earth Environ, 5, 53, https://doi.org/10.1038/s43247-024-01212-1, 2024.

Atkinson, J., King, N. G., Wilmes, S. B., and Moore, P. J.: Summer and Winter Marine Heatwaves Favor an Invasive Over Native Seaweeds, Journal of Phycology, 56, 1591–1600, https://doi.org/10.1111/jpy.13051, 2020.

Avens, L., Goshe, L., Harms, C., Anderson, E., Goodman Hall, A., Cluse, W., Godfrey, M., Braun-McNeill, J., Stacy, B., Bailey, R., and Lamont, M.: Population characteristics, age structure, and growth dynamics of neritic juvenile green turtles in the northeastern Gulf of Mexico, Mar. Ecol. Prog. Ser., 458, 213–229, https://doi.org/10.3354/meps09720, 2012.

Avila, M., De Zarate, C., Clement, A., Carbonell, P., and Pérez, F.: Efecto de factores abióticos en el crecimiento vegetativo de Alexandrium catenella proveniente de quistes en laboratorio, Rev. biol. mar. oceanogr., 50, 177–185, https://doi.org/10.4067/S0718-19572015000200004, 2015.

Bao, W. and Moffat, C.: Impact of shallow sills on circulation regimes and submarine melting in glacial fjords, The Cryosphere, 18, 187–203, https://doi.org/10.5194/tc-18-187-2024, 2024.

Barange, M. and Cochrane, K.: Chapter 28: Impacts of climate change on fisheries and aquaculture: conclusions, 611–628, 2018.

Barbeaux, S. J., Holsman, K., and Zador, S.: Marine Heatwave Stress Test of Ecosystem-Based Fisheries Management in the Gulf of Alaska Pacific Cod Fishery, Front. Mar. Sci., 7, 703, https://doi.org/10.3389/fmars.2020.00703, 2020.

Barlow, D. R., Klinck, H., Ponirakis, D., Branch, T. A., and Torres, L. G.: Environmental conditions and marine heatwaves influence blue whale foraging and reproductive effort, Ecology and Evolution, 13, https://doi.org/10.1002/ece3.9770, 2023.

Barría, C., Vásquez-Calderón, P., Lizama, C., Herrera, P., Canto, A., Conejeros, P., Beltrami, O., Suárez-Isla, B. A., Carrasco, D., Rubilar, I., Guzmán, L., Durán, L. R., and Oliva, D.: Spatial Temporal Expansion of Harmful Algal Blooms in Chile: A Review of 65 Years Records, JMSE, 10, 1868, https://doi.org/10.3390/jmse10121868, 2022.

Barth, A., Beckers, J.-M., Troupin, C., Alvera-Azcárate, A., and Vandenbulcke, L.: divand-1.0: n-dimensional variational data analysis for ocean observations, Geosci. Model Dev., 7, 225–241, https://doi.org/10.5194/gmd-7-225-2014, 2014.

Bass, A. V. and Falkenberg, L. J.: Seasonal effects and trophic pressure shape the responses of species interactions in a tropical seagrass meadow to marine heatwaves, Oikos, 2024, e10382, https://doi.org/10.1111/oik.10382, 2024.

Batten, S. D., Ostle, C., Hélaouët, P., and Walne, A. W.: Responses of Gulf of Alaska plankton communities to a marine heat wave, Deep Sea Research Part II: Topical Studies in Oceanography, 195, 105002, https://doi.org/10.1016/j.dsr2.2021.105002, 2022.

Bayoumy, M., Nilsen, F., and Skogseth, R.: Marine Heatwaves Characteristics in the Barents Sea Based on High Resolution Satellite Data (1982–2020), Front. Mar. Sci., 9, 821646, https://doi.org/10.3389/fmars.2022.821646, 2022.

Becerra, S., Arriagada-Solimano, M., Escobar-Aguirre, S., Palomino, J., Aedo, J., Estrada, J. M., Barra-Valdebenito, V., Zuloaga, R., Valdes, J. A., and Dettleff, P.: High temperature induces oxidative damage, immune modulation, and atrophy in the gills and skeletal muscle of the teleost fish black cusk-eel (Genypterus maculatus), Developmental & Comparative Immunology, 164, 105332, https://doi.org/10.1016/j.dci.2025.105332, 2025.

Beck, K. K., Nierste, J., Schmidt-Grieb, G. M., Lüdtke, E., Naab, C., Held, C., Nehrke, G., Steinhoefel, G., Laudien, J., Richter, C., and Wall, M.: Ontogenetic differences in the response of the cold-water coral Caryophyllia huinayensis to ocean acidification, warming and food availability, Science of The Total Environment, 900, 165565, https://doi.org/10.1016/j.scitotenv.2023.165565, 2023.

Beck, K. K., Schmidt-Grieb, G. M., Kayser, A. S., Wendels, J., Kler Lago, A., Meyer, S., Laudien, J., Häussermann, V., Richter, C., and Wall, M.: Cold-water coral energy reserves and calcification in contrasting fjord environments, Sci Rep, 14, 5649, https://doi.org/10.1038/s41598-024-56280-2, 2024.

Beckers, J. M. and Rixen, M.: EOF Calculations and Data Filling from Incomplete Oceanographic Datasets, Journal of Atmospheric and Oceanic Technology, 20, 1839–1856, 2003.

Bell, J. J., Micaroni, V., Strano, F., Ryan, K. G., Mitchell, K., Mitchell, P., Wilkinson, S., Thomas, T., Bachtiar, R., and Smith, R. O.: Marine heatwave-driven mass mortality and microbial community reorganisation in an ecologically important temperate sponge, Global Change Biology, 30, e17417, https://doi.org/10.1111/gcb.17417, 2024.

Benfey, T. J., Gonen, S., Bartlett, C. B., and Garber, A. F.: Thermal tolerance has high heritability in Atlantic salmon, Salmo salar, Aquaculture Reports, 37, 102249, https://doi.org/10.1016/j.aqrep.2024.102249, 2024.

Bennett, S., Duarte, C. M., Marbà, N., and Wernberg, T.: Integrating within-species variation in thermal physiology into climate change ecology, Phil. Trans. R. Soc. B, 374, 20180550, https://doi.org/10.1098/rstb.2018.0550, 2019.

Benthuysen, J., Feng, M., and Zhong, L.: Spatial patterns of warming off Western Australia during the 2011 Ningaloo Niño: Quantifying impacts of remote and local forcing, Continental Shelf Research, 91, 232–246, https://doi.org/10.1016/j.csr.2014.09.014, 2014.

Benthuysen, J. A., Smith, G. A., Spillman, C. M., and Steinberg, C. R.: Subseasonal prediction of the 2020 Great Barrier Reef and Coral Sea marine heatwave, Environ. Res. Lett., 16, 124050, https://doi.org/10.1088/1748-9326/ac3aa1, 2021.

Bernardes Batista, M., Batista Anderson, A., Franzan Sanches, P., Simionatto Polito, P., Lima Silveira, T., Velez-Rubio, G., Scarabino, F., Camacho, O., Schmitz, C., Martinez, A., Ortega, L., Fabiano, G., Rothman, M., Liu, G., Ojeda, J., Mansilla, A., Barreto, L., Assis, J., Serrão, E., Santos, R., and Antunes Horta, P.: Kelps' Long-Distance Dispersal: Role of Ecological/Oceanographic Processes and Implications to Marine Forest Conservation, Diversity, 10, 11, https://doi.org/10.3390/d10010011, 2018.

Berntsson, E. V. C., Stevik, T. K., Bergheim, A., Persson, D., Stormoen, M., and Liland, K. H.: Managing the Dissolved Oxygen Balance of Open Atlantic Salmon Sea Cages: A Narrative Review, Reviews in Aquaculture, 17, e12992, https://doi.org/10.1111/raq.12992, 2025.

Bertrand, A., Habasque, J., Hattab, T., Hintzen, N. T., Oliveros-Ramos, R., Gutiérrez, M., Demarcq, H., and Gerlotto, F.: 3-D habitat suitability of jack mackerel Trachurus murphyi in the Southeastern Pacific, a comprehensive study, Progress in Oceanography, 146, 199–211, https://doi.org/10.1016/j.pocean.2016.07.002, 2016.

Betti, F., Enrichetti, F., Bavestrello, G., Costa, A., Moreni, A., Bo, M., Ortiz Saini, P., and Daneri, G.: Hard-Bottom Megabenthic Communities of a Chilean Fjord System: Sentinels for Climate Change?, Front. Mar. Sci., 8, 635430, https://doi.org/10.3389/fmars.2021.635430, 2021.

Bianchi, T. S., Arndt, S., Austin, W. E. N., Benn, D. I., Bertrand, S., Cui, X., Faust, J. C., Koziorowska-Makuch, K., Moy, C. M., Savage, C., Smeaton, C., Smith, R. W., and Syvitski, J.: Fjords as Aquatic Critical Zones (ACZs), Earth-Science Reviews, 203, 103145, https://doi.org/10.1016/j.earscirev.2020.103145, 2020.

Bianucci, L., Jackson, J. M., Allen, S. E., Krassovski, M. V., Giesbrecht, I. J. W., and Callendar, W. C.: Fjord circulation permits a persistent subsurface water mass in a long, deep mid-latitude inlet, Ocean Sci., 20, 293–306, https://doi.org/10.5194/os-20-293-2024, 2024.

Birnie-Gauvin, K., Thorstad, E. B., and Aarestrup, K.: Overlooked aspects of the Salmo salar and Salmo trutta lifecycles, Rev Fish Biol Fisheries, 29, 749–766, https://doi.org/10.1007/s11160-019-09575-x, 2019.

Black, E., Blackburn, M., Harrison, G., Hoskins, B., and Methven, J.: Factors contributing to the summer 2003 European heatwave, Weather, 59, 217–223, https://doi.org/10.1256/wea.74.04, 2004.

Bloshkina, E. V., Pavlov, A. K., and Filchuk, K.: Warming of Atlantic Water in three west Spitsbergen fjords: recent patterns and century-long trends, Polar Research, 40, https://doi.org/10.33265/polar.v40.5392, 2021.

Boening, C., Willis, J. K., Landerer, F. W., Nerem, R. S., and Fasullo, J.: The 2011 La Niña: So strong, the oceans fell, Geophysical Research Letters, 39, 2012GL053055, https://doi.org/10.1029/2012GL053055, 2012.

Boisier, J. P., Rondanelli, R., Garreaud, R. D., and Muñoz, F.: Anthropogenic and natural contributions to the Southeast Pacific precipitation decline and recent megadrought in central Chile, Geophysical Research Letters, 43, 413–421, https://doi.org/10.1002/2015GL067265, 2016.

Bond, N. A., Cronin, M. F., Freeland, H., and Mantua, N.: Causes and impacts of the 2014 warm anomaly in the NE Pacific, Geophysical Research Letters, 42, 3414–3420, https://doi.org/10.1002/2015GL063306, 2015.

Brauko, K. M., Cabral, A., Costa, N. V., Hayden, J., Dias, C. E. P., Leite, E. S., Westphal, R. D., Mueller, C. M., Hall-Spencer, J. M., Rodrigues, R. R., Rörig, L. R., Pagliosa, P. R., Fonseca, A. L., Alarcon, O. E., and Horta, P. A.: Marine Heatwaves, Sewage and Eutrophication Combine to Trigger Deoxygenation and Biodiversity Loss: A SW Atlantic Case Study, Front. Mar. Sci., 7, 590258, https://doi.org/10.3389/fmars.2020.590258, 2020.

Breitburg, D., Levin, L. A., Oschlies, A., Grégoire, M., Chavez, F. P., Conley, D. J., Garçon, V., Gilbert, D., Gutiérrez, D., Isensee, K., Jacinto, G. S., Limburg, K. E., Montes, I., Naqvi, S. W. A., Pitcher, G. C., Rabalais, N. N., Roman, M. R., Rose, K. A., Seibel, B. A., Telszewski, M., Yasuhara, M., and Zhang, J.: Declining oxygen in the global ocean and coastal waters, Science, 359, https://doi.org/10.1126/science.aam7240, 2018.

Brooks, M., Fergusson, E., Rogers, M., Strasburger, W., and Suryan, R.: Juvenile salmon body condition in Southeast Alaska is buffered during marine heatwaves, Mar. Ecol. Prog. Ser., 760, 135–149, https://doi.org/10.3354/meps14850, 2025.

Bruning, M. J., Véliz, D., Rojas-Hernández, N., Garcés-Vargas, J., Garrido, I., Cid, M. J., Paschke, K., and Pardo, L. M.: The timing of marine heatwaves during the moulting cycle affects performance of decapod larvae, Sci Rep, 14, 29800, https://doi.org/10.1038/s41598-024-81258-5, 2024.

Buchan, S. J., Pérez-Santos, I., Narváez, D., Castro, L., Stafford, K. M., Baumgartner, M. F., Valle-Levinson, A., Montero, P., Gutiérrez, L., Rojas, C., Daneri, G., and Neira, S.: Intraseasonal variation in southeast Pacific blue whale acoustic presence, zooplankton backscatter, and oceanographic variables on a feeding ground in Northern Chilean Patagonia, Progress in Oceanography, 199, 102709, https://doi.org/10.1016/j.pocean.2021.102709, 2021.

Burger, F. A., Terhaar, J., and Frölicher, T. L.: Compound marine heatwaves and ocean acidity extremes, Nat Commun, 13, 4722, https://doi.org/10.1038/s41467-022-32120-7, 2022.

Burt, K., Hamoutene, D., Perez-Casanova, J., Kurt Gamperl, A., and Volkoff, H.: The effect of intermittent hypoxia on growth, appetite and some aspects of the immune response of Atlantic salmon (*Salmo salar*), Aquac Res, 45, 124–137, https://doi.org/10.1111/j.1365-2109.2012.03211.x, 2013.

Buschmann, A., Farías, L., Tapia, F., Varela, D., and Vásquez, M.: Scientific report on the 2016 southern Chile red tide, Chilean Department of Economy, 66, 2016.

Buschmann, A. H., Camus, C., Infante, J., Neori, A., Israel, Á., Hernández-González, M. C., Pereda, S. V., Gomez-Pinchetti, J. L., Golberg, A., Tadmor-Shalev, N., and Critchley, A. T.: Seaweed production: overview of the global state of exploitation, farming and emerging research activity, European Journal of Phycology, 52, 391–406, https://doi.org/10.1080/09670262.2017.1365175, 2017.

Buschmann, A. H., Niklitschek, E. J., and Pereda, S. V.: Aquaculture and Its Impacts on the Conservation of Chilean Patagonia, in: Conservation in Chilean Patagonia, vol. 19, edited by: Castilla, J. C., Armesto Zamudio, J. J., Martínez-Harms, M. J., and Tecklin, D., Springer International Publishing, Cham, 303–320, https://doi.org/10.1007/978-3-031-39408-9_12, 2023.

Bustos, C. A., Landaeta, M. F., and Balbontín, F.: Spawning and early nursery areas of anchoveta Engraulis ringens Jenyns, 1842 in fjords of southern Chile, Rev. biol. mar. oceanogr., 43, https://doi.org/10.4067/S0718-19572008000200014, 2008.

Calado, R., Mota, V. C., Madeira, D., and Leal, M. C.: Summer Is Coming! Tackling Ocean Warming in Atlantic Salmon Cage Farming, Animals, 11, 1800, https://doi.org/10.3390/ani11061800, 2021.

Calcagno, J. A., Lovrich, G. A., Thatje, S., Nettelmann, U., and Anger, K.: First year growth in the lithodids Lithodes santolla and Paralomis granulosa reared at different temperatures, Journal of Sea Research, 54, 221–230, https://doi.org/10.1016/j.seares.2005.04.004, 2005.

Calvete, C. and Sobarzo, M.: Quantification of the surface brackish water layer and frontal zones in southern Chilean fjords between Boca del Guafo (43°30'S) and Estero Elefantes (46°30'S), Continental Shelf Research, 31, 162–171, https://doi.org/10.1016/j.csr.2010.09.013, 2011.

Capotondi, A., Rodrigues, R. R., Sen Gupta, A., Benthuysen, J. A., Deser, C., Frölicher, T. L., Lovenduski, N. S., Amaya, D. J., Le Grix, N., Xu, T., Hermes, J., Holbrook, N. J., Martinez-Villalobos, C., Masina, S., Roxy, M. K., Schaeffer, A., Schlegel, R. W., Smith, K. E., and Wang, C.: A global overview of marine heatwaves in a changing climate, Commun Earth Environ, 5, 701, https://doi.org/10.1038/s43247-024-01806-9, 2024.

Caputi, N., Kangas, M., Denham, A., Feng, M., Pearce, A., Hetzel, Y., and Chandrapavan, A.: Management adaptation of invertebrate fisheries to an extreme marine heat wave event at a global warming hot spot, Ecology and Evolution, 6, 3583–3593, https://doi.org/10.1002/ece3.2137, 2016.

Caputi, N., Kangas, M., Chandrapavan, A., Hart, A., Feng, M., Marin, M., and Lestang, S. D.: Factors Affecting the Recovery of Invertebrate Stocks From the 2011 Western Australian Extreme Marine Heatwave, Front. Mar. Sci., 6, 484, https://doi.org/10.3389/fmars.2019.00484, 2019.

Carrasco, D., Pizarro, O., Jacques-Coper, M., and Narváez, D. A.: Main drivers of marine heat waves in the eastern South Pacific, Front. Mar. Sci., 10, https://doi.org/10.3389/fmars.2023.1129276, 2023.

Carvalho, K. S., Smith, T. E., and Wang, S.: Bering Sea marine heatwaves: Patterns, trends and connections with the Arctic, Journal of Hydrology, 600, 126462, https://doi.org/10.1016/j.jhydrol.2021.126462, 2021.

Cascarano, M. C., Stavrakidis-Zachou, O., Mladineo, I., Thompson, K. D., Papandroulakis, N., and Katharios, P.: Mediterranean Aquaculture in a Changing Climate: Temperature Effects on Pathogens and Diseases of Three Farmed Fish Species, Pathogens, 10, 1205, https://doi.org/10.3390/pathogens10091205, 2021.

Castilla, J., Armesto, J., and Martínez-Harms, M. J.: Conservación en la Patagonia chilena: evaluación del conocimiento, oportunidades y desafíos, Santiago, Chile: Ediciones Universidad Católica., 600 pp., 2021.

Castilla, J. C., Uribe, M., Bahamonde, N., Clarke, M., Desqueyroux-Faündez, R., Kong, I., Moyano, H., Rozbaczylo, N., Santelices, B., Valdovinos, C., and Zavala, P.: Down under the southeastern Pacific: marine non-indigenous species in Chile, Biol Invasions, 7, 213–232, https://doi.org/10.1007/s10530-004-0198-5, 2005.

Castilla, J. C., Armesto Zamudio, J. J., Martínez-Harms, M. J., and Tecklin, D. (Eds.): Conservation in Chilean Patagonia: Assessing the State of Knowledge, Opportunities, and Challenges, Springer International Publishing, Cham, https://doi.org/10.1007/978-3-031-39408-9, 2023.

Castillo, M. I., Pizarro, O., Cifuentes, U., Ramirez, N., and Djurfeldt, L.: Subtidal dynamics in a deep fjord of southern Chile, Continental Shelf Research, 49, 73–89, https://doi.org/10.1016/j.csr.2012.09.007, 2012.

Castillo, M. I., Cifuentes, U., Pizarro, O., Djurfeldt, L., and Caceres, M.: Seasonal hydrography and surface outflow in a fjord with a deep sill: the Reloncaví fjord, Chile, Ocean Sci., 12, 533–544, https://doi.org/10.5194/os-12-533-2016, 2016.

Castro, L. and Gironás, J.: Precipitation, Temperature and Evaporation, in: Water Resources of Chile, vol. 8, edited by: Fernández, B. and Gironás, J., Springer International Publishing, Cham, 31–60, https://doi.org/10.1007/978-3-030-56901-3_3, 2021.

Castro, L., Salinas, G., and Hernández, E.: Environmental influences on winter spawning of the anchoveta Engraulis ringens off central Chile, Mar. Ecol. Prog. Ser., 197, 247–258, https://doi.org/10.3354/meps197247, 2000.

Cavanaugh, K. C., Kellner, J. R., Forde, A. J., Gruner, D. S., Parker, J. D., Rodriguez, W., and Feller, I. C.: Poleward expansion of mangroves is a threshold response to decreased frequency of extreme cold events, Proc. Natl. Acad. Sci. U.S.A., 111, 723–727, https://doi.org/10.1073/pnas.1315800111, 2014.

Cavole, L., Demko, A., Diner, R., Giddings, A., Koester, I., Pagniello, C., Paulsen, M.-L., Ramirez-Valdez, A., Schwenck, S., Yen, N., Zill, M., and Franks, P.: Biological Impacts of the 2013–2015 Warm-Water Anomaly in the Northeast Pacific: Winners, Losers, and the Future, Oceanog, 29, https://doi.org/10.5670/oceanog.2016.32, 2016.

Ceballos-Concha, A., Asche, F., and Cárdenas-Retamal, R.: Salmon Aquaculture in Chile: Production Growth and Socioeconomic Impacts, Reviews in Aquaculture, 17, e12993, https://doi.org/10.1111/raq.12993, 2025.

Cerrano, C., Bavestrello, G., Bianchi, C. N., Cattaneo-vietti, R., Bava, S., Morganti, C., Morri, C., Picco, P., Sara, G., Schiaparelli, S., Siccardi, A., and Sponga, F.: A catastrophic mass-mortality episode of gorgonians and other organisms in the Ligurian Sea (North-western Mediterranean), summer 1999, Ecology Letters, 3, 284–293, https://doi.org/10.1046/j.1461-0248.2000.00152.x, 2000.

Cervantes, B. T., Fewings, M. R., and Risien, C. M.: Subsurface Temperature Anomalies Off Central Oregon During 2014–2021, JGR Oceans, 129, e2023JC020565, https://doi.org/10.1029/2023JC020565, 2024.

Chandrapavan, A., Caputi, N., and Kangas, M. I.: The Decline and Recovery of a Crab Population From an Extreme Marine Heatwave and a Changing Climate, Front. Mar. Sci., 6, 510, https://doi.org/10.3389/fmars.2019.00510, 2019.

Chapron, L., Galand, P. E., Pruski, A. M., Peru, E., Vétion, G., Robin, S., and Lartaud, F.: Resilience of cold-water coral holobionts to thermal stress, Proc. R. Soc. B., 288, 20212117, https://doi.org/10.1098/rspb.2021.2117, 2021.

Chatterjee, S., Nuncio, M., and Satheesan, K.: ENSO related SST anomalies and relation with surface heat fluxes over south Pacific and Atlantic, Clim Dyn, 49, 391–401, https://doi.org/10.1007/s00382-016-3349-3, 2017.

Chavez, F. P., Bertrand, A., Guevara-Carrasco, R., Soler, P., and Csirke, J.: The northern Humboldt Current System: Brief history, present status and a view towards the future, Progress in Oceanography, 79, 95–105, https://doi.org/10.1016/j.pocean.2008.10.012, 2008.

Chen, N., Thual, S., and Stuecker, M. F.: El Niño and the Southern Oscillation: Theory, in: Reference Module in Earth Systems and Environmental Sciences, Elsevier, B9780124095489117658, https://doi.org/10.1016/B978-0-12-409548-9.11765-8, 2019.

Chen, Q., Li, D., Feng, J., Zhao, L., Qi, J., and Yin, B.: Understanding the compound marine heatwave and low-chlorophyll extremes in the western Pacific Ocean, Front. Mar. Sci., 10, 1303663, https://doi.org/10.3389/fmars.2023.1303663, 2023.

Chen, Y., Shen, C., Zhao, H., and Pan, G.: The impact of marine heatwaves on surface phytoplankton chlorophyll-a in the South China Sea, Science of The Total Environment, 949, 175099, https://doi.org/10.1016/j.scitotenv.2024.175099, 2024.

Cheng, Y., Zhang, M., Song, Z., Wang, G., Zhao, C., Shu, Q., Zhang, Y., and Qiao, F.: A quantitative analysis of marine heatwaves in response to rising sea surface temperature, Science of The Total Environment, 881, 163396, https://doi.org/10.1016/j.scitotenv.2023.163396, 2023.

Cheung, W. W. L. and Frölicher, T. L.: Marine heatwaves exacerbate climate change impacts for fisheries in the northeast Pacific, Sci Rep, 10, 6678, https://doi.org/10.1038/s41598-020-63650-z, 2020.

Choi, H.-Y., Park, M.-S., Kim, H.-S., and Lee, S.: Marine heatwave events strengthen the intensity of tropical cyclones, Commun Earth Environ, 5, https://doi.org/10.1038/s43247-024-01239-4, 2024.

Cisek, M., Makuch, P., and Petelski, T.: Comparison of meteorological conditions in Svalbard fjords: Hornsund and Kongsfjorden, Oceanologia, 59, 413–421, https://doi.org/10.1016/j.oceano.2017.06.004, 2017.

Clement, A., Lincoqueo, L., Saldivia, M., Brito, C. G., Muñoz, F., Fernández, C., Pérez, F., Maluje, C. P., Correa, N., Moncada, V., and Contreras, G.: Exceptional summer conditions and HABs of Pseudochattonella in Southern Chile create record impacts on salmon farms., Harful Allgal News, 53, 1–3, 2016.

Coleman, M. A., Minne, A. J. P., Vranken, S., and Wernberg, T.: Genetic tropicalisation following a marine heatwave, Sci Rep, 10, 12726, https://doi.org/10.1038/s41598-020-69665-w, 2020.

Combe, M., Reverter, M., Caruso, D., Pepey, E., and Gozlan, R. E.: Impact of Global Warming on the Severity of Viral Diseases: A Potentially Alarming Threat to Sustainable Aquaculture Worldwide, Microorganisms, 11, 1049, https://doi.org/10.3390/microorganisms11041049, 2023.

Cook, F., Smith, R. O., Roughan, M., Cullen, N. J., Shears, N., and Bowen, M.: Marine heatwaves in shallow coastal ecosystems are coupled with the atmosphere: Insights from half a century of daily in situ temperature records, Front. Clim., 4, 1012022, https://doi.org/10.3389/fclim.2022.1012022, 2022.

Cook, K. M., Dunn, M. R., Behrens, E., Pinkerton, M. H., Law, C. S., and Cummings, V. J.: The impacts of marine heatwaves on ecosystems and fisheries in Aotearoa New Zealand, New Zealand Journal of Marine and Freshwater Research, 59, 1530–1560, https://doi.org/10.1080/00288330.2024.2436661, 2025.

Cooley, K. M., Fewings, M. R., Lerczak, J. A., O'Neill, L. W., and Brown, K. S.: Role of Sea Surface Physical Processes in Mixed-Layer Temperature Changes During Summer Marine Heat Waves in the Chile-Peru Current System, JGR Oceans, 127, https://doi.org/10.1029/2021jc018338, 2022.

Cordes, E. and Mienis, F. (Eds.): Cold-Water Coral Reefs of the World, Springer International Publishing, Cham, https://doi.org/10.1007/978-3-031-40897-7, 2023.

Cortina, M. and Madeira, C.: Exposures to climate change's physical risks in Chile, Latin American Journal of Central Banking, 4, 100090, https://doi.org/10.1016/j.latcb.2023.100090, 2023.

Couch, C. S., Burns, J. H. R., Liu, G., Steward, K., Gutlay, T. N., Kenyon, J., Eakin, C. M., and Kosaki, R. K.: Mass coral bleaching due to unprecedented marine heatwave in Papahānaumokuākea Marine National Monument (Northwestern Hawaiian Islands), PLoS ONE, 12, e0185121, https://doi.org/10.1371/journal.pone.0185121, 2017.

Crawford, D. W., Montero, P., and Daneri, G.: Blooms of Alexandrium catenella in Coastal Waters of Chilean Patagonia: Is Subantarctic Surface Water Involved?, Front. Mar. Sci., 8, 612628, https://doi.org/10.3389/fmars.2021.612628, 2021.

Crosswell, J. R., Bravo, F., Pérez-Santos, I., Carlin, G., Cherukuru, N., Schwanger, C., Gregor, R., and Steven, A. D. L.: Geophysical controls on metabolic cycling in three Patagonian fjords, Progress in Oceanography, 207, 102866, https://doi.org/10.1016/j.pocean.2022.102866, 2022.

Cruces, E., Huovinen, P., and Gómez, I.: Interactive effects of UV radiation and enhanced temperature on photosynthesis, phlorotannin induction and antioxidant activities of two sub-Antarctic brown algae, Mar Biol, 160, 1–13, https://doi.org/10.1007/s00227-012-2049-8, 2013.

Cubillos, L.: Crecimiento estacional de peces pelágicos en Talcahuano, Chile (37°S, 73°W): ¿consecuencia de su estrategia reproductiva a un sistema de surgencia estacional ?, Aquatic Living Resources, 14, 115–124, https://doi.org/10.1016/S0990-7440(01)01112-3, 2001.

Cubillos, L. and Arcos, D. F.: Recruitment of common sardine (Strangomera bentincki) and anchovy (Engraulis ringens) off central-south Chile in the 1990s and the impact of the 1997–1998 El Niño, Aquatic Living Resources, 15, 87–94, https://doi.org/10.1016/S0990-7440(02)01158-0, 2002.

Cuevas, L. A., Tapia, F. J., Iriarte, J. L., González, H. E., Silva, N., and Vargas, C. A.: Interplay between freshwater discharge and oceanic waters modulates phytoplankton size-

structure in fjords and channel systems of the Chilean Patagonia, Progress in Oceanography, 173, 103–113, https://doi.org/10.1016/j.pocean.2019.02.012, 2019.

Dabulevičienė, T. and Servaitė, I.: Characteristics of Marine Heatwaves in the Southeastern Baltic Sea Based on Long-Term In Situ and Satellite Observations, JMSE, 12, 1109, https://doi.org/10.3390/jmse12071109, 2024.

Dalsin, M., Walter, R. K., and Mazzini, P. L. F.: Effects of basin-scale climate modes and upwelling on nearshore marine heatwaves and cold spells in the California Current, Sci Rep, 13, 12389, https://doi.org/10.1038/s41598-023-39193-4, 2023.

Dalton, S. J., Carroll, A. G., Sampayo, E., Roff, G., Harrison, P. L., Entwistle, K., Huang, Z., Salih, A., and Diamond, S. L.: Successive marine heatwaves cause disproportionate coral bleaching during a fast phase transition from El Niño to La Niña, Science of The Total Environment, 715, 136951, https://doi.org/10.1016/j.scitotenv.2020.136951, 2020.

Darmaraki, S., Somot, S., Sevault, F., and Nabat, P.: Past Variability of Mediterranean Sea Marine Heatwaves, Geophysical Research Letters, 46, 9813–9823, https://doi.org/10.1029/2019gl082933, 2019.

Deser, C., Phillips, A. S., Alexander, Michael. A., Amaya, D. J., Capotondi, A., Jacox, M. G., and Scott, J. D.: Future Changes in the Intensity and Duration of Marine Heat and Cold Waves: Insights from Coupled Model Initial-Condition Large Ensembles, Journal of Climate, 37, 1877–1902, https://doi.org/10.1175/JCLI-D-23-0278.1, 2024.

Deutsch, C., Ferrel, A., Seibel, B., Pörtner, H.-O., and Huey, R. B.: Climate change tightens a metabolic constraint on marine habitats, Science, 348, 1132–1135, https://doi.org/10.1126/science.aaa1605, 2015.

Di Lorenzo, E. and Mantua, N.: Multi-year persistence of the 2014/15 North Pacific marine heatwave, Nature Clim Change, 6, 1042–1047, https://doi.org/10.1038/nclimate3082, 2016.

Díaz, P. A. and Figueroa, R. I.: Toxic Algal Bloom Recurrence in the Era of Global Change: Lessons from the Chilean Patagonian Fjords, Microorganisms, 11, 1874, https://doi.org/10.3390/microorganisms11081874, 2023.

Díaz, P. A., Álvarez, G., Varela, D., Pérez-Santos, I., Díaz, M., Molinet, C., Seguel, M., Aguilera-Belmonte, A., Guzmán, L., Uribe, E., Rengel, J., Hernández, C., Segura, C., and Figueroa, R. I.: Impacts of harmful algal blooms on the aquaculture industry: Chile as a case study, pip, 6, 39–50, https://doi.org/10.1127/pip/2019/0081, 2019.

Díaz, P. A., Álvarez, G., Figueroa, R. I., Garreaud, R., Pérez-Santos, I., Schwerter, C., Díaz, M., López, L., Pinto-Torres, M., and Krock, B.: From lipophilic to hydrophilic toxin producers: Phytoplankton succession driven by an atmospheric river in western Patagonia, Marine Pollution Bulletin, 193, 115214, https://doi.org/10.1016/j.marpolbul.2023.115214, 2023a.

Díaz, P. A., Pérez-Santos, I., Basti, L., Garreaud, R., Pinilla, E., Barrera, F., Tello, A., Schwerter, C., Arenas-Uribe, S., Soto-Riquelme, C., Navarro, P., Díaz, M., Álvarez, G., Linford, P. M., Altamirano, R., Mancilla-Gutiérrez, G., Rodríguez-Villegas, C., and Figueroa, R. I.: The impact of local and climate change drivers on the formation, dynamics, and potential recurrence of a massive fish-killing microalgal bloom in Patagonian fjord, Science of The Total Environment, 865, 161288, https://doi.org/10.1016/j.scitotenv.2022.161288, 2023b.

Díaz, P. A., Rosales, S. A., Molinet, C., Niklitschek, E. J., Marín, A., Varela, D., Seguel, M., Díaz, M., Figueroa, R. I., Basti, L., Hernández, C., Carbonell, P., Cantarero, B., and Álvarez, G.: Are Alexandrium catenella Blooms Spreading Offshore in Southern Chile? An In-Depth Analysis of the First PSP Outbreak in the Oceanic Coast, Fishes, 9, 340, https://doi.org/10.3390/fishes9090340, 2024.

Diehl, N., Roleda, M. Y., Bartsch, I., Karsten, U., and Bischof, K.: Summer Heatwave Impacts on the European Kelp Saccharina latissima Across Its Latitudinal Distribution Gradient, Front. Mar. Sci., 8, https://doi.org/10.3389/fmars.2021.695821, 2021.

Dodds, L., Black, K., Orr, H., and Roberts, J.: Lipid biomarkers reveal geographical differences in food supply to the cold-water coral Lophelia pertusa (Scleractinia), Mar. Ecol. Prog. Ser., 397, 113–124, https://doi.org/10.3354/meps08143, 2009.

Dodds, L. A., Roberts, J. M., Taylor, A. C., and Marubini, F.: Metabolic tolerance of the cold-water coral Lophelia pertusa (Scleractinia) to temperature and dissolved oxygen change, Journal of Experimental Marine Biology and Ecology, 349, 205–214, https://doi.org/10.1016/j.jembe.2007.05.013, 2007.

Dorey, N., Gjelsvik, Ø., Kutti, T., and Büscher, J. V.: Broad Thermal Tolerance in the Cold-Water Coral Lophelia pertusa From Arctic and Boreal Reefs, Front. Physiol., 10, 1636, https://doi.org/10.3389/fphys.2019.01636, 2020.

Dowd, S. C., Van Putten, I., Colburn, L. L., Pecl, G. T., Mullany, B., Holbrook, N. J., Hobday, A. J., and Nye, J. A.: Rising Heat, Rising Risks: Understanding the Nexus of Marine Heatwaves, Fishing Dependence, and Vulnerability to Coastal Communities, Global Change Biology, 31, e70454, https://doi.org/10.1111/gcb.70454, 2025.

Duarte, C., Navarro, J. M., Acuña, K., Torres, R., Manríquez, P. H., Lardies, M. A., Vargas, C. A., Lagos, N. A., and Aguilera, V.: Combined effects of temperature and ocean acidification on the juvenile individuals of the mussel Mytilus chilensis, Journal of Sea Research, 85, 308–314, https://doi.org/10.1016/j.seares.2013.06.002, 2014.

Dzwonkowski, B., Coogan, J., Fournier, S., Lockridge, G., Park, K., and Lee, T.: Compounding impact of severe weather events fuels marine heatwave in the coastal ocean, Nat Commun, 11, 4623, https://doi.org/10.1038/s41467-020-18339-2, 2020.

Egea, L. G., Jiménez-Ramos, R., Romera-Castillo, C., Casal-Porras, I., Bonet-Melià, P., Yamuza-Magdaleno, A., Cerezo-Sepúlveda, L., Pérez-Lloréns, J. L., and Brun, F. G.: Effect of marine heat waves on carbon metabolism, optical characterization, and bioavailability of dissolved organic carbon in coastal vegetated communities, Limnology & Oceanography, 68, 467–482, https://doi.org/10.1002/lno.12286, 2023.

Elliott, J. M. and Elliott, J. A.: Temperature requirements of Atlantic salmon Salmo salar, brown trout Salmo trutta and Arctic charr Salvelinus alpinus: predicting the effects of climate change, Journal of Fish Biology, 77, 1793–1817, https://doi.org/10.1111/j.1095-8649.2010.02762.x, 2010.

Elzahaby, Y. and Schaeffer, A.: Observational Insight Into the Subsurface Anomalies of Marine Heatwaves, Front. Mar. Sci., 6, 745, https://doi.org/10.3389/fmars.2019.00745, 2019.

Espíndola, F., Vega, R., and Yáñez, E.: Identification of the spatial-temporal distribution pattern of swordfish (Xiphias gladius) in the southeastern Pacific, LAJAR, 37, 43–57, https://doi.org/10.3856/vol37-issue1-fulltext-4, 2009.

Estay, S. A. and Lima, M.: Combined effect of ENSO and SAM on the population dynamics of the invasive yellowjacket wasp in central Chile, Population Ecology, 52, 289–294, https://doi.org/10.1007/s10144-009-0179-8, 2010.

European Food Safety Authority (EFSA), Engel, K., Kukuła-Koch, W., Maciuk, A., Pelaez, C., Pilegaard, K., van Loveren, H., Laganaro, M., Turla, E., and Beneventi, E.: Technical Report on the notification of dried fronds of Durvillaea incurvata (Suhr) Macaya as a traditional food from a third country pursuant to Article 14 of Regulation (EU) 2015/2283, EFS3, 22, https://doi.org/10.2903/sp.efsa.2025.EN-9279, 2025.

European Union-Copernicus Marine Service: Global Ocean OSTIA Sea Surface Temperature and Sea Ice Analysis, https://doi.org/10.48670/MOI-00165, 2015.

European Union-Copernicus Marine Service: Global Ocean Physics Reanalysis, https://doi.org/10.48670/MOI-00021, 2018.

Falk, K. and Aamelfot, M.: Infectious salmon anaemia., in: Fish viruses and bacteria: pathobiology and protection, edited by: Woo, P. T. K. and Cipriano, R. C., CABI, UK, 68–78, https://doi.org/10.1079/9781780647784.0068, 2017.

Fan, H., Pein, J., Chen, W., Staneva, J., and Cheng, H.: Effects of heatwave events on dissolved oxygen in the Elbe Estuary, Water Research, 286, 124125, https://doi.org/10.1016/j.watres.2025.124125, 2025.

FAO: Fishery and Aquaculture Statistics. Global aquaculture production 1950-2017 (FishstatJ)., In: FAO Fisheries and Aquaculture Department [online]., 2019.

FAO: The State of World Fisheries and Aquaculture 2024, FAO, https://doi.org/10.4060/cd0683en, 2024.

Félix-Loaiza, A. C., Rodríguez-Bravo, L. M., Beas-Luna, R., Lorda, J., De La Cruz-González, E., and Malpica-Cruz, L.: Marine heatwaves facilitate invasive algae takeover as foundational kelp, Botanica Marina, 65, 315–319, https://doi.org/10.1515/bot-2022-0037, 2022.

Fernández, B. and Gironás, J. (Eds.): Water Resources of Chile, Springer International Publishing, Cham, https://doi.org/10.1007/978-3-030-56901-3, 2021.

Fernández-Álvarez, B., Barceló-Llull, B., and Pascual, A.: Tracking Marine Heatwaves in the Balearic Sea: Temperature Trends and the Role of Detection Methods, https://doi.org/10.5194/egusphere-2024-4065, 22 January 2025.

Ferreira, A. P., Francelino, A. C., and Costa, T. M.: Effects of marine heatwaves on primary and secondary production in macroalgae-amphipod systems, Marine Environmental Research, 209, 107231, https://doi.org/10.1016/j.marenvres.2025.107231, 2025.

Field, C. B., Barros, V., Stocker, T. F., and Dahe, Q. (Eds.): Managing the Risks of Extreme Events and Disasters to Advance Climate Change Adaptation: Special Report of the Intergovernmental Panel on Climate Change, 1st ed., Cambridge University Press, https://doi.org/10.1017/cbo9781139177245, 2012.

Fierro, J. J.: Tides in the austral Chilean channels and fjords, in: Progress in the oceanographic knowledge of Chilean inner waters, from Puerto Montt to Cape Horn, 63–66, 2008.

Figueroa, V., Farfán, M., and Aguilera, J. M.: Seaweeds as Novel Foods and Source of Culinary Flavors, Food Reviews International, 39, 1–26, https://doi.org/10.1080/87559129.2021.1892749, 2023.

Figueroa-Muñoz, G., Molinet, C., Díaz, M., and De Los Ríos-Escalante, P.: Decapods Associated with the Southern King Crab (Lithodes santolla) Fishery in Central Patagonia (44° S, Chile), JMSE, 9, 1353, https://doi.org/10.3390/jmse9121353, 2021.

Filbee-Dexter, K., Wernberg, T., Grace, S. P., Thormar, J., Fredriksen, S., Narvaez, C. N., Feehan, C. J., and Norderhaug, K. M.: Marine heatwaves and the collapse of marginal North Atlantic kelp forests, Sci Rep, 10, 13388, https://doi.org/10.1038/s41598-020-70273-x, 2020.

FishfarmingExpert: Algal blooms cause three fish die-offs in Chile, 2021a.

FishfarmingExpert: Chilean farmer hit again by algal bloom, 2021b.

Flores-Aqueveque, V., Rojas, M., Aguirre, C., Arias, P. A., and González, C.: South Pacific Subtropical High from the late Holocene to the end of the 21st century: insights from climate proxies and general circulation models, Clim. Past, 16, 79–99, https://doi.org/10.5194/cp-16-79-2020, 2020.

Fogarty, M., Incze, L., Hayhoe, K., Mountain, D., and Manning, J.: Potential climate change impacts on Atlantic cod (Gadus morhua) off the northeastern USA, Mitig Adapt Strateg Glob Change, 13, 453–466, https://doi.org/10.1007/s11027-007-9131-4, 2008.

Fordyce, A. J., Ainsworth, T. D., Heron, S. F., and Leggat, W.: Marine Heatwave Hotspots in Coral Reef Environments: Physical Drivers, Ecophysiological Outcomes, and Impact Upon Structural Complexity, Front. Mar. Sci., 6, 498, https://doi.org/10.3389/fmars.2019.00498, 2019.

Försterra, G., Häussermann, V., Laudien, J., Jantzen, C., Sellanes, J., and Muñoz, P.: Mass die-off of the cold-water coral <I>Desmophyllum dianthus</I> in the Chilean Patagonian fjord region, BMS, 90, 895–899, https://doi.org/10.5343/bms.2013.1064, 2014.

Fossheim, M., Primicerio, R., Johannesen, E., Ingvaldsen, R. B., Aschan, M. M., and Dolgov, A. V.: Recent warming leads to a rapid borealization of fish communities in the Arctic, Nature Clim Change, 5, 673–677, https://doi.org/10.1038/nclimate2647, 2015.

Fragkopoulou, E., Sen Gupta, A., Costello, M. J., Wernberg, T., Araújo, M. B., Serrão, E. A., De Clerck, O., and Assis, J.: Marine biodiversity exposed to prolonged and intense subsurface heatwaves, Nat. Clim. Chang., 13, 1114–1121, https://doi.org/10.1038/s41558-023-01790-6, 2023.

Franco, J., Wernberg, T., Bertocci, I., Duarte, P., Jacinto, D., Vasco-Rodrigues, N., and Tuya, F.: Herbivory drives kelp recruits into 'hiding' in a warm ocean climate, Mar. Ecol. Prog. Ser., 536, 1–9, https://doi.org/10.3354/meps11445, 2015.

Free, C. M., Anderson, S. C., Hellmers, E. A., Muhling, B. A., Navarro, M. O., Richerson, K., Rogers, L. A., Satterthwaite, W. H., Thompson, A. R., Burt, J. M., Gaines, S. D., Marshall, K. N., White, J. W., and Bellquist, L. F.: Impact of the 2014–2016 marine heatwave on US and Canada West Coast fisheries: Surprises and lessons from key case studies, Fish and Fisheries, 24, 652–674, https://doi.org/10.1111/faf.12753, 2023.

Freedman, R. M., Brown, J. A., Caldow, C., and Caselle, J. E.: Marine protected areas do not prevent marine heatwave-induced fish community structure changes in a temperate transition zone, Sci Rep, 10, 21081, https://doi.org/10.1038/s41598-020-77885-3, 2020.

Freitas, C., Olsen, E. M., Knutsen, H., Albretsen, J., and Moland, E.: Temperature-associated habitat selection in a cold-water marine fish, Journal of Animal Ecology, 85, 628–637, https://doi.org/10.1111/1365-2656.12458, 2016.

Frölicher, T. L. and Laufkötter, C.: Emerging risks from marine heat waves, Nat Commun, 9, 650, https://doi.org/10.1038/s41467-018-03163-6, 2018.

Frölicher, T. L., Fischer, E. M., and Gruber, N.: Marine heatwaves under global warming, Nature, 560, 360–364, https://doi.org/10.1038/s41586-018-0383-9, 2018.

Fuentes-Grünewald, C., Clement, A., and Aguilera B., A.: Alexandrium catenella Bloom and the Impact on Fish Farming in the XI region, Chile, in: Books of proceedings of 12th International Conference on Harmful Algae, vol. 183–186, Copenhagen, 2008.

Gairn, L.: Harmful algal bloom in Chile triggers mass salmon mortality event, WEAREAQUACULTURE, 2024.

Galletti Vernazzani, B., Jackson, J. A., Cabrera, E., Carlson, C. A., and Brownell, R. L.: Estimates of Abundance and Trend of Chilean Blue Whales off Isla de Chiloé, Chile, PLoS ONE, 12, e0168646, https://doi.org/10.1371/journal.pone.0168646, 2017.

Galván, D. E., Bovcon, N. D., Cochia, P. D., González, R. A., Lattuca, M. E., Reinaldo, M. O., Rincón-Díaz, M. P., Romero, M. A., Vanella, F. A., Venerus, L. A., and Svendsen, G. M.: Changes in the Specific and Biogeographic Composition of Coastal Fish Assemblages in Patagonia, Driven by Climate Change, Fishing, and Invasion by Alien Species, in: Global Change in Atlantic Coastal Patagonian Ecosystems, edited by: Helbling, E. W., Narvarte, M. A., González, R. A., and Villafañe, V. E., Springer International Publishing, Cham, 205–231, https://doi.org/10.1007/978-3-030-86676-1_9, 2022.

Gamperl, A. K., Ajiboye, O. O., Zanuzzo, F. S., Sandrelli, R. M., Peroni, E. D. F. C., and Beemelmanns, A.: The impacts of increasing temperature and moderate hypoxia on the

production characteristics, cardiac morphology and haematology of Atlantic Salmon (Salmo salar), Aquaculture, 519, 734874, https://doi.org/10.1016/j.aquaculture.2019.734874, 2020.

Gamperl, A. K., Zrini, Z. A., and Sandrelli, R. M.: Atlantic Salmon (Salmo salar) Cage-Site Distribution, Behavior, and Physiology During a Newfoundland Heat Wave, Front. Physiol., 12, 719594, https://doi.org/10.3389/fphys.2021.719594, 2021.

Gao, G., Zhao, X., Jiang, M., and Gao, L.: Impacts of Marine Heatwaves on Algal Structure and Carbon Sequestration in Conjunction With Ocean Warming and Acidification, Front. Mar. Sci., 8, 758651, https://doi.org/10.3389/fmars.2021.758651, 2021.

Garrabou, J., Coma, R., Bensoussan, N., Bally, M., Chevaldonné, P., Cigliano, M., Diaz, D., Harmelin, J. G., Gambi, M. C., Kersting, D. K., Ledoux, J. B., Lejeusne, C., Linares, C., Marschal, C., Pérez, T., Ribes, M., Romano, J. C., Serrano, E., Teixido, N., Torrents, O., Zabala, M., Zuberer, F., and Cerrano, C.: Mass mortality in Northwestern Mediterranean rocky benthic communities: effects of the 2003 heat wave, Global Change Biology, 15, 1090–1103, https://doi.org/10.1111/j.1365-2486.2008.01823.x, 2009.

Garrabou, J., Gómez-Gras, D., Medrano, A., Cerrano, C., Ponti, M., Schlegel, R., Bensoussan, N., Turicchia, E., Sini, M., Gerovasileiou, V., Teixido, N., Mirasole, A., Tamburello, L., Cebrian, E., Rilov, G., Ledoux, J., Souissi, J. B., Khamassi, F., Ghanem, R., Benabdi, M., Grimes, S., Ocaña, O., Bazairi, H., Hereu, B., Linares, C., Kersting, D. K., La Rovira, G., Ortega, J., Casals, D., Pagès-Escolà, M., Margarit, N., Capdevila, P., Verdura, J., Ramos, A., Izquierdo, A., Barbera, C., Rubio-Portillo, E., Anton, I., López-Sendino, P., Díaz, D., Vázquez-Luis, M., Duarte, C., Marbà, N., Aspillaga, E., Espinosa, F., Grech, D., Guala, I., Azzurro, E., Farina, S., Cristina Gambi, M., Chimienti, G., Montefalcone, M., Azzola, A., Mantas, T. P., Fraschetti, S., Ceccherelli, G., Kipson, S., Bakran-Petricioli, T., Petricioli, D., Jimenez, C., Katsanevakis, S., Kizilkaya, I. T., Kizilkaya, Z., Sartoretto, S., Elodie, R., Ruitton, S., Comeau, S., Gattuso, J., and Harmelin, J.: Marine heatwaves drive recurrent mass mortalities in the Mediterranean Sea, Global Change Biology, 28, 5708–5725, https://doi.org/10.1111/gcb.16301, 2022.

Garreaud, R.: A plausible atmospheric trigger for the 2017 coastal El Niño, Intl Journal of Climatology, 38, https://doi.org/10.1002/joc.5426, 2018a.

Garreaud, R.: Record-breaking climate anomalies lead to severe drought and environmental disruption in western Patagonia in 2016, Clim. Res., 74, 217–229, https://doi.org/10.3354/cr01505, 2018b.

Garreaud, R.: Record-breaking climate anomalies lead to severe drought and environmental disruption in western Patagonia in 2016, Clim. Res., 74, 217–229, https://doi.org/10.3354/cr01505, 2018c.

Garreaud, R. and Aceituno, P.: Atmospheric Circulation and Climatic Variability, Thephysical geography of South America, 45, 2007.

Garreaud, R., Vuille, M., Compagnucci, R., and Marengo, J.: Present-day South American climate, Palaeogeography, Palaeoclimatology, Palaeoecology, 281, 180–195, https://doi.org/10.1016/j.palaeo.2007.10.032, 2009.

Garreaud, R., Lopez, P., Minvielle, M., and Rojas, M.: Large-Scale Control on the Patagonian Climate, Journal of Climate, 26, 215–230, https://doi.org/10.1175/JCLI-D-12-00001.1, 2013a.

Garreaud, R., Lopez, P., Minvielle, M., and Rojas, M.: Large-Scale Control on the Patagonian Climate, Journal of Climate, 26, 215–230, https://doi.org/10.1175/JCLI-D-12-00001.1, 2013b.

Garreaud, R., Boisier, J. P., Rondanelli, R., Montecinos, A., Sepúlveda, H. H., and Veloso-Aguila, D.: The Central Chile Mega Drought (2010–2018): A climate dynamics perspective, Int J Climatol, 40, 421–439, https://doi.org/10.1002/joc.6219, 2020.

Gierens, R., Kneifel, S., Shupe, M. D., Ebell, K., Maturilli, M., and Löhnert, U.: Low-level mixed-phase clouds in a complex Arctic environment, Atmos. Chem. Phys., 20, 3459–3481, https://doi.org/10.5194/acp-20-3459-2020, 2020.

Gillett, N. P. and Thompson, D.: Simulation of Recent Southern Hemisphere Climate Change, Science, 302, 273–275, https://doi.org/10.1126/science.1087440, 2003.

Gironás, J., Fernández, B., and Saldías, J.: Country Profile, in: Water Resources of Chile, vol. 8, edited by: Fernández, B. and Gironás, J., Springer International Publishing, Cham, 1–5, https://doi.org/10.1007/978-3-030-56901-3_1, 2021.

Glaropoulos, A., Stien, L. H., Folkedal, O., Dempster, T., and Oppedal, F.: Welfare, behaviour and feasibility of farming Atlantic salmon in submerged cages with weekly surface access to refill their swim bladders, Aquaculture, 502, 332–337, https://doi.org/10.1016/j.aquaculture.2018.12.065, 2019.

Glibert, P. and Burford, M.: Globally Changing Nutrient Loads and Harmful Algal Blooms: Recent Advances, New Paradigms, and Continuing Challenges, Oceanog., 30, 58–69, https://doi.org/10.5670/oceanog.2017.110, 2017.

Glibert, P. M.: Harmful algae at the complex nexus of eutrophication and climate change, Harmful Algae, 91, 101583, https://doi.org/10.1016/j.hal.2019.03.001, 2020.

Gobler, C. J.: Climate Change and Harmful Algal Blooms: Insights and perspective, Harmful Algae, 91, 101731, https://doi.org/10.1016/j.hal.2019.101731, 2020.

Gobler, C. J., Doherty, O. M., Hattenrath-Lehmann, T. K., Griffith, A. W., Kang, Y., and Litaker, R. W.: Ocean warming since 1982 has expanded the niche of toxic algal blooms in the North Atlantic and North Pacific oceans, Proc. Natl. Acad. Sci. U.S.A., 114, 4975–4980, https://doi.org/10.1073/pnas.1619575114, 2017.

Godoy, M. G., Kibenge, M. J., Suarez, R., Lazo, E., Heisinger, A., Aguinaga, J., Bravo, D., Mendoza, J., Llegues, K. O., Avendaño-Herrera, R., Vera, C., Mardones, F., and Kibenge, F. S.: Infectious salmon anaemia virus (ISAV) in Chilean Atlantic salmon (Salmo salar) aquaculture: emergence of low pathogenic ISAV-HPR0 and re-emergence of virulent ISAV-HPRΔ: HPR3 and HPR14, 2013.

Godwin, S. C., Fast, M. D., Kuparinen, A., Medcalf, K. E., and Hutchings, J. A.: Increasing temperatures accentuate negative fitness consequences of a marine parasite, Sci Rep, 10, 18467, https://doi.org/10.1038/s41598-020-74948-3, 2020.

Gomes, D. G. E., Ruzicka, J. J., Crozier, L. G., Huff, D. D., Brodeur, R. D., and Stewart, J. D.: Marine heatwaves disrupt ecosystem structure and function via altered food webs and energy flux, Nat Commun, 15, https://doi.org/10.1038/s41467-024-46263-2, 2024.

Gómez, C. E., Gori, A., Weinnig, A. M., Hallaj, A., Chung, H. J., and Cordes, E. E.: Natural variability in seawater temperature compromises the metabolic performance of a reef-forming cold-water coral with implications for vulnerability to ongoing global change, Coral Reefs, 41, 1225–1237, https://doi.org/10.1007/s00338-022-02267-2, 2022.

Gomez, F., Montecinos, A., Hormazabal, S., Cubillos, L. A., Correa-Ramirez, M., and Chavez, F. P.: Impact of spring upwelling variability off southern-central Chile on common sardine (*Strangomera bentincki*) recruitment, Fisheries Oceanography, 21, 405–414, https://doi.org/10.1111/j.1365-2419.2012.00632.x, 2012.

Gong, D. and Wang, S.: Definition of Antarctic Oscillation index, Geophysical Research Letters, 26, 459–462, https://doi.org/10.1029/1999GL900003, 1999.

Gong, T., Feldstein, S. B., and Luo, D.: The Impact of ENSO on Wave Breaking and Southern Annular Mode Events, Journal of the Atmospheric Sciences, 67, 2854–2870, https://doi.org/10.1175/2010JAS3311.1, 2010.

Gonzalez-Aragon, D., Rivadeneira, M. M., Lara, C., Torres, F. I., Vásquez, J. A., and Broitman, B. R.: A species distribution model of the giant kelp *Macrocystis pyrifera* : Worldwide changes and a focus on the Southeast Pacific, Ecology and Evolution, 14, e10901, https://doi.org/10.1002/ece3.10901, 2024.

Gori, A., Ferrier-Pagès, C., Hennige, S. J., Murray, F., Rottier, C., Wicks, L. C., and Roberts, J. M.: Physiological response of the cold-water coral *Desmophyllum dianthus* to thermal stress and ocean acidification, PeerJ, 4, e1606, https://doi.org/10.7717/peerj.1606, 2016.

Gorska, N., Schmidt, B., Węsławski, J. M., Grabowski, M., Dragan-Górska, A., Szczucka, J., and Beszczynska-Möller, A.: Fish in Kongsfjorden under the influence of climate warming, Front. Mar. Sci., 10, 1213081, https://doi.org/10.3389/fmars.2023.1213081, 2023.

Graham, M., Buschmann, A., and Vásquez, J.: Global Ecology of the Giant Kelp Macrocystis: from ecotypes to ecosystems, Oceanography and Marine Biology, 20074975, 39–88, https://doi.org/10.1201/9781420050943.ch2, 2007.

Graiff, A., Karsten, U., Meyer, S., Pfender, D., Tala, F., and Thiel, M.: Seasonal variation in floating persistence of detached *Durvillaea antarctica* (Chamisso) Hariot thalli, Botanica Marina, 56, 3–14, https://doi.org/10.1515/bot-2012-0193, 2013.

Green, T. J.: Ontogeny and water temperature influences the antiviral response of the Pacific oyster, Crassostrea gigas, 2014.

Greenhough, H., Vignier, J., Smith, K. F., Brown, C. M., Kenny, N. J., and Rolton, A.: Multi-stressor dynamics: Effects of marine heatwave stress and harmful algal blooms on juvenile mussel (Perna canaliculus) survival and physiology, Science of The Total Environment, 964, 178590, https://doi.org/10.1016/j.scitotenv.2025.178590, 2025.

Gröger, M., Dutheil, C., Börgel, F., and Meier, M. H. E.: Drivers of marine heatwaves in a stratified marginal sea, Clim Dyn, 62, 3231–3243, https://doi.org/10.1007/s00382-023-07062-5, 2024.

Groves, L., Whyte, S., Purcell, S., Michaud, D., Cai, W., Garber, A., and Fast, M.: Temperature impacts Atlantic salmon's (Salmo salar) immunological response to infectious salmon anemia virus (ISAv)., Fish and Shellfish Immunology Reports, 4, 100099, https://doi.org/10.1016/j.fsirep.2023.100099, 2023.

Gruber, N., Boyd, P. W., Frölicher, T. L., and Vogt, M.: Biogeochemical extremes and compound events in the ocean, Nature, 600, 395–407, https://doi.org/10.1038/s41586-021-03981-7, 2021.

Guillemin, M.-L., Faugeron, S., Destombe, C., Viard, F., Correa, J. A., and Valero, M.: Genetic Variation in Wild and Cultivated populations of the Haploid-Diploid Red Alga Gracilaria chilensis: How Farming Practices Favor Asexual Reproduction and Heterozygosity, Evolution, 62, 1500–1519, https://doi.org/10.1111/j.1558-5646.2008.00373.x, 2008.

Gunderson, A. R. and Leal, M.: A conceptual framework for understanding thermal constraints on ectotherm activity with implications for predicting responses to global change, Ecology Letters, 19, 111–120, https://doi.org/10.1111/ele.12552, 2016.

Guo, X., Gao, Y., Zhang, S., Wu, L., Chang, P., Cai, W., Zscheischler, J., Leung, L. R., Small, J., Danabasoglu, G., Thompson, L., and Gao, H.: Threat by marine heatwaves to adaptive large marine ecosystems in an eddy-resolving model, Nat. Clim. Chang., 12, 179–186, https://doi.org/10.1038/s41558-021-01266-5, 2022.

Guo, X., Gao, Y., Zhang, S., Cai, W., Chen, D., Leung, L. R., Zscheischler, J., Thompson, L., Davis, K., Qu, B., Gao, H., and Wu, L.: Intensification of future subsurface marine heatwaves in an

eddy-resolving model, Nat Commun, 15, https://doi.org/10.1038/s41467-024-54946-z, 2024.

Gupta, H., Sil, S., Gangopadhyay, A., and Gawarkiewicz, G.: Observed surface and subsurface Marine Heat Waves in the Bay of Bengal from in-situ and high-resolution satellite data, Clim Dyn, 62, 203–221, https://doi.org/10.1007/s00382-023-06913-5, 2024.

Gurumoorthi, K. and Luis, A. J.: Southern Ocean marine heatwaves: variability, hotspots and teleconnections, J Oceanogr, https://doi.org/10.1007/s10872-025-00769-5, 2025.

Gutiérrez, M. H., Narváez, D., Daneri, G., Montero, P., Pérez-Santos, I., and Pantoja, S.: Linking Seasonal Reduction of Microbial Diversity to Increase in Winter Temperature of Waters of a Chilean Patagonia Fjord, Front. Mar. Sci., 5, 277, https://doi.org/10.3389/fmars.2018.00277, 2018.

Gúzman, L. and Lembeye, G.: Estudios sobre un florecimiento toxico causado por Gonyaulax catenella en Magallanes, An. Inst. Patagon., 6, 209–223, 1975.

Guzmán, L., Pacheco, H., Pizarro, G., and Alárcon, C.: Alexandrium catenella y veneno paralizante de los mariscos en Chile, in: Floraciones Algales Nocivas en el Cono Sur Americano., edited by: Ferrario, M. E. and Reguera, B., Madrid, 235–255, 2002.

Haberle, S.: Postglacial formation and dynamics of North Patagonian Rainforest in the Chonos Archipelago, Southern Chile, Quaternary Science Reviews, 23, 2433–2452, https://doi.org/10.1016/j.quascirev.2004.03.001, 2004.

Hall, S. and Thatje, S.: Global bottlenecks in the distribution of marine Crustacea: temperature constraints in the family Lithodidae, Journal of Biogeography, 36, 2125–2135, https://doi.org/10.1111/j.1365-2699.2009.02153.x, 2009.

Hamdeno, M. and Alvera-Azcaráte, A.: Marine heatwaves characteristics in the Mediterranean Sea: Case study the 2019 heatwave events, Front. Mar. Sci., 10, https://doi.org/10.3389/fmars.2023.1093760, 2023.

Hamdeno, M., Nagy, H., Ibrahim, O., and Mohamed, B.: Responses of Satellite Chlorophyll-a to the Extreme Sea Surface Temperatures over the Arabian and Omani Gulf, Remote Sensing, 14, 4653, https://doi.org/10.3390/rs14184653, 2022.

Hansen, L. P. and Quinn, T. P.: The marine phase of the Atlantic salmon (*Salmo salar*) life cycle, with comparisons to Pacific salmon, Can. J. Fish. Aquat. Sci., 55, 104–118, https://doi.org/10.1139/d98-010, 1998.

Hart, L. C., Goodman, M. C., Walter, R. K., Rogers-Bennett, L., Shum, P., Garrett, A. D., Watanabe, J. M., and O'Leary, J. K.: Abalone Recruitment in Low-Density and Aggregated Populations Facing Climatic Stress, Journal of Shellfish Research, 39, 359, https://doi.org/10.2983/035.039.0218, 2020.

Häussermann, V. and Försterra, G.: Large assemblages of cold-water corals in Chile: a summary of recent findings and potential impacts, Bulletin of Marine Science, 81, 195–207, 2007.

Häussermann, V. and Försterra, G.: Marine benthic fauna of chilean Patagonia: illustrated identification guide, Nature in focus, Puerto Montt, 2009.

Häussermann, V., Gutstein, C. S., Beddington, M., Cassis, D., Olavarria, C., Dale, A. C., Valenzuela-Toro, A. M., Perez-Alvarez, M. J., Sepúlveda, H. H., McConnell, K. M., Horwitz, F. E., and Försterra, G.: Largest baleen whale mass mortality during strong El Niño event is likely related to harmful toxic algal bloom, PeerJ, 5, e3123, https://doi.org/10.7717/peerj.3123, 2017.

Häussermann, V., Försterra, G., and Laudien, J.: Hard Bottom Macrobenthos of Chilean Patagonia: Emphasis on Conservation of Sublitoral Invertebrate and Algal Forests, in: Conservation in Chilean Patagonia, vol. 19, edited by: Castilla, J. C., Armesto Zamudio, J. J., Martínez-Harms, M. J., and Tecklin, D., Springer International Publishing, Cham, 263–284, https://doi.org/10.1007/978-3-031-39408-9_10, 2023.

Hay, C. H.: The distribution of *Macrocystis* (Phaeophyta: Laminariales) as a biological indicator of cool sea surface temperature, with special reference to New Zealand waters, Journal of the Royal Society of New Zealand, 20, 313–336, https://doi.org/10.1080/03036758.1990.10426716, 1990.

Hayashida, H., Matear, R. J., and Strutton, P. G.: Background nutrient concentration determines phytoplankton bloom response to marine heatwaves, Global Change Biology, 26, 4800–4811, https://doi.org/10.1111/gcb.15255, 2020a.

Hayashida, H., Matear, R. J., Strutton, P. G., and Zhang, X.: Insights into projected changes in marine heatwaves from a high-resolution ocean circulation model, Nat Commun, 11, 4352, https://doi.org/10.1038/s41467-020-18241-x, 2020b.

He, Q., Zhan, W., Feng, M., Gong, Y., Cai, S., and Zhan, H.: Common occurrences of subsurface heatwaves and cold spells in ocean eddies, Nature, 634, 1111–1117, https://doi.org/10.1038/s41586-024-08051-2, 2024.

Heran, T., Laudien, J., Waller, R. G., Häussermann, V., Försterra, G., González, H. E., and Richter, C.: Life cycle of the cold-water coral Caryophyllia huinayensis, Sci Rep, 13, 2593, https://doi.org/10.1038/s41598-023-29620-x, 2023.

Hernández, C., Díaz, P. A., and Molinet, C.: Exceptional climate anomalies and northwards expansion of Paralytic Shellfish Poisoning outbreaks in Southern Chile, Harmful Algal News, 54, 2016.

Hersbach, H., Bell, B., Berrisford, P., Biavati, G., Horányi, A., Muñoz Sabater, J., Nicolas, J., Peubey, C., Radu, R., Rozum, I., Schepers, D., Simmons, A., Soci, C., Dee, D., and Thépaut, J.-N.: ERA5 hourly data on single levels from 1940 to present. (Copernicus Climate Change Service (C3S) Climate Data Store (CDS)), https://doi.org/10.24381/cds.adbb2d47, 2023.

Hevrøy, E. M., Waagbø, R., Torstensen, B. E., Takle, H., Stubhaug, I., Jørgensen, S. M., Torgersen, T., Tvenning, L., Susort, S., Breck, O., and Hansen, T.: Ghrelin is involved in voluntary anorexia in Atlantic salmon raised at elevated sea temperatures, General and Comparative Endocrinology, 175, 118–134, https://doi.org/10.1016/j.ygcen.2011.10.007, 2012.

Hirata, H., Kawamura, R., and Nonaka, M.: Effects of a marine heatwave associated with the Kuroshio Extension large meander on extreme precipitation in September 2023, Sci Rep, 15, https://doi.org/10.1038/s41598-025-88294-9, 2025.

Hobday, A., Alexander, L. V., Perkins, S. E., Smale, D. A., Straub, S. C., Oliver, E. C. J., Benthuysen, J. A., Burrows, M. T., Donat, M. G., Feng, M., Holbrook, N. J., Moore, P. J., Scannell, H. A., Sen Gupta, A., and Wernberg, T.: A hierarchical approach to defining marine heatwaves, Progress in Oceanography, 141, 227–238, https://doi.org/10.1016/j.pocean.2015.12.014, 2016.

Hobday, A., Oliver, E., Sen Gupta, A., Benthuysen, J., Burrows, M., Donat, M., Holbrook, N., Moore, P., Thomsen, M., Wernberg, T., and Smale, D.: Categorizing and Naming Marine Heatwaves, Oceanog, 31, https://doi.org/10.5670/oceanog.2018.205, 2018a.

Hobday, A., Oliver, E., Sen Gupta, A., Benthuysen, J., Burrows, M., Donat, M., Holbrook, N., Moore, P., Thomsen, M., Wernberg, T., and Smale, D.: Categorizing and Naming Marine Heatwaves, Oceanog, 31, 162–173, https://doi.org/10.5670/oceanog.2018.205, 2018b.

Holbrook, N. J., Scannell, H. A., Sen Gupta, A., Benthuysen, J. A., Feng, M., Oliver, E. C. J., Alexander, L. V., Burrows, M. T., Donat, M. G., Hobday, A. J., Moore, P. J., Perkins-Kirkpatrick, S. E., Smale, D. A., Straub, S. C., and Wernberg, T.: A global assessment of marine heatwaves and their drivers, Nat Commun, 10, 2624, https://doi.org/10.1038/s41467-019-10206-z, 2019.

Holbrook, N. J., Claar, D. C., Hobday, A. J., McInnes, K. L., Oliver, E. C. J., Gupta, A. S., Widlansky, M. J., and Zhang, X.: ENSO-Driven Ocean Extremes and Their Ecosystem Impacts, in: Geophysical Monograph Series, edited by: McPhaden, M. J., Santoso, A., and Cai, W., Wiley, 409–428, https://doi.org/10.1002/9781119548164.ch18, 2020a.

Holbrook, N. J., Sen Gupta, A., Oliver, E. C. J., Hobday, A. J., Benthuysen, J. A., Scannell, H. A., Smale, D. A., and Wernberg, T.: Keeping pace with marine heatwaves, Nat Rev Earth Environ, 1, 482–493, https://doi.org/10.1038/s43017-020-0068-4, 2020b.

Hollarsmith, J. A., Buschmann, A. H., Camus, C., and Grosholz, E. D.: Varying reproductive success under ocean warming and acidification across giant kelp (Macrocystis pyrifera) populations, Journal of Experimental Marine Biology and Ecology, 522, 151247, https://doi.org/10.1016/j.jembe.2019.151247, 2020.

Hu, L.: A Global Assessment of Coastal Marine Heatwaves and Their Relation With Coastal Urban Thermal Changes, Geophysical Research Letters, 48, e2021GL093260, https://doi.org/10.1029/2021GL093260, 2021.

Hu, S., Li, S., Zhang, Y., Guan, C., Du, Y., Feng, M., Ando, K., Wang, F., Schiller, A., and Hu, D.: Observed strong subsurface marine heatwaves in the tropical western Pacific Ocean, Environ. Res. Lett., 16, 104024, https://doi.org/10.1088/1748-9326/ac26f2, 2021.

Hu, Z.-Z., Kumar, A., Xue, Y., and Jha, B.: Why were some La Niñas followed by another La Niña?, Clim Dyn, 42, 1029–1042, https://doi.org/10.1007/s00382-013-1917-3, 2014.

Huang, B., L'Heureux, M., Hu, Z., and Zhang, H.: Ranking the strongest ENSO events while incorporating SST uncertainty, Geophysical Research Letters, 43, 9165–9172, https://doi.org/10.1002/2016GL070888, 2016.

Huang, B., Liu, C., Banzon, V., Freeman, E., Graham, G., Hankins, B., Smith, T., and Zhang, H.-M.: Improvements of the Daily Optimum Interpolation Sea Surface Temperature (DOISST) Version 2.1, Journal of Climate, 34, 2923–2939, https://doi.org/10.1175/JCLI-D-20-0166.1, 2021a.

Huang, B., Wang, Z., Yin, X., Arguez, A., Graham, G., Liu, C., Smith, T., and Zhang, H.: Prolonged Marine Heatwaves in the Arctic: 1982–2020, Geophysical Research Letters, 48, https://doi.org/10.1029/2021gl095590, 2021b.

Huang, Z., Feng, M., Dalton, S. J., and Carroll, A. G.: Marine heatwaves in the Great Barrier Reef and Coral Sea: their mechanisms and impacts on shallow and mesophotic coral ecosystems, Science of The Total Environment, 908, 168063, https://doi.org/10.1016/j.scitotenv.2023.168063, 2024.

Hucke-Gaete, R., Osman, L. P., Moreno, C. A., Findlay, K. P., and Ljungblad, D. K.: Discovery of a blue whale feeding and nursing ground in southern Chile, Proc. R. Soc. Lond. B, 271, https://doi.org/10.1098/rsbl.2003.0132, 2004.

Hucke-Gaete, R., Haro, D., Torres-Florez, J. P., Montecinos, Y., Viddi, F., Bedriñana-Romano, L., Nery, M. F., and Ruiz, J.: A historical feeding ground for humpback whales in the eastern South Pacific revisited: the case of northern Patagonia, Chile, Aquatic Conservation, 23, 858–867, https://doi.org/10.1002/aqc.2343, 2013.

Ignatz, E. H., Sandrelli, R. M., Vadboncoeur, É., Zanuzzo, F. S., Perry, G. M. L., Rise, M. L., and Gamperl, A. K.: The Atlantic salmon's (Salmo salar) incremental thermal maximum is a more relevant and sensitive indicator of family-based differences in upper temperature tolerance than its critical thermal maximum, Aquaculture, 574, 739628, https://doi.org/10.1016/j.aquaculture.2023.739628, 2023.

IPCC: Summary for Policymakers, in: Climate Change 2021 – The Physical Science Basis, Cambridge University Press, 3–32, https://doi.org/10.1017/9781009157896.001, 2021.

Iriarte, J. L.: Natural and Human Influences on Marine Processes in Patagonian Subantarctic Coastal Waters, Front. Mar. Sci., 5, 360, https://doi.org/10.3389/fmars.2018.00360, 2018.

Iriarte, J. L., González, H. E., and Nahuelhual, L.: Patagonian Fjord Ecosystems in Southern Chile as a Highly Vulnerable Region: Problems and Needs, AMBIO, 39, 463–466, https://doi.org/10.1007/s13280-010-0049-9, 2010.

Iriarte, J. L., Pantoja, S., and Daneri, G.: Oceanographic Processes in Chilean Fjords of Patagonia: From small to large-scale studies, Progress in Oceanography, 129, 1–7, https://doi.org/10.1016/j.pocean.2014.10.004, 2014.

Ishida, K., Tachibana, M., Yao, Y., Wada, Y., and Noda, T.: The impact of marine heatwaves on rocky intertidal communities: evidence of accumulative carryover effects of marine heatwaves, Front. Mar. Sci., 10, 1146148, https://doi.org/10.3389/fmars.2023.1146148, 2023.

Jackson, J. M., Johnson, G. C., Dosser, H. V., and Ross, T.: Warming From Recent Marine Heatwave Lingers in Deep British Columbia Fjord, Geophysical Research Letters, 45, 9757–9764, https://doi.org/10.1029/2018GL078971, 2018.

Jackson, J. M., Bianucci, L., Hannah, C. G., Carmack, E. C., and Barrette, J.: Deep Waters in British Columbia Mainland Fjords Show Rapid Warming and Deoxygenation From 1951 to 2020, Geophysical Research Letters, 48, e2020GL091094, https://doi.org/10.1029/2020GL091094, 2021.

Jacox, M. G., Hazen, E. L., Zaba, K. D., Rudnick, D. L., Edwards, C. A., Moore, A. M., and Bograd, S. J.: Impacts of the 2015–2016 El Niño on the California Current System: Early assessment and comparison to past events, Geophysical Research Letters, 43, 7072–7080, https://doi.org/10.1002/2016GL069716, 2016.

Jacox, M. G., Alexander, M. A., Bograd, S. J., and Scott, J. D.: Thermal displacement by marine heatwaves, Nature, 584, 82–86, https://doi.org/10.1038/s41586-020-2534-z, 2020.

Jahnsen-Guzmán, N., Lagos, N. A., Lardies, M. A., Vargas, C. A., Fernández, C., San Martín, V. A., Saavedra, L., Cuevas, L. A., Quijón, P. A., and Duarte, C.: Environmental refuges increase performance of juvenile mussels Mytilus chilensis: Implications for mussel seedling and farming strategies, Science of The Total Environment, 751, 141723, https://doi.org/10.1016/j.scitotenv.2020.141723, 2021.

Jangir, B., Mishra, A. K., and Strobach, E.: The interplay between medicanes and the Mediterranean Sea in the presence of sea surface temperature anomalies, Atmospheric Research, 310, 107625, https://doi.org/10.1016/j.atmosres.2024.107625, 2024.

Jantzen, C., Häussermann, V., Försterra, G., Laudien, J., Ardelan, M., Maier, S., and Richter, C.: Occurrence of a cold-water coral along natural pH gradients (Patagonia, Chile), Mar Biol, 160, 2597–2607, https://doi.org/10.1007/s00227-013-2254-0, 2013.

Jones, S., Bruno, D., Madsen, L., and Peeler, E.: Disease management mitigates risk of pathogen transmission from maricultured salmonids, Aquacult. Environ. Interact., 6, 119–134, https://doi.org/10.3354/aei00121, 2015.

Jones, T., Parrish, J. K., Peterson, W. T., Bjorkstedt, E. P., Bond, N. A., Ballance, L. T., Bowes, V., Hipfner, J. M., Burgess, H. K., Dolliver, J. E., Lindquist, K., Lindsey, J., Nevins, H. M., Robertson, R. R., Roletto, J., Wilson, L., Joyce, T., and Harvey, J.: Massive Mortality of a Planktivorous Seabird in Response to a Marine Heatwave, Geophysical Research Letters, 45, 3193–3202, https://doi.org/10.1002/2017GL076164, 2018.

Jones, T., Divine, L. M., Renner, H., Knowles, S., Lefebvre, K. A., Burgess, H. K., Wright, C., and Parrish, J. K.: Unusual mortality of Tufted puffins (Fratercula cirrhata) in the eastern Bering Sea, PLoS ONE, 14, e0216532, https://doi.org/10.1371/journal.pone.0216532, 2019.

Jordà-Molina, È., Renaud, P. E., Silberberger, M. J., Sen, A., Bluhm, B. A., Carroll, M. L., Ambrose, W. G., Cottier, F., and Reiss, H.: Seafloor warm water temperature anomalies impact benthic macrofauna communities of a high-Arctic cold-water fjord, Marine Environmental Research, 189, 106046, https://doi.org/10.1016/j.marenvres.2023.106046, 2023.

Keeling, R. F., Körtzinger, A., and Gruber, N.: Ocean Deoxygenation in a Warming World, Annu. Rev. Mar. Sci., 2, 199–229, https://doi.org/10.1146/annurev.marine.010908.163855, 2010.

Kendrick, G. A., Nowicki, R. J., Olsen, Y. S., Strydom, S., Fraser, M. W., Sinclair, E. A., Statton, J., Hovey, R. K., Thomson, J. A., Burkholder, D. A., McMahon, K. M., Kilminster, K., Hetzel, Y., Fourqurean, J. W., Heithaus, M. R., and Orth, R. J.: A Systematic Review of How Multiple Stressors From an Extreme Event Drove Ecosystem-Wide Loss of Resilience in an Iconic Seagrass Community, Front. Mar. Sci., 6, 455, https://doi.org/10.3389/fmars.2019.00455, 2019.

Khangaonkar, T., Nugraha, A., Yun, S. K., Premathilake, L., Keister, J. E., and Bos, J.: Propagation of the 2014–2016 Northeast Pacific Marine Heatwave Through the Salish Sea, Front. Mar. Sci., 8, 787604, https://doi.org/10.3389/fmars.2021.787604, 2021.

Kilpeläinen, T., Vihma, T., and Ólafsson, H.: Modelling of spatial variability and topographic effects over Arctic fjords in Svalbard, Tellus A: Dynamic Meteorology and Oceanography, 63, 223, https://doi.org/10.1111/j.1600-0870.2010.00481.x, 2011.

Kohlman, C., Cronin, M. F., Dziak, R., Mellinger, D. K., Sutton, A., Galbraith, M., Robert, M., Thomson, J., Zhang, D., and Thompson, L.: The 2019 Marine Heatwave at Ocean Station Papa: A Multi-Disciplinary Assessment of Ocean Conditions and Impacts on Marine Ecosystems, JGR Oceans, 129, e2023JC020167, https://doi.org/10.1029/2023JC020167, 2024.

Korus, J., Filgueira, R., and Grant, J.: Influence of temperature on the behaviour and physiology of Atlantic salmon (Salmo Salar) on a commercial farm, Aquaculture, 589, 740978, https://doi.org/10.1016/j.aquaculture.2024.740978, 2024.

Kumagai, J. A., Goodman, M. C., Villaseñor-Derbez, J. C., Schoeman, D. S., Cavanuagh, K. C., Bell, T. W., Micheli, F., De Leo, G., and Arafeh-Dalmau, N.: Marine Protected Areas That Preserve Trophic Cascades Promote Resilience of Kelp Forests to Marine Heatwaves, Global Change Biology, 30, e17620, https://doi.org/10.1111/gcb.17620, 2024.

Kuroda, H., Azumaya, T., Setou, T., and Hasegawa, N.: Unprecedented Outbreak of Harmful Algae in Pacific Coastal Waters off Southeast Hokkaido, Japan, during Late Summer 2021 after Record-Breaking Marine Heatwaves, JMSE, 9, 1335, https://doi.org/10.3390/jmse9121335, 2021.

Laboy-Nieves, E. N., Klein, E., Conde, J. E., Losada, F., and Bone, D.: Mass mortality of tropical marine communities in Morrocoy, Venezuela, BULLETIN OF MARINE SCIENCE, 68, 2001.

Ladah, L. B. and Zertuche-González, J. A.: Survival of microscopic stages of a perennial kelp (Macrocystis pyrifera) from the center and the southern extreme of its range in the Northern Hemisphere after exposure to simulated El Niño stress, Mar Biol, 152, 677–686, https://doi.org/10.1007/s00227-007-0723-z, 2007.

Landaeta, M. F., Bustos, C. A., Palacios Fuentes, P., Rojas, P., and Balbontin, F.: Distribucion del ictioplancton en la Patagonia austral de Chile: potenciales efectos del deshielo de Campos de Hielo Sur, lajar, 39, 236–249, https://doi.org/10.3856/vol39-issue2-fulltext-5, 2011.

Lara, C., Saldías, G. S., Tapia, F. J., Iriarte, J. L., and Broitman, B. R.: Interannual variability in temporal patterns of Chlorophyll–a and their potential influence on the supply of mussel larvae to inner waters in northern Patagonia (41–44°S), Journal of Marine Systems, 155, 11–18, https://doi.org/10.1016/j.jmarsys.2015.10.010, 2016.

Laufkötter, C., Zscheischler, J., and Frölicher, T. L.: High-impact marine heatwaves attributable to human-induced global warming, Science, 369, 1621–1625, https://doi.org/10.1126/science.aba0690, 2020.

Lazo-Andrade, J., Barría, P., and Urzúa, Á.: Bioenergetic status of swordfish (Xiphias gladius) during the El Niño Southern Oscillation (ENSO) in the Southeast Pacific Ocean: An

interannual scale, Science of The Total Environment, 918, 170354, https://doi.org/10.1016/j.scitotenv.2024.170354, 2024.

Le, D. M., Desmond, M. J., Pritchard, D. W., and Hepburn, C. D.: Effect of temperature on sporulation and spore development of giant kelp (Macrocystis pyrifera), PLoS ONE, 17, e0278268, https://doi.org/10.1371/journal.pone.0278268, 2022.

Le Grix, N., Zscheischler, J., Laufkötter, C., Rousseaux, C. S., and Frölicher, T. L.: Compound high-temperature and low-chlorophyll extremes in the ocean over the satellite period, Biogeosciences, 18, 2119–2137, https://doi.org/10.5194/bg-18-2119-2021, 2021.

Lee, D. Y., Petersen, M. R., and Lin, W.: The Southern Annular Mode and Southern Ocean Surface Westerly Winds in E3SM, Earth and Space Science, 6, 2624–2643, https://doi.org/10.1029/2019EA000663, 2019.

Leggat, W. P., Camp, E. F., Suggett, D. J., Heron, S. F., Fordyce, A. J., Gardner, S., Deakin, L., Turner, M., Beeching, L. J., Kuzhiumparambil, U., Eakin, C. M., and Ainsworth, T. D.: Rapid Coral Decay Is Associated with Marine Heatwave Mortality Events on Reefs, Current Biology, 29, 2723-2730.e4, https://doi.org/10.1016/j.cub.2019.06.077, 2019.

Lellouche, J.-M., Greiner, E., Bourdallé-Badie, R., Garric, G., Melet, A., Drévillon, M., Bricaud, C., Hamon, M., Le Galloudec, O., Regnier, C., Candela, T., Testut, C.-E., Gasparin, F., Ruggiero, G., Benkiran, M., Drillet, Y., and Le Traon, P.-Y.: The Copernicus Global 1/12° Oceanic and Sea Ice GLORYS12 Reanalysis, Front. Earth Sci., 9, 698876, https://doi.org/10.3389/feart.2021.698876, 2021.

Lenaerts, J. T. M., Van Den Broeke, M. R., Van Wessem, J. M., Van De Berg, W. J., Van Meijgaard, E., Van Ulft, L. H., and Schaefer, M.: Extreme Precipitation and Climate Gradients in Patagonia Revealed by High-Resolution Regional Atmospheric Climate Modeling, Journal of Climate, 27, 4607–4621, https://doi.org/10.1175/JCLI-D-13-00579.1, 2014.

León-Muñoz, J., Marcé, R., and Iriarte, J.: Influence of hydrological regime of an Andean river on salinity, temperature and oxygen in a Patagonia fjord, Chile, New Zealand Journal of Marine and Freshwater Research, 47, 515–528, https://doi.org/10.1080/00288330.2013.802700, 2013.

León-Muñoz, J., Urbina, M. A., Garreaud, R., and Iriarte, J. L.: Hydroclimatic conditions trigger record harmful algal bloom in western Patagonia (summer 2016), Sci Rep, 8, 1330, https://doi.org/10.1038/s41598-018-19461-4, 2018.

León-Muñoz, J., Aguayo, R., Marcé, R., Catalán, N., Woelfl, S., Nimptsch, J., Arismendi, I., Contreras, C., Soto, D., and Miranda, A.: Climate and Land Cover Trends Affecting Freshwater Inputs to a Fjord in Northwestern Patagonia, Front. Mar. Sci., 8, 628454, https://doi.org/10.3389/fmars.2021.628454, 2021.

León-Muñoz, J., Aguayo, R., Corredor-Acosta, A., Tapia, F. J., Iriarte, J. L., Reid, B., and Soto, D.: Hydrographic shifts in coastal waters reflect climate-driven changes in hydrological regimes across Northwestern Patagonia, Sci Rep, 14, 20632, https://doi.org/10.1038/s41598-024-71008-y, 2024.

Letelier, J., Pizarro, O., and Nuñez, S.: Seasonal variability of coastal upwelling and the upwelling front off central Chile, J. Geophys. Res., 114, https://doi.org/10.1029/2008JC005171, 2009.

Li, C., Huang, J., Liu, X., Ding, L., He, Y., and Xie, Y.: The ocean losing its breath under the heatwaves, Nat Commun, 15, 6840, https://doi.org/10.1038/s41467-024-51323-8, 2024.

Li, C., Cao, X., Ji, J., Yao, Y., and Hu, Y.: More intense and prolonged bottom marine cold-spells than surface: evidence from the continental shelf of China, Environ. Res. Lett., 20, 084026, https://doi.org/10.1088/1748-9326/ade81b, 2025.

Li, G., Li, C., Tan, Y., and Bai, T.: Seasonal evolution of dominant modes in south pacific SST and relationship with ENSO, Adv. Atmos. Sci., 29, 1238–1248, https://doi.org/10.1007/s00376-012-1191-z, 2012.

Li, G., Cheng, L., Zhu, J., Trenberth, K. E., Mann, M. E., and Abraham, J. P.: Increasing ocean stratification over the past half-century, Nat. Clim. Chang., 10, 1116–1123, https://doi.org/10.1038/s41558-020-00918-2, 2020.

Li, X. and Donner, S. D.: Lengthening of warm periods increased the intensity of warm-season marine heatwaves over the past 4 decades, Clim Dyn, 59, 2643–2654, https://doi.org/10.1007/s00382-022-06227-y, 2022.

Li, X., Hu, Z., McPhaden, M. J., Zhu, C., and Liu, Y.: Triple-Dip La Niñas in 1998–2001 and 2020–2023: Impact of Mean State Changes, JGR Atmospheres, 128, e2023JD038843, https://doi.org/10.1029/2023JD038843, 2023.

Lian, Z., Yang, T., Leung, J. C.-H., and Zhang, B.: East Asian monsoon and Pacific basin dynamics jointly regulate boreal winter marine cold spells in the Taiwan Strait, Sci Rep, 14, 26010, https://doi.org/10.1038/s41598-024-75479-x, 2024.

Lien, V. S., Raj, R. P., and Chatterjee, S.: Surface and bottom marine heatwave characteristics in the Barents Sea: a model study, State Planet, 4-osr8, 1–11, https://doi.org/10.5194/sp-4-osr8-8-2024, 2024.

Lim, Y. K., Park, B. S., Kim, J. H., Baek, S.-S., and Baek, S. H.: Effect of marine heatwaves on bloom formation of the harmful dinoflagellate Cochlodinium polykrikoides: Two sides of the same coin?, Harmful Algae, 104, 102029, https://doi.org/10.1016/j.hal.2021.102029, 2021.

Lima, F. P. and Wethey, D. S.: Three decades of high-resolution coastal sea surface temperatures reveal more than warming, Nat Commun, 3, https://doi.org/10.1038/ncomms1713, 2012.

Lindhal, O.: A dividable hose for phytoplankton sampling. Report of the working group on phytoplankton and management of their effects., International Council for the exploration of the sea, 1986.

Linford, P., Pérez-Santos, I., Montes, I., Dewitte, B., Buchan, S., Narváez, D., Saldías, G., Pinilla, E., Garreaud, R., Díaz, P., Schwerter, C., Montero, P., Rodríguez-Villegas, C., Cáceres-Soto, M., Mancilla-Gutiérrez, G., and Altamirano, R.: Recent Deoxygenation of Patagonian Fjord Subsurface Waters Connected to the Peru–Chile Undercurrent and Equatorial Subsurface Water Variability, Global Biogeochemical Cycles, 37, e2022GB007688, https://doi.org/10.1029/2022GB007688, 2023.

Linford, P., Pérez-Santos, I., Montero, P., Díaz, P. A., Aracena, C., Pinilla, E., Barrera, F., Castillo, M., Alvera-Azcárate, A., Alvarado, M., Soto, G., Pujol, C., Schwerter, C., Arenas-Uribe, S., Navarro, P., Mancilla-Gutiérrez, G., Altamirano, R., San Martín, J., and Soto-Riquelme, C.: Oceanographic processes driving low-oxygen conditions inside Patagonian fjords, Biogeosciences, 21, 1433–1459, https://doi.org/10.5194/bg-21-1433-2024, 2024.

Lipiatou, E. and Granéli, E.: Eurohab – Science initiative. Part B, Research and infrastructural needs. National European and international programmes, edited by: Lipiatou, E. and Granéli, E., Publications Office, 2002.

Liu, B., Zhou, Z., Wang, L., Zhang, X., Xu, Z., Liu, Z., Hu, J., Fu, W., and Zhong, Z.: The heatwaves weaken the effect of light on the growth, photosynthesis, and reproductive capacity of Ulva prolifera, Marine Environmental Research, 209, 107163, https://doi.org/10.1016/j.marenvres.2025.107163, 2025.

Liu, H., Nie, X., Shi, J., and Wei, Z.: Marine heatwaves and cold spells in the Brazil Overshoot show distinct sea surface temperature patterns depending on the forcing, Commun Earth Environ, 5, 102, https://doi.org/10.1038/s43247-024-01258-1, 2024.

Lobo, A., Torres, D., and Acevedo, J.: Los mamíferos marinos de Chile: I. Cetacea, Serie Científica INACH, 48, 19–159, 1998.

Lonhart, S. I., Jeppesen, R., Beas-Luna, R., Crooks, J. A., and Lorda, J.: Shifts in the distribution and abundance of coastal marine species along the eastern Pacific Ocean during marine heatwaves from 2013 to 2018, Mar Biodivers Rec, 12, 13, https://doi.org/10.1186/s41200-019-0171-8, 2019.

López, B. A., Macaya, E. C., Rivadeneira, M. M., Tala, F., Tellier, F., and Thiel, M.: Epibiont communities on stranded kelp rafts of *Durvillaea antarctica* (Fucales, Phaeophyceae)—Do positive interactions facilitate range extensions?, Journal of Biogeography, 45, 1833–1845, https://doi.org/10.1111/jbi.13375, 2018.

Lovegrove, T.: An improved form of sedimentation apparatus for use with an inverted microscope, J. Cons. Int. Explor. Mer., 25, 279–284, 1960.

Lutz, K., Jacobeit, J., and Rathmann, J.: Atlantic warm and cold water events and impact on African west coast precipitation, Intl Journal of Climatology, 35, 128–141, https://doi.org/10.1002/joc.3969, 2015.

Macreadie, P. I., Jarvis, J., Trevathan-Tackett, S. M., and Bellgrove, A.: Seagrasses and Macroalgae: Importance, Vulnerability and Impacts, in: Climate Change Impacts on Fisheries and Aquaculture, edited by: Phillips, B. F. and Pérez-Ramírez, M., Wiley, 729–770, https://doi.org/10.1002/9781119154051.ch22, 2017.

Magel, C. L., Chan, F., Hessing-Lewis, M., and Hacker, S. D.: Differential Responses of Eelgrass and Macroalgae in Pacific Northwest Estuaries Following an Unprecedented NE Pacific Ocean Marine Heatwave, Front. Mar. Sci., 9, 838967, https://doi.org/10.3389/fmars.2022.838967, 2022.

Mansilla, A. O., Avila, M., and Cáceres, J.: Reproductive biology of Durvillaea antarctica (Chamisso) Hariot in the sub-Antarctic ecoregion of Magallanes (51–56° S), J Appl Phycol, 29, 2567–2574, https://doi.org/10.1007/s10811-017-1077-7, 2017.

Mantua, N. J. and Hare, S. R.: The Pacific Decadal Oscillation, Journal of Oceanography, 58, 35–44, https://doi.org/10.1023/A:1015820616384, 2002.

Mantua, N. J., Hare, S. R., Zhang, Y., Wallace, J. M., and Francis, R. C.: A Pacific Interdecadal Climate Oscillation with Impacts on Salmon Production, Bull. Amer. Meteor. Soc., 78, 1069–1079, https://doi.org/10.1175/1520-0477(1997)078<1069:APICOW>2.0.CO;2, 1997.

Marbà, N. and Duarte, C. M.: Mediterranean warming triggers seagrass (*Posidonia oceanica*) shoot mortality, Global Change Biology, 16, 2366–2375, https://doi.org/10.1111/j.1365-2486.2009.02130.x, 2010.

Mardones, J.: Chile: Causes, impacts and management of a "hot spot" for toxic algal blooms, in: Abstract book of the 19th International Conference on Harmful Algae, edited by: Band-Schmidt, C. J. and Rodríguez-Gómez, C. F., La Paz, B.C.S., Mexico, 10, 2021.

Mardones, J., Clement, A., Rojas, X., and Aparicio, C.: Alexandrium catenella during 2009 in Chilean waters, and recent expansion to coastal ocean, Harmful Algae News, 41, 8–9, 2010.

Marin, M., Bindoff, N. L., Feng, M., and Phillips, H. E.: Slower Long-Term Coastal Warming Drives Dampened Trends in Coastal Marine Heatwave Exposure, JGR Oceans, 126, https://doi.org/10.1029/2021jc017930, 2021.

Marochi, M. Z., De Grande, F. R., Farias Pardo, J. C., Montenegro, Á., and Costa, T. M.: Marine heatwave impacts on newly-hatched planktonic larvae of an estuarine crab, Estuarine, Coastal and Shelf Science, 278, 108122, https://doi.org/10.1016/j.ecss.2022.108122, 2022.

Marquet, P. A., Buschmann, A. H., Corcoran, D., Díaz, P. A., Fuentes-Castillo, T., Garreaud, R., Pliscoff, P., and Salazar, A.: Global Change and Acceleration of Anthropic Pressures on

Patagonian Ecosystems, in: Conservation in Chilean Patagonia, vol. 19, edited by: Castilla, J. C., Armesto Zamudio, J. J., Martínez-Harms, M. J., and Tecklin, D., Springer International Publishing, Cham, 33–65, https://doi.org/10.1007/978-3-031-39408-9_2, 2023.

Márquez Porras, R.: La fiebre de las algas. Forma y dinámicas del extractivismo en la costa chilena., RAA, 57–71, https://doi.org/10.12795/RAA.2019.17.03, 2019.

Marshall, G. J.: Trends in the Southern Annular Mode from Observations and Reanalyses, Journal of Climate, 16, 4134–4143, 2003.

Martel, S. I., Fernández, C., Lagos, N. A., Labra, F. A., Duarte, C., Vivanco, J. F., García-Herrera, C., and Lardies, M. A.: Acidification and high-temperature impacts on energetics and shell production of the edible clam Ameghinomya antiqua, Front. Mar. Sci., 9, 972135, https://doi.org/10.3389/fmars.2022.972135, 2022.

Martínez, V., Lara, C., Silva, N., Gudiño, V., and Montecino, V.: Variability of environmental heterogeneity in northern Patagonia, Chile: effects on the spatial distribution, size structure and abundance of chlorophyll-a, Rev. biol. mar. oceanogr., 50, 39–52, https://doi.org/10.4067/S0718-19572015000100004, 2015.

Marzonie, M. R., Bay, L. K., Bourne, D. G., Hoey, A. S., Matthews, S., Nielsen, J. J. V., and Harrison, H. B.: The effects of marine heatwaves on acute heat tolerance in corals, Global Change Biology, 29, 404–416, https://doi.org/10.1111/gcb.16473, 2023.

Maturana-Martínez, C., Fernández, C., González, H. E., and Galand, P. E.: Different Active Microbial Communities in Two Contrasted Subantarctic Fjords, Front. Microbiol., 12, 620220, https://doi.org/10.3389/fmicb.2021.620220, 2021.

Maulu, S., Hasimuna, O. J., Haambiya, L. H., Monde, C., Musuka, C. G., Makorwa, T. H., Munganga, B. P., Phiri, K. J., and Nsekanabo, J. D.: Climate Change Effects on Aquaculture Production: Sustainability Implications, Mitigation, and Adaptations, Front. Sustain. Food Syst., 5, 609097, https://doi.org/10.3389/fsufs.2021.609097, 2021.

Mayr, C., Rebolledo, L., Schulte, K., Schuster, A., Zolitschka, B., Försterra, G., and Häussermann, V.: Responses of nitrogen and carbon deposition rates in Comau Fjord (42°S, southern Chile) to natural and anthropogenic impacts during the last century, Continental Shelf Research, 78, 29–38, https://doi.org/10.1016/j.csr.2014.02.004, 2014.

Mazzini, P. L. F. and Pianca, C.: Marine Heatwaves in the Chesapeake Bay, Front. Mar. Sci., 8, 750265, https://doi.org/10.3389/fmars.2021.750265, 2022.

Mazzotti, F. J., Cherkiss, M. S., Parry, M., Beauchamp, J., Rochford, M., Smith, B., Hart, K., and Brandt, L. A.: Large reptiles and cold temperatures: Do extreme cold spells set distributional limits for tropical reptiles in Florida?, Ecosphere, 7, e01439, https://doi.org/10.1002/ecs2.1439, 2016.

McCabe, R. M., Hickey, B. M., Kudela, R. M., Lefebvre, K. A., Adams, N. G., Bill, B. D., Gulland, F. M. D., Thomson, R. E., Cochlan, W. P., and Trainer, V. L.: An unprecedented coastwide toxic algal bloom linked to anomalous ocean conditions, Geophysical Research Letters, 43, https://doi.org/10.1002/2016GL070023, 2016.

McPhaden, M. J.: Genesis and Evolution of the 1997-98 El Niño, Science, 283, 950–954, https://doi.org/10.1126/science.283.5404.950, 1999.

McPhee, J., MacDonell, S., and Casassa, G.: Snow Cover and Glaciers, in: Water Resources of Chile, vol. 8, edited by: Fernández, B. and Gironás, J., Springer International Publishing, Cham, 129–151, https://doi.org/10.1007/978-3-030-56901-3_6, 2021.

McPherson, M. L., Finger, D. J. I., Houskeeper, H. F., Bell, T. W., Carr, M. H., Rogers-Bennett, L., and Kudela, R. M.: Large-scale shift in the structure of a kelp forest ecosystem co-occurs with an epizootic and marine heatwave, Commun Biol, 4, https://doi.org/10.1038/s42003-021-01827-6, 2021.

Meehl, G. A., Arblaster, J. M., Chung, C. T. Y., Holland, M. M., DuVivier, A., Thompson, L., Yang, D., and Bitz, C. M.: Sustained ocean changes contributed to sudden Antarctic sea ice retreat in late 2016, Nat Commun, 10, 14, https://doi.org/10.1038/s41467-018-07865-9, 2019.

Meng, H., Hayashida, H., Norazmi-Lokman, N. H., and Strutton, P. G.: Benefits and detrimental effects of ocean warming for Tasmanian salmon aquaculture, Continental Shelf Research, 246, 104829, https://doi.org/10.1016/j.csr.2022.104829, 2022.

Merkouriadi, I. and Leppäranta, M.: Influence of sea ice on the seasonal variability of hydrography and heat content in Tvärminne, Gulf of Finland, Ann. Glaciol., 56, 274–284, https://doi.org/10.3189/2015AoG69A003, 2015.

Michaud, K. M., Reed, D. C., and Miller, R. J.: The Blob marine heatwave transforms California kelp forest ecosystems, Commun Biol, 5, 1143, https://doi.org/10.1038/s42003-022-04107-z, 2022.

Mignot, A., Von Schuckmann, K., Landschützer, P., Gasparin, F., Van Gennip, S., Perruche, C., Lamouroux, J., and Amm, T.: Decrease in air-sea CO2 fluxes caused by persistent marine heatwaves, Nat Commun, 13, 4300, https://doi.org/10.1038/s41467-022-31983-0, 2022.

Millner, R. and Whiting, L.: Long-term changes in growth and population abundance of sole in the North Sea from 1940 to the present, ICES Journal of Marine Science, 53, 1185–1195, https://doi.org/10.1006/jmsc.1996.0143, 1996.

Mills, K., Pershing, A., Brown, C., Chen, Y., Chiang, F.-S., Holland, D., Lehuta, S., Nye, J., Sun, J., Thomas, A., and Wahle, R.: Fisheries Management in a Changing Climate: Lessons From the 2012 Ocean Heat Wave in the Northwest Atlantic, oceanog, 26, https://doi.org/10.5670/oceanog.2013.27, 2013.

Ministerio de Economía, Fomento y Reconstrucción, and Subsecretaría de Pesca: Reglamiento sobre Parques Marinos y Reservas Marinas de la Ley General de Pesca y Acuicultura, Decreto 238, 2004.

Ministerio de Economía, Fomento y Reconstrucción and Subsecretaría de Pesca: Resolución 3612 Extenta, Aprueba Resolución que Fija las Metodologías para Elaborar la Caracterización Preliminar de Sitio (CPS) y la Información Ambiental (INFA), Law "Resolución 3612 Extenta," 2009.

Ministerio de Salud and Secretaría Regional Ministerial Región de Los Lagos: Apprueba procedimientos de fiscalización de productos del mar afectos a toxinas marinas, 43817, 2024.

Ministerio de Salud and Subsecretaría de Salud Pública: Proroga vigencia del decreto N°38, de 6 de Abril de 2022, del Ministerio de Salud, que decreta alerta sanitaria por el preíodo que se señala y otorga faculdades extraodinarias que indica por presencia de marea roja en las regiones de Los Lagos y de Aysén, 2022.

Miyama, T., Minobe, S., and Goto, H.: Marine Heatwave of Sea Surface Temperature of the Oyashio Region in Summer in 2010–2016, Front. Mar. Sci., 7, 576240, https://doi.org/10.3389/fmars.2020.576240, 2021.

Molinet, C., Lafon, A., Lembeye, G., and Moreno, C. A.: Patrones de distribución espacial y temporal de floraciones de Alexandrium catenella (Whedon & Kofoid) Balech 1985, en aguas interiores de la Patagonia noroccidental de Chile, Rev. chil. hist. nat., 76, https://doi.org/10.4067/S0716-078X2003000400011, 2003.

Molinet, C., Olguín, A., Gebauer, P., Díaz, P. A., Díaz, M., Matamala, T., Mora, P., and Paschke, K.: Upswing and expansion of the southern king crab (Lithodes santolla) fishery in Northwest Patagonia: Drivers, trends and opportunities for management, Regional Studies in Marine Science, 34, 101073, https://doi.org/10.1016/j.rsma.2020.101073, 2020.

Molinet, C., Astorga, M., Cares, L., Diaz, M., Hueicha, K., Marín, S., Matamala, T., and Soto, D.: Vertical distribution patterns of larval supply and spatfall of three species of Mytilidae in a

Chilean fjord used for mussel farming: Insights for mussel spatfall efficiency, Aquaculture, 535, 736341, https://doi.org/10.1016/j.aquaculture.2021.736341, 2021.

Molinet, C., Soto, D., León-Muñoz, J., Díaz, M., Espinoza, K., Henríquez, J., and Matamala, T.: Climate-driven changes in freshwater inputs to a Northern patagonia Fjord and overfishing of wild mussel seed could threaten Chilean mussel farming, Climatic Change, 178, 119, https://doi.org/10.1007/s10584-025-03956-x, 2025.

Molinet Flores, C. A. M., Gomez, M. A. D., Muñoz, C. B. A., Pérez, L. E. C., Arribas, S. L. M., Opazo, M. P. A., and Huaquin, E. J. E. N.: Spatial distribution pattern of Mytilus chilensis beds in the Reloncaví fjord: hypothesis on associated processes, Rev. Chil. de Hist. Nat., 88, 11, https://doi.org/10.1186/s40693-015-0041-7, 2015.

Montecinos, A. and Gomez, F.: ENSO modulation of the upwelling season off southern-central Chile, Geophysical Research Letters, 37, 2009GL041739, https://doi.org/10.1029/2009GL041739, 2010.

Montero, P. M., Daneri, G., Tapia, F., Iriarte, J. L., and Crawford, D.: Diatom blooms and primary production in a channel ecosystem of central Patagonia, lajar, 45, 999–1016, https://doi.org/10.3856/vol45-issue5-fulltext-16, 2017.

Montie, S.: Marine heatwave impacts on New Zealand algal populations and their associations with obligate and facultative epibiota., University of Canterbury, https://doi.org/10.26021/15100, 2023.

Montie, S., Schiel, D. R., and Thomsen, M. S.: Shifts in foundation species dominance and altered interaction networks after compounding seismic uplift and extreme marine heatwaves, Marine Environmental Research, 202, 106738, https://doi.org/10.1016/j.marenvres.2024.106738, 2024.

Moore, S. K., Mantua, N. J., Hickey, B. M., and Trainer, V. L.: Recent trends in paralytic shellfish toxins in Puget Sound, relationships to climate, and capacity for prediction of toxic events, Harmful Algae, 8, 463–477, https://doi.org/10.1016/j.hal.2008.10.003, 2009.

Morato, T., González-Irusta, J., Dominguez-Carrió, C., Wei, C., Davies, A., Sweetman, A. K., Taranto, G. H., Beazley, L., García-Alegre, A., Grehan, A., Laffargue, P., Murillo, F. J., Sacau, M., Vaz, S., Kenchington, E., Arnaud-Haond, S., Callery, O., Chimienti, G., Cordes, E., Egilsdottir, H., Freiwald, A., Gasbarro, R., Gutiérrez-Zárate, C., Gianni, M., Gilkinson, K., Wareham Hayes, V. E., Hebbeln, D., Hedges, K., Henry, L., Johnson, D., Koen-Alonso, M., Lirette, C., Mastrototaro, F., Menot, L., Molodtsova, T., Durán Muñoz, P., Orejas, C., Pennino, M. G., Puerta, P., Ragnarsson, S. Á., Ramiro-Sánchez, B., Rice, J., Rivera, J., Roberts, J. M., Ross, S. W., Rueda, J. L., Sampaio, Í., Snelgrove, P., Stirling, D., Treble, M. A., Urra, J., Vad, J., Van Oevelen, D., Watling, L., Walkusz, W., Wienberg, C., Woillez, M., Levin, L. A., and Carreiro-Silva, M.: Climate-induced changes in the suitable habitat of cold-water corals and commercially important deep-sea fishes in the North Atlantic, Global Change Biology, 26, 2181–2202, https://doi.org/10.1111/gcb.14996, 2020.

Muller-Karger, F. E.: The Spring 1998 Northeastern Gulf of Mexico (NEGOM) Cold Water Event: Remote Sensing Evidence for Upwelling and for Eastward Advection of Mississippi Water (or: How an Errant Loop Current Anticyclone Took the NEGOM for a Spin), goms, 18, https://doi.org/10.18785/goms.1801.06, 2000.

Muñoz, R., Vergara, O. A., Figueroa, P. A., Mardones, P., Sobarzo, M., and Saldías, G. S.: On the phenology of coastal upwelling off central-southern Chile, Dynamics of Atmospheres and Oceans, 104, 101405, https://doi.org/10.1016/j.dynatmoce.2023.101405, 2023.

Myers, T. A., Mechoso, C. R., Cesana, G. V., DeFlorio, M. J., and Waliser, D. E.: Cloud Feedback Key to Marine Heatwave off Baja California, Geophysical Research Letters, 45, 4345–4352, https://doi.org/10.1029/2018GL078242, 2018.

Napitupulu, G.: Eddy-induced modulation of marine heatwaves and cold spells in a tropical region: a case study in the natuna sea area, Ocean Dynamics, 75, 28, https://doi.org/10.1007/s10236-025-01673-8, 2025.

Narváez, D. A., Vargas, C. A., Cuevas, L. A., García-Loyola, S. A., Lara, C., Segura, C., Tapia, F. J., and Broitman, B. R.: Dominant scales of subtidal variability in coastal hydrography of the Northern Chilean Patagonia, Journal of Marine Systems, 193, 59–73, https://doi.org/10.1016/j.jmarsys.2018.12.008, 2019.

NASA OBPG: MODIS Aqua Global Level 3 Mapped SST. Ver. 2019.0., https://doi.org/10.5067/MODAM-8D4N9, 2020.

Naumann, M. S., Orejas, C., and Ferrier-Pagès, C.: High thermal tolerance of two Mediterranean cold-water coral species maintained in aquaria, Coral Reefs, 32, 749–754, https://doi.org/10.1007/s00338-013-1011-7, 2013.

Navarro, J. M., Duarte, C., Manríquez, P. H., Lardies, M. A., Torres, R., Acuña, K., Vargas, C. A., and Lagos, N. A.: Ocean warming and elevated carbon dioxide: multiple stressor impacts on juvenile mussels from southern Chile, ICES Journal of Marine Science, 73, 764–771, https://doi.org/10.1093/icesjms/fsv249, 2016.

Newman, M., Alexander, M. A., Ault, T. R., Cobb, K. M., Deser, C., Di Lorenzo, E., Mantua, N. J., Miller, A. J., Minobe, S., Nakamura, H., Schneider, N., Vimont, D. J., Phillips, A. S., Scott, J. D., and Smith, C. A.: The Pacific Decadal Oscillation, Revisited, Journal of Climate, 29, 4399–4427, https://doi.org/10.1175/JCLI-D-15-0508.1, 2016.

Nissar, S., Bakhtiyar, Y., Arafat, M. Y., Andrabi, S., Bhat, A. A., and Yousuf, T.: A review of the ecosystem services provided by the marine forage fish, Hydrobiologia, 850, 2871–2902, https://doi.org/10.1007/s10750-022-05033-1, 2023.

NOAA Climate, (National Oceanic and Atmospheric Administration Climate): Record-setting bloom of toxic algae in North Pacific, https://www.climate.gov/news-features/event-tracker/record-setting-bloom-toxic-algae-north-pacific, 2015.

Noël, B., Lhermitte, S., Wouters, B., and Fettweis, X.: Poleward shift of subtropical highs drives Patagonian glacier mass loss, Nat Commun, 16, 3795, https://doi.org/10.1038/s41467-025-58974-1, 2025.

Nuic, B., English, C., Bowden, A., Wade, N. M., Koster, L., Kawasaki, M., Williams, A., Mendoza-Porras, O., Barnes, A. C., Franklin, C. E., Smullen, R., and Cramp, R. L.: Physiological and immunological biomarkers of chronic thermal stress in post-smolt Atlantic salmon, Salmo salar, Aquaculture, 609, 742850, https://doi.org/10.1016/j.aquaculture.2025.742850, 2025.

Olita, A., Sorgente, R., Natale, S., Gaberšek, S., Ribotti, A., Bonanno, A., and Patti, B.: Effects of the 2003 European heatwave on the Central Mediterranean Sea: surface fluxes and the dynamical response, Ocean Sci., 3, 273–289, https://doi.org/10.5194/os-3-273-2007, 2007.

Oliver, E. C. J.: Mean warming not variability drives marine heatwave trends, Clim Dyn, 53, 1653–1659, https://doi.org/10.1007/s00382-019-04707-2, 2019.

Oliver, E. C. J., Benthuysen, J. A., Bindoff, N. L., Hobday, A. J., Holbrook, N. J., Mundy, C. N., and Perkins-Kirkpatrick, S. E.: The unprecedented 2015/16 Tasman Sea marine heatwave, Nat Commun, 8, 16101, https://doi.org/10.1038/ncomms16101, 2017.

Oliver, E. C. J., Donat, M. G., Burrows, M. T., Moore, P. J., Smale, D. A., Alexander, L. V., Benthuysen, J. A., Feng, M., Sen Gupta, A., Hobday, A. J., Holbrook, N. J., Perkins-Kirkpatrick, S. E., Scannell, H. A., Straub, S. C., and Wernberg, T.: Longer and more frequent marine heatwaves over the past century, Nat Commun, 9, 1324, https://doi.org/10.1038/s41467-018-03732-9, 2018a.

Oliver, E. C. J., Lago, V., Hobday, A. J., Holbrook, N. J., Ling, S. D., and Mundy, C. N.: Marine heatwaves off eastern Tasmania: Trends, interannual variability, and predictability, Progress in Oceanography, 161, 116–130, https://doi.org/10.1016/j.pocean.2018.02.007, 2018b.

Oliver, E. C. J., Burrows, M. T., Donat, M. G., Sen Gupta, A., Alexander, L. V., Perkins-Kirkpatrick, S. E., Benthuysen, J. A., Hobday, A. J., Holbrook, N. J., Moore, P. J., Thomsen, M. S., Wernberg, T., and Smale, D. A.: Projected Marine Heatwaves in the 21st Century and the Potential for Ecological Impact, Front. Mar. Sci., 6, https://doi.org/10.3389/fmars.2019.00734, 2019.

Oyarzún, P. A., Toro, J. E., Nuñez, J. J., Ruiz-Tagle, G., and Gardner, J. P. A.: The Mediterranean Mussel Mytilus galloprovincialis (Mollusca: Bivalvia) in Chile: Distribution and Genetic Structure of a Recently Introduced Invasive Marine Species, Animals, 14, 823, https://doi.org/10.3390/ani14060823, 2024.

Palma, S. and Silva, N.: Distribution of siphonophores, chaetognaths, euphausiids and oceanographic conditions in the fjords and channels of southern Chile, Deep Sea Research Part II: Topical Studies in Oceanography, 51, 513–535, https://doi.org/10.1016/j.dsr2.2004.05.001, 2004.

Palmas, F., Cariccia, F., Pasquini, V., Cabiddu, S., Addis, P., and Pusceddu, A.: Marine heatwaves effects on quantity, composition, and turnover of sedimentary organic matter in a Mediterranean coastal lagoon: A benthocosm study, Estuarine, Coastal and Shelf Science, 318, 109252, https://doi.org/10.1016/j.ecss.2025.109252, 2025.

Pansch, C., Scotti, M., Barboza, F. R., Al-Janabi, B., Brakel, J., Briski, E., Bucholz, B., Franz, M., Ito, M., Paiva, F., Saha, M., Sawall, Y., Weinberger, F., and Wahl, M.: Heat waves and their significance for a temperate benthic community: A near-natural experimental approach, Global Change Biology, 24, 4357–4367, https://doi.org/10.1111/gcb.14282, 2018.

Pantoja, S., Luis Iriarte, J., and Daneri, G.: Oceanography of the Chilean Patagonia, Continental Shelf Research, 31, 149–153, https://doi.org/10.1016/j.csr.2010.10.013, 2011.

Pardo, L. M., Rubilar, P. S., and Fuentes, J. P.: North Patagonian estuaries appear to function as nursery habitats for marble crab (Metacarcinus edwardsii), Regional Studies in Marine Science, 36, 101315, https://doi.org/10.1016/j.rsma.2020.101315, 2020.

Paredes-Mella, J., Mardones, J. I., Norambuena, L., Fuenzalida, G., Labra, G., Espinoza-González, O., and Guzmán, L.: Toxic Alexandrium catenella expanding northward along the Chilean coast: New risk of paralytic shellfish poisoning off the Bío-Bío region (36° S), Marine Pollution Bulletin, 172, 112783, https://doi.org/10.1016/j.marpolbul.2021.112783, 2021.

Parra Núñez, S.: Fabricación y experimentación de biotextiles a base de cochayuyo, Universidad de Chile, 94 pp., 2024.

Paschke, K., Cumillaf, J. P., Chimal, M. E., Díaz, F., Gebauer, P., and Rosas, C.: Relationship between age and thermoregulatory behaviour of Lithodes santolla (Molina, 1782) (Decapoda, Lithodidae) juveniles, Journal of Experimental Marine Biology and Ecology, 448, 141–145, https://doi.org/10.1016/j.jembe.2013.06.018, 2013.

Pathmeswaran, C., Sen Gupta, A., Perkins-Kirkpatrick, S. E., and Hart, M. A.: Exploring Potential Links Between Co-occurring Coastal Terrestrial and Marine Heatwaves in Australia, Front. Clim., 4, 792730, https://doi.org/10.3389/fclim.2022.792730, 2022.

Pavlov, A. K., Tverberg, V., Ivanov, B. V., Nilsen, F., Falk-Petersen, S., and Granskog, M. A.: Warming of Atlantic Water in two west Spitsbergen fjords over the last century (1912–2009), Polar Research, 32, 11206, https://doi.org/10.3402/polar.v32i0.11206, 2013.

Peal, R., Worsfold, M., and Good, S.: Comparing global trends in marine cold spells and marine heatwaves using reprocessed satellite data, State Planet, 1-osr7, 1–10, https://doi.org/10.5194/sp-1-osr7-3-2023, 2023.

Pearce, A., Lenanton, R., Jackson, G., Moore, J., Feng, M., and Gaughan, D.: The "marine heat wave" off Western Australia during the summer of 2010/1, 2011.

Pearce, A. F. and Feng, M.: The rise and fall of the "marine heat wave" off Western Australia during the summer of 2010/2011, Journal of Marine Systems, 111–112, 139–156, https://doi.org/10.1016/j.jmarsys.2012.10.009, 2013.

Pecuchet, L., Mohamed, B., Hayward, A., Alvera-Azcárate, A., Dörr, J., Filbee-Dexter, K., Kuletz, K. J., Luis, K., Manizza, M., Miller, C. E., Staehr, P. A. U., Szymkowiak, M., and Wernberg, T.: Arctic and Subarctic marine heatwaves and their ecological impacts, Front. Environ. Sci., 13, 1473890, https://doi.org/10.3389/fenvs.2025.1473890, 2025.

Pellizzari, F. M., Santos, K. C., Osaki, S., and Rosa, L. H.: Marine heatwaves and changes in macroalgae richness and composition from Antarctic Peninsula and South Shetland Islands: concise review, An. Acad. Bras. Ciênc., 97, e20240580, https://doi.org/10.1590/0001-3765202520240580, 2025.

Perez-Quezada, J. F., Moncada, M., Barrales, P., Urrutia-Jalabert, R., Pfeiffer, M., Herrera, A. F., and Sagardía, R.: How much carbon is stored in the terrestrial ecosystems of the Chilean Patagonia?, Austral Ecology, 48, 893–903, https://doi.org/10.1111/aec.13331, 2023.

Pérez-Santos, I.: Deep ventilation event during fall and winter 2015 in the Puyuhuapi Fjord (44.6 S), lajar, 45, 223–227, https://doi.org/10.3856/vol45-issue1-fulltext-25, 2017.

Pérez-Santos, I., Garcés-Vargas, J., Schneider, W., Ross, L., Parra, S., and Valle-Levinson, A.: Double-diffusive layering and mixing in Patagonian fjords, Progress in Oceanography, 129, 35–49, https://doi.org/10.1016/j.pocean.2014.03.012, 2014.

Pérez-Santos, I., Castro, L., Ross, L., Niklitschek, E., Mayorga, N., Cubillos, L., Gutierrez, M., Escalona, E., Castillo, M., Alegría, N., and Daneri, G.: Turbulence and hypoxia contribute to dense biological scattering layers in a Patagonian fjord system, Ocean Sci., 14, 1185–1206, https://doi.org/10.5194/os-14-1185-2018, 2018.

Pérez-Santos, I., Seguel, R., Schneider, W., Linford, P., Donoso, D., Navarro, E., Amaya-Cárcamo, C., Pinilla, E., and Daneri, G.: Synoptic-scale variability of surface winds and ocean response to atmospheric forcing in the eastern austral Pacific Ocean, Ocean Sci., 15, 1247–1266, https://doi.org/10.5194/os-15-1247-2019, 2019.

Pérez-Santos, I., Díaz, P. A., Silva, N., Garreaud, R., Montero, P., Henríquez-Castillo, C., Barrera, F., Linford, P., Amaya, C., Contreras, S., Aracena, C., Pinilla, E., Altamirano, R., Vallejos, L., Pavez, J., and Maulen, J.: Oceanography time series reveals annual asynchrony input between oceanic and estuarine waters in Patagonian fjords, Science of The Total Environment, 798, 149241, https://doi.org/10.1016/j.scitotenv.2021.149241, 2021.

Perkins, S. E. and Alexander, L. V.: On the Measurement of Heat Waves, Journal of Climate, 26, 4500–4517, https://doi.org/10.1175/jcli-d-12-00383.1, 2013.

Perkins-Kirkpatrick, S. E., King, A. D., Cougnon, E. A., Holbrook, N. J., Grose, M. R., Oliver, E. C. J., Lewis, S. C., and Pourasghar, F.: The Role of Natural Variability and Anthropogenic Climate Change in the 2017/18 Tasman Sea Marine Heatwave, Bulletin of the American Meteorological Society, 100, S105–S110, https://doi.org/10.1175/BAMS-D-18-0116.1, 2019.

Peters, A. F. and Breeman, A. M.: Temperature tolerance and latitudinal range of brown algae from temperate Pacific South America, Marine Biology, 115, 143–150, https://doi.org/10.1007/BF00349396, 1993.

Piatt, J. F., Parrish, J. K., Renner, H. M., Schoen, S. K., Jones, T. T., Arimitsu, M. L., Kuletz, K. J., Bodenstein, B., García-Reyes, M., Duerr, R. S., Corcoran, R. M., Kaler, R. S. A., McChesney,

G. J., Golightly, R. T., Coletti, H. A., Suryan, R. M., Burgess, H. K., Lindsey, J., Lindquist, K., Warzybok, P. M., Jahncke, J., Roletto, J., and Sydeman, W. J.: Extreme mortality and reproductive failure of common murres resulting from the northeast Pacific marine heatwave of 2014-2016, PLoS ONE, 15, e0226087, https://doi.org/10.1371/journal.pone.0226087, 2020.

Pickard, G. L.: Some Physical Oceanographic Features of Inlets of Chile, J. Fish. Res. Bd. Can., 28, 1077–1106, https://doi.org/10.1139/f71-163, 1971.

Pietri, A., Colas, F., Mogollon, R., Tam, J., and Gutierrez, D.: Marine heatwaves in the Humboldt current system: from 5-day localized warming to year-long El Niños, Sci Rep, 11, https://doi.org/10.1038/s41598-021-00340-4, 2021.

Pikitch, E. K., Rountos, K. J., Essington, T. E., Santora, C., Pauly, D., Watson, R., Sumaila, U. R., Boersma, P. D., Boyd, I. L., Conover, D. O., Cury, P., Heppell, S. S., Houde, E. D., Mangel, M., Plagányi, É., Sainsbury, K., Steneck, R. S., Geers, T. M., Gownaris, N., and Munch, S. B.: The global contribution of forage fish to marine fisheries and ecosystems, Fish and Fisheries, 15, 43–64, https://doi.org/10.1111/faf.12004, 2014.

Pilo, G. S., Holbrook, N. J., Kiss, A. E., and Hogg, A. McC.: Sensitivity of Marine Heatwave Metrics to Ocean Model Resolution, Geophysical Research Letters, 46, 14604–14612, https://doi.org/10.1029/2019GL084928, 2019.

Pinilla, E., Soto, G., Soto-Riquelme, C., Venegas, O., and Salas, P.: Determinación de las escalas de intercambio de agua en fiordos y canales de la Patagonia, Etapa II (Región de Aysén), 2019.

Pinilla, E., Castillo, M. I., Pérez-Santos, I., Venegas, O., and Valle-Levinson, A.: Water age variability in a Patagonian fjord, Journal of Marine Systems, 210, 103376, https://doi.org/10.1016/j.jmarsys.2020.103376, 2020.

Pinilla, E., Soto, G., Soto-Riquelme, C., Venegas, O., Salas, P., and Cortés, J.: Determinación de las escalas de intercambio de agua en fiordos y canales de la región de Los Lagos y región de Aysén, Subsecretaría de Economía y Empresas de Menor Tamaño, https://doi.org/10.13140/RG.2.2.17813.65762, 2021.

Pinochet, J., Brante, A., Daguin-Thiébaut, C., Tellier, F., and Viard, F.: Investigating the risk of non-indigenous species introduction through ship hulls in Chile, MBI, 14, 156–177, https://doi.org/10.3391/mbi.2023.14.1.09, 2023.

Piñones, A., Aziares-Aguayo, N., Amador-Véliz, P., Mercado-Peña, O., González-Reyes, A., Valdivia, N., Garcés-Vargas, J., Garrido, I., Pardo, L. M., and Höfer, J.: Local and Remote Atmosphere-Ocean Coupling During Extreme Warming Events Impacting Subsurface Ocean Temperature in an Antarctic Embayment, JGR Oceans, 129, e2023JC020735, https://doi.org/10.1029/2023JC020735, 2024.

Pirhalla, D. E., Sheridan, S. C., Ransibrahmanakul, V., and Lee, C. C.: Assessing Cold-Snap and Mortality Events in South Florida Coastal Ecosystems: Development of a Biological Cold Stress Index Using Satellite SST and Weather Pattern Forcing, Estuaries and Coasts, 38, 2310–2322, https://doi.org/10.1007/s12237-014-9918-y, 2015.

Pizarro A, O., Hormazabal F, S., Gonzalez C, A., and Yañez R, E.: Variabilidad del viento, nivel del mar y temperatura en la costa norte de Chile, Investig. mar., 22, https://doi.org/10.4067/S0717-71781994002200007, 1994.

Plecha, S. M. and Soares, P. M. M.: Global marine heatwave events using the new CMIP6 multi-model ensemble: from shortcomings in present climate to future projections, Environ. Res. Lett., 15, 124058, https://doi.org/10.1088/1748-9326/abc847, 2020.

Pontoppidan, M., De Falco, C., Mooney, P. A., Nummelin, A., and Tjiputra, J.: Added value of a regional coupled model: the case study for marine heatwaves in the Caribbean, Clim Dyn, 61, 3569–3579, https://doi.org/10.1007/s00382-023-06758-y, 2023.

Porter, C. and Santana, A.: Rápido Retroceso, en el Siglo 20, del ventisquero Marinelli en el campo de Hielo de la Cordillera Darwin. Rapid 20th Century Retreat of Ventisquero Marinelli in the Cordillera Darwin Icefield., Anales Del Instituto De La Patagonia, 37, 17–26, 2014.

Poston, H. A. and Williams, R. C.: Interrelations of Oxygen Concentration, Fish Density, and Performance of Atlantic Salmon in an Ozonated Water Reuse System, The Progressive Fish-Culturist, 50, 69–76, https://doi.org/10.1577/1548-8640(1988)050<0069:IOOCFD>2.3.CO;2, 1988.

Preti, A., Muhling, B. A., DiNardo, G. T., Pierce, G. J., Lyons, K., and Stohs, S. M.: Foraging ecology of swordfish in the California Current Large Marine Ecosystem during an ecosystem regime shift, ICES Journal of Marine Science, 82, fsaf139, https://doi.org/10.1093/icesjms/fsaf139, 2025.

Pretterebner, K., Pardo, L. M., and Paschke, K.: Temperature-dependent seminal recovery in the southern king crab *Lithodes santolla*, R. Soc. open sci., 6, 181700, https://doi.org/10.1098/rsos.181700, 2019.

Pujol, C., Pérez-Santos, I., Barth, A., and Alvera-Azcárate, A.: Marine Heatwaves Offshore Central and South Chile: Understanding Forcing Mechanisms During the Years 2016-2017, Front. Mar. Sci., 9, 800325, https://doi.org/10.3389/fmars.2022.800325, 2022.

Pujol, C., Barth, A., Pérez-Santos, I., Muñoz-Linford, P., and Alvera-Azcárate, A.: Overcoming Challenges in Coastal Marine Heatwave Detection: Integrating In Situ and Satellite Data in Complex Coastal Environment, https://doi.org/10.5194/egusphere-2025-1421, 3 April 2025.

Pun, I.-F., Hsu, H.-H., Moon, I.-J., Lin, I.-I., and Jeong, J.-Y.: Marine heatwave as a supercharger for the strongest typhoon in the East China Sea, npj Clim Atmos Sci, 6, https://doi.org/10.1038/s41612-023-00449-5, 2023.

Purcell-Meyerink, D., Packer, M. A., Wheeler, T. T., and Hayes, M.: Aquaculture Production of the Brown Seaweeds Laminaria digitata and Macrocystis pyrifera: Applications in Food and Pharmaceuticals, Molecules, 26, 1306, https://doi.org/10.3390/molecules26051306, 2021.

Quiñones, R. A., Fuentes, M., Montes, R. M., Soto, D., and León-Muñoz, J.: Environmental issues in Chilean salmon farming: a review, Reviews in Aquaculture, 11, 375–402, https://doi.org/10.1111/raq.12337, 2019.

Rahn, D. A. and Garreaud, R. D.: A synoptic climatology of the near-surface wind along the west coast of South America, Intl Journal of Climatology, 34, 780–792, https://doi.org/10.1002/joc.3724, 2014.

Rathore, S., Goyal, R., Jangir, B., Ummenhofer, C. C., Feng, M., and Mishra, M.: Interactions Between a Marine Heatwave and Tropical Cyclone Amphan in the Bay of Bengal in 2020, Front. Clim., 4, 861477, https://doi.org/10.3389/fclim.2022.861477, 2022.

Raymond, C., Matthews, T., and Horton, R. M.: The emergence of heat and humidity too severe for human tolerance, Sci. Adv., 6, eaaw1838, https://doi.org/10.1126/sciadv.aaw1838, 2020.

Reboita, M. S., Ambrizzi, T., and Rocha, R. P. D.: Relationship between the southern annular mode and southern hemisphere atmospheric systems, Rev. bras. meteorol., 24, 48–55, https://doi.org/10.1590/S0102-77862009000100005, 2009.

Ren, X., Wang, Q., Shao, H., Xu, Y., Liu, P., and Li, J.: Effects of Low Temperature on Shrimp and Crab Physiology, Behavior, and Growth: A Review, Front. Mar. Sci., 8, 746177, https://doi.org/10.3389/fmars.2021.746177, 2021.

Reyes–Mendoza, O., Manta, G., and Carrillo, L.: Marine heatwaves and marine cold-spells on the Yucatan Shelf-break upwelling region, Continental Shelf Research, 239, 104707, https://doi.org/10.1016/j.csr.2022.104707, 2022.

Rich, W. A., Carvalho, S., and Berumen, M. L.: Coral bleaching due to cold stress on a central Red Sea reef flat, Ecology and Evolution, 12, e9450, https://doi.org/10.1002/ece3.9450, 2022.

Rind, D., Chandler, M., Lerner, J., Martinson, D. G., and Yuan, X.: Climate response to basin-specific changes in latitudinal temperature gradients and implications for sea ice variability, J. Geophys. Res., 106, 20161–20173, https://doi.org/10.1029/2000JD900643, 2001.

Rivera, A., Aravena, J. C., Urra, A., and Reid, B.: Chilean Patagonian Glaciers and Environmental Change, in: Conservation in Chilean Patagonia: Assessing the State of Knowledge, Opportunities, and Challenges, edited by: Castilla, J. C., Armesto Zamudio, J. J., Martínez-Harms, M. J., and Tecklin, D., Springer International Publishing, Cham, 393–407, https://doi.org/10.1007/978-3-031-39408-9_15, 2023.

Roberts, S. D., Van Ruth, P. D., Wilkinson, C., Bastianello, S. S., and Bansemer, M. S.: Marine Heatwave, Harmful Algae Blooms and an Extensive Fish Kill Event During 2013 in South Australia, Front. Mar. Sci., 6, 610, https://doi.org/10.3389/fmars.2019.00610, 2019a.

Roberts, S. D., Van Ruth, P. D., Wilkinson, C., Bastianello, S. S., and Bansemer, M. S.: Marine Heatwave, Harmful Algae Blooms and an Extensive Fish Kill Event During 2013 in South Australia, Front. Mar. Sci., 6, 610, https://doi.org/10.3389/fmars.2019.00610, 2019b.

Robinson, N., Winberg, P., and Kirkendale, L.: Genetic improvement of macroalgae: status to date and needs for the future, J Appl Phycol, 25, 703–716, https://doi.org/10.1007/s10811-012-9950-x, 2013.

Rodolfo-Metalpa, R., Montagna, P., Aliani, S., Borghini, M., Canese, S., Hall-Spencer, J. M., Foggo, A., Milazzo, M., Taviani, M., and Houlbrèque, F.: Calcification is not the Achilles' heel of cold-water corals in an acidifying ocean, Global Change Biology, 21, 2238–2248, https://doi.org/10.1111/gcb.12867, 2015.

Rodrigo, C.: Submarine topography in the Chilean North Patagonian channels, in: Progress in the oceanographic knowledge of Chilean inner waters, from Puerto Montt to Cape Horn, 19–23, 2008.

Rodrigues, R. R., Taschetto, A. S., Sen Gupta, A., and Foltz, G. R.: Common cause for severe droughts in South America and marine heatwaves in the South Atlantic, Nat. Geosci., 12, 620–626, https://doi.org/10.1038/s41561-019-0393-8, 2019.

Rodríguez-Morata, C., Díaz, H. F., Ballesteros-Canovas, J. A., Rohrer, M., and Stoffel, M.: The anomalous 2017 coastal El Niño event in Peru, Clim Dyn, 52, 5605–5622, https://doi.org/10.1007/s00382-018-4466-y, 2019.

Rodríguez-Villegas, C., Pérez-Santos, I., Díaz, P. A., Baldrich, Á. M., Lee, M. R., Saldías, G. S., Mancilla-Gutiérrez, G., Urrutia, C., Navarro, C. R., Varela, D. A., Ross, L., and Figueroa, R. I.: Deep Turbulence as a Novel Main Driver for Multi-Specific Toxic Algal Blooms: The Case of an Anoxic and Heavy Metal-Polluted Submarine Canyon That Harbors Toxic Dinoflagellate Resting Cysts, Microorganisms, 12, 2015, https://doi.org/10.3390/microorganisms12102015, 2024.

Roemmich, D., Gilson, J., Sutton, P., and Zilberman, N.: Multidecadal Change of the South Pacific Gyre Circulation, Journal of Physical Oceanography, 46, 1871–1883, https://doi.org/10.1175/JPO-D-15-0237.1, 2016.

Rogers-Bennett, L. and Catton, C. A.: Marine heat wave and multiple stressors tip bull kelp forest to sea urchin barrens, Sci Rep, 9, 15050, https://doi.org/10.1038/s41598-019-51114-y, 2019.

Rojas-Hernandez, N., Veliz, D., Riveros, M. P., Fuentes, J. P., and Pardo, L. M.: Highly Connected Populations and Temporal Stability in Allelic Frequencies of a Harvested Crab from the Southern Pacific Coast, PLoS ONE, 11, e0166029, https://doi.org/10.1371/journal.pone.0166029, 2016.

Rollins, H. B.: The peruvian anchoveta and its upwelling ecosystem: Three Decades of Change. D. Pauly and I. Tsukayama, Eds., 1987, International Center for Living Aquatic Resources Management (available from International Specialized Book Services, P.O. Box 1632, Beaverton, OR 970751, 351 pp., $36.00, Georchaeology, 3, 306–307, https://doi.org/10.1002/gea.3340030411, 1988.

Ross Brown, A., Lilley, M. K. S., Shutler, J., Widdicombe, C., Rooks, P., McEvoy, A., Torres, R., Artioli, Y., Rawle, G., Homyard, J., Tyler, C. R., and Lowe, C.: Harmful Algal Blooms and their impacts on shellfish mariculture follow regionally distinct patterns of water circulation in the western English Channel during the 2018 heatwave, Harmful Algae, 111, 102166, https://doi.org/10.1016/j.hal.2021.102166, 2022.

Rosselló, P., Pascual, A., and Combes, V.: Assessing marine heat waves in the Mediterranean Sea: a comparison of fixed and moving baseline methods, Front. Mar. Sci., 10, 1168368, https://doi.org/10.3389/fmars.2023.1168368, 2023.

Rossi, S., Bramanti, L., Gori, A., and Orejas, C. (Eds.): Marine Animal Forests: The Ecology of Benthic Biodiversity Hotspots, Springer International Publishing, Cham, https://doi.org/10.1007/978-3-319-21012-4, 2017.

Rothäusler, E., Gómez, I., Hinojosa, I. A., Karsten, U., Tala, F., and Thiel, M.: Effect of Temperature and Grazing on Growth and reproduction of Floating Macrocystis Spp. (Phaeophycaea) along a Latitudinal Gradient, Journal of Phycology, 45, 547–559, https://doi.org/10.1111/j.1529-8817.2009.00676.x, 2009.

Ruthrof, K. X., Breshears, D. D., Fontaine, J. B., Froend, R. H., Matusick, G., Kala, J., Miller, B. P., Mitchell, P. J., Wilson, S. K., Van Keulen, M., Enright, N. J., Law, D. J., Wernberg, T., and Hardy, G. E. St. J.: Subcontinental heat wave triggers terrestrial and marine, multi-taxa responses, Sci Rep, 8, 13094, https://doi.org/10.1038/s41598-018-31236-5, 2018.

Rutterford, L. A., Simpson, S. D., Jennings, S., Johnson, M. P., Blanchard, J. L., Schön, P.-J., Sims, D. W., Tinker, J., and Genner, M. J.: Future fish distributions constrained by depth in warming seas, Nature Clim Change, 5, 569–573, https://doi.org/10.1038/nclimate2607, 2015.

Sae-Lim, P., Kause, A., Mulder, H. A., and Olesen, I.: BREEDING AND GENETICS SYMPOSIUM: Climate change and selective breeding in aquaculture1, Journal of Animal Science, 95, 1801–1812, https://doi.org/10.2527/jas.2016.1066, 2017.

Sajid, Z., Gamperl, A. K., Parrish, C. C., Colombo, S. M., Santander, J., Mather, C., Neis, B., Holmen, I. M., Filgueira, R., McKenzie, C. H., Cavalli, L. S., Jeebhay, M., Gao, W., López Gómez, M. A., Ochs, C., Lehnert, S., Couturier, C., Knott, C., Romero, J. F., Caballero-Solares, A., Cembella, A., Murray, H. M., Fleming, I. A., Finnis, J., Fast, M. D., Wells, M., and Singh, G. G.: An aquaculture risk model to understand the causes and consequences of Atlantic Salmon mass mortality events: A review, Reviews in Aquaculture, 16, 1674–1695, https://doi.org/10.1111/raq.12917, 2024.

Salazar, Á., Thatcher, M., Goubanova, K., Bernal, P., Gutiérrez, J., and Squeo, F.: CMIP6 precipitation and temperature projections for Chile, Clim Dyn, 62, 2475–2498, https://doi.org/10.1007/s00382-023-07034-9, 2024.

Saldías, G. S., Sobarzo, M., and Quiñones, R.: Freshwater structure and its seasonal variability off western Patagonia, Progress in Oceanography, 174, 143–153, https://doi.org/10.1016/j.pocean.2018.10.014, 2019.

Saldías, G. S., Hernández, W., Lara, C., Muñoz, R., Rojas, C., Vásquez, S., Pérez-Santos, I., and Soto-Mardones, L.: Seasonal Variability of SST Fronts in the Inner Sea of Chiloé and Its Adjacent Coastal Ocean, Northern Patagonia, Remote Sensing, 13, 181, https://doi.org/10.3390/rs13020181, 2021.

Saldías, G. S., Figueroa, P. A., Carrasco, D., Narváez, D. A., Pérez-Santos, I., and Lara, C.: Satellite-Derived Variability of Sea Surface Salinity and Geostrophic Currents off Western Patagonia, Remote Sensing, 16, 1482, https://doi.org/10.3390/rs16091482, 2024.

Salgado, H., Bailey, J., Tiller, R., and Ellis, J.: Stakeholder perceptions of the impacts from salmon aquaculture in the Chilean Patagonia, Ocean & Coastal Management, 118, 189–204, https://doi.org/10.1016/j.ocecoaman.2015.07.016, 2015.

Salinger, M. J., Renwick, J., Behrens, E., Mullan, A. B., Diamond, H. J., Sirguey, P., Smith, R. O., Trought, M. C. T., Alexander, L., Cullen, N. J., Fitzharris, B. B., Hepburn, C. D., Parker, A. K., and Sutton, P. J.: The unprecedented coupled ocean-atmosphere summer heatwave in the New Zealand region 2017/18: drivers, mechanisms and impacts, Environ. Res. Lett., 14, 044023, https://doi.org/10.1088/1748-9326/ab012a, 2019.

Salmonexpert: Activan plan de contingencia por mortalidad masiva en centro de Marine Farm, 2020a.

Salmonexpert: Ingresan segunda ronda de peces en jaula sumergible Atlantis, 2020b.

Salmonexpert: Jaula sumergible chilena para salmonicultura oceánica revela positivos resultados, 2021.

Santora, J. A., Mantua, N. J., Schroeder, I. D., Field, J. C., Hazen, E. L., Bograd, S. J., Sydeman, W. J., Wells, B. K., Calambokidis, J., Saez, L., Lawson, D., and Forney, K. A.: Habitat compression and ecosystem shifts as potential links between marine heatwave and record whale entanglements, Nat Commun, 11, 536, https://doi.org/10.1038/s41467-019-14215-w, 2020.

Santos, R. O., Rehage, J. S., Boucek, R., and Osborne, J.: Shift in recreational fishing catches as a function of an extreme cold event, Ecosphere, 7, e01335, https://doi.org/10.1002/ecs2.1335, 2016.

Santoso, A., Mcphaden, M. J., and Cai, W.: The Defining Characteristics of ENSO Extremes and the Strong 2015/2016 El Niño, Reviews of Geophysics, 55, 1079–1129, https://doi.org/10.1002/2017RG000560, 2017.

Saurral, R. I., García-Serrano, J., Doblas-Reyes, F. J., Díaz, L. B., and Vera, C. S.: Decadal predictability and prediction skill of sea surface temperatures in the South Pacific region, Clim Dyn, 54, 3945–3958, https://doi.org/10.1007/s00382-020-05208-3, 2020.

Sauter, T.: Revisiting extreme precipitation amounts over southern South America and implications for the Patagonian Icefields, Hydrol. Earth Syst. Sci., 24, 2003–2016, https://doi.org/10.5194/hess-24-2003-2020, 2020.

Scannell, H. A., Pershing, A. J., Alexander, M. A., Thomas, A. C., and Mills, K. E.: Frequency of marine heatwaves in the North Atlantic and North Pacific since 1950, Geophysical Research Letters, 43, 2069–2076, https://doi.org/10.1002/2015gl067308, 2016.

Scannell, H. A., Johnson, G. C., Thompson, L., Lyman, J. M., and Riser, S. C.: Subsurface Evolution and Persistence of Marine Heatwaves in the Northeast Pacific, Geophysical Research Letters, 47, https://doi.org/10.1029/2020gl090548, 2020.

Schär, C., Vidale, P. L., Lüthi, D., Frei, C., Häberli, C., Liniger, M. A., and Appenzeller, C.: The role of increasing temperature variability in European summer heatwaves, Nature, 427, 332–336, https://doi.org/10.1038/nature02300, 2004.

Schlegel, R. W. and Smit, A. J.: heatwaveR: A central algorithm for the detection of heatwaves and cold-spells, JOSS, 3, 821, https://doi.org/10.21105/joss.00821, 2018.

Schlegel, R. W., Oliver, E. C. J., Hobday, A. J., and Smit, A. J.: Detecting Marine Heatwaves With Sub-Optimal Data, Front. Mar. Sci., 6, https://doi.org/10.3389/fmars.2019.00737, 2019.

Schlegel, R. W., Darmaraki, S., Benthuysen, J. A., Filbee-Dexter, K., and Oliver, E. C. J.: Marine cold-spells, Progress in Oceanography, 198, 102684, https://doi.org/10.1016/j.pocean.2021.102684, 2021.

Schloss, I. R., Pizarro, G., Cadaillon, A. M., Giesecke, R., Hernando, M. P., Almandoz, G. O., Latorre, M. P., Malits, A., Flores-Melo, X., Saravia, L. A., Martín, J., Guzmán, L., Iachetti, C. M., and Ruiz, C.: Alexandrium catenella dynamics and paralytic shellfish toxins distribution along the Beagle Channel (southern Patagonia), Journal of Marine Systems, 239, 103856, https://doi.org/10.1016/j.jmarsys.2022.103856, 2023.

Schneider, W., Pérez-Santos, I., Ross, L., Bravo, L., Seguel, R., and Hernández, F.: On the hydrography of Puyuhuapi Channel, Chilean Patagonia, Progress in Oceanography, 129, 8–18, https://doi.org/10.1016/j.pocean.2014.03.007, 2014.

Schneider, W., Donoso, D., Garcés-Vargas, J., and Escribano, R.: Water-column cooling and sea surface salinity increase in the upwelling region off central-south Chile driven by a poleward displacement of the South Pacific High, Progress in Oceanography, 151, 38–48, https://doi.org/10.1016/j.pocean.2016.11.004, 2017.

Seguel, M. and Pavés, H. J.: Sighting patterns and habitat use of marine mammals at Guafo Island, Northern Chilean Patagonia during eleven austral summers, Rev. biol. mar. oceanogr., 53, 237–250, https://doi.org/10.22370/rbmo.2018.53.2.1296, 2018.

Sellanes, J., Quiroga, E., and Neira, C.: Megafauna community structure and trophic relationships at the recently discovered Concepción Methane Seep Area, Chile, ~36°S, ICES Journal of Marine Science, 65, 1102–1111, https://doi.org/10.1093/icesjms/fsn099, 2008.

Sen Gupta, A., Thomsen, M., Benthuysen, J. A., Hobday, A. J., Oliver, E., Alexander, L. V., Burrows, M. T., Donat, M. G., Feng, M., Holbrook, N. J., Perkins-Kirkpatrick, S., Moore, P. J., Rodrigues, R. R., Scannell, H. A., Taschetto, A. S., Ummenhofer, C. C., Wernberg, T., and Smale, D. A.: Drivers and impacts of the most extreme marine heatwave events, Sci Rep, 10, 19359, https://doi.org/10.1038/s41598-020-75445-3, 2020.

SERNAPESCA: Balance de la Situación Sanitaria de la Anemia Infecciosa dem Salmón en Chile de Julio del 2007 a Julio del 2008, 2008.

SERNAPESCA: Sistema de Alerta Temprana de Sernapesca: Mortalidad masiva por FAN afecta centro en la Isla de Chiloé, 2019.

SERNAPESCA: Sernapesca realiza seguimiento diario de las acciones que la empresa Aquachile S.A. ha implementado ante evento de Mortalidad de peces en centro ubicado en el canal Puyuhuapi, 2020.

SERNAPESCA: Sernapesca actualiza información de mortalidad por FAN en Los Lagos, 2021a.

SERNAPESCA: Sernapesca informa activación de planes de contingencia por mortalidad masiva en la región de Aysén, 2021b.

SERNAPESCA: Sernapesca mantuvo monitoreo durante el fin de semana y no se presentaron nuevos eventos de mortalidad masiva, 2021c.

SERNAPESCA: Sernapesca: Se ha retirado un 95% de mortalidad por contingencia FAN, 2021d.

SERNAPESCA: Aysén: Sernapesca actualiza estado de la contingencia de mortalidad masiva por FAN, 2022a.

SERNAPESCA: Concluye retiro y disposición final de mortalidad de salmones afectados por floraciones algales nocivas en Aysén, 2022b.

SERNAPESCA: SERNAPESCA fiscaliza contingencia de mortalidad de salmónidos en un centro de Los Lagos, 2022c.

Serrano, O., Arias-Ortiz, A., Duarte, C. M., Kendrick, G. A., and Lavery, P. S.: Impact of Marine Heatwaves on Seagrass Ecosystems, in: Ecosystem Collapse and Climate Change, vol. 241, edited by: Canadell, J. G. and Jackson, R. B., Springer International Publishing, Cham, 345–364, https://doi.org/10.1007/978-3-030-71330-0_13, 2021.

Seto, D. S., Karp-Boss, L., and Wells, M. L.: Effects of increasing temperature and acidification on the growth and competitive success of Alexandrium catenella from the Gulf of Maine, Harmful Algae, 89, 101670, https://doi.org/10.1016/j.hal.2019.101670, 2019.

Shanks, A. L., Rasmuson, L. K., Valley, J. R., Jarvis, M. A., Salant, C., Sutherland, D. A., Lamont, E. I., Hainey, M. A. H., and Emlet, R. B.: Marine heat waves, climate change, and failed spawning by coastal invertebrates, Limnology & Oceanography, 65, 627–636, https://doi.org/10.1002/lno.11331, 2020.

Shen, J., Li, L., Zhu, D., Liao, E., and Guo, X.: Observation of abnormal coastal cold-water outbreak in the Taiwan Strait and the cold event at Penghu waters in the beginning of 2008, Journal of Marine Systems, 204, 103293, https://doi.org/10.1016/j.jmarsys.2019.103293, 2020.

Shi, H., García-Reyes, M., Jacox, M. G., Rykaczewski, R. R., Black, B. A., Bograd, S. J., and Sydeman, W. J.: Co-occurrence of California Drought and Northeast Pacific Marine Heatwaves Under Climate Change, Geophysical Research Letters, 48, https://doi.org/10.1029/2021gl092765, 2021.

Shi, J., Chen, Z., Ding, S., and Lu, Y.: A Hot Blob Eastward of New Zealand in December 2019, Atmosphere, 11, 1267, https://doi.org/10.3390/atmos11121267, 2020.

Short, J., Foster, T., Falter, J., Kendrick, G. A., and McCulloch, M. T.: Crustose coralline algal growth, calcification and mortality following a marine heatwave in Western Australia, Continental Shelf Research, 106, 38–44, https://doi.org/10.1016/j.csr.2015.07.003, 2015.

Shunk, N. P., Mazzini, P. L. F., and Walter, R. K.: Impacts of Marine Heatwaves on Subsurface Temperatures and Dissolved Oxygen in the Chesapeake Bay, JGR Oceans, 129, e2023JC020338, https://doi.org/10.1029/2023JC020338, 2024.

Sievers, H.: Temperature and salinity in the austral Chilean channels and fjords, in: Progress in the oceanographic knowledge of Chilean inner waters, from Puerto Montt to Cape Horn, 31–35, 2008.

Sievers, H. and Silva, N.: Water masses and circulation in austral Chilean channels, in: Progress in the oceanographic knowledge of Chilean inner waters, from Puerto Montt to Cape Horn, 53–58, 2008.

Silva, C., Yáñez, E., Barbieri, M. A., Bernal, C., and Aranis, A.: Forecasts of swordfish (Xiphias gladius) and common sardine (Strangomera bentincki) off Chile under the A2 IPCC climate change scenario, Progress in Oceanography, 134, 343–355, https://doi.org/10.1016/j.pocean.2015.03.004, 2015.

Silva, C., Andrade, I., Yáñez, E., Hormazabal, S., Barbieri, M. Á., Aranis, A., and Böhm, G.: Predicting habitat suitability and geographic distribution of anchovy (Engraulis ringens) due to climate change in the coastal areas off Chile, Progress in Oceanography, 146, 159–174, https://doi.org/10.1016/j.pocean.2016.06.006, 2016.

Silva, N.: Dissolved oxygen, pH, and nutrients in the austral Chilean channels and fjords, in: Progress in the oceanographic knowledge of Chilean inner waters, from Puerto Montt to Cape Horn, 37–43, 2008.

Silva, N. and Vargas, C. A.: Hypoxia in Chilean Patagonian Fjords, Progress in Oceanography, 129, 62–74, https://doi.org/10.1016/j.pocean.2014.05.016, 2014.

Silva, N., Calvete, C., and Sievers, H.: Masas de agua y circulación general para algunos canales australes entre Puerto Montt y Laguna San Rafael, Ciencia y Tecnologia del Mar, 21, 17–48, 1998.

Silva, N., Rojas, N., and Fedele, A.: Water masses in the Humboldt Current System: Properties, distribution, and the nitrate deficit as a chemical water mass tracer for Equatorial Subsurface Water off Chile, Deep Sea Research Part II: Topical Studies in Oceanography, 56, 1004–1020, https://doi.org/10.1016/j.dsr2.2008.12.013, 2009.

Sims, D. W., Wearmouth, V. J., Genner, M. J., Southward, A. J., and Hawkins, S. J.: Low-temperature-driven early spawning migration of a temperate marine fish, Journal of Animal Ecology, 73, 333–341, https://doi.org/10.1111/j.0021-8790.2004.00810.x, 2004.

Skogseth, R., Olivier, L. L. A., Nilsen, F., Falck, E., Fraser, N., Tverberg, V., Ledang, A. B., Vader, A., Jonassen, M. O., Søreide, J., Cottier, F., Berge, J., Ivanov, B. V., and Falk-Petersen, S.: Variability and decadal trends in the Isfjorden (Svalbard) ocean climate and circulation – An indicator for climate change in the European Arctic, Progress in Oceanography, 187, 102394, https://doi.org/10.1016/j.pocean.2020.102394, 2020.

Smale, D. A. and Wernberg, T.: Extreme climatic event drives range contraction of a habitat-forming species, Proc. R. Soc. B., 280, 20122829, https://doi.org/10.1098/rspb.2012.2829, 2013.

Smale, D. A., Wernberg, T., Oliver, E. C. J., Thomsen, M., Harvey, B. P., Straub, S. C., Burrows, M. T., Alexander, L. V., Benthuysen, J. A., Donat, M. G., Feng, M., Hobday, A. J., Holbrook, N. J., Perkins-Kirkpatrick, S. E., Scannell, H. A., Sen Gupta, A., Payne, B. L., and Moore, P. J.: Marine heatwaves threaten global biodiversity and the provision of ecosystem services, Nat. Clim. Chang., 9, 306–312, https://doi.org/10.1038/s41558-019-0412-1, 2019.

Smith, J. G., Free, C. M., Lopazanski, C., Brun, J., Anderson, C. R., Carr, M. H., Claudet, J., Dugan, J. E., Eurich, J. G., Francis, T. B., Hamilton, S. L., Mouillot, D., Raimondi, P. T., Starr, R. M., Ziegler, S. L., Nickols, K. J., and Caselle, J. E.: A marine protected area network does not confer community structure resilience to a marine heatwave across coastal ecosystems, Global Change Biology, 29, 5634–5651, https://doi.org/10.1111/gcb.16862, 2023a.

Smith, K. E., Burrows, M. T., Hobday, A. J., Sen Gupta, A., Moore, P. J., Thomsen, M., Wernberg, T., and Smale, D. A.: Socioeconomic impacts of marine heatwaves: Global issues and opportunities, Science, 374, eabj3593, https://doi.org/10.1126/science.abj3593, 2021.

Smith, K. E., Burrows, M. T., Hobday, A. J., King, N. G., Moore, P. J., Sen Gupta, A., Thomsen, M. S., Wernberg, T., and Smale, D. A.: Biological Impacts of Marine Heatwaves, Annu. Rev. Mar. Sci., 15, 119–145, https://doi.org/10.1146/annurev-marine-032122-121437, 2023b.

Smith, K. E., Aubin, M., Burrows, M. T., Filbee-Dexter, K., Hobday, A. J., Holbrook, N. J., King, N. G., Moore, P. J., Sen Gupta, A., Thomsen, M., Wernberg, T., Wilson, E., and Smale, D. A.: Global impacts of marine heatwaves on coastal foundation species, Nat Commun, 15, 5052, https://doi.org/10.1038/s41467-024-49307-9, 2024.

Smith, K. E., Sen Gupta, A., Amaya, D., Benthuysen, J. A., Burrows, M. T., Capotondi, A., Filbee-Dexter, K., Frölicher, T. L., Hobday, A. J., Holbrook, N. J., Malan, N., Moore, P. J., Oliver, E. C. J., Richaud, B., Salcedo-Castro, J., Smale, D. A., Thomsen, M., and Wernberg, T.: Baseline matters: Challenges and implications of different marine heatwave baselines, Progress in Oceanography, 231, 103404, https://doi.org/10.1016/j.pocean.2024.103404, 2025.

Soares, M. O., Rabelo, E. F., and Gurgel, A. L.: Marine heatwaves lead to bleaching and mass mortality in a key zoantharian, Mar. Biodivers., 53, 11, https://doi.org/10.1007/s12526-022-01319-8, 2023.

Sobarzo, M., Bravo, L., Donoso, D., Garcés-Vargas, J., and Schneider, W.: Coastal upwelling and seasonal cycles that influence the water column over the continental shelf off central Chile, Progress in Oceanography, 75, 363–382, https://doi.org/10.1016/j.pocean.2007.08.022, 2007.

Soga, M. and Gaston, K. J.: Shifting baseline syndrome: causes, consequences, and implications, Frontiers in Ecol & Environ, 16, 222–230, https://doi.org/10.1002/fee.1794, 2018.

Solas, M., Correa, R. A., Barría, F., Garcés, C., Camus, C., and Faugeron, S.: Assessment of local adaptation and outbreeding risks in contrasting thermal environments of the giant kelp, Macrocystis pyrifera, J Appl Phycol, 36, 471–483, https://doi.org/10.1007/s10811-023-03119-4, 2024.

Sorte, C. J. B., Williams, S. L., and Carlton, J. T.: Marine range shifts and species introductions: comparative spread rates and community impacts, Global Ecology and Biogeography, 19, 303–316, https://doi.org/10.1111/j.1466-8238.2009.00519.x, 2010.

Soto, D., León-Muñoz, J., Dresdner, J., Luengo, C., Tapia, F. J., and Garreaud, R.: Salmon farming vulnerability to climate change in southern Chile: understanding the biophysical, socioeconomic and governance links, Reviews in Aquaculture, 11, 354–374, https://doi.org/10.1111/raq.12336, 2019.

Soto, D., Chávez, C., León-Muñoz, J., Luengo, C., and Soria-Galvarro, Y.: Chilean salmon farming vulnerability to external stressors: The COVID 19 as a case to test and build resilience, Marine Policy, 128, https://doi.org/10.1016/j.marpol.2021.104486, 2021.

Soto-Mardones, L., Letelier, J., Salinas, S., Pinillas, E., and Belmar, J. P.: Analisis de Parametros oceanograficos y atmosfericos del seno de Reloncavi, Gayana (Concepc.), 73, https://doi.org/10.4067/S0717-65382009000100017, 2009.

Soto-Riquelme, C., Pinilla, E., and Ross, L.: Wind influence on residual circulation in Patagonian channels and fjords, Continental Shelf Research, 254, 104905, https://doi.org/10.1016/j.csr.2022.104905, 2023.

Souto Cavalli, L., Tapia-Jopia, C., Ochs, C., López Gómez, M. A., and Neis, B.: Salmon mass mortality events and occupational health and safety in Chilean aquaculture, All Life, 16, 2207772, https://doi.org/10.1080/26895293.2023.2207772, 2023.

Spillman, C. M. and Smith, G. A.: A New Operational Seasonal Thermal Stress Prediction Tool for Coral Reefs Around Australia, Front. Mar. Sci., 8, https://doi.org/10.3389/fmars.2021.687833, 2021.

Spyksma, A. J. P., Miller, K. I., and Shears, N. T.: Marine heatwave promotes population expansion of the invasive ascidian Symplegma brakenhielmi, Biol Invasions, 26, 1987–1995, https://doi.org/10.1007/s10530-024-03296-4, 2024.

Steneck, R. S. and Johnson, C.: Kelp forests: Dynamic patterns, processes, and feedbacks, Marine Community Ecology and Conservation, 315–336, 2013.

Stowhas Salinas, P., Carlton, J., Thiel, M., Santibañez, J., Sáez, R., Puga, A., Munizaga, M., and Brante, A.: Marine bioinvasions in Chile: A national research and conservation management agenda, MBI, 14, 595–618, https://doi.org/10.3391/mbi.2023.14.4.02, 2023.

Stramma, L., Peterson, R. G., and Tomczak, M.: The South Pacific Current, J. Phys. Oceanogr., 25, 77–91, https://doi.org/10.1175/1520-0485(1995)025<0077:TSPC>2.0.CO;2, 1995.

Straub, S. C., Wernberg, T., Thomsen, M. S., Moore, P. J., Burrows, M. T., Harvey, B. P., and Smale, D. A.: Resistance, Extinction, and Everything in Between – The Diverse Responses of Seaweeds to Marine Heatwaves, Front. Mar. Sci., 6, 763, https://doi.org/10.3389/fmars.2019.00763, 2019.

Strub, P. T., James, C., Montecino, V., Rutllant, J. A., and Blanco, J. L.: Ocean circulation along the southern Chile transition region (38°–46°S): Mean, seasonal and interannual variability, with a focus on 2014–2016, Progress in Oceanography, 172, 159–198, https://doi.org/10.1016/j.pocean.2019.01.004, 2019.

Su, Z., Pilo, G. S., Corney, S., Holbrook, N. J., Mori, M., and Ziegler, P.: Characterizing Marine Heatwaves in the Kerguelen Plateau Region, Front. Mar. Sci., 7, 531297, https://doi.org/10.3389/fmars.2020.531297, 2021a.

Su, Z., Pilo, G. S., Corney, S., Holbrook, N. J., Mori, M., and Ziegler, P.: Characterizing Marine Heatwaves in the Kerguelen Plateau Region, Front. Mar. Sci., 7, 1119, https://doi.org/10.3389/fmars.2020.531297, 2021b.

SUBPESCA: Informe Sectorial de Pesca y Acuicultura, Subsecretaría de Pesca y Acuicultura, 2025.

Subrahmanyam, M. V.: Impact of typhoon on the north-west Pacific sea surface temperature: a case study of Typhoon Kaemi (2006), Nat Hazards, 78, 569–582, https://doi.org/10.1007/s11069-015-1733-7, 2015.

Subsecretaría del Trabajo, Gobierno de Chile and Observatorio Laboral de la Región de Aysén: EQUIPO OBSERVATORIO LABORAL AYSÉN, 2024.

Sully, S., Burkepile, D. E., Donovan, M. K., Hodgson, G., and Van Woesik, R.: A global analysis of coral bleaching over the past two decades, Nat Commun, 10, 1264, https://doi.org/10.1038/s41467-019-09238-2, 2019.

Sun, D., Jing, Z., Li, F., and Wu, L.: Characterizing global marine heatwaves under a spatio-temporal framework, Progress in Oceanography, 211, 102947, https://doi.org/10.1016/j.pocean.2022.102947, 2023a.

Sun, D., Li, F., Jing, Z., Hu, S., and Zhang, B.: Frequent marine heatwaves hidden below the surface of the global ocean, Nat. Geosci., 16, 1099–1104, https://doi.org/10.1038/s41561-023-01325-w, 2023b.

Sun, W., Yang, Y., Wang, Y., Yang, J., Ji, J., and Dong, C.: Characterization and future projection of marine heatwaves under climate change in the South China Sea, Ocean Modelling, 188, 102322, https://doi.org/10.1016/j.ocemod.2024.102322, 2024a.

Sun, W., Wang, Y., Yang, Y., Yang, J., Ji, J., and Dong, C.: Marine Heatwaves/Cold-Spells Associated With Mixed Layer Depth Variation Globally, Geophysical Research Letters, 51, e2024GL112325, https://doi.org/10.1029/2024GL112325, 2024b.

Sundfjord, A., Albretsen, J., Kasajima, Y., Skogseth, R., Kohler, J., Nuth, C., Skarðhamar, J., Cottier, F., Nilsen, F., Asplin, L., Gerland, S., and Torsvik, T.: Effects of glacier runoff and wind on surface layer dynamics and Atlantic Water exchange in Kongsfjorden, Svalbard; a model study, Estuarine, Coastal and Shelf Science, 187, 260–272, https://doi.org/10.1016/j.ecss.2017.01.015, 2017.

Szeligowska, M., Trudnowska, E., Boehnke, R., Dąbrowska, A. M., Wiktor, J. M., Sagan, S., and Błachowiak-Samołyk, K.: Spatial Patterns of Particles and Plankton in the Warming Arctic Fjord (Isfjorden, West Spitsbergen) in Seven Consecutive Mid-Summers (2013–2019), Front. Mar. Sci., 7, 584, https://doi.org/10.3389/fmars.2020.00584, 2020.

Szuwalski, C. S., Aydin, K., Fedewa, E. J., Garber-Yonts, B., and Litzow, M. A.: The collapse of eastern Bering Sea snow crab, Science, 382, 306–310, https://doi.org/10.1126/science.adf6035, 2023.

Takagi, S., Kuroda, H., Hasegawa, N., Watanabe, T., Unuma, T., Taniuchi, Y., Yokota, T., Izumida, D., Nakagawa, T., Kurokawa, T., and Azumaya, T.: Controlling factors of large-scale harmful algal blooms with Karenia selliformis after record-breaking marine heatwaves, Front. Mar. Sci., 9, 939393, https://doi.org/10.3389/fmars.2022.939393, 2022.

Tala, F., Gómez, I., Luna-Jorquera, G., and Thiel, M.: Morphological, physiological and reproductive conditions of rafting bull kelp (Durvillaea antarctica) in northern-central Chile (30°S), Mar Biol, 160, 1339–1351, https://doi.org/10.1007/s00227-013-2186-8, 2013.

Tala, F., Velásquez, M., Mansilla, A., Macaya, E. C., and Thiel, M.: Latitudinal and seasonal effects on short-term acclimation of floating kelp species from the South-East Pacific,

Journal of Experimental Marine Biology and Ecology, 483, 31–41, https://doi.org/10.1016/j.jembe.2016.06.003, 2016.

Tala, F., López, B. A., Velásquez, M., Jeldres, R., Macaya, E. C., Mansilla, A., Ojeda, J., and Thiel, M.: Long-term persistence of the floating bull kelp Durvillaea antarctica from the South-East Pacific: Potential contribution to local and transoceanic connectivity, Marine Environmental Research, 149, 67–79, https://doi.org/10.1016/j.marenvres.2019.05.013, 2019.

Tanaka, K. R. and Van Houtan, K. S.: The recent normalization of historical marine heat extremes, PLOS Clim, 1, e0000007, https://doi.org/10.1371/journal.pclm.0000007, 2022.

Tanaka, K. R., Van Houtan, K. S., Mailander, E., Dias, B. S., Galginaitis, C., O'Sullivan, J., Lowe, C. G., and Jorgensen, S. J.: North Pacific warming shifts the juvenile range of a marine apex predator, Sci Rep, 11, 3373, https://doi.org/10.1038/s41598-021-82424-9, 2021.

Tapella, F. and Lovrich, G. A.: Asentamiento de estadios tempranos de las centollas Lithodes santolla y Paralomis granulosa (Decapoda: Lithodidae) en colectores artificiales pasivos en el Canal Beagle, Argentina, Investig. mar., 34, https://doi.org/10.4067/S0717-71782006000200005, 2006.

Tassone, S. J. and Pace, M. L.: Increased Frequency of Sediment Heatwaves in a Virginia Seagrass Meadow, Estuaries and Coasts, 47, 656–669, https://doi.org/10.1007/s12237-023-01314-7, 2024.

Tecklin, D., Farías, A., Peña, M. P., Gélvez, X., Castilla, J. C., Sepúlveda, M., Viddi, F. A., and Hucke-Gaete, R.: Coastal-Marine Protection in Chilean Patagonia: Historical Progress, Current Situation, and Challenges, in: Conservation in Chilean Patagonia, vol. 19, edited by: Castilla, J. C., Armesto Zamudio, J. J., Martínez-Harms, M. J., and Tecklin, D., Springer International Publishing, Cham, 205–232, https://doi.org/10.1007/978-3-031-39408-9_8, 2023.

Thiel, M., Macaya, E., Acuña, E., Arntz, W., Bastias, H., Brokordt, K., Camus, P., Castilla, J. C., Castro, L., Cortes, M., Dumont, C., Escribano, R., Fernandez, M., Gajardo, J., Gaymer, C., Gomez, I., González, A., González, H., Haye, P., Illanes, J.-E., Iriarte, J., Lancellotti, D., Luna-Jorquera, G., Luxoro, C., Manriquez, P., Marín, V., Muñoz, P., Navarrete, S., Perez, E., Poulin, E., Sellanes, J., Sepulveda, H., Stotz, W., Tala, F., Thomas, A., Vargas, C., Vasquez, J., and Vega, A.: The Humboldt Current System of Northern and Central Chile: Oceanographic Processes, Ecological Interactions And Socioeconomic Feedback, in: Oceanography and Marine Biology, vol. 20074975, edited by: Gibson, R., Atkinson, R., and Gordon, J., CRC Press, 195–344, https://doi.org/10.1201/9781420050943.ch6, 2007.

Thompson, A. R., Ben-Aderet, N. J., Bowlin, N. M., Kacev, D., Swalethorp, R., and Watson, W.: Putting the Pacific marine heatwave into perspective: The response of larval fish off southern California to unprecedented warming in 2014–2016 relative to the previous 65 years, Global Change Biology, 28, 1766–1785, https://doi.org/10.1111/gcb.16010, 2022.

Thompson, D. W. J. and Wallace, J. M.: Annular Modes in the Extratropical Circulation. Part I: Month-to-Month Variability*, J. Climate, 13, 1000–1016, https://doi.org/10.1175/1520-0442(2000)013<1000:AMITEC>2.0.CO;2, 2000.

Thompson-Saud, G., Grech, A., Choukroun, S., Vásquez, S. I., Salas, C., and Ospina-Alvarez, A.: The biophysical dynamics of giant kelp, Macrocystis pyrifera : Seasonal patterns and dispersal mechanisms in the southeast Pacific, Journal of Biogeography, 51, 2198–2210, https://doi.org/10.1111/jbi.14980, 2024.

Thomsen, M. S., Mondardini, L., Alestra, T., Gerrity, S., Tait, L., South, P. M., Lilley, S. A., and Schiel, D. R.: Local Extinction of Bull Kelp (Durvillaea spp.) Due to a Marine Heatwave, Front. Mar. Sci., 6, 84, https://doi.org/10.3389/fmars.2019.00084, 2019.

Tietbohl, M. D., Genevier, L. G. C., Krieger, E. C., Kattan, A., Wang, Y., Gokul, E. A., Rodriguez Bravo, L. M., Palm, L., Mele, G., Hoteit, I., and Johnson, M. D.: Extreme marine heatwave linked to mass fish kill in the Red Sea, Science of The Total Environment, 975, 179073, https://doi.org/10.1016/j.scitotenv.2025.179073, 2025.

Traiger, S. B., Bodkin, J. L., Coletti, H. A., Ballachey, B., Dean, T., Esler, D., Iken, K., Konar, B., Lindeberg, M. R., Monson, D., Robinson, B., Suryan, R. M., and Weitzman, B. P.: Evidence of increased mussel abundance related to the Pacific marine heatwave and sea star wasting, Marine Ecology, 43, https://doi.org/10.1111/maec.12715, 2022.

Trainer, V. L., Moore, S. K., Hallegraeff, G., Kudela, R. M., Clement, A., Mardones, J. I., and Cochlan, W. P.: Pelagic harmful algal blooms and climate change: Lessons from nature's experiments with extremes, Harmful Algae, 91, 101591, https://doi.org/10.1016/j.hal.2019.03.009, 2020.

Troupin, C., Machín, F., Ouberdous, M., Sirjacobs, D., Barth, A., and Beckers, J. -M.: High-resolution climatology of the northeast Atlantic using Data-Interpolating Variational Analysis (Diva), J. Geophys. Res., 115, 2009JC005512, https://doi.org/10.1029/2009JC005512, 2010.

Tunsjø, H. S., Paulsen, S. M., Mikkelsen, H., L'Abée-Lund, T. M., Skjerve, E., and Sørum, H.: Adaptive response to environmental changes in the fish pathogen Moritella viscosa, Research in Microbiology, 158, 244–250, https://doi.org/10.1016/j.resmic.2006.11.014, 2007.

Urban, H.-J.: Upper temperature tolerance of ten bivalve species off Peru and Chile related to El Nino, Mar. Ecol. Prog. Ser., 107, 139–145, https://doi.org/10.3354/meps107139, 1994.

Usandizaga, S., Camus, C., Kappes, J. L., Guillemin, M.-L., and Buschmann, A. H.: Effect of temperature variation in Agarophyton chilensis: contrasting the response of natural and farmed populations, J Appl Phycol, 31, 2709–2717, https://doi.org/10.1007/s10811-019-1757-6, 2019.

Utermöhl, H.: Zur Vervollkommnung der quantitativen Phytoplankton-Methodik: Mit 1 Tabelle und 15 abbildungen im Text und auf 1 Tafel, SIL Communications, 1953-1996, 9, 1–38, https://doi.org/10.1080/05384680.1958.11904091, 1958.

Vadboncoeur, É.: Low Temperatures Typical of Winter Cage-Site Conditions in Atlantic Canada Impact the Growth, Physiology, Health and Welfare of Atlantic Salmon (Salmo salar), Memorial University of Newfoundland and Labrador, 2023.

Valdés-Pineda, R., Cañón, J., and Valdés, J. B.: Multi-decadal 40- to 60-year cycles of precipitation variability in Chile (South America) and their relationship to the AMO and PDO signals, Journal of Hydrology, 556, 1153–1170, https://doi.org/10.1016/j.jhydrol.2017.01.031, 2018.

Valdivia, I. M., Chávez, R. A., and Oliva, M. E.: Metazoan parasites of Engraulis ringens as tools for stock discrimination along the Chilean coast, Journal of Fish Biology, 70, 1504–1511, https://doi.org/10.1111/j.1095-8649.2007.01429.x, 2007.

Valiñas, M. S., Blum, R., Galván, D. E., Varisco, M., and Martinetto, P.: Global Change Effects on Biological Interactions: Nutrient Inputs, Invasive Species, and Multiple Drivers Shape Marine Patagonian Communities, in: Global Change in Atlantic Coastal Patagonian Ecosystems, edited by: Helbling, E. W., Narvarte, M. A., González, R. A., and Villafañe, V. E., Springer International Publishing, Cham, 291–316, https://doi.org/10.1007/978-3-030-86676-1_12, 2022.

Valle-Levinson, A., Sarkar, N., Sanay, R., and Soto, D.: Spatial Structure of Hydrography and Flow in a Chilean Fjord, Estuario Reloncaví, Estuaries and Coasts, 30, 113–126, https://doi.org/10.1007/BF02782972, 2007.

Varas, E. C. and Varas, E. V.: Surface Water Resources, in: World Water Resources, Springer International Publishing, Cham, 61–92, https://doi.org/10.1007/978-3-030-56901-3_4, 2021.

Varela, R., Rodríguez-Díaz, L., De Castro, M., and Gómez-Gesteira, M.: Influence of Eastern Upwelling systems on marine heatwaves occurrence, Global and Planetary Change, 196, 103379, https://doi.org/10.1016/j.gloplacha.2020.103379, 2021.

Vásquez, S. I., De La Torre, M. B., Saldías, G. S., and Montecinos, A.: Meridional Changes in Satellite Chlorophyll and Fluorescence in Optically-Complex Coastal Waters of Northern Patagonia, Remote Sensing, 13, 1026, https://doi.org/10.3390/rs13051026, 2021.

Velásquez, M., Fraser, C. I., Nelson, W. A., Tala, F., and Macaya, E. C.: Concise review of the genus Durvillaea Bory de Saint-Vincent, 1825, J Appl Phycol, 32, 3–21, https://doi.org/10.1007/s10811-019-01875-w, 2020.

Venegas, R. M., Acevedo, J., and Treml, E. A.: Three decades of ocean warming impacts on marine ecosystems: A review and perspective, Deep Sea Research Part II: Topical Studies in Oceanography, 212, 105318, https://doi.org/10.1016/j.dsr2.2023.105318, 2023.

Viale, M. and Garreaud, R.: Orographic effects of the subtropical and extratropical Andes on upwind precipitating clouds, JGR Atmospheres, 120, 4962–4974, https://doi.org/10.1002/2014JD023014, 2015.

Viale, M., Bianchi, E., Cara, L., Ruiz, L. E., Villalba, R., Pitte, P., Masiokas, M., Rivera, J., and Zalazar, L.: Contrasting Climates at Both Sides of the Andes in Argentina and Chile, Front. Environ. Sci., 7, https://doi.org/10.3389/fenvs.2019.00069, 2019.

Viddi, F. A., Hucke-Gaete, R., Torres-Florez, J. P., and Ribeiro, S.: Spatial and seasonal variability in cetacean distribution in the fjords of northern Patagonia, Chile, ICES Journal of Marine Science, 67, 959–970, https://doi.org/10.1093/icesjms/fsp288, 2010.

Vilela, R. A. N., Giulianelli, S., Zabala, S., Bigatti, G., and Márquez, F.: Lethal Consequences and Embryo Shell Shape Alterations in the Marine Gastropod Trophon geversianus Due to Elevated Temperatures, Zoological Studies, 2024.

Villaseñor-Derbez, J. C., Arafeh-Dalmau, N., and Micheli, F.: Past and future impacts of marine heatwaves on small-scale fisheries in Baja California, Mexico, Commun Earth Environ, 5, https://doi.org/10.1038/s43247-024-01696-x, 2024.

Vimeux, F., Maignan, F., Reutenauer, C., and Pouyaud, B.: Evaluation of cloudiness over Monte San Valentín, Northern Patagonia Icefield, from 2000 to 2008 using MODIS satellite images: implications for paleoclimate investigations from ice cores, J. Glaciol., 57, 221–230, https://doi.org/10.3189/002214311796405915, 2011.

Vogt, L., Burger, F. A., Griffies, S. M., and Frölicher, T. L.: Local Drivers of Marine Heatwaves: A Global Analysis With an Earth System Model, Front. Clim., 4, 847995, https://doi.org/10.3389/fclim.2022.847995, 2022.

Wade, N. M., Clark, T. D., Maynard, B. T., Atherton, S., Wilkinson, R. J., Smullen, R. P., and Taylor, R. S.: Effects of an unprecedented summer heatwave on the growth performance, flesh colour and plasma biochemistry of marine cage-farmed Atlantic salmon (Salmo salar), Journal of Thermal Biology, 80, 64–74, https://doi.org/10.1016/j.jtherbio.2018.12.021, 2019.

Walter, R. K., Dalsin, M., Mazzini, P. L. F., and Pianca, C.: Compound marine cold spells and hypoxic events in a nearshore upwelling system, Estuarine, Coastal and Shelf Science, 300, 108706, https://doi.org/10.1016/j.ecss.2024.108706, 2024.

Wang, D., Xu, T., Fang, G., Jiang, S., Wang, G., Wei, Z., and Wang, Y.: Characteristics of Marine Heatwaves in the Japan/East Sea, Remote Sensing, 14, 936, https://doi.org/10.3390/rs14040936, 2022a.

Wang, S., Jing, Z., Sun, D., Shi, J., and Wu, L.: A New Model for Isolating the Marine Heatwave Changes under Warming Scenarios, Journal of Atmospheric and Oceanic Technology, 39, 1353–1366, https://doi.org/10.1175/JTECH-D-21-0142.1, 2022b.

Wang, Y. and Zhou, Y.: Seasonal dynamics of global marine heatwaves over the last four decades, Front. Mar. Sci., 11, 1406416, https://doi.org/10.3389/fmars.2024.1406416, 2024.

Wang, Y., Kajtar, J. B., Alexander, L. V., Pilo, G. S., and Holbrook, N. J.: Understanding the Changing Nature of Marine Cold-Spells, Geophysical Research Letters, 49, e2021GL097002, https://doi.org/10.1029/2021GL097002, 2022c.

Wang, Y., Holbrook, N. J., and Kajtar, J. B.: Predictability of Marine Heatwaves off Western Australia Using a Linear Inverse Model, Journal of Climate, 36, 6177–6193, https://doi.org/10.1175/jcli-d-22-0692.1, 2023.

Warren-Myers, F., Folkedal, O., Vågseth, T., Stien, L. H., Fosse, J. O., Dempster, T., and Oppedal, F.: Efficiency of salmon production in submerged cages with air domes matches standard surface cages when environments are similar, Aquaculture, 586, 740751, https://doi.org/10.1016/j.aquaculture.2024.740751, 2024.

WBG: Climate Risk Country Profile: Chile (2021), World Bank Group, Washington DC, USA, 2021.

Weitzman, B., Konar, B., Iken, K., Coletti, H., Monson, D., Suryan, R., Dean, T., Hondolero, D., and Lindeberg, M.: Changes in Rocky Intertidal Community Structure During a Marine Heatwave in the Northern Gulf of Alaska, Front. Mar. Sci., 8, 556820, https://doi.org/10.3389/fmars.2021.556820, 2021.

Wells, M. L., Trainer, V. L., Smayda, T. J., Karlson, B. S. O., Trick, C. G., Kudela, R. M., Ishikawa, A., Bernard, S., Wulff, A., Anderson, D. M., and Cochlan, W. P.: Harmful algal blooms and climate change: Learning from the past and present to forecast the future, Harmful Algae, 49, 68–93, https://doi.org/10.1016/j.hal.2015.07.009, 2015.

Wells, M. L., Karlson, B., Wulff, A., Kudela, R., Trick, C., Asnaghi, V., Berdalet, E., Cochlan, W., Davidson, K., De Rijcke, M., Dutkiewicz, S., Hallegraeff, G., Flynn, K. J., Legrand, C., Paerl, H., Silke, J., Suikkanen, S., Thompson, P., and Trainer, V. L.: Future HAB science: Directions and challenges in a changing climate, Harmful Algae, 91, 101632, https://doi.org/10.1016/j.hal.2019.101632, 2020.

Wernberg, T. and Filbee-Dexter, K.: Missing the marine forest for the trees, Mar. Ecol. Prog. Ser., 612, 209–215, https://doi.org/10.3354/meps12867, 2019.

Wernberg, T., Smale, D. A., Tuya, F., Thomsen, M. S., Langlois, T. J., De Bettignies, T., Bennett, S., and Rousseaux, C. S.: An extreme climatic event alters marine ecosystem structure in a global biodiversity hotspot, Nature Clim Change, 3, 78–82, https://doi.org/10.1038/nclimate1627, 2013.

Wernberg, T., Bennett, S., Babcock, R. C., De Bettignies, T., Cure, K., Depczynski, M., Dufois, F., Fromont, J., Fulton, C. J., Hovey, R. K., Harvey, E. S., Holmes, T. H., Kendrick, G. A., Radford, B., Santana-Garcon, J., Saunders, B. J., Smale, D. A., Thomsen, M. S., Tuckett, C. A., Tuya, F., Vanderklift, M. A., and Wilson, S.: Climate-driven regime shift of a temperate marine ecosystem, Science, 353, 169–172, https://doi.org/10.1126/science.aad8745, 2016.

Westley, P. A. H.: Documentation of *en route* mortality of summer chum salmon in the Koyukuk River, Alaska and its potential linkage to the heatwave of 2019, Ecology and Evolution, 10, 10296–10304, https://doi.org/10.1002/ece3.6751, 2020.

Whalen, M. A., Starko, S., Lindstrom, S. C., and Martone, P. T.: Heatwave restructures marine intertidal communities across a stress gradient, Ecology, 104, e4027, https://doi.org/10.1002/ecy.4027, 2023.

Wild, S., Krützen, M., Rankin, R. W., Hoppitt, W. J. E., Gerber, L., and Allen, S. J.: Long-term decline in survival and reproduction of dolphins following a marine heatwave, Current Biology, 29, R239–R240, https://doi.org/10.1016/j.cub.2019.02.047, 2019.

Winckler-Grez, P. W., Aguirre, C., Farías, L., Contreras-López, M., and Masotti, Í.: Evidence of climate-driven changes on atmospheric, hydrological, and oceanographic variables along the Chilean coastal zone, Climatic Change, 163, 633–652, https://doi.org/10.1007/s10584-020-02805-3, 2020.

WMO: Guide to Climatological Practices, World Meteorological Organization,., Geneva, Switzerland, 2023.

Wyatt, A. M., Resplandy, L., and Marchetti, A.: Ecosystem impacts of marine heat waves in the northeast Pacific, Biogeosciences, 19, 5689–5705, https://doi.org/10.5194/bg-19-5689-2022, 2022.

Xie, M., Ji, Q., Zheng, Q., Meng, Z., Wang, Y., and Gao, M.: Spatial and Temporal Characteristics and Mechanisms of Marine Heatwaves in the Changjiang River Estuary and Its Surrounding Coastal Regions, JMSE, 12, 653, https://doi.org/10.3390/jmse12040653, 2024.

Xu, Q., Liu, K., Wang, H., and Chen, X.: Vertical structures and drivers of marine heatwaves and cold-spells in the Kuroshio Extension region, Environ. Res. Lett., 19, 054015, https://doi.org/10.1088/1748-9326/ad3b26, 2024.

Yáñez, E., Lagos, N. A., Norambuena, R., Silva, C., Letelier, J., Muck, K., Martin, G. S., Benítez, S., R. Broitman, B., Contreras, H., Duarte, C., Gelcich, S., Labra, F. A., Lardies, M. A., Manríquez, P. H., Quijón, P. A., Ramajo, L., González, E., Molina, R., Gómez, A., Soto, L., Montecino, A., Barbieri, M. Á., Plaza, F., Sánchez, F., Aranis, A., Bernal, C., and Böhm, G.: Impacts of Climate Change on Marine Fisheries and Aquaculture in Chile, in: Climate Change Impacts on Fisheries and Aquaculture, edited by: Phillips, B. F. and Pérez-Ramírez, M., Wiley, 239–332, https://doi.org/10.1002/9781119154051.ch10, 2017a.

Yáñez, E., Lagos, N. A., Norambuena, R., Silva, C., Letelier, J., Muck, K.-P., Martin, G. S., Benítez, S., R. Broitman, B., Contreras, H., Duarte, C., Gelcich, S., Labra, F. A., Lardies, M. A., Manríquez, P. H., Quijón, P. A., Ramajo, L., González, E., Molina, R., Gómez, A., Soto, L., Montecino, A., Barbieri, M. Á., Plaza, F., Sánchez, F., Aranis, A., Bernal, C., and Böhm, G.: Impacts of Climate Change on Marine Fisheries and Aquaculture in Chile, in: Climate Change Impacts on Fisheries and Aquaculture, vol. 1, edited by: Phillips, B. F. and Pérez-Ramírez, M., John Wiley & Sons, Ltd, Chichester, UK, 239–332, https://doi.org/10.1002/9781119154051.ch10, 2017b.

Yang, B., Emerson, S. R., and Peña, M. A.: The effect of the 2013–2016 high temperature anomaly in the subarctic Northeast Pacific (the "Blob") on net community production, Biogeosciences, 15, 6747–6759, https://doi.org/10.5194/bg-15-6747-2018, 2018.

Yao, Y. and Wang, C.: Marine heatwaves and cold-spells in global coral reef zones, Progress in Oceanography, 209, 102920, https://doi.org/10.1016/j.pocean.2022.102920, 2022.

Yao, Y. and Wang, C.: Subsurface Marine Heatwaves in the South China Sea, JGR Oceans, 129, e2024JC021356, https://doi.org/10.1029/2024JC021356, 2024.

Yao, Y., Wang, C., and Fu, Y.: Global Marine Heatwaves and Cold-Spells in Present Climate to Future Projections, Earth's Future, 10, e2022EF002787, https://doi.org/10.1029/2022EF002787, 2022.

Yu, S., Wang, Z., Jiang, Z., Li, T., Ding, X., Wei, X., and Liu, D.: Marine Heatwave and Terrestrial Drought Reduced CO2 Uptake in the East China Sea in 2022, Remote Sensing, 16, 849, https://doi.org/10.3390/rs16050849, 2024.

Zhang, N., Lan, J., and Dong, C.: Subsurface Heatwaves and Cold Spells in the South China Sea Regulated by ENSO: Role of the South China Sea Throughflow, Geophysical Research Letters, 52, e2025GL114692, https://doi.org/10.1029/2025GL114692, 2025.

Zhang, Y., Du, Y., Feng, M., and Hobday, A. J.: Vertical structures of marine heatwaves, Nat Commun, 14, 6483, https://doi.org/10.1038/s41467-023-42219-0, 2023.

Zhao, Z. and Marin, M.: A MATLAB toolbox to detect and analyze marine heatwaves, JOSS, 4, 1124, https://doi.org/10.21105/joss.01124, 2019.

Zhou, X., Xu, K., Ashok, K., Shi, J., Zhang, L., Yu, J.-Y., Liu, B., Tam, C.-Y., Xu, H., and Wang, W.: Compound marine heatwaves and tropical cyclones delay the onset of the Bay of Bengal summer monsoon, npj Clim Atmos Sci, 8, 162, https://doi.org/10.1038/s41612-025-01061-5, 2025.

Zhou, Z., Steiner, N., Fivash, G. S., Cozzoli, F., Blok, D. B., Van IJzerloo, L., Van Dalen, J., Ysebaert, T., Walles, B., and Bouma, T. J.: Temporal dynamics of heatwaves are key drivers of sediment mixing by bioturbators, Limnology & Oceanography, 68, 1105–1116, https://doi.org/10.1002/lno.12332, 2023.

Ziegler, S. L., Johnson, J. M., Brooks, R. O., Johnston, E. M., Mohay, J. L., Ruttenberg, B. I., Starr, R. M., Waltz, G. T., Wendt, D. E., and Hamilton, S. L.: Marine protected areas, marine heatwaves, and the resilience of nearshore fish communities, Sci Rep, 13, 1405, https://doi.org/10.1038/s41598-023-28507-1, 2023.

Zou, Y. and Xi, X.: An ongoing cooling in the eastern Pacific linked to eastward migrations of the Southeast Pacific Subtropical Anticyclone, Environ. Res. Lett., 16, 034020, https://doi.org/10.1088/1748-9326/abd819, 2021.

CHAPTER 11.   ANNEXES

This section presents additional material, while not essential for a general understanding of the work, might be of interest to readers seeking a more detailed description of the in situ-based temperature climatology introduced in <u>Chapter 3</u>.

Annexes contain vertical profile plots of the temperature from the in situ-based climatology, maps of the temperature climatology for the entire Northern Patagonia at every depth computed, and the list and origin of all the in situ data used for the construction of the climatology.

Annexes are available only for the PDF version of this thesis.

1.Profile plots

Here, the vertical structure of Northern Patagonia is illustrated using the in situ-based climatology. A map showing the locations of the different profile plots is first presented, followed by the corresponding profiles.

1:Reloncavi fjord head
2:Reloncavi
3:Reloncavi-Ancud
4:Ancud
5:Comau mouth
6:Canal Chacao Est
7:Canal Chacao West
8:Corcovado
9:Boca del Guafo
10:Corcovado 2
11:Channel South
12:Puyuhuapi
13:Puyuhuapi head
14:Aysen mouth
15:Aysen
16:Aysen head
17:Elefantes
18:Pacific West of Chiloé
19:Pacific
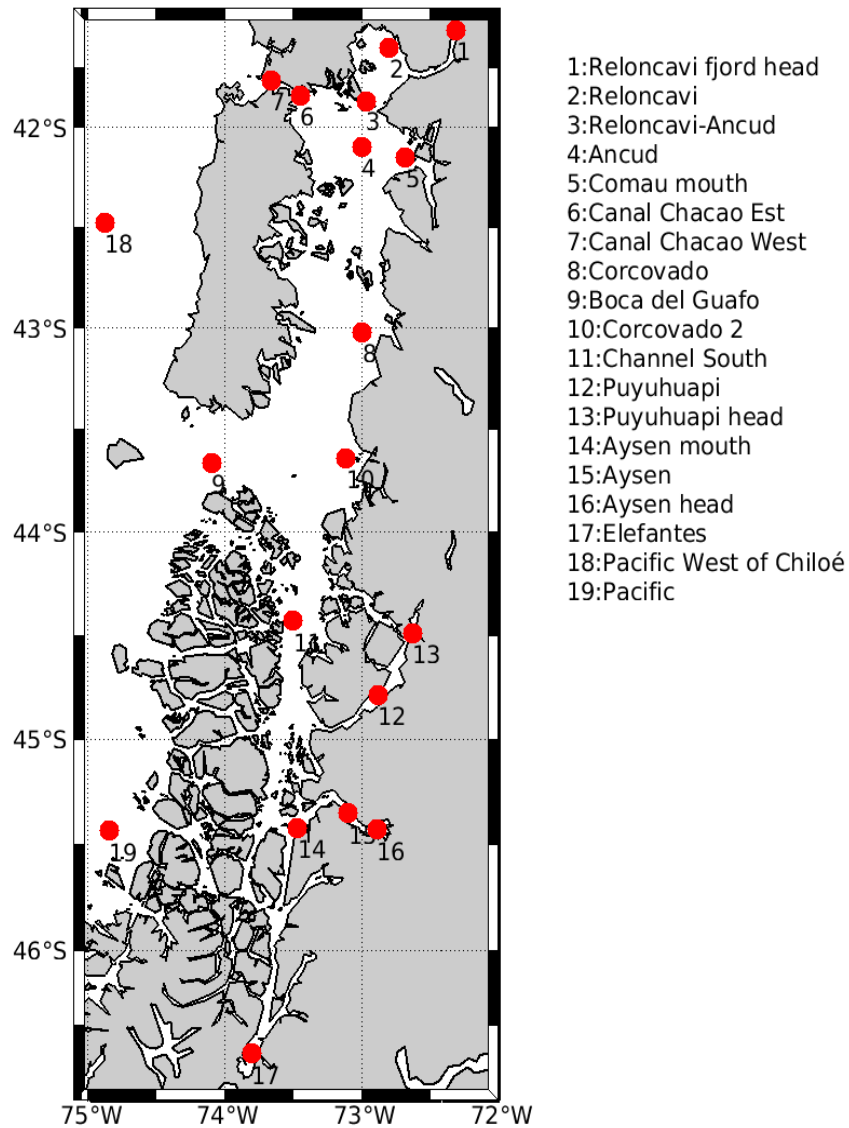
Figure Annexe 1: Location of the different profile plots following this figure.
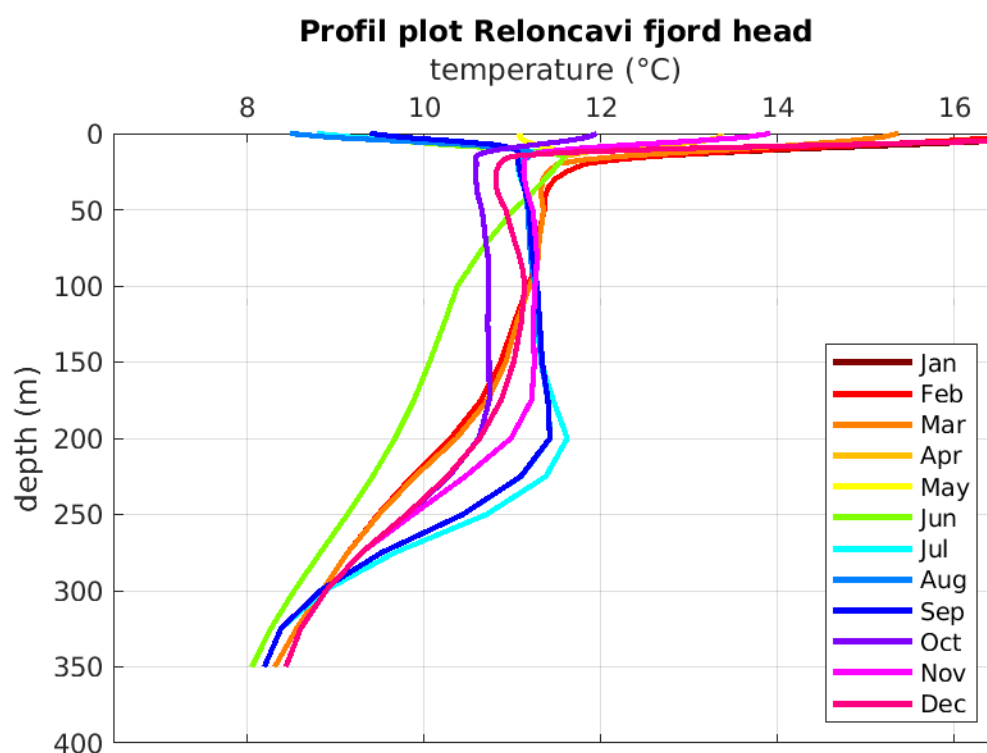
Figure Annexe 2: Profile plots of the monthly temperature from the in situ-based climatology at Reloncaví Fjord's head (point 1 on the map).
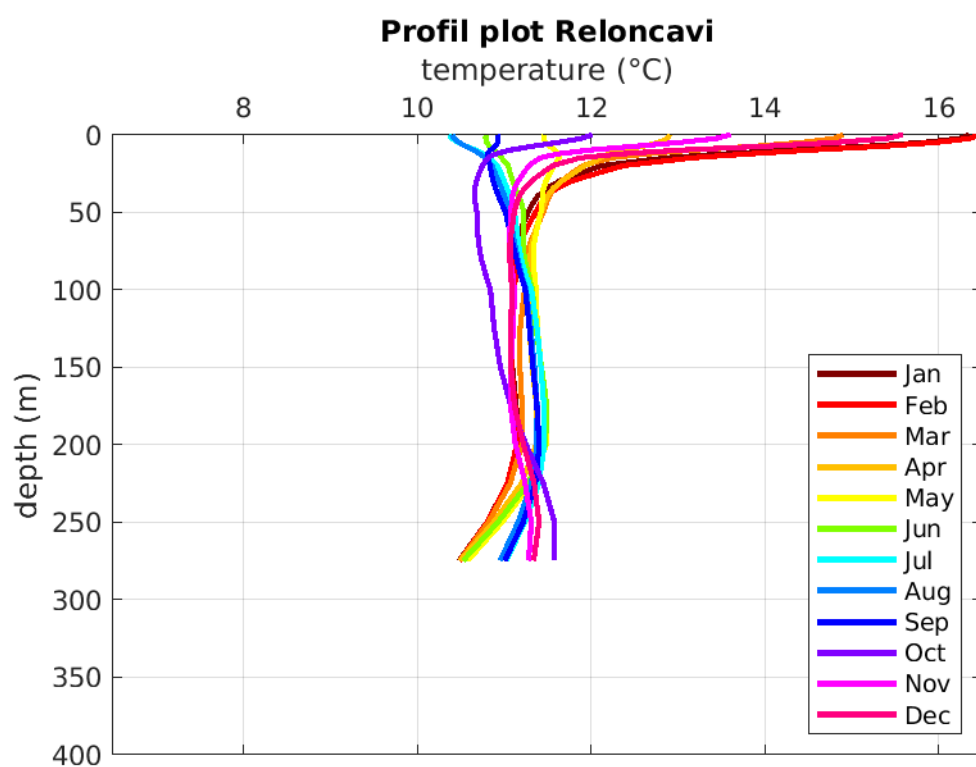
Figure Annexe 3: Profile plots of the monthly temperature from the in situ-based climatology in Reloncaví Sound (point 2 on the map).
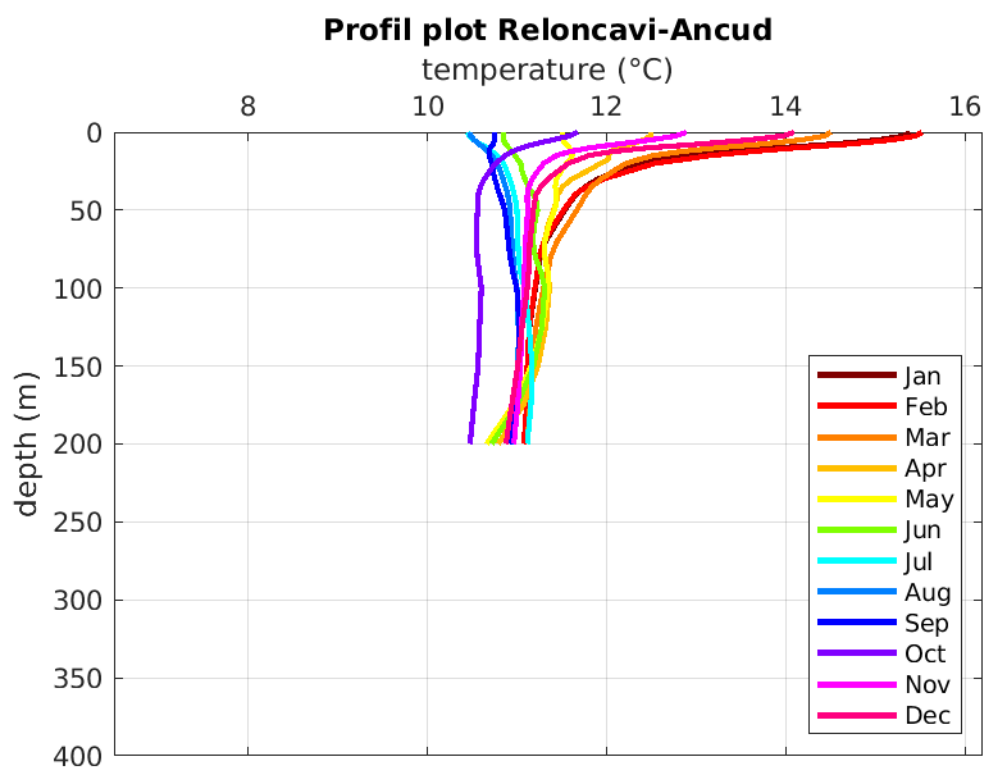
Figure Annexe 5: Profile plots of the monthly temperature from the in situ-based climatology between Reloncaví Sound and Ancud Gulf (point 3 on the map).
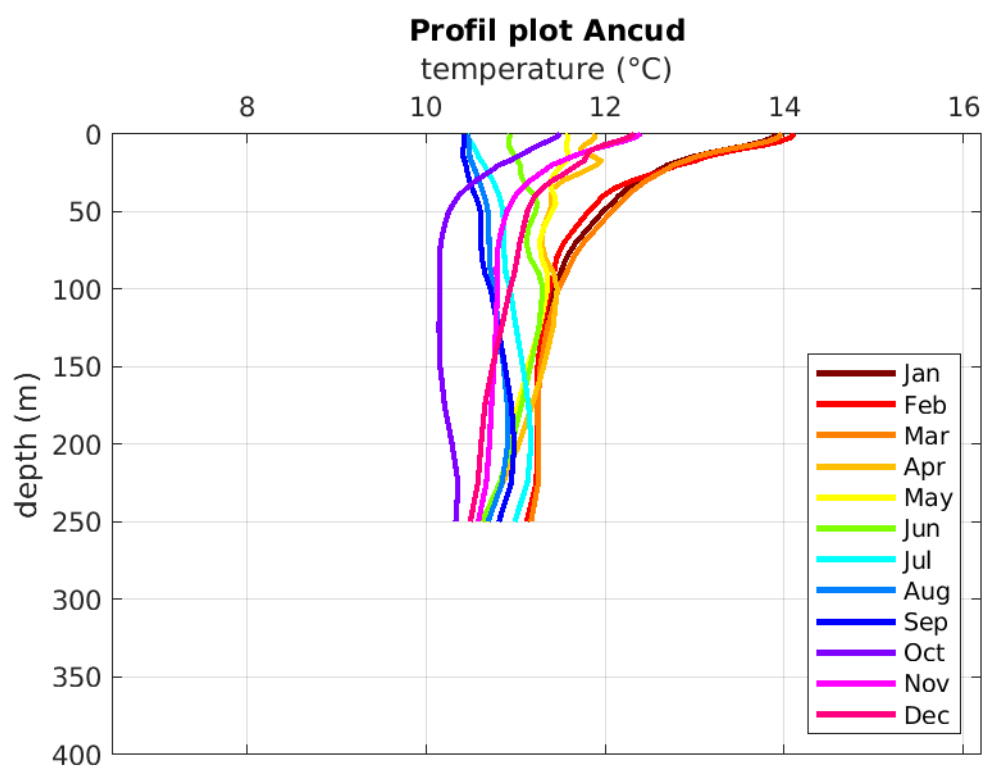
Figure Annexe 4: Profile plots of the monthly temperature from the in situ-based climatology in Ancud Gulf (point 4 on the map).
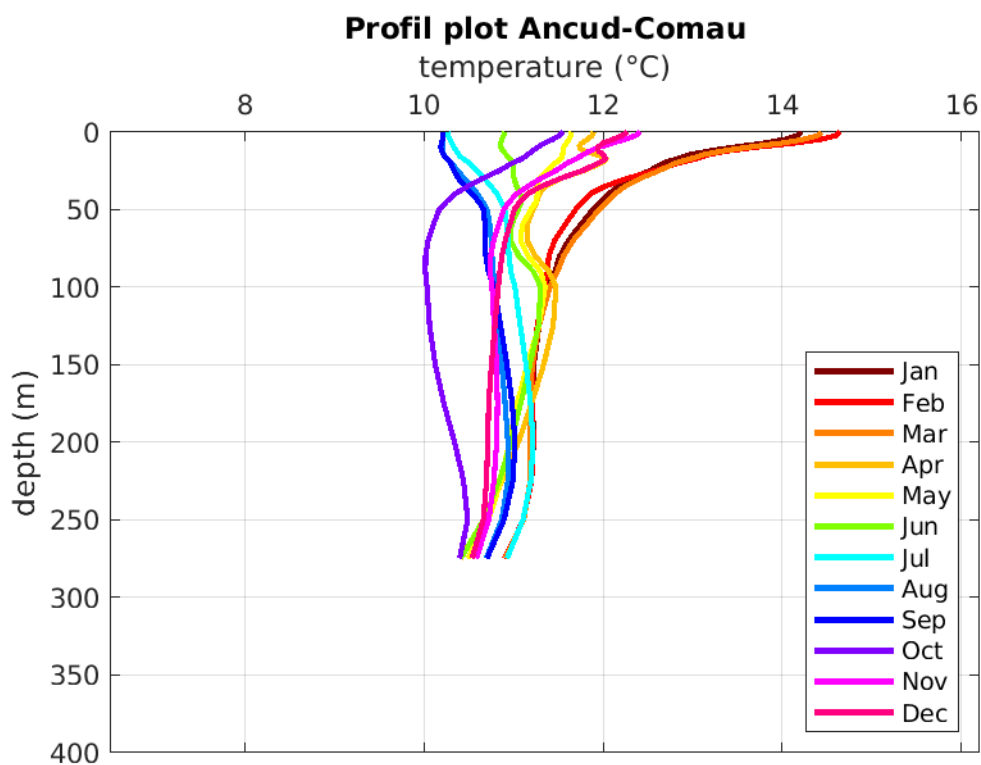
Figure Annexe 6: Profile plots of the monthly temperature from the in situ-based climatology in Comau Fjord's mouth (point 5 on the map).
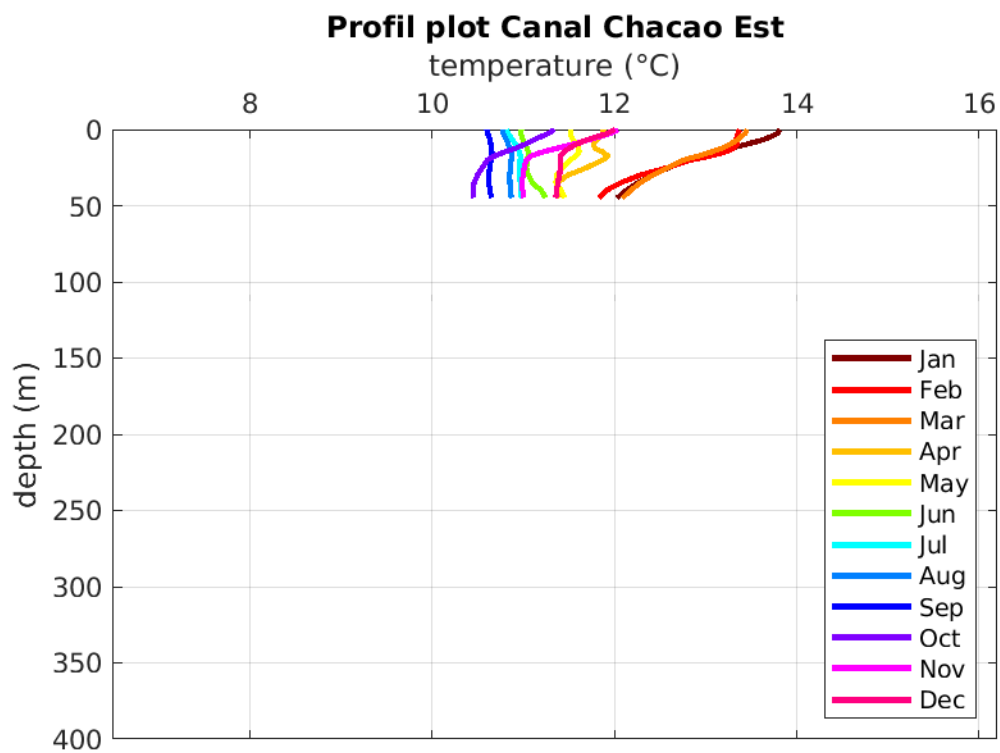
Figure Annexe 7: Profile plots of the monthly temperature from the in situ-based climatology East of Chacao Channel (point 6 on the map).
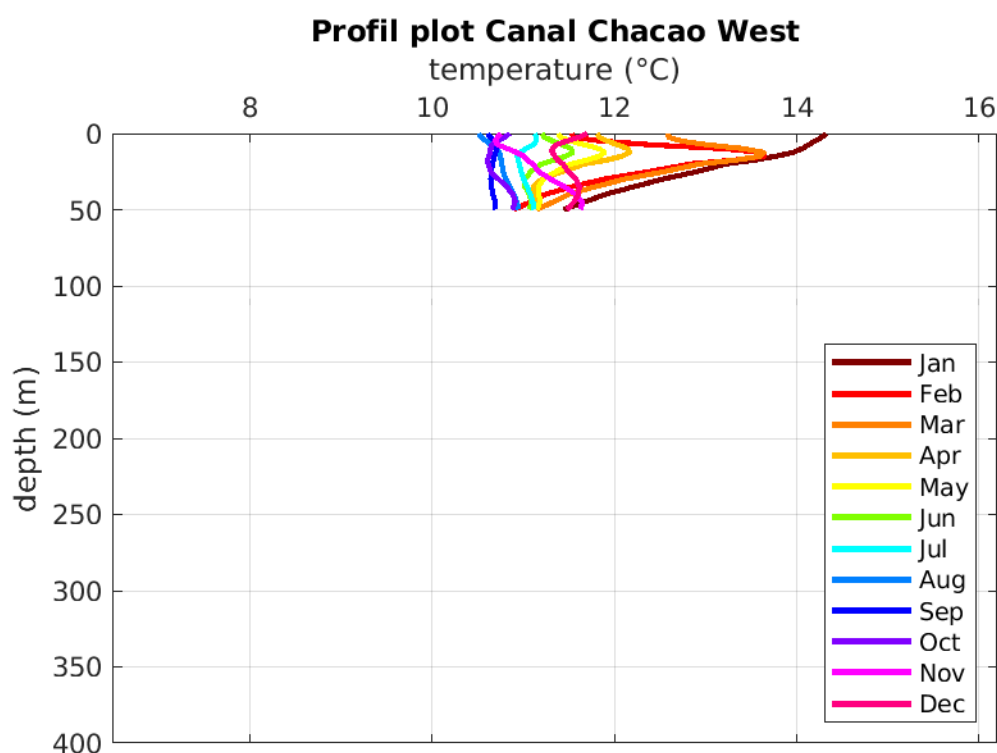
Figure Annexe 8: Profile plots of the monthly temperature from the in situ-based climatology West of Chacao Channel (point 7 on the map).
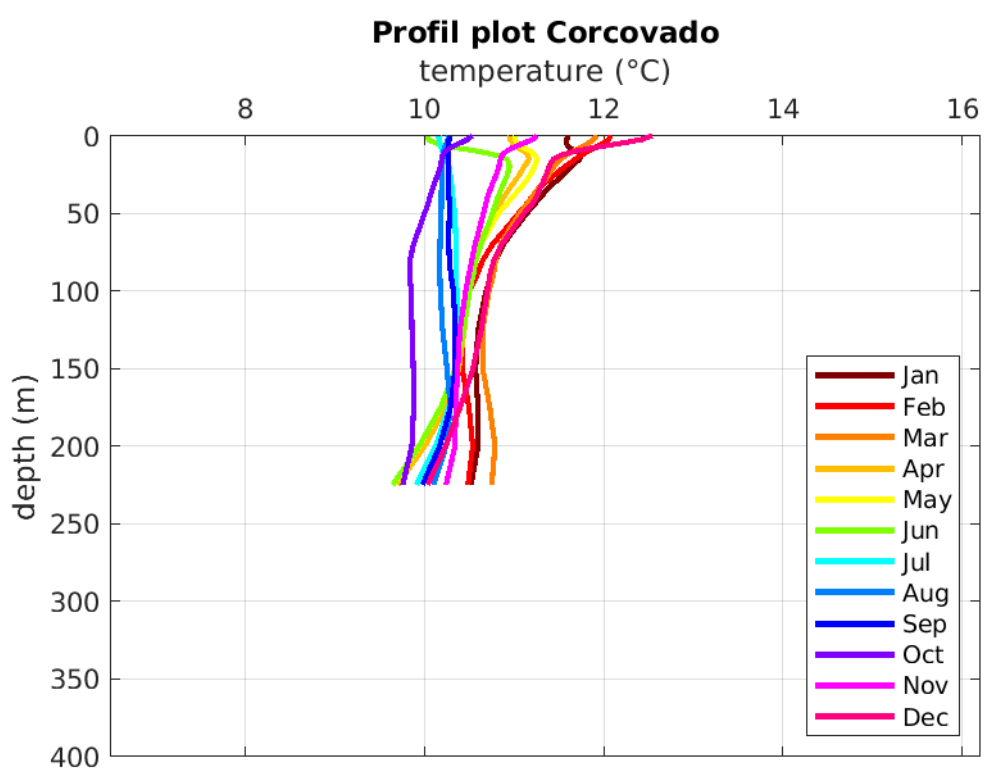
Figure Annexe 9: Profile plots of the monthly temperature from the in situ-based climatology in Corcovado Gulf (point 8 on the map).
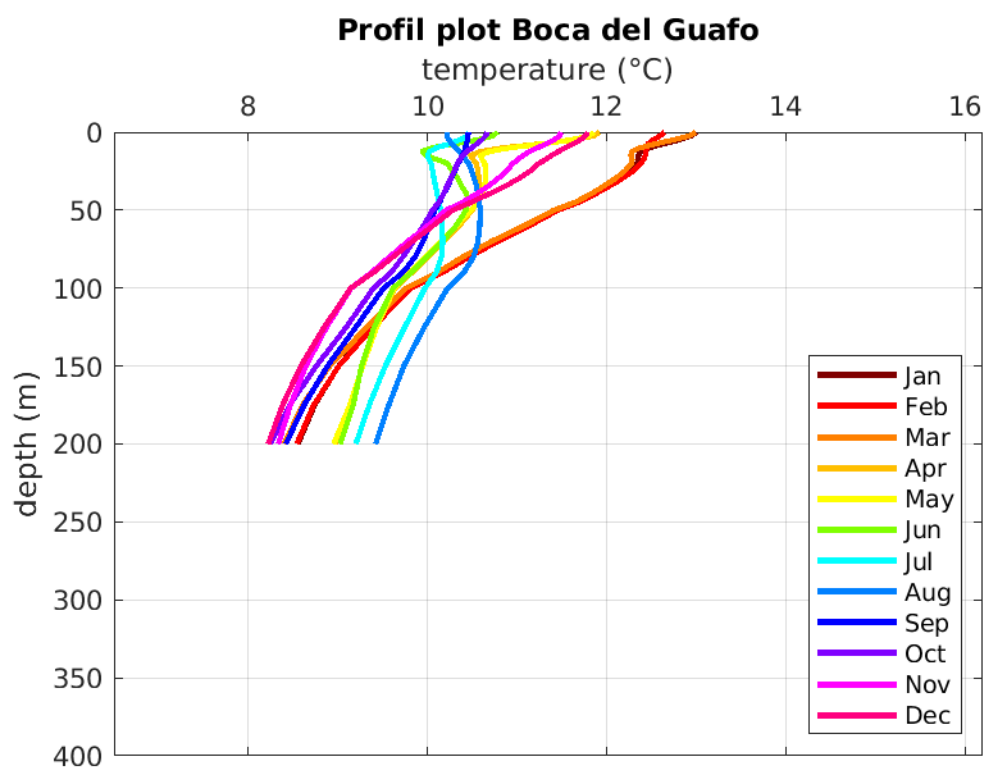
Figure Annexe 11: Profile plots of the monthly temperature from the in situ-based climatology in Guafo Mouth (point 9 on the map).
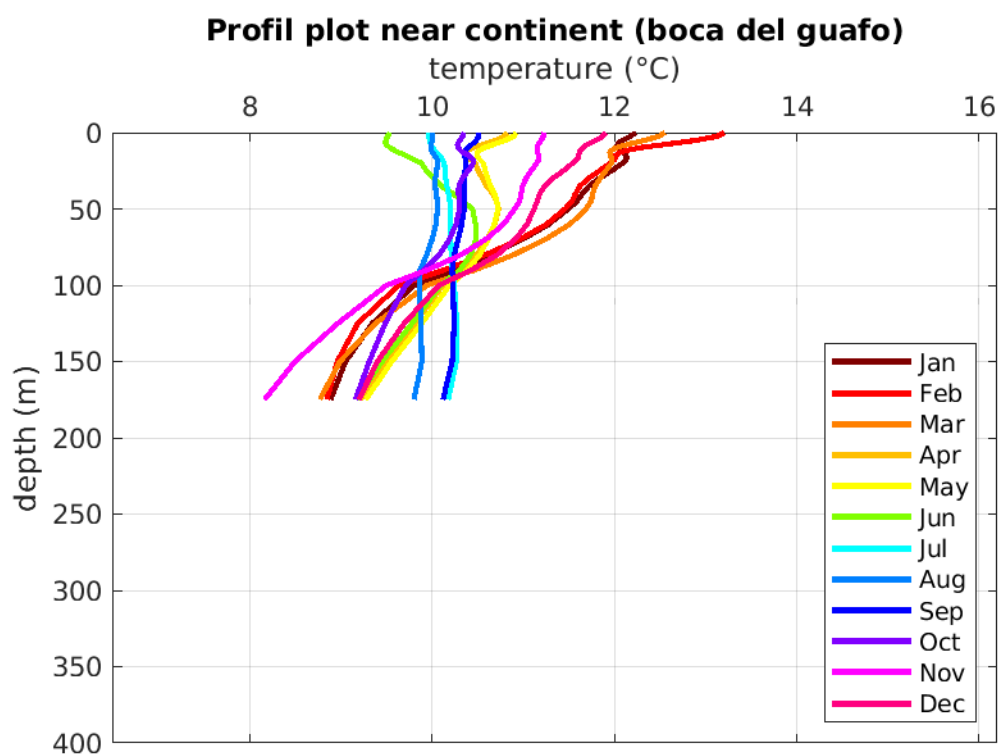
Figure Annexe 10: Profile plots of the monthly temperature from the in situ-based climatology in south Corcovado Gulf (point 10 on the map).
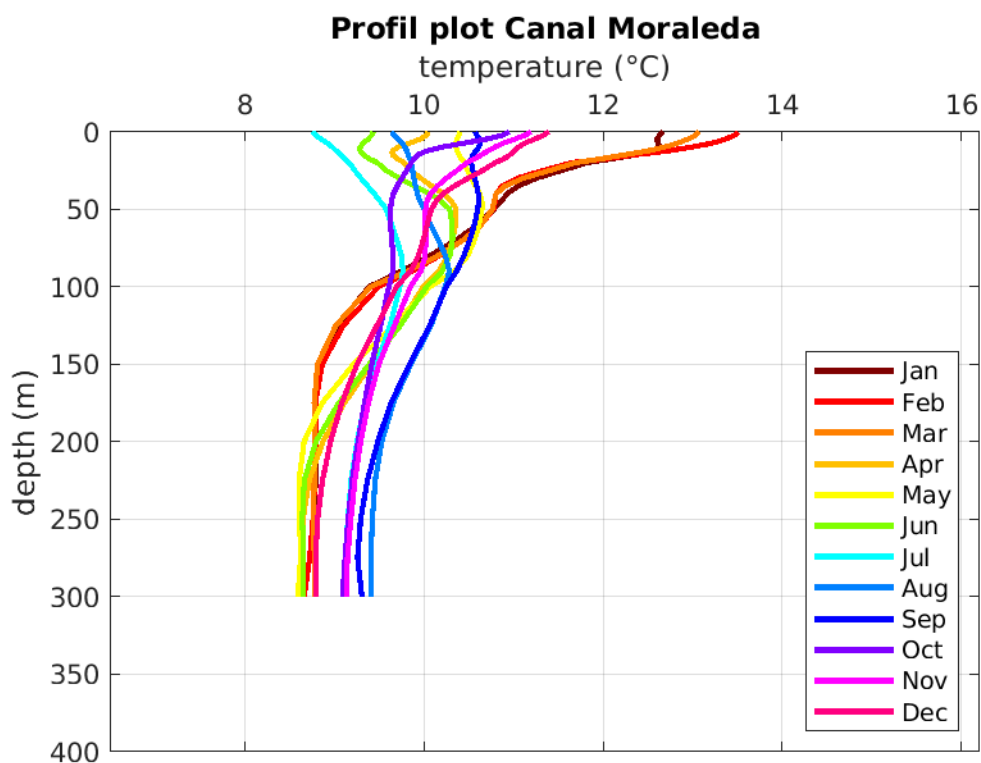
Figure Annexe 13: Profile plots of the monthly temperature from the in situ-based climatology in Moraleda Channel (point 11 on the map).
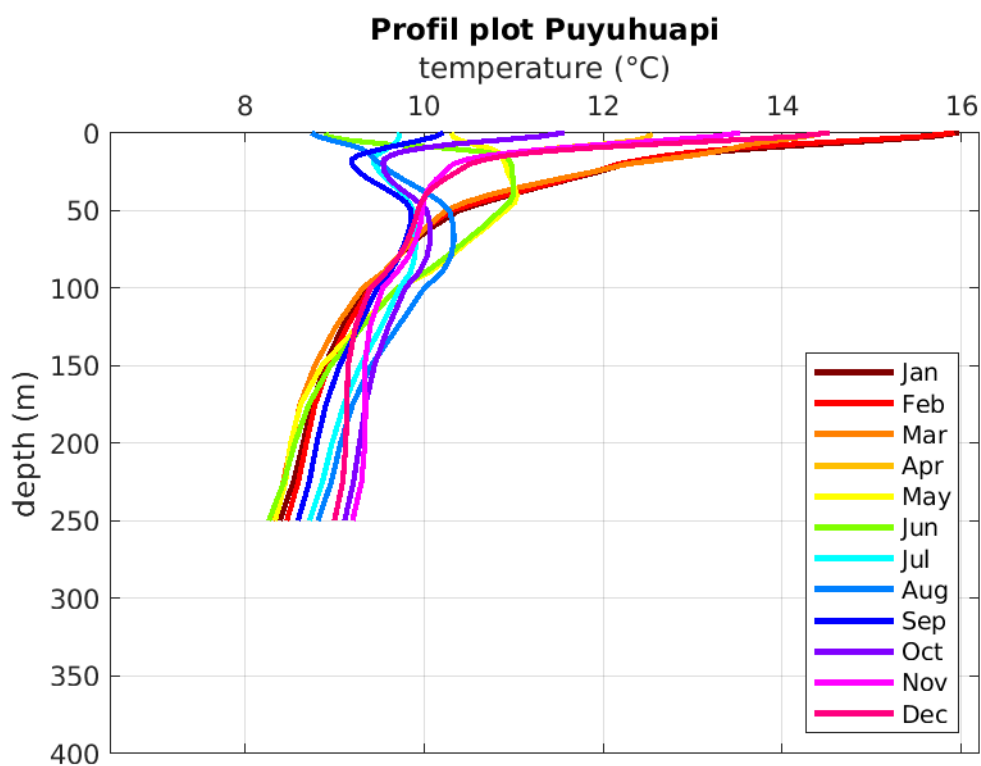
Figure Annexe 12: Profile plots of the monthly temperature from the in situ-based climatology in Puyuhuapi Fjord (point 12 on the map).
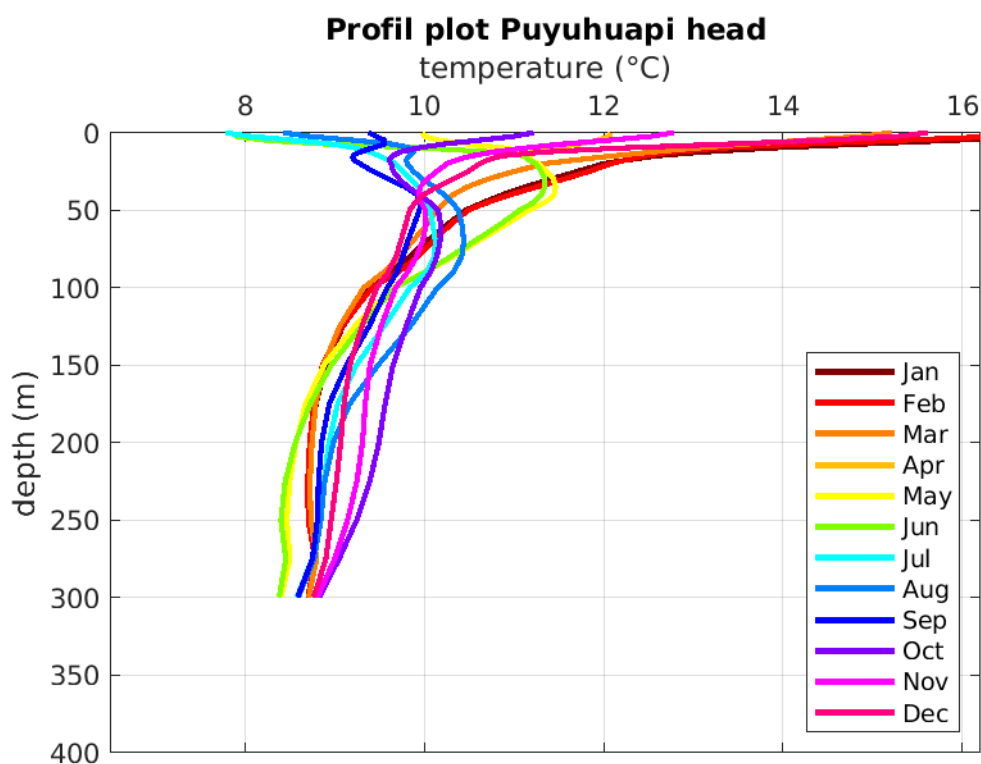
Figure Annexe 15: Profile plots of the monthly temperature from the in situ-based climatology in Puyuhuapi Fjord's head (point 13 on the map).
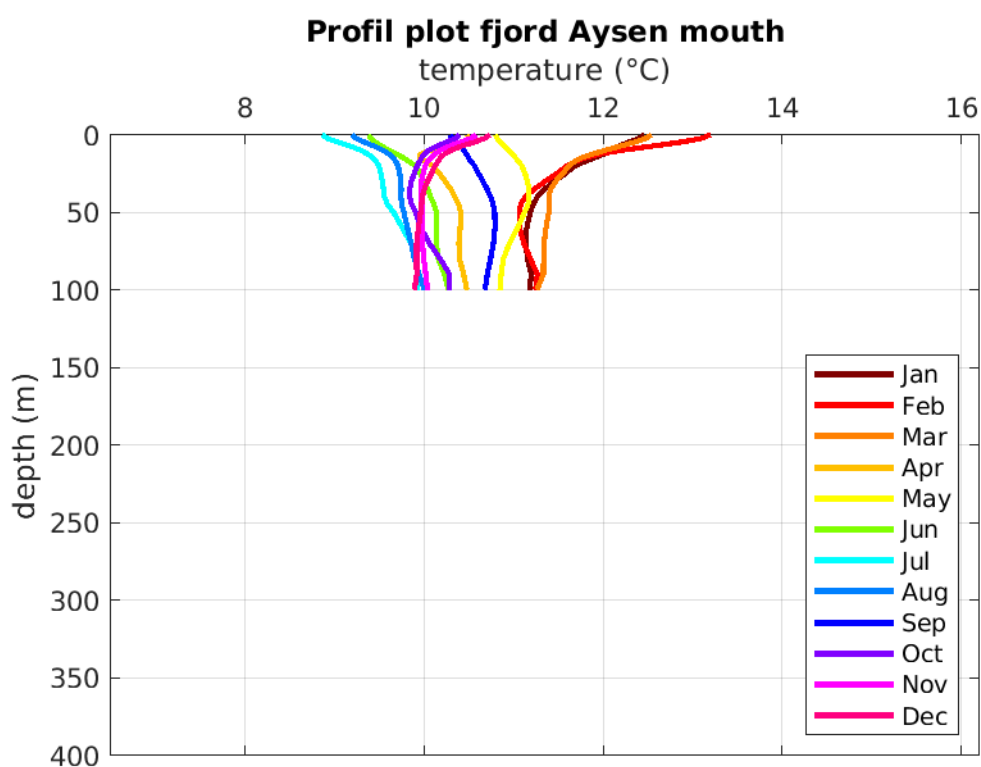
Figure Annexe 14 : Profile plots of the monthly temperature from the in situ-based climatology in Aysén Fjord's Mouth (point 14 on the map).
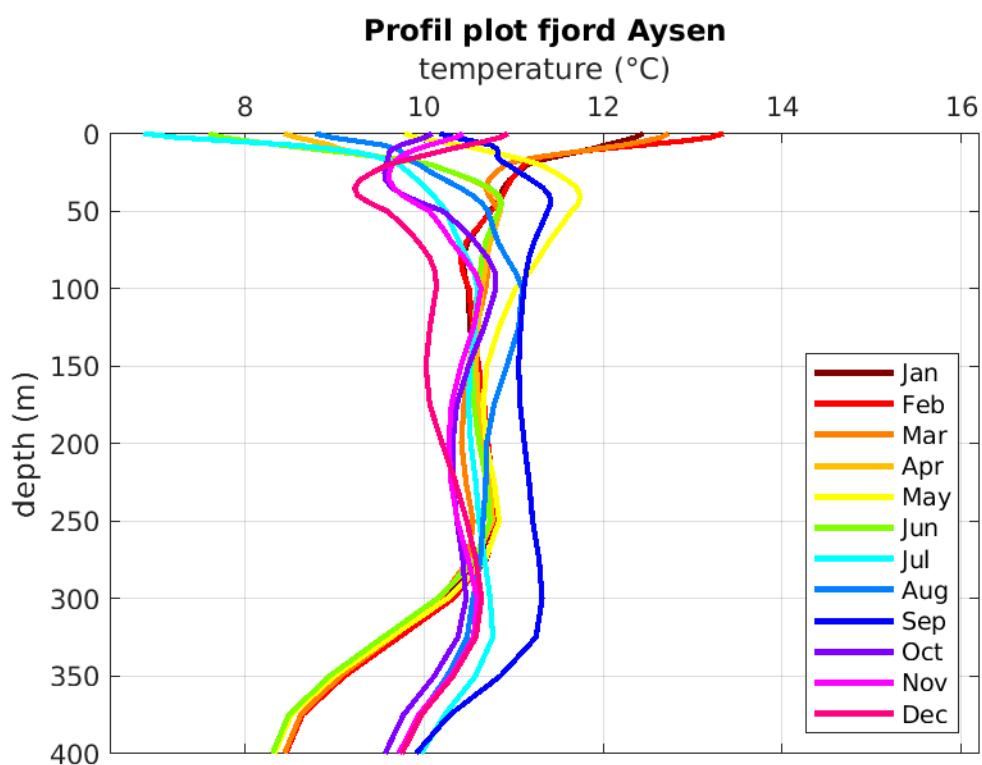
Figure Annexe 16: Profile plots of the monthly temperature from the in situ-based climatology in Aysén Fjord (point 51 on the map).
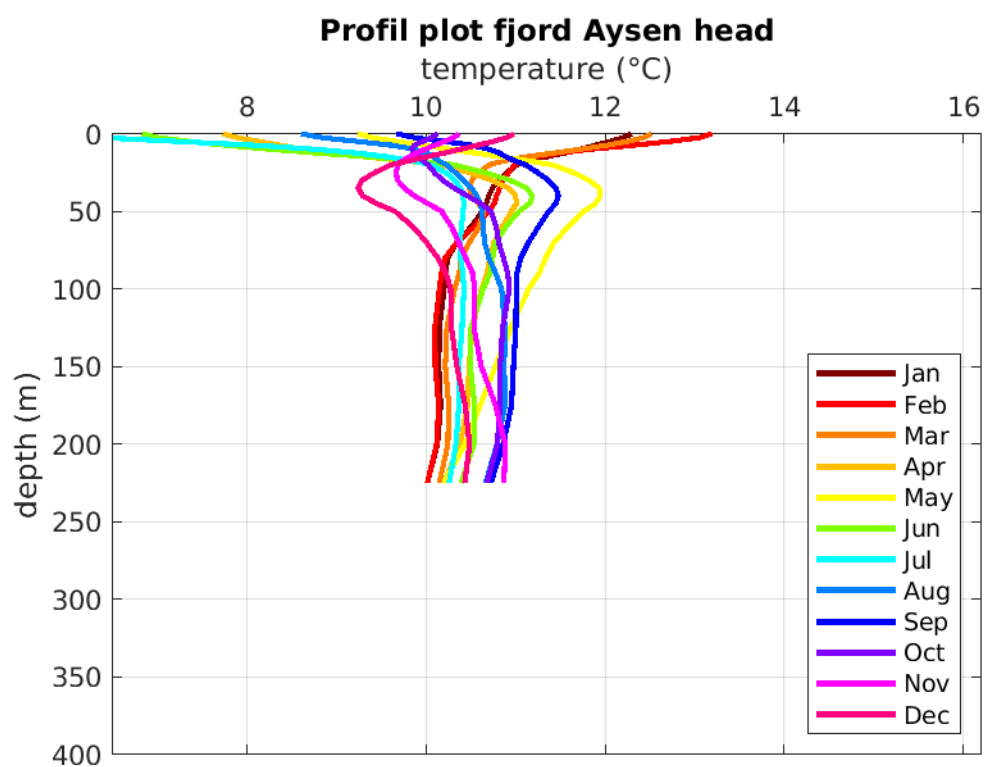
Figure Annexe 17: Profile plots of the monthly temperature from the in situ-based climatology in Aysén Fjord's head (point 16 on the map).

x
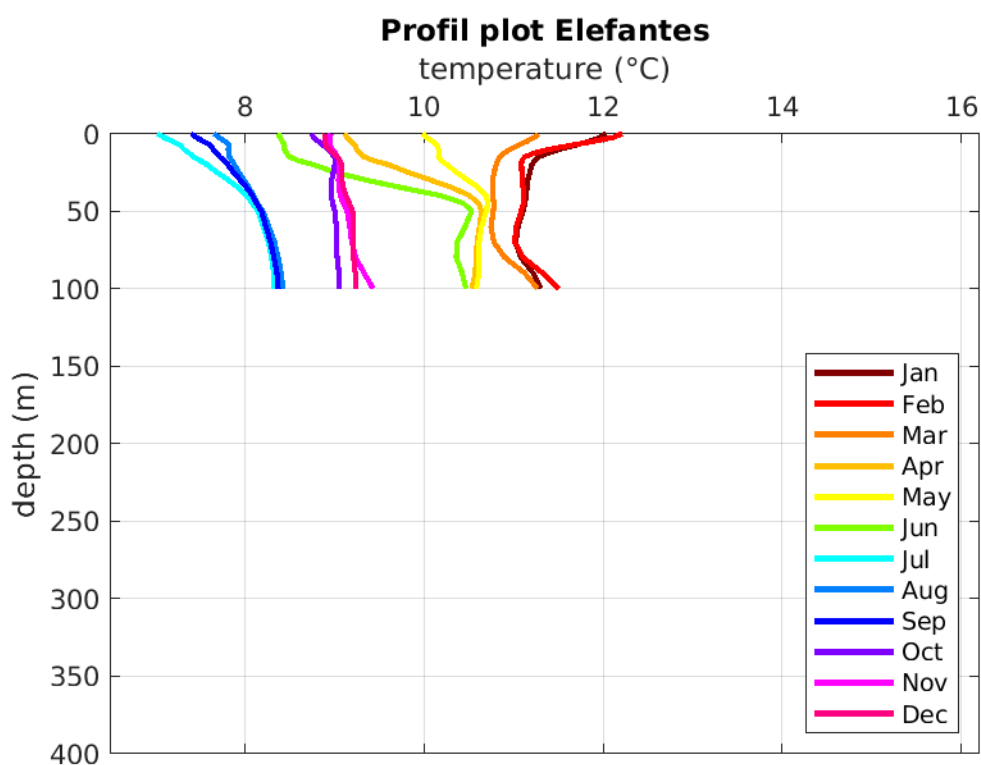
Figure Annexe 19: Profile plots of the monthly temperature from the in situ-based climatology in Elefantes Channel (point 17 on the map).
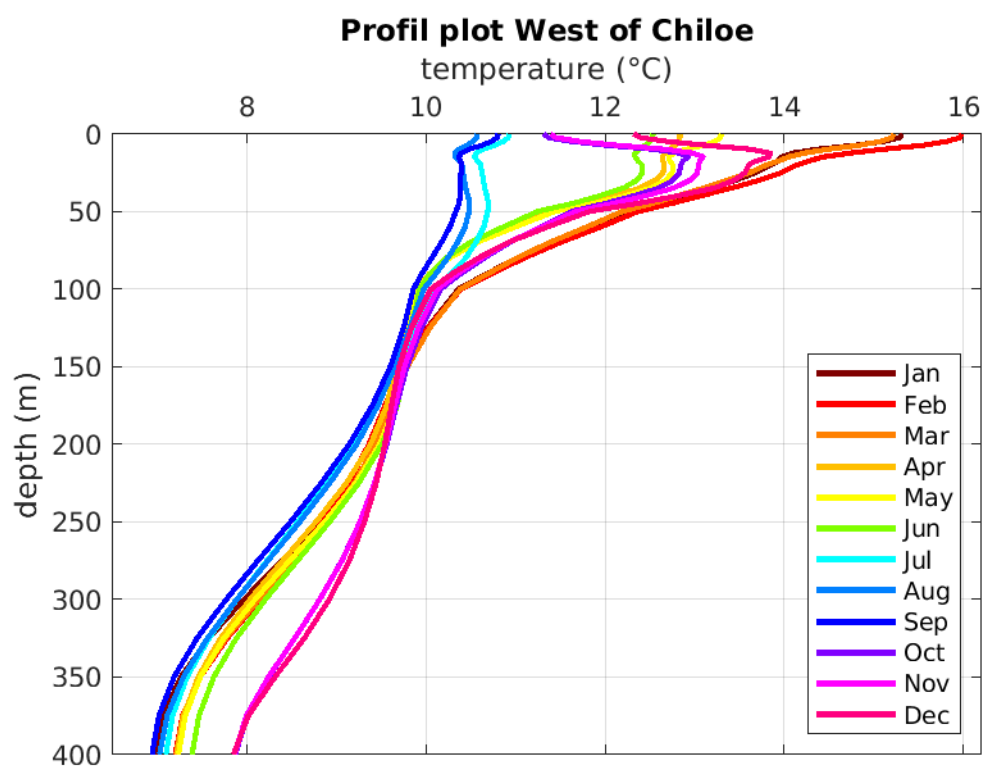
Figure Annexe 18: Profile plots of the monthly temperature from the in situ-based climatology in the Pacific Ocean west of Chiloé Island (point 18 on the map).
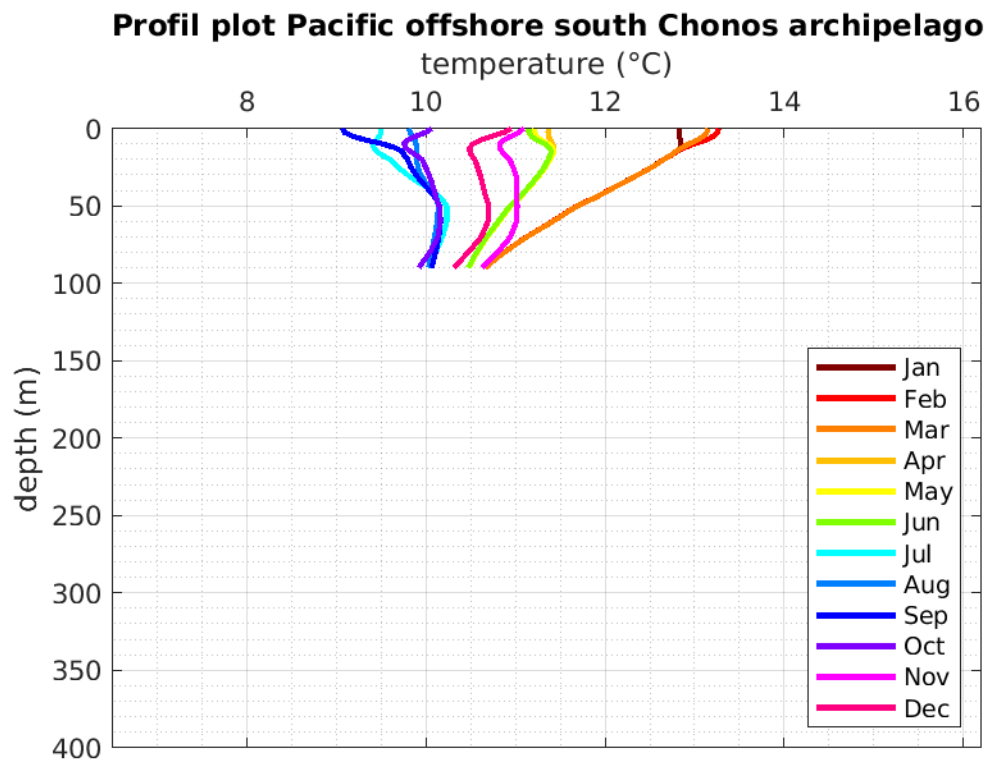
Figure Annexe 20: Profile plots of the monthly temperature from the in situ-based climatology in the Pacific Ocean West of Chonos Archipelago (point 19 on the map).

2.Spatial representation of the temperature climatology

This section provides the full temperature climatology corresponding to section 3.3.2 of the manuscript. While only 3 depths are presented there (0, 30 and 100m), here the results are shown for all depths at which the monthly climatology has been calculated.
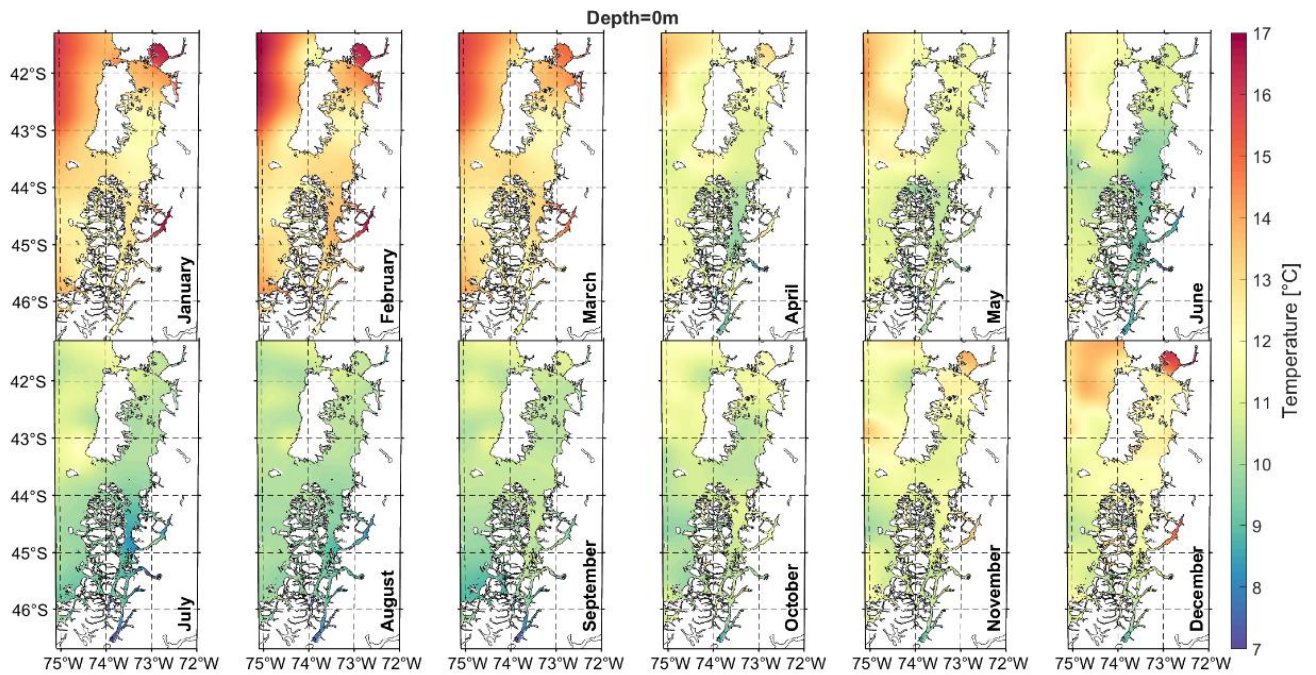
Figure Annexe 21: Monthly climatology of the sea temperature at 0m depth.
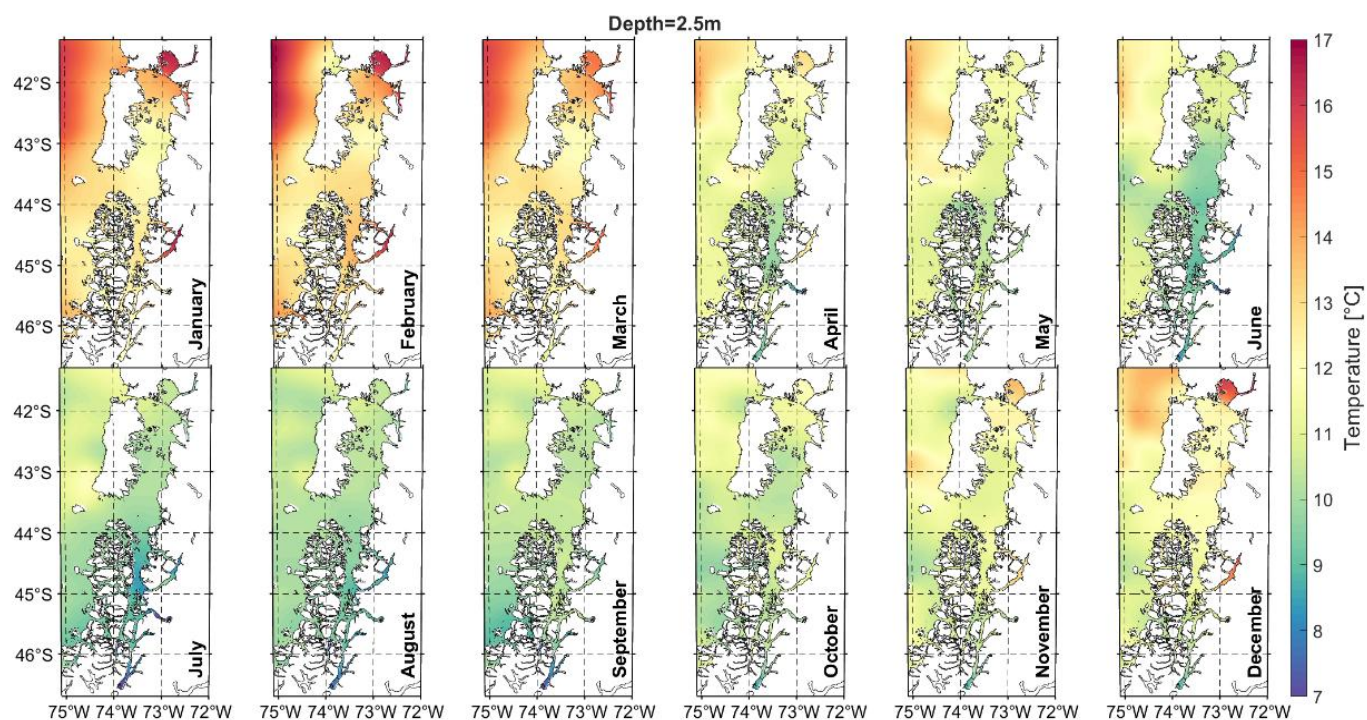
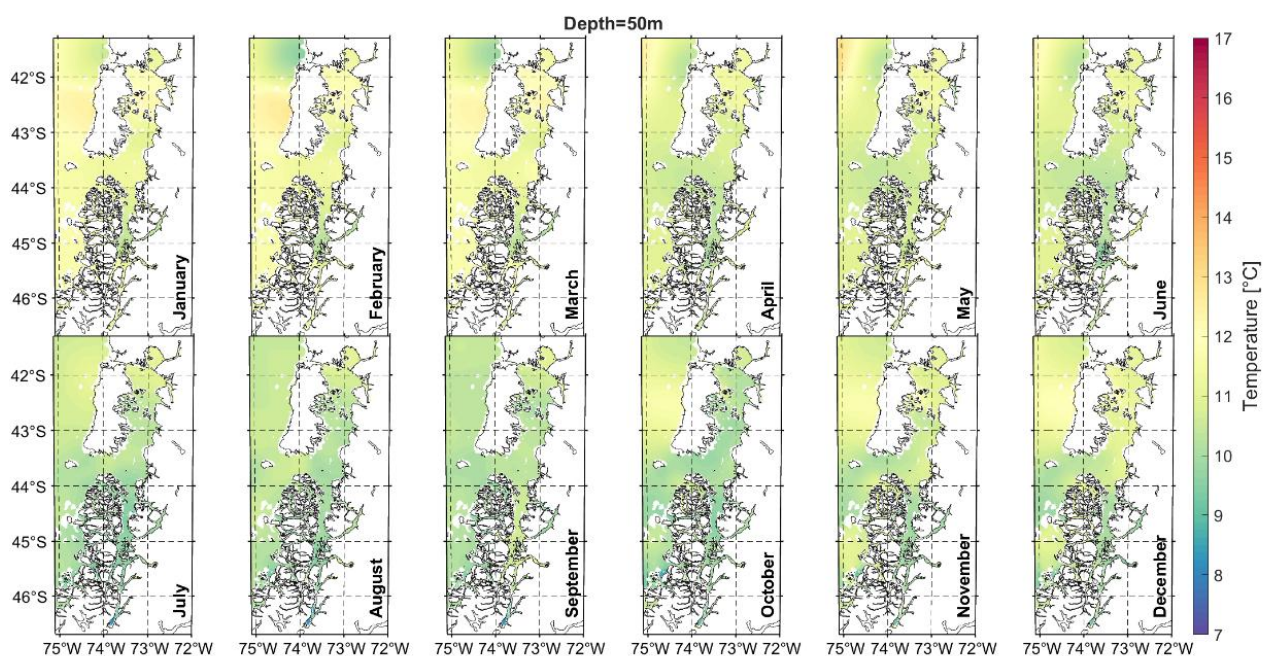*Figure Annexe 22: Monthly climatology of the sea temperature at 2.5m depth.*
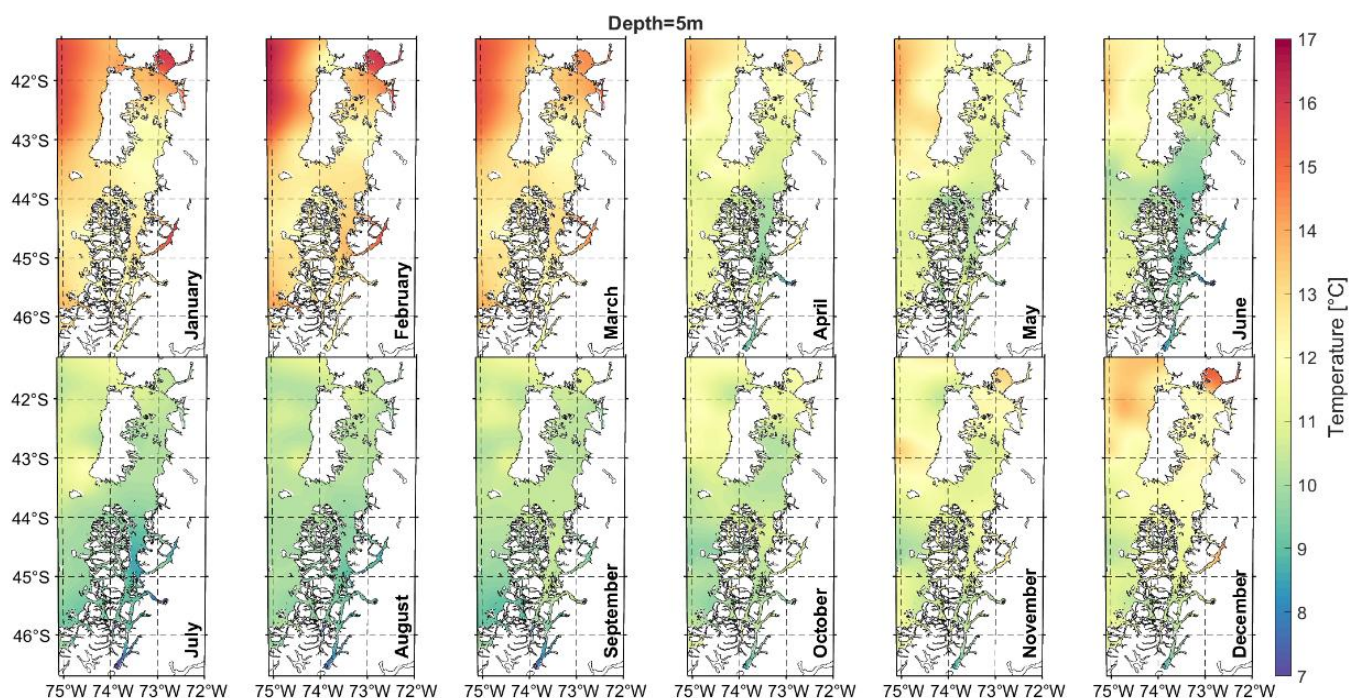
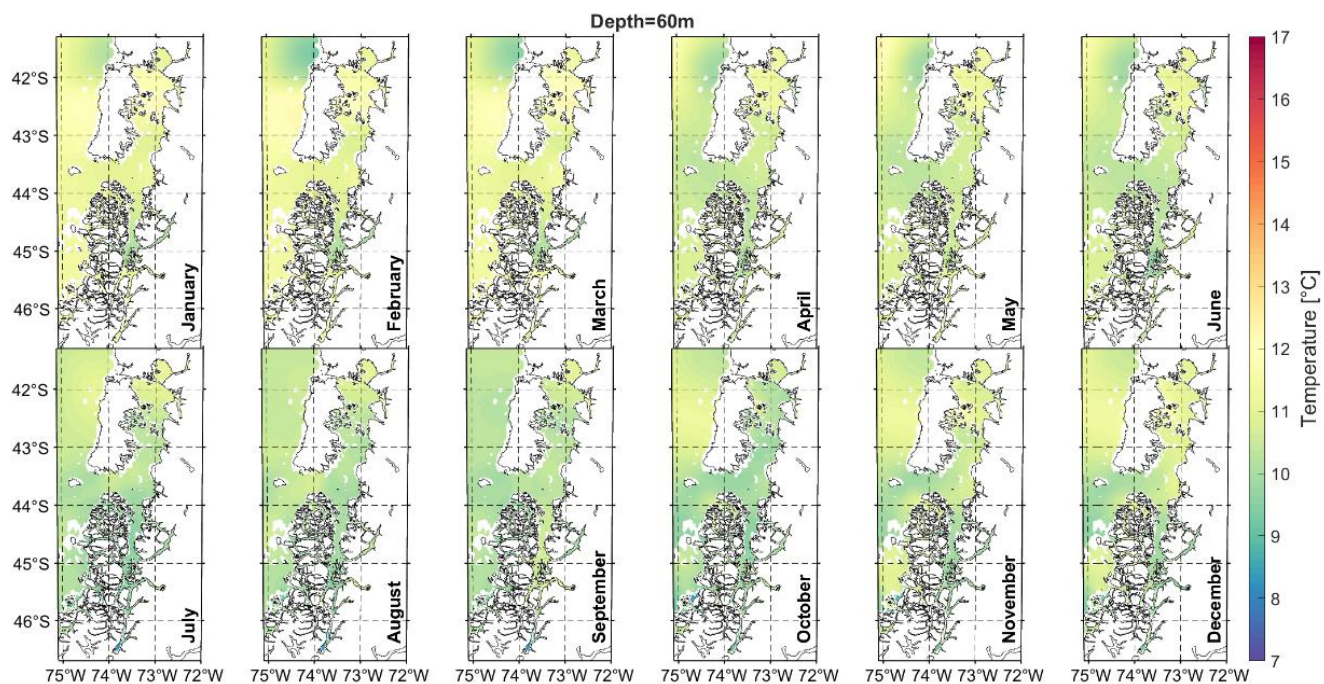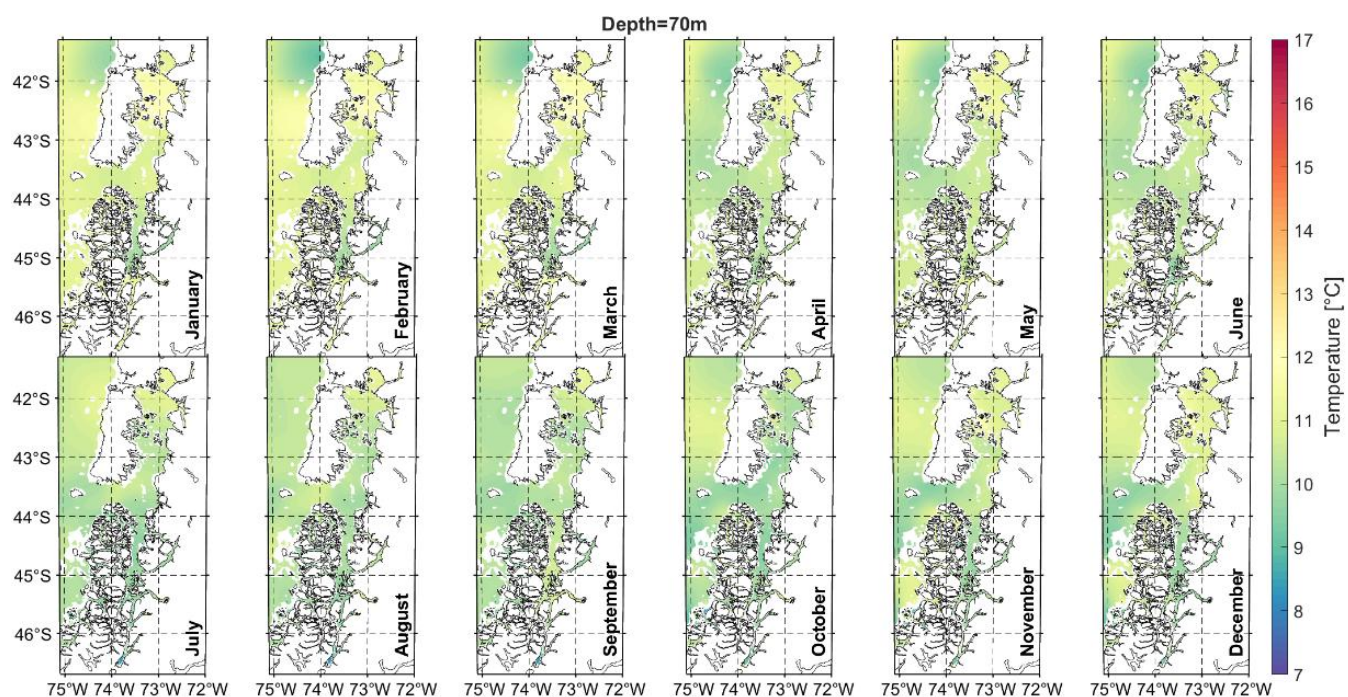*Figure Annexe 23: Monthly climatology of the sea temperature at 5m depth.*
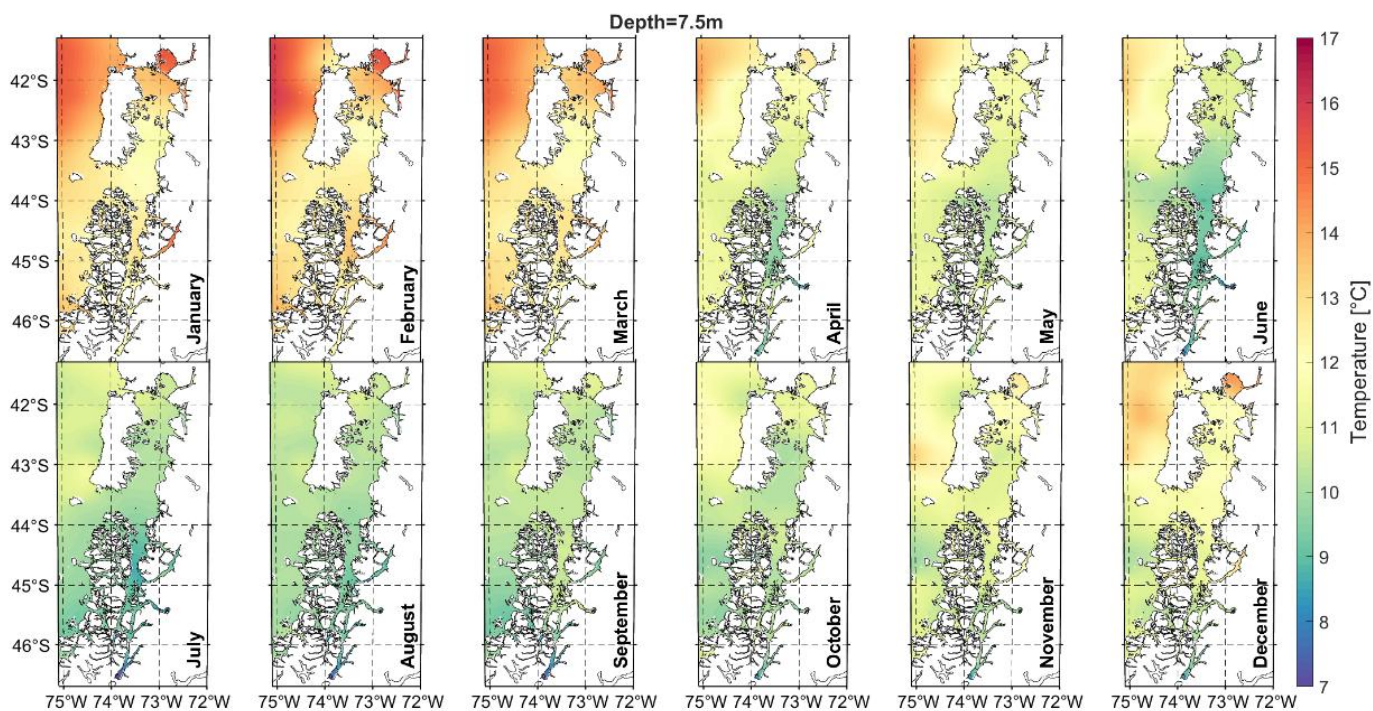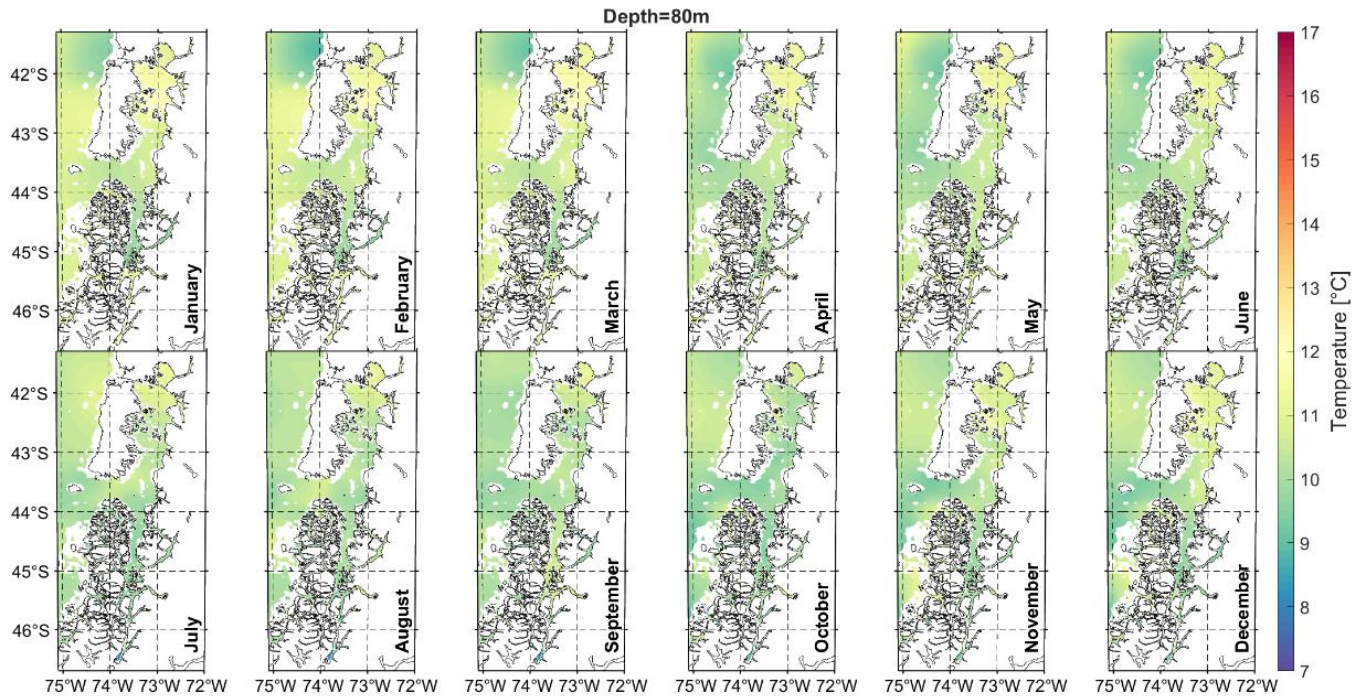
Figure Annexe 24: Monthly climatology of the sea temperature at 7.5m depth.
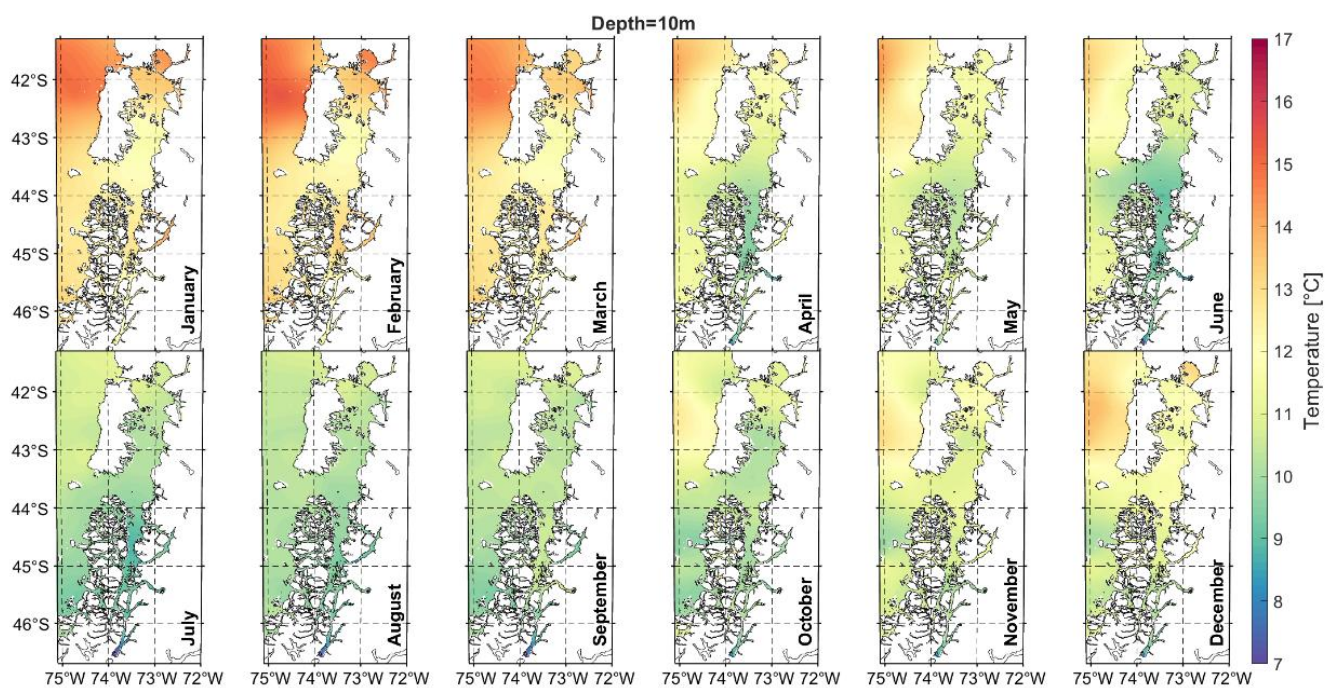
Figure Annexe 25: Monthly climatology of the sea temperature at 10m depth
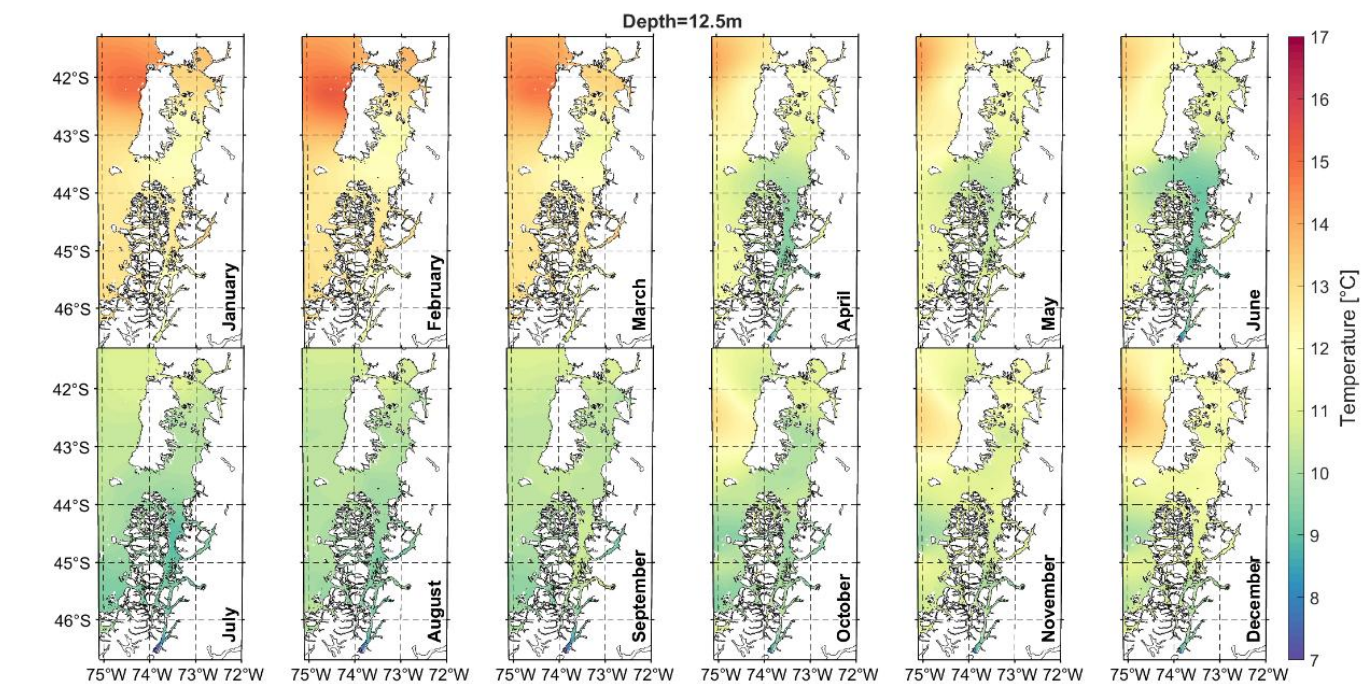
Figure Annexe 26: Monthly climatology of the sea temperature at 12.5m depth.
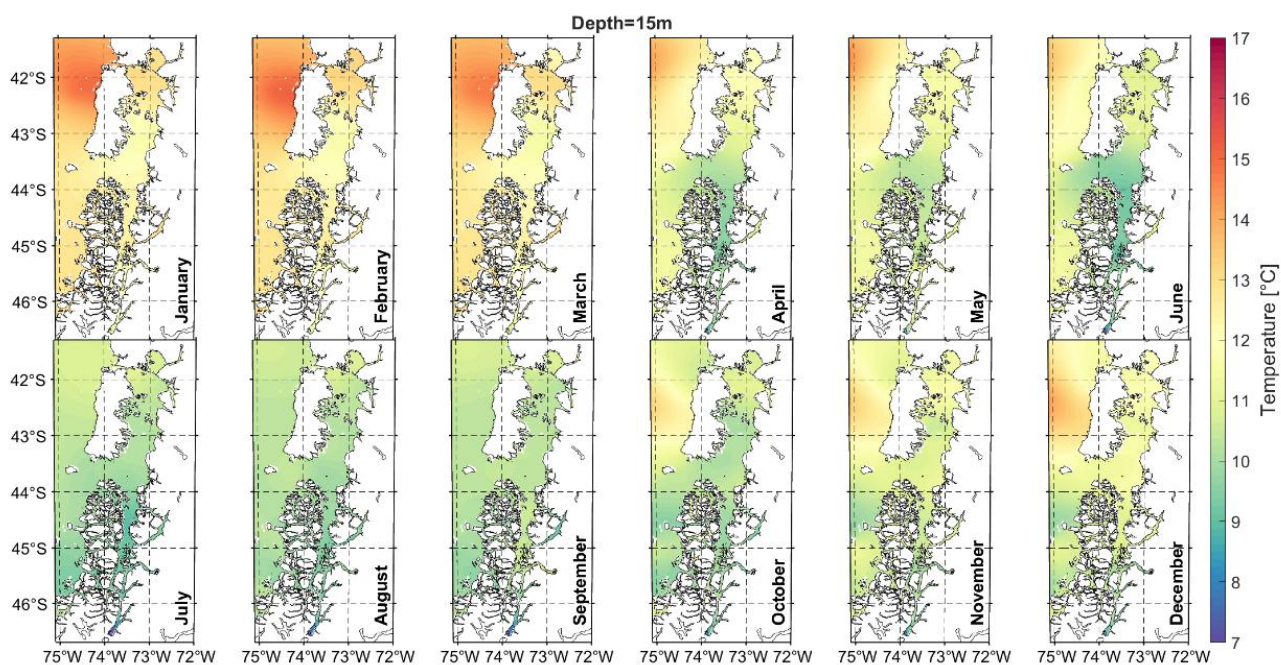
Figure Annexe 27: Monthly climatology of the sea temperature at 15m depth.
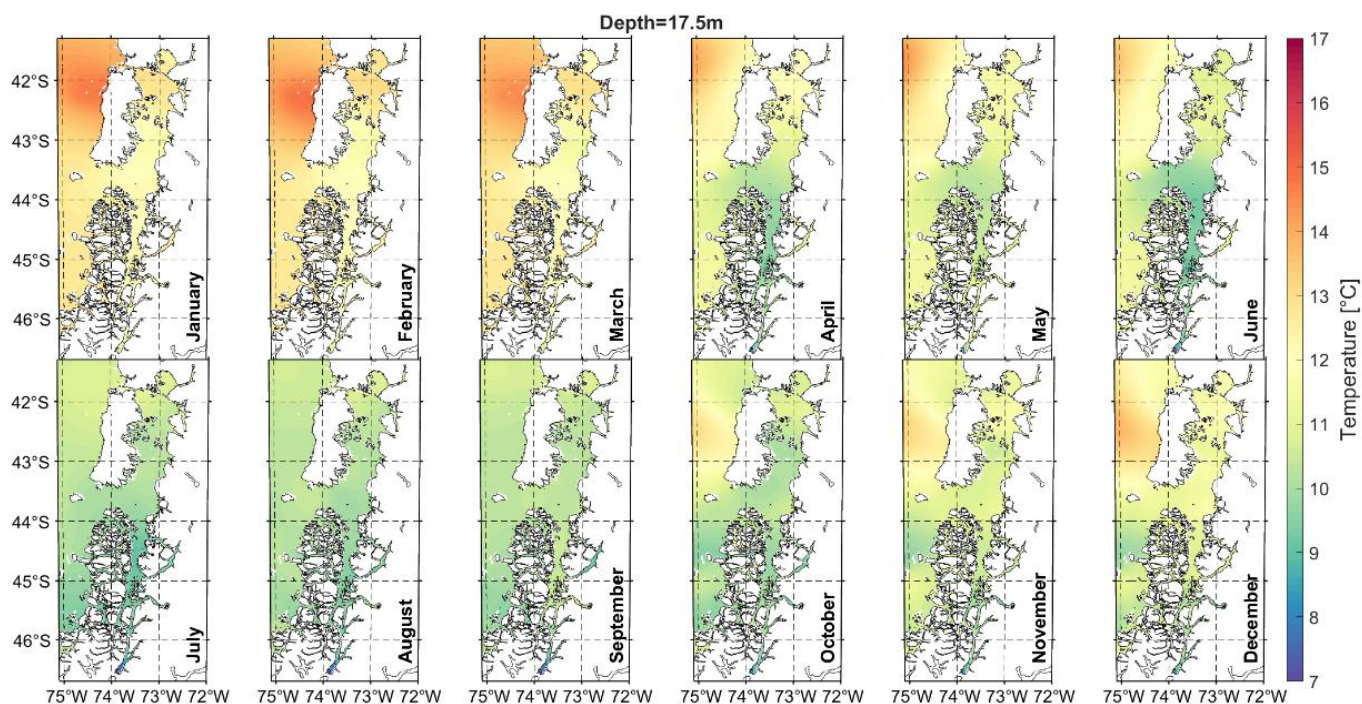
Figure Annexe 28: Monthly climatology of the sea temperature at 17.5m depth.
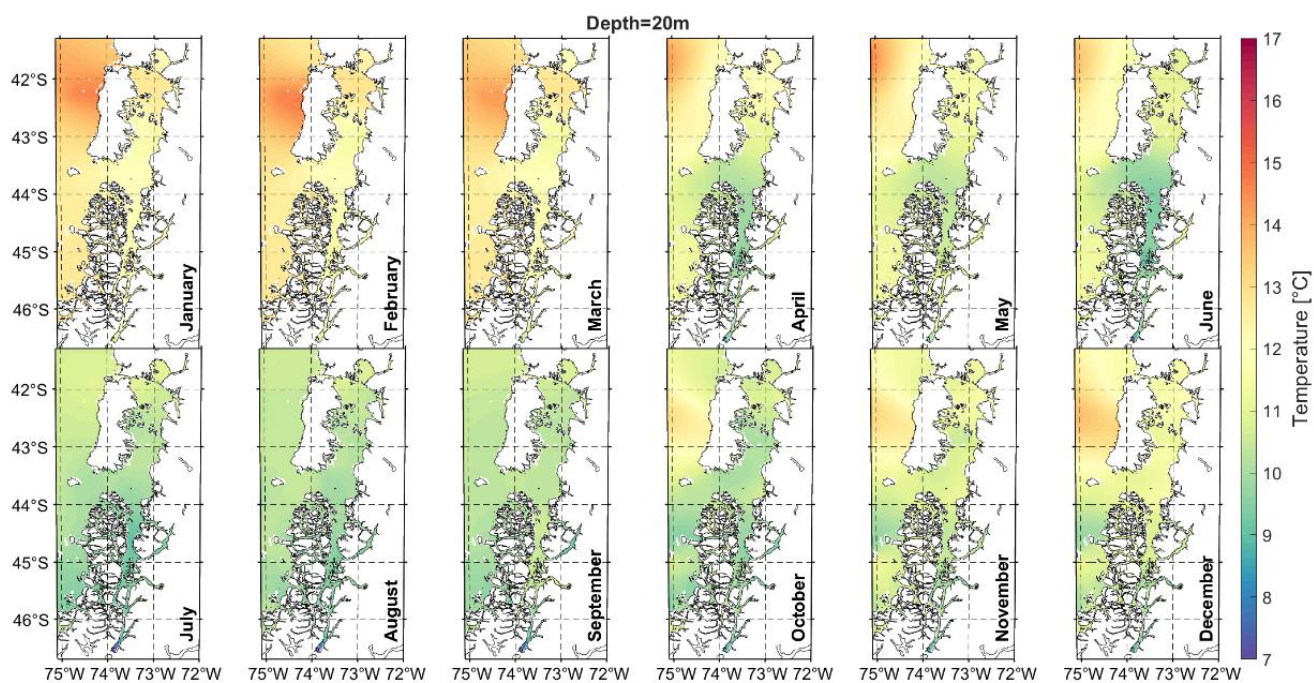
Figure Annexe 29: Monthly climatology of the sea temperature at 20m depth.
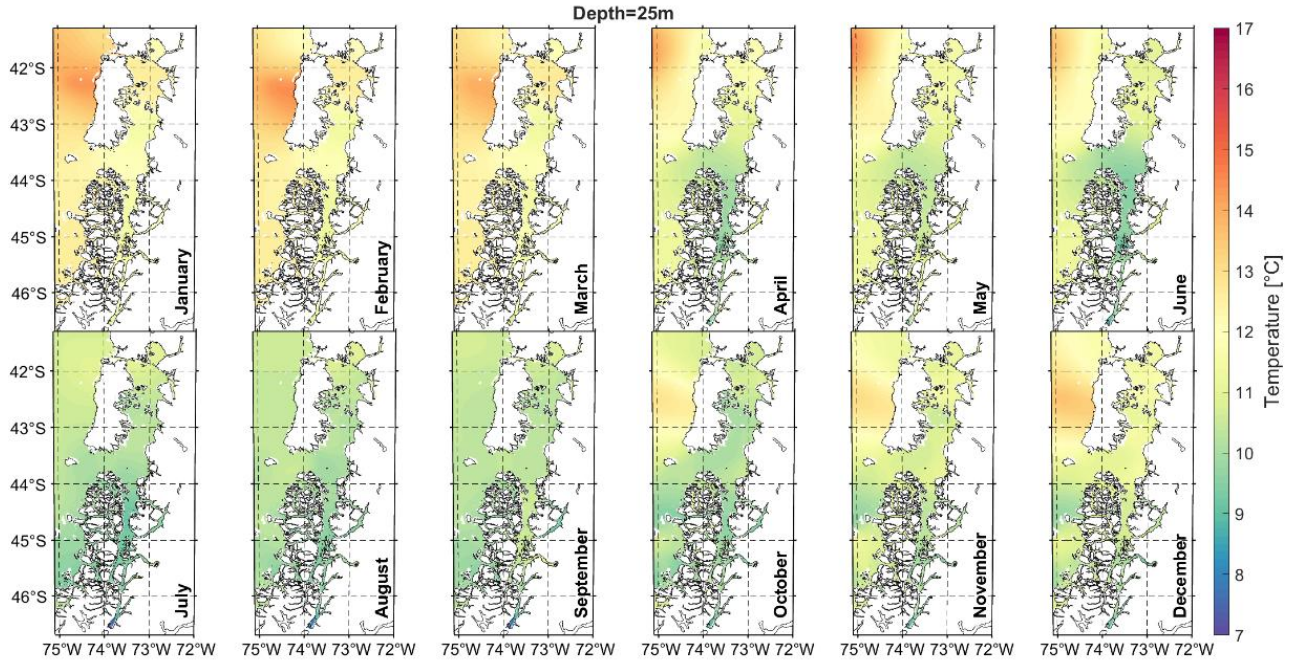
Figure Annexe 30: Monthly climatology of the sea temperature at 25m depth.
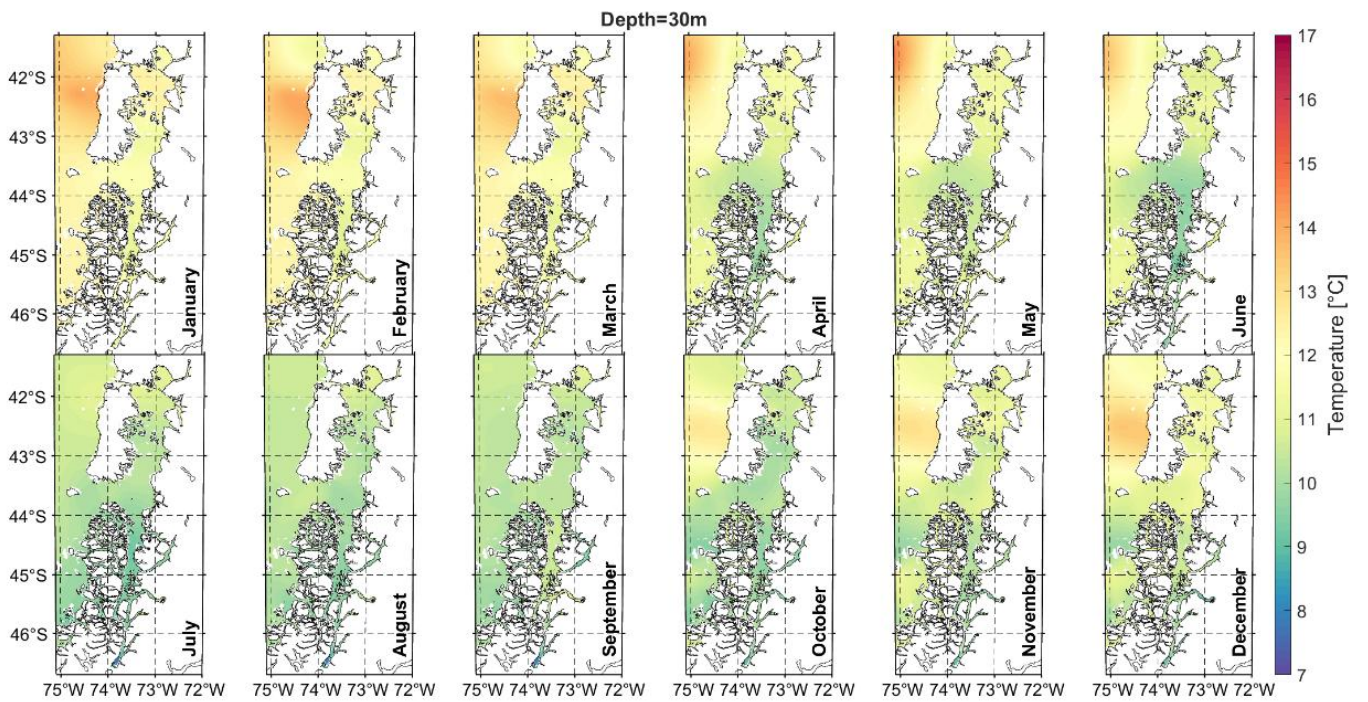
Figure Annexe 31: Monthly climatology of the sea temperature at 30m depth.
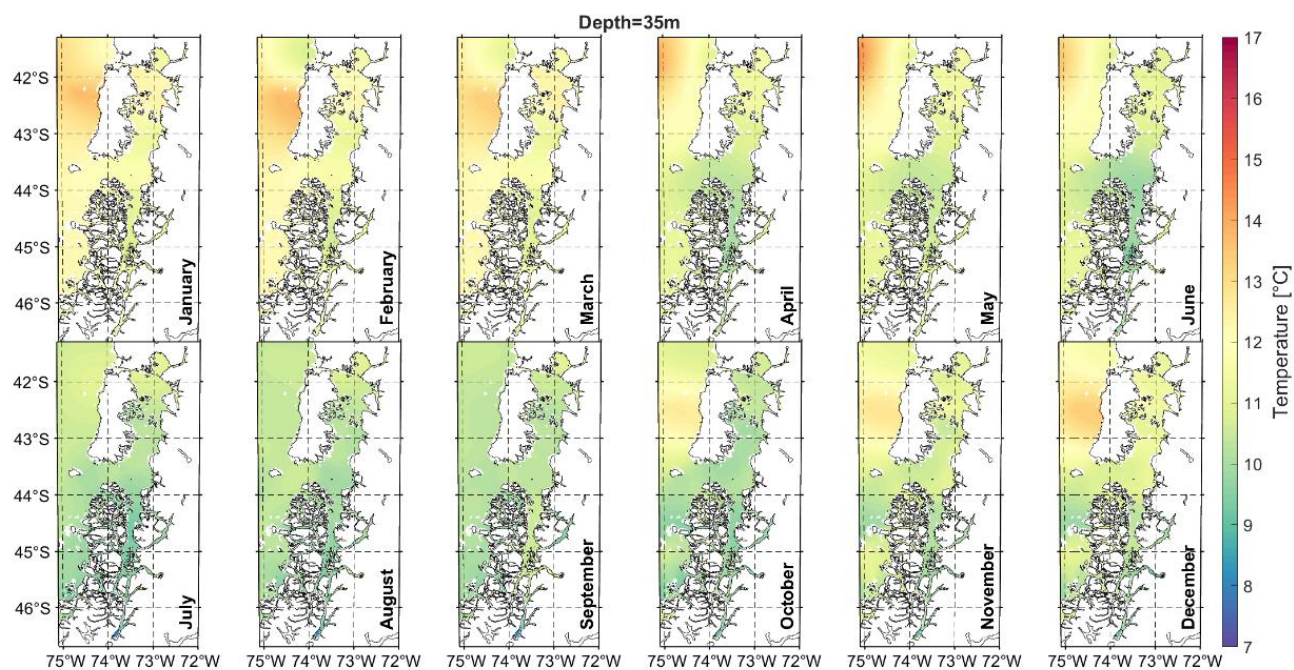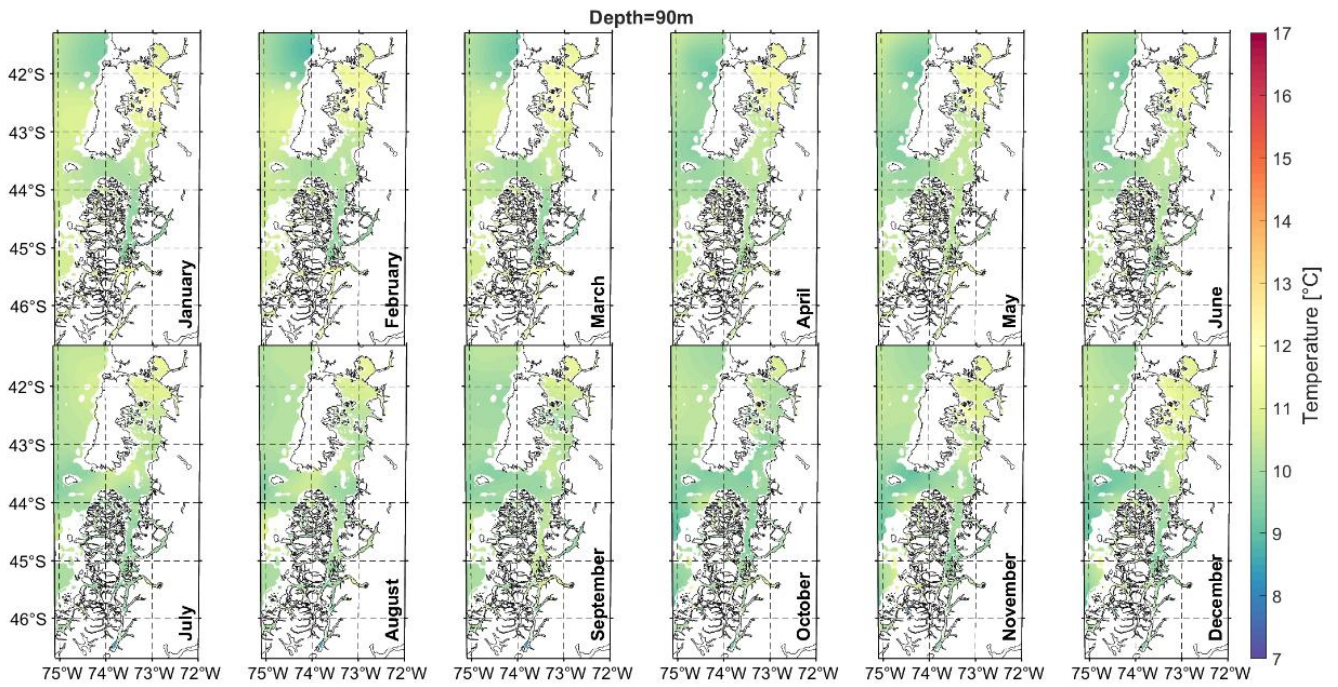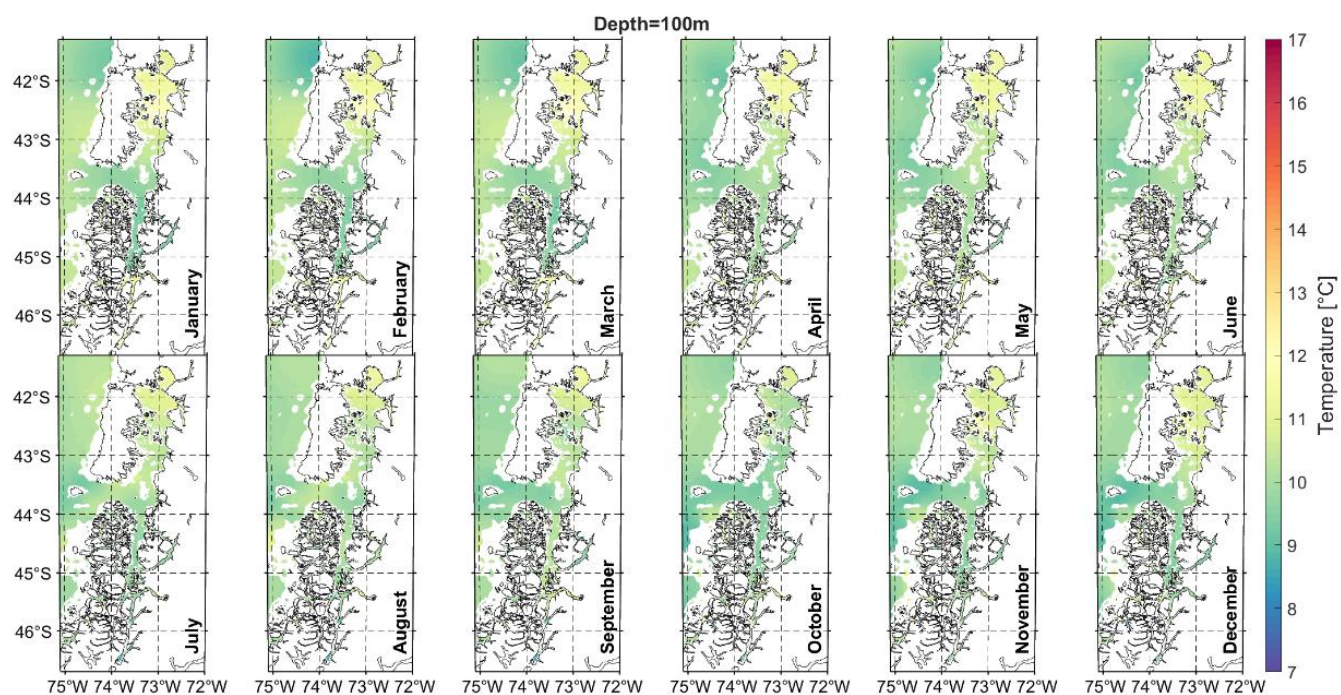
Figure Annexe 32: Monthly climatology of the sea temperature at 35m depth.
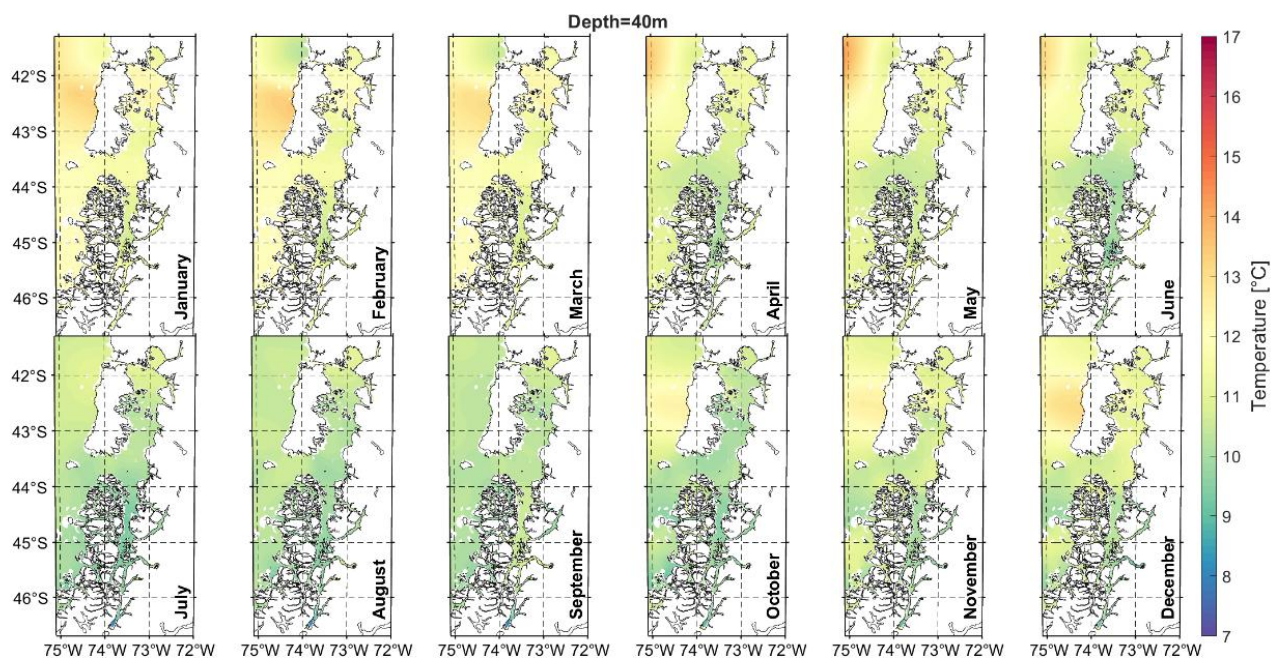
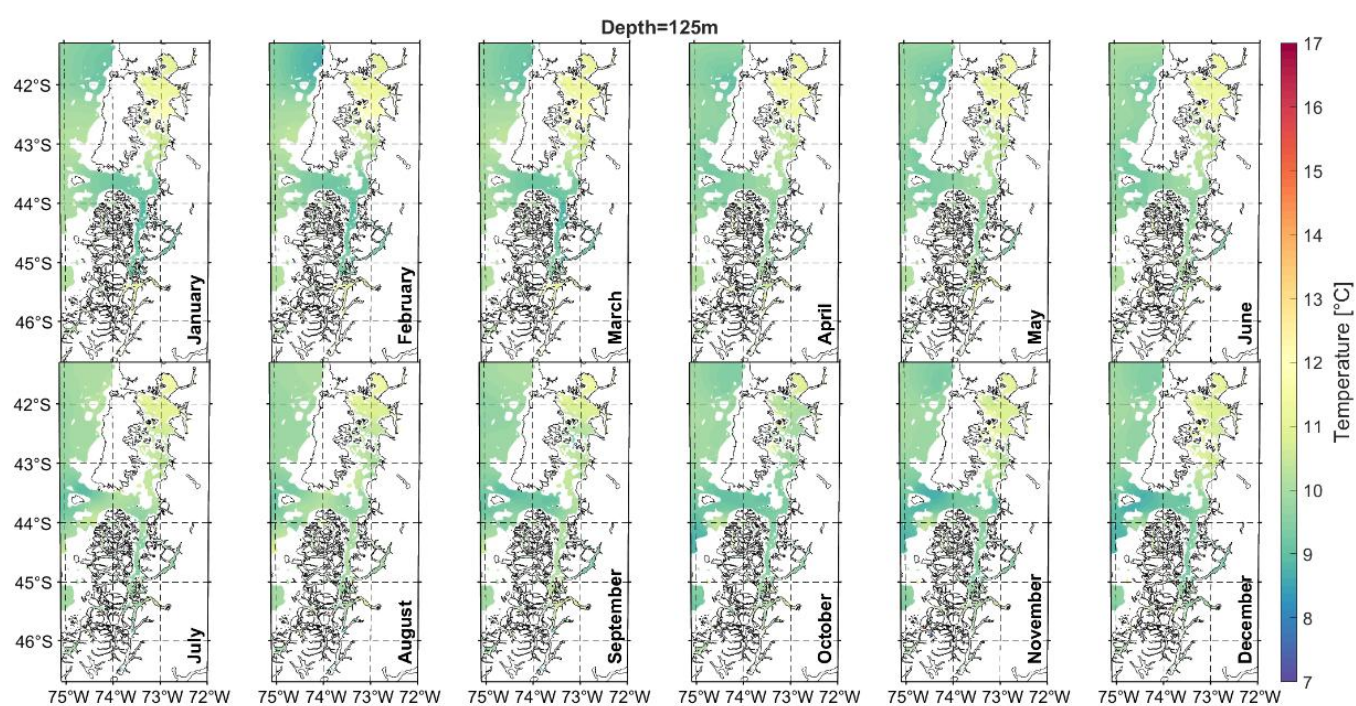*Figure Annexe 33: Monthly climatology of the sea temperature at 40m depth.*
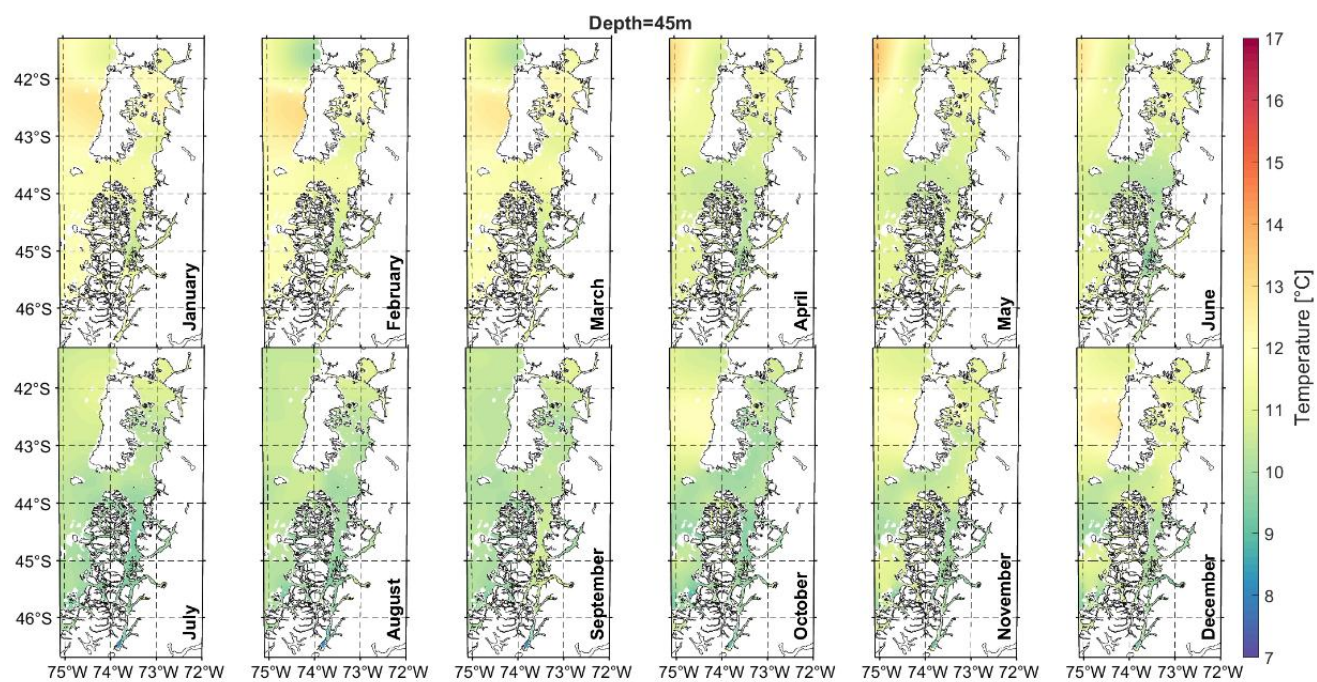
Figure Annexe 34: Monthly climatology of the sea temperature at 45m depth.

Figure Annexe 35: Monthly climatology of the sea temperature at 50m depth.

Figure Annexe 36: Monthly climatology of the sea temperature at 60m depth.
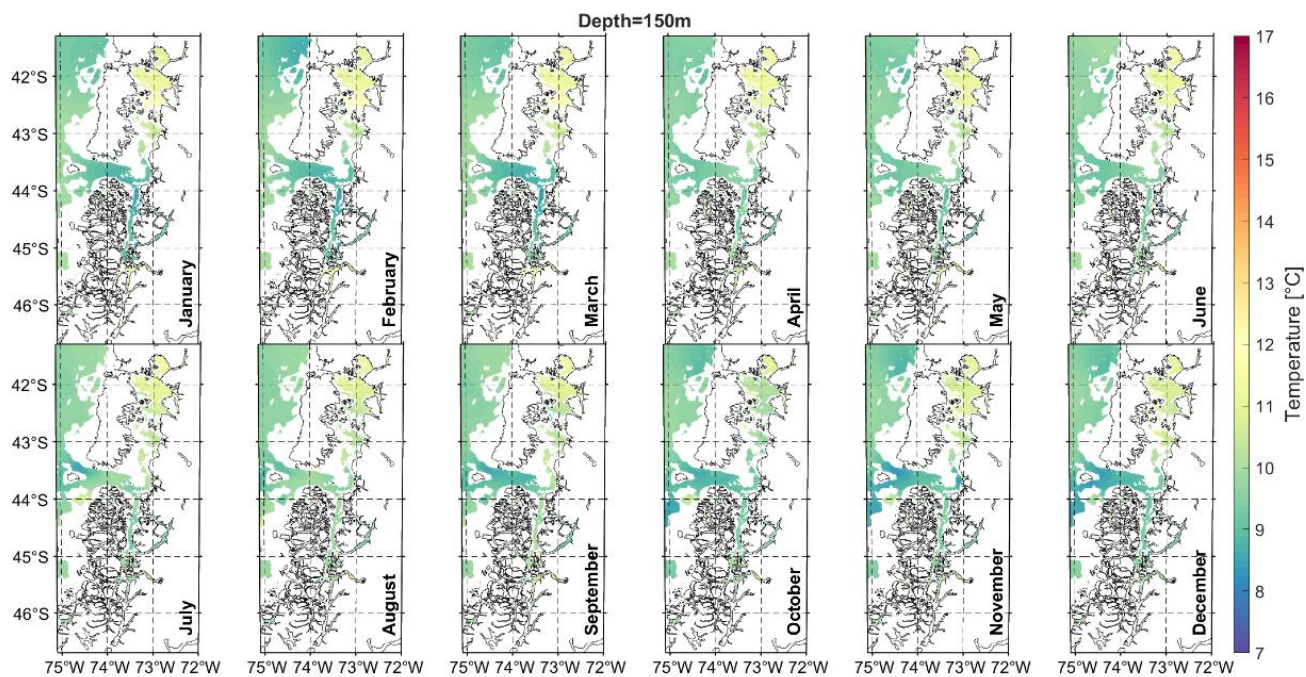

Figure Annexe 37: Monthly climatology of the sea temperature at 70m depth.

Figure Annexe 39: Monthly climatology of the sea temperature at 80m depth.

Figure Annexe 38: Monthly climatology of the sea temperature at 90m depth.

Figure Annexe 40: Monthly climatology of the sea temperature at 100m depth.

Figure Annexe 41: Monthly climatology of the sea temperature at 125m depth.

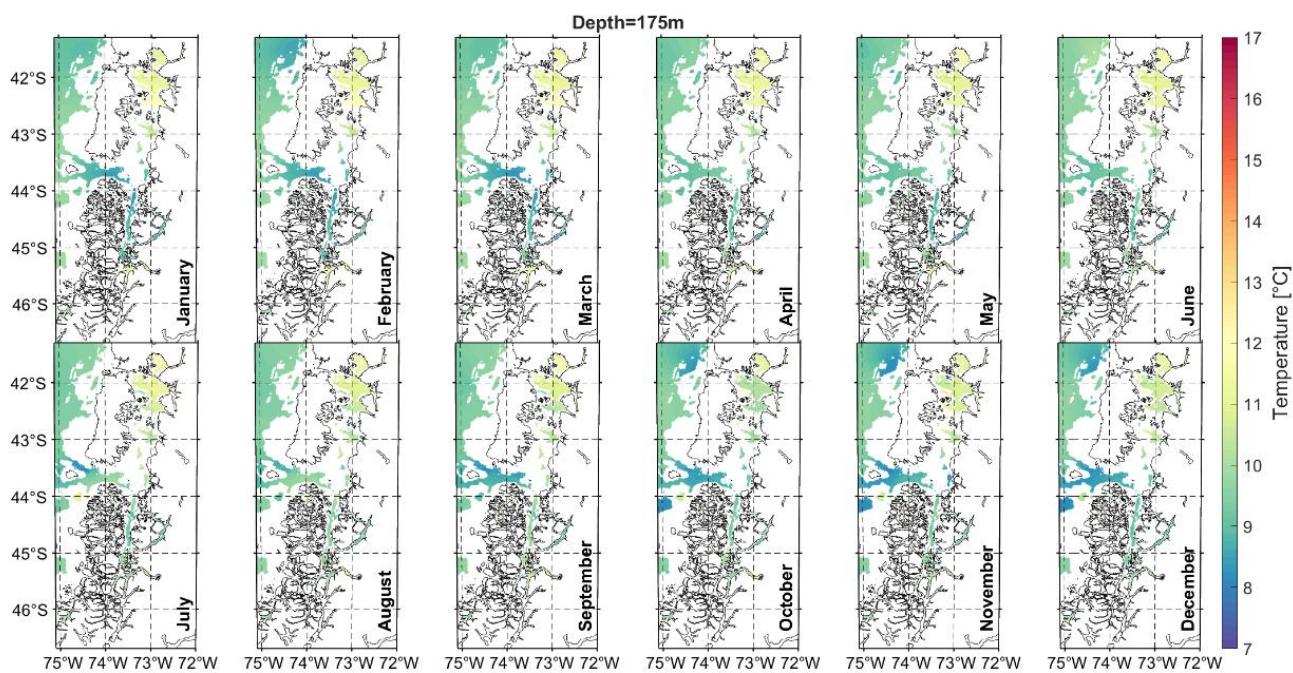*Figure Annexe 42: Monthly climatology of the sea temperature at 150m depth.*

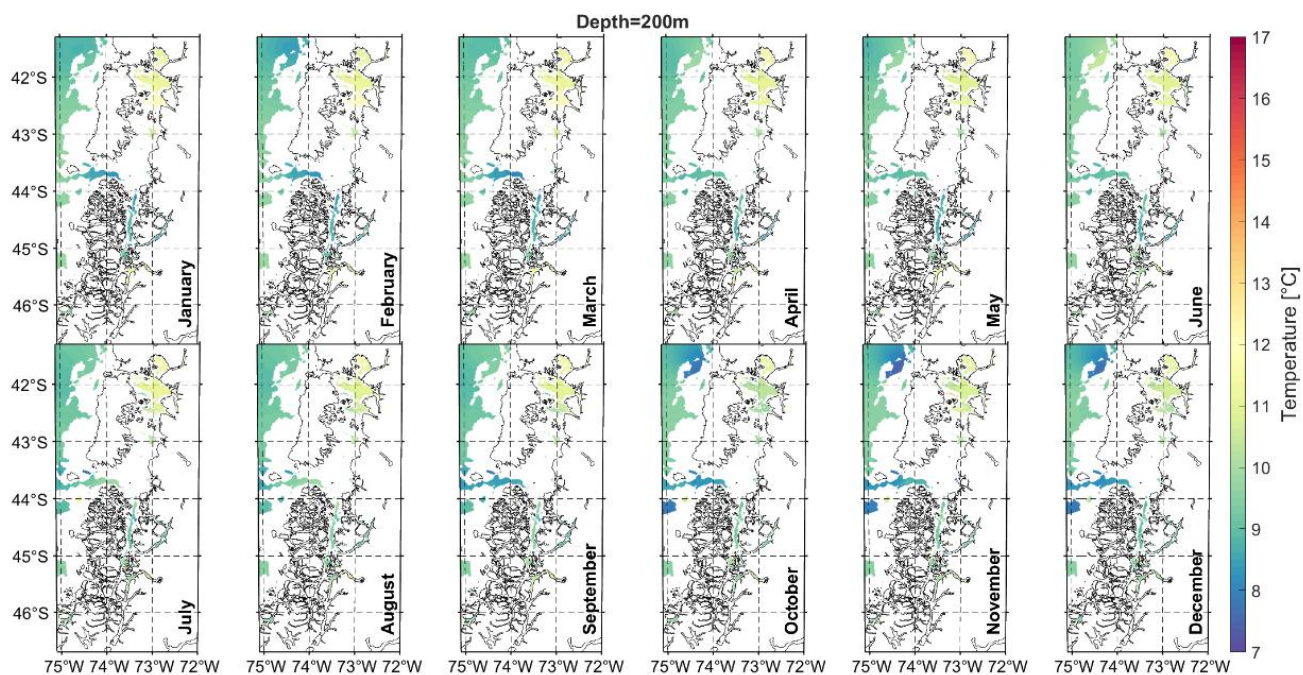*Figure Annexe 43: Monthly climatology of the sea temperature at 175m depth.*

Figure Annexe 44: Monthly climatology of the sea temperature at 200m depth.
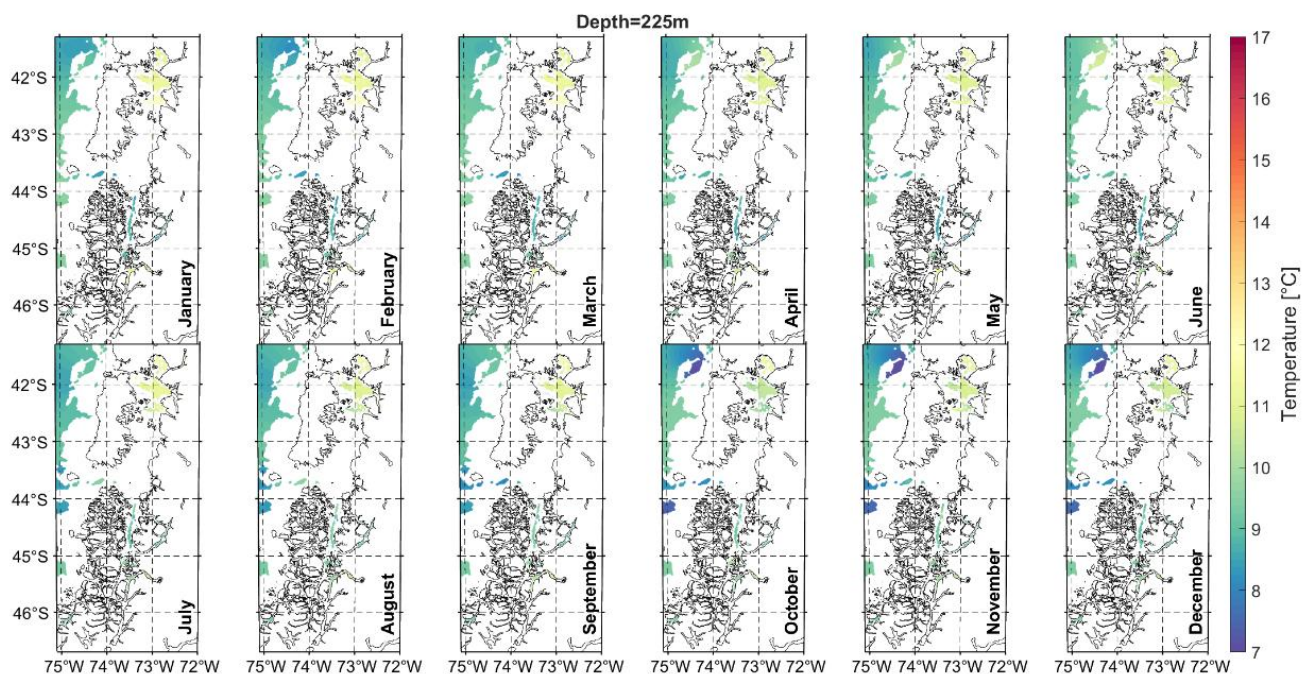

Figure Annexe 45: Monthly climatology of the sea temperature at 225m depth.

Figure Annexe 46: Monthly climatology of the sea temperature at 250m depth.

Figure Annexe 47: Monthly climatology of the sea temperature at 275m depth.

Figure Annexe 49: Monthly climatology of the sea temperature at 300m depth.

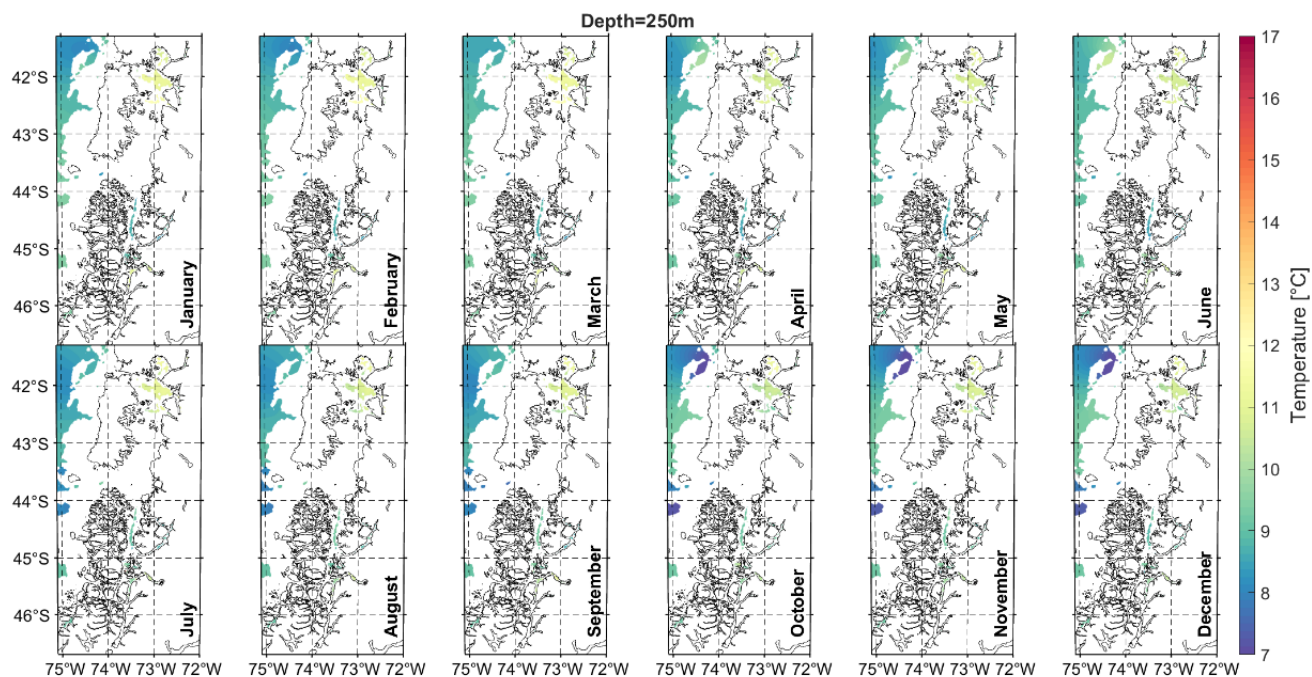*Figure Annexe 48: Monthly climatology of the sea temperature at 325m depth.*

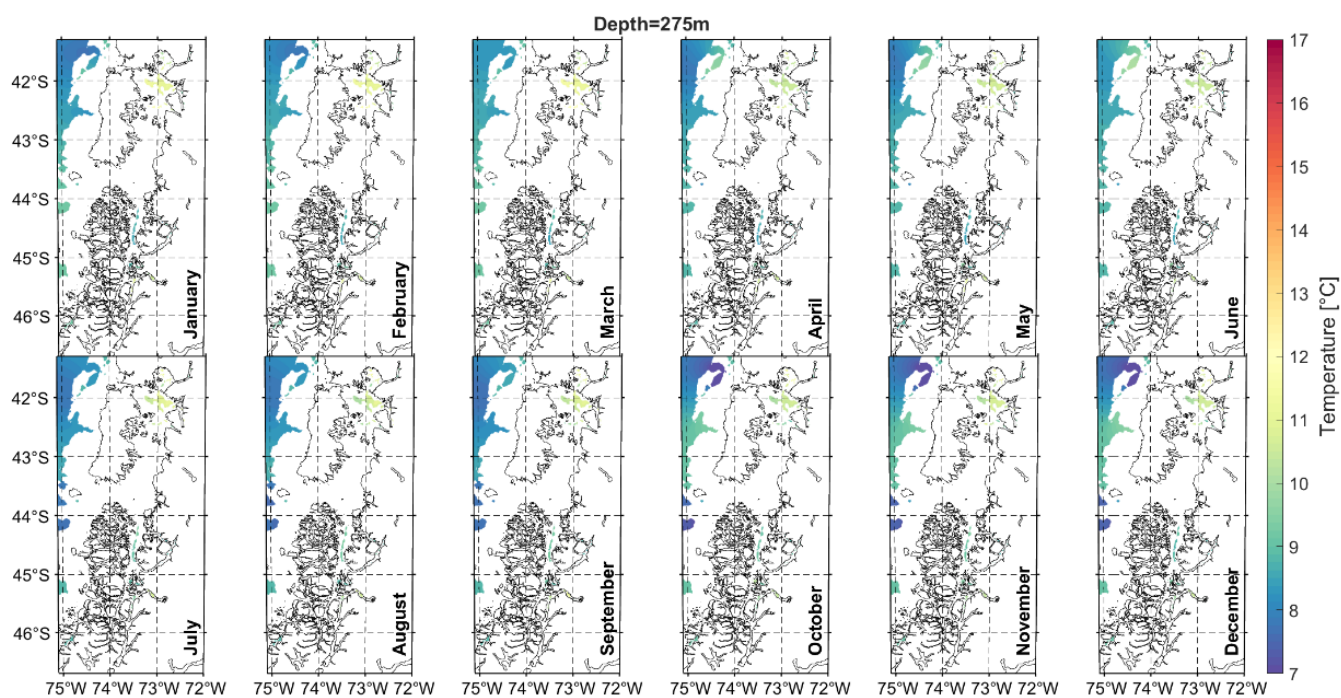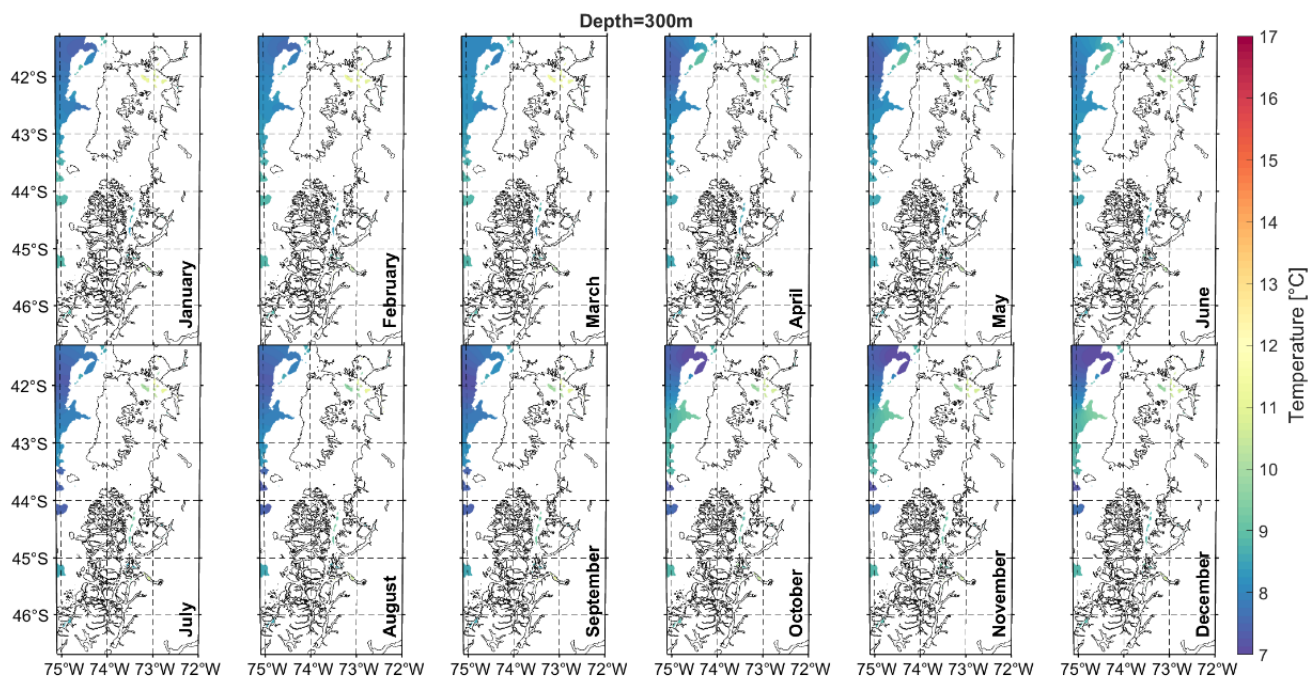*Figure Annexe 51: Monthly climatology of the sea temperature at 350m depth.*

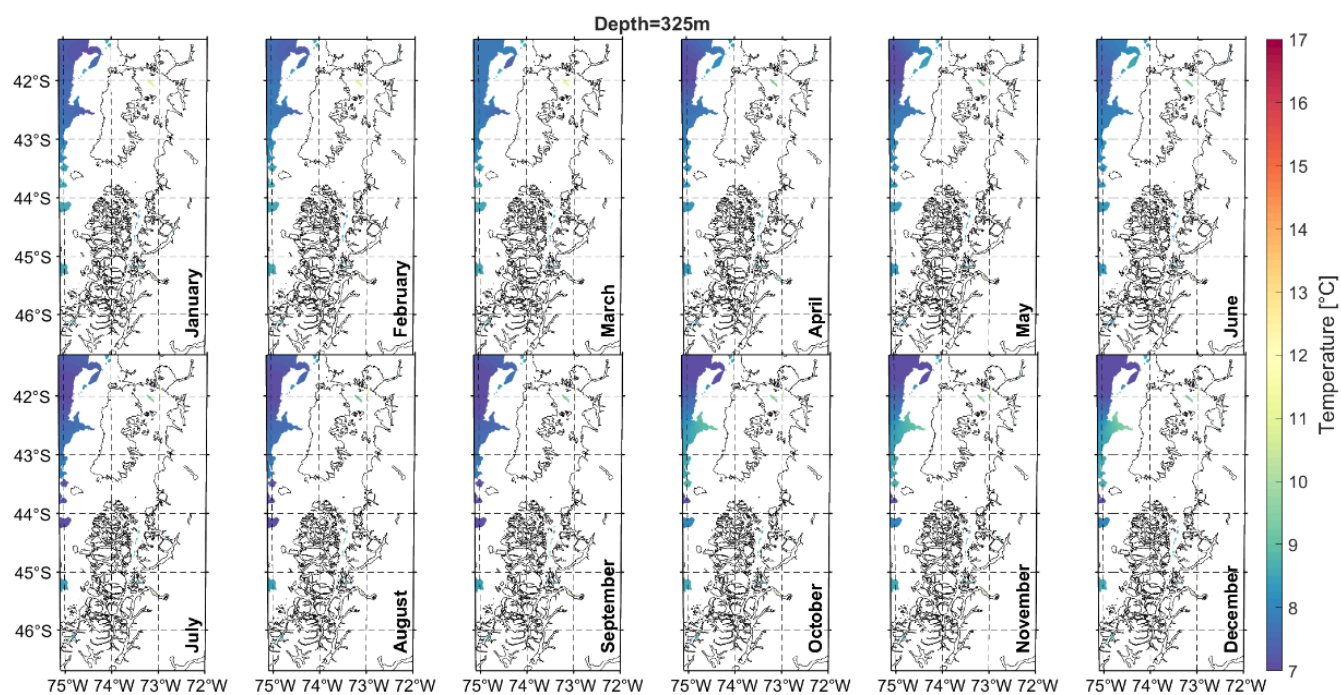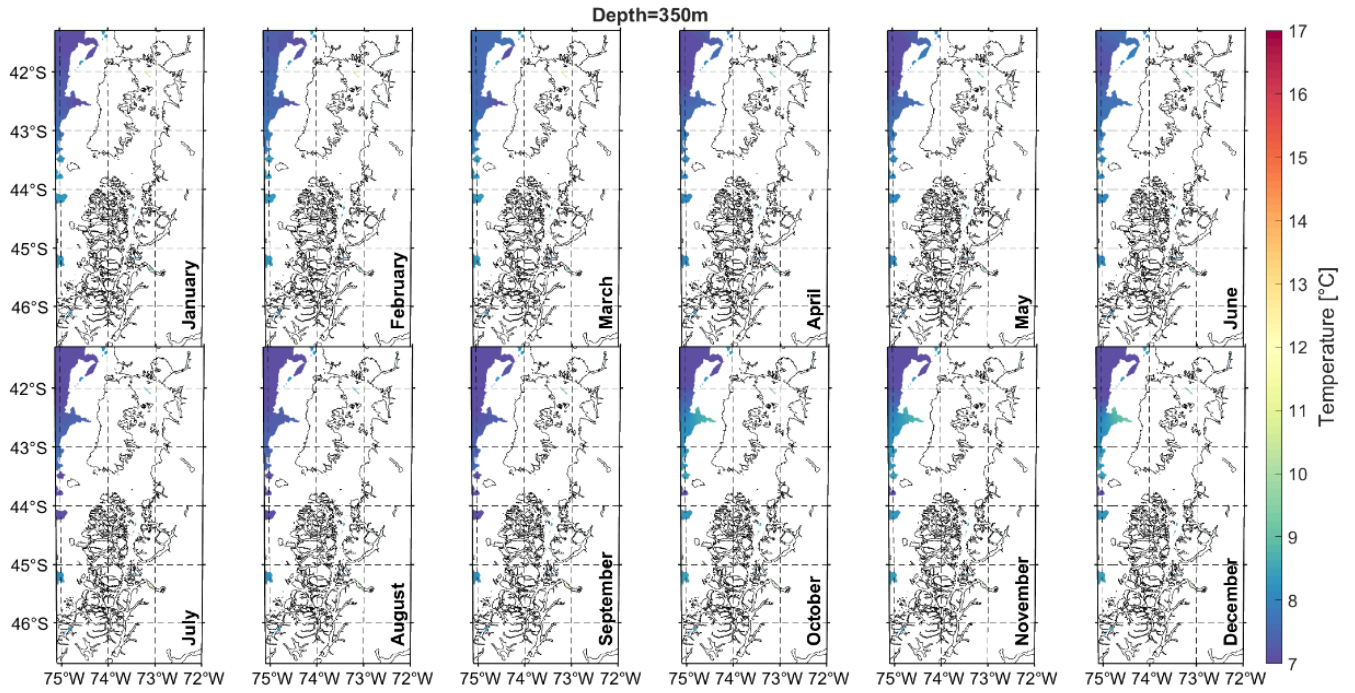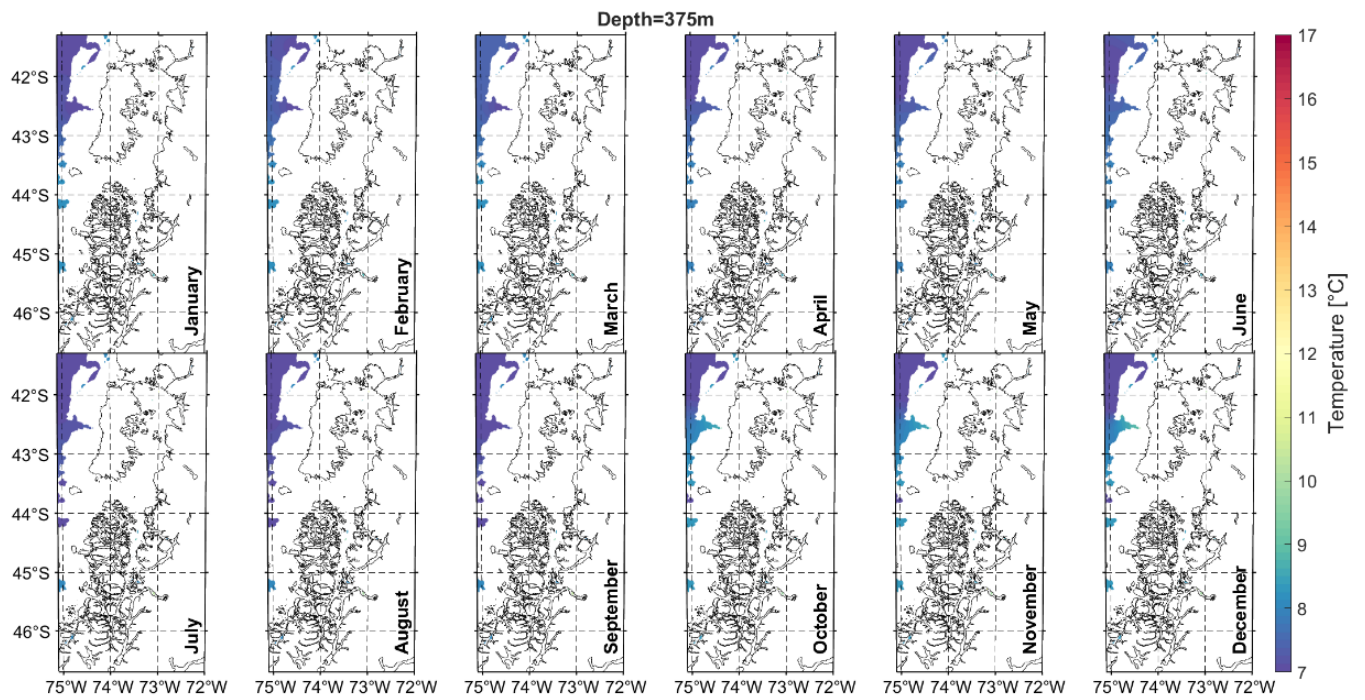
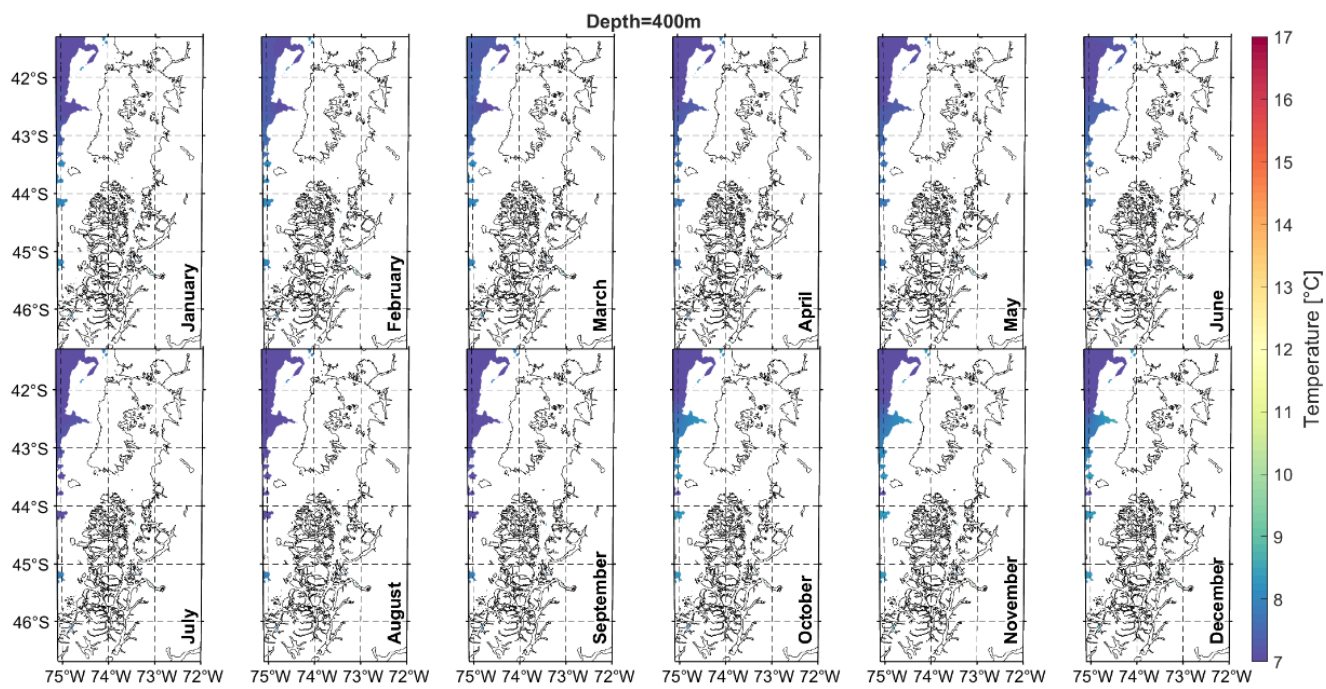*Figure Annexe 50: Monthly climatology of the sea temperature at 375m depth.*

Figure Annexe 52: Monthly climatology of the sea temperature at 400m depth.

3.Availability of in situ data

In section 3.2.2, we described the use of in situ data to build the temperature climatology. The following table lists all the sources of the in situ data, along with information on the platform type, the institute that conducted the campaigns (if available), and the spatial and temporal extent of the samples.

Table Annexe 1: Origin and information about the in situ data used for the construction of the climatology.

Source/ Provider	Platform type	Institute	Temporal extent	Spatial extend	References
CMEMS	Drifters	/	1950-01-01 to 2021-12-31	All study area	Szekely et al., 2023[1]
	CTD				
Pangaea	Shallow water monitoring stations	Wagner institute Huinay Scientific Field Station	2009-04-07 to 2014-02-11	Fjord Comau	[2] to [54]
				Fjord Renihue	
				Fjord Piti Palena	
				Repollal Islands	
EMODnet	Drifting buoys	/	2016-09-20 to 2021-05-31	All study area	[55] to [59]
World Ocean Database (WOD)	CTD (conductivity temperature depth)	/	1948-11-23 to 2020-05-12	Open Ocean, West of the Sea of Chiloé	Boyer et al., 2018[60]
	OSD (ocean station data)				
	XBT (expandable bathythermograph)				
	MBT (Mechanical Bathythermograph)				
	APB (Autonomous Pinniped Bathythermographs				

	)				
	PFL (Profiling Floats)				
Centro de datos oceanográficos y meteorológicos (CDOM)	Anchored buoy	COPAS Sur-Austral	2013-03-09 to 2014-06-19	Reloncaví Fjord (Cochamo) -72,31E, -41,52N	http://cdom.cl/
			2010-07-01 to 2018-04-06	Puyuhuapi Fjord -72.72E, -44.58N	
Centro de investigaciónes i~mar	Anchored buoy	Centro de investigaciones i~mar	2017-04-28 to 2023-09-01	Reloncaví Sound -72.8345E, -41.6364N	http://cdom.cl/
		COPAS Sur-Austral			
Centro de investigaciónes i~mar	CTD	Centro de Instrucción y Capacitación Maritima (CIMAR)	1970-03-20 to 2022-09-01	All study area (especially interior Sea of Chiloé)	...
	Microprofiler	Centro de investigaciones i~mar			
		Instituto de Fomento Pesquero (IFOP)			

The following pages list the different sources and/or DOIs for the in situ data shown in the table above.

3.1 CMEMS

[1]Szekely Tanguy, Gourrion Jerome, Pouliquen Sylvie, Reverdin Gilles (2023). CORA, Coriolis Ocean Dataset for Reanalysis. SEANOE. https://doi.org/10.17882/46219

3.2 Pangaea

Coming from shallow depth monitoring stations in different fjords of the north of the Inner Sea of Chiloé. Listed by localisation.

Comau

[2]2009 Laudien, Jürgen; Jantzen, Carin; Häussermann, Verena; Försterra, Günter; Funke, Tobias; Richter, Claudio (2018): Physical oceanographic profiles of CTD casts at X-Huinay and Punta Gruesa (Comau Fjord) in April 2009. Alfred Wegener Institute, Helmholtz Centre for Polar and Marine Research, Bremerhaven, PANGAEA, https://doi.org/10.1594/PANGAEA.894699

[3]2011 Laudien, Jürgen; Jantzen, Carin; Häussermann, Verena; Försterra, Günter; Sswat, Michael; Baumgarten, Sebastian; Richter, Claudio (2017): Physical oceanographic profiles of seven CTD casts from Gulf of Ancud into Comau Fjord in 2011. Alfred Wegener Institute, Helmholtz Centre for Polar and Marine Research, Bremerhaven, PANGAEA, https://doi.org/10.1594/PANGAEA.884120

[4]2012 Fillinger, Laura; Richter, Claudio (2013): Physical oceanography during expedition Comau2012. Alfred Wegener Institute, Helmholtz Centre for Polar and Marine Research, Bremerhaven, PANGAEA, https://doi.org/10.1594/PANGAEA.811832

[5]2012 phys oce Fillinger, Laura; Richter, Claudio (2013): Physical oceanography during expedition Comau2012. Alfred Wegener Institute, Helmholtz Centre for Polar and Marine Research, Bremerhaven, PANGAEA, https://doi.org/10.1594/PANGAEA.811832

[6]2013 Laudien, Jürgen; Häussermann, Verena; Försterra, Günter; Goehlich, Henry (2017): Physical oceanographic profiles of 14 CTD casts from Gulf of Ancud into Comau Fjord in 2013. Alfred Wegener Institute, Helmholtz Centre for Polar and Marine Research, Bremerhaven, PANGAEA, https://doi.org/10.1594/PANGAEA.874259

[7]2014 Laudien, Jürgen; Häussermann, Verena; Försterra, Günter; Goehlich, Henry (2014): Physical oceanographic profiles of seven CTD casts from Gulf of Ancud into Comau Fjord in 2014. Alfred Wegener Institute, Helmholtz Centre for Polar and Marine Research, Bremerhaven, PANGAEA, https://doi.org/10.1594/PANGAEA.832187

Huinay

[8]2010 Laudien, Jürgen; Baumgarten, Sebastian; Jantzen, Carin; Richter, Claudio; Steinmetz, Richard; Häussermann, Verena; Försterra, Günter (2012): Water temperature at station Huinay, Comau Fjord, Patagonia, Chile in 2010. Alfred Wegener Institute, Helmholtz Centre for Polar and Marine Research, Bremerhaven, PANGAEA, https://doi.org/10.1594/PANGAEA.783633

[9]2012-13 Laudien, Jürgen; Jantzen, Carin; Häussermann, Verena; Försterra, Günter (2013):

Water temperature at time series station Huinay Jetty, Comau Fjord, Patagonia, Chile in 2012/2013. Alfred Wegener Institute, Helmholtz Centre for Polar and Marine Research, Bremerhaven, PANGAEA, https://doi.org/10.1594/PANGAEA.843752

[10]2013-14 Laudien, Jürgen; Häussermann, Verena; Försterra, Günter (2014): Water temperature at time series station Huinay Jetty, Comau Fjord, Patagonia, Chile in 2013/2014. Alfred Wegener Institute, Helmholtz Centre for Polar and Marine Research, Bremerhaven, PANGAEA, https://doi.org/10.1594/PANGAEA.843753

[11]2014-15 Laudien, Jürgen; Häussermann, Verena; Försterra, Günter (2015): Water temperature at time series station Huinay Jetty, Comau Fjord, Patagonia, Chile in 2014/2015. Alfred Wegener Institute, Helmholtz Centre for Polar and Marine Research, Bremerhaven, PANGAEA, https://doi.org/10.1594/PANGAEA.843770

[12]2015-16 Laudien, Jürgen; Häussermann, Verena; Försterra, Günter; Richter, Claudio (2017): Water temperature at time series station Huinay Jetty, Comau Fjord, Patagonia, Chile in 2015/2016. Alfred Wegener Institute, Helmholtz Centre for Polar and Marine Research, Bremerhaven, PANGAEA, https://doi.org/10.1594/PANGAEA.872935

Liliguapi

[13]2010 Laudien, Jürgen; Baumgarten, Sebastian; Jantzen, Carin; Richter, Claudio; Steinmetz, Richard; Häussermann, Verena; Försterra, Günter (2012): Water temperature at time series station Liliguapi, Paso Comau, Patagonia, Chile in 2010. Alfred Wegener Institute, Helmholtz Centre for Polar and Marine Research, Bremerhaven, PANGAEA, https://doi.org/10.1594/PANGAEA.783296

[14]2011-12 Laudien, Jürgen; Jantzen, Carin; Häussermann, Verena; Försterra, Günter (2012): Water temperature at time series station Liliguapi, Paso Comau, Patagonia, Chile in 2011/2012. Alfred Wegener Institute, Helmholtz Centre for Polar and Marine Research, Bremerhaven, PANGAEA, https://doi.org/10.1594/PANGAEA.777752

[15]2012-13 Laudien, Jürgen; Jantzen, Carin; Häussermann, Verena; Försterra, Günter (2013): Water temperature at time series station Liliguapi, Paso Comau, Patagonia, Chile in 2012/2013. Alfred Wegener Institute, Helmholtz Centre for Polar and Marine Research, Bremerhaven, PANGAEA, https://doi.org/10.1594/PANGAEA.818388

[16]2013-14 Laudien, Jürgen; Jantzen, Carin; Häussermann, Verena; Försterra, Günter (2014): Water temperature at time series station Liliguapi, Paso Comau, Patagonia, Chile in 2013/2014. Alfred Wegener Institute, Helmholtz Centre for Polar and Marine Research, Bremerhaven, PANGAEA, https://doi.org/10.1594/PANGAEA.830086

[17]2014-15 Laudien, Jürgen; Häussermann, Verena; Försterra, Günter (2015): Water temperature at time series station Liliguapi, Paso Comau, Patagonia, Chile in 2014/2015. Alfred Wegener Institute, Helmholtz Centre for Polar and Marine Research, Bremerhaven, PANGAEA, https://doi.org/10.1594/PANGAEA.843773

[18]2015 02 Laudien, Jürgen; Häussermann, Verena; Försterra, Günter (2015): Water temperature at time series station Liliguapi, Paso Comau, Patagonia, Chile in 2015-02. Alfred Wegener Institute, Helmholtz Centre for Polar and Marine Research, Bremerhaven, PANGAEA, https://doi.org/10.1594/PANGAEA.845259

[19]2015-16 Laudien, Jürgen; Häussermann, Verena; Försterra, Günter (2017): Water temperature at time series station Liliguapi, Paso Comau, Patagonia, Chile in 2015/2016. Alfred Wegener

Institute, Helmholtz Centre for Polar and Marine Research, Bremerhaven, PANGAEA, https://doi.org/10.1594/PANGAEA.872161

[20]2016-17 Laudien, Jürgen; Häussermann, Verena; Försterra, Günter (2017): Water temperature at time series station Liliguapi, Paso Comau, Patagonia, Chile in 2016/2017. Alfred Wegener Institute, Helmholtz Centre for Polar and Marine Research, Bremerhaven, PANGAEA, https://doi.org/10.1594/PANGAEA.872121

[21]2017-18 Laudien, Jürgen; Häussermann, Verena; Försterra, Günter (2021): Water temperature at time series station Liliguapi, Paso Comau, Patagonia, Chile in 2017/2018. Alfred Wegener Institute, Helmholtz Centre for Polar and Marine Research, Bremerhaven, PANGAEA, https://doi.org/10.1594/PANGAEA.933275

Near Swall

[22]Laudien, Jürgen; Schmidt, Gertraud; González Estay, Humberto; Höfer, Juan; Häussermann, Verena; Försterra, Günter; Richter, Claudio (2017): Water temperature at time series station Near SWALL, Comau Fjord, Patagonia, Chile in 2016/2017. Alfred Wegener Institute, Helmholtz Centre for Polar and Marine Research, Bremerhaven, PANGAEA, https://doi.org/10.1594/PANGAEA.872480

Pirate Cove

[23]2016-17 Laudien, Jürgen; Schmidt, Gertraud; González Estay, Humberto; Höfer, Juan; Häussermann, Verena; Försterra, Günter; Richter, Claudio (2017): Water temperature at time series station Pirate Cove, Comau Fjord, Patagonia, Chile in 2016/2017. Alfred Wegener Institute, Helmholtz Centre for Polar and Marine Research, Bremerhaven, PANGAEA, https://doi.org/10.1594/PANGAEA.872482

Punta Gruesa

[24]2010 Laudien, Jürgen; Baumgarten, Sebastian; Jantzen, Carin; Richter, Claudio; Steinmetz, Richard; Häussermann, Verena; Försterra, Günter (2012): Water temperature at station Punta Gruesa, Comau Fjord, Patagonia, Chile in 2010. Alfred Wegener Institute, Helmholtz Centre for Polar and Marine Research, Bremerhaven, PANGAEA, https://doi.org/10.1594/PANGAEA.783293

Rio Tambor

[25]Laudien, Jürgen; Schmidt, Gertraud; González Estay, Humberto; Höfer, Juan; Häussermann, Verena; Försterra, Günter; Richter, Claudio (2017): Water temperature at time series station Rio Tambor, Comau Fjord, Patagonia, Chile in 2016/2017. Alfred Wegener Institute, Helmholtz Centre for Polar and Marine Research, Bremerhaven, PANGAEA, https://doi.org/10.1594/PANGAEA.872483

Soledad

[26]2015-17 Laudien, Jürgen; Häussermann, Verena; Försterra, Günter (2017): Water temperature at time series station Soledad, Paso Comau, Patagonia, Chile in 2015/2017. Alfred Wegener

Institute, Helmholtz Centre for Polar and Marine Research, Bremerhaven, PANGAEA, https://doi.org/10.1594/PANGAEA.872183

Swall

[27]2010 Laudien, Jürgen; Baumgarten, Sebastian; Jantzen, Carin; Richter, Claudio; Steinmetz, Richard; Häussermann, Verena; Försterra, Günter (2012): Water temperature at station SWALL, Comau Fjord, Patagonia, Chile in 2010. Alfred Wegener Institute, Helmholtz Centre for Polar and Marine Research, Bremerhaven, PANGAEA, https://doi.org/10.1594/PANGAEA.783302

X-Huinay North

[28]2014-15 Laudien, Jürgen; Häussermann, Verena; Försterra, Günter (2015): Water temperature at time series station X-Huinay North, Comau Fjord, Patagonia, Chile in 2014/2015. Alfred Wegener Institute, Helmholtz Centre for Polar and Marine Research, Bremerhaven, PANGAEA, https://doi.org/10.1594/PANGAEA.845371

[29]2015-16 Laudien, Jürgen; Häussermann, Verena; Försterra, Günter; Richter, Claudio (2017): Water temperature at time series station X-Huinay North, Comau Fjord, Patagonia, Chile in 2015/2016. Alfred Wegener Institute, Helmholtz Centre for Polar and Marine Research, Bremerhaven, PANGAEA, https://doi.org/10.1594/PANGAEA.872936

[30]2016-17 Laudien, Jürgen; Häussermann, Verena; Försterra, Günter (2017): Water temperature at time series station X-Huinay North, Comau Fjord, Patagonia, Chile in 2016/2017. Alfred Wegener Institute, Helmholtz Centre for Polar and Marine Research, Bremerhaven, PANGAEA, https://doi.org/10.1594/PANGAEA.872157

X-Huinay

[31]2010 Laudien, Jürgen; Baumgarten, Sebastian; Jantzen, Carin; Richter, Claudio; Steinmetz, Richard; Häussermann, Verena; Försterra, Günter (2012): Water temperature at station X-Huinay, Comau Fjord, Patagonia, Chile in 2010. Alfred Wegener Institute, Helmholtz Centre for Polar and Marine Research, Bremerhaven, PANGAEA, https://doi.org/10.1594/PANGAEA.783284

[32]2011-12 Laudien, Jürgen; Jantzen, Carin; Häussermann, Verena; Försterra, Günter (2012): Water temperature at station X-Huinay, Comau Fjord, Patagonia, Chile in 2011/2012. Alfred Wegener Institute, Helmholtz Centre for Polar and Marine Research, Bremerhaven, PANGAEA, https://doi.org/10.1594/PANGAEA.777693

[33]2012 Laudien, Jürgen; Jantzen, Carin; Häussermann, Verena; Försterra, Günter (2013): Water temperature at time series station X-Huinay, Comau Fjord, Patagonia, Chile in 2012. Alfred Wegener Institute, Helmholtz Centre for Polar and Marine Research, Bremerhaven, PANGAEA, https://doi.org/10.1594/PANGAEA.818434

[34]2013-14 Laudien, Jürgen; Jantzen, Carin; Häussermann, Verena; Försterra, Günter (2014): Water temperature at station X-Huinay, Comau Fjord, Patagonia, Chile in 2013/2014. Alfred Wegener Institute, Helmholtz Centre for Polar and Marine Research, Bremerhaven, PANGAEA, https://doi.org/10.1594/PANGAEA.830087

[35]2014-15 Laudien, Jürgen; Häussermann, Verena; Försterra, Günter (2015): Water temperature at time series station X-Huinay, Comau Fjord, Patagonia, Chile in 2014/2015. Alfred Wegener Institute, Helmholtz Centre for Polar and Marine Research, Bremerhaven, PANGAEA,

https://doi.org/10.1594/PANGAEA.845260

[36]2015-16 Laudien, Jürgen; Häussermann, Verena; Försterra, Günter; Richter, Claudio (2017): Water temperature at time series station X-Huinay, Comau Fjord, Patagonia, Chile in 2015/2016. Alfred Wegener Institute, Helmholtz Centre for Polar and Marine Research, Bremerhaven, PANGAEA, https://doi.org/10.1594/PANGAEA.872937

[37]2016-17 Laudien, Jürgen; Häussermann, Verena; Försterra, Günter (2017): Water temperature at time series station X-Huinay, Comau Fjord, Patagonia, Chile in 2016/2017. Alfred Wegener Institute, Helmholtz Centre for Polar and Marine Research, Bremerhaven, PANGAEA, https://doi.org/10.1594/PANGAEA.872155

[38]2017-18 Laudien, Jürgen; Häussermann, Verena; Försterra, Günter; Heran, Thomas (2021): Water temperature at time series station X-Huinay, Comau Fjord, Patagonia, Chile in 2017/2018. Alfred Wegener Institute, Helmholtz Centre for Polar and Marine Research, Bremerhaven, PANGAEA, https://doi.org/10.1594/PANGAEA.933272

X-Telele

[39]2016-17 Laudien, Jürgen; Schmidt, Gertraud; González Estay, Humberto; Höfer, Juan; Häussermann, Verena; Försterra, Günter; Richter, Claudio (2017): Water temperature at time series station X-Telele (deep), Comau Fjord, Patagonia, Chile in 2016/2017. Alfred Wegener Institute, Helmholtz Centre for Polar and Marine Research, Bremerhaven, PANGAEA, https://doi.org/10.1594/PANGAEA.872484

[40]2017 05 Laudien, Jürgen; Schmidt, Gertraud; González Estay, Humberto; Höfer, Juan; Häussermann, Verena; Försterra, Günter; Richter, Claudio (2017): Water temperature at time series station X-Telele-deep, Comau Fjord, Patagonia, Chile, 2017-05-17 to 2017-08-07. Alfred Wegener Institute, Helmholtz Centre for Polar and Marine Research, Bremerhaven, PANGAEA, https://doi.org/10.1594/PANGAEA.883954

[41]2016-17 Laudien, Jürgen; Schmidt, Gertraud; González Estay, Humberto; Höfer, Juan; Häussermann, Verena; Försterra, Günter; Richter, Claudio (2017): Water temperature at time series station X-Telele (shallow), Comau Fjord, Patagonia, Chile in 2016/2017. Alfred Wegener Institute, Helmholtz Centre for Polar and Marine Research, Bremerhaven, PANGAEA, https://doi.org/10.1594/PANGAEA.872486

[42]2017 01 Laudien, Jürgen; Schmidt, Gertraud; González Estay, Humberto; Höfer, Juan; Häussermann, Verena; Försterra, Günter; Richter, Claudio (2017): Water temperature at time series station X-Telele, Comau Fjord, Patagonia, Chile, 2017-01-19 to 2017-01-26. Alfred Wegener Institute, Helmholtz Centre for Polar and Marine Research, Bremerhaven, PANGAEA, https://doi.org/10.1594/PANGAEA.872485

Fjord Pillan

[43]2012-13 Laudien, Jürgen; González-Diaz, Felipe; Bellhoff, David; Reichel, Lisa (2013): Water temperature at time series station Punta Pillan, Brazo Pillan, Region Aysén, Chile, in 2012/2013. Alfred Wegener Institute, Helmholtz Centre for Polar and Marine Research, Bremerhaven, PANGAEA, https://doi.org/10.1594/PANGAEA.818389

[44]2013-14 Laudien, Jürgen; González-Diaz, Felipe (2014): Water temperature at time series station Punta Pillan, Brazo Pillan, Region Aysén, Chile, in 2013/2014. Alfred Wegener Institute, Helmholtz Centre for Polar and Marine Research, Bremerhaven, PANGAEA,

https://doi.org/10.1594/PANGAEA.830092

[45]2014-15 Laudien, Jürgen; González-Diaz, Felipe; Heran Arce, Thomas (2015): Water temperature at time series station Punta Pillan, Brazo Pillan, Region Aysén, Chile, in 2014/2015. Alfred Wegener Institute, Helmholtz Centre for Polar and Marine Research, Bremerhaven, PANGAEA, https://doi.org/10.1594/PANGAEA.843774

Anihue

[46]2012 Laudien, Jürgen; Müller, Jens; González-Diaz, Felipe; Bellhoff, David (2012): Physical oceanographic profiles of 20 CTD casts from Las Hermanas Island, Palena Bay, Chile via fjord Piti Palena to Brazo Pian, Region Aysén. Alfred Wegener Institute, Helmholtz Centre for Polar and Marine Research, Bremerhaven, PANGAEA, https://doi.org/10.1594/PANGAEA.783931

Piti Palena fjord, Ensenada de las islas

[47]2012-13 Laudien, Jürgen; González-Diaz, Felipe; Bellhoff, David; Reichel, Lisa (2013): Water temperature at time series station Ensenada de Las Islas, Piti Palena Fjord, Region Aysén, Chile in 2012/2013. Alfred Wegener Institute, Helmholtz Centre for Polar and Marine Research, Bremerhaven, PANGAEA, https://doi.org/10.1594/PANGAEA.818387

[48]2013-14 Laudien, Jürgen; González-Diaz, Felipe (2014): Water temperature at time series station Ensenada de Las Islas, Piti Palena Fjord, Region Aysén, Chile in 2013/2014. Alfred Wegener Institute, Helmholtz Centre for Polar and Marine Research, Bremerhaven, PANGAEA, https://doi.org/10.1594/PANGAEA.830085

[49]2014-15 Laudien, Jürgen; González-Diaz, Felipe; Heran Arce, Thomas (2015): Water temperature at time series station Ensenada de Las Islas, Piti Palena Fjord, Region Aysén, Chile in 2014/2015. Alfred Wegener Institute, Helmholtz Centre for Polar and Marine Research, Bremerhaven, PANGAEA, https://doi.org/10.1594/PANGAEA.843772

Renihue

[50]2013 Laudien, Jürgen; González-Diaz, Felipe; Goehlich, Henry (2017): Physical oceanographic profiles of six CTD casts from Reñihue Fjord in 2013. Alfred Wegener Institute, Helmholtz Centre for Polar and Marine Research, Bremerhaven, PANGAEA, https://doi.org/10.1594/PANGAEA.874261

Anihue

[51]2012 Laudien, Jürgen; Müller, Jens; González-Diaz, Felipe; Bellhoff, David (2012): Physical oceanographic profiles of 20 CTD casts from Las Hermanas Island, Palena Bay, Chile via fjord Piti Palena to Brazo Pian, Region Aysén. Alfred Wegener Institute, Helmholtz Centre for Polar and Marine Research, Bremerhaven, PANGAEA, https://doi.org/10.1594/PANGAEA.783931

[52]2013 Laudien, Jürgen; González-Diaz, Felipe; Häussermann, Verena; Försterra, Günter (2017): Physical oceanographic profiles of 20 CTD casts from Gulf of Corcovado via fjord Piti Palena to Brazo Pian (Region Aysén) in 2013. Alfred Wegener Institute, Helmholtz Centre for Polar and Marine Research, Bremerhaven, PANGAEA, https://doi.org/10.1594/PANGAEA.874034

[53]2014 Laudien, Jürgen; González-Diaz, Felipe; Goehlich, Henry (2014): Physical oceanographic

profiles of 30 CTD casts from Gulf of Corcovado via fjord Piti Palena to Brazo Pian (Region Aysén) in 2014. Alfred Wegener Institute, Helmholtz Centre for Polar and Marine Research, Bremerhaven, PANGAEA, https://doi.org/10.1594/PANGAEA.832226

<u>Isla Garza</u>

[54]2014-15 Laudien, Jürgen; González-Diaz, Felipe; Heran Arce, Thomas (2015): Water temperature at time series station Islotes Alloupa, Golfo Corcovado, Patagonia, Chile in 2014/2015. Alfred Wegener Institute, Helmholtz Centre for Polar and Marine Research, Bremerhaven, PANGAEA, https://doi.org/10.1594/PANGAEA.843771

3.3 EMODnet

The dataset was extracted from the Ocean Browser EMODnet (European Marine Observation and Data Network, URL: https://emodnet.ec.europa.eu/en/physics/; last access in 2022)

[55]https://doi.org/10.13155/59938

[56]https://doi.org/10.13155/40846

[57]https://doi.org/10.13155/53381

[58]https://doi.org/10.13155/36230

[59]https://doi.org/10.13155/43494

3.4 World Ocean Database (WOD)

[60]Boyer, T.P., O.K. Baranova, C. Coleman, H.E. Garcia, A. Grodsky, R.A. Locarnini, A.V. Mishonov, C.R. Paver, J.R. Reagan, D. Seidov, I.V. Smolyar, K. Weathers, M.M. Zweng,(2018): World Ocean Database 2018. A.V. Mishonov, Technical Ed., NOAA Atlas NESDIS 87.